

SEDIMENTOLOGY, ICHNOLOGY,
SEQUENCE STRATIGRAPHY
AND VERTEBRATE PALEONTOLOGY
OF THE BELLY RIVER GROUP,
SOUTHWESTERN SASKATCHEWAN
CANADA

A Thesis Submitted to the College of
Graduate Studies and Postdoctoral Studies
in Partial Fulfillment of the Requirements
for the Degree of Doctor of Philosophy
in the Department of Geological Sciences
University of Saskatchewan,
Saskatoon

By

Meagan Michelle Gilbert

©Copyright Meagan Michelle Gilbert, April 2019. All Rights Reserved.

Permission to Use,

In presenting this thesis in partial fulfilment of the requirements for a Postgraduate degree from the University of Saskatchewan, I agree that the Libraries of this University may make it freely available for inspection. I further agree that permission for copying of this thesis in any manner, in whole or in part, for scholarly purposes may be granted by the professor or professors who supervised my thesis work or, in their absence, by the Head of the Department or the Dean of the College in which my thesis work was done. It is understood that any copying or publication or use of this thesis or parts thereof for financial gain shall not be allowed without my written permission. It is also understood that due recognition shall be given to me and to the University of Saskatchewan in any scholarly use which may be made of any material in my thesis. Requests for permission to copy or to make other use of material in this thesis in whole or part should be addressed to:

Dean
College of Graduate and Postdoctoral Studies
University of Saskatchewan
116 Thorvaldson Building
110 Science Place
Saskatoon, Saskatchewan S7N 5C9
Canada

Head of the Department of Geological Sciences
University of Saskatchewan
114 Science Place
Saskatoon, Saskatchewan S7N 5E2
Canada

Abstract

The Belly River Group (BRG) in southwestern Saskatchewan records the interplay of accommodation space and base level in an epicontinental seaway. The Belly River Group has been the focus of numerous studies concerned with sedimentology, stratigraphy, and paleontology in Alberta and Montana, due to extensive badlands exposure, exceptional three-dimensional preservation of many sedimentary features, and the vast paleontologic data available from the deposits. The BRG has been studied with far less detail in Saskatchewan, due to the poor and sporadic nature of available outcrop, and comparatively little subsurface data. This study synthesizes all available data for the BRG in southwestern Saskatchewan, effectively characterizing the sedimentology, stratigraphy, ichnology, and paleontology and provides a comprehensive framework for these deposits in the province. This study provides critical insights into the BRG, particularly in regards to sequence stratigraphy. During the Campanian, the Western Interior Seaway bisected North America, and its western shore was located in southern Saskatchewan. This study provides critical insights into shoreline dynamics, both from a geologic and paleontologic perspective, and how these dynamics influence deposits further inland not directly in contact with the seaway. This study highlights the utility of integrating multiple, distinct datasets to understand depositional evolution along coastal plains, and its effects on biodiversity.

McLean (1971) characterized the uppermost deposits of the BRG (then called the Judith River Group) in the Cypress Hills as being deposited in an extensive delta plain. In Chapter 3, detailed facies analysis indicates the upper DPF does not record sedimentation in a delta system. A reinterpretation determines the DPF was deposited in a low-relief coastal plain with a wave-dominated, tidally influenced, fluvially modified shoreline. Marginal-marine facies, interpreted

as lagoons, tidal flats and estuaries, display a typical brackish-water trace-fossil assemblage, including *Asterosoma* isp., *Chondrites* isp., *Cylindrichnus concentricus*, *Teichichnus rectus*, and *Skolithos* isp. Fine-grained sandstone deposited in an estuarine mouth-bar and barrier-island complex protected the coast from wave reworking. As the seaway transgressed across the coast, fully marine wave-dominated parasequences replaced those of the coastal plain. Typical trace fossils include *Asterosoma* isp., *Chondrites* isp., *Diplocraterion* isp., *Nereites missouriensis*, *Phycosiphon incertum*, *Planolites* isp., *Rhizocorallium* isp., and *Zoophycos* isp., reflecting open, fully marine conditions.

In Chapter 4, the Belly River Group and its associated formations are formally recognized for the first time in Saskatchewan with facies, depositional environments, and sequence stratigraphic framework interpreted to provide a concise treatment of the deposits in southwestern Saskatchewan. A new lithostratigraphic unit within the uppermost Dinosaur Park Formation is recognized based on laterally extensive barrier island, lagoon, and estuary basin deposits. The Manâtakâw Member is established as a means to aide in discussing the transition from nonmarine clastics of the BRG to marine shales of the overlying Bearpaw Formation. Unincised and incised valley systems are explored in detail, with lowstand systems tract deposits compared and contrasted between the Oldman and Dinosaur Park formations.

Chapters 5 and 6 discuss microvertebrate localities from the Dinosaur Park Formation, one at Lake Diefenbaker (Ch. 5), and the other at Woodpile Coulee (Ch. 6). Palynology, ichnology, sedimentology, and vertebrate paleontology are integrated to determine paleoenvironmental and paleoecological conditions in the two regions and their stratigraphic positions. Both sites are interpreted as having been deposited at different times during transgression of the encroaching Bearpaw Sea. Though well studied and sampled in Alberta, the

Dinosaur Park Formation is poorly exposed with little known associated vertebrate assemblages in Saskatchewan. These discoveries from the microvertebrate sites offer new insights into Late Cretaceous ecosystems near paleocoastlines, allowing for future studies of spatial diversity patterns relative to Albertan faunas.

Acknowledgements

For anyone who knows me and is familiar with my sojourn through grad school, I am truly as surprised as any of you that this project is “finished.” When I so naively set out on this journey, I had just completed my undergraduate research project on the Lake Diefenbaker microsite. As a result of that study, I had realized the geology of the Belly River Group in Saskatchewan was poorly constrained and grossly understudied. Thus, my Master of Science project was conceived, which turned into a PhD, which has turned into many (undisclosed) years and a life’s obsession. This project was so vast and all-consuming it felt insurmountable, and that there certainly would never be an end. But here we are, thank goodness.

I have had a tremendous amount of help and support from many great people along the way. Firstly, I would like to thank Tim Tokaryk of the Royal Saskatchewan Museum, who is the reason I started studying microvertebrate assemblages and the Belly River Group. My supervisors Luis Buatois and Robin Renaut - without your support this never would have happened. Your patience knows no bounds, especially for the times when I was definitely the ghost of your research group. Both of you were always able to support me in the ways I needed when I needed it, and that is a rare gift. To Dennis Braman and Don Brinkman of the Royal Tyrrell Museum - I owe you both so much for your support and guidance.

To Gabriela Mángano and Tracy Marchant, I don’t know if either of you can fully understand and appreciate how much you’ve influenced me through my years at the University of Saskatchewan. I am a much better teacher, researcher, and overall well-rounded human for your influence in my life.

My most sincere thanks to Zoë Vestrum and Brittany Laing for all the support in its varying forms. My friend and kindred spirit Chantal Crossman for being the unsung hero of the Geological Sciences Department (and my life). Michael Cuggy for his never-ending encouragement and emails with job postings - it always helped to know there might be life after grad school. Tim Prokupuik for everything that you are, including our upbeat and hopeful discussions on humanity. I can absolutely and without any hesitation say that I owe my trajectory to you. To Emily Bamforth for years of friendship, discussions, patience, and help; many aspects of the vertebrate microfossil component of this thesis would not have been possible without you.

I would like to thank my parents, both as a parental unit and as individuals. To my dad, Robert, who inspired my love of history, science, and the Cypress Hills. To my mom Leanne, who taught me social skills, empathy, and how to tell a good ‘yarn’. Daniel Princz for our technicolor dreamworld friendship. To my partner Tiakohl, who has boundlessly encouraged me to strive for better and to follow my goals, regardless of the obstacles, challenges, or where it takes me. I wouldn’t have finished my PhD without you.

Lastly, I want to thank my students, past, present, and future.
Inspiring the next generation of Earth scientists is the reason I do this.

This is for anyone who has ever found themselves in the middle of nowhere.

Table of Contents

Permission to use	i
Abstract	ii
Acknowledgements	v
Dedication	vi
Table of Contents	vii
List of Figures	xv
List of Tables	xix
List of Abbreviations	xxi
Chapter 1: Introduction	1
Thesis Structure	2
Transition	
Chapter 2: Geological Setting and Methodology	5
2.1 Depositional History and Tectonic Setting	5
2.2 Outcrop Pattern and Structural Geology	11
2.3 Previous Work	13
2.3.1 Nomenclature	13
2.3.2 Belly River Group Sedimentology and Stratigraphy	15
2.3.3 Belly River Group in Saskatchewan	17
2.4 Paleogeography and Paleoclimate	20

2.5 Paleontology	20
2.5.1 Palynology	20
2.5.2 Ichnology	23
2.5.3 Vertebrate Paleontology	25
2.6 Fieldwork Methods	28
2.7 Surface Data Collection Methods	30
2.8 Diversity Analysis	34
2.8.1 Quantifying Diversity	34
2.8.2 Non-Parametric Species Estimators	36
Tables	37
References	39
Transition	
Chapter 3: Ichnology and Depositional Environments of the Upper Cretaceous Dinosaur Park – Bearpaw Formation transition in the Cypress Hills region of Southwestern Saskatchewan, Canada	
Title	48
Abstract	48
1. Introduction	50
2. Geological Background	51
3. Methods	54
4. Results	56

4.1 Facies descriptions and interpretations	52
4.2 Facies associations	77
4.3 Ichnofabric characterizations	83
5. Discussion	88
5.1 Trace fossil distribution	87
5.2 Ichnodiversity and bioturbation of epicontinental seaways	89
5.3 Depositional Processes and paleoenvironments	90
5.4 Redefining the Dinosaur Park - Bearpaw Formation contact	92
5.5 Stratigraphic correlations and depositional evolution	94
6. Conclusions	99
Funding and Acknowledgments	100
Tables	101
References	108

Transition

Chapter 4: Sequence Stratigraphy and Depositional Environments of the Belly River Group (Campanian) in southwestern Saskatchewan, Canada: Incised and Unincised Fluvial Systems along an Epicontinental Seaway

Title	118
Abstract	118
4.1 Introduction	120

4.2 Geological Background and Dataset	122
4.3 Historical Stratigraphic Nomenclature	128
4.4 Stratigraphic and Sedimentary Environments	130
Foremost Formation	132
Oldman Formation	142
Dinosaur Park Formation	148
Manâtakâw Member	154
Bearpaw Formation	158
4.5 Discussion	161
Sequence Stratigraphy	160
4.6 Summary and Conclusions	174
Acknowledgements	177
Tables	178
References	190
Transition	
Chapter 5: Paleoecology and sedimentology of a vertebrate microfossil assemblage from the easternmost Dinosaur Park Formation (Late Cretaceous, Upper Campanian) Saskatchewan, Canada: Reconstructing diversity in a coastal ecosystem	
Title	198
Abstract	198
5.1. Introduction	199

5.2. Material and Methods	202
2.1 Geological Setting	202
2.2 History of fossil collection	206
2.3 Data collection and specimen identification	207
2.4 Diversity Analysis	208
5.3. Results	209
3.1 Facies descriptions and interpretations	209
3.2 Palynology and biostratigraphy	217
3.3 Vertebrate paleontology	218
5.4. Discussion	218
4.1 Paleoecology	218
4.2 Estimated species diversity	228
4.3 Depositional evolution	229
5.5. Conclusions	231
Acknowledgements	232
Tables	233
References	245
Transition	
Chapter 6: A New Dinosaur Park Formation (Campanian, Late Cretaceous)	
Microvertebrate Locality from the Cypress Hills region of Southwest	

Saskatchewan: Implications for paleoenvironmental controls on species alpha diversity

Title	258
Abstract	258
1. Introduction	260
2. Geological Setting	261
3. Materials and Methods	265
3.1 Data Collection	265
3.2 Diversity Analysis	267
4. Results	270
4.1 Site Description	270
4.2 Sedimentology	271
4.2.1 Sedimentology of the Belly River Group at Woodpile Coulee	271
4.2.2 Sedimentology of the Dinosaur Park Formation at Woodpile Coulee	274
4.3 Paleopedology	278
4.4 Biostratigraphy	279
4.5 Paleontology	282
5. Discussion	282
5.1 Vertebrate paleontology	282
5.2 Invertebrate paleontology	286

5.3 Palynological reconstruction	287
5.4 Vertebrate alpha diversity of Woodpile Coulee	288
5.5 Paleoecological Implications	289
6. Conclusions	293
Acknowledgements	294
Tables	295
References	300
Transition	
Chapter 7: A Review of Hydrocarbon Resources associated with the Belly River Group in Saskatchewan	307
Tables	312
References	314
Chapter 8: Conclusions	315
Appendix A: Dinosaur Park – Bearpaw Formation Facies Picks	318
Appendix B: Supplementary Cross Sections, Dinosaur Park - Bearpaw Transition	326
Appendix C: Supplementary Palynology Data, Dinosaur Park - Bearpaw Transition	332
Appendix D: Supplementary Cross Sections, Belly River Group	338
Appendix E: Belly River Group Formation Picks	365
Appendix F: Systematic Paleontology	356

List of Figures

Chapter 2

Figure 2.1	6
Figure 2.2	7
Figure 2.3	9
Figure 2.4	29
Figure 2.5	31
Figure 2.6	32

Chapter 3

Figure 3.1	52
Figure 3.2	53
Figure 3.3	56
Figure 3.4	57
Figure 3.5	58
Figure 3.6	60
Figure 3.7	63
Figure 3.8	66
Figure 3.9	67
Figure 3.10	69
Figure 3.11	78
Figure 3.12	80
Figure 3.13	93
Figure 3.14	95

Figure 3.15	96
Figure 3.16	98
Chapter 4	
Figure 4.1	121
Figure 4.2	123
Figure 4.3	125
Figure 4.4	127
Figure 4.5	129
Figure 4.6	131
Figure 4.7	133
Figure 4.8A	135
Figure 4.8B	136
Figure 4.8C	137
Figure 4.8D	138
Figure 4.8E	139
Figure 4.9	141
Figure 4.10	145
Figure 4.11	150
Figure 4.12	152
Figure 4.13	155
Figure 4.14A	159
Figure 4.14B	160
Figure 4.15	162

Figure 4.16	163
Figure 4.17	165
Figure 4.18	172
Chapter 5	
Figure 5.1	201
Figure 5.2	203
Figure 5.3	205
Figure 5.4	210
Figure 5.5	212
Figure 5.6	216
Figure 5.7	222
Figure 5.8	226
Chapter 6	
Figure 6.1	262
Figure 6.2	264
Figure 6.3	266
Figure 6.4	268
Figure 6.5	269
Figure 6.6	272
Figure 6.7	273
Figure 6.8	275
Figure 6.9	277
Figure 6.10	281

Figure 6.11	284
Chapter 7	
Figure 7.1	309
Figure 7.2	310

List of Tables

Chapter 2

Table 2.1	38
Table 2.1	39

Chapter 3

Table 3.1	101
Table 3.2	102
Table 3.3	106

Chapter 4

Table 4.1	178
Table 4.2	179
Table 4.3	181
Table 4.4	184
Table 4.5	186
Table 4.6	187
Table 4.7	189

Chapter 5

Table 5.1	233
Table 5.2	237
Table 5.3	244

Chapter 6

Table 6.1	295
-----------	-----

Table 6.2	297
Table 6.3	299
Chapter 7	
Table 7.1	312
Table 7.2	313

List of Abbreviations

10^6m^3 – million cubic meters; 10^9m^3 – billion cubic meters; ACE – Abundance-based Coverage Estimator; API – American Petroleum Institute (gamma ray); BF – Bearpaw Formation; BRG – Belly River Group; C – Coal; DPF – Dinosaur Park Formation; DPP – Dinosaur Provincial Park; FE-LDPF – Fluvio-Estuarine Lower Dinosaur Park Formation; FF – Foremost Formation; FSS – Fine-grained Sandstone; FSST – Falling Stage Systems Tract; GIP – gas in place; HST – Highstand Systems Tract; IHS – Inclined Heterolithic Stratification; LD – Lake Diefenbaker Site; LP – Lea Park Formation; LST – Lowstand Systems Tract; m – meter; M – Mudstone; MM – Manâtakâw Member; MMS – Medium-grained Sandstone; M-UDPF – Muddy Upper Dinosaur Park Formation; OF – Oldman Formation; RCM – Ribstone Creek Member; RSM – Royal Saskatchewan Museum; RTMP – Royal Tyrrell Museum of Paleontology; Sh – Shale; Si – Siltstone; Tcf – trillion cubic feet; TST – Transgressive Systems Tract; WIS – Western Interior Seaway; WPC – Woodpile Coulee Site

Introduction

The Upper Cretaceous Belly River Group (BRG) of the Western Canadian Sedimentary Basin is a vast siliciclastic deposit recording the last major regressive - transgressive cycle of the Western Interior Seaway in southern Alberta and Saskatchewan, Canada, extending into northern Montana in the United States. In Alberta and Montana, these deposits have been the focus of several sedimentologic and stratigraphic studies due to exceptional outcrop exposure and extensive subsurface data. The Saskatchewan extension of the Belly River Group has not been studied in as much detail, in part due to a lack of quality surface exposure. Available outcrop and subsurface data have been integrated, along with palynology, ichnology, vertebrate and invertebrate paleontology to provide the first comprehensive picture of the BRG in southwestern Saskatchewan since McLean (1971). Understanding the easternmost expression of the BRG has meaningful, large-scale implications which furthers our understanding of sequence stratigraphic signatures across an epicontinental basin, and what impact these changes had on organismal diversity across space and time.

The interplay of accommodation space, sediment supply, and shoreline morphology resulted in significant paleoenvironmental shifts along the western edge of the Western Interior Seaway shoreline during this time. These shifts are recorded in Belly River Group deposits in southwestern Saskatchewan. A robust depositional model and sequence stratigraphic framework for the Saskatchewan extent of the BRG and its associated formations (in ascending order, the Foremost, Oldman, and Dinosaur Park formations) has been developed for the first time in Saskatchewan, and utilizes ichnology, invertebrate and vertebrate paleontology. The results of this study contribute to a broader understanding of Late Cretaceous geology and paleontology not only in Saskatchewan, but across the Western Interior Sedimentary Basin. This thesis sheds

light on global problems concerning large-scale sequence stratigraphy, coastline morphology, and faunal turnovers associated with transgression, a problem of increasing relevance due to modern sea level rise.

The objectives of this study are to: 1) revise stratigraphic nomenclature of the group and its formations and members within Saskatchewan; 2) document the sedimentary facies; 3) characterize facies associations and their corresponding depositional environments; 4) develop a sequence stratigraphic framework; 5) document trace fossil occurrences and their significance to reconstructing depositional environments; 6) document the vertebrate and invertebrate assemblages and report on their occurrences; 7) analyze community alpha-diversity of vertebrate communities utilizing vertebrate microsite material; and 8) where possible, integrate palynologic data to augment environmental interpretations and constrain stratigraphic interpretation.

Thesis Structure

This is a manuscript-based thesis, with Chapters 3 - 6 corresponding to a manuscript submitted or prepared for submission to a peer-reviewed journal. Chapter 2 provides a brief literature review concerning the geologic background and previous research done on the BRG to date. This chapter also discusses methods used in the field and in the lab to compile the various datasets used throughout this thesis.

Chapter 3 highlights the Dinosaur Park - Bearpaw formation transition in the Cypress Hills of southwestern Saskatchewan, featuring both surface and subsurface datasets, and utilizes stratigraphic and ichnologic concepts. This chapter provides a detailed treatment of transgression across a low relief eperic coastline, providing a framework from which the sequence stratigraphy

of chapter 4 is based. This manuscript has been published in the June 2019 volume of *Cretaceous Research*.

Chapter 4 provides a detailed lithostratigraphic treatment of each of the formations in the Belly River Group (from oldest to youngest these are the Foremost, Oldman, and Dinosaur Park formations), and deals with placing the BRG into a sequence stratigraphic framework. Of particular significance is the formal recognition of all three formations in Saskatchewan, the proposed establishment of a new stratigraphic member in the upper Dinosaur Park (Manataka Member), and a discussion on lowstand systems tracts and their variability in epicontinental seaways. This has been submitted to *Bulletin of Canadian Petroleum Geology*.

Chapter 5 focuses on the Lake Diefenbaker site, which represents the easternmost extension of the BRG in Canada. This paper discusses local stratigraphy, an associated vertebrate microfossil assemblage, and vertebrate alpha diversity. This manuscript has been published in the May 2018 volume of *Palaeogeography, Palaeoclimatology, Palaeoecology*.

Chapter 6 discusses the geology of the BRG at Woodpile Coulee on the southern flanks of the Cypress Hills, and the biostratigraphy of the site interpreted through palynological samples. The Dinosaur Park Formation is discussed in detail, and invertebrate and vertebrate paleontology is considered. This chapter discusses various aspects of the vertebrate assemblage and the depositional environments preserved there. This has been prepared for submission, and will be submitted to *Palaeogeography, Palaeoclimatology, Palaeoecology*.

Several appendices at the end of this thesis are dedicated to the varying datasets used throughout this thesis. All vertebrate taxa, well log picks, and palynology data is provided in a raw format, for those who wish to use these datasets for future studies and scrutiny.

Transition

Chapter 1 presented an introduction to the thesis topic and information regarding the structure of the thesis. Chapter 2 provides a general background of the geological setting, and the history of work focused on the Belly River Group and its associated members and formations in western Canada and Montana. The Belly River Group has been studied for both its geologic and paleontologic significance for over a century. The vast amount of literature available on the topic underscore its significance to our modern understanding of geology and paleontology at a regional and global scale. As well as setting the geologic context, this chapter provides a background for different methodologies utilized when collecting and analyzing data used throughout this thesis.

Geological Setting and Methodology

2.1 Depositional History and Tectonic Setting

Deposition of Cretaceous and Cenozoic sediments in the Western Canada Sedimentary Basin occurred in two depocenters separated by the Bow Island Arch. These are the Williston Basin to the east and the Alberta Foreland Basin to the west (Fig. 2.1) (Dawson et al., 1994). During the Laramide Orogeny, collisional accretion of microcontinents on the western coast of North America caused thrust sheet loading, forming an orogenic belt along the western coast of North America (Price, 1994). This loading flexed the craton, producing a deeply subsiding asymmetric foredeep supplied by sediments derived from the building Rocky Mountains (Catuneanu et al., 2000). This resulted in the deposition of cyclical marine and terrestrial clastic sediments in transgressive-regressive tectonically controlled stacking patterns (Fig. 2.2; Leckie and Smith, 1992). Deposition of the Belly River Group (BRG) is interpreted to represent the fourth of five cycles of foreland basin deposition (Embry, 1990; Miall, 1991; Leckie and Smith, 1992).

The BRG overlies the marine Lea Park Formation, and underlies marine sediments of the Bearpaw Formation. Marine deposits of the underlying and interfingering Lea Park Formation (also known as the Claggett and/or Pakowki Formation) were deposited during a time of tectonic quiescence (Leckie and Smith, 1992). In contrast, deposition of terrestrial sediments of the BRG reflects an event that resulted in large amounts of sediment being supplied to the basin (Cant and Stockmal,

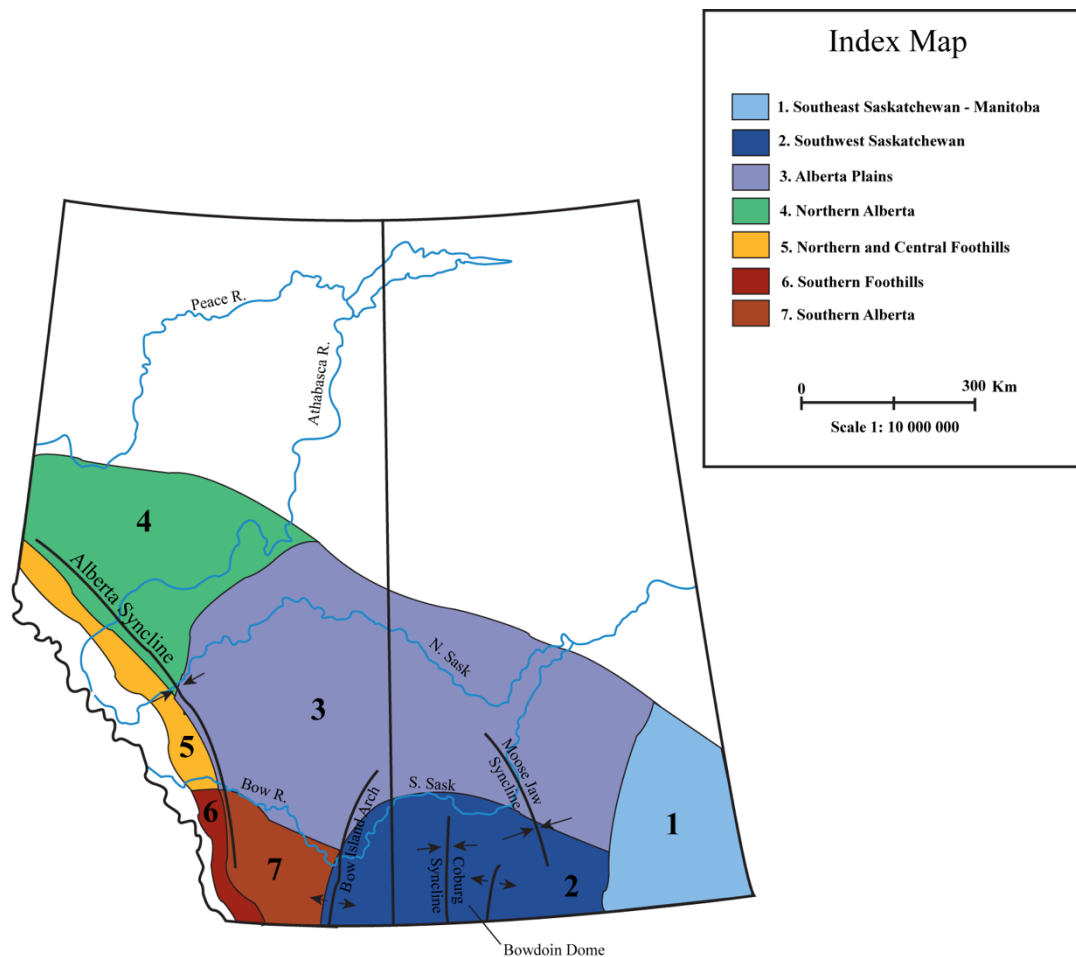


Figure 2.1: General map indicating different regional structural features, geographic areas and regions of different nomenclature throughout Alberta and Saskatchewan. Modified from Dawson et al. (1994).

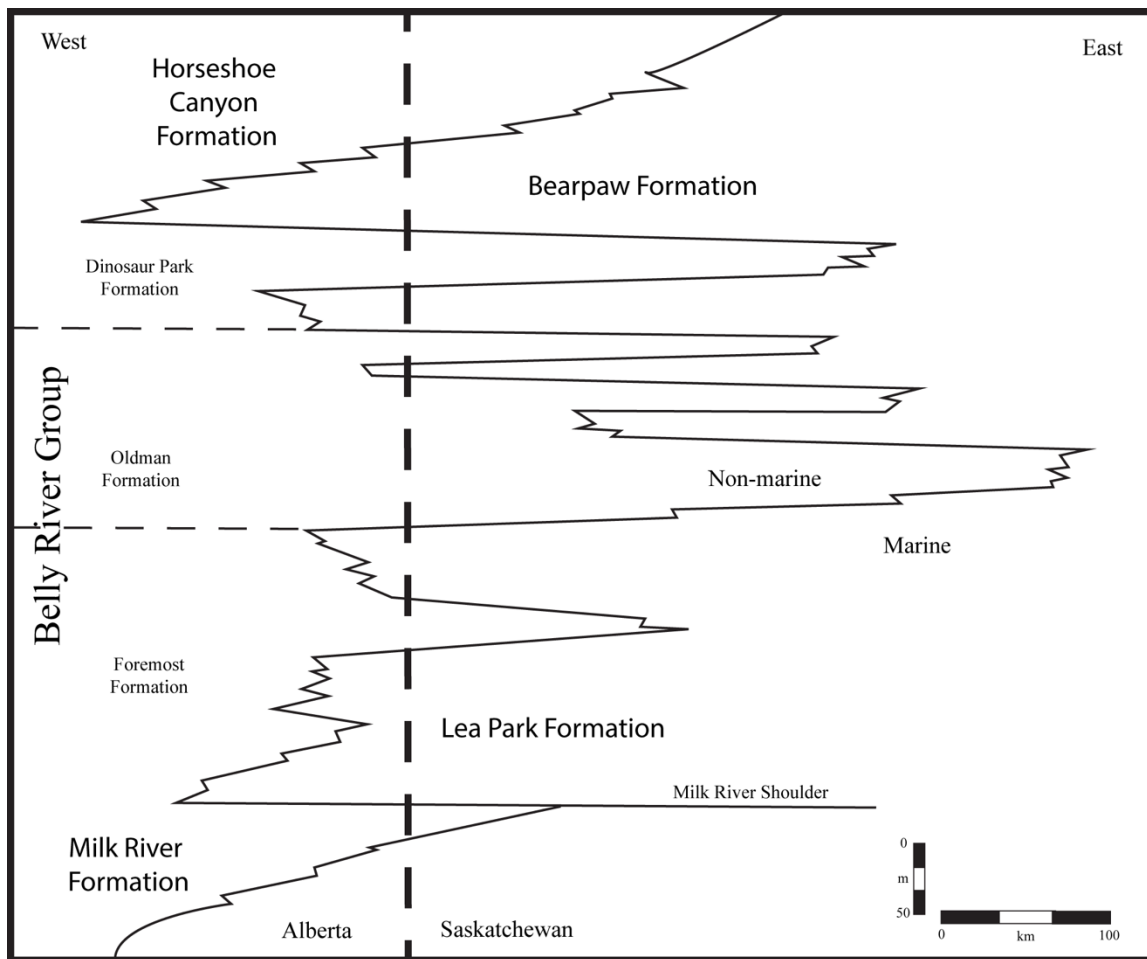


Figure 2.2: Simplified schematic cross section of the Upper Cretaceous Series through southern Alberta and southern Saskatchewan. Modified from McLean (1971). The Saskatchewan – Alberta border runs concurrent with the 4th meridian (110°W longitude) along its entirety.

1989). Rapid marine sedimentation of the conformably overlying Bearpaw Formation is believed to have resulted from rapid basin subsidence.

Regional correlations of Late Cretaceous and Cenozoic sedimentation events within southern Saskatchewan and the Alberta Plains are generally consistent, with some variation in stratigraphic nomenclature. The marine Pakowki Formation of Alberta is referred to as the Lea Park Formation in Saskatchewan. Terrestrial deposits of the Eastend, Frenchman, and Ravenscrag formations of Saskatchewan are equivalent to the Horseshoe Canyon, Scollard and Paskapoo formations of Alberta, respectively. Regional variations in nomenclature, as well as regional extent of formations and ages are included in Figure 2.3.

The Milk River Formation occurs stratigraphically below the base of the Lea Park Formation (Dawson et al., 1994). The contact between the coarser terrestrial clastics of the Milk River Formation and the marine shales of the Lea Park Formation are sharp in outcrop. A distinctive resistivity well log signature known as the Milk River (Eagle) Shoulder is used to identify this contact between the two formations. The contact is correlative to the top of the Milk River Formation and is used as the datum for stratigraphic cross sections prepared within this thesis.

Regressive deposits of the Lea Park Formation are predominantly shelf shales with occasional sandstone shoreface facies (Ogunyomi and Hills, 1977; Gordon, 2000). Contact between the interfingering Lea Park Formation and BRG is often inconsistently defined. Gordon (2000) and Dawson et al. (1994) identified the contact as the “base of the first coarsening upwards cycle capped by a major sandstone greater than two meters

thick.” In some parts of Alberta, the McKay coal zone is used to define the base between the two formations.

The BRG is overlain by the Bearpaw Formation, which forms a northwestward-thinning wedge of marine shale and shoreface sandstone (e.g., Beechy Sandcastle near Beechy, Saskatchewan). Contact between the two units is generally sharp and is characterized by an abrupt upward change in lithology from a heterogeneous sequence of interbedded siltstone, sandstone, carbonaceous mudstone and coal to a relatively homogeneous succession of mudstone or shale (Eberth, 2005). Over much of the Alberta Plains the Lethbridge Coal Zone, a succession of thin coal seams interbedded with mudstone, siltstone and bentonite, is present in the upper portion of the Dinosaur Park Formation (DPF). Where coal is not present, there is commonly a zone of interbedded bentonite and carbonaceous mudstone immediately below the overlying contact with the Bearpaw Formation. Traditionally, the base of the Bearpaw Formation is placed at the first succession of shale characteristic of this unit directly overlying the Lethbridge Coal Zone (Russell and Landes, 1940). However, marine sandstone is known to occur within the lower Bearpaw in some regions (such as the Cypress Hills). Previously, coarsening-upwards sandstone situated above the Lethbridge Coal Zone has been included within the Bearpaw Formation rather than the underlying Dinosaur Park Formation (Glombick, 2010). This thesis redefines this contact in the Cypress Hills, which is investigated in full in Chapter 3.

This thesis will follow the formational nomenclature of Hamblin and Abrahamson (1996). The term Judith River Formation of McLean (1971) is dropped, with the clastic wedge between the Lea Park and Bearpaw formations being elevated to Group status in Saskatchewan, as has been done in Alberta (Eberth and Hamblin, 1993). All Belly River equivalents are included in the Belly River Group, to conform to nomenclature used in Alberta. The division of

the BRG follows Eberth and Hamblin (1993). From oldest to youngest these units are the Foremost, Oldman, and Dinosaur Park formations. In Saskatchewan, the lowermost Foremost Formation is generally represented as marine shoreface successions, with evidence of paralic channel fill near the Alberta – Saskatchewan border (Gordon, 2000). The Foremost Formation gradationally overlies shales of the Lea Park Formation. The Oldman Formation is composed of pale yellow alluvial sandstone and mudstone, and records the maximum regression of the Western Interior Seaway. The Dinosaur Park Formation is dominated by sandstone and mudstone, consisting of alluvial, estuarine, and paralic facies (Eberth, 2005). The general lithology and known paleoenvironmental parameters of these formations will be discussed in more detail below.

2.2 Outcrop Pattern and Structural Geology

Along the western edge of the foreland basin in the Alberta Foothills, extensive folding, faulting, and erosion occurred during the last stages of the Laramide Orogeny (Fig. 2.1). To the east of the foothills lies the trough-like Alberta Syncline, the western limb of which dips to the west, and was formed due to overthrusting linked to the development of the Rocky Mountains (Dawson et al., 1994).

Strata gently dip westward between the axis of the Alberta Syncline and the Bow Island Arch. Thicker Cretaceous-Cenozoic successions imply more compressional tectonism has occurred along the Alberta Syncline than in other regions along the Rocky Mountains (Dawson et al., 1994). Structural elevation in southeastern Alberta is controlled by the Bow Island Arch, which causes Cretaceous and Cenozoic strata to dip gently to the east and west on either side of the structure. Erosion over the Arch has caused units as old as the Milk River Formation to be exposed along its axis (Dawson et al., 1994).

In southern Saskatchewan, strata of the Williston Basin dip towards the basin centre in northeastern North Dakota. The Williston Basin forms the southeastern extremity of the Western Canada Sedimentary Basin, consisting of Phanerozoic successions located in Manitoba, Saskatchewan, the Dakotas, and Montana (Kent and Christopher, 1994). The eastern limit is the Sioux Arch, which runs through the Dakotas and into southeastern Manitoba. The western limit is the Sweetgrass Arch of northern Montana and southeastern Alberta, a large structural complex active throughout geologic time (Herbaly, 1974; Kent and Christopher, 1994). Therefore, the BRG in Saskatchewan straddles the Alberta Basin to the west, and the Williston Basin to the east. During the Cretaceous, the Sweetgrass Arch was believed to be undergoing uplift due to intrusion caused by the Laramide Orogeny (Kent and Christopher, 1994). This would have undoubtedly had a significant impact on sedimentation in the Cypress Hills region, immediately east of the Sweetgrass Arch.

Several regional and local structural features occur throughout southwestern Saskatchewan in the study area, many of which are believed to have formed by salt dissolution in older strata (particularly Devonian beds). These regional features include the Bowdoin Dome, Coburg Syncline, and the Moose Jaw Syncline (Fig. 2.1). Local features include folding and block faulting (McLean, 1971; Dawson et al., 1994). These features are reflected in regional thickening and thinning of facies adjacent to these structures.

2.3 Previous Work

2.3.1 Nomenclature

Dawson (1883) was the first to publish on BRG, studying outcrops along the Milk River in southern Alberta. Naming the outcrop the Belly River Series, he subdivided the series into an upper unit called the Pale and Yellow Beds and lower unit referred to as the Sombre Beds.

Correlation of outcrop from Montana was completed by Stanton and Hatcher (1905), who demonstrated that the Judith River Formation of Montana is equivalent to the Belly River of Alberta. Stanton and Hatcher (1905) showed that the Belly River in Alberta was underlain by Lea Park (Claggett or Pakowki) equivalent marine strata and overlain by Bearpaw equivalent marine strata, as in the Judith River Formation of Montana.

Dowling (1915) furthered Dawson's (1883) work by combining the Pale and Yellow Beds into the Pale Beds and renamed the Sombre Beds as the Foremost Beds. Dowling (1917) identified three stratigraphically different coal zones in the Belly River of Alberta that were subsequently named by Crockford (1949). In descending order, these coal zones are referred to as the Lethbridge, Taber, and McKay. Dowling's Foremost Beds were elevated to formation status and the Pale Beds were renamed the Oldman Formation by Russell and Landes (1940).

McLean (1971) named the clastic wedge between the Lea Park and Bearpaw Formations the Judith River Formation. He did not agree with the division of the Belly River into the Foremost and Oldman, citing inconsistency in lithological definition. He also proposed the name Belly River be used strictly in the foothills of Alberta where the Belly River and Milk River formations are undifferentiated (not separated by the Lea Park Formation). McLean (1971) proposed that subdivision of the Judith River should be discontinued until recognition of formational status units could be justified over a large geographic area.

Eberth and Hamblin (1993) raised the Judith River Formation to group status, and divided it into the Foremost, Oldman, and Dinosaur Park formations. The Dinosaur Park Formation is the newest and uppermost unit that had not been differentiated prior to their publication. The name Belly River is commonly used in the oil industry, therefore Hamblin and Abrahamson (1996) proposed the name Judith River Group be dropped in favor of BRG. The

Ribstone Creek Member of southwestern Saskatchewan is included within the Foremost Formation. Jerzykiewicz and Norris (1994) correlated the BRG of the Alberta Plains with the Belly River Formation of the Alberta Foothills. This was resolved by discovery of previously unknown deposits of the marine Lea Park Formation underlying the Belly River Formation.

Original reference to the Judith River beds in northern Montana was published by Meek and Hayden (1856), with Hayden (1856) officially proposing the term Judith Group. In the first comprehensive study of the Judith River Formation in Montana, Stanton and Hatcher (1905) identified the type area and described the lithology. The term Judith River Formation began to be employed in the early 1900s and has been used in Montana ever since (Lamb, 1907; Peale, 1912; Bowen, 1915; Rogers, 1995; Rogers et al., 2016). Rogers et al. (2016) identified four members within the Judith River Group in northern Montana. From oldest to youngest, these are the Parkman Sandstone, McClelland Ferry, Coal Ridge, and the Woodhawk members (Rogers et al., 2016).

2.3.2 Belly River Group Sedimentology and Stratigraphy

The Foremost Formation is paralic to non-marine in Alberta, and paralic to shallow marine in Saskatchewan, and reflects a major phase of basinward progradation of the BRG. The lower half of the formation consists of coarsening-upwards parasequences that interfinger with the Lea Park Formation, varying from progradational to aggradational. This parasequence stacking pattern reflects a complex relationship between sediment supply and accommodation space at the time of deposition (Speelman and Hills, 1980; Wasser, 1988; Gordon, 2000; Eberth, 2005). In Alberta, this Foremost Formation contains the McKay and Taber coal zones, at the bottom and top, respectively, and the Herronton Sandstone Zone, which overlies the Taber Coal Zone.

Contact between the Foremost and Oldman formations is historically placed at the top of the Taber Coal Zone. For consistency, the overlying Herronton Sandstone is placed within the Foremost, defining the contact between the Oldman and Foremost formations (Eberth, 2005).

The transition to the Oldman Formation is easily recognized in both subsurface data and outcrop. In outcrop, the Oldman Formation is characterized by fining-upward, lenticular to sheet-shaped paleochannel sandstones, and a complex variety of tabular, fine-grained members representing channel top, channel margin, and overbank facies (Eberth, 2005). Due to high calcite content, the Oldman Formation appears yellow and steep-faced with blocky surfaces (Eberth, 2005). In subsurface well logs, a strong, sometimes multi-cyclic increase in gamma response signals transition between the two formations (Hamblin, 1997a, 1997b). Oldman sediments contain mature fine- to very fine-grained sandstones with no extraformational pebbles or cobbles. This formation is exclusively alluvial in Alberta and records the maximum basinward extent of a regressive cycle in the BRG (Hamblin, 1997b).

The Oldman Formation is subdivided into three informal stratigraphic units based on paleochannel geometry and stacking patterns. The lower units display lenticular paleochannel geometries and were previously interpreted as deposited during a time of modest accommodation space (Eberth, 2005). The middle unit (Comrey Sandstone) consists of decameter-thick, amalgamated sandstone bodies with sheet-like to lenticular geometries. Tidal features in the upper Comrey Sandstone in southeastern Alberta imply potential marine influence (Noad, 1993; Troke, 1993; Eberth, 2005). In the upper unit above the Comrey Sandstone, paleochannels are well separated, with sub-equal paleochannel-overbank ratio indicating increased accommodation (Eberth, 2002, 2005). Paleocurrent data and southwest formation thickening suggest northwestern Montana as the primary source of sedimentation (Eberth and Hamblin, 1993).

The contact between the Oldman and Dinosaur Park formation is diachronous north to south, signaling the onset of progradation of the DPF clastic wedge. A regional discontinuity recognized in both outcrop and subsurface marks the transition between the two formations. In geophysical well logs, contact between the Oldman and DPF is marked by an abrupt, leftward deflection in gamma-ray across the discontinuity. The boundary is placed at the first major leftward gamma-ray deflection following a maximum rightward gamma-ray peak throughout the Oldman Formation (Eberth and Hamblin, 1993). In outcrop, lithofacies of the DPF are thicker and more laterally extensive than those of the Oldman Formation, and are easily divided into fine and coarse members dominated by claystone and sandstone respectively (Wood, 1989; Eberth and Hamblin, 1993).

The DPF consists of sandstone and mudstone, with lower sandy alluvial paleochannel deposits overlaying an upper, muddy overbank-facies-dominated, coaly succession (Lethbridge Coal Zone). Somber gray, brown, and green characterize DPF sediments that starkly contrast with the pale yellow-colored, mature sediments of the Oldman Formation in outcrop. Predominantly, the lower unit crops out as muddy sandstones with highly riled surfaces. Outcrops are meter- to decameter-thick, fossiliferous, straight- to meandering-paleochannel deposits containing trough-cross-bedded clean sandstone, extraformational pebbles, inclined heterolithic strata, carbonaceous drapes, and *in situ* and reworked ironstone. The upper mudstone-dominated unit contains tidally influenced mud-filled incised valleys resulting from high-order changes in relative sea level (Eberth, 1996). Laterally extensive and smectite-clay-rich, green-gray overbank facies are common (Eberth, 2005). Paleocurrent data indicates paleochannel flow from the east-southeast, with clastics derived from the north (Eberth and

Hamblin, 1993). Progradation of the lower DPF is followed by retrogradation in the upper DPF due to rapid transgression of the Bearpaw Sea (Chapters 3 and 4).

2.3.3 Belly River Group in Saskatchewan

Sparse exposures of the BRG are known to outcrop throughout western Saskatchewan in the North and South Saskatchewan River Valleys, Muddy Lake in west-central Saskatchewan, and the Cypress Hills in extreme southwestern Saskatchewan (McLean, 1971). These sediments represent the most eastern extent of the BRG and record passage of the terrestrial BRG into fully marine Bearpaw Shale of the Western Interior Seaway (Caldwell, 1968; Dawson et al., 1994). Outcrops of the BRG are rare in Saskatchewan south of 52° north latitude (McLean, 1971).

In the northern extent of the Cypress Hills, exposures are known along Boxelder Creek. In the southern extent, outcrops are recorded along two or three small creeks adjacent to the United States/Canada boundary. The best exposures in this region occur at Woodpile Coulee, where the entirety of the Group is exposed in roughly inclined strata associated with a Pleistocene thrust structure. It is uncertain to what extent these beds are displaced (McLean, 1971). Furnival (1946) studied the Cypress Lake region using the names Oldman and Foremost formations for the beds and correlated them to the Judith River Formation of Montana. A suitable division point between the two formations was not recognized, and therefore they described them together (Furnival, 1946).

Caldwell's (1968) study of the Bearpaw Formation along the South Saskatchewan River includes a brief summary of the underlying BRG. The beds were mentioned as closely resembling the Oldman and Foremost formations of Alberta (Caldwell, 1968). Little is mentioned other than being exposed as outcrops in decreasing thickness towards the east,

eventually pinching out into the Bearpaw Formation. Sediments are described as consisting of sandstone, siltstone, and claystone.

McLean (1971) incorporated both surface and subsurface data in an extensive study of the BRG. This study extended Russell and Landes's (1940) work into northern Montana and western Saskatchewan. The Foremost and Oldman formations were considered difficult to distinguish, and were grouped together as the Judith River Formation. The name "Judith River" was considered to have priority over Belly River, due to its priority in Montana and its consistent usage. The Judith River Formation was dropped with Eberth and Hamblin's (1993) division of the BRG into the Foremost, Oldman, and Dinosaur Park formations in Alberta. This thesis formally extends the nomenclature and recognition of these formations into Saskatchewan for the first time.

At Muddy Lake in south-central Saskatchewan, a 55 m thick section represents the northeastern-most documented exposure of the BRG. This section was divided into two informal subunits based on lithology, a lower "A" and upper "B" by Eberth et al. (1990). Unit A is characterized by trough cross-stratification, rare inclined heterolithic stratification (IHS), thinly interbedded sequences of sandstone and mudstone, and drab-colored mudstones. Unit B was described as containing IHS, inclined bedded sandstone, mudstone, and abundant organic-rich mudstone and bentonite. Unit B is muddier and darker than Unit A and contains extraformational pebbles and cobbles (Eberth et al., 1990). In a later publication, Eberth and Hamblin (1993) suggested these two units represent the Oldman and Dinosaur Park formations, respectively. These exposures record east-west shoreline fluctuations of the Bearpaw transgression not seen in Alberta and Montana (Eberth et al., 1990).

Gordon (2000) examined the Foremost Formation from a sequence stratigraphic perspective in southwestern Saskatchewan and southeastern Alberta. Subsurface information in Saskatchewan was linked to outcrops in the Pinhorn Grazing Pasture along the Milk River in southeastern Alberta. Subsurface mapping was utilized to explore stacking patterns and facies architecture during deposition of the easternmost Foremost Formation. This research suggested incised sandstone shoreface deposits formed due to progradation at times of stillstand conditions.

Frank (2010) used core and well logs to evaluate coal and carbonaceous mudstone distribution in the Saskatchewan extent of the BRG in the Cypress Hills. Coal was found to be concentrated in the upper part of the Belly River Group, particularly in the extreme southwest. No attempt to distinguish between formations or expand on depositional environments was made, but evaluation of the dataset by the author determines most of the mapped coal can be correlated to the upper Dinosaur Park Formation.

2.4 Paleogeography and Paleoclimate

Geography has changed significantly since deposition of the Group. Due to plate movement, Saskatchewan deposits are several degrees more northerly than during the Campanian, with the region located between 45° and 55° north latitude (Caldwell et al., 1982; Eberth, 2005). The western interior of North America was covered in a vast inland sea that episodically stretched from the Gulf of Mexico to the Arctic Ocean. Oxygen isotope analysis of fossil shells indicates water temperatures were between 15° and 27° Celsius (Caldwell et al., 1982). Western shorelines fluctuated over time due to changes in tectonic activity associated with the Laramide Orogeny. The Saskatchewan extent of the BRG was located at the most distal end of a broad, low-lying alluvial plain extending from the highlands in the west, to the coast of the Western Interior

Seaway in the east. Drainage was provided by paleorivers that flowed away from the rising Cordillera (Eberth, 2005).

Humidity is believed to have increased through time, particularly by the end of the Dinosaur Park Formation. Abundant caliche beds in the Oldman Formation are interpreted as signifying seasonal aridity (Jerzykiewicz and Sweet, 1988; D. Eberth, personal communication, 2012). Studies of growth rings in petrified wood, teeth, and vertebrae from Dinosaur Provincial Park further suggest seasonal climates (Caldwell et al., 1982). Increased diversity in pollen species upsection, especially evident in the DPF, implies decreased environmental stressors on plant diversity (Jerzykiewicz and Sweet, 1988). This evidence is further supported by abundant taphonomic studies conducted in Dinosaur Provincial Park.

Varying deposition styles of the Oldman and DPF suggest changing climates throughout the Belly River Group. Non-marine sediments of the Oldman Formation were deposited as part of an arid climate featuring braided stream systems with low sinuosity punctuated by massive flooding events. Evidence for catastrophic flooding is based on the style of preservation and distribution of dinosaur macrofossils (D. Eberth, personal communication, 2012). Most macrofossils from the Oldman Formation consist of bone beds made up of disarticulated fragments of tens to hundreds of individuals. Preservation and taphonomic features of the bones suggest slow burial, extensive scavenging, and re-exposure by channel migration. In contrast, DPF deposition occurred in a highly sinuous meandering stream system, suggesting a climate with more consistent rainfall if not a more humid climate. Many DPF macrofossils consist of articulated individuals, suggesting rapid burial, restricted scavenging, and limited reworking by fluvial systems (D. Eberth, personal communication, 2012).

2.5 Paleontology

2.5.1 Palynology

Subdivision of the Late Cretaceous successions based on palynomorphs has been suggested by several authors (Nichols et al., 1985; Sweet et al., 1989; Nichols and Sweet, 1993; Nichols, 1994; Braman and Sweet, 2012). Palynological studies of the Late Cretaceous have been conducted throughout Alberta, offering not only biostratigraphic information, but also paleoecological and paleoenvironmental insight (Nichols et al., 1982; Jerzykiewicz and Sweet, 1988; Braman and Sweet, 2012). Of particular relevance to this study is the palynomorphs recovered from Dinosaur Provincial Park.

Diversity of Dinosaur Provincial Park (DPP) palynomorphs is enormous, with over 500 species identified, representing mosses, hornworts, liverworts, lycopods, horsetails, ferns, tree ferns, conifers, gnetophytes, and a wide variety of flowering plants (Braman and Koppelhus, 2005). Due to low preservation of plants in the BRG, pollen offers a glimpse into paleoecological and paleogeographical variation. Due to pollen high preservation in both marine and non-marine settings, it allows for fine-tuned stratigraphic resolution not possible with other biostratigraphic taxa.

Species making a first appearance in the Foremost Formation include *Cirratiradites luminosus*, *Aquilapollenites funkhousei*, *Pulcheripollenites krempii* and *Aquilapollenites mtchedlishvili*. *Aquilapollenites rigidus* reaches an acme in the lower portion of the formation, but virtually disappears at the top of the Foremost Formation, with only extremely rare specimens seen in overlying units. Verrucate specimens of *Siberiapollis* first appear in the Oldman Formation. *Fibulapollis scabratus* has not been recovered from the Dinosaur Park Formation. New appearances in the DPP include *Accratipollis macrosolenoides*, *Anacolosidites grandis*, *Aquilapollenites augustus* and *Dynadnopites reticulatus*. Near the top of the DPP,

Kurtzipites sp. 1, *Aquilapollenites parallelus*, *Senipites drumhellerensis*, *Orbiculapollis globosus*, *Liliacidites complexus* and *Aquilapollenites leucocephalus* first appear and *Integricorpus bellus* has a last occurrence. Two undescribed species of *Accuratipollis* have relatively short ranges within the upper part of the formation. *Gleicheniidites* sp. 1 first appears in the uppermost layers of the DPF (Braman and Koppelhus, 2005; Braman and Sweet, 2012). First appearances near the base of the formation include *Aquilapollenites sentus* and *Mancicorpus glaber*. *Accuratipollis macrosolenoides* and *Anacolosidites grandis* have their last occurrences in the lower part of the Bearpaw Formation.

The only formal palynology study conducted on the BRG in Saskatchewan was by Eberth et al. (1990) in an attempt to correlate stratigraphic sequences from Muddy Lake, Saskatchewan to successions in Alberta and Montana. The assemblage compared closely with those in DPP, but did contain palynomorphs not found in the park (Eberth et al., 1990). Two species, *Mancicorpus tripodiformis* and *Expressipollis* sp., were identified that appeared to offer potential as biostratigraphic markers for these sections. The Muddy Lake assemblage was found to fit within the *Siberiapollis montanensis* Subzone of the *Aquilapollenites quadrilobus* Interval Zone of Nichols et al. (1982), which is biostratigraphically equivalent to the lower Judith River Formation in Montana (Eberth et al., 1990). However, much of the biostratigraphic zonation has been changed since the time of this publication (e.g., Braman and Sweet, 2012), and re-examination of the data set is of relevance to this study.

2.5.2 Ichnology

Ichnology is the study of trace fossils, the record of organismal behavior preserved on or within a substrate (Bromley, 1990, 1996; Pemberton et al., 1992). Organisms (whether they be animals or plants) respond directly to their environments, and the record of these responses (essentially,

fossilized evidence of behaviour) is thus invaluable to determining paleoenvironmental parameters not otherwise obvious in the paleontologic and geologic record. A summary of prior studies that included ichnologic analysis of the BRG is summarized below.

Multiple subsurface studies focusing on the ‘basal Belly River’ and Foremost Formation have been conducted, largely due to oil and gas interests in north-central and central Alberta (e.g., Hansen, 2007; Jones, 2013). Trace fossils produced by brackish-water ichnofaunas (e.g., *Teichichnus* isp.) have been of utility in identifying marine-bounded discontinuity surfaces and small-scale transgressive-regressive cycles throughout the basal Belly River (Jones, 2013). In southwestern Saskatchewan, Gordon (2010) integrated basic ichnologic concepts to facies descriptions and interpretations in the Foremost Formation and Ribstone Creek Member. Bioturbation is common throughout the Foremost Formation and basal Belly River, and is attributed to the dominance of marginal-marine conditions at the time of deposition.

Trace fossils produced by freshwater unionid bivalves and terrestrial organisms (e.g., *Taenidium*, *Skolithos* likely produced by beetles) are associated with paleosols, crevasse splay sandstones, and freshwater fluvial channels (Johnston and Hendry, 2005). This assemblage characterizes the coastal plain environments of the Oldman Formation. Bioturbation is common in crevasse splay deposits, and laterally accreting freshwater fluvial deposits containing unionid bivalves whose biogenic structures demonstrate short-term variability in sediment accumulation within channel systems. Cylindrical trace fossils with back-filled laminae with scratch surfaces and walls lined with fecal pellets are abundant in many of the ripple-laminated, fine-grained sandstones and siltstones that cap paleochannel and splay deposits. Vertically oriented, conical ironstone root traces are common in the mudstone deposits (Eberth and Hamblin, 1993).

The DPF, in contrast, generally preserves a high-density, low-diversity assemblage of very simple types of bioturbation. Root and plant material are preserved throughout, but do not necessarily accompany paleosol development or freshwater environments. Higher diversity and potential brackish-water forms (e.g., *Teichichnus*) appear abruptly above the Lethbridge Coal Zone (LCZ). Progradational, coarsening-upwards units of siltstone and very fine-grained sandstone contain comparatively small *Skolithos* and abundant terrestrial plant detritus. Trace fossils in the DPF tend to be simple (e.g., *Planolites*) and cryptic bioturbation that is commonly associated with shallow-marine and brackish-water settings (e.g., MacEachern and Gingras, 2007; Pemberton et al., 2008). Drapes of clay and small plant fragments on rhythmic laminae are associated with high-density, very small horizontal burrows (*Planolites*) (Scott et al., 2012). Thin units of low-angle cross-bedded sandstone above the LCZ within the park have been interpreted as upper shoreface to foreshore deposits. These deposits preserve *Macaronichnus* and large *Skolithos*, and are marine (Scott et al., 2012).

2.5.3 Vertebrate Paleontology

The BRG, particularly in Dinosaur Provincial Park, has yielded one of the most remarkable fossilized terrestrial ecosystems yet discovered. Approximately 45 dinosaur species are known, with the main groups including theropods, ceratopsians and hadrosaurs. Freshwater invertebrates are rare but consist of gastropods and bivalves (Johnston and Hendry, 2005). Chondrichthyans (sharks, skates, and rays), Acipenseriformes (sturgeon and paddlefish), holostean-grade fishes (bowfin, gars, etc.), and teleosts dominate the freshwater assemblage (Brinkman, 2005). Representative amphibians include anurans (frogs) and caudates (salamanders) (Gardiner, 2005). Turtles, squamates (snakes and lizards), crocodilians, plesiosaurs, pterosaurs, and choristoderes (champsosaurs) are abundant (Brinkman, 2005; Caldwell, 2005; Gao and Brinkman, 2005; Sato

et al., 2005). Multituberculates, marsupials, and eutherian mammals are known from isolated teeth (Fox, 2005).

Stratigraphic distribution of vertebrate fossils in the park has been well studied on both the macro and microfossil level. Macrofossil distribution is of little relevance to Saskatchewan studies, as macrofossils are poorly represented in the easternmost outcrops (for those interested in macrofossil remains recovered from the BRG, the reader is referred to Currie and Koppelhus, 2005). In contrast, Saskatchewan microfossil assemblages are known, with some localities collected and bulk sampled prior to the beginning of this thesis by Royal Saskatchewan Museum (RSM) staff.

Vertebrate microfossil assemblages (microsites; microvertebrates; microvertebrate assemblage) represent distinct locations where an assortment of small bones and teeth of a variety of organisms has collected, often due to hydrologic sorting (Brinkman, 2005). Microfossil assemblages have been instrumental in furthering understanding of paleocommunity structure and changes to community composition through time. The Belly River Group in general has yielded a rich assortment of these localities, and has been pivotal in furthering advancement of paleoecologic studies based on these sites. Initial taxonomic studies of these assemblages throughout the different formations of the BRG eventually allowed for comparison of taxonomic compositions through time and across space.

Several studies from Dinosaur Provincial Park have investigated sedimentologic and taphonomic interpretations of microsites from the Oldman and Dinosaur Park formations. Paleoecological studies were first undertaken by Dodson (1983, 1987), who focused on localities in DPP, utilizing these sites to reconstruct dinosaur diversity in the park. Brinkman (1990) recognized stratigraphic changes in microfossil abundance and diversity upsection throughout

Dinosaur Provincial Park. Vertebrate microfossil taxa with similar stratigraphic distribution were divided into coastal and inland paleocommunity assemblages, based on modern faunal ecology. Due to the park's transgressive depositional history, more inland species were presumed to be in abundance at the top of the Oldman and bottom of the Dinosaur Park Formation. In contrast, assemblages at the top of the DPF were interpreted as belonging to coastal paleocommunities.

Brinkman's (1990) study assumed that differences in faunal composition of vertebrate microfossil localities in DPP were biologic rather than taphonomic in nature. This was questioned by Blob and Fiorillo (1996), and were addressed by Peng (1998), who used size frequency data to test taphonomic equivalency. Though no connection could be found between size and abundance of taxa, a strong correlation between abundance and stratigraphic position was noted, supporting Brinkman's (1990) original study.

Prior to this thesis, little of the vertebrate microfossil material collected from the Saskatchewan BRG deposits had been documented in the literature. Eberth et al. (1990) included a list of taxa recovered from Muddy Lake, Saskatchewan. All were considered to be consistent with taxa known from BRG exposures in Alberta, with the exception of *Melvius* and a possible new species of ceratopsian dinosaur. Overall, the taxa recovered from Muddy Lake was of considerably lower diversity than age-equivalent sites in Alberta (Eberth et al., 1990).

2.6 Fieldwork Methods

Outcrop was logged for detailed sedimentologic, paleontologic, and stratigraphic information during summers of 2012–2016 (Fig. 2.4). Detailed sediment logs included Brunton© compass and Jacob's Staff measurements. Standard sedimentological information (grain size, clast shape, sedimentary structures, paleocurrent indicators, bed geometry, bed contacts, body fossils, trace fossils) was recorded after outcrop surfaces were cleaned. Sediment color was assigned using the

Munsell color chart (Munsell, 2000). Emily Bamforth, Tim Prokopiuk, and Frank McDougall assisted in the field sporadically throughout the 2012–2016 field excursions. Outcrop from Lake Diefenbaker (Fig. 2.5A), Woodpile Coulee (Fig. 2.5B), Muddy Lake (Fig. 2.6A), and Sandy Point, Alberta (Fig. 2.6B) was logged and facies/facies associations were mapped both vertically and laterally. Full-page figures of all sedimentary logs constructed for this study are included in Appendix D.

Palynology samples were collected when stratigraphic measurements were made. Three sub-samples from each stratigraphic horizon were collected for palynological analysis and sent to Global Geolabs Ltd. (<http://www.globalgeolab.com>) in Medicine Hat, Alberta, for processing. The resulting slides were analyzed and the palynomorphs identified by Dennis Braman of the Royal Tyrrell Museum in Drumheller, Alberta. The palynological samples are currently catalogued and stored at that location. Samples from Woodpile Coulee, Sandy Point, and Muddy Lake were collected from 1989-1991 by Dennis Braman and subsequently shared with the author for the purposes of this study. A full list of palynology taxa identified for this study are included in Appendix E.

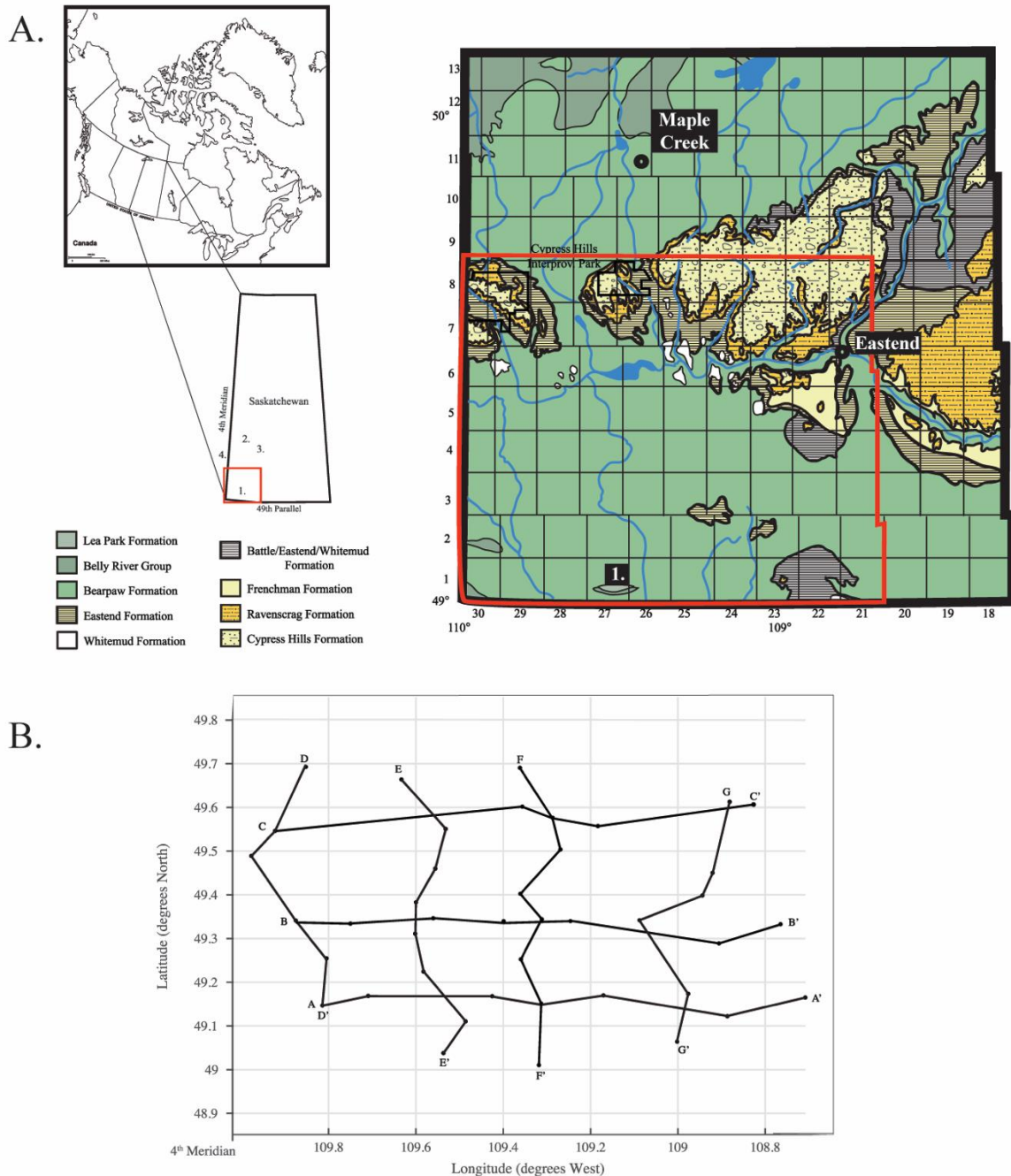


Figure 2.4: A. Boundaries of the Cypress Hills region and approximate location of exposed outcrop at 1. Woodpile Coulee, Saskatchewan; 2. Muddy Lake, Saskatchewan; 3. Herschel, Saskatchewan; 4. Sandy Point, Alberta; Regional map of the Cypress Hills region in context to regional landmarks. Based on maps from the Saskatchewan Geological Survey; B. Map of wells used to make cross-section correlations used in this study, plotted against latitude and longitude (Appendix A and C). Cross-sections B and F are included in text as figures in Chapter 3. A, C-E, and G are included as Appendix B and D.

Microvertebrate fossil material was both picked at the surface and shoveled out in a mass, a strategy known as bulk collecting. Bulk material was screen-washed with a #18 U.S. standard size sieve with 1 mm openings and picked under a dissection microscope. Fossil material was identified and catalogued at the RSM by Tim Tokaryk, John Storer, Meagan Gilbert, Emily Bamforth and Terra Lekach, and at McGill University by Sarah Popov and Hans Larsson. All material was identified to the lowest possible taxonomic level, and the abundance of each type of faunal element was determined. The collections are housed at the Royal Saskatchewan Museum T. rex Discovery Centre in Eastend, Saskatchewan. Those wishing to view the original raw data can contact the lead author for access to the excel documents.

2.7 Subsurface Data Collection Methods

The subsurface study area extends from the United States border north to township 8, and from the Alberta border to range 21W3, encompassing most of the Saskatchewan extent of the Cypress Hills (Fig. 2.4). Where possible, a minimum of one well per township was picked, resulting in a database of 258 wells. Seven subsurface cores (Table 2.1) and outcrop exposures (township 1, range 27 along Woodpile Coulee; townships 22 and 23, range 2W4 at Sandy Point, Alberta; townships 38 and 39, range 23W3 at Muddy Lake, Saskatchewan; township 17, range 28W3 at Herschel, Saskatchewan; and township 20, range 16W3) were included to provide a more robust dataset of depositional patterns across the basin.

No continuous core through the BRG was available (late 2018) in the study area, therefore geophysical well logs were used to correlate major contacts. Well logs,

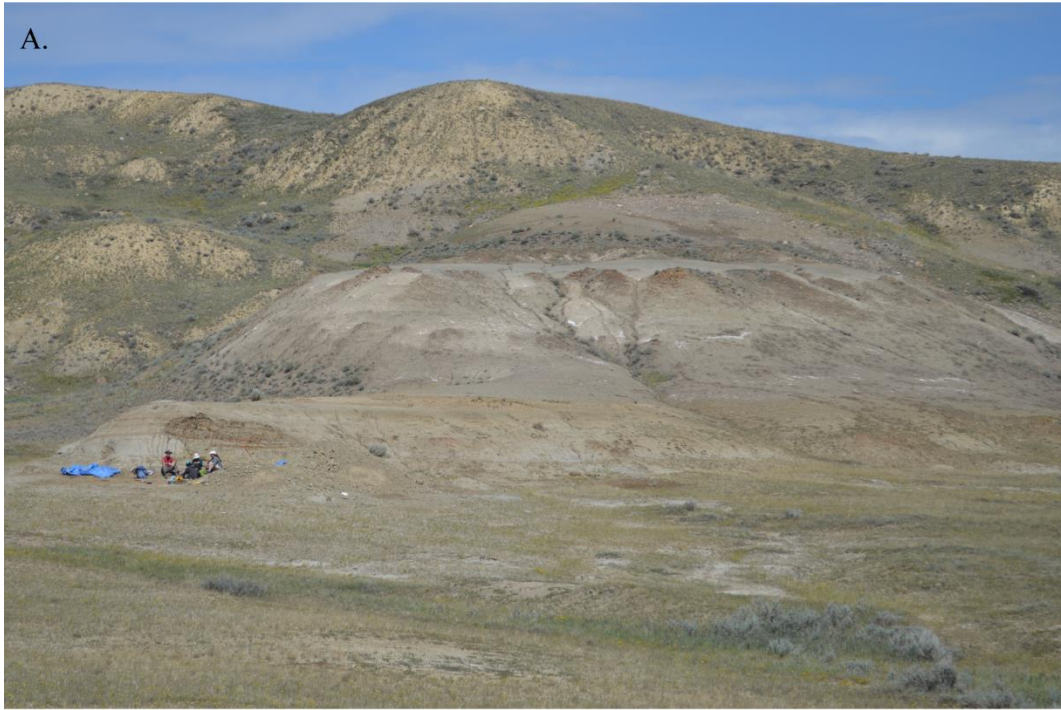


Figure 2.5: Selected photos of measured outcrop localities utilized for this thesis. A. The Lake Diefenbaker site in Saskatchewan Landing Provincial Park. This photo spans the DPF-BP contact; B. Woodpile Coulee in extreme southwestern Saskatchewan. This photo spans the DPF-OF contact, with the DPF to the left side of the photograph. Note the inclined nature of the strata.



Figure 2.6: Selected photos of measured outcrop localities utilized for this thesis. A. The Muddy Lake site south of Unity, Saskatchewan. This photo spans the DPF-OF contact; B. Sandy Point near the Alberta-Saskatchewan boundary north of Medicine Hat, Alberta. This photo spans the DPF-OF contact.

subsurface core, and outcrop data were integrated to develop composite sections for paleoenvironmental interpretations. Results were compared with those of Dawson et al. (1994), Eberth and Hamblin (1993), Hamblin (1997a, 1997b), Gordon (2000), and Rogers et al. (2016). Facies were described in terms of sedimentology attributes and, where possible, ichnologic and paleontologic information. Cores were logged at the Subsurface Geological Laboratory in Regina, Saskatchewan. Isopach maps of the uppermost Foremost Formation, Ribstone Creek Member, Oldman Formation, Dinosaur Park Formation, and the newly erected Manâtakâw Member were constructed using MATLAB version R2017b (MathWorks, 2018) to provide insights to wedge geometry and basin evolution. Individual log picks were made using GeoScout (geoLOGIC Systems Ltd., 2018) and open-source well logs (Appendix A and C).

The gamma-density-resistivity suite of logs was used to pick the tops of the associated formations in the study area. This suite of logs is the most reliable for picking coals, which are a defining feature of the Dinosaur Park Formation and the Ribstone Creek Member in the Cypress Hills. Criteria for picks are illustrated in Chapter 4 of this thesis, and Table 2.2. Wells without the full suite of logs and those that were not drilled vertically were rejected. Wells that did not contain a complete log from the mid to lower Bearpaw Formation to the ‘Milk River Shoulder’ were removed from the isopach study.

The Milk River Shoulder (MRS) marks the boundary between the Milk River Formation and the Lea Park Formation. This regional stratigraphic marker is a marine flooding surface, with the Milk River Formation composed of wave-dominated shoreface sandstones (Power and Walker, 1996). The MRS has a distinct signature on gamma-ray and resistivity logs and is laterally continuous across the entire study area. Therefore, the MRS was chosen as the datum

for the subsurface data, in common with other studies focusing on the Belly River Group (Eberth and Hamblin, 1993; Power and Walker, 1996; Hamblin, 1997a, 1997b; Hamblin and Abrahamson, 1996; Gordon, 2000).

2.8 Diversity Analysis

Several chapters within this thesis utilize diversity analysis to quantify paleofaunal assemblages preserved as vertebrate microfossil localities. Vertebrate microfossil localities are distinct localities in which small bones and teeth of a variety of vertebrates have been deposited and concentrated (Brinkman, 2005). These sites are commonly utilized by paleontologists as a means of testing paleoecologic hypotheses not easily discerned from body fossils alone. The Belly River Group in Alberta has been critical in the advancement of paleoecological studies utilizing microvertebrate localities (e.g., Brinkman, 1990; Eberth and Brinkman, 1997; Peng, 1998; Brinkman et al., 2005; Cullen et al., 2016), and therefore it seemed natural to include such analysis in this thesis. Vertebrate microfossil localities within the Dinosaur Park Formation were identified and collected from Woodpile Coulee, Lake Diefenbaker, and Muddy Lake field sites in southwestern Saskatchewan. The Woodpile Coulee and Lake Diefenbaker microsite collections were utilized extensively for this thesis.

2.8.1 Quantifying Diversity

Both ecology and paleontology can be used to assess diversity based on the number of individuals of a given taxa, known as ‘abundance based’, or the number of individuals in a given sample, referred to as ‘occurrence based’ (Colwell, 2013). This study utilized alpha diversity, a common paleoecologic means of assessing within-site, local-scale diversity. In the context of the studies conducted in this thesis, alpha diversity is defined as within-microsite diversity, following Bamforth (2014) and Vavrek (2011). In the context of microsites, beta diversity is

defined as two or more microsites deposited within different stratigraphic units (Hammer and Harper, 2006; Bamforth, 2014), and draws on patterns underlying alpha diversity in a given habitat (Whittaker, 1972). Beta diversity is beyond the scope of the research conducted in this thesis, but is part of an ongoing research program undertaken by the author (e.g., Bamforth and Gilbert, 2018, 2019).

In Chapters 5 and 6 of this thesis, alpha diversity is calculated using non-parametric species estimators based on abundance data. A major problem when dealing with fossil populations is the inherent incompleteness of the fossil record and the uncertainty in knowing how many species are absent in any given microvertebrate sample. In spite of these limitations, information can be extrapolated to provide meaningful information on species richness for a paleocommunity (Colwell and Coddington, 1994; Vavrek, 2011). Non-parametric species estimators account for some of the inherent bias associated with taphonomic processes and sampling problems affecting vertebrate microfossil assemblages. Non-parametric estimators are useful to incomplete datasets in that they are not restricted to any particular parameterized distribution. The data itself is utilized, with the distribution calculated as an empirical distribution. Non-parametric species estimators extrapolate how many species would be present if a sample were complete by utilizing the number of rare taxa in a given sample (Colwell and Coddington, 1994). Essentially, this method estimates the number of missing or undiscovered taxa in alpha diversity analysis, by differentiating between common and rare taxa (Vavrek, 2011).

2.8.2 Non-Parametric Species Estimators

The Chao-1 (Chao, 1984), Abundance-based Coverage Estimator (ACE) (Chao and Lee, 1992; Chao et al., 1993; Lee and Chao, 1994), and second-order Jackknife estimator (Smith and

van Belle, 1984) have been found to perform best for alpha diversity analysis (e.g., Bamforth, 2014). All three estimators were applied and compared to the Dinosaur Park Formation microsites, and were calculated in R using the ‘spp.est’ function in `fossil` (Vavrek, 2011). Much of what is covered in this section is outlined in greater detail by Bamforth (2014), and the reader is directed there for further discussion of non-parametric species estimators and their utility in analyzing vertebrate microfossil assemblages.

Chao-1 species estimator (Chao, 1984) is described with the following equation:

$$S_1 = S_{\text{obs}} + (F_1^2/2F_2)$$

where S_{obs} is the number of species, F_1 is the number of species that are represented by one specimen (referred to as singletons), and F_2 is the number of species represented by exactly two specimens (referred to as doubletons).

Abundance-based Coverage Estimator (ACE) (Chao and Lee, 1992; Chao et al., 1993; Lee and Chao, 1994) is described with the following equation:

$$S_{\text{ace}} = S_{\text{common}} - (S_{\text{rare}}/C_{\text{ace}}) + ((F_1/C_{\text{ace}})Y_{\text{ace}}^2)$$

where S_{common} are species represented by more than ten specimens, S_{rare} are species that occur fewer than ten times, C_{ace} is the sample coverage estimator, and Y_{ace}^2 is the estimated coefficient of variation for the singletons (F_1) of rare species.

The second-order jackknife estimator (Jackknife-2) (Smith and van Belle, 1984) is a variation on the jackknife estimator of Burnham and Overton (1978, 1979) and is described with the equation:

$$S_{\text{jack2}} = S_{\text{obs}} + ((Q_1 (2m-3)/m) - ((Q(m-2)^2)/m)m-1))$$

where S_{obs} is the observed number of species, Q_1 is the number of doubletons, and m is the total number of specimens in the sample.

Well Name	Location	Depths Cored
Nexen Battle Creek	W 111/07-02-04-27W3	185 – 243 m
Renaissance Senate	W 101/10-10-02-27W3	219 – 235 and 241 – 248 m
Nexen Vidora	W 111/06-04-05-25W3	225 – 280 m
Canadian Landmaster Cypress Hills	W 141/06-31-06-25W3	330 – 372 m
Renaissance Vidora	W 111/02-15-04-26W3	237 – 246 m
Canadian Landmaster Belanger	W141/10-23-07-25W3	385 – 415 m

Table 2.1: Summary of core logged for the purpose of this study.

Formation	Lower Contact	Upper Contact
Bearpaw Formation	GR - Rightward deflection R- Rightward deflection BD -Minimal rightward deflection to no change	N/A
Manâtakâw Member	GR - Rightward deflection R- Leftward deflection BD -Minimal leftward deflection	GR - Gradual leftward increase followed by sharp rightward deflection R- Sharp rightward deflection BD -Minimal rightward deflection to no change
Dinosaur Park Formation	GR - Sharp to gradual leftward deflection R- Sharp rightward deflection BD -Sharp to gradual rightward deflection	GR - Rightward deflection R- Leftward deflection BD -Minimal leftward deflection
Oldman Formation	GR - Sharp rightward deflection R- Sharp rightward deflection BD - Sharp to gradual leftward deflection	GR - Sharp to gradual leftward deflection R- Sharp rightward deflection BD -Sharp to gradual rightward deflection
Foremost Formation	GR - Leftward Deflection R- Leftward Deflection BD -Minimal leftward deflection to no change	GR - Gradual leftward deflection followed by sharp right at the FF/OF contact R- No change, followed by sharp rightward deflection BD - Gradual leftward deflection, followed by consistent leftward deflection at the FF/OF contact
Ribstone Creek Member	GR - Consistent shift to higher leftward deflection signatures R- Rightward deflection near the top contact with LP BD -Minimal leftward deflection at base with increasing intensity upwards	GR - Sharp rightward deflection at LP contact R- Sharp leftward deflection BD -Sharp rightward deflection at LP contact

Table 2.2: Summary of gamma-density-resistivity well log signatures utilized for picking formation tops for the purpose of this study. A summary of the upper and lower contact picking criteria are provided. GR - Gamma ray; R - Resistivity; BD - Bulk Density; N/A – Not available.

References

- Bamforth, E. (2014). *Paleoecology and paleoenvironmental trends immediately prior to the end-Cretaceous extinction in the Latest Maastrichtian (66 Ma) Frenchman Formation, Saskatchewan, Canada* (Unpublished doctoral dissertation). Montreal, Quebec: McGill University Libraries.
- Bamforth, E. L. and Gilbert M. M. (2018). Large-scale Spatial Beta Diversity Trends in the Late Campanian Dinosaur Park Formation of Western Canada. *Journal of Vertebrate Paleontology, Program and Abstracts*, 2018, (p. 85).
- Bamforth, E. L., & Gilbert, M. M. (2019). Campanian conundrum: Large-scale spatial diversity patterns elucidate Judith River and Dinosaur Park Formation equivalents in Saskatchewan, Canada. In *7th Annual Meeting Canadian Society of Vertebrate Palaeontology, May 10-13, 2019, Grande Prairie, Alberta* (p. 9).
- Blob, R. W., & Fiorillo, A. R. (1996). The significance of vertebrate microfossil size and shape distributions for faunal abundance reconstructions: A Late Cretaceous example. *Paleobiology*, 22(3), 422-435.
- Braman, D. R., & Koppelhus, E. B. (2005). Campanian palynomorphs. In *Dinosaur Provincial Park: A spectacular ancient ecosystem revealed* (pp. 101-130). Bloomington & Indianapolis, IN: Indiana University Press.
- Braman, D., & Sweet, A. (2012). Biostratigraphically useful Late Cretaceous–Paleocene terrestrial palynomorphs from the Canadian Western Interior Sedimentary Basin. *Palynology*, 36(1), 8-35.
- Brinkman, D. B. (1990). Paleoecology of the Judith River Formation (Campanian) of Dinosaur Provincial Park, Alberta, Canada: Evidence from vertebrate microfossil localities. *Palaeogeography, Palaeoclimatology, Palaeoecology*, 78(1), 37-54.
- Brinkman, D. B. (2005). Turtles: Diversity, paleoecology, and distribution. In *Dinosaur Provincial Park: A spectacular ancient ecosystem revealed* (pp. 202-220). Bloomington & Indianapolis, IN: Indiana University Press.
- Brinkman, D. B., Braman, D. R., Neuman, A. G., Ralrick, P. E., & Sato, T. (2005). A vertebrate assemblage from the marine shales of the Lethbridge Coal Zone. In *Dinosaur Provincial Park: A spectacular ancient ecosystem revealed* (pp. 486-500). Bloomington & Indianapolis, IN: Indiana University Press.
- Bromley, R. G. (1990). *Trace fossils. Biology and taphonomy*. London, UK: Unwin Hyman.
- Bromley, R. G. (1996). *Trace fossils. Biology, taphonomy, and applications*. London, UK: Chapman & Hall.

- Burnham, K. P., & Overton, W. S. (1978). Estimation of the size of a closed population when capture probabilities vary among animals. *Biometrika*, 65, 625-633.
- Burnham, K. P., & Overton, W. S. (1979). Robust estimation of population size when capture probabilities vary among animals. *Ecology*, 60, 927-936.
- Caldwell, M. W. (2005). The Squamates: Origins, phylogeny, and paleoecology. In *Dinosaur Provincial Park: A spectacular ancient ecosystem revealed* (pp. 235-248). Bloomington & Indianapolis, IN: Indiana University Press.
- Caldwell, W. G. E. (1968). *The Late Cretaceous Bearpaw Formation in the South Saskatchewan River valley*. Saskatchewan Research Council, Geology Division, Report No. 8, 86 p.
- Caldwell, W. G. E. (1982). The Cretaceous system in the Williston Basin: A modern appraisal. In C. E. Dunn, D. M. Kent & J. A. Lorisong (Eds.), *Fourth International Williston Basin Symposium* (pp. 295-312). Saskatchewan Geological Society, Special Publication No. 6.
- Cant, D. J., & Stockmal, G. S. (1989). The Alberta foreland basin: Relationship between stratigraphy and Cordilleran terrane-accretion events. *Canadian Journal of Earth Sciences*, 26(10), 1964-1975.
- Catuneanu, O., Sweet, A. R., & Miall, A. D. (2000). Reciprocal stratigraphy of the Campanian–Paleocene western interior of North America. *Sedimentary Geology*, 134(3-4), 235-255.
- Chao, A. (1984). Non-parametric estimation of the number of classes in a population. *Scandinavian Journal of Statistics*, 11, 265-270.
- Chao, A., & Lee, S. M. (1992). Estimating the number of classes via sample coverage. *Journal of the American Statistical Association*, 87, 210-217.
- Chao, A., Ma, M. C., & Yang, M. C. K. (1993). Stopping rules and estimation for recapture debugging with unequal failure rates. *Biometrika*, 80, 193-201.
- Cobban, W. A., Walaszczyk, I., Obradovich, J. D., & McKinney, K. C. (2006). *A USGS zonal table for the Upper Cretaceous Middle Cenomanian–Maastrichtian of the western interior of the United States based on ammonites, inoceramids, and radiometric ages*. U.S. Geological Survey, Open-File Report 2006-1250, 46 p.
- Colwell, R. K. (2013). Estimates: Statistical estimation of species richness and shared species from samples. User's Guide and application, published at <http://purl.oclc.org/estimates>.
- Colwell, R. K., & Coddington, J. A. (1994). Estimating terrestrial biodiversity through extrapolation. *Philosophical Transactions of the Royal Society, B* 345(1311), 101-118.
- Crockford, M. B. B. (1949). Oldman and Foremost formations of southern Alberta. *AAPG Bulletin*, 33(4), 500-510.

- Cullen, T. M., Fanti, F., Capobianco, C., Ryan, M. J., & Evans, D. C. (2016). A vertebrate microsite from a marine-terrestrial transition in the Foremost Formation (Campanian) of Alberta, Canada, and the use of faunal assemblage data as a paleoenvironmental indicator. *Palaeogeography, palaeoclimatology, palaeoecology*, 444, 101-114.
- Currie, P. J., & Koppelhus, E. B. (Eds.). (2005). *Dinosaur Provincial Park: A spectacular ancient ecosystem revealed*. Bloomington & Indianapolis, IN: Indiana University Press.
- Dawson, G. M. (1883). Glacial deposits of the Bow and Belly river country. *Science*, 1(17), 477-479.
- Dawson, F. M., Evans, C. G., Marsh, R., & Richardson, R. (1994). Uppermost Cretaceous and Tertiary strata of the Western Canada Sedimentary Basin. In G. D. Mossop & I. Shetson (Comps.), *Geological atlas of the Western Canada Sedimentary Basin* (pp. 387-406). Calgary, Alberta: Canadian Society of Petroleum Geologists and Alberta Research Council.
- Dodson, P. (1983). A faunal review of the Judith River (Oldman) Formation, Dinosaur Provincial Park, Alberta. *Mosasaurs*, 1, 89-118.
- Dodson, P., Currie, P. J., & Koster, E. (1987). Microfaunal studies of dinosaur paleoecology, Judith River Formation of southern Alberta. In *Fourth symposium on Mesozoic terrestrial ecosystems: Short papers* (Vol. 3, pp. 70-75). Tyrrell Museum of Palaeontology, issue 1987 of Occasional paper of the Tyrrell Museum of Palaeontology.
- Eberth, D. A. (1996). Origin and significance of mud-filled incised valleys (Upper Cretaceous) in southern Alberta, Canada. *Sedimentology*, 43(3), 459-477.
- Eberth, D. A. (2005). The geology. In *Dinosaur Provincial Park: A spectacular ancient ecosystem revealed* (pp. 54-82). Bloomington & Indianapolis, IN: Indiana University Press.
- Eberth, D. A., Braman, D. R., & Tokaryk, T. T. (1990). Stratigraphy, sedimentology and vertebrate paleontology of the Judith River Formation (Campanian) near Muddy Lake, west-central Saskatchewan. *Bulletin of Canadian Petroleum Geology*, 38(4), 387-406.
- Eberth, D. A., & Brinkman, D. B. (1997). Paleoecology of an estuarine, incised-valley fill in the Dinosaur Park Formation (Judith River Group, Upper Cretaceous) of southern Alberta, Canada. *Palaios*, 43-58.
- Eberth, D. A., & Hamblin, A. P. (1993). Tectonic, stratigraphic, and sedimentologic significance of a regional discontinuity in the upper Judith River Group (Belly River wedge) of southern Alberta, Saskatchewan, and northern Montana. *Canadian Journal of Earth Sciences*, 30(1), 174-200.
- Embry, A. (1990). A tectonic origin for third order depositional sequences in extensional basins - Implications for basin modeling. In *Quantitative dynamic stratigraphy* (pp. 491-501). New Jersey, NJ: Prentice Hall.

- Fox, R. C. (2005). Late Cretaceous mammals. In *Dinosaur Provincial Park: A spectacular ancient ecosystem revealed* (pp. 417-435). Bloomington & Indianapolis, IN: Indiana University Press.
- Frank, M. C. (2006). *Coal distribution in the Upper Cretaceous (Campanian) Belly River Group of southwest Saskatchewan*. Saskatchewan Industry and Resources, Open File Report 2005-33, CD-ROM.
- Furnival, G. M. (1946). *Cypress Lake map area*. Geological Survey of Canada, Memoir 242.
- Gao, K., & Brinkman, D. B. (2005). Choristoderes from the park and its vicinity. In *Dinosaur Provincial Park: A spectacular ancient ecosystem revealed* (pp. 221-234). Bloomington & Indianapolis, IN: Indiana University Press.
- Glombick, P. M. (2010). *Top of the Belly River Group in the Alberta Plains: Subsurface stratigraphic picks and modelled surface*. Energy Resources Conservation Board, ERCB/AGS, Open File Report 2010-10, 27 p.
- Gordon, J. (2000). *Stratigraphy and sedimentology of the Foremost Formation in southeastern Alberta and southwestern Saskatchewan* (Unpublished master's thesis). University of Regina, Saskatchewan.
- Hamblin, A. P. (1997a). Stratigraphic architecture of the Oldman Formation, Belly River Group, surface and subsurface of southern Alberta. *Bulletin of Canadian Petroleum Geology*, 45(2), 155.
- Hamblin, A. P. (1997b). Regional distribution and dispersal of the Dinosaur Park Formation, Belly River Group, surface and subsurface of southern Alberta. *Bulletin of Canadian Petroleum Geology*, 45(3), 377-399.
- Hamblin, A. P., & Abrahamson, B. (1996). Stratigraphic architecture of "Basal Belly River" cycles, Foremost Formation, Belly River Group, subsurface of southern Alberta and southwestern Saskatchewan. *Bulletin of Canadian Petroleum Geology*, 44(4), 654-673.
- Hammer, Ø., & Harper, D. A. T. (2006). *Paleontological data analysis*. Malden, ME: Blackwell Publishing.
- Hansen, C. D. (2007). *Facies characterization and depositional architecture of a mixed-influence asymmetric delta lobe: Upper Cretaceous basal Belly River Formation, central Alberta* (Unpublished doctoral thesis). Simon Fraser University, Vancouver, British Columbia.
- Herbaly, E. L. (1974). Petroleum geology of Sweetgrass arch, Alberta. *AAPG Bulletin*, 58(11), 2227-2244.

- Jerzykiewicz, T., & Norris, D. K. (1994). Stratigraphy, structure and syntectonic sedimentation of the Campanian 'Belly River' clastic wedge in the southern Canadian Cordillera. *Cretaceous Research*, 15(4), 367-399.
- Jerzykiewicz, T., & Sweet, A. R. (1988). Sedimentological and palynological evidence of regional climatic changes in the Campanian to Paleocene sediments of the Rocky Mountain Foothills, Canada. *Sedimentary Geology*, 59(1-2), 29-76.
- Johnston, P. A., & Hendry, A. J. W. (2005). Paleoecology of mollusks from the Belly River Group. In *Dinosaur Provincial Park: A spectacular ancient ecosystem revealed* (pp. 139-166). Bloomington & Indianapolis, IN: Indiana University Press.
- Jones, B. (2013). *Integrated ichnology and sedimentology of mixed river- and wave-influenced delta complexes, Upper Cretaceous Basal Belly River Formation, central Alberta, Canada* (Unpublished master's thesis). Simon Fraser University, Vancouver, British Columbia.
- Kent, D. M., & Christopher, J. E. (1994). Geological history of the Williston Basin and Sweetgrass Arch. In G. D. Mossop & I. Shetsen (Comps.), *Geological atlas of the Western Canada Sedimentary Basin* (pp. 421-429). Calgary, Alberta: Canadian Society of Petroleum Geologists and Alberta Research Council.
- Leckie, D. A., & Smith, D. G. (1992). Regional setting, evolution, and depositional cycles of the Western Canada Foreland Basin. In R. W. Macqueen & D. A. Leckie (Eds.), *Foreland basins and fold belts* (pp. 9-46). American Association of Petroleum Geologists, AAPG Memoir Vol. 55.
- Lee, S. M. & Chao, A. (1994). Estimating population size via sample coverage for closed capture-recapture models. *Biometrics*, 50, 88-97.
- Lerbekmo, J. F., & Braman, D. R. (2002). Magnetostratigraphic and biostratigraphic correlation of late Campanian and Maastrichtian marine and continental strata from the Red Deer Valley to the Cypress Hills, Alberta, Canada. *Canadian Journal of Earth Sciences*, 39(4), 539-557.
- MacEachern, J. A., & Gingras, M. K. (2007). Recognition of brackish-water trace fossil suites in the Cretaceous Western Interior Seaway of Alberta, Canada. In R. G. Bromley, L. A. Buatois, G. Mángano, J. F. Genise & R. N. Melchor (Eds.), *Sediment-organism interaction: A multifaceted ichnology* (pp. 149-193). Society for Sedimentary Geology, SEPM Special Publication No. 88.
- MathWorks (2018). Massachusetts. *United States*.
- McLean, J. R. (1971). *Stratigraphy of the Upper Cretaceous Judith River Formation in the Canadian Great Plains*. Saskatchewan Research Council, Geology Division, Report No. 11, 96 p.

- Miall, A. D. (1991). Stratigraphic sequences and their chronostratigraphic correlation. *Journal of Sedimentary Research*, 61(4), 497-505.
- Munsell soil color charts. (2000). New Windsor, NY: Gretag Macbeth.
- Nichols, D. J., Jacobson, S. R., & Tschudy, R. H. (1982). Cretaceous palynomorph biozones for the Central and Northern Rocky Mountain region of the United States. In *Geologic studies of the Cordilleran thrust belt* (Vol II, pp. 721-733). Denver, CO: Rocky Mountain Association of Geologists.
- Nichols, D., Perry Jr, W., & Haley, J. (1985). Reinterpretation of the palynology and age of Laramide syntectonic deposits, southwestern Montana, and revision of the Beaverhead Group. *Geology*, 13(2), 149-153.
- Nichols, D. J., & Sweet, A. R. (1993). Biostratigraphy of Upper Cretaceous non-marine palynofloras in a north-south transect of the Western Interior Basin. In *Evolution of the Western Interior Basin* (pp. 539-584). Geological Association of Canada, Special Paper #39.
- Noad, J. J. (1993). *An analysis of changes in fluvial architecture through the upper Oldman Member, Judith River Formation of the Upper Cretaceous, southern Alberta, Canada* (Unpublished master's thesis). Birkbeck College, University of London, UK.
- Ogunyomi, O., & Hills, L. (1977). Depositional environments, Foremost Formation (Late Cretaceous), Milk River area, southern Alberta. *Bulletin of Canadian Petroleum Geology*, 25(5), 929-968.
- Pemberton, S. G., Frey, R. W., Ranger M. J., & MacEachern, J. (2008). The conceptual framework of ichnology. In S. G. Pemberton (Ed.), *Applications of ichnology to petroleum exploration: A core workshop* (pp. 1-32). Society for Sedimentary Geology, SEPM Core Workshop No. 17.
- Pemberton, S. G., MacEachern, J. A., Dashtgard, S. E., Bann, K. L., Gingras, M. K., & Zonneveld, J. P. (2012). Shorefaces. In D. Knaust & R. G. Bromley (Eds.), *Developments in sedimentology* (Vol. 64, pp. 563-603). Elsevier.
- Peng, J. (1997). *Palaeoecology of vertebrate assemblages from the Upper Cretaceous Judith River Group (Campanian) of southeastern Alberta, Canada*. (Unpublished master's thesis). University of Calgary, Calgary, Alberta.
- Power, B. A., & Walker, R. G. (1996). Allostratigraphy of the Upper Cretaceous Lea Park-Belly River transition in central Alberta, Canada. *Bulletin of Canadian Petroleum Geology*, 44(1), 14-38.
- Price, R. A. (1994). Cordilleran tectonics and the evolution of the Western Canada Sedimentary Basin. In G. D. Mossop & I. Shetson (Comps.), *Geological atlas of the Western Canada*

- Sedimentary Basin* (pp. 13-24). Calgary, Alberta: Canadian Society of Petroleum Geologists and Alberta Research Council.
- Rogers, R. R., Kidwell, S. M., Deino, A. L., Mitchell, J. P., Nelson, K., & Thole, J. T. (2016). Age, correlation, and lithostratigraphic revision of the Upper Cretaceous (Campanian) Judith River Formation in its type area (north-central Montana), with a comparison of low- and high-accommodation alluvial records. *The Journal of Geology*, 124(1), 99-135.
- Russell, L., & Landes, R. (1940). *Geology of the southern Alberta plains*. Geological Survey of Canada, Memoir 221.
- Sato, T., Eberth, D., Nicholls, E., & Manabe, M. (2005). Plesiosaurian remains from non-marine to paralic sediments. In *Dinosaur Provincial Park: A spectacular ancient ecosystem revealed* (pp. 249-276). Bloomington & Indianapolis, IN: Indiana University Press.
- Scott, J. J., Gingras, M. K., Eberth, D. A., & Pemberton, S. G. (2012). The freshwater to brackish channel-dominated transgressive Belly River Group, Dinosaur Provincial Park, Alberta. Paper presented at CSPG Geoconvention Core Conference, Calgary, Alberta.
- Slipper, S. E., & Hunter, H. M. (1931). Stratigraphy of Foremost, Pakowki, and Milk River formations of southern plains of Alberta. *AAPG Bulletin*, 15(10), 1181-1196.
- Smith E. P. & van Belle, G. (1984). Nonparametric estimation of species richness. *Biometrics* 40, 119-129.
- Speelman, J. D., & Hills, L. V. (1980). Megaspore paleoecology: Pakowki, Foremost and Oldman formations (Upper Cretaceous), southeastern Alberta. *Bulletin of Canadian Petroleum Geology*, 28(4), 522-541.
- Stanton, T. W., Hatcher, J. B., & Knowlton, F. H. (1905). *Geology and paleontology of the Judith River beds* (No. 257). U.S. Government Printing Office.
- Sweet, A. R., Ricketts, B. D., Cameron, A. R., & Norris, D. K. (1989). An integrated analysis of the Brackett coal basin, Northwest Territories. In *Current Research Part G, Frontier Geoscience Program, Arctic Canada* (pp. 85-99). Geological Survey of Canada, Paper no. 89-1G.
- Troke, C. (1993). *Sedimentology, stratigraphy and calcretes of the Comrey Member, Oldman Formation (Campanian), Milk River Canyon, southeastern Alberta* (Unpublished master's thesis). University of Calgary, Alberta.
- Vavrek, M. J. (2011). Fossil: Palaeoecological and palaeogeographical analysis tools. *Palaeontologia Electronica*, 14(1), 16.
- Wasser, G. G. M. (1988). A geological evaluation of the Judith River Formation (Belly River Formation) in the Pembina region. In D. P. James & D. A. Leckie (Eds.), *Sequences*,

stratigraphy, sedimentology: Surface and subsurface, Proceedings of a Canadian Society of Petroleum Geologists Technical Meeting, Calgary, Alberta, September 14-16, 1988 (pp. 563-569). Canadian Society of Petroleum Geologists, Memoir 15.

Whittaker, R. H. (1972). Evolution and measurement of species diversity. *Taxon*, 21, 213-251.

Wood, J. M. (1989). Alluvial architecture of the Upper Cretaceous Judith River Formation, Dinosaur Provincial Park, Alberta, Canada. *Bulletin of Canadian Petroleum Geology*, 37(2), 169-181.

Transition

Chapter 2 presented the geological setting and a brief history of noteworthy studies conducted on the Belly River Group in western Canada and Montana, providing context for the region under investigation. Chapter 3 investigates the ichnology and sedimentology of the transition from terrestrial clastics of the Dinosaur Park Formation to marine clastics of the Bearpaw Formation in the Cypress Hills region of southwestern Saskatchewan. Previous studies have noted the presence of large, hydrocarbon-rich sandbodies running parallel to mudstone- and siltstone-dominated paleoshorelines, but have failed to provide a mechanism to explain their depositional history. These deposits are characterized for the first time utilizing sedimentology and ichnology, and a detailed discussion of the paleoenvironment and paleoecology is provided. Overall, the region records a marine transgression, characterized by barrier islands, lagoons, and estuaries. M. Gilbert conducted the field and laboratory work, interpreted the sedimentologic and ichnologic dataset, wrote the manuscript, and prepared all tables and figures.

Ichnology and Depositional Environments of the Upper Cretaceous Dinosaur Park – Bearpaw Formation Transition in the Cypress Hills Region of Southwestern Saskatchewan, Canada

Abstract

The upper Campanian Dinosaur Park Formation (DPF) is a south- and eastward-thinning fluvial to marginal-marine clastic wedge in the Western Canada Sedimentary Basin. The DPF is overlain by the Bearpaw Formation (BF), a fully marine clastic succession representing the final major transgression of this epicontinental sea across western North America. In southwestern Saskatchewan, the DPF is comprised of marginal-marine coal, carbonaceous shale, and heterolithic siltstone and sandstone grading vertically into marine sandstone and shale of the BF. Historically these deposits have been interpreted as the record of fluvial delta systems along a paleocoastline. This study revisits this interpretation using integration of ichnologic, sedimentologic, and sequence-stratigraphic concepts.

Detailed facies analysis indicates the upper DPF does not record sedimentation in a delta system, but rather was deposited in a low-relief coastal plain with a wave-dominated, tidally influenced, fluvially modified shoreline. Marginal-marine facies, interpreted as lagoons, tidal flats and estuaries, are bioturbated, showing a typical brackish-water trace-fossil assemblage, including *Asterosoma* isp., *Chondrites* isp., *Cylindrichnus concentricus*, *Teichichnus rectus*, and *Skolithos* isp. Fine-grained sandstone was deposited in an estuarine mouth-bar and barrier-island complex that protected the coast from wave reworking. As the seaway transgressed across the coast, fully marine wave-dominated parasequences replaced those of the coastal plain. Typical trace fossils include *Asterosoma* isp., *Chondrites* isp., *Diplocraterion* isp., *Nereites*

missouriensis, *Phycosiphon incertum*, *Planolites* isp., *Rhizocorallium* isp., and *Zoophycos* isp., reflecting open, fully marine conditions. This study provides new insights into the evolution of depositional environments in the Late Cretaceous of southwestern Saskatchewan, and provides a framework for further geological and paleontological studies ongoing in the region.

3.1 Introduction

The Upper Cretaceous Dinosaur Park Formation (DPF) and Bearpaw Formation (BF) are part of the infill of the Western Canada Sedimentary Basin in southern Alberta and Saskatchewan. In Alberta and Montana, both formations have been the focus of several sedimentologic and stratigraphic studies reflecting exceptional outcrop exposure and a wealth of subsurface data (e.g., McLean, 1971; Wood, 1985, 1989; Eberth & Hamblin, 1993; Tsujita, 1995; Catuneanu et al., 1997; Hamblin, 1997; Rogers et al., 2016). The Dinosaur Park-Bearpaw (DPF-BF) transition, which is exposed in the Cypress Hills of southwestern Saskatchewan, has received little attention. There, it records a transgressive shoreline controlled largely by contemporary tectonics in the Canadian Cordillera. Interplay of accommodation space, sediment supply, and shoreline morphology resulted in major environmental changes in Alberta and Saskatchewan. This investigation of the DPF-BF transition, using outcrop and subsurface data, provides new understanding of depositional trends and the evolving coastal paleogeography in the Cypress Hills and across the Western Canada Sedimentary Basin. Historically, the Saskatchewan deposits have been interpreted as the record of deltaic systems along a paleocoastline (McLean, 1971). This study revises this interpretation by the integrating of modern ichnologic, sedimentologic, and stratigraphic concepts. The objectives of this study are to: 1) characterize the facies and facies associations during the transition between the coastal-plain deposits of the DPF and the shallow-marine strata of the BF; 2) identify the controlling depositional processes that prevailed in the region during transgression; 3) discuss the paleoenvironmental evolution of the area of study; and 4) highlight the significance of ichnologic data in interpreting the processes and environments.

The results will aid in understanding the variability recorded in transgressive marginal-marine and coastal-plain facies in different regions of a single sedimentary basin. This study

highlights the regional diversity in facies associations and ichnofaunas – from sandy barrier bars to muddy and clayey heterolithic settings, to wave-dominated shorelines – all of which are recorded across the region during the transition from coastal-plain to shallow-marine strata. Results allow us to present a detailed depositional model for the transition between the DPF and BF in southwestern Saskatchewan.

3.2 Geological Background

Most Cretaceous and Paleogene sedimentation in the Western Canada Sedimentary Basin occurred in two depocenters separated by the Bow Island Arch: the Williston Basin to the east, and the Foreland Basin to the west (Dawson et al., 1994). During the Laramide Orogeny (~70–80 Ma), collisional accretion of microcontinents onto the western coast of North America caused thrust-sheet loading, resulting in formation of an orogenic belt (Price, 1994). These tectonic processes flexed the craton to produce a deeply subsiding, asymmetric foredeep fed by sediments from the tectonically induced slope (Catuneanu et al., 2000). In west-central North America, this resulted in deposition of abundant marine and nonmarine clastic sediments in transgressive-regressive, wedge-cycles (Fig. 3.1; Leckie & Smith, 1992). The Belly River Group (BRG) is the fourth of five recognized cycles of foreland basin deposition (Embry, 1990; Miall, 1991; Leckie & Smith, 1992; Hamblin, 1997; Eberth, 2005; Gilbert et al., 2018).

Deposition of the Campanian BRG is characterized by large sediment supply to the basin, producing an eastward-thinning paralic (interfingering marine and coastal) to nonmarine clastic succession (Cant & Stockmal, 1989). The lower half of the BRG is assigned to the regressive extent of the Claggett Cycle, and the upper deposits to the transgressive Bearpaw Cycle (Kauffman & Caldwell, 1993). Radiometric ages from $^{40}\text{Ar}/^{39}\text{Ar}$ and K-Ar dating of sanidine, plagioclase, and biotite phenocrysts from the top of the Oldman Formation to the base of the BF

spans 76.5–74.8 Ma (Eberth & Deino, 1992; Eberth, 2005). Three formations from this period are formally recognized in the western Canadian plains. In ascending order, these are the Foremost, Oldman and the Dinosaur Park formations (Eberth & Hamblin, 1993). Each formation is bounded on its lower and upper contacts by a disconformity, and has distinctive sedimentologic and petrographic signatures that reflect tectonic controls of sediment supply (Eberth, 2005).

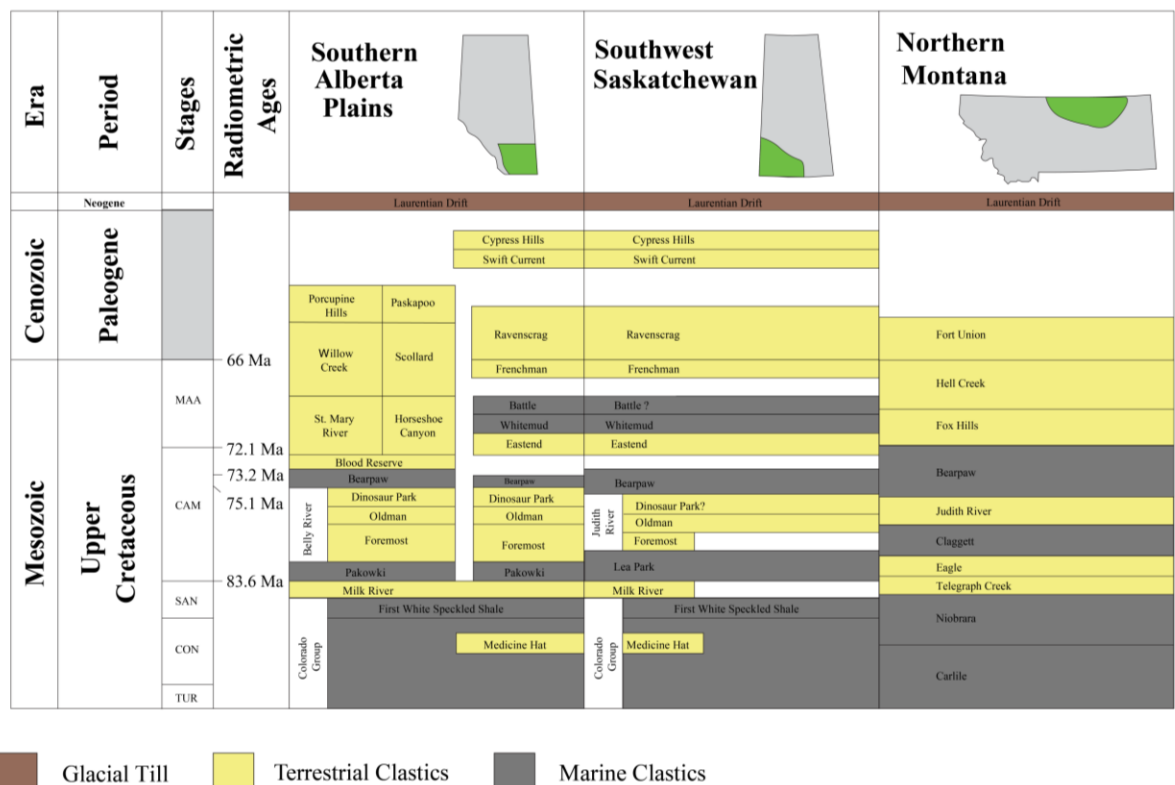
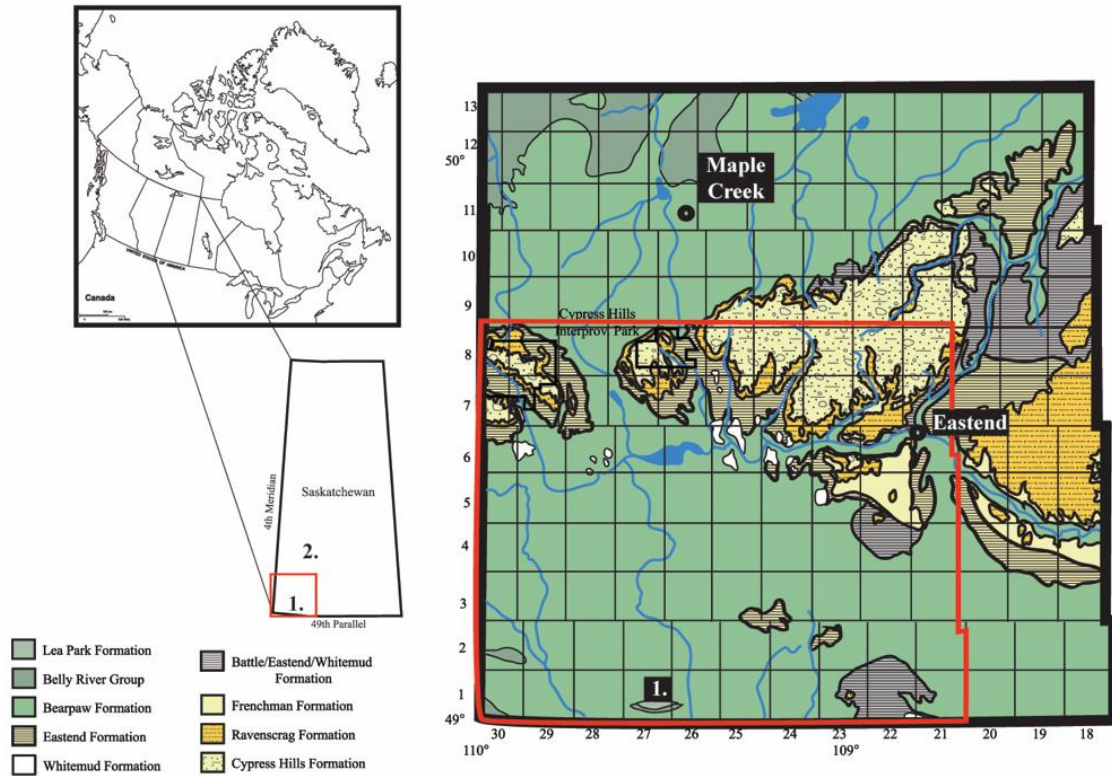


Figure 3.1: Stratigraphic nomenclature utilized in southeastern Alberta and southwestern Saskatchewan through the Upper Cretaceous Series in the Western Canada Sedimentary Basin. Radiometric and biostratigraphic dates (Ma): 66: K-T boundary (Gradstein et al., 2012); 72.1: Campanian – Maastrichtian boundary (Gradstein et al., 2012); 73.2±0.4: Dorothy Bentonite (Lerbekmo & Braman, 2002); 75.1: *Exileoceras jenneyi* (Cobban et al., 2006); 83.6: Campanian – Santonian boundary (Gradstein et al., 2012). After Gilbert et al. (2018). TUR - Turonian; CON - Coniacian; SAN - Santonian; CAM - Campanian; MAA - Maastrichtian.

A.



B.

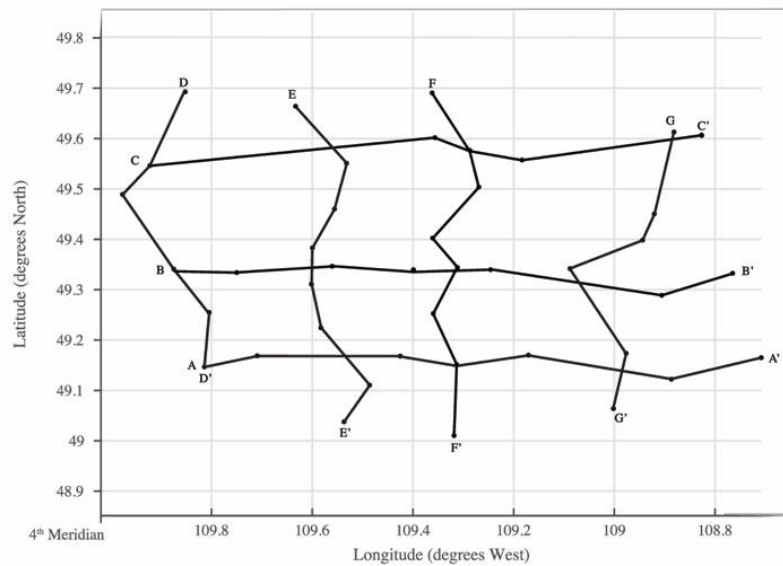


Figure 3.2: **A.** Left: Geographic location of Saskatchewan in context to regional landmarks and boundaries of the Cypress Hills region and location of exposed outcrop at 1. Woodpile Coulee and 2. Herschel, Saskatchewan. Right: Regional map of the Cypress Hills region in context to regional landmarks. Based on maps from the Saskatchewan Geological Survey. **B.** Map of wells used to make cross-section correlations used in this study, plotted against latitude and longitude. Cross-sections B and F are included in this chapter as figures 14 and 15; the remaining cross-sections are included in Appendix B.

Sparse exposures of the BRG crop out throughout western Saskatchewan in the North and South Saskatchewan River valleys, at sites near Muddy Lake and Herschel in west-central Saskatchewan, and in the Cypress Hills in the southwestern corner of Saskatchewan. Those sediments, which record the easternmost extent of the BRG in Saskatchewan, record the passage of the terrestrial BRG into fully marine shale and sandstone of the BF (McLean, 1971; Eberth et al., 1990; Tsujita, 1995; Gilbert et al., 2018). Outcrops of the BRG are rare in Saskatchewan south of 52° N latitude (McLean, 1971).

3.3 Methods

The main study area extends from the United States border north to township 8 and from range 21 west of the third meridian (21W3) to the Alberta border, encompassing most of the Cypress Hills in Saskatchewan (Fig. 3.2). Where possible, a minimum of one well per township was used, resulting in a database of 258 wells (Appendix A). Six subsurface cores (Table 3.1) and outcrop exposure in township 1, range 27W3 along Woodpile Coulee (Fig. 3.2) was integrated to assist subsurface correlation. A small, but well exposed outcrop of the DPF - BF transition in township 17, range 28W3 (Fig. 3.2) was included to provide a more robust dataset of depositional patterns across the basin. Subsurface core (Fig. 3.3 and 3.4) and outcrop exposures (Fig. 3.5) were logged and interpreted based on sedimentology and ichnology, enabling 15 discrete facies and 4 facies associations to be recognized (Table 3.2). Two hundred and fifty-eight subsurface logs were picked to identify the contact between the Oldman - Dinosaur Park and the Dinosaur Park - Bearpaw formations, and facies associations (Fig. 3.6; Appendix A and B). Bioturbation intensity uses the Bioturbation Index (BI) of Taylor and Goldring (1993), with 0 defining complete absence of bioturbation, and 6 reflecting complete reworking of the substrate. Table 3.3 summarizes the trace-fossil distribution among the different facies.

The semiquantitative coastal classification scheme proposed by Ainsworth et al. (2011) is used to classify the dominant depositional processes that occurred during the DPF-BP transition. This system aims to provide meaningful comparison between different depositional systems in dynamic coastal environments, and expands the classic tripartite model long used to include coastal plain deposits. This system effectively subdivides the plot into nine fields based on the relative importance of wave, tidal, and fluvial processes. Twenty-two (22) potential classification categories are possible in the classification (see Ainsworth et al., 2011).

3.4 Results

3.4.1 Facies Descriptions and Interpretations

F1: Shale

Description

This facies consists of fissile, thinly parallel-laminated, brown to gray shale. Bioturbation is pervasive throughout (BI 4–6). The ichnofauna is dominated by deep-tier trace fossils, including *Zoophycos* isp. and *Chondrites* isp. *In situ* marine bivalves are abundant, and sandy and/or silty millimeter-scale stringers are common throughout. Shale of Facies 1 typically grades upwards into mudstone and interbedded siltstone of Facies 2. Facies intervals are 1–5.2 m thick.

Interpretation

Shale is associated with low-energy suspension fallout, but thin siltstone and sandstone stringers are attributed to turbidity currents triggered during storm activity (Davis & Hayes, 1984; Roy et al., 1994; Plint, 2010; Buatois & Mángano, 2011). These deposits are intensely bioturbated by a low-diversity, deep-tier, trace-fossil assemblage representative of the *Zoophycos* Ichnofacies

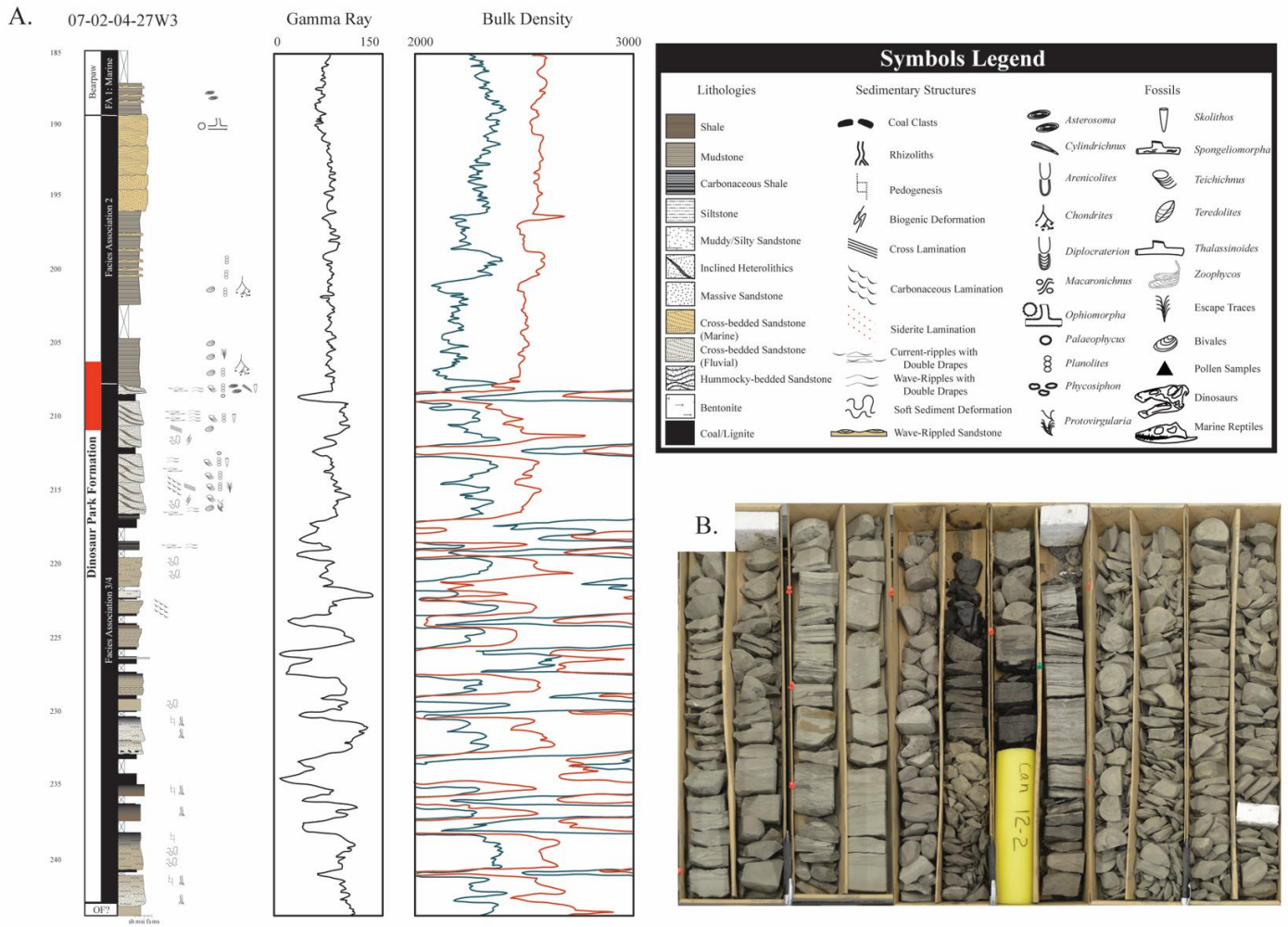


Figure 3.3: A. Representative lithostratigraphic log profiles of Nexen Battle Creek 07-02-004-27W3 and corresponding gamma (API) and bulk density log (K/M3). Red fill in column signifies location of cored section in part B of figure. B. Cored section through the transition between inclined heterolithic deposits of F7 and lagoonal/estuarine basin fill of F8. C - Coal; Sh - Shale/claystone; M - Mudstone; Si - Siltstone; FSS - Fine-grained sandstone; MSS - Medium-grained sandstone.

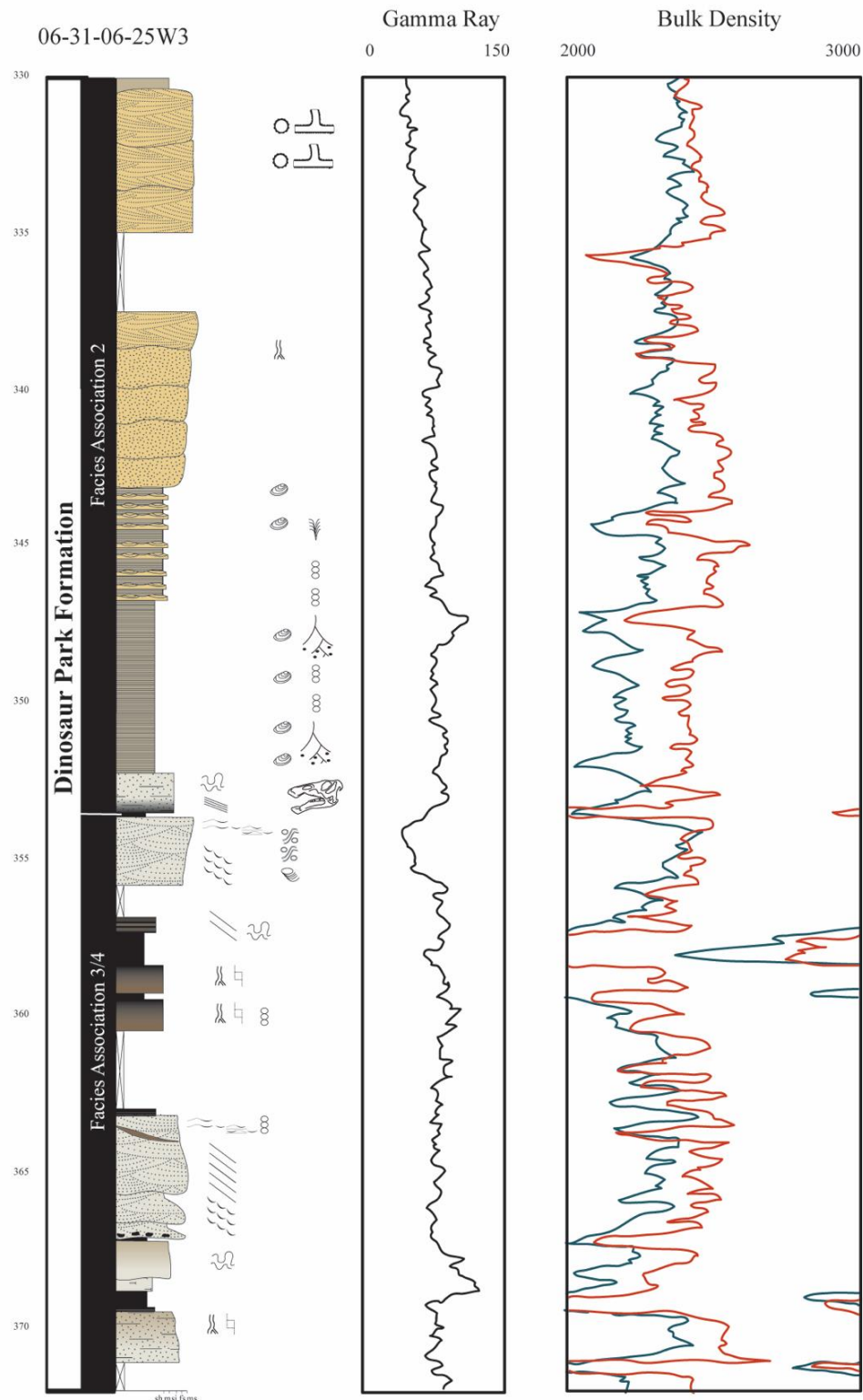


Figure 3.4: Representative lithostratigraphic log profiles of Canadian Landmaster Cypress Hills 06-31-06-25W3 and corresponding gamma (API) and bulk density log (K/M3). C - Coal; Sh - Shale/claystone; M - Mudstone; Si - Siltstone; FSS - Fine-grained sandstone; MSS - Medium-grained sandstone. For symbols legend see Figure 3.

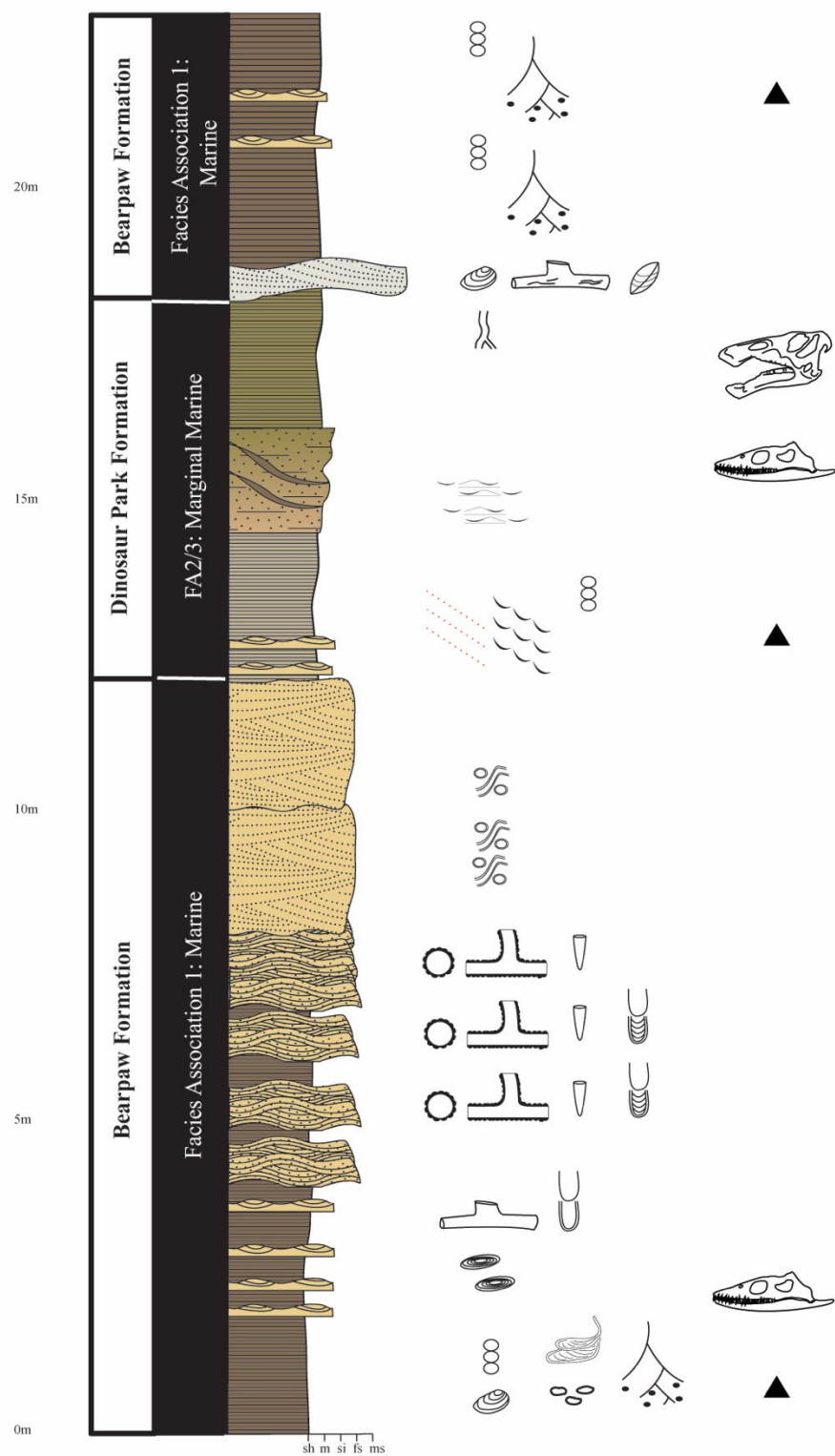


Figure 3.5: Representative composite lithostratigraphic log profile of exposed outcrop near Herschel, Saskatchewan. C - Coal; Sh - Shale/claystone; M - Mudstone; Si - Siltstone; FSS - Fine-grained sandstone; MSS - Medium-grained sandstone. For symbols legend, see Figure 3.

(MacEachern et al., 1999; Pemberton et al., 2001; Buatois & Mángano, 2011). The ichnological and sedimentological evidence indicates a shelf environment (i.e., below storm wave base) with anoxic to dysoxic subsurface conditions.

F2: Mudstone and interbedded siltstone

Description

This facies is composed of massive brown to dark gray shale and mudstone with local interbedded, thinly laminated sandstone and siltstone lenses and layers 0.5–5.2 cm thick.

Abundance and thickness of discrete sandstone and siltstone beds increases upwards, with sharp bases where not reworked by bioturbation. Shell debris is common throughout, and carbonaceous laminae can be observed rarely in the coarser-grained deposits. This facies is moderately to heavily bioturbated (BI 3–6), making discrete trace-fossil identification difficult. A wide variety of infaunal, deep-tier trace fossils (e.g., *Chondrites* isp. and *Zoophycos* isp.) dominates the assemblage in this facies (Fig. 3.7A). Facies intervals are 2–4.5 m thick.

Interpretation

This facies is interpreted as having been deposited between storm- and fair-weather wave base in a shallow-marine, wave-dominated setting. Sandstone and siltstone are consistent with distal storm beds in an offshore environment (Roy et al., 1994; Buatois & Mángano, 2003; Plint, 2010; Wesolowski et al., 2018). F2 displays a higher ichnodiversity compared to the shale of Facies 1. Trace fossils identified in this facies are consistent with a distal *Cruziana* Ichnofacies (MacEachern et al., 1999, 2007, 2010; Buatois & Mángano, 2003). These deposits record low-energy suspension fallout during fair-weather conditions, punctuated by storm events. F2 is interpreted as having formed in the lower offshore.

Canadian Landmaster Belanger
10-23-007-25W3

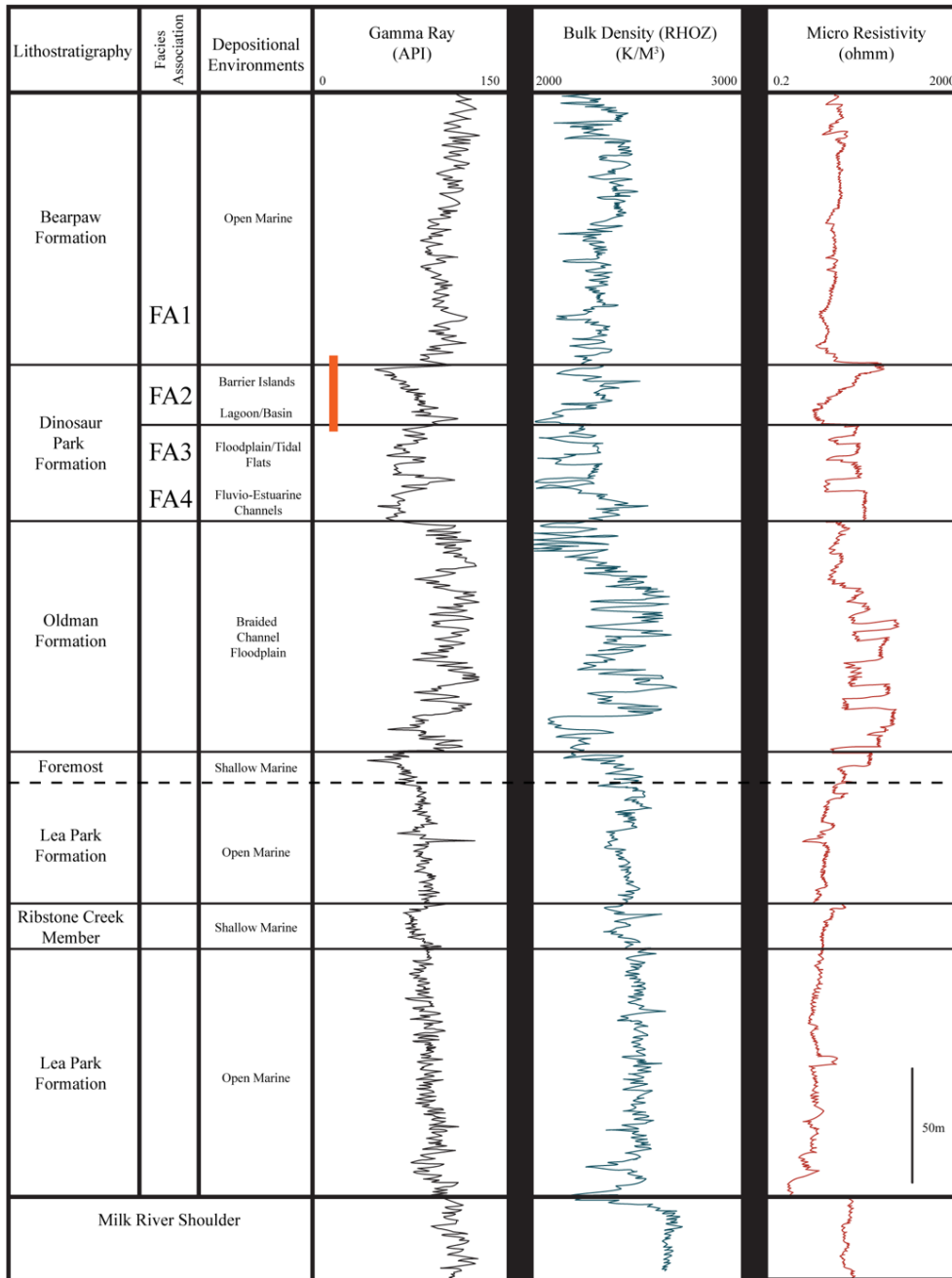


Figure 3.6: Representative well log highlighting stratigraphy, facies associations, and depositional environments of the Belly River Group in the subsurface of southwestern Saskatchewan (Canadian Landmaster Belanger – 10-23-007-25W3). This well illustrates the typical gamma ray - bulk density - resistivity log signatures of the Belly River Group. Dashed line of the Foremost Formation indicates its sporadic occurrence throughout the study area. Red line indicates available core that was logged for this study.

F3: Bioturbated muddy and sandy siltstone

Description

Facies 3 consists of light gray, muddy and sandy siltstone with rare mudstone interbeds. This facies occurs in 1–2 m thick packages, with individual silty and sandy beds being thicker than those in F2 (0.8–7.2 cm thick). Sandstone and siltstone beds have erosional sharp bases and locally are massive. Identifiable sedimentary structures are rare, but where observed consist of micro-hummocky and symmetrical ripples. Mudstone layers (1–2.8 cm thick) and carbonaceous drapes and laminae are commonly associated with sandy siltstone lenses that show symmetrical ripple cross-lamination. Mudstone is heavily bioturbated (BI 5–6). A high-diversity trace-fossil assemblage, including *Asterosoma* isp., *Diplocraterion* isp. and *Rhizocorallium* isp. (Fig. 3.7B), among other ichnotaxa, is present, particularly towards the tops of silty beds and within the mudstone (Table 2). F3 gradationally overlies F2 and is identified by an increase in thickness of individual sandstone beds.

Interpretation

Alternating thin, heavily bioturbated mudstone with sandy siltstone and sandstone indicate suspension fallout punctuated by storm activity, respectively (Pemberton et al., 2001; Buatois & Mángano, 2003, 2011). Micro-hummocky and wave-ripples imply oscillatory flow in a shallow-marine, wave-dominated, storm-influenced, upper-offshore environment (Duke et al., 1991; MacEachern et al., 1999; Buatois & Mángano, 2011). Lack of bioturbation at the base of storm deposits is consistent with other wave-dominated upper-offshore environments described previously (Buatois & Mángano, 2003; Buatois et al., 2006; Wesolowski et al., 2018), supporting an interpretation of a high-energy environment. The ichnofauna at the top of the tempestites and

within the mudstone is ascribed to the *Cruziana* Ichnofacies, reflecting bioturbation during fair-weather conditions and long colonization windows (Buatois & Mángano, 2011).

F4: Fine-grained sandstone and siltstone

Description

This facies consists of fine-grained, light gray, interbedded sandstone and siltstone with low-angle lamination, oscillatory wave-ripples, and an erosive base. Mudstone beds show high bioturbation intensities (BI 5–6), with sandstone beds recording moderate bioturbation near the top (BI 2–3), but with relatively undisturbed bioturbation at the base (BI 1–2). The overall lower bioturbation preserves many primary sedimentary structures. Sandstones have sharp bases, with hummocky cross-stratification, and with individual beds 0.2–0.6 m thick. Marine bivalve shells, intact and fragmented, are preserved locally, but typically at the base of sandstones. Thin, discrete mudstone intervals (1–2.8 cm thick), mudstone laminae (0.2–1.1 cm thick), and mudstone drapes are rare. The diverse trace-fossil assemblage recorded in this facies includes *Asterosoma* isp., *Diplocraterion* isp., *Rhizocorallium* isp., and *Thalassinoides* isp. (Fig. 3.7C and D). This composition is typical of an archetypal *Cruziana* Ichnofacies. Local suspension-feeding trace fossils, such as *Skolithos* and *Ophiomorpha* isp., are preserved throughout the beds. Facies intervals are 1 to 2.5 m thick. This facies overlies F3 and underlies F5 with gradational upper and lower contacts.

Interpretation

Scoured-based sandstone with HCS and oscillatory ripples, alternating with rare bioturbated mudstone, indicate an offshore transitional environment (Aigner, 1985; Pemberton et al., 2001).

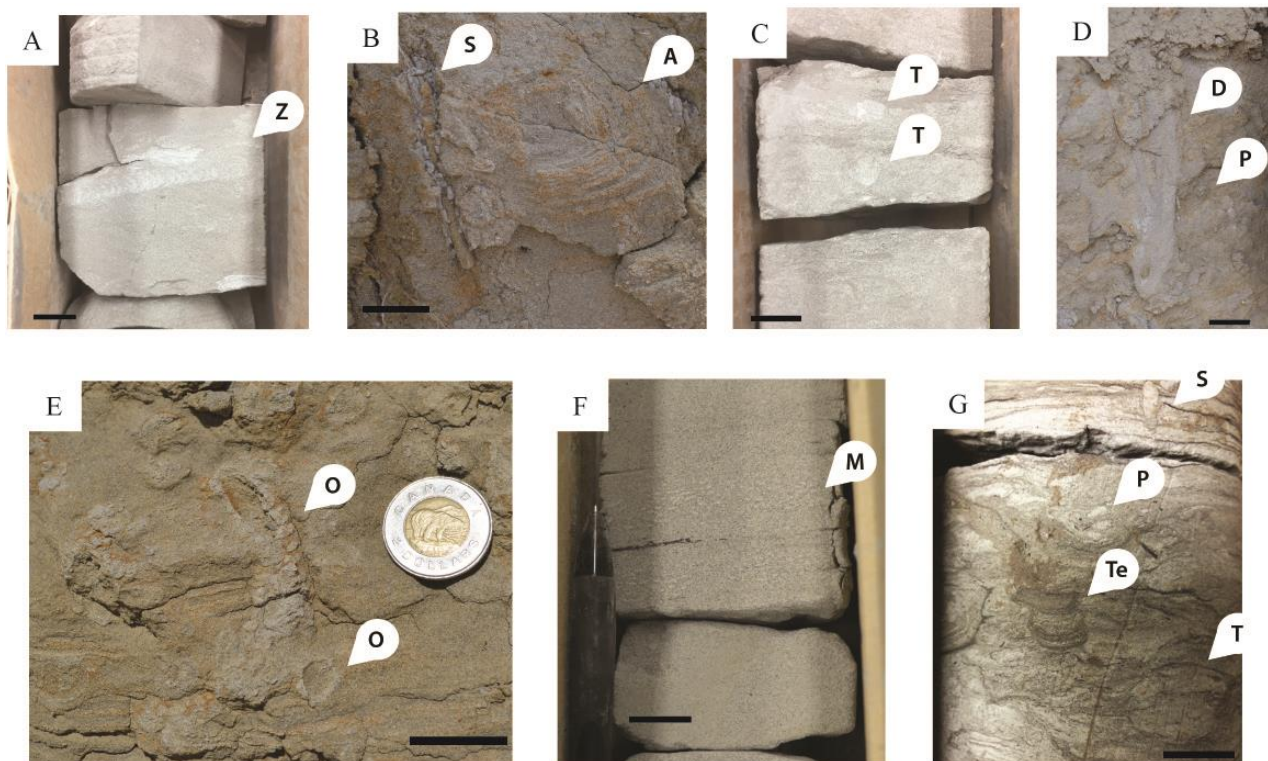


Figure 3.7: Selected photos of core and outcrop highlighting different ichnofossils from the Dinosaur Park and Bearpaw formations in both core and outcrop. A. *Zoophycos* isp. in mudstone and siltstone beds, F2. Note protrusive spreiten (Core 07-02-004-27W3); B. *Asterosoma* isp. displaying diagnostic concentric infill around a central axis in F3 (Herschel, Saskatchewan); C. *Thalassinoides* isp. in F4 (Core 07-02-004-27W3); D. Vertical, U-shaped burrow with spreite assigned to *Diplocarterion* isp. in F4 (Herschel, Saskatchewan); E. Cylindrical passively filled burrows with walls reinforced with fecal pellets assigned to *Ophiomopha* isp. in F5 (Herschel, Saskatchewan); F. Sinuous, densely packed, sub-horizontal to sub-vertical cylindrical burrows assigned to *Macaronichnus* isp. in F6 (Core 02-15-04-26W3); G. Bioturbated inclined heterolithic sediments (IHS) exhibiting traces characteristic of the brackish water trace fossil assemblage of F7 (Core 10-10-002-27W3). A - *Asterosoma* isp.; D - *Diplocarterion* isp.; M - *Macaronichnus* isp.; O - *Ophiomopha* isp.; P - *Planolites* isp.; S - *Skolithos* isp., T - *Thalassinoides* isp.; Te - *Teichichnus* isp. All scale bars = 2 cm.

The offshore transition lies above the upper offshore and below fair-weather wave base (MacEachern et al., 1999; Pemberton et al., 2001; Buatois & Mángano, 2011). Fluctuations in wave intensity led to an alternation of high- and low-energy conditions, resulting in deposition of sand with oscillatory structures, punctuated by low-energy mud deposition. The presence of the archetypal *Cruziana* Ichnofacies throughout F4 traces of suspension-feeders in the storm-generated sandstone is consistent with this interpretation (MacEachern et al., 1999; Pemberton et al., 2001; Buatois & Mángano, 2011).

F5: Amalgamated hummocky cross-stratified sandstone

Description

Facies 5 comprises light gray to greenish-gray, erosive-based, hummocky cross-stratified, very fine- to fine-grained sandstone beds (0.1–0.8 m thick) amalgamated in thick (1–2.3 m) packages (Fig. 3.8A). Coarsening upwards is observed, within both beds and bedsets. Rare bioturbation (BI 0–1) is dominated exclusively by *Skolithos* and *Ophiomorpha* isp. (Fig. 3.7E). F5 gradationally overlies F4, and underlies F6.

Interpretation

The shoreface, located above fair-weather wave base, experiences constant agitation by wave activity (Walker & Plint, 1992; Schwarz & Howell, 2005; James & Dalrymple, 2010).

Amalgamated hummocky cross-stratified sandstone is attributed to deposits of the lower- to middle-shoreface (MacEachern & Pemberton, 1992; Plint, 2010; Buatois & Mángano, 2011).

Most sediments were deposited by waves and during storms. Bioturbation in this setting is rare because of constant wave reworking (Pemberton et al., 2001). Where trace fossils are present, the producers are suspension feeders adapted to high-energy environments (MacEachern et al., 1999; Pemberton et al., 2001; Buatois & Mángano, 2011).

F6: Amalgamated trough cross-stratified sandstone

Description

Light gray to greenish-gray, tabular cross-bedded and trough cross-bedded fine-grained sandstone beds (0.7–4.2 m thick) are amalgamated into packages 0.5–1 m thick (Fig. 3.8B). This facies coarsens upwards, at both bed and bedset scales. Bioturbation is rare (BI 0–1), and traces are represented by monospecific examples of *Macaronichnus* isp. (Fig. 3.7F). Reworked *Ophiomorpha* isp. are common at the base of troughs. F6 abruptly overlies F5 and F9, and is overlain by F9 and F4, either gradationally or abruptly.

Interpretation

Cross-bedded and trough cross-bedded fine-grained sandstone with erosive or gradational beds and bedsets is consistent with deposition in the upper shoreface. In upper shoreface environments, high-energy conditions prevail, with longshore currents, fair-weather wave action, and storm activity proliferating migration of longshore bars. These processes resulted in migration of two- and three-dimensional dunes linked to unidirectional flows (Clifton et al., 1971; Walker & Plint, 1992). *Macaronichnus* is representative of deposit- or epigranular-feeding polychaetes associated with nearshore high-energy environments (Coates, 2002; Pemberton et al., 2001; Quiroz et al., 2010; Buatois & Mángano, 2011; Uchman et al., 2016).

F7: Massive shale, mudstone and laminated siltstone

Description

This facies consists of massive, medium to dark gray, mudstone and shale (Fig. 3.9). The mudstone and shale are generally structureless, with local, 3–5 mm thick, siltstone and very fine-grained sandstone stringers with oscillatory ripples. F7 displays considerable variability, both at bed and facies scales. Lithology ranges from carbonaceous-rich shale and mudstone to mudstone

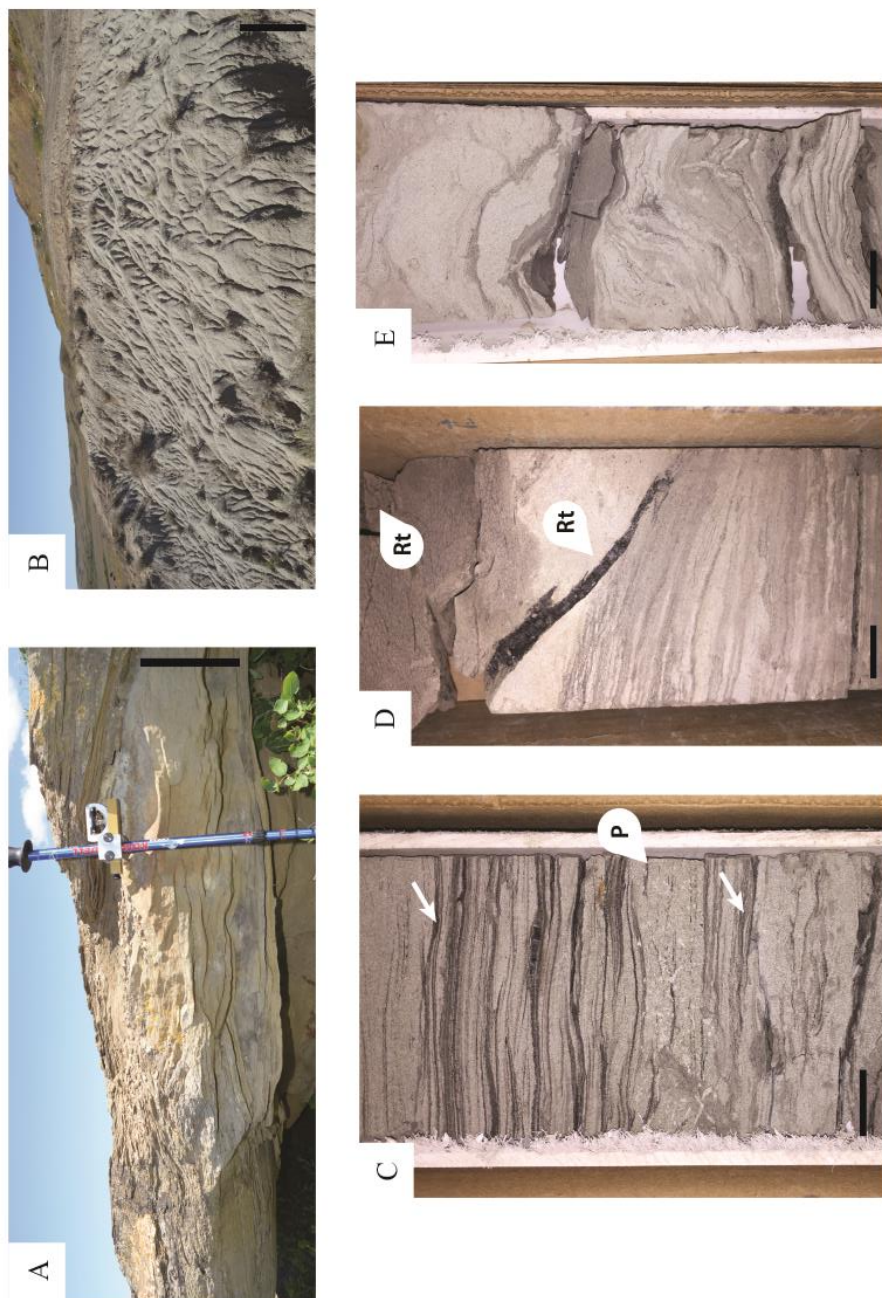


Figure 3.8: Selected photos of core and outcrop from the Dinosaur Park and Bearpaw formations. **A.** Amalgamated hummocky cross-stratified sandstone, F5 (Herschel, Saskatchewan; scale = 0.5 m). **B.** Amalgamated trough cross-stratified sandstone, F6 (Herschel, Saskatchewan; scale = 0.5 m). **C.** Carbonaceous/mudstone drapes and current- and wave-rippled fine-grained sandstone, F9 (Core 07-02-004-27W3). Small *Planolites* isp. visible within the laminae. Double mudstone drapes are present throughout (indicated by arrow) (Core 07-02-004-27W3). **D.** Rooted mudstones and siltstones, F10 (Core 07-02-004-27W3). **E.** Convolute mudstone, siltstone, and sandstone, F11 (Core 07-02-004-27W3). P - *Planolites* isp.; RT - Root trace fossil. All scale bars on core = 2 cm.



Figure 3.9: Representative compiled photographs of Facies Association 2 (FA2) and Facies Association 3 (FA3) showing vertical facies stacking. This core distinctly highlights the flooding of a coastal plain, as heterolithic deposits of F9 are replaced by mudstones and shales of F7. The very top of the core transitions into a fine-grained sandstone, and is interpreted as the base of a barrier island deposit. Nexen Battle Creek Core 07-02-004-27W3

with interbedded siltstone and very fine-grained sandstone in a ratio of 8:1. Small *in situ* bivalves are interspersed throughout. Bioturbation is irregular, and represented by *Planolites* isp. and rare *Chondrites* isp. (BI 0–1). Facies intervals are 0.5–5.2 m thick, display both sharp-based and gradational contacts, and commonly overlie F9 and F10.

Interpretation

This facies, dominated by muds and clays, records sedimentation under low-energy conditions where mud and clay settled from suspension. A coarsening-upward trend to heterolithic siltstone and sandstone implies a shift to higher-energy conditions. Carbonaceous organic matter indicates a sediment source near a terrestrial setting (Leckie et al., 1989; Vakarelov et al., 2012; Jones, 2013). Small marine bivalves and a diminutive monospecific trace-fossil assemblage with a low bioturbation index is evidence of a stressed environment (Gingras et al., 1999; Pearson & Gingras, 2006; MacEachern & Gingras, 2007; Lettley et al., 2009; Buatois & Mángano, 2011). F7 is interpreted as being deposited in estuarine and lagoonal basins.

F8: Bioturbated fine- to medium-grained sandstone

Description

F8 comprises medium gray to greenish-gray, fine- to medium-grained sandstone with patches of bioturbation (BI 0–3). Beds (0.6–1.3 m) are massive to structureless, but low-angle cross-bedding with rare symmetrical ripples and trough- and planar cross-bedding is present locally. This facies is 1.4–6.3 m thick, and display both gradational and erosive lower contacts. Rare glauconite grains, carbonaceous laminae, coal clasts, and lignitic plant debris are locally present. Deep, coalified root traces are present in some of the logged sections, and monospecific assemblages of *Macaronichnus* isp. appear in discrete horizons between unbioturbated sandstone (Fig. 3.9).

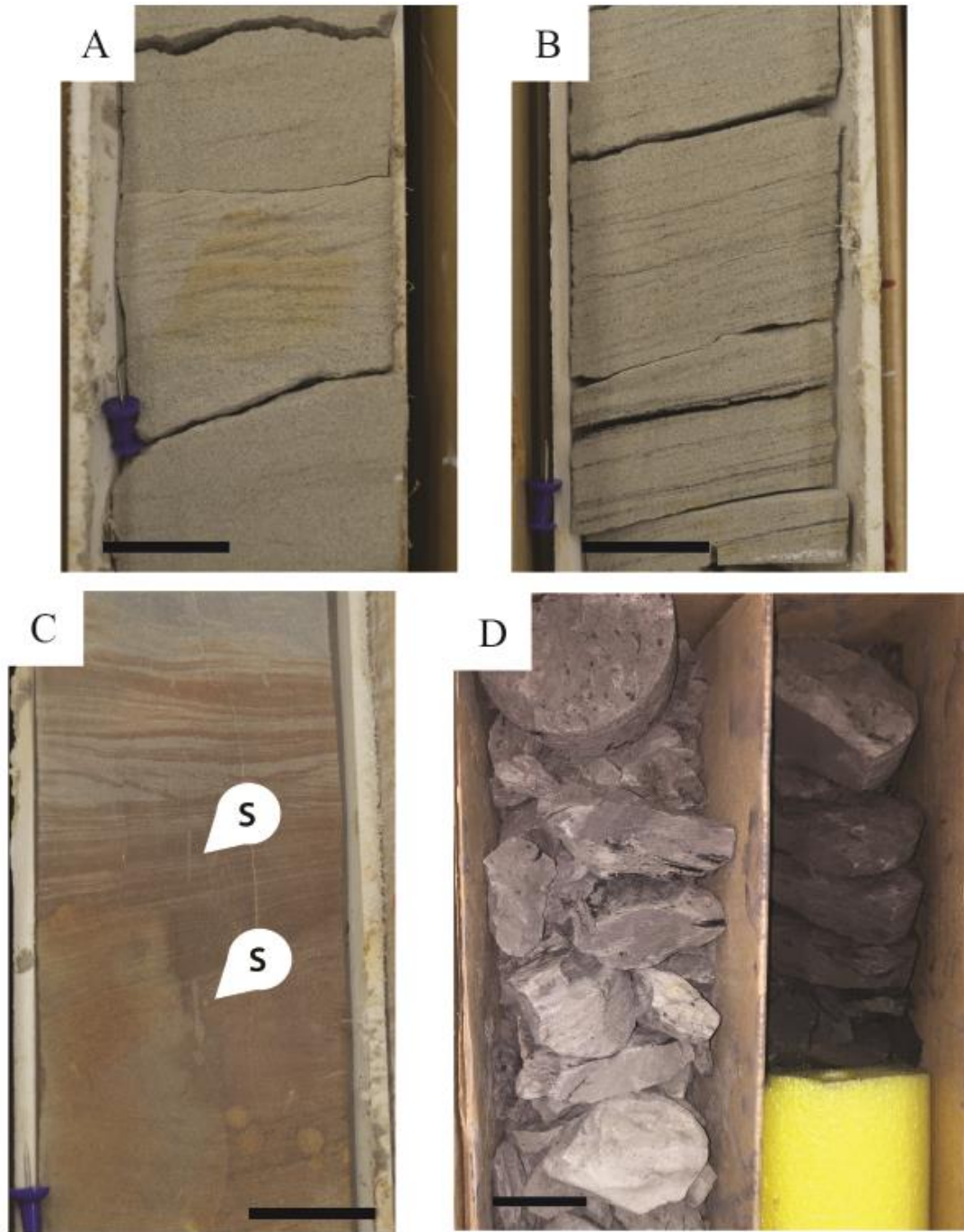


Figure 3.10: Selected photos of core in the Dinosaur Park Formation. A. Current rippled fine-grained sandstone, F12; B. Cross-bedded fine-grained sandstone with associated carbonaceous laminae, F12; C. Current-rippled sandstone with siderite. Small *Skolithos* isp. present at the top of bedsets, F12; D. Carbonaceous mudstone, siltstone, and coal, F13. All scale bars = 2 cm.

Interpretation

Massive, low-angle, and cross-bedded sandstone with rare symmetrical ripples indicates a high-energy environment mostly affected by unidirectional currents with subordinate oscillatory flows (Dalrymple et al., 1992; Dalrymple, 2010; Reinson, 2010; Davis et al., 2011; Daidu et al., 2013). Structureless sandstones are attributed to mass-flow deposition, high sedimentation rates, and (or) complete biogenic reworking (Thomas & Mack, 1982; Reading & Collinson, 1996; Odezulu et al., 2018). As mentioned, *Macaronichnus* represents deposit-feeding or epigranular-feeding polychaetes commonly associated with high-energy, nearshore environments (Coates, 2002; Pemberton et al., 2001; Quiroz et al., 2010; Buatois & Mángano, 2011; Uchman et al., 2016). Root traces near the top of some beds indicate periodic subaerial exposure and environmental conditions favorable for plant colonization. This facies is compatible with deposition in offshore estuarine mouth-bars and barrier-island bars.

F9: Sparsely bioturbated heterolithic deposits

Description

This facies consists of medium to light gray, inclined, thinly laminated, 1.2 centimeter- to millimeter-scale, fine to very-fine sandstones and siltstone. Beds are tabular to lenticular, exhibit parallel-lamination, current- and wave-ripple cross-lamination, and are erosionally based (Fig. 3.9). Mud and carbonaceous drapes are pervasive, and are associated with both wave- and current-ripples. Bidirectional current ripples are discernible in silty and sandy intervals. Thick, silty and sandy layers alternate with light brown to brownish-gray mudstone and claystone with carbonaceous laminae (Fig. 3.8C). Beds and bedsets exhibit inclination between 2 and 4° and are oriented towards the east and southeast. This is consistent with the definition of inclined heterolithic stratification (Thomas et al., 1987). Facies intervals are 0.7 to 3.4 m thick, displaying

fining-upward trends. These fining-upward trends result in a gradational change up-section from flaser to wavy, to lenticular bedding. Intensity of bioturbation varies (BI 0–3), with some beds displaying discrete trace fossils (e.g., *Asterosoma* isp., *Cylindrichnus concentricus*, *Teichichnus rectus*, *Thalassinoides* isp.), while others show a mottled texture, and some beds are unburrowed (Fig. 3.7G).

Interpretation

Inclined, parallel-laminated and ripple cross-laminated, sandstone, siltstone and mudstone, forming fining-upward intervals with erosive bases, are characteristic of tidally influenced point-bar deposits and intertidal channels. Bidirectional ripples with mudstone and carbonaceous drapes indicate changes in flow velocity and direction, and are associated with many tidally influenced settings, including tidal flats and tidal sandbars (Wood, 1989; Lettley & Pemberton, 2004; Dalrymple & Choi, 2007; Davis et al., 2011; Daidu et al., 2013). Inclined heterolithic sediments with flaser, wavy, and lenticular bedding are typical of tidally influenced coastal-plain channels (Lettley & Pemberton, 2004; Dalrymple & Choi, 2007; Dalrymple, 2010; Reinson, 2010; Davis et al., 2011). Trace fossils in this facies (Table 2) are typical of brackish-water trace-fossil assemblages. Sporadic bioturbation intensity, combined with alternating inclined sands, silts and muds, reflects variability in turbidity, salinity and suspended sediment load.

Fluctuations in environmental parameters such as temperature, suspended sediment load, and salinity can be stressful for organisms that bioturbate sediment (MacEachern et al., 2007; Buatois & Mángano, 2011). F9 is interpreted to have formed in upper and middle estuarine and intertidal channels.

F10: Wave-, current-, and cross-bedded bioturbated sandstone

Description

F10 consists of medium to light gray, current- and wave-rippled, and cross-stratified medium to fine-grained sandstone. Lower facies contacts are sharp based and sediments fine upwards. A decrease in sedimentary structures is noted, going from cross-stratification to ripples. Mud and carbonaceous drapes and horizontal mud laminae are present. Reactivation surfaces are locally present. Bioturbation is sporadic (BI 0–3), consisting of *Macaronichnus* isp. and *Skolithos* isp. F10 ranges in thickness from 0.4–1.5 m.

Interpretation

Medium-grained sandstones, cross-stratification, sharp bases, and reactivation surfaces are evidence of high-energy conditions. The presence of mud and carbonaceous drapes, horizontal mud laminae, and reactivation surfaces indicates periods of suspension fallout during slackwater conditions. Dominance of suspension feeding traces suggests a high-energy setting where particulate matter was suspended in the water column. This facies is interpreted as migrating dunes in a bay-head–delta complex that formed at the innermost part of an estuary system.

F11: Rooted massive and thinly laminated carbonaceous mudstone and muddy siltstone

Description

F11 consists of medium to light gray and gray-brown, massive mudstone and siltstone beds 0.2–2.5 m thick, with thin siltstone and very fine-grained sandstone laminations. Individual beds have sharp to gradational bases, and are 0.2–1.1 m thick. This facies contains abundant plant debris, coal clasts, millimeter- to centimeter-scale silt and very fine-grained planar lamination and stringers, slickensides, and soft-sediment deformation (Fig. 3.8E). Contacts between individual beds within this facies are both gradational and erosive. Coal clasts are common at the base of beds, as F11 is commonly over- and/or underlain by coal. Haloed, coalified root traces and

evidence of pedogenesis in the form of slickensides are common, giving this facies a blocky appearance. Bioturbation is absent to rare, with the exception of root trace fossils.

Interpretation

F11 is dominated by fine-grained sediments, plant debris, coal fragments, and root trace fossils. This suggests deposition in a low-energy setting where there is a high potential for the accumulation of plant material (Retallack, 1988). Silty and sandy stringers, laminations, and soft-sediment deformation structures indicate periods of event-style deposition (Slingerland & Smith, 2004; Miall, 2013). Root trace fossils and slickensides suggest periods of subaerial exposure, with enough time elapsing to allow for pedogenic alteration of the sediment. Haloed root trace fossils are commonly associated with gleysols, which indicate soil development in an environment with a high water table in humid, mid-latitude climates (Kraus, 1999; Retallack, 2008). Facies 11 is interpreted as floodplain deposits with paleosol formation in a humid environment.

F12: Current-rippled and convolute-bedded fine-grained sandstone

Description

Facies 12 consists of light gray, fine-grained sandstone and silty sandstone (Fig. 3.10A). This facies ranges in thickness from 0.62–1.7 m, and displays both gradational and sharp, erosive contacts. Discrete and amalgamated beds of current-rippled, cross-laminated sandstone with rare muddy and silty laminations near the tops of beds, form fining-upward intervals. Individual beds are 0.1–0.6 m thick, with minor cross-lamination, aggradational climbing ripples, and more commonly convolute bedding (Fig. 3.8E). Moderate to abundant carbonaceous laminae, organic debris, and mudstone rip-up clasts are present throughout F12.

Interpretation

Current ripples and trough cross-bedding indicate deposition from unidirectional currents. The presence of aggradational climbing ripples signifies occasional periods of high sediment load in suspension. Silty and muddy drapes at the tops of beds indicate decreased energy, allowing for the deposition of fine-grained silts and muds otherwise suspended. Carbonaceous material and small root trace fossils suggest a periodic subaerial exposure and minor pedogenesis (Leckie et al., 1989; Kraus, 1999; Eberth, 2005). F12 is interpreted as being deposited in coastal plain fluvial channels and crevasse splays.

F13: Trough cross-bedded and current-rippled sandstone

Description

Light gray, current-rippled and trough cross-bedded to structureless, fine-grained sandstone with erosional bases, comprising 0.45–0.7 m thick beds and 0.45–3.7 m thick bedsets (Fig. 3.10A, B). Carbonaceous lamination, coal fragments, and mudstone rip-up clasts are common throughout. Individual beds are amalgamated and with erosive bases, and display normal grading. Muddy and silty drapes, separated by thin sandstone laminae, are isolated and rare. Bioturbation is nearly absent (BI 0–1) with very rare *Skolithos* isp. and local, small root trace fossils restricted to the topmost beds in the facies interval (Fig. 3.10C).

Interpretation

Current ripples and cross-bedding, combined with the presence of fine-grained sands support an interpretation of sediment transport by relatively steady, unidirectional moderate energy flow. Fining-upward sediment patterns, coupled with current-ripple lamination, indicate a decrease in flow velocity over time. Carbonaceous detritus and coal clasts suggests deposition in a terrestrial environment (Wood, 1985, 1989; Leckie et al., 1989; Eberth et al., 1990; Eberth & Hamblin,

1993). Rare mudstone and siltstone drapes separated by thin sands are possible tidal couplets, suggesting tidal influence (Visser, 1980; Nio & Yang, 1991; Dalrymple, 2010). A lack of bioturbation indicates a highly stressful environment, and root traces indicate occasional subaerial exposure. F13 is interpreted as freshwater channels under tidal influence.

F14: Carbonaceous shale, silt and coal

Description

This facies is highly variable, locally consisting of coal, carbonaceous shale, mudstone, silty mudstone, sandy mudstone, siltstone, muddy sandstone, and silty sandstone (Fig. 3.10D, 11). Individual beds are 0.1–1 m thick, forming 0.3–3 m thick packages. Due to varying organic content, color varies from black to brownish-black, brown, dark gray, medium gray, and gray. Dominantly, this facies displays horizontal laminations and massive, organic-rich, structureless bedding. Convolute bedding is abundant, and consists predominantly of mixtures of mudstone, siltstone, and very fine-grained sandstone. Locally, this facies displays current ripples, horizontal planar lamination, wave ripples, and silty and sandy stringers. Local slickensides are observed throughout this facies. Thin (0.3 m) to thick (<2 m) coal beds are common. Coals range from lignitic to bright-banded. Distinct, coalified branches, seeds, leaves and conifer needles are discernible and relatively common. Siderite nodules and layers are sporadically distributed throughout this facies. Bioturbation is predominantly absent (BI 0–1), except for very rare *Teredolites* isp., *Cochlichnus* isp., *Gordia* isp., *Planolites* isp. and root trace fossils.

Interpretation

The predominance of fine-grained sediments, coupled with high amounts of organic material, suggest deposition in a quiet-water, terrestrial setting with frequent subaerial exposure (Colombera et al., 2013; Burns et al., 2017). Sandstones and siltstones displaying current ripples

are attributed to unidirectional flow and indicate periodic high-energy conditions. Rare oscillatory ripples indicate wind activity in open, shallow pools of standing water. *Cochlichnus* isp., *Gordia* isp. and *Planolites* isp. were observed on the bedding plane and within the substrate, respectively. All are indicative of freshwater continental conditions and the *Mermia* Ichnofacies (Buatois & Mángano, 1995). The abundance of soft-sediment deformation is a result of rapid deposition of sediments in a water-saturated substrate, or by degassing of organic-rich sediment due to decaying plant material (Shanmugam, 2017). Rare root trace fossils and slickensides indicate subaerial exposure significant enough to result in pedogenesis of the substrate (Krauss, 1999; Retallack, 2008). The presence of *Teredolites* isp. at the top of some beds, particularly where overlain by F7 and F9, indicates rapid inundation of a terrestrial coastal plain by marine waters (Bromley et al., 1984; Savrda, 1991; Buatois & Mángano, 2011). F14 is interpreted as floodplain, peat-forming mires, swamps, bogs, and/or marshes periodically affected by brackish-water conditions, as indicated by the presence of *Teredolites* isp.

F15: Bentonite

Description

Seams of green-gray to light gray bentonitic-rich mudstones occur in 0.08 to 0.4 m thick layers. These beds can be fissile or massive, with some exhibiting grains of biotite, quartz and feldspar. This facies has sharp lower boundaries, and sharp to gradational upper contacts (Fig. 3.11). Overlying facies locally have bentonitic clasts from these layers incorporated into their base.

Interpretation

The presence of bentonite is attributed to air fallout of ash from volcanic eruptions. During the Late Cretaceous, the Laramide Orogeny was ongoing, and volcanic activity on the west coast is known to have occurred (Price, 1994). These ash layers are undoubtedly a result of that process.

The presence of accumulated ash, wedged between floodplain-related deposits, indicates preservation in sheltered, poorly drained swamps and marshes.

3.4.2 Facies Association Descriptions and Interpretations

Facies association 1: Wave-dominated shallow marine

Facies association 1 (FA1) consists of Facies 1–6, representing suspension fallout and wave and storm deposition controlled by basin slope and relative sea level. Sedimentological and ichnologic evidence indicates that FA1 was deposited in a moderately storm-affected shallow-marine environment (Wesolowski, 2018) subject to longshore currents. FA1 records deposition in a wave-dominated shallow-marine environment ranging from the lower offshore to the upper shoreface. Distal deposits result from low-energy suspension fallout with intermittent silty and very fine-grained sandstone tempestites, with frequency of deposition in relation to proximity of storm-weather wave base. Decreased thickness and abundance of shale and mudstone, combined with the presence of structures indicative of oscillatory flows, such as micro-hummocky, hummocky, and wave-ripple cross-laminated siltstone and sandstone, indicates a landward increase in wave and storm influence due to shallowing. Bioturbation intensity is high (BI 5–6) in offshore deposits, and decreases landward (to a minimum of BI 0–1), reflecting environmental controls on the benthos in high-energy settings, and the difficulty in colonizing shifting sediments (MacEachern et al., 2007). Barrier island sandstones are interpreted as having been deposited by longshore currents, which acted to protect the coastal plain and amplify tides. Shoreface and seaward portions of barrier island and bar complexes are dominated by occurrences of *Ophiomorpha* isp. and *Skolithos* isp., commonly near the top of storm beds. This assemblage is consistent with the *Skolithos* Ichnofacies, associated with shifting, sandy substrates in high-energy environments (Buatois & Mángano, 2011). Bioturbation is pervasive

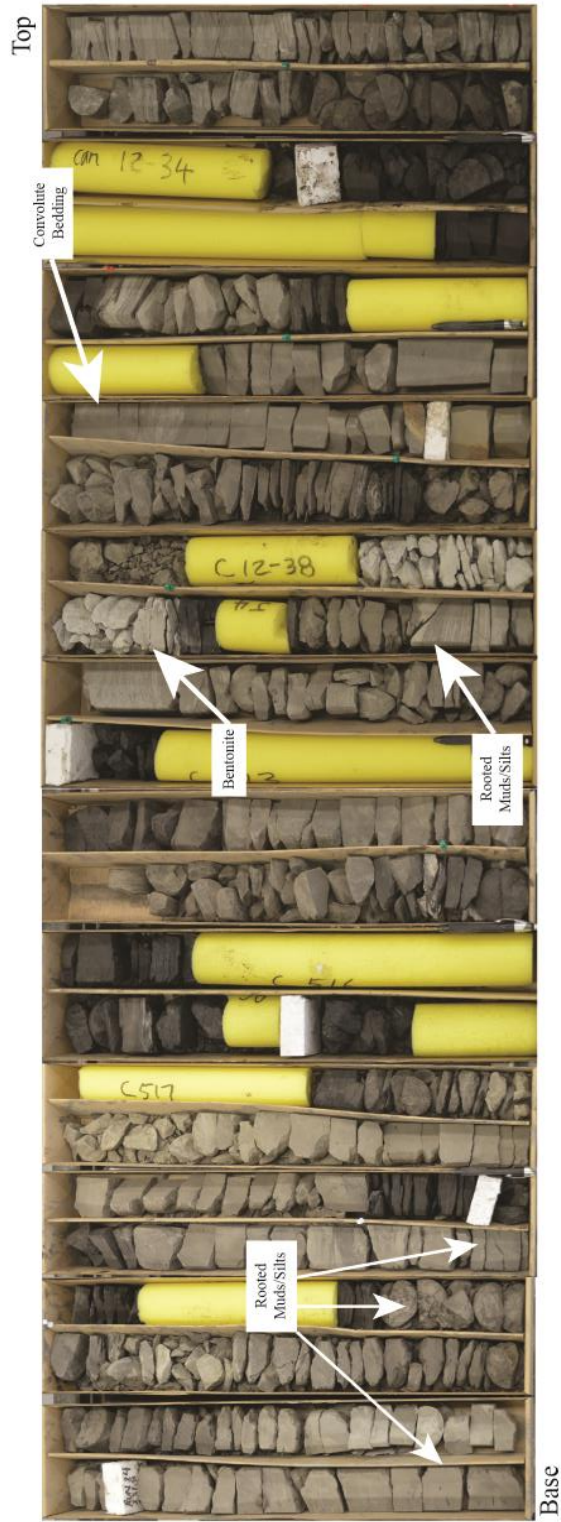


Figure 3.11: Representative photographs of Facies Association 3 (FA3) and Facies Association 4 (FA4) highlighting vertical facies stacking. The base of the Dinosaur Park Formation is often dominated by fluvial sandstone in the Cypress Hills. This is replaced by stacking, lenticular, laterally restricted fine-grained sandstones, grading upwards into laminated siltstones and mudstones. Pedogenically altered mudstones and coal cap these repeating depositional cycles. These are interpreted as representing regional transgression controlled by subsidence. Nexen Battle Creek Core 07-02-004-27W3.

throughout the offshore facies, commonly obliterating primary sedimentary features. This indicates significant colonization windows, allowing for complete reworking of the substrate between storm events. The offshore deposits are dominated by deep-tier trace fossils of the *Zoophycos* and *Cruziana* ichnofacies. This facies assemblage occurs in the BF throughout the entirety of the study area.

Facies association 2: Wave-dominated, tide-influenced, barrier island–lagoon complex

Facies Association 2 (FA2) consists of Facies 7–8, and overlies heterolithic tidally influenced sediments. FA2 is attributed to estuarine and lagoonal basins and barrier-island deposits. The presence of lagoons, barrier islands, and sand bars aligned parallel to the coast indicates that wave energy was the dominant control on coastal morphology, with tides and fluvial processes contributing subordinately (Boyd et al., 1992; Dalrymple et al., 1992; Dalrymple, 2010).

Massive, structureless shale indicates suspension fallout during fair-weather conditions. Barrier islands would have protected lagoon and estuary deposits from all but the most severe of storm-weather conditions. Mudstone with siltstone laminae is interpreted as resulting from washover during storm conditions. The appearance of localized *Chondrites* isp. suggests that lagoon and estuary waters periodically underwent episodes of low dissolved oxygen content. *Macaronichnus* is commonly present in nearshore and barrier-island environments (Coates, 2002; Pemberton et al., 2001; Quiroz et al., 2010; Uchman et al., 2016). Coal and root trace fossils at the top of these sandstones indicate subaerial exposure long enough to promote the growth of significant plants along the tops of the bars. This facies association is interpreted as having formed in wave-dominated, tidally influenced estuary basins, lagoons and barrier-island bars. This facies association occurs in the DPF, and was mapped in the subsurface with an isopach map constructed of the total thickness (Fig. 3.12).

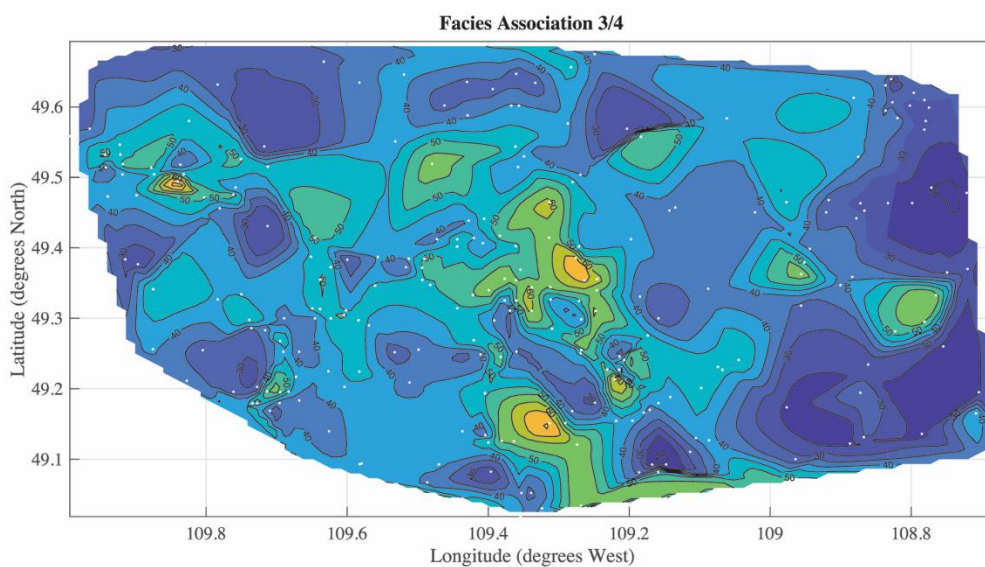
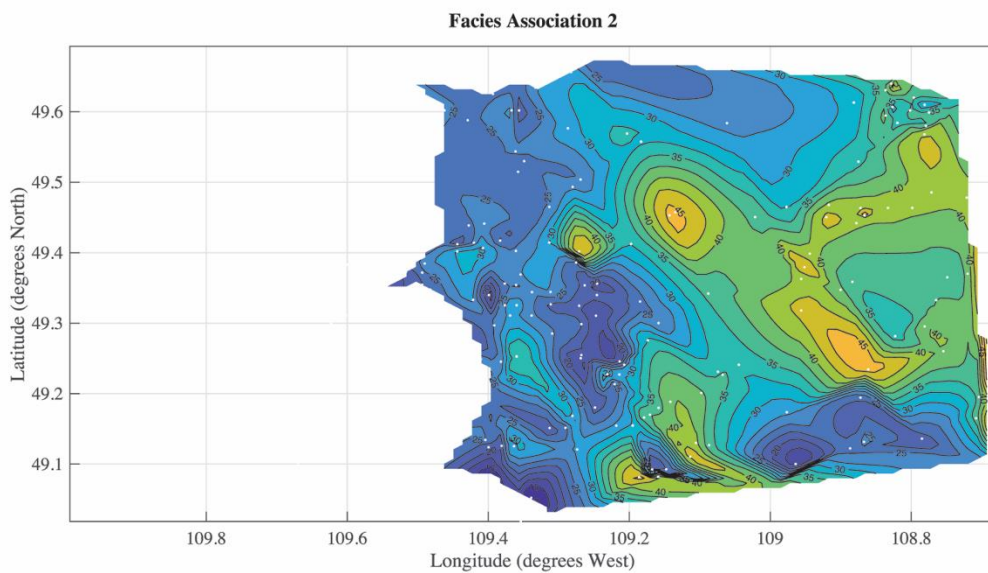


Figure 3.12: Isopach maps based on well log picks of the different facies associations found within the Dinosaur Park - Bearpaw Formation transition. FA3/4 was mapped together due to the complexity of differentiating the two facies associations in well logs. Contour interval is x m; darkest blue indicates thinnest strata.

Facies association 3: Wave-dominated, tide-influenced, fluvial-affected marginal marine

Facies association 3 (FA3) consists of Facies 9–10, and is characterized by fining-upward successions of structureless, current-rippled, and/or cross-bedded sandstone, followed by organic-rich, upward-fining, inclined silty and muddy heterolithic deposits. This is interpreted as reflecting deposition in laterally migrating estuarine and intertidal channels. Syneresis cracks, current-ripple cross-lamination with mudstone drapes, and a brackish-water trace-fossil assemblage (the so-called depauperate mixed *Skolithos* and *Cruziana* ichnofacies) indicate admixing of fresh and saline waters. Bioturbation was intermittent and dominated by diminutive trace fossils. Facies 9 is occasionally overlain by F10. The scarcity of F10 suggests that fluvial input to the coast was a tertiary influence to coastline morphology, with tides and waves playing a more active role. This facies association is interpreted as recording deposition in wave-dominated, tidally influenced fluvio-estuarine settings, encompassing tidal flats adjacent to estuary basins, lagoons, and barrier islands. Wave energy is reduced in this facies association due to protection of the coast by barrier island–sandbar complexes farther basinwards. Inclined heterolithic deposits are interpreted as representing laterally migrating point bars within channel fills (Thomas et al., 1987). Muddy heterolithic, tidally influenced sediments were deposited as broad, shallow-marine lagoons, tidal flats, and small estuary complexes. This association is characterized by organic-rich heterolithic deposits, fine-grained sandstone with mudstone drapes, wave-reworked asymmetrical ripples, and a brackish-water ichnofauna. Microtidal influence is observed in all outcrop and core in the Cypress Hills region near the top of the DPF.

Facies association 4: Coastal plain

Facies association 4 (FA4), consisting of F11–15, is characterized by fine-grained, high-organic-content deposits, displaying significant lithological variability. Siltstone, mudstone, and shale

alternate with thick- to thin-bedded, bright-banded to lignitic coal layers. Pedogenesis is common in this association, and gleysol root development can be observed throughout several of the facies. Interbedded heterolithic sediments, horizontal lamination, convolute lamination and units of massive appearance are pervasive. Trace fossils are exceptionally rare, comprising simple vertical (*Skolithos* isp.) and horizontal (e.g., *Planolites* isp.) burrows, as well as simple grazing trails (e.g., *Mermia carickensis*, *Cochlichnus anguineus*, *Gordia marina*), the latter suite illustrating the *Mermia* Ichnofacies. The presence of this ichnofacies suggests the establishment in the coastal plain of freshwater bodies. Rare mudstone drapes in fluvial sandstone indicates a low-gradient coast where even a small tidal range impacted a large area. Rare fine- and very fine-grained sandstone laminae, stringers, and convolute lamination indicate periodic sediment influx resulting from crevasse-splay deposition (Elliot, 1986). Splay deposits are commonly formed when levees are breached during flooding. Splays are common components of meandering stream environments, which commonly occur in areas with low gradients (Slingerland & Smith, 2004; Miall, 2010, 2013). The prevalence of mud, silt, and organic detritus in this facies association indicates deposition in a low-energy environment with significant surrounding plant growth. Large volumes of sediments were periodically deposited in overbank flooding events (Miall, 2013). Widespread peatmires, bogs, marshes and swamps developed into 0.1–3.3 m thick coal layers, which extend throughout the Cypress Hills region into Alberta and Montana (Frank, 2006). The extent of the coalbeds indicates deposition in a low-lying, low-gradient environment. One of these coal seams immediately underlying lagoon deposits contains a monospecific suite of the bivalve boring *Teredolites*, representing the *Homonymous* Ichnofacies (Bromley et al., 1984). This boring is also present in associated wood fragments near the DPF-BF transition. The presence of *Teredolites* indicates times of marine

influence. Siderite layers and nodules are a common feature in waterlogged soils (Retallack, 2008). The vegetation responsible for the coal beds most likely developed during periods of aggradation during 5th order sea-level rise. Subaerial exposure long enough to permit soil development is indicated by gleying, root development, slickensides, and mottling. An isopach map was constructed to illustrate total thickness of FA3/4. These facies associations were combined due to similarities in well-log signatures (Fig. 3.12). FA4 occurs in the DPF.

3.4.3 Ichnofabric Characterization

Chondrites ichnofabric

Description

This ichnofabric is dominated by deep-tier *Chondrites* isp. in mudstone and shale of Facies 1–2.

Chondrites isp. commonly reworks mid- and shallow-tier burrows, such as *Planolites* isp., *Rhizocorallium* isp., and *Asterosoma* isp. Occasionally, discrete, well-defined *Phycosiphon incertum*, *Nereites missouriensis*, and *Zoophycos* isp. are observed. Reworking of the sediment is extremely high (BI 5–6), commonly obscuring all identifiable ichnotaxa within the host facies.

Interpretation

The dominance of deep-tier ichnogenera is attributed to steady background sedimentation in a shelf environment below storm-weather wave base. *Chondrites* is indicative of climax ecological conditions (Bromley, 2012). Steady sedimentation resulted in vertical migration of deep-tier organisms and subsequent reworking and overprinting of shallower trace fossils. Other deep-tier trace fossils, such as *Zoophycos* isp., were preserved with little to no reworking. This is attributed to the fact that the producers of *Zoophycos* isp. occupy deep tiers together with those that produce *Chondrites*, therefore increasing their preservation potential. This ichnofabric indicates long, stable windows of colonization with little environmental disturbance.

Chondrites - Planolites ichnofabric

Description

This ichnofabric is dominated by the deep-tier trace fossil *Chondrites* isp. and the shallow-tier trace fossil *Planolites* isp. in Facies 7. *Planolites* isp. occurs sporadically throughout this facies, but do not always co-occur with *Chondrites* isp. The *Chondrites-Planolites* ichnofabric is present in moderately bioturbated deposits (BI = 3) that alternate with unbioturbated deposits (BI = 0).

Interpretation

Localized horizons with *Chondrites* isp. and *Planolites* isp. indicate periods of lagoon anoxia and/or euxinia. Monospecific occurrences of *Chondrites* isp. are typical of poorly oxygenated environments and the trace maker(s) is believed to be able to live in euxinic to anoxic sediments as a chemosymbiont (Seilacher, 1990; Bhattacharya & Banerjee, 2014). Very low ichnodiversity, coupled with opportunistic deep-tier chemosymbionts, suggests a highly stressful environment and, potentially, short colonization windows.

Asterosoma ichnofabric

Description

The *Asterosoma* ichnofabric is moderately diverse and records a moderate to high bioturbation index (BI 3–6). This ichnofabric is present in mudstone and silty mudstone of Facies 3–5.

Deposits containing this ichnofabric exhibit varying degrees of bioturbation within and between beds. A mid- to deep-tier assemblage of *Asterosoma* isp., *Chondrites* isp., and *Thalassinoides* isp. overprints shallower-tier ichnotaxa, such as *Rhizocorallium* isp., *Diplocraterion* isp., *Skolithos* isp., and *Rosselia* isp.

Interpretation

The *Asterosoma* ichnofabric characterizes the various offshore deposits identified. A variety of vertical and horizontal forms reflect detritus and suspension feeding organisms, indicating a variety of trophic types in this environment. Typical intense bioturbation indicates open colonization windows during fair-weather conditions.

Ophiomorpha ichnofabric

Description

This ichnofabric occurs in fine-grained sandstone deposits of Facies 5, displays low diversity, and is present in deposits characterized by low bioturbation index (BI 0–1). Trace fossils identified in this ichnofabric include *Ophiomorpha* isp., *Arenicolites* isp., and *Skolithos* isp. Smaller trace fossils, such as *Arenicolites* isp. and *Skolithos* isp., are typically found at the top of hummocky bedded sandstone. *Ophiomorpha* isp. represents a deep-tier, actively constructed and maintained burrow, commonly crossing into underlying beds and bedsets.

Interpretation

This ichnofabric represents well-oxygenated, high-energy environments, with shifting, sandy substrate (Pollard et al., 1993; Bromley, 1996). Producers of *Arenicolites* isp. and *Skolithos* isp. are commonly attributed to suspension feeding organisms favoring high-energy environments (Pemberton et al., 1992). *Ophiomorpha* is regarded as a dwelling trace produced by callianassids, who reinforce their burrow walls in unstable substrates with fecal pellets (Frey et al., 1978).

Macaronichnus ichnofabric

Description

Bioturbation in trough cross-bedded marine sandstone of Facies 6 is represented by monospecific occurrences of deep-tier *Macaronichnus* isp. The *Macaronichnus* ichnofabric is present in deposits with alternating degrees of bioturbation (BI 1–3). This ichnotaxon consists of irregular, sinuous, unbranched burrows with a light core and thin mantle.

Interpretation

Macaronichnus isp. is representative of vagile, deposit-feeding or epigranular-feeding polychaetes associated with high-energy environments close to shore (Coates, 2002; Pemberton et al., 2001; Quiroz et al., 2010; Uchman et al., 2016). The producers were able to thrive in conditions of high energy, effectively colonizing shifting two- and three-dimensional dunes. These organisms would have to cope with high sedimentation rates, shifting substrate, and episodic storm events. Complete or nearly-complete reworking of sandstone is punctuated by episodes of no bioturbation.

Teichichnus ichnofabric

Description

This ichnofabric is present in the heterolithic deposits of Facies 7. It is dominated by mid-tier *Teichichnus rectus* and *Planolites* isp., and occasional mid- to shallow-tier *Asterosoma* isp., *Cylindrichnus concentricus*, *Palaeophycus* isp., *Protovirgularia* isp., *Thalassinoides* isp., and *Skolithos* isp. Degree of bioturbation and ichnodiversity vary. Bioturbation index ranges from 0 to 3. Trace fossils are of small size and depauperate, with mid- to shallow-tier forms, such as *Asterosoma* isp., *Cylindrichnus concentricus* and *Palaeophycus* isp., preferentially occurring at the tops of silty and sandy beds. Both *Teichichnus rectus* and *Planolites* isp. occur throughout Facies 7, with no discernible preference for beds or sediment types, whereas the other trace fossils show a preference for tide- and wave-reworked siltstone and sandstone units.

Interpretation

This ichnofabric records sporadic colonization in tidally affected heterolithic deposits. Characteristics of this ichnofabric are consistent with colonization by deposit feeders in a marginal-marine environment experiencing variation in turbidity, temperature, salinity, and oxygen (Croghan & Funnell, 1983; MacEachern & Pemberton, 1994; MacEachern & Gingras, 2007).

3.5 Discussion

3.5.1 Trace Fossil Distribution

Trace-fossil diversity and bioturbation intensity vary considerably between the different facies associations (Table 3). Fully marine deposits of FA1 show high to moderate bioturbation intensity and include the most diverse trace-fossil assemblage. Collectively, these assemblages illustrate the *Zoophycos*, *Cruziana*, and *Skolithos* ichnofacies. These associations are dominated by trace fossils of deposit- and suspension-feeding organisms in fully marine environments (Frey & Pemberton, 1984; Pemberton et al., 2001). Identification of discrete ichnotaxa was often obscured by complete or near-complete reworking of the sediment, indicating a significant colonization window (Bromley, 1996). Ichnotaxa identified landward of the barrier island sandstones were smaller than their marine counterparts, a reflection of size reduction in marine fauna experiencing stressful environmental conditions (Pemberton et al., 1982; MacEachern & Pemberton, 1992; Buatois & Mángano, 2011).

FA2 displays low ichnodiversity with sporadic and opportunistic colonization. The appearance of localized *Chondrites* isp. is interpreted as periods of anoxia within the lagoon. *Chondrites* isp. is most commonly found in poorly oxygenated shelf environments, where the trace producers can live in anoxic sediments as a chemosymbiont (Seilacher, 1990; Bhattacharya

& Banerjee, 2014). In modern lagoon environments, anoxia can occur during times of high environmental temperatures, increased organic content, and low water turbidity (Cioffi et al., 1995; Harzallah & Chapelle, 2002). Euxinia can develop when anoxia is coupled with the presence of organic matter, sulfate ions, and sulfur-reducing bacteria, and is a common phenomenon in restricted saltwater bodies, such as barrier island–lagoon complexes, where there is a source of freshwater input from rivers and streams (Nägler et al., 2011). This would suggest the producer of *Chondrites* isp. is an opportunistic colonizer in this facies association, favoring restricted saltwater environments during times of low dissolved oxygen content. *Planolites* isp. occurs throughout F7 and is likely related to more stable conditions.

Facies association 3 exhibits moderate to low ichnodiversity and sporadic, irregular bioturbation, illustrating a depauperate mixed *Skolithos* and *Cruziana* ichnofacies. Ichnotaxa recognized in this assemblage are characteristic of the brackish-water trace-fossil assemblage, which exhibits: 1) small size, 2) reduced diversity, 3) infaunal habit, 4) monospecific assemblages, 5) mixture of *Skolithos* and *Cruziana* ichnofacies, and 6) trophic generalists (Wightman et al., 1987; Pemberton & Wightman, 1992; MacEachern & Pemberton, 1994; Gingras et al., 1999; Buatois & Mángano, 2003). Trace fossils present in this facies association are consistent with a marginal-marine environment experiencing variation in turbidity, temperature, salinity, and oxygen (Pemberton et al., 1982; Croghan & Funnell, 1983; Pemberton & Wightman, 1992; Lettley, 2004; MacEachern & Pemberton, 1994; Lettley et al., 2009).

Coastal plain deposits of FA4 are nearly void of identifiable trace fossils. The localized presence of elements of the *Mermia* Ichnofacies provides evidence of freshwater conditions in some of the coastal plain water bodies. Root trace fossils are relatively abundant and indicate water-saturated soils with a high water table at the time of deposition (Retallack, 2008). The

Teredolites Ichnofacies, as well as the presence of this boring in wood logs, provides evidence of times of marine influence.

3.5.2 Ichnodiversity and Bioturbation Intensity of Epicontinental Seaways

The Western Interior Seaway represents a shallow, epicontinental seaway where regional sea level was controlled by cordilleran tectonics to the west. Studies on modern infaunal communities have indicated consolidation of the substrate, organic matter, and oxygen content as some of the main limiting factors burrowing organisms must overcome in marine settings (Bromley, 1996). Upper Campanian deposits in Saskatchewan host trace-fossil assemblages dominated by mid- and deep-tier ichnotaxa. This dominance reflects a preservational bias, as shallower-tier trace fossils have been reworked and overprinted by deeply emplaced burrows. Bioturbation intensity is highest in the shelf and offshore facies, so much that discrete ichnogenera are often difficult to identify. Obliteration of shallower tiers indicates prolonged colonization windows with background sedimentation dominating below storm wave base. Above storm wave base, deposition of tempestites can cause erosion of shallow tiers, particularly in the upper offshore. Above fair-weather wave base, simple ichnofabrics dominate, and consist of low-diversity suites preserved in deposits showing low bioturbation intensities. Erosion and rapid deposition in these environments either prevent bioturbation, or remove shallower tiers to obliterate evidence of colonization. *Macaronichnus* isp. was identified in both barrier sandbars and upper shoreface deposits, associated with high-energy migrating dunes. Colonization is sporadic, but high bioturbation intensity is locally observed. This suggests single-tier colonization and short-term colonization windows (Pearson et al., 2013).

Ichnodiversity decreases landward, with marginal-marine deposits hosting sporadically bioturbated fabrics and continental facies hosting few identifiable ichnogenera. Central basin and

lagoonal deposits are sparsely bioturbated, commonly consisting of monospecific occurrences of *Planolites* isp. and *Chondrites* isp. This is attributed to low water circulation and fluctuating temperature and water salinity. Tidally influenced heterolithic deposits are sporadically bioturbated and display simple ichnofabrics, suggesting sporadic colonization due to fluctuations in salinity, turbidity, and sedimentation. Continental trace fossils are rare, and consist predominantly of *Planolites* isp., *Skolithos* isp., and root traces, with rare *Cochlichnus anguineus*, *Gordia marina* and *Mermia carickensis* occurring locally.

Previous studies have indicated the Western Interior Seaway in Saskatchewan underwent episodic anoxic bottom-water conditions at times (Schröder-Adams et al., 2001). Studies on foraminiferal plankton from the Cenomanian to Campanian of eastern Saskatchewan indicate the water column was stratified, with anoxic bottom-water conditions reaching the photic zone (Schröder-Adams et al., 2001). Water stratification of this magnitude would likely be caused by influx of freshwater to the basin, and was likely perpetuated by freshwater runoff and fluvial discharge. Evidence from southwestern Saskatchewan suggests these conditions existed in other parts of the basin, as both shelf and lagoon deposits contain monospecific or near-monospecific occurrences of *Chondrites* isp. These conditions were evidently episodic, as monospecific occurrences are punctuated by the appearance of more diverse trace fossil assemblages indicative of well-oxygenated conditions. Ichnologic evidence illustrates that anoxic pulses extended to southwestern Saskatchewan. Further investigation of trace-fossil assemblages from the BF would be of significant value for understanding epeiric seaway anoxia and euxinia.

3.5.3 Depositional Processes and Paleoenvironments

Marginal systems are highly complex, as they are influenced by several processes related to both fluvial and marine effects (Boyd et al; 1992; Dalrymple et al., 1992; Bhattacharya & Giosan,

2003; Dashtgard et al., 2009; Ainsworth et al., 2011). The integration of facies analysis, stratigraphy and ichnology provides a more robust understanding of the region than simply employing facies analysis alone. Where ichnofossils are present, trace fossil analysis offers a valuable tool for identifying subtle changes in depositional systems not otherwise readily deduced (Pemberton et al., 1992; Buatois & Mángano, 2011).

This succession exhibits well-preserved sedimentary structures, allowing assignment of dominant depositional processes during sedimentation. Estimated percentages of sedimentary structures generated by each process have been calculated for the DPF-BP transition, and the results shown in ternary plots (Fig. 3.13). The relative proportions of wave-, tide-, and fluvial-generated structures are 60%, 27%, and 13%, respectively, indicating a wave-dominated, tide-influenced, and fluvially affected depositional system (Fig. 3.13).

Though wave-dominated, tide-influenced, fluvially affected systems have been rarely documented in the literature, they are quite common in modern coastal environments (Vakarelov et al., 2012). In modern environments, these systems are associated with wide, shallow continental shelves (Vakarelov et al., 2012). This is consistent with the morphology of the Western Interior Seaway, as true abyssal conditions were largely absent at the time of deposition. A similar study investigated deposits in Alberta representative of the subsequent regression of the Bearpaw Formation, and its replacement with the marginal-marine to coastal-plain Horseshoe Canyon Formation (Vakarelov et al., 2012). In that study, the Bearpaw - Horseshoe Canyon transition was identified as wave-dominated and tidally influenced, with minor fluvial input (Vakarelov et al., 2012).

Though the DPF-BP transition overall adheres to the example provided by Vakarelov et al. (2012), the study area deviates from the model via the presence of widespread barrier-island

sandbars. This is likely due to significant regional storm activity coupled with coastline morphology. Barrier islands can be formed by a number of mechanisms, with sediment supply, the nature of transport, coastal profile, tidal range, wave conditions, and relative changes in sea level being important factors (Hayes et al., 2005). In the Holocene, barrier islands have generally been produced by transgression and the subsequent reworking of pre-existing sand deposits, and are known to expand during storm surges (Hayes et al., 2005). Given that the Bearpaw - Horseshoe Canyon formation transition is regressive, it is reasonable to assume that this process is the cause of the coastline difference. At the time of deposition, the Sweetgrass Arch to the west and the Bowdoin Dome to the east were relatively prevalent topographic features (Kent and Christopher, 1994). These features may have exacerbated regional shoreline tide and longshore current effects by funneling waters in a north-south direction.

3.5.4 Redefining the Dinosaur Park - Bearpaw Formation Contact

There has been no consistent constraint on the subsurface criteria used to pick the bounding surfaces of the Dinosaur Park Formation in Saskatchewan. This is in part due to 1) the interdigitating, diachronous nature of the contacts; and 2) the DPF has previously not been formally recognized in Saskatchewan. Frank (2006) considered tongues of sandstone less than 20 meters above the main Belly River sequence as part of the BRG. Any tongue that contained coal was automatically considered part of the BRG. In this study, a consistent gamma ray-density-resistivity signature was identified that correlated with FA2 (Figure 3.14). The upper contact of

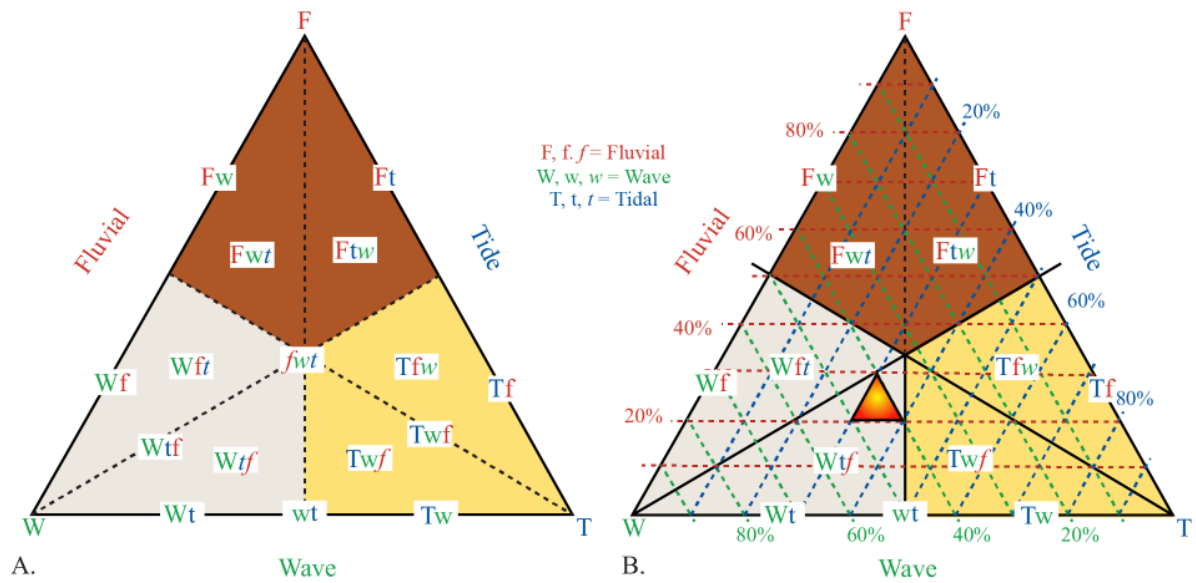


Figure 3.13: Conceptual ternary plots of wave, tide, and fluvial depositional environments (modified from Ainsworth et al., 2011). Figure **13A** illustrates the full classification with nomenclature reflecting the dominant processes from left to right. **B.** Simplified classification with environment plotted in red and yellow triangle. The red and yellow triangle indicates where the DPF-BP shoreline plots on the diagram, and suggests wave-dominated, tide-influenced, fluvial-affected processes (Wtf). For more detailed information regarding the nomenclature and abbreviations, see Ainsworth et al. (2011).

the Belly River Group/Dinosaur Park Formation correlates with the upper boundary of FA2 (Appendix A and B). Where FA2 is not present west of range 28W3, the uppermost heterolithic and coal-bearing beds identifiable in both outcrop and subsurface logs of FA3 and 4 are used to pick the top of the BRG.

3.5.5 Stratigraphic Correlations and Depositional Evolution

Correlations were focused on major bounding surfaces due to significant spacing between cored intervals, available outcrop, and adjacent wells. Despite the limitations, subsurface correlations were made to establish regional geometry and lateral extension of the different facies associations in the study area (Fig. 3.14, 15). This study relied heavily on the gamma-density-resistivity suite of logs to make broad facies association picks. The Milk River Shoulder (MRS) was chosen as the datum, which is consistent with other studies focusing on the Belly River Group (Eberth & Hamblin, 1993; Power & Walker, 1996; Hamblin, 1997; Hamblin & Abrahamson, 1996). The MRS has a distinct signature on both gamma-ray and resistivity logs, and is laterally continuous across the entire study area.

Cross-section B-B' is oriented in a down-dip direction and runs west to east through township 4 (Fig. 3.14). The base of the Dinosaur Park Formation is characterized by FA4, which exhibits low radioactivity in well logs and consists of trough cross-bedded and current-rippled fine-grained sandstone in outcrop and core. These deposits are interpreted as tidally influenced meandering fluvio-estuarine fill, and form progradational stacking patterns. Both adjacent to and overlying the fluvio-estuarine sandstones, fine-grained floodplain deposits containing abundant coal seams, carbonaceous mudstones, siltstones and sandstones are ubiquitous throughout the study area. Like the underlying sandstones, this unit thins and progrades to the east, before backstepping westward towards the Alberta–Saskatchewan border. This is consistent with the

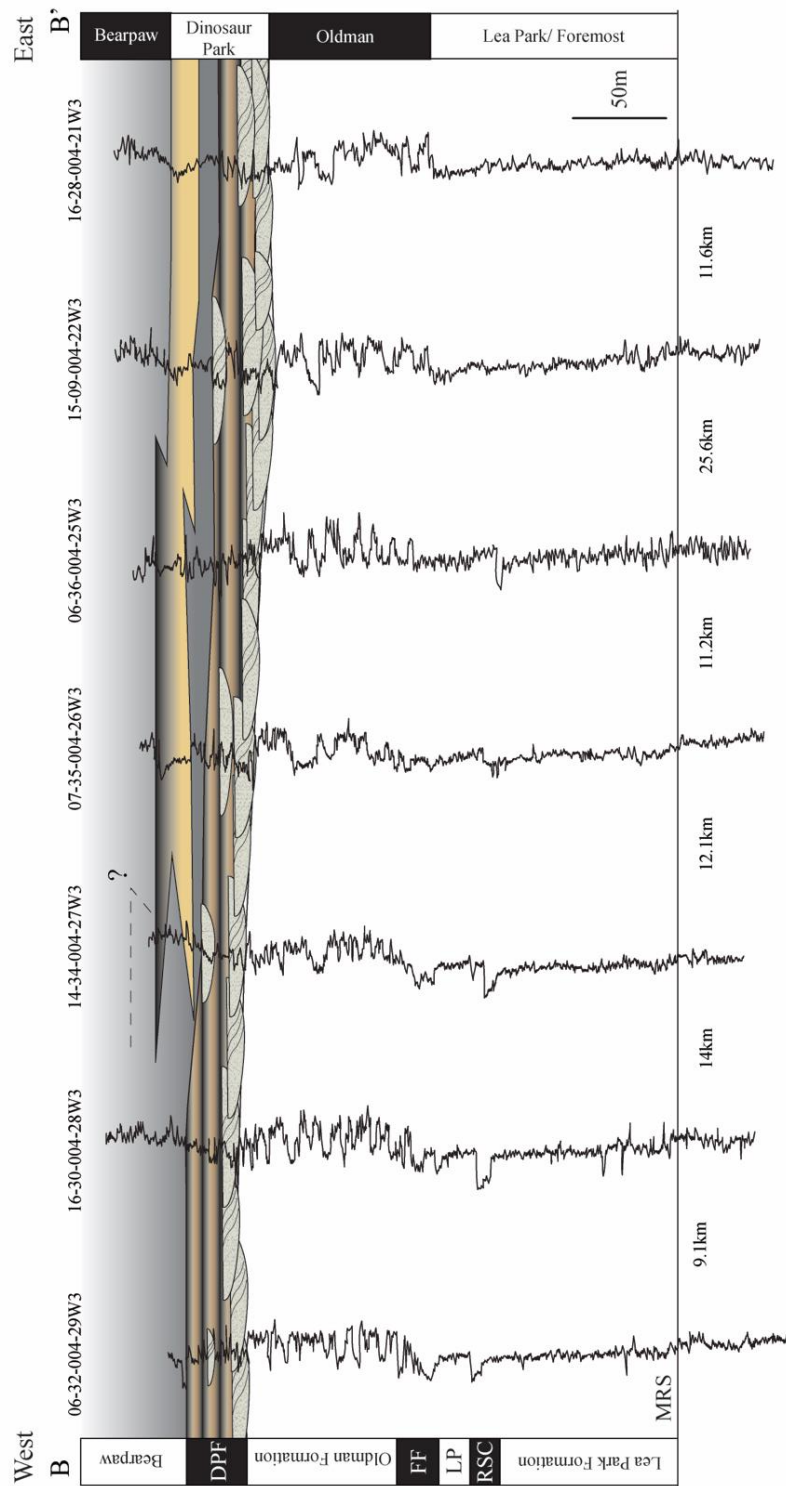


Figure 3.14: Cross-section B-B' represents a dip-oriented transect through township 4. Coastal plain facies of the Dinosaur Park Formation are replaced by backstepping packages of FA2 and 3. Marine shales and mudstones of the Bearpaw Formation ubiquitously overlie the Dinosaur Park Formation in the region.

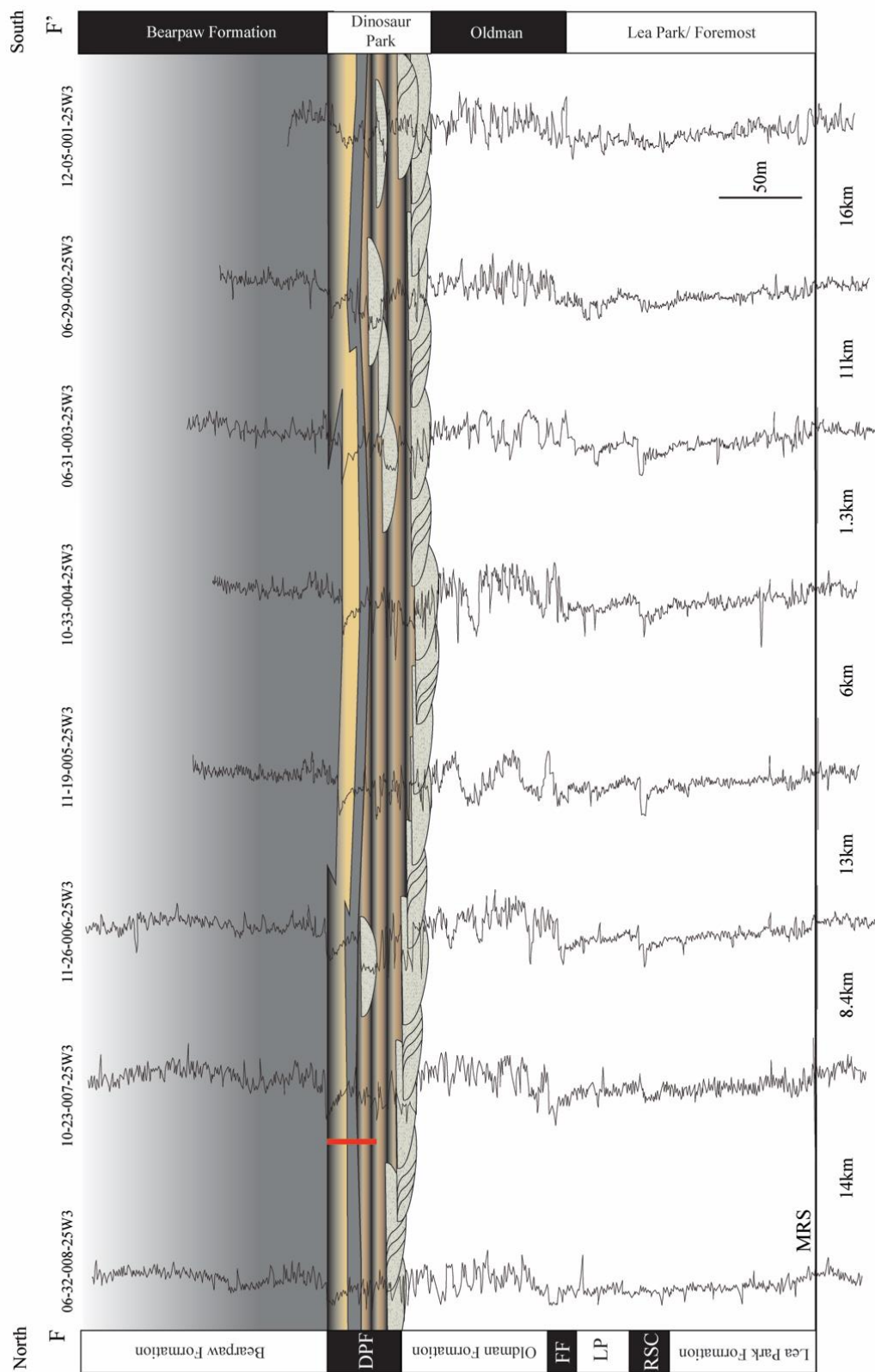


Figure 3.15: Cross-section F-F' represents a strike-oriented transect through range 25W3. Coastal plain facies of the Dinosaur Park Formation are replaced by backstepping packages of FA2 and 3. Marine shales and mudstones of the Bearpaw Formation ubiquitously overlie the Dinosaur Park Formation in the region.

inner incised valley (segment 3) of Zaitlin et al. (1994). Wedge backstepping and thick coal seams in the coastal plain are interpreted as signaling the onset of marine transgression.

Marginal-marine facies of FA2 and 3 cap coastal plain deposits of FA4, forming a retrogradational backstepping stacking pattern. Sporadically bioturbated interstratified sandstone, siltstone, mudstone and claystone pass upwards into sparsely bioturbated shales and mudstones characteristic of estuaries and lagoons. This corresponds to middle incised valley-fill (segment 2), and represents transgressive estuarine and lagoon facies (Zaitlin et al., 1994). Backstepping barrier island sandstones of FA2 pass upward into shoreface sandstones and thick packages of wave-dominated, open-marine deposits of FA1, signaling the marine extent of segment 1 (Zaitlin et al., 1994). Transgression of the Bearpaw Sea continued across the Western Interior, reaching its maximum geographic extent in Alberta. Final regression of the seaway is signaled by progradation of terrestrial clastics from Alberta into Saskatchewan during the Maastrichtian (Eberth and Braman, 2012). The disappearance of FA2 west of ranges 27 and 28W3 indicates the Western Interior Seaway transgressed across the coastal plain in short amounts of time. This suggests episodic flooding of large sections of the coast, likely due to tectonic controls in the Canadian Cordillera.

Cross-section F-F' (Fig. 3.15) runs parallel to strike, and is oriented north to south through range 25W3. Transgression is illustrated by the replacement of sandstones, siltstones, mudstones, and coal seams with deepening-upwards, retrogradational packages of tidally influenced heterolithic sediments, sparsely bioturbated shales and mudstones, capped by barrier-island sandstones. Both cross-sections illustrate deposition consistent with transgression of a mixed wave-dominated, tidally influenced, river-affected shoreline.

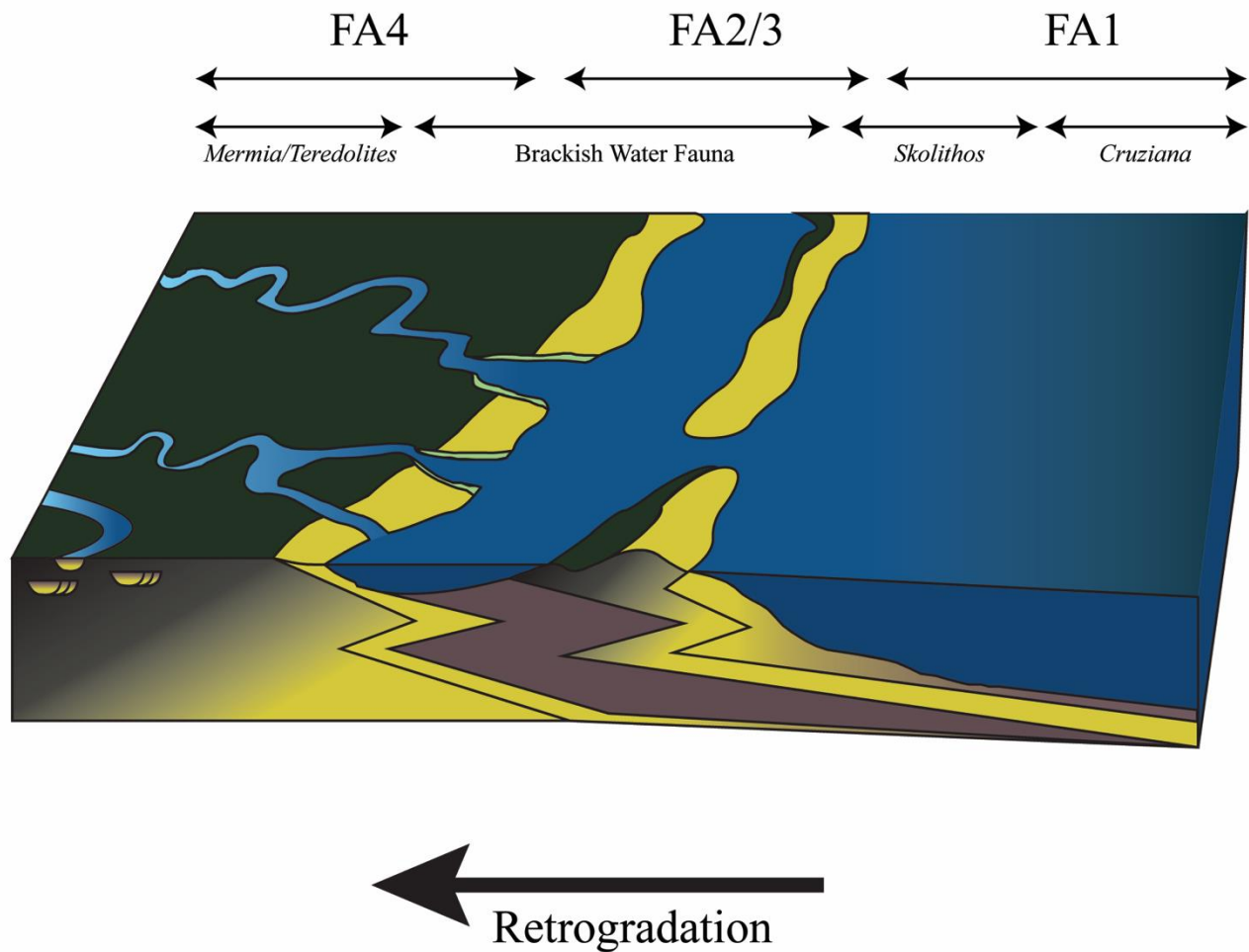


Figure 3.16: Paleoenvironmental diagram of the Dinosaur Park - Bearpaw Formation transition in the Cypress Hills region of southwestern Saskatchewan, Canada. FA1 - Facies association 1: Wave-dominated shallow marine; FA2 - Facies association 2: Wave-dominated, tide-influenced, marginal-marine deposits; FA3 - Facies association 3: Coastal plain deposits.

3.6 Conclusions

- 1) Detailed facies analysis reveals the Dinosaur Park - Bearpaw Formation contact in southwestern Saskatchewan as the base of a transgressive, barrier island–estuarine complex (Fig. 3.16). The morphology of the coastline was largely controlled by storm surges and wave action, and influenced by mesotidal effects. Though meandering fluvial channels were active at the time of deposition, fluvial processes had subordinate control on sedimentation and shoreline morphology.
- 2) Facies analysis and distribution and ichnology of trace fossils have been integrated to provide context to the depositional history of the region. The fining-upward succession of the facies reveals: 1) wave and storm reworking in shallow-marine environments; 2) tidal influence indicated by the amalgamated nature of the upper and lower shoreface, and heterolithic deposits along lagoons and estuaries; 3) subordinate fluvial control on sedimentation; 4) fluvial channels themselves were heavily influenced by tidal processes, as evidenced by inclined heterolithic stratification and mudstone drapes in fluvial facies most distal from the coastline. This system fits within the wave-dominated, tidally influenced facies model of Ainsworth et al. (2011), departing only with the presence of barrier-island sandstones along the shore.
- 3) Integration of ichnofacies and ichnofabrics has suggested that the Western Interior Seaway underwent episodic, regional anoxia/euxinia in nearshore, restricted environments.
- 4) Along-strike and down-dip subsurface well-log correlations provide a regional picture of depositional geometry during transgression of the Western Interior Seaway, resulting in proposal of a modern depositional model. This model is of utility for understanding

depositional history of these deposits in the Montana and Alberta extensions of these formations. It also provides an explanation for isolated, 'stacked shoreface' deposits known throughout Alberta and Saskatchewan in the lower Bearpaw Formation.

Funding and Acknowledgements

Funding was provided by the University of Saskatchewan. Special thanks to Zoe Vestrum, who assisted with isopachs created in MATLAB, and Emily Bamforth for many discussions concerning this topic both in and out of the field. MMG also wishes to thank the Saskatchewan Geological Survey, particularly Richard Wood, for help with finding available core and providing core tables. Thank you to Alfred Uchman and Renata Netto for their thoughtful comments in reviewing this manuscript.

Well Name	Location	Depths Cored
Nexen Battle Creek	W 111/07-02-04-27W3	185 – 243 m
Renaissance Senate	W 101/10-10-02-27W3	219 – 235 and 241 – 248 m
Nexen Vidora	W 111/06-04-05-25W3	225 – 280 m
Canadian Landmaster Cypress Hills	W 141/06-31-06-25W3	330 – 372 m
Renaissance Vidora	W 111/02-15-04-26W3	237 – 246 m
Canadian Landmaster Belanger	W141/10-23-07-25W3	385 – 415 m

Table 3.1: Summary of core logged for this study. Location is provided according to township and range, a standard of the oil and gas industry. Depths cored is what was logged for the purpose of this study.

Lithofacies Association	Lithofacies	Lithology, Sedimentary Structures and Body Fossil Content	Trace fossils	BI	Sedimentary Processes and Depositional Conditions	Sedimentary Environment
Bearpaw Formation FA 1: Wave-dominated shallow marine	FI Shale	Fissile, thinly parallel-laminated, brown to grey shale. Sandy and/or silty stringers, and in situ marine bivalves. Thickness ranges from <1m to 5.2m.	<i>Chondrites</i> isp., <i>Phycosiphon incertum</i> , <i>Planolites</i> isp., <i>Zoophycos</i> isp.	4-6	Low energy suspension fallout below storm wave base.	Shelf
	F2 Mudstone and interbedded siltstone	Brown to dark grey shale and mudstone with interbedded siltstone and rare very fine-grained sandstone laminae. Symmetrical ripples, carbonaceous laminae, shell debris and in situ bivalves are preserved throughout. Siltstone and sandstone laminae are 0.5 to 5.2 cm thick. This facies ranges in thickness from <2 to 4.5 m thick.	<i>Asterosoma</i> isp., <i>Chondrites</i> isp., <i>Nereites missouriensis</i> , <i>Planolites</i> isp., <i>Rhizocorallium</i> isp., <i>Zoophycos</i> isp.	2-5	Low energy suspension fallout punctuated by storms right above storm wave base.	Lower Offshore
	F3 Bioturbated muddy and sandy siltstone	Fine-grained, light grey, alternating muddy and sandy siltstone. Rare micro-hummocky and symmetrical ripples, interstitial mudstone layers (>1-2.8 cm) and carbonaceous drapes. Bed thickness ranges from <1m to 2.5m.	<i>Asterosoma</i> isp., <i>Chondrites</i> isp., <i>Diplocraterion</i> isp., <i>Nereites missouriensis</i> , <i>Planolites</i> isp., <i>Rhizocorallium</i> isp., <i>Rosselia</i> isp.	3-5	Shallow marine, wave dominated environment between fair weather and storm weather wave base.	Upper Offshore
	F4 Fine-grained sandstone and siltstone	Very fine- to fine-grained light grey sandstone and siltstone. Where discernible, beds are erosive based, and preserve low angle lamination and wave ripples ranging in thickness from 0.5-8 cm. Commonly, beds are heavily bioturbated at the top, with sedimentary structures discernible at the base of beds. Rare marine bivalve debris throughout. Mudstones ranging in thickness from 1.1-3.6 cm occur as discrete layers and drapes, but are rare.	<i>Asterosoma</i> isp., <i>Chondrites</i> isp., <i>Diplocraterion</i> isp., <i>Planolites</i> isp., <i>Rhizocorallium</i> isp., <i>Skolithos</i> isp., <i>Thalassinoides</i> isp.	2-6	Shallow marine, wave dominated environment periodically affected by storms. Erosive sands are interpreted as tempestites, with siltstone deposited under fair-weather conditions.	Offshore Transition
	F5 Amalgamated hummocky cross-stratified sandstone	Light grey to greenish-grey, fine-grained, hummocky cross-stratified sandstone. Rare trace fossils. Erosive bases and scours. Forms packages upwards of 6.8 m thick.	<i>Arenicolites</i> isp., <i>Ophiomorpha</i> isp., <i>Skolithos</i> isp.	0-1	Shallow marine wave dominated shoreline with periodic storm waves. High energy oscillatory flows. Storm surges result in	Lower Shoreface

					unidirectional flow producing migrating 3D dunes.	
	F6 Amalgamated trough cross-stratified sandstone	Light grey to greenish-grey, tabular, cross-bedded and trough cross-bedded fine-grained sandstone beds 0.7-4.2m thick. Both beds and bedsets coarsen upwards. Bed contacts are erosive based or gradational. Beds are amalgamated into packages 0.5-1 m thick	<i>Macaronichnus</i> isp.	0-1	Shallow marine shoreline with periodic storm activity. High energy, with predominant longshore currents producing 2D and 3D dunes in longshore bar deposits.	Upper Shoreface
Dinosaur Park Formation FA2: Wave-dominated, tide influenced barrier island-lagoon complex	F7 Massive shale, mudstone and laminated silt	Massive medium to dark grey dominantly structureless shale with localized silt and sand stringers with rare oscillatory ripples 3-5 mm in thickness. Small in situ bivalves are present throughout. Small Lucinidae and Ostreidae bivalves are preserved throughout. This facies is 0.5-5.2 m thick.	<i>Chondrites</i> isp. <i>Planolites</i> isp.	0-1	Quiet waters in a central basin catchment restricted from storms and tidal influence.	Restricted central estuary basin and coastal lagoons
	F8 Fine to Medium grained bioturbated sandstone	Medium grey to greenish-grey, fine to medium grained sandstone. Low angle and cross bedding, and local glauconitic grains. Wave ripples, locally coal clasts, carbonaceous laminae, and local plant debris. Root traces at top of some beds. Bed thickness ranges from 1.4-6.3 m.	<i>Macaronichnus</i> isp., root traces	0-3	High-energy environment with unidirectional and oscillatory wave action produced by migration of dunes and ripples.	Outer estuarine mouth bar complex and barrier island bars
FA3: Wave-dominated tide influenced marginal marine fluvial affected	F9 Sparsely bioturbated heterolithic deposits	Medium to light grey, thinly laminated, tabular to lenticular, fine- to very fine-grained sandstone interbedded with light grey to grey-brown mudstone, silty mudstone, and silt. Cross-lamination and current ripples (locally wave reworked), syneresis cracks, slickensides and convolute bedding occur throughout. Coal clasts, carbonaceous laminae and plant debris occur throughout. Vertebrate microfossil assemblages are associated with this facies. Bed thickness ranges from 0.7-3.4 m.	<i>Asterosoma</i> isp. <i>Cylindrichnus concentricus</i> , <i>Palaeophycus</i> isp., <i>Planolites</i> isp., <i>Protovirgularia</i> isp., <i>Teichichnus rectus</i> , <i>Thalassinoides</i> isp., <i>Skolithos</i> isp.	0-3	Current ripples and low angle bedding indicate dominant unidirectional flow. Mud deposition during intermittent, slack water conditions between ebb and flow Low salinity brackish conditions.	Upper and middle estuarine channels, intertidal channels

	F10 Wave, current, and cross-stratified bioturbated sandstone	Medium to light grey, current, wave rippled, and cross stratified medium to fine-grained sandstone. Beds are erosionally based and reactivation surfaces are locally present. Mud drapes and horizontal mud laminae are present. When present, is always overlain by F7.	<i>Macaronichnus</i> isp., <i>Skolithos</i> isp	0-1	Migration of subaqueous, unidirectional flow dunes punctuated by slack-water conditions and occasional wind-driven oscillatory flows.	Bayhead delta
FA4: Coastal Plain	F11 Rooted massive and thinly laminated carbonaceous mudstone and muddy siltstone	Medium to light grey and grey-brown massive mudstone and siltstone with abundant plant debris, coal clasts, slickensides, and soft sediment deformation. Lamination is thin alternating mud, silt, and carbonaceous debris and is unbioturbated. Commonly bounded by coal and containing coalified haloed root traces in places. Bed thickness ranges from 0.2-2.5 m.	Root traces, <i>Cochlichnus</i> isp., <i>Mermia</i> isp., <i>Planolites</i> isp.,	0-1	Suspension fallout of mud, silt and sand in a low energy environment. Gleysols indicate waterlogged conditions and a high water-table.	Floodplain
	F12 Current rippled and convolute bedded fine-grained sandstone	Light grey current ripple and trough cross bedded fine-grained sandstone and silty sandstone. Beds display both gradational and erosive bases with abundant carbonaceous debris, coal fragments, mudstone rip-up clasts, and convolute bedding. Rare Unionid bivalves and <i>Viviparus</i> sp., <i>Goniobasis</i> sp. and <i>Hydrobia</i> sp. gastropods are locally preserved both as isolated shells, and as coquina beds. Vertebrate microfossil assemblages are associated with this facies. Bed thickness ranges from 0.62-1.7 m.	Root traces, <i>Mermia</i> isp.	0-1	Episodic deposits due to levee failure along a fluvial channel resulting in sheetflooding onto the floodplain.	Lower fluvial and distributary channels and crevasse splays
	F13 Trough and current rippled sandstone	Light grey fine grained current rippled, trough cross bedded, and structureless sandstone. Carbonaceous detritus, mud rip-up clasts, and coal fragments are locally present. Vertebrate microfossil assemblages are associated with this facies. Erosive-based packages range in thickness from 0.45- 3.7 m.	Root traces, <i>Skolithos</i> isp.,	0-1	Lowermost portion of a meandering stream in a low gradient coastal plain environment. Rare evidence of intermittent tidal influence in channels.	Freshwater channels

	F14 Carbonaceous shale, silt, and coal	Highly variable, intercalated coal seams and coaly laminae. Coal ranges from shaly to bright- banded. Planar laminae, current ripples, slickensides, siderite, and convolute bedding. Thickness ranges from 0.38-3 m.	Root traces, <i>Cochlichnus</i> isp., <i>Mermia</i> isp., <i>Teredolites</i> isp.	0-1	High accumulation of plant debris in a coastal plain environment.	Floodplain, peat forming mires, swamps, and marshes.
	F15 Bentonitic mudstone	Seams of green-grey to light grey bentonite rich mudstone. Fissile to massive, with phenocrysts of biotite, quartz, and feldspar. Thickness ranges from 0.08-0.4 m.	N/A	0	Air fallout of ash from volcanic activity.	Sheltered, poorly drained swamps and marshes.

Table 3.2: Summary of facies, facies associations, and inferred depositional environments of the Dinosaur Park - Bearpaw Formation transition. BI - Bioturbation Index

Ichnofauna	FA1					FA2			FA3		FA4				
	F1	F2	F3	F4	F5	F6	F7	F8	F9	F10	F11	F12	F13	F14	F15
<i>Arenicolites</i> isp.					R										
<i>Asterosoma</i> isp.		C	C	R					R						
<i>Chondrites</i> isp.	A	A	C	R			C								
<i>Cochlichnus</i> isp.											R			R	
<i>Cylindrichnus concentricus</i>									R						
<i>Diplocraterion</i> isp.			R	C		R									
<i>Macaronichnus</i> isp.								C		C					
<i>Mermia</i> isp.											R	R		R	
<i>Nereites missouriensis</i>	R	R													
<i>Ophiomorpha</i> isp.					R	A									
<i>Palaeophycus</i> isp.									R						
<i>Phycosiphon incertum</i>	R														
<i>Planolites</i> isp.	A	A	A			R	C		C		R				
<i>Protovirgularia</i> isp.									R						
<i>Rhizocorallium</i> isp.		R	R												
<i>Rosselia</i> isp.		R													
<i>Skolithos</i> isp.				R	R	R		R	R	R			R		
<i>Teichichnus rectus</i>									C						
<i>Teredolites</i> isp.														R	
<i>Thalassinoides</i> isp.				R					R						
<i>Zoophycos</i> isp.	R	R													
Root traces								C			C			R	
Indeterminate infaunal burrows	A	A	A	C	C	R	C	R	C	R	R	C	R	C	

Table 3.3: Trace-fossil distribution and relative abundance in the different sedimentary facies from the Upper Cretaceous Dinosaur Park - Bearpaw Formation transition in the Cypress Hills region, southwestern Saskatchewan. F1: Shale; F2: Mudstone and interbedded siltstone; F3: Bioturbated muddy and sandy siltstone; F4: Fine-grained sandstone and siltstone; F5: Amalgamated hummocky cross-stratified sandstone; F6: Amalgamated trough cross-stratified sandstone; F7: Massive shale, mudstone and laminated silt; F8: Fine to Medium grained bioturbated sandstone; F9: Sparsely bioturbated heterolithic deposits; F10: Wave, current, and cross-stratified bioturbated sandstone; F11: Rooted massive and thinly laminated carbonaceous mudstone and muddy siltstone; F12: Current rippled and convolute bedded fine-grained sandstone; and F13: Trough and current rippled sandstone; Facies 14: Carbonaceous shale, silt, and coal; Facies 15: Bentonitic mudstone. A: abundant; C: common; R: rare.

References

- Aigner, T. (1985). Storm sedimentation in offshore shelf areas, German Bay, North Sea. *Storm Depositional Systems: Berlin, Springer-Verlag*, 30-158.
- Ainsworth, R., Vakarelov, B., & Nanson, R. (2011). Dynamic spatial and temporal prediction of changes in depositional processes on clastic shorelines; toward improved subsurface uncertainty reduction and management. *AAPG Bulletin*, 95(2), 267-297.
- Bhattacharya, B., & Banerjee, S. (2014). *Chondrites* isp. indicating late Paleozoic atmospheric anoxia in eastern peninsular India. *The Scientific World Journal*, 2014, Article ID 434672, 9 p. <http://dx.doi.org/10.1155/2014/434672>
- Bhattacharya, J., & Giosan, L. (2003). Wave-influenced deltas; geomorphological implications for facies reconstruction. *Sedimentology*, 50(1), 187-210.
- Boyd, R., Dalrymple, R., & Zaitlin, B. A. (1992). Classification of clastic coastal depositional environments. *Sedimentary Geology*, 80(3-4), 139-150.
- Bromley, R. G. (1996). *Trace fossils. Biology, taphonomy, and applications* (2nd ed.). London ; New York: Chapman & Hall.
- Bromley, R., Pemberton, S., & Rahmani, R. (1984). A Cretaceous woodground: The Teredolites ichnofacies. *Journal of Paleontology*, 58(2), 488-498.
- Buatois & Mángano, 1995 (section 3.4.1, F14)
- Buatois, L. A., & Mángano, M. G. (2003). Sedimentary facies, depositional evolution of the Upper Cambrian–Lower Ordovician Santa Rosita Formation in northwest Argentina. *Journal of South American Earth Sciences*, 16(5), 343-363.
- Buatois, L. A., & Mángano, M. G. (2011). *Ichnology: Organism-substrate interactions in space and time*. Cambridge, UK: Cambridge University Press.
- Buatois, L. A., Zeballo, F. J., Albanesi, G. L., Ortega, G., Vaccari, N. E., & Mangano, M. G. (2006). Depositional environments and stratigraphy of the Upper Cambrian-Lower Ordovician Santa Rosita Formation at the Alfarcito area, Cordillera Oriental, Argentina: integration of biostratigraphic data within a sequence stratigraphic framework. *Latin American journal of sedimentology and basin analysis*, 13(1), 1-29.
- Burns, C. E., Mountney, N. P., Hodgson, D. M., & Colombero, L. (2017). Anatomy and dimensions of fluvial crevasse-splay deposits: Examples from the Cretaceous Castlegate Sandstone and Neslen Formation, Utah, USA. *Sedimentary Geology*, 351, 21-35.

- Cant, D. J., & Stockmal, G. S. (1989). The Alberta foreland basin: Relationship between stratigraphy and Cordilleran terrane-accretion events. *Canadian Journal of Earth Sciences*, 26(10), 1964-1975.
- Catuneanu, O., Sweet, A. R., & Miall, A. D. (1997). Reciprocal architecture of Bearpaw TR sequences, uppermost Cretaceous, Western Canada Sedimentary Basin. *Bulletin of Canadian Petroleum Geology*, 45(1), 75-94.
- Catuneanu, O., Sweet, A. R., & Miall, A. D. (2000). Reciprocal stratigraphy of the Campanian–Paleocene western interior of North America. *Sedimentary Geology*, 134(3-4), 235-255.
- Cioffi, D., Di Eugenio, A., & Gallerano, F. (1995). A new representation of anoxic crises in hypertrophic lagoons. *Applied Mathematical Modelling*, 19(11), 685-695.
- Clifton, H. E., Hunter, R. E., & Phillips, R. L. (1971). Depositional structures and processes in the non-barred high-energy nearshore. *Journal of Sedimentary Research*, 41(3), 651-670.
- Coates, L. (2002). *The ichnological-sedimentological signature of wave- and river-dominated deltas: Dunvegan and Basal Belly River formations, west-central Alberta* (Unpublished master's thesis). Simon Fraser University, Vancouver, Canada.
- Cobban, W. A., Walaszczyk, I., Obradovich, J. D., & McKinney, K. C. (2006). *A USGS zonal table for the Upper Cretaceous Middle Cenomanian–Maastrichtian of the western interior of the United States based on ammonites, inoceramids, and radiometric ages*. U.S. Geological Survey, Open-File Report 2006-1250.
- Colombera, L., Mountney, N. P., & McCaffrey, W. D. (2013). A quantitative approach to fluvial facies models: methods and example results. *Sedimentology*, 60(6), 1526-1558.
- Croghan, P., & Funnell, B. (1983). Osmotic regulation and the evolution of brackish- and fresh-water faunas. *Journal of the Geological Society of London*, 140(1), 39-46.
- Daidu, F., Yuan, W., & Min, L. (2013). Classifications, sedimentary features and facies associations of tidal flats. *Journal of Palaeogeography*, 2(1), 66-80.
- Dalrymple, R. W. (2006). Incised valleys in time and space: An introduction to the volume and an examination of the controls on valley formation and filling. In R. W. Dalrymple, D. A. Leckie & R. W. Tillman (Eds.), *Incised valleys in time and space* (pp. 5-12). Society for Sedimentary Geology, SEPM Special Publication No. 85.
- Dalrymple, R. W. (2010). Tidal depositional systems. In N. P. James & R. W. Dalrymple (Eds.), *Facies models* (4th ed., pp. 201-231). St. John's, Newfoundland: Geological Association of Canada.

- Dalrymple, R. W., & Choi, K. (2007). Morphologic and facies trends through the fluvial–marine transition in tide-dominated depositional systems: A schematic framework for environmental and sequence-stratigraphic interpretation. *Earth Science Reviews*, 81(3-4), 135-174.
- Dalrymple, R. W., Zaitlin, B. A., & Boyd, R. (1992). Estuarine facies models: Conceptual basis and stratigraphic implications. *Journal of Sedimentary Petrology*, 62(6), 1130-1146.
- Dashtgard, S., Gingras, M., MacEachern, J., & Dashtgard, S. E. (2009). Tidally modulated shorefaces. *Journal of Sedimentary Research*, 79(11), 793-807.
- Davis Jr., R. A., & Hayes, M. O. (1984). What is a wave-dominated coast? *Marine Geology*, 60(1-4), 313-329.
- Davis et al., 2011 (section 3.4.1, F8, F9)
- Dawson, F. M., Evans, C. G., Marsh, R., & Richardson, R. (1994). Uppermost Cretaceous and Tertiary strata of the Western Canada Sedimentary Basin. In G. D. Mossop & I. Shetson (Comps.), *Geological atlas of the Western Canada Sedimentary Basin* (pp. 387-406). Calgary, Alberta: Canadian Society of Petroleum Geologists and Alberta Research Council.
- Duke et al., 1991 (section 3.4.1, F3)
- Eberth, D. A. (2005). The geology. In P. J. Currie & E. B. Koppelhus (Eds.), *Dinosaur Provincial Park: A spectacular ancient ecosystem revealed* (pp. 54-82). Bloomington & Indianapolis, IN: Indiana University Press.
- Eberth, D. A., & Braman, D. R. (2012). A revised stratigraphy and depositional history for the Horseshoe Canyon Formation (Upper Cretaceous), southern Alberta plains. *Canadian Journal of Earth Sciences*, 49(9), 1053-1086.
- Eberth, D. A., Braman, D. R., & Tokaryk, T. T. (1990). Stratigraphy, sedimentology and vertebrate paleontology of the Judith River Formation (Campanian) near Muddy Lake, west-central Saskatchewan. *Bulletin of Canadian Petroleum Geology*, 38(4), 387-406.
- Eberth, D. A., & Deino, A. L. (1992). A geochronology of the non-marine Judith River Formation of southern Alberta. In R. M. Flores (Ed.), *Mesozoic of the Western Interior: field guidebook: SEPM 1992 Theme Meeting* (pp. 24-25). Society for Sedimentary Geology, Rocky Mountain Section.
- Eberth, D. A., & Hamblin, A. P. (1993). Tectonic, stratigraphic, and sedimentologic significance of a regional discontinuity in the upper Judith River Group (Belly River wedge) of southern Alberta, Saskatchewan, and northern Montana. *Canadian Journal of Earth Sciences*, 30(1), 174-200.
- Elliot, T. (1986). Deltas. In H. G. Reading (Ed.), *Sedimentary environments and facies* (2nd ed., pp. 113-154). Oxford, UK: Blackwell Scientific Publications.

- Embry, A. (1990). A tectonic origin for third order depositional sequences in extensional basins - Implications for basin modeling. In *Quantitative dynamic stratigraphy* (pp. 491-501). New Jersey, NJ: Prentice Hall.
- Frank, M. C. (2006). *Coal distribution in the Upper Cretaceous (Campanian) Belly River Group of southwest Saskatchewan*. Saskatchewan Industry and Resources, Open File Report 2005-33, CD-ROM.
- Frey, R. W., Howard, J. D., & Pryor, W. A. (1978). *Ophiomorpha*: Its morphologic, taxonomic, and environmental significance. *Palaeogeography, Palaeoclimatology, Palaeoecology*, 23, 199-229.
- Frey, R. W., & Pemberton, S. G. (1984). Trace fossils facies models. In R. G. Walker (Ed.), *Facies models* (2nd ed., pp. 189-207). Tulsa, OK: American Association of Petroleum Geologists.
- Gilbert, M. M., Bamforth, E. L., Buatois, L. A., & Renaut, R. W. (2018). Paleoeology and sedimentology of a vertebrate microfossil assemblage from the easternmost Dinosaur Park Formation (Late Cretaceous, Upper Campanian,) Saskatchewan, Canada: Reconstructing diversity in a coastal ecosystem. *Palaeogeography, Palaeoclimatology, Palaeoecology*, 495, 227-244.
- Gingras, M. K., Pemberton, S. G., Saunders, T., & Clifton, H. E. (1999). The ichnology of modern and Pleistocene brackish-water deposits at Willapa Bay, Washington; variability in estuarine settings. *Palaaios*, 14(4), 352-374.
- Gradstein, F. M., Ogg, J. G., Schmitz, M. D., & Ogg, G. M. (2012). *The geologic time scale 2012* (Vol. 1-2). Elsevier B.V.
- Hamblin, A. P. (1997). Regional distribution and dispersal of the Dinosaur Park Formation, Belly River Group, surface and subsurface of southern Alberta. *Bulletin of Canadian Petroleum Geology*, 45(3), 377-399.
- Hamblin, A. P., & Abrahamson, B. (1996). Stratigraphic architecture of “Basal Belly River” cycles, Foremost Formation, Belly River Group, subsurface of southern Alberta and southwestern Saskatchewan. *Bulletin of Canadian Petroleum Geology*, 44(4), 654-673.
- Harzallah, A., & Chapelle, A. (2002). Contribution of climate variability to occurrences of anoxic crises ‘malaïgues’ in the Thau lagoon (southern France). *Oceanologica Acta*, 25(2), 79-86.
- Hayes, M., Schwartz, M. L., Fairbridge, R. W., & Rampino, M. R. (2005). Barrier islands. In *Encyclopedia of coastal science* (Encyclopedia of earth science series, pp. 117-119). Dordrecht, Netherlands: Springer.

- Jones, B. (2013). *Integrated ichnology and sedimentology of mixed river- and wave-influenced delta complexes, Upper Cretaceous Basal Belly River Formation, central Alberta, Canada* (Unpublished master's thesis). Simon Fraser University, Vancouver, Canada.
- Kauffman, E., & Caldwell, W. (1993). The Western Interior Basin in space and time. In W. G. E. Caldwell & E. G. Kauffman (Eds.), *Evolution of the Western Interior Basin* (pp. 1-30). Geological Association of Canada, Special Paper #39.
- Kent, D. M., & Christopher, J. E. (1994). Geological history of the Williston Basin and Sweetgrass Arch. In G. D. Mossop & I. Shetson (Comps.), *Geological atlas of the Western Canada Sedimentary Basin* (pp. 421-429). Calgary, Alberta: Canadian Society of Petroleum Geologists and Alberta Research Council.
- Kraus, M. J. (1999). Paleosols in clastic sedimentary rocks: their geologic applications. *Earth-Science Reviews*, 47(1-2), 41-70.
- Leckie, D. A., & Smith, D. G. (1992). Regional setting, evolution, and depositional cycles of the Western Canada Foreland Basin. In R. W. Macqueen & D. A. Leckie (Eds.), *Foreland basins and fold belts* (pp. 9-46). American Association of Petroleum Geologists, AAPG Memoir 55.
- Leckie, D., Fox, C., & Tarnocai, C. (1989). Multiple paleosols of the late Albian Boulder Creek Formation, British Columbia, Canada. *Sedimentology*, 36(2), 307-323.
- Lerbekmo, J. F., & Braman, D. R. (2002). Magnetostratigraphic and biostratigraphic correlation of late Campanian and Maastrichtian marine and continental strata from the Red Deer Valley to the Cypress Hills, Alberta, Canada. *Canadian Journal of Earth Sciences*, 39(4), 539-557.
- Lettley, C. D. (2004). Speciation of McMurray Formation inclined heterolithic strata: Varying depositional character along a riverine estuary system. In *CSPG/ CSEG / CWLS Convention 2004, Innovation, Collaboration, Exploration: Building to the Future, May 31 - June 4*, Calgary, Alberta, Proceedings.
- Lettley, C. D., Pemberton, S. G., Gingras, M. K., Ranger, M. J., & Blakney, B. J. (2009). Integrating sedimentology and ichnology to shed light on the system dynamics and paleogeography of an ancient riverine estuary. In J. A. MacEachern, K. L. Bann, M. K. Gingras & S. G. Pemberton (Eds.), *Applied ichnology* (pp. 144-162). Society for Sedimentary Geology, SEPM Short Course Notes, Vol. 52 (2005).
- MacEachern, J. A., Bann, K. L., Pemberton, S. G., & Gingras, M. K. (2007). The ichnofacies paradigm: High-resolution paleoenvironmental interpretation of the rock record. In *Applied ichnology* (pp. 27-64). Society for Sedimentary Geology, SEPM Short Course Notes.

- MacEachern, J. A., & Gingras, M. K. (2007). Recognition of brackish-water trace fossil suites in the Cretaceous Western Interior Seaway of Alberta, Canada. In R. G. Bromley, L. A. Buatois, G. Mángano, J. F. Genise & R. N. Melchor (Eds.), *Sediment-organism interaction: A multifaceted ichnology* (pp. 149-193). Society for Sedimentary Geology, SEPM Special Publication No. 88.
- MacEachern, J. A., & Pemberton, S. G. (1992). Ichnological aspects of Cretaceous shoreface successions and shoreface variability in the Western Interior Seaway of North America. In S. G. Pemberton (Ed.), *Applications of ichnology to petroleum exploration: A core workshop* (pp. 57-84). Society for Sedimentary Geology, SEPM Core Workshop No. 17.
- MacEachern, J. A., & Pemberton, S. G. (1994). Ichnological aspects of incised-valley fill systems from the Viking Formation of the Western Canada Sedimentary Basin, Alberta, Canada. In R. W. Dalrymple, R. Boyd & B. A. Zaitlin (Eds.), *Incised-valley systems: Origin and sedimentary sequences* (pp. 129-157). Society for Sedimentary Geology, SEPM Special Publication No. 51.
- MacEachern, J. A., Zaitlin, B. A., & Pemberton, S. G. (1999). A sharp-based sandstone of the Viking Formation, Joffre Field, Alberta, Canada: Criteria for recognition of transgressively incised shoreface complexes. *Journal of Sedimentary Research*, 69, 876-892.
- MacEachern, J. A., Pemberton, S. G., Gingras, M. K., Bann, K. L., James, N. P., & Dalrymple, R. W. (2010). Ichnology and facies models. *Facies models*, 4, 19-58.
- Mángano and Buatois, 2003 (section 3.5.1; should be Buatois and Mángano 2003 perhaps?)
- McLean, J. R. (1971). *Stratigraphy of the Upper Cretaceous Judith River Formation in the Canadian Great Plains*. Saskatchewan Research Council, Geology Division, Report No. 11.
- Miall, A. D. (1991). Stratigraphic sequences and their chronostratigraphic correlation. *Journal of Sedimentary Research*, 61(4), 497-505.
- Miall, A. D. (2010) Alluvial models. In N. P. James & R. W. Dalrymple (Eds.), *Facies models* (4th ed., pp. 201-231). St. John's, Newfoundland: Geological Association of Canada.
- Miall, A. D. (2013). *The geology of fluvial deposits: Sedimentary facies, basin analysis, and petroleum geology*. Springer.
- Nägler, T. F., Neubert, N., Böttcher, M. E., Dellwig, O., & Schnetger, B. (2011). Molybdenum isotope fractionation in pelagic euxinia: Evidence from the modern Black and Baltic seas. *Chemical Geology*, 289(1-2), 1-11.
- Nio, S. D., & Yang, C. S. (1991). Diagnostic attributes of clastic tidal deposits: a review.

- Odezulu, C. I., Lorenzo-Trueba, J., Wallace, D. J., & Anderson, J. B. (2018). Follets Island: a case of unprecedented change and transition from rollover to subaqueous shoals. In *Barrier dynamics and response to changing climate* (pp. 147-174). Springer, Cham.
- Pearson, N. J., & Gingras, M. K. (2006). An ichnological and sedimentological facies model for muddy point-bar deposits. *Journal of Sedimentary Research*, 76(5), 771-782.
- Pearson, N. J., Mángano, M. G., Buatois, L. A., Casadío, S., & Raising, M. R. (2013). Environmental variability of *Macaronichnus* ichnofabrics in Eocene tidal-embayment deposits of southern Patagonia, Argentina. *Lethaia*, 46(3), 341-354.
- Pemberton, S. G., Flach, P. D., & Mossop, G. D. (1982). Trace fossils from the Athabasca oil sands, Alberta, Canada. *Science*, 217(4562), 825-827.
- Pemberton, S. G., MacEachern, J. A., Dashtgard, S. E., Bann, K. L., Gingras, M. K., & Zonneveld, J. P. (2012). Shorefaces. In D. Knaust & R. G. Bromley (Eds.), *Developments in sedimentology* (Vol. 64, pp. 563-603). Elsevier.
- Pemberton, S. G., Spila, M., Pulham, A. J., Saunders, T., MacEachern, J. A., Robbins, D., & Sinclair, I. K. (2001). *Ichnology & sedimentology of shallow to marginal marine systems. Ben Nevis and Avalon reservoirs, Jeanne d'Arc Basin*. Geological Association of Canada, Short Course Notes, 15. St. John's, Newfoundland: Geological Association of Canada.
- Pemberton, S. G., Van Wagoner, J. C., & Wach, G. D. (1992). Ichnofacies of a wave-dominated shoreline. In S. G. Pemberton (Ed.), *Applications of ichnology to petroleum exploration: A core workshop* (pp. 339-382). Society for Sedimentary Geology, SEPM Core Workshop No. 17.
- Pemberton, S. G., & Wightman, D. M. (1992). Ichnological characteristics of brackish water deposits. In S. G. Pemberton (Ed.), *Application of ichnology to petroleum exploration: A core workshop* (pp. 141-167). Society for Sedimentary Geology, SEPM Core Workshop No. 17.
- Plint, A. G. (2010). Wave- and storm-dominated shoreline and shallow-marine systems. In N. P. James & R. W. Dalrymple (Eds.), *Facies models* (4th ed., pp. 167-199). St. John's, Newfoundland: Geological Association of Canada.
- Pollard, J. E., Goldring, R., & Buck, S. G. (1993). Ichnofabrics containing *Ophiomorpha*: Significance in shallow-water facies interpretation. *Journal of the Geological Society*, 150(1), 149-164.
- Power, B. A., & Walker, R. G. (1996). Allostratigraphy of the Upper Cretaceous Lea Park-Belly River transition in central Alberta, Canada. *Bulletin of Canadian Petroleum Geology*, 44(1), 14-38.

- Price, R. A. (1994). Cordilleran tectonics and the evolution of the Western Canada Sedimentary Basin. In G. D. Mossop & I. Shetson (Comps.), *Geological atlas of the Western Canada Sedimentary Basin* (pp. 13-24). Calgary, Alberta: Canadian Society of Petroleum Geologists and Alberta Research Council.
- Quiroz, L. I., Buatois, L. A., Mángano, M. G., Jaramillo, C. A., & Santiago, N. (2010). Is the trace fossil *Macaronichnus* an indicator of temperate to cold waters? Exploring the paradox of its occurrence in tropical coasts. *Geology*, 38(7), 651-654.
- Reading, H. G., & Collinson, J. D. (1996). Clastic coasts. In H. G. Reading (Ed.), *Sedimentary environments: Processes, facies, and stratigraphy* (3rd ed., pp. 154-231). Oxford, UK: Blackwell Scientific Publications.
- Reinson, G. E. (2010). Barriers and estuaries. In N. P. James & R. W. Dalrymple (Eds.), *Facies models* (4th ed., pp. 201-231). St. John's, Newfoundland: Geological Association of Canada.
- Retallack, G. J. (1988). Field recognition of paleosols. In J. Reinhardt & W. R. Sigleo (Eds.), *Paleosols and weathering through geologic time: Principles and applications* (pp. 1-20). Geological Society of America, GSA Special Papers, 216.
- Retallack, G. J. (2008). *Soils of the past: An introduction to paleopedology*. John Wiley & Sons.
- Rogers, R. R., Kidwell, S. M., Deino, A. L., Mitchell, J. P., Nelson, K., & Thole, J. T. (2016). Age, correlation, and lithostratigraphic revision of the Upper Cretaceous (Campanian) Judith River Formation in its type area (north-central Montana), with a comparison of low- and high-accommodation alluvial records. *The Journal of Geology*, 124(1), 99-135.
- Roy, P. S., Cowell, P. J., Ferland, M. A., & Thom, B. G. (1994). Wave-dominated coasts. In R. W. G. Carter & C. D. Woodroffe (Eds.), *Coastal evolution: Late Quaternary shoreline morphodynamics* (pp. 121-186). Cambridge, UK: Cambridge University Press.
- Savrda, C. E. (1991). Teredolites, wood substrates, and sea-level dynamics. *Geology*, 19(9), 905-908.
- Schröder-Adams, C. J., Cumbaa, S. L., Bloch, J., Leckie, D. A., Craig, J., Seif, E. D. S., ... Kenig, F. (2001). Late Cretaceous (Cenomanian to Campanian) paleoenvironmental history of the eastern Canadian margin of the Western Interior Seaway: Bonebeds and anoxic events. *Palaeogeography, Palaeoclimatology, Palaeoecology*, 170(3-4), 261-289.
- Schwarz, E., & Howell, J. A. (2005). Sedimentary evolution and depositional architecture of a lowstand sequence set: the Lower Cretaceous Mulichinco Formation, Neuquén Basin, Argentina. *Geological Society, London, Special Publications*, 252(1), 109-138.
- Seilacher, A. (1990). Aberrations in bivalve evolution related to photo- and chemosymbiosis. *Historical Biology*, 4, 289-311.

- Shanmugam, G. (2017). Global case studies of soft-sediment deformation structures (SSDS): Definitions, classifications, advances, origins, and problems. *Journal of Palaeogeography*, 6(4), 251-320.
- Slingerland, R., & Smith, N. D. (2004). River avulsions and their deposits. *Annual Review of Earth and Planetary Science*, 32, 257-285.
- Taylor, A. M., & Goldring, R. (1993). Description and analysis of bioturbation and ichnofabric. *Journal of the Geological Society*, 150(1), 141-148.
- Thomas, R. G., Smith, D. G., Wood, J. M., Visser, J., Calverley-Range, E. A., & Koster, E. H. (1987). Inclined heterolithic stratification—terminology, description, interpretation and significance. *Sedimentary Geology*, 53(1-2), 123-179.
- Thomas, W. A., & Mack, G. H. (1982). Paleogeographic relationship of a Mississippian barrier-island and shelf-bar system (Hartselle Sandstone) in Alabama to the Appalachian-Ouachita orogenic belt. *Geological Society of America Bulletin*, 93(1), 6-19.
- Tsujita, J. C. (1995). *Stratigraphy, taphonomy and paleoecology of the Upper Cretaceous Bearpaw Formation in southern Alberta* (Unpublished doctoral dissertation). McMaster University, Hamilton, Canada.
- Uchman, A., Johnson, M. E., Rebelo, A. C., Melo, C., Cordeiro, R., Ramalho, R. S., & Ávila, S. P. (2016). Vertically-oriented trace fossil *Macaronichnus segregatis* from Neogene of Santa Maria Island (Azores; NE Atlantic) records vertical fluctuations of the coastal groundwater mixing zone on a small oceanic island. *Geobios*, 49(3), 229-241.
- Vakarelov, B. K., Ainsworth, R. B., & MacEachern, J. A. (2012). Recognition of wave-dominated, tide-influenced shoreline systems in the rock record: Variations from a microtidal shoreline model. *Sedimentary Geology*, 279, 23-41.
- Visser, M. (1980). Neap-spring cycles reflected in Holocene subtidal large-scale bedform deposits; a preliminary note. *Geology*, 8(11), 543-546.
- Walker, R. G., & Plint, A. G. (1992). Wave- and storm-dominated shallow marine systems. In R. G. Walker & N. P. James (Eds.), *Facies models, response to sea level change* (pp. 219-238). St. John's, Newfoundland: Geological Association of Canada.
- Wesolowski, L. J. N. (2018). *Trace fossils, sedimentary facies and parasequence architecture from the Lower Cretaceous Mulichinco Formation of Argentina: The role of fair-weather waves in shoreface deposits* (Unpublished master's thesis). University of Saskatchewan, Saskatoon, Canada.

- Wightman, D. M., Pemberton, S. G., & Singh, C. (1987). Depositional modelling of the Upper Mannville Lower Cretaceous east central Alberta: Implications for the recognition of brackish water deposits. In R. W. Tillman & K. J. Weber (Eds.), *Reservoir sedimentology* (pp. 189-220). Society for Sedimentary Geology, SEPM Special Publication No. 40.
- Wood, J. M. (1985). *Sedimentology of the Late Cretaceous Judith River Formation, "Cathedral" area, Dinosaur Provincial Park, Alberta* (Unpublished master's thesis). University of Calgary, Canada.
- Wood, J. M. (1989). Alluvial architecture of the Upper Cretaceous Judith River Formation, Dinosaur Provincial Park, Alberta, Canada. *Bulletin of Canadian Petroleum Geology*, 37(2), 169-181.
- Zaitlin, B., Dalrymple, R., & Boyd, R. (1994). The stratigraphic organization of incised-valley systems associated with relative sea-level change. In R. W. Dalrymple, R. Boyd & B. A. Zaitlin (Eds.), *Incised-valley systems: Origin and sedimentary sequences* (pp. 45-60). Society for Sedimentary Geology, SEPM Special Publication No. 51.

Transition

Chapter 3 discusses the sedimentology and ichnology of the Dinosaur Park - Bearpaw transition in the Cypress Hills region of southwestern Saskatchewan. This provides a detailed treatment of the Dinosaur Park and lowermost Bearpaw formations, which acts as a framework for larger-picture sequence-stratigraphic and paleoenvironmental interpretations of the Belly River Group in its entirety. Chapter 4 details an extensive study of the Belly River Group as a whole as it is expressed in southwestern Saskatchewan, from the Foremost Formation at the base, Oldman Formation in the middle, and Dinosaur Park Formation at the top. A new member is erected in the Dinosaur Park Formation, herein named the Manâtakâw Member. The Manâtakâw Member is named in honor of the Plains Cree word for the Cypress Hills, meaning ‘beautiful uplands.’ The Cypress Hills, or Manâtakâw as they are called by the Cree, are of archeological, historical, cultural, and spiritual significance to many indigenous Plains groups in North America. A complete sedimentologic, ichnologic, and sequence-stratigraphic framework is presented for the Belly River Group in Saskatchewan for the first time, with implications for evolution of the sedimentary basin. A discussion of incised and unincised lowstand systems tracts and their stratigraphic and paleoenvironmental significance is provided. M. Gilbert conducted both field and laboratory work, analyzed the data, wrote the manuscript, and created the figures and tables used in the chapter.

Sequence Stratigraphy and Depositional Environments of the Belly River Group (Campanian) in Southwestern Saskatchewan, Canada: Incised and Unincised Fluvial Systems along an Epicontinental Seaway

Abstract

The Campanian Belly River Group (BRG) is a nonmarine clastic cycle in the Western Canada Sedimentary Basin. In southern and central Alberta, the BRG has been subdivided in ascending order into the Foremost, Oldman, and Dinosaur Park formations based on distinctive lithologic, petrographic, and geometric characteristics. Regional surface and subsurface correlation of the BRG reveals the three formations are discernible in southwestern Saskatchewan. The Belly River Group and its associated formations are formally recognized for the first time in Saskatchewan with facies, depositional environments, and sequence-stratigraphic framework interpreted to provide a concise treatment of the Group in southwestern Saskatchewan. A new lithostratigraphic unit within the uppermost Dinosaur Park Formation is recognized based on laterally extensive barrier island, lagoon, and estuary basin deposits. The Manâtakâw Member is established as a means to aid in discussing the transition from nonmarine clastics of the BRG to marine shales of the overlying Bearpaw Formation.

Unincised and incised valley systems are explored in detail, with lowstand systems tract deposits compared and contrasted between the Oldman and Dinosaur Park formations. Lowstand deposits of the Oldman Formation display as braided channel fill, and are interpreted as being deposited on an unincised alluvial to coastal plain. Isopachs constructed from subsurface data, coupled with core and outcrop features, indicate lowstand deposits of the Dinosaur Park

Formation were deposited in incised fluvial valleys. Differences in lowstand systems tracts as expressed in epicontinental seaways is explored, particularly in relation to climate and tectonic controls on changes in base level.

4.1 Introduction

The Upper Cretaceous Belly River Group (BRG) represents part of the infill of the Western Canada Sedimentary Basin in southern Alberta and Saskatchewan, extending into northern Montana in the United States. In Alberta and Montana, these deposits have been the focus of several sedimentologic and stratigraphic studies due to exceptional outcrop exposure and extensive subsurface data (e.g., McLean, 1971; Eberth & Hamblin, 1993; Catuneanu et al., 1997; Hamblin, 1997a, 1997b; Rogers et al., 2016; Gilbert et al., 2018; Gilbert et al., 2019). The Saskatchewan extension of these deposits has not been studied in as much detail. The interplay of accommodation space, sediment supply, and shoreline morphology resulted in significant paleoenvironmental shifts in Alberta and Saskatchewan during this time. An investigation of the Belly River Group and adjacent units formed in the Western Interior Seaway (WIS) (underlying Lea Park and overlying Bearpaw formations) based on outcrop and subsurface data provides insight into depositional trends and paleogeographic parameters of marginal-marine coastlines in both the Cypress Hills and across the Western Canada Sedimentary Basin. The objectives of this study are to: 1) characterize the facies and facies associations of the Belly River Group in Saskatchewan; 2) update the stratigraphic nomenclature to reflect modern understanding of the Group; 3) discuss the sequence-stratigraphic and paleoenvironmental evolution of these deposits in the Saskatchewan extent of the Western Canada Sedimentary Basin; and 4) discuss the significance of unincised vs. incised valley systems, and their significance to paleoenvironmental interpretation and the petroleum industry. The results of this study contribute to a broader understanding of Late Cretaceous geology in Saskatchewan and across the Western Canada Sedimentary Basin. A robust depositional model and sequence-stratigraphic framework for the Saskatchewan part of the

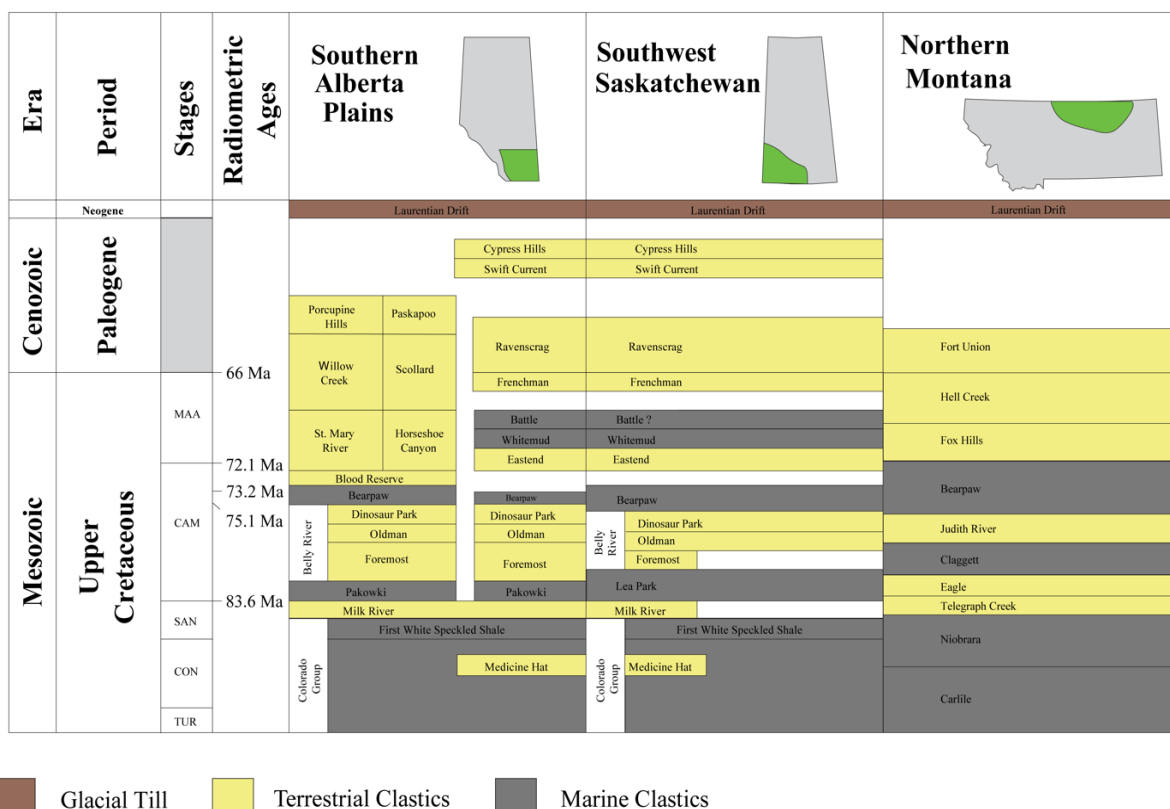


Figure 4.1: Stratigraphic nomenclature utilized in southeastern Alberta and southwestern Saskatchewan through the Upper Cretaceous Series in the Western Canada Sedimentary Basin. Radiometric and biostratigraphic dates (Ma): 66: K-T boundary (Gradstein et al., 2012); 72.1: Campanian–Maastrichtian boundary (Gradstein et al., 2012); 73.2 ± 0.4: Dorothy Bentonite (Lerbekmo & Braman, 2002); 75.1: *Exileoceras jenneyi* (Cobban et al., 2006); 83.6: Campanian–Santonian boundary (Gradstein et al., 2012). After Gilbert et al. (2018). TUR - Turonian; CON - Coniacian; SAN - Santonian; CAM - Campanian; MAA - Maastrichtian.

Group has been developed. This refines understanding of more-distal Belly River Group deposits in the Western Canada Sedimentary Basin, and provides context for deposits in Alberta that do not record subtle changes in base level due to distance from the paleocoastline. This study also provides a framework for regional and local geologic and paleontologic studies in Saskatchewan, and insight into unincised vs. incised lowstand systems, and its broader implications for sequence stratigraphy.

4.2 Geologic Background and Dataset

Cretaceous and Paleogene sedimentation in the Western Interior Sedimentary Basin occurred in two depocenters separated by the Bow Island Arch: the Williston Basin to the east and the Foreland Basin to the west (Dawson et al., 1994). During the Laramide Orogeny (~ 70–80 Ma), collisional accretion of microcontinents onto the west coast of North America caused thrust-sheet loading, resulting in formation of an orogenic belt (Price, 1994). This flexed the craton to produce a deeply subsiding asymmetric foredeep fed by sediments from the tectonically induced slope (Catuneanu et al., 2000). In west-central North America, this resulted in deposition of large amounts of marine and nonmarine clastic sediments (Fig. 4.1) in transgressive-regressive, tectonically controlled wedge-cycles (Leckie & Smith, 1992). The Belly River Group (BRG) is the fourth of five recognized cycles of foreland basin deposition (Embry, 1990; Leckie & Smith, 1992; Kauffman & Caldwell, 1993).

Deposition of the Campanian Belly River Group resulted from large sediment supply to the basin, producing an eastward-thinning paralic marginal-marine to nonmarine clastic succession (Cant & Stockmal, 1989). Three formations from this period are recognized formally in the western Canadian plains. In ascending order, these are the Foremost (FF),

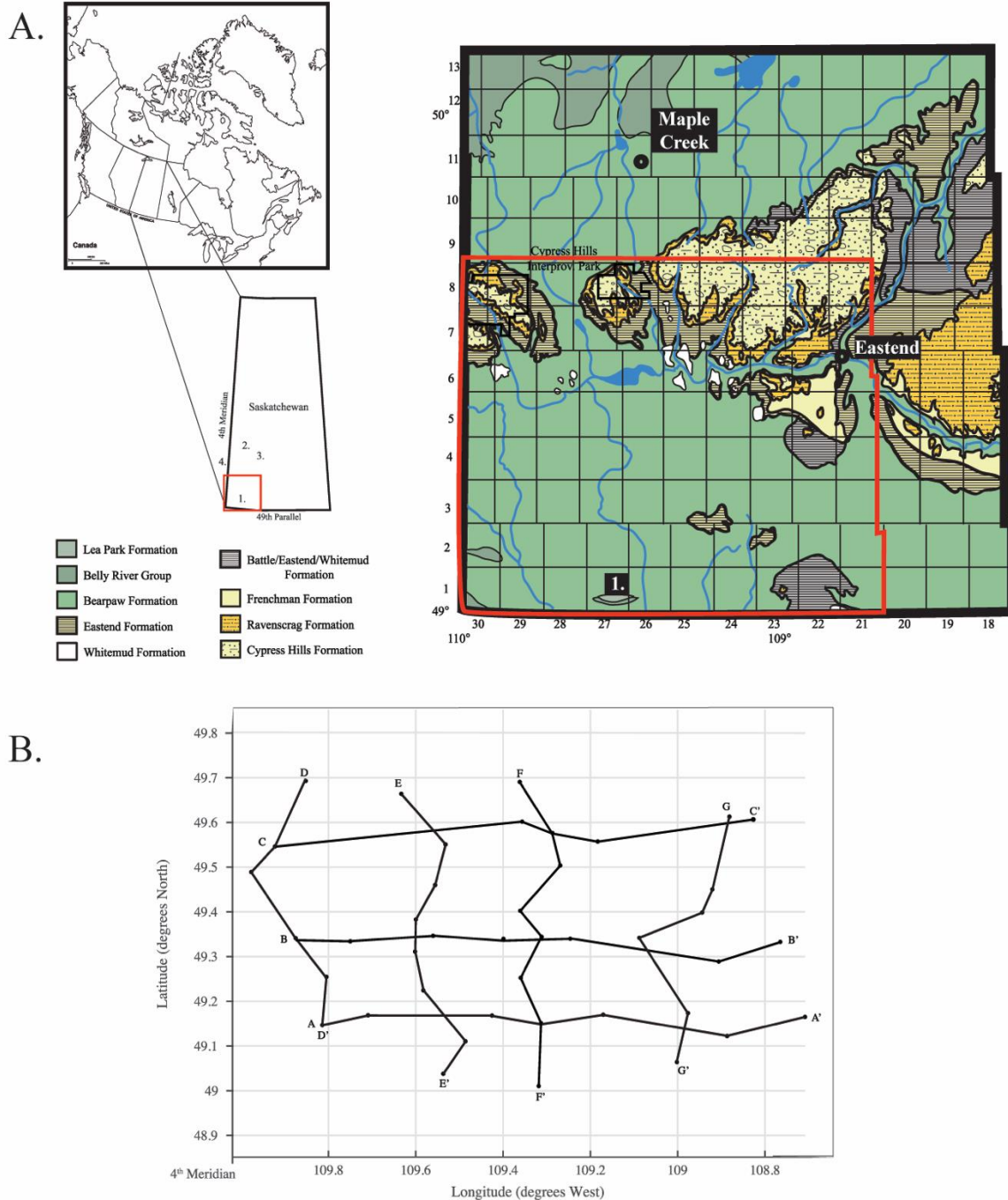


Figure 4.2: **A.** Left: Boundaries of the Cypress Hill region and approximate location of exposed outcrop at 1. Woodpile Coulee, Saskatchewan; 2. Muddy Lake, Saskatchewan; 3. Herschel, Saskatchewan; 4. Sandy Point, Alberta. Right: Regional map of the Cypress Hills region in context to regional landmarks. Based on maps from the Saskatchewan Geological Survey. **B.** Map of wells used to make cross-section correlations used in this study plotted against latitude and longitude. Cross-sections B and F are included in chapter as Figures 4.17 and 4.16; cross-sections A, C to E, and G are included as Appendix D.

Oldman (OF) and Dinosaur Park (DPF) formations (Eberth & Hamblin, 1993). Each formation is bound by a disconformity, and has distinctive sedimentologic and petrographic signatures that reflect tectonic controls of sediment supply (Eberth, 2005).

Sparse exposures of the Belly River Group crop out throughout western Saskatchewan in the North and South Saskatchewan River valleys, Muddy Lake and Herschel in west-central Saskatchewan, and the Cypress Hills in southwestern Saskatchewan (Fig. 4.2). These sediments represent the easternmost extent of the Group and record the transition of the terrestrial BRG into the fully marine Bearpaw Formation of the Western Interior Seaway (McLean, 1971; Eberth et al., 1990; Gilbert et al., 2018). Outcrops of the BRG are rare in Saskatchewan south of 52° N latitude (McLean, 1971).

The main study area extends from the United States border north to township 8 and from the Alberta border to range 21 west of the third meridian (21W3), encompassing most of the Saskatchewan extent of the Cypress Hills (Fig. 4.2). Where possible, a minimum of one well per township was used, resulting in a database of 212 wells. Seven subsurface cores (Table 4.1; Fig. 4.3) and outcrop exposures in township 1, range 27W3 along Woodpile Coulee (Fig. 4.4), townships 22 and 23, range 2W4 at Sandy Point, Alberta (Fig. 4.5), townships 38 and 39, range 23W3 at Muddy Lake, Saskatchewan (Fig. 4.4), and township 17, range 28W3 at Herschel, Saskatchewan (Fig. 4.5) were included to provide a more robust dataset of depositional patterns across the basin.

No continuous core through the BRG was available (late 2018) in the study area, therefore geophysical well logs were used to correlate major contacts. Well logs, core data, and outcrop data were integrated to develop composite sections for paleoenvironmental interpretations. Results were compared with those of Dawson et al. (1994), Eberth and Hamblin

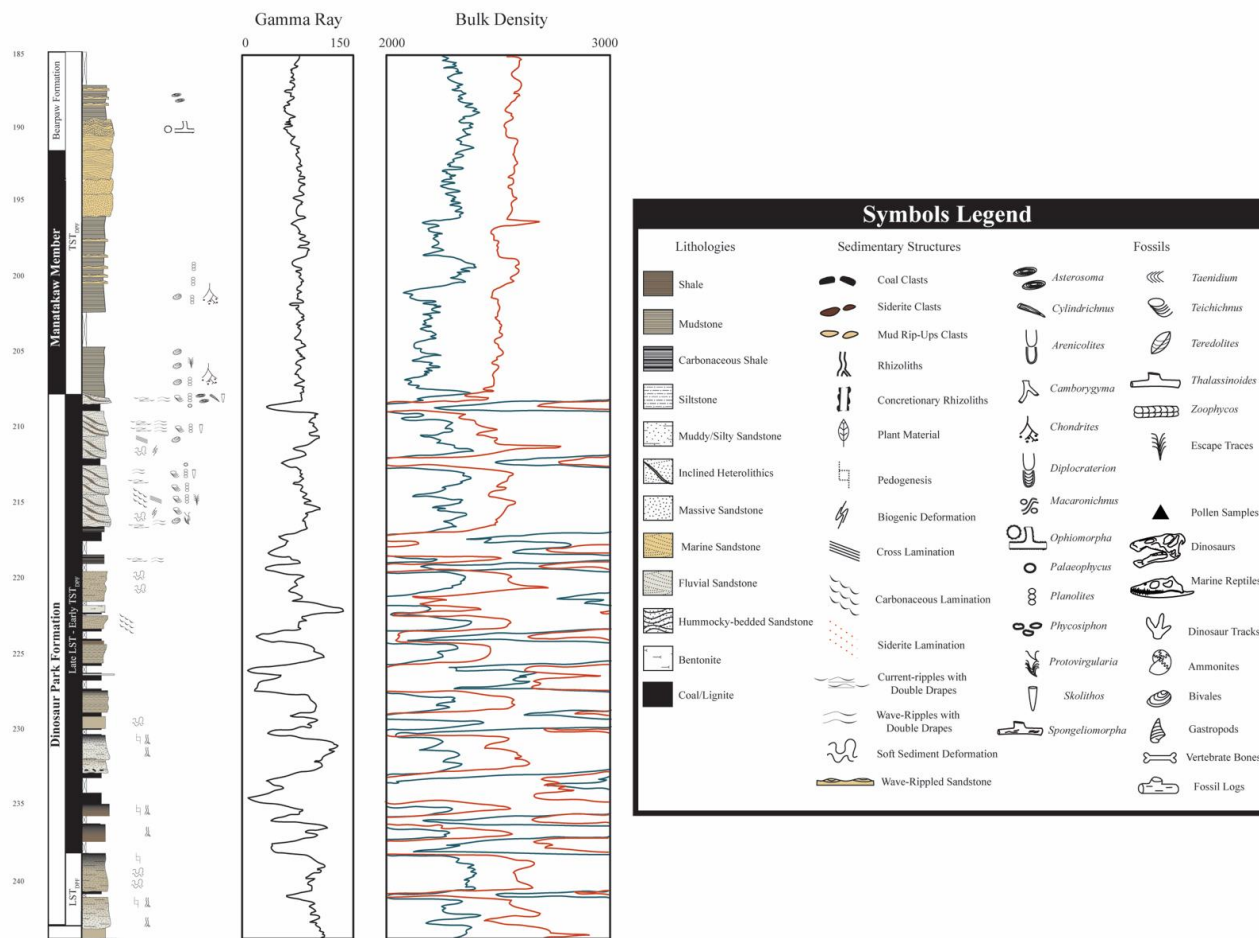


Figure 4.3: Representative lithostratigraphic log profiles of Nexen Battle Creek 07-02-004-27W3 and corresponding gamma (API) and bulk density log (K/M3). C - Coal; Sh - Shale/claystone; M - Mudstone; Si - Siltstone; FSS - Fine-grained sandstone; MSS - Medium-grained sandstone. LST - Lowstand Systems Tract; TST - Transgressive Systems Tract.

(1993), Hamblin (1997a, 1997b), Gordon (2000), and Rogers et al. (2016). Each facies was described in terms of sedimentology attributes and, where possible, ichnologic and paleontologic information. Cores were logged at the Subsurface Geological Laboratory in Regina, Saskatchewan. Isopach maps of the uppermost Foremost Formation, Ribstone Creek Member (RSC), Oldman Formation, Dinosaur Park Formation, and the newly erected Manâtakâw Member (MM) were constructed using MATLAB version R2017b (MathWorks, 2018) to provide insights to wedge geometry and basin evolution. Individual log picks were made using GeoScout (geoLOGIC Systems Ltd., 2018) and open-source well logs (Appendix C).

The gamma-density-resistivity suite of logs was used to pick the tops of the associated formations in the study area. This suite of logs is the most reliable for picking coals, which are a defining feature of the Dinosaur Park Formation and the Ribstone Creek Member in the Cypress Hills. Criteria for picks are illustrated in Fig. 4.6. Wells without the full suite of logs and those that were not drilled vertically were rejected. Wells that did not contain a complete log from the mid to lower Bearpaw Formation to the ‘Milk River Shoulder’ were removed from the isopach study. The Milk River Shoulder (MRS) marks the boundary between the Milk River Formation and the Lea Park Formation. This regional stratigraphic marker is a marine flooding surface, with the Milk River Formation composed of wave-dominated shoreface sandstones (Power & Walker, 1996). The MRS has a distinct signature on gamma-ray and resistivity logs and is laterally continuous across the entire study area (Fig. 4.6). Therefore, the MRS was chosen as the datum for the subsurface data, in common with other studies focusing on the Belly River Group (Eberth & Hamblin, 1993; Power & Walker, 1996; Hamblin, 1997a, 1997b; Hamblin & Abrahamson, 1996; Gordon, 2000).

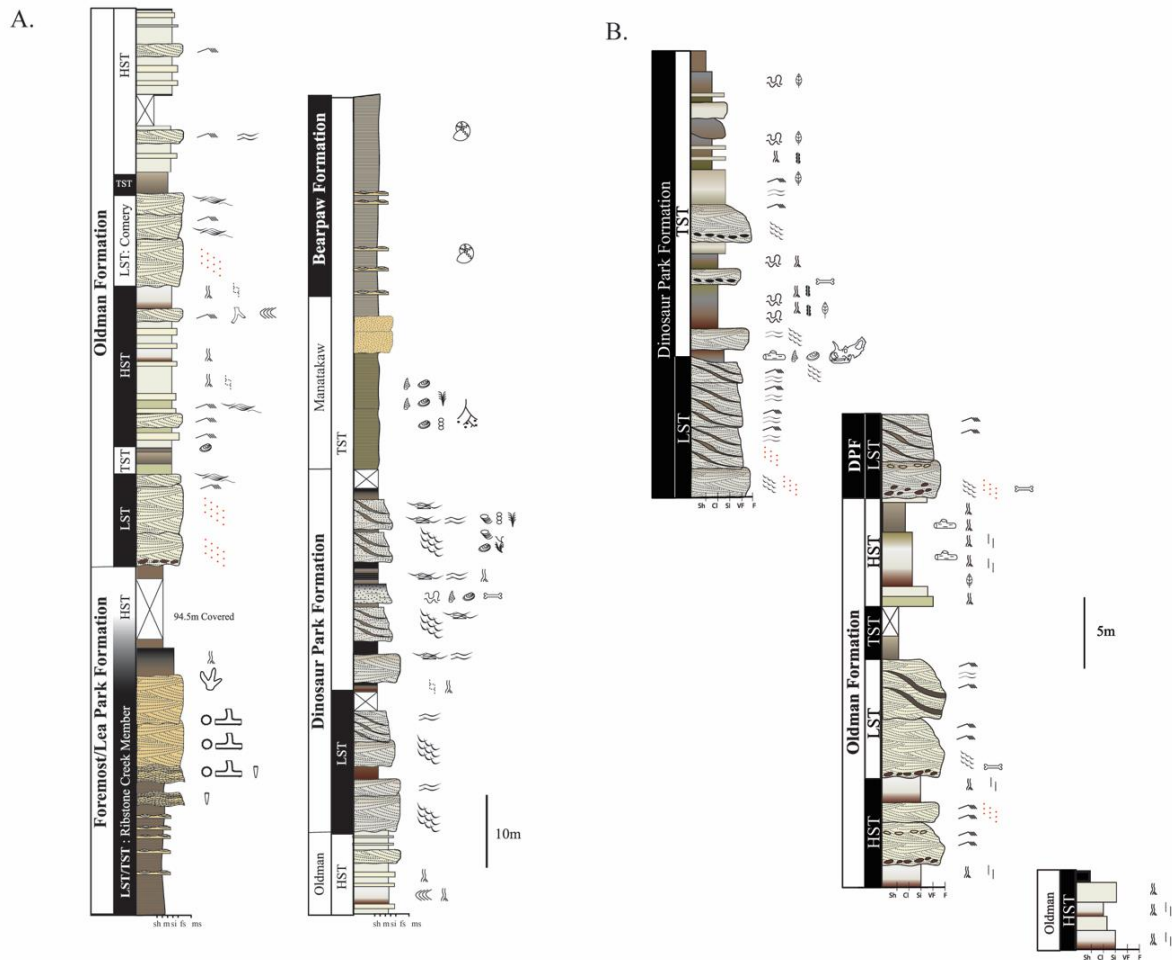


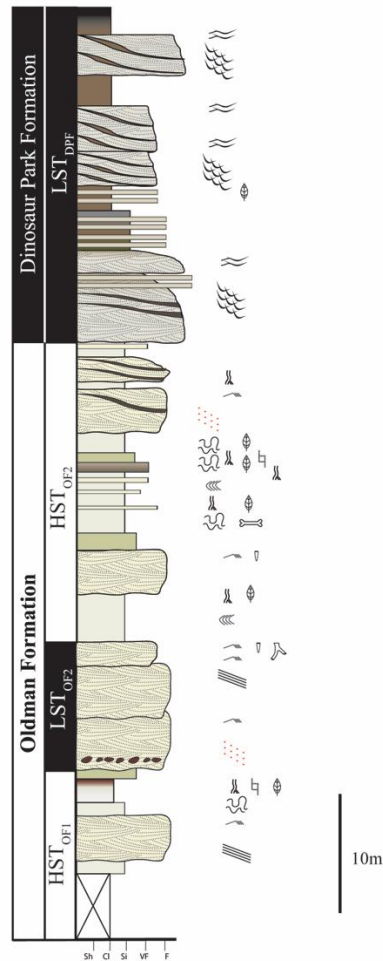
Figure 4.4: Representative composite lithostratigraphic log profiles of exposed outcrop near **A.** Woodpile Coulee, Saskatchewan and **B.** Muddy Lake, Saskatchewan. C - Coal; Sh - Shale/claystone; M - Mudstone; Si - Siltstone; FSS - Fine-grained sandstone; MSS - Medium-grained sandstone; LST - Lowstand Systems Tract; TST - Transgressive Systems Tract; HST - Highstand Systems Tract. For symbol legend, see Figure 4.3.

4.3 Historical Stratigraphic Nomenclature

The BRG in Alberta was first referred to as the Belly River ‘series’ by Dawson (1883) who described nonmarine deposits along the Milk River in southern Alberta. He divided the ‘series’ into the ‘lower Sombre Beds’ and ‘upper Pale Beds’. Slipper and Hunter (1931) renamed the upper Pale Beds as the Oldman Formation; Russell and Landes (1940) renamed the lower Sombre Beds as the Foremost Formation. McLean (1971) considered the Foremost and Oldman formations difficult to distinguish, and combined them as the Judith River Formation, a name that had priority in Montana. Eberth and Hamblin (1993) elevated the Judith River Formation to Group status, and subdivided it into the Foremost, Oldman, and Dinosaur Park formations, in ascending order. Jerzykiewicz and Norris (1994) renamed the Belly River Series the Belly River Group, which included all sediments between the Pakowki Formation (Lea Park Formation of Saskatchewan) and Bearpaw Formation. This terminology was adopted by the petroleum industry: Hamblin and Abrahamson (1996) then used this nomenclature for deposits in southern Alberta. Subsequently the name ‘Judith River Group’ was dropped in favor of the Belly River Group. The Judith River Formation (Bowen 1915; Rogers, 1995; Rogers et al., 2016) is nonetheless still used in Montana.

Original reference to the Judith River beds in northern Montana was published by Meek and Hayden (1856), with Hayden (1856) officially proposing the term Judith Group. In the first comprehensive study of the Judith River Formation in Montana, Stanton and Hatcher (1905) identified the type area and described the lithology. The term Judith River Formation began to be employed in the early 1900s and has been used in Montana ever since (Lambe, 1907; Peale, 1912; Bowen, 1915; Rogers, 1995; Rogers et al., 2016). Rogers et al. (2016) identified four

A.



B.

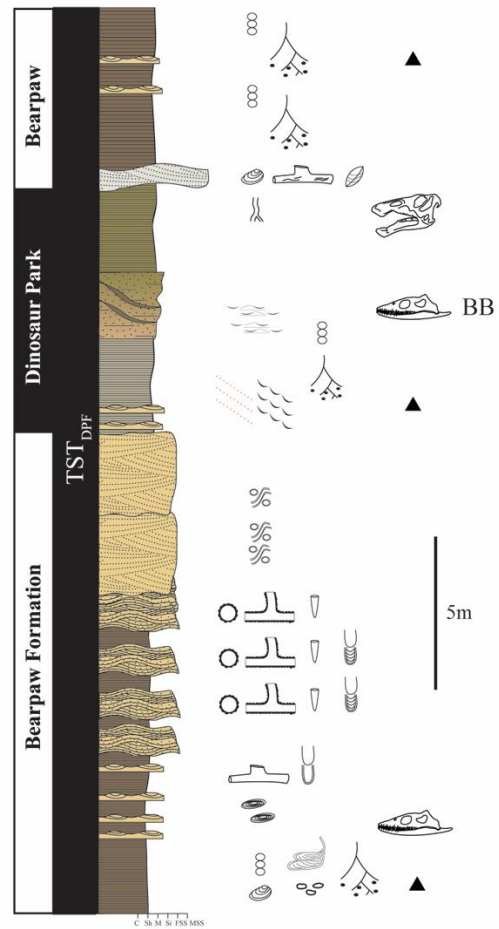


Figure 4.5. Representative composite lithostratigraphic log profiles of exposed outcrop near **A.** Sandy Point, Alberta and **B.** Herschel, Saskatchewan. C - Coal; Sh - Shale/claystone; M - Mudstone; Si - Siltstone; FSS - Fine-grained sandstone; MSS - Medium-grained sandstone; LST - Lowstand Systems Tract; TST - Transgressive Systems Tract; HST - Highstand Systems Tract; BB – bone bed. For symbol legend, see Figure 4.3.

The Belly River Group and adjacent formations record alluvial and coastal plain, marginal-marine, and wave-dominated shallow-marine deposition. In describing the formations and members of the Belly River Group, we propose a revision to the formal nomenclature for these deposits in Saskatchewan. In ascending order, we recognize the Foremost, Oldman, and Dinosaur Park formations established by Eberth and Hamblin (1993). The Judith River Formation of McLean (1971) is dropped, and we treat the clastic wedge as the Belly River Group as recognized in Alberta (Hamblin & Abrahamson, 1996; Eberth, 2005). A new stratigraphic member within the DPF is identified and described in the Cypress Hills and is similar to the Woodhawk Member of Rogers et al. (2016). The Manâtakâw Member is named in recognition of the Plains Cree, and is their traditional name for the Cypress Hills.

4.4 Stratigraphy and Sedimentary Environments

The Belly River Group records fluvial to marginal-marine deposition in several transgressive-regressive cycles. When interpreting depositional setting, we use the environmental framework for 1) wave-dominated shorelines; 2) wave-dominated, tidally influenced, river-affected coastlines; and (3) fluvial channels and their associated floodplain deposits (Gilbert et al., 2019). Each formation has distinct depositional cycles and patterns, reflecting variations in accommodation space, sediment supply, and contemporary climate.

Canadian Landmaster Belanger
10-23-007-25W3

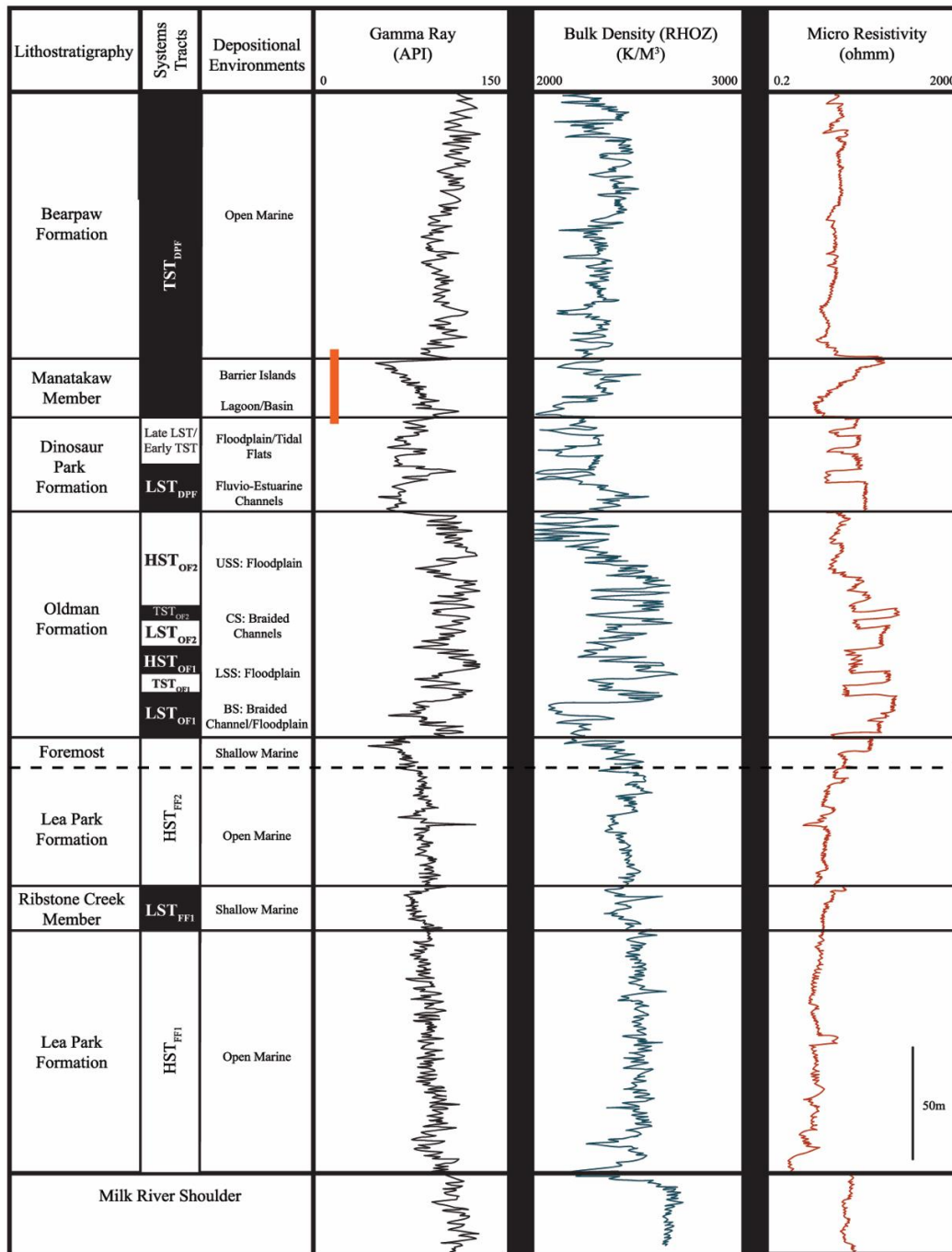


Figure 4.6: Representative well log highlighting stratigraphy, systems tracts, and depositional environments of the Belly River Group in the subsurface of southwestern Saskatchewan (Canadian Landmaster Belanger – 10-23-007-25W3). This well illustrates the typical gamma ray - bulk density - resistivity log signatures of the Belly River Group. Dashed line of the Foremost Formation indicates its sporadic occurrence throughout the study area. Red line indicates available core that was logged for this study.

4.4.1 Foremost Formation

The Foremost Formation crops out at Woodpile Coulee and can be traced in the subsurface throughout southwestern Saskatchewan. It has been defined as any formation between the Milk River Shoulder and Oldman formations capped by a sandstone bed thicker than two meters (Gordon, 2000). The FF comprises coarsening-upwards, wave-dominated, shallow-marine successions in both well logs and outcrop. In well logs, interfingering units of the FF are recognized by a leftward gamma shift (Fig. 4.6), indicating a decreased gamma value (Gordon, 2000). In Alberta, the Foremost Formation is paralic to nonmarine, and reflects a major regressive phase of the Belly River Group (Eberth, 2005). In western Saskatchewan, the FF underlies the Oldman Formation but thins to the east, becoming a series of interfingering parasequences within the Lea Park Formation, and is not everywhere in contact with the OF. The Ribstone Creek Member (RSC), a distinct shoreface succession within the FF capped by backshore carbonaceous shale and coal, was identified and mapped throughout the study area.

Boundaries

The Foremost Formation interfingers with the Lea Park Formation at the base and is represented by coarsening-upwards successions and associated flooding surfaces. These successions are identified in logs by a decreasing gamma signature coupled with a bulk density and resistivity signature for sandstone (Fig. 4.6). The base of the RSC represents a disconformity. The upper boundary of the FF is overlain unconformably by the erosive-based Oldman Formation.

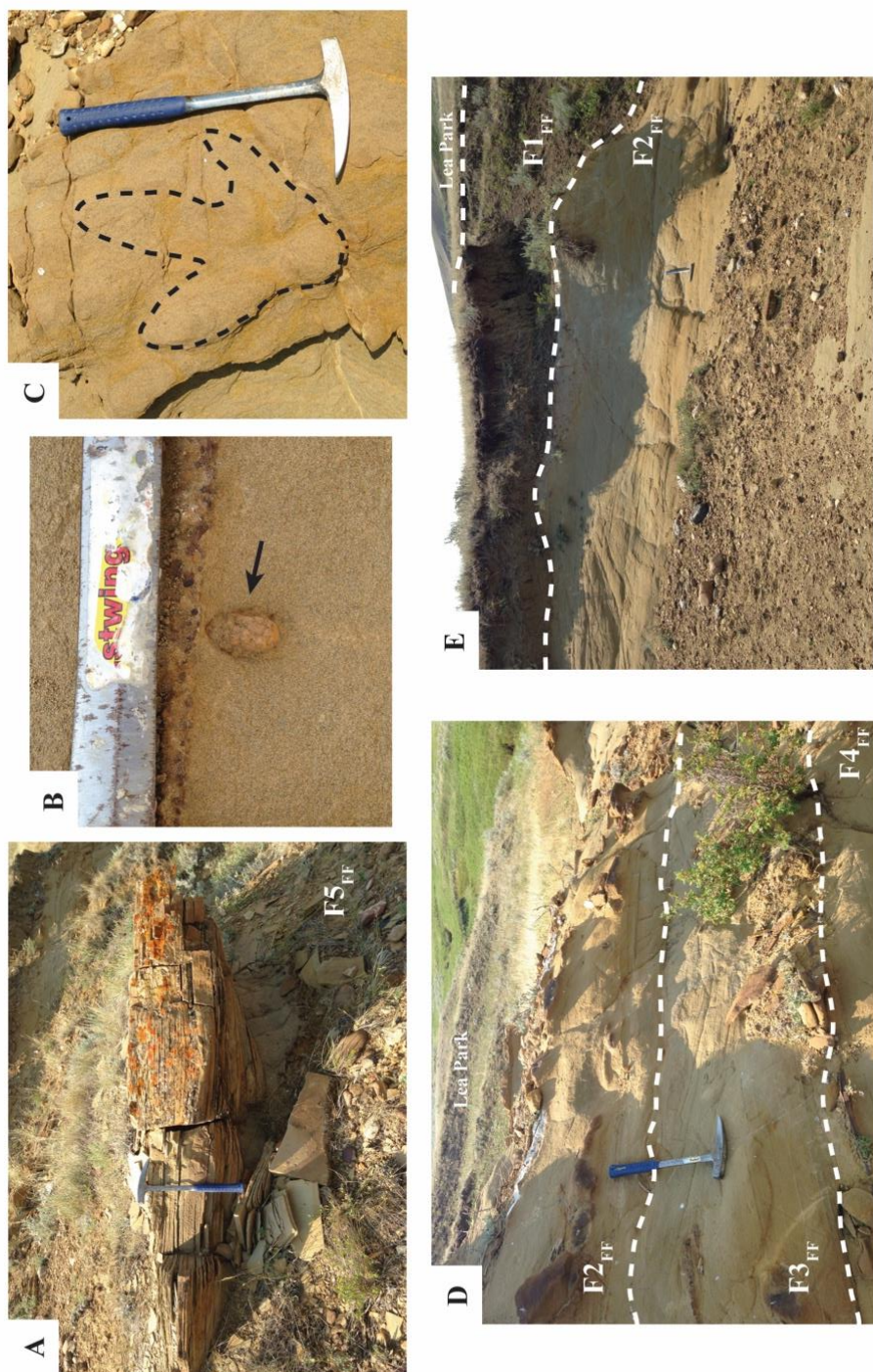


Figure 4.7: Selected photos of outcrop highlighting different facies and ichnofossils from the Foremost Formation (Ribstone Creek Member) in Woodpile Coulee, Saskatchewan. **A.** Hummocky cross-stratification from offshore transition deposits of F5_{FF}. **B.** *Ophiomorpha* isp. burrows in F4_{FF}. **C.** Dinosaur track preserved in foreshore facies of F2_{FF}. **D.** Foreshore, Upper shoreface, and lower shoreface deposits of F2-F5_{FF}. Note the overlying Lea Park Member in the background. **E.** Foreshore sandstones and backshore shales and coals of the Ribstone Creek Member immediately overlain by shales of the Lea Park Formation. Upper dashed line denotes a marine flooding surface.

Description

The Foremost Formation is characterized by massive mudstone with interbedded sandstone, siltstone and mudstone, very fine- to fine-grained sandstone, carbonaceous shale and coal, consisting of seven facies (F1_{FF} to F7_{FF}) that form coarsening-upwards successions. Rare fining-upward intervals near the Alberta border noted in well logs were not described due to lack of core and outcrop data. The lower cycles are composed of interbedded mudstone, siltstone, and sandstone with symmetrical ripples, micro-hummocky, and hummocky cross-stratification. Trace fossils in mudstone are dominated by horizontal to subhorizontal forms including *Chondrites* isp. and *Planolites* isp. Mudstone is heavily bioturbated, obscuring discrete trace-fossil identification. Coarse-grained, hummocky cross-stratified sandstone beds increase in abundance and thickness upwards. The upper portion of this formation consists of amalgamated, fine- to medium-grained sandstone beds displaying hummocky and trough cross-bedding, planar lamination and low-angle bedding (Fig. 4.7A, D, E). Some successions are capped with carbonaceous shale and coal (Fig. 4.7D). Trace fossils in the sandy intervals consist of vertical forms, such as *Ophiomorpha* isp. and *Skolithos* isp (Fig. 4.7B). Dinosaur tracks were identified in backshore facies, at Woodpile Coulee (Fig. 4.7C).

Sedimentary environment

The facies identified from the Foremost Formation (Table 4.2) are characteristic of clastic shallow-marine successions (Gordon, 2000). F1_{FF} to F6_{FF} gradationally and sequentially overlie one another, indicating a continuous succession of sub-environments in progradational stacking patterns bounded by flooding surfaces. Trace fossils identified throughout the study area are those of the *Cruziana* and *Skolithos* ichnofacies and are associated with offshore and shoreface facies, respectively (Buatois & Mángano, 2011). The combination of lithological characteristics

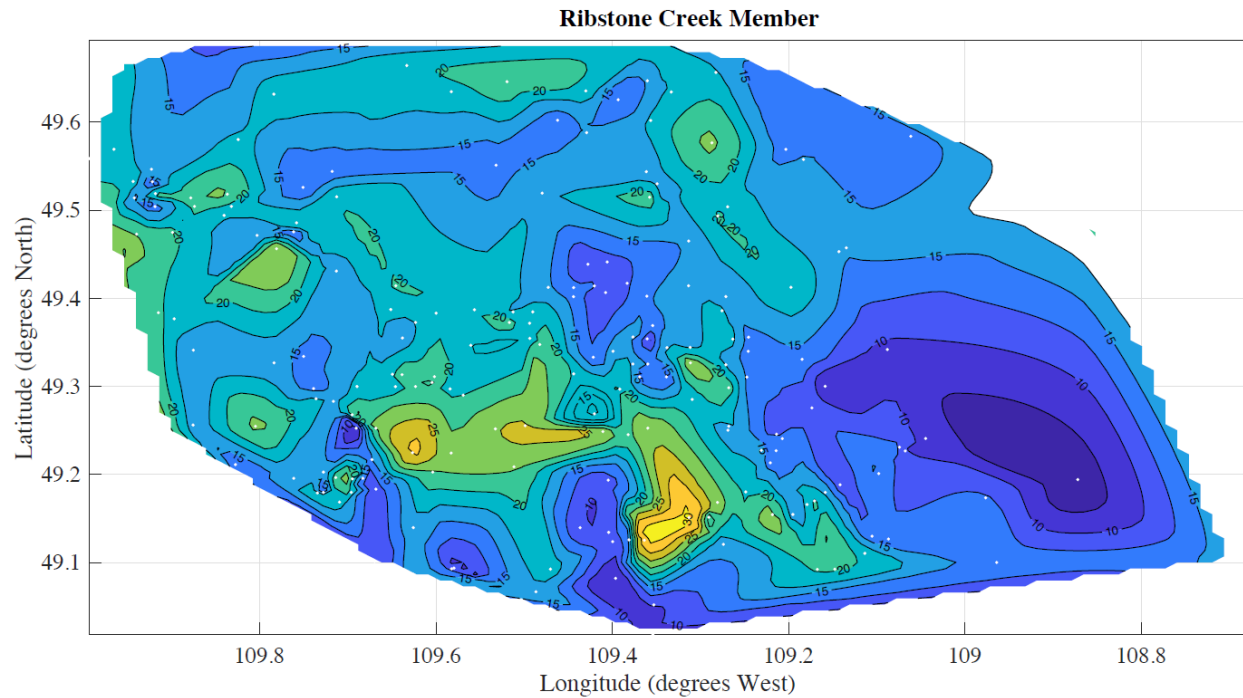


Figure 4.8A: Isopach map of the Ribstone Creek Member in the Cypress Hills study area. The bottom x-axis represents the 49th parallel, or the international border with the United States. The y axis represents the boundary between the 3rd and 4th meridian, or the provincial border between Alberta to the left, and Saskatchewan. Gap in extreme southwest corner is due to lack of subsurface data. The member thickens to the west, where it is known to amalgamate with the marginal-marine to terrestrial Foremost Formation. Darkest blue indicates thinnest strata.

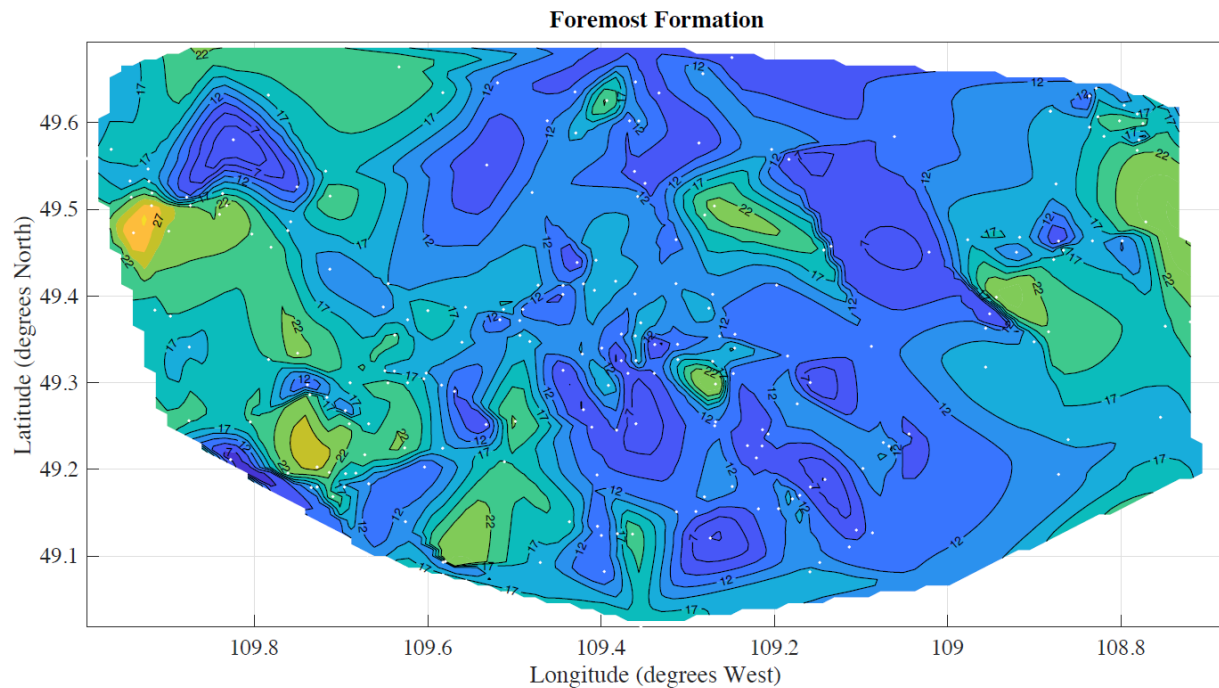


Figure 4.8B: Isopach map of the Foremost Formation in the Cypress Hills study area. The bottom x-axis represents the 49th parallel, or the international border with the United States. The y axis represents the boundary between the 3rd and 4th meridian, or the provincial border between Alberta to the left, and Saskatchewan. Gap in extreme southwest corner is due to lack of subsurface data. Inconsistency in thickness is due to erosional downcutting of the Oldman Formation into underlying FF deposits. This formation continues into Montana, where it is loosely correlated with the Parkman Sandstone Member.

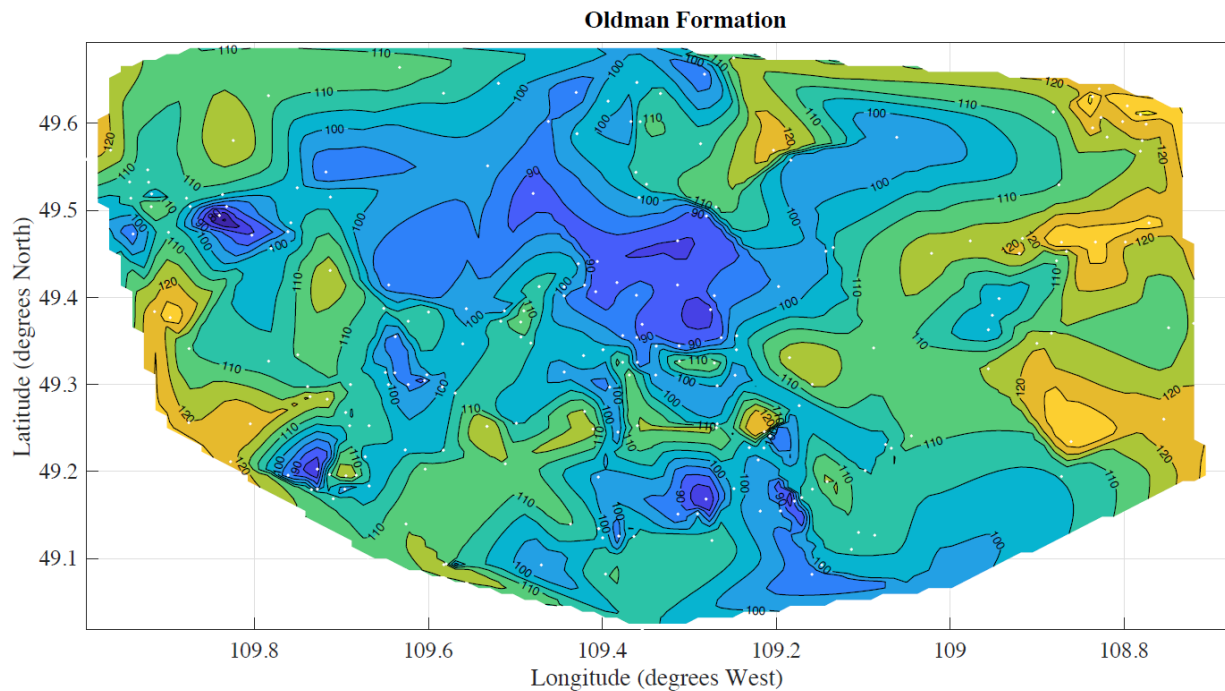


Figure 4.8C: Isopach map of the Oldman Formation in the Cypress Hills study area. The bottom x-axis represents the 49th parallel, or the international border with the United States. The y axis represents the boundary between the 3rd and 4th meridian, or the provincial border between Alberta to the left, and Saskatchewan. Gap in extreme southwest corner is due to lack of subsurface data. Note a decrease in thickness trending northwest – southeast, which is interpreted as reflecting 1) fluvial input from the southwest draining to the northeast during OF deposition, and 2) downcutting of the DPF into the OF. This formation continues into Montana, where it correlates with the McClelland Ferry Member.

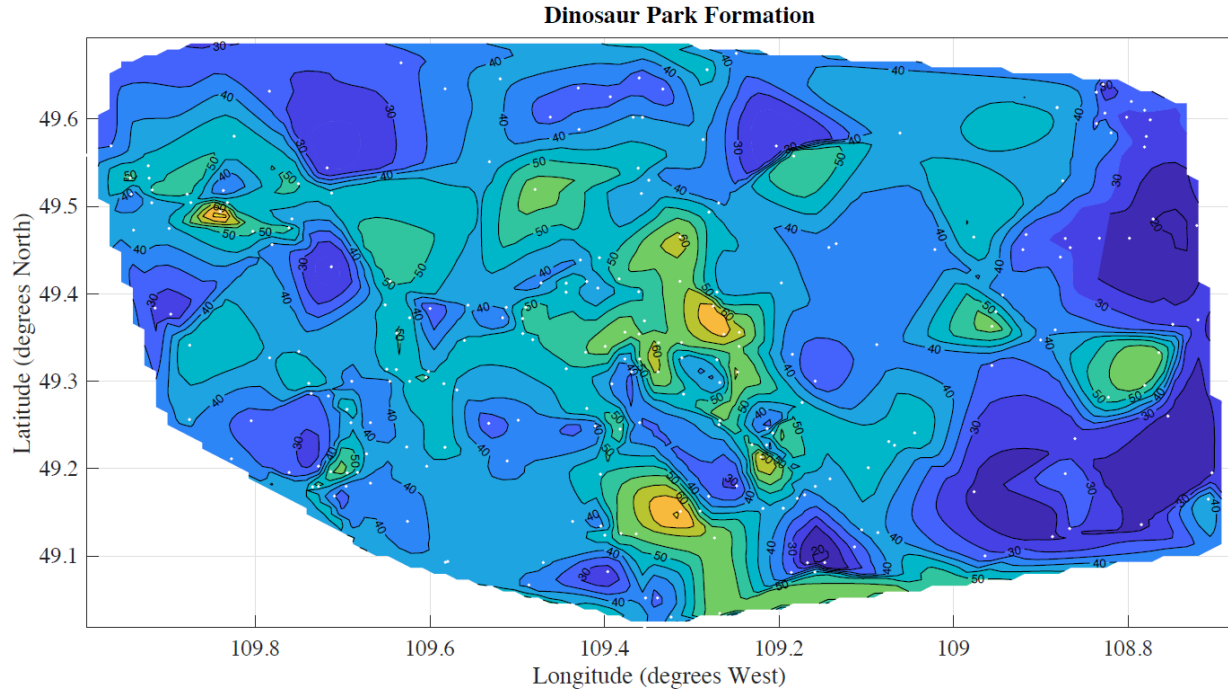


Figure 4.8D: Isopach map of the Dinosaur Park Formation in the Cypress Hills study area. The bottom x-axis represents the 49th parallel, or the international border with the United States. The y axis represents the boundary between the 3rd and 4th meridian, or the provincial border between Alberta to the left, and Saskatchewan. Gap in extreme southwest corner is due to lack of subsurface data. Increased thickness in a northwest – southeast trend is interpreted as 1) infill of an incised valley cut during a significant base-level fall and its subsequent infill during base-level rise and, 2) cannibalization of sediments in the eastern portion of the study area with advancement of the WIS transgression. This formation continues into Montana, where it correlates with the Coal Ridge Member.

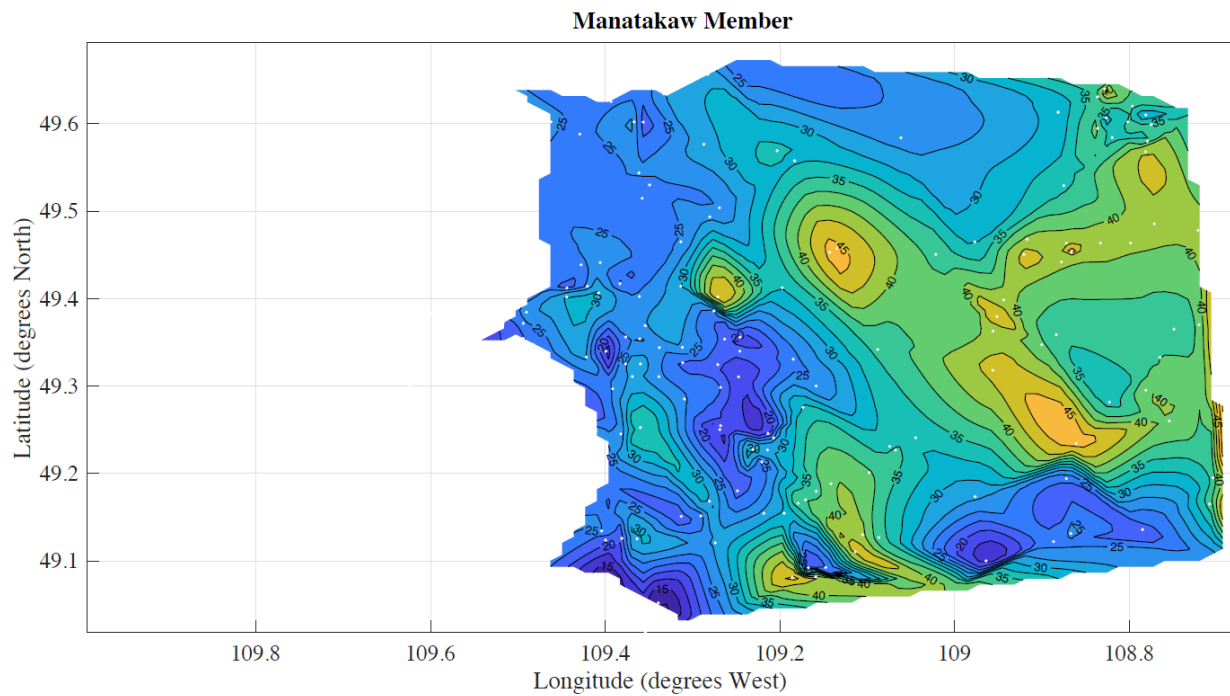


Figure 4.8E: Isopach map of the Manâtakâw Member in the Cypress Hills study area. The bottom x-axis represents the 49th parallel, or the international border with the United States. The y axis represents the boundary between the 3rd and 4th meridian, or the provincial border between Alberta to the left, and Saskatchewan. Gap in extreme southwest corner is due to lack of subsurface data. This member decreases in thickness towards the west, where it eventually terminates against the DPF due to flooding of the WIS. This formation continues into Montana, where it correlates with the Woodhawk Member, which are interpreted as shoreface deposits.

and ichnology suggests a fully marine, wave-dominated environment periodically affected by storms and subaerial exposure at maximum regression. F7_{FF}, identified at the top of some parasequences, contains marine bivalves reworked during flooding events. Fining-upwards cycles identified in well logs have previously been interpreted as estuarine channel fill (Gordon, 2000). Overall, this stratigraphic succession records a progradational transition from fully marine shale of the Lea Park Formation, to shoreface and estuarine deposits of the Foremost Formation. The oldest deposits are found on the western margins of the study area, closest to the Alberta border, with the youngest on the eastern edge of the study area (Gordon, 2000).

Formation geometry

Isopach maps were constructed for the Ribstone Creek Member and the uppermost Foremost Formation (clastics directly underlying the Oldman Formation). The Ribstone Creek Member (Fig. 4.8A) is 4.4–29.4 m thick, thinning significantly towards the east and moderately towards the southeast. The presence or absence of the upper FF (Fig. 4.8B) and its highly variable thickness are a result of 1) eastward thinning of the lobe as it approached the WIS, and 2) downcutting and erosion due to base-level fall immediately preceding advancement of OF fluvial clastics. The boundary between the Foremost and Oldman formations in southwestern Saskatchewan represents a sequence boundary. The thickness of the FF varies greatly throughout the study area due to downcutting and erosion, with evidence preserved by the basal fluvial deposits of the overlying Oldman Formation.

The Ribstone Creek Member represents progradation of a complete wave-dominated parasequence, recording shelf deposits at the base and shallowing to coastal plain mudstones and coals at the top. The member is 6.3–30.6 m thick, thinning to the east and southeast (Fig. 4.8A). The base of the RSC is interpreted as a sequence boundary, indicative of downcutting and



Figure 4.9: Selected panoramic outcrop photos of the Oldman and Dinosaur Park formations. **A.** The lower ‘basal sandstone’ of southwestern Saskatchewan in Woodpile Coulee. This contact sits directly above shales of the Lea Park Formation. Note the basal contact of the Comrey Sandstone roughly 20 m to the south. Both sandstones are resistant to weathering, and can be traced laterally for ~1 km to the east and west before terminating against the fault’s edge. Formations are dipping at roughly 30°. **B.** Steep, block-faced siltstones and sandstones of the Oldman Formation overlain by recessive, somber-colored sandstones and mudstones of the Dinosaur Park Formation at Sandy Point, Alberta. The lower dashed line indicates the contact between the two formations. The upper dashed line indicates erosional downcutting by overlying glacial till deposits. Note the truncation of floodplain deposits against buff-colored braided isolated channels in the Oldman Formation. Leached paleosols of the OF appear as whitish horizons. **C.** Oldman and Dinosaur Park contact at Sandy Point, Alberta. The lower dashed line denotes the upper contact of the Comrey Sandstone, which crops out in the valley. Upper dashed line indicates the contact between the DPF and OF.

subsequent progradation of a clastic wedge following base-level fall. The RSC terminates between ranges 22 and 21W3, downlapping onto marine mudstone and shale of the Lea Park Formation.

4.4.2 Oldman Formation

The Oldman Formation consists of eight facies (Table 4.3), and is characterized by resistant, buff- to pale yellow-colored sandstone and mudstone. The OF crops out at Woodpile Coulee in the Cypress Hills, at Sandy Point in the South Saskatchewan River Valley near the Alberta-Saskatchewan border, and at Muddy Lake in west-central Saskatchewan (Fig. 4.4, 4.5). Despite its high sandstone content, the Oldman Formation is identifiable in well logs by a strong gamma-ray signature attributed to high potassium feldspar content (Gordon, 2000; Eberth, 2005; Hamblin, 1997a). In Alberta, the OF is exclusively alluvial and records maximum regression and subsequent progradation of the Belly River Group in Alberta and Saskatchewan. In previous studies, the OF was found to thicken towards the southwest, indicating Montana as the primary sediment source area (Eberth & Hamblin, 1993; Hamblin, 1997a; Eberth, 2005).

Boundaries

In Alberta, the base of the Oldman Formation is placed at the top of a series of amalgamated paleochannel deposits within the Foremost Formation known as the Herronton Sandstone. The Herronton Sandstone is absent in Saskatchewan as it is in southeastern Alberta, so this criterion cannot be used (Hamblin, 1997a). Therefore, in well logs, the base of the OF is placed at the first major gamma deflection to the right. In outcrop, the base is placed at the first blocky-faced, buff-colored amalgamated fluvial sandstone or floodplain siltstone directly overlying darker shallow-marine to paralic deposits of the Foremost or Lea Park formations (Fig. 4.9A, B). Erosional amalgamated sandstone containing abundant intraformational siderite pebbles incises the

underlying Foremost and Lea Park formations throughout much of the study area (Fig. 4.4A, 4.9A). These paleochannels and their associated floodplains are recognized as the lower contact of the OF, and their deposits are referred to herein as the ‘basal sandstones’ (Fig. 4.9A).

The uppermost OF contact is unconformable and strongly diachronous from north to south with overlying deposits of the Dinosaur Park Formation (Eberth & Hamblin, 1993; Hamblin, 1997a; Eberth, 2005). This contact represents a disconformity, and records considerable paleoenvironmental and base-level changes between the two formations.

Description

The Oldman Formation contains eight facies (F1_{OF} to F8_{OF}; Table 4.3), forming fining-upwards packages of pale sandstone, interbedded siltstone and sandstone, and mudstone (Fig. 4.9B). In southwestern Saskatchewan, the OF can be divided into three informal units in outcrop and subsurface logs. The basal and topmost units are dominantly fine-grained siltstones and lenticular fine-grained sandstones, with the basal sandstone included in the lower unit. The middle unit consists of a thick succession of amalgamated paleochannel deposits and is interpreted as lithostratigraphically equivalent to the Comrey Sandstone (CS) of southern Alberta.

The basal and topmost units are composed of amalgamated, lenticular sandstone, fine-grained sandstone, interbedded sandstone, siltstone and mudstone, massive light mudstone, and dark muddy shale of F2_{OF} to F8_{OF} (Fig. 4.9B). Sandstone beds are tabular to lenticular, displaying erosive bases, trough cross-bedding, current- and climbing ripples and parallel lamination. Mudstone laminae and intraclasts are rare. Siltstone and mudstone layers are tabular, and commonly appear as massive. Where exhibiting structures, these beds preserve planar lamination and current ripples. Mudstone beds are massive to contorted and laterally

discontinuous, locally terminating against lenticular sandstone of F2_{OF} (Fig. 4.9B). Prominent white layers of siliceous siltstone and sandy siltstone are common, and associated with clay-lined, deeply penetrating vertical root trace fossils. In well logs, the upper and lower units are characterized by strong overall gamma-ray deflections to the right, with local leftward deflections (Fig. 4.6).

The basal and middle interval consists of amalgamated, medium to very-fine grained sandstone sheets 0.5–1.3 m thick. The ‘basal sandstone’ dominates the lower ~5–10 m of the OF, and consists of amalgamated, erosive-based, trough cross-bedded, fine- to medium-grained sandstone with intraformational siderite clasts at its base (Fig. 4.9A, C). In well logs, this unit is identified by a sharp deflection to the left, and a steady upwards shift to the right, characteristic of fluvial deposits (Fig. 4.6). The Comrey Sandstone crops out as sheets of trough cross-bedded and current-ripple cross-laminated, fine- to medium-grained sandstone (Fig. 4.9C). Data from unidirectional sedimentary structures indicate a paleocurrent towards the east-northeast (Eberth et al., 1990; Eberth & Hamblin, 1993). Rare root trace fossils and *Skolithos* isp. are found at the top of some beds within the amalgamated channels (Fig. 4.10A). Basal lags consisting of any combination of calcrete nodules, mudstone rip-ups, dinosaur bones, coalified wood, and bivalve and gastropod shells are common. In well logs, the base of the Comrey Sandstone is marked by a sharp gamma-ray deflection to the right, coupled with a bulk-density signature for sandstone (ranging in thickness from ~5–15 m thick) that remains consistent through the entirety of the unit (Fig. 4.6).

F3_{OF}-F8_{OF} are found within the upper and lower Oldman Formation. Siderite-cemented and mud-lined root trace fossils, *Skolithos* isp., *Planolites* isp. and meniscate backfilled *Taenidium* isp. are associated with F3_{OF}-F5_{OF}. *Taenidium* isp. (Fig. 4.10B, C) has been observed

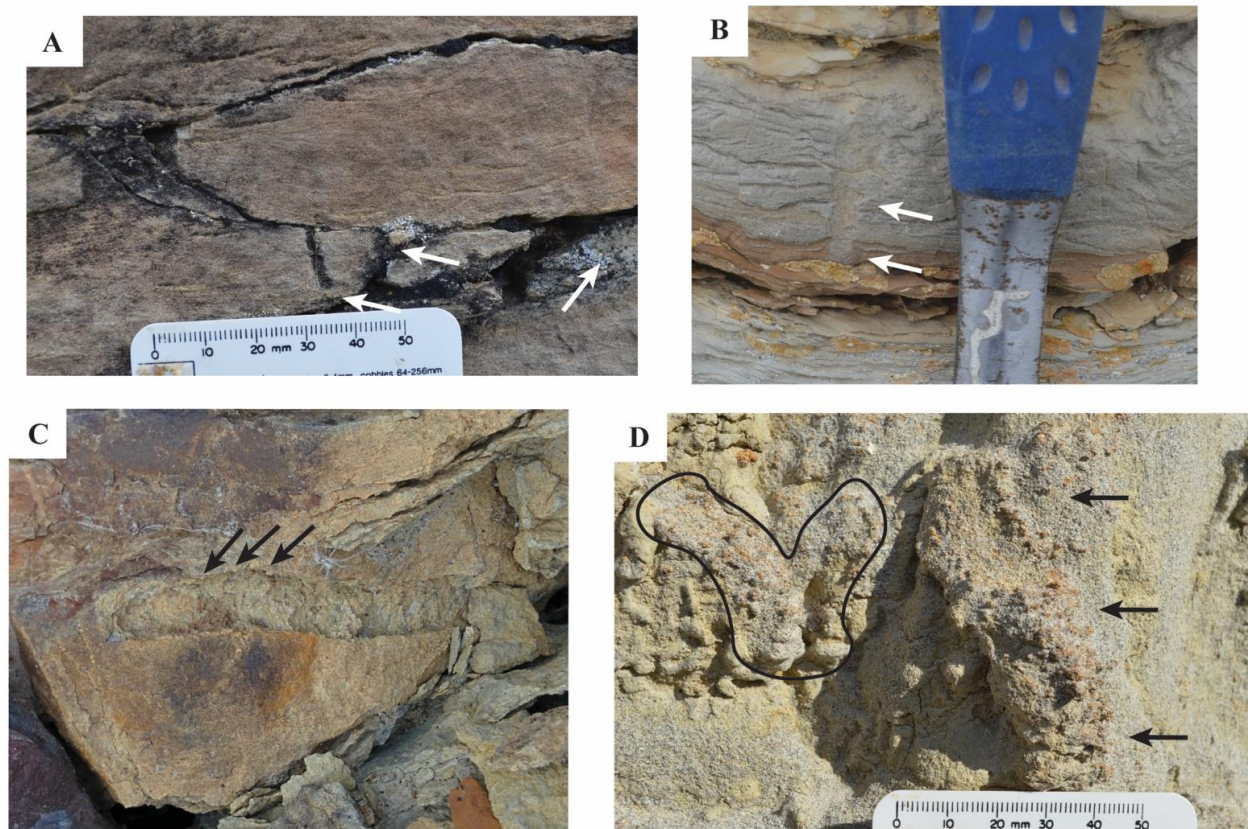


Figure 4.10: Selected photos of biogenic structures in the Oldman Formation. **A.** *Skolithos* isp. burrows between bedsets in the Comrey Sandstone at Sandy Point, Alberta. **B.** *Taenidium* isp. burrows crosscutting isolated braided sandstones in the upper HST_{OF2} at Woodpile Coulee, Saskatchewan. This trace was likely colonizing upper floodplain deposits, and downcutting into underlying fluvial deposits. **C.** *Taenidium* isp. in floodplain deposits of HST_{OF2} at Sandy Point, Alberta. Note the spreiten backfill and fecal pellets that characterize this ichnogenus. **D.** *Camborygma* isp. made by freshwater crayfish in the Comrey Sandstone (LST_{OF2}) at Sandy Point, Alberta. Note the fecal pellets used to reinforce the walls (arrows), and the y-shaped burrow bifurcation. Reinforcing the burrow wall indicates this species was living in turbulent conditions with shifting, sandy substrate conditions.

in outcrop to cut into underlying beds and crosscutting older fluvial sandstones. F8_{OF} is closely associated with the Comrey and basal sandstones, and is found exclusively at the top of these units. F1_{OF} is restricted to the Comrey and basal sandstone, and F2_{OF} is found throughout the formation. Rare *Camborygma* isp. and common *Skolithos* isp. are present within F2_{OF} (Fig. 4.10A, D).

Sedimentary environment

The Oldman Formation records fluvial channels, levees, crevasse splays, floodplains, paleosols, and rare episodic marine incursion in a well-drained, highly seasonal floodplain (Eberth & Hamblin, 1993; Noad, 1993; Eberth, 2005). In the upper and lower portions of the formation, fine-grained deposits of interbedded sandstone, siltstone and mudstone, and massive mudstones of F3_{OF} to F6_{OF} are interpreted as levee, splay, and floodplain deposits. Silica-rich siltstone and sandy siltstone of F4_{OF} are interpreted as leached paleosols (Eberth, 2005). In levees and crevasse-splay deposits, deep clay-lined root traces and meniscate backfilled burrows indicate that the sediment experienced periodic subaerial exposure and periods of flooding, with a fluctuating water table (Frey et al., 1984; Frey & Pemberton, 1987; Buatois & Mángano, 2011). Bulk density logs denote thin and laterally discontinuous coal beds in the upper silty beds of the OF in the Cypress Hills, a trend that is observed in the upper OF at Muddy Lake, Saskatchewan (Fig. 4.4B). Dark gray and greenish-gray mudstone of F8_{OF} is interpreted as marginal-marine deposits. In well logs, strong rightward gamma-ray signatures represent siltstone-dominated floodplain deposits, with leftward deflections interpreted as associated sand-dominated braided streams.

Sandstone ranges from single, isolated, lenticular channel-fills, to amalgamated, multistorey tabular beds. Isolated channels are common in the upper and lower fine-grained

portions of the OF and display evidence of periodic exposure, recorded by *Taenidium* isp. and root traces at the top of beds. Amalgamated paleochannels commonly found at the base of the OF in the study area are not evident in Alberta. These deposits are overlain by F8_{OF} in Woodpile Coulee, and are interpreted as marginal-marine mudstone and shale. Large- and medium-scale, trough cross-bedded strata at Sandy Point (Fig. 4.9C) and Woodpile Coulee correlate with easily discernible low gamma-ray radioactivity in the middle portion of the formation. This unit is assigned to the Comrey Sandstone and can be correlated across the study area. This facies records shallow, low-sinuosity ephemeral stream deposits in a semi-arid environment (Eberth & Hamblin, 1993; Hamblin, 1997a; Eberth, 2005). In southeastern Alberta, Troke (1993) gathered sedimentologic evidence that suggests tidal influence and a possible marine incursion at the top of the Comrey Sandstone. Noad (1993) reported rare lateral-accretion deposits in the upper 10 m of the Oldman Formation, implying migrating paleochannels. This is also observed in the OF at Muddy Lake, where upper OF fluvial channels display lateral accretion and inclined heterolithic stratification (IHS). Amalgamated and laterally accreting paleochannels indicate periods of low accommodation, whereas isolated channels signal high or increasing accommodation in fluvial environments (Catuneanu et al., 2009 or Catuneanu, 2006?).

Evidence from Saskatchewan further supports the interpretation of marine incursion during OF deposition. Two small minor transgressions are believed to have occurred, with one at the top of the basal sandstone, and another at the top of the CS. Both amalgamated sandstones are directly and abruptly overlain by ~ 1 m of shale and mudstone (F8_{OF}), which implies estuarine deposition during a period when accommodation was available. Evidence for tidal influence at the top of the Comrey Sandstone in southeastern Alberta supports this hypothesis (Troke, 1993).

Formation geometry

The Oldman Formation is 73.7–132.1 m thick, thickening southwards (Fig. 4.8C). This pattern agrees with previous studies that propose southwestern Montana and southeastern British Columbia as probable sediment source areas for the OF (Eberth & Hamblin, 1993). This is also supported by paleocurrent data from Woodpile Coulee, Sandy Point, and Muddy Lake, all of which show paleocurrent drainage towards the east-northeast. Localized northeast-southwest thinning of the OF in the study area is interpreted as downcutting by incised valleys (Fig. 4.8C, D) of the overlying Dinosaur Park Formation.

4.4.3 Dinosaur Park Formation

In Saskatchewan, the Dinosaur Park Formation consists of six facies, and is characterized by immature sandstone, heterolithic deposits, mudstone, and abundant coal seams. The DPF crops out at Woodpile Coulee, and to varying extents along the North and South Saskatchewan River valleys, Sandy Point, Alberta, and Muddy Lake and Herschel, Saskatchewan (Eberth et al., 1990; McLean, 1971; Gilbert et al., 2018). The DPF is identified in well logs by sandstone with low gamma-ray radioactivity and high coal content, identified via bulk density logs. The DPF is fluvio-estuarine at its base and increasingly marginal-marine at the top, recording onset of the 2nd order Bearpaw Cycle transgression of the Western Interior Seaway (Kauffman & Caldwell, 1993; Tsujita, 1995). The DPF thickens to the north and northwest, indicating northwestern Alberta – northeastern British Columbia as the main sediment source area (Eberth & Hamblin, 1993; Hamblin, 1997b). Lagoon, estuarine, and barrier island sandstone forms thick, easily recognizable successions between ranges 21 and 28W3. These distinctive deposits are here given Member status in southwestern Saskatchewan, and are described separately. All known

vertebrate fossil localities of Campanian age in Saskatchewan have been recovered from the DPF (Eberth et al., 1990; Gilbert et al., 2018).

Boundaries

The base of the DPF is sharp, diachronous north to south, and disconformable. In well logs, this is recognized by a sharp gamma-ray deflection to the left, coupled with a bulk density signature for sandstone (Fig. 4.6). In outcrop (Fig. 4.9B, C), the base is placed at the appearance of somber gray, laterally accreting fluvial sandstone commonly with extraformational chert pebbles at the base (Eberth & Hamblin, 1993). The upper contact of the Dinosaur Park Formation is conformable with the lower mudstone and shale of the Bearpaw Formation. East of range 28W3, the boundary between the DPF and BP is placed at the top of the barrier-island sandstones, distinct in both core and well log signatures (Fig. 4.6). These deposits are recognized as a discrete member within the DPF (Manâtakâw Member). West of range 28W3, where the Manâtakâw Member is absent, a high gamma-ray signature and a termination of coal beds marks the transition to the marine Bearpaw Formation in the subsurface.

Description

The Dinosaur Park Formation is characterized by fine-grained sandstone and mudstone, high organic content and considerable lithologic variability (Table 4.4). Erosionally based, planar- and trough cross-bedded, and current-rippled somber gray, fine-grained sandstone dominates the base of the formation (Fig. 4.11A). Basal sandstones are tabular, with sheet geometry, and range from single to multi-storied with bed thickness of 0.62–1.7 m. Inclined bedded sandstone is preserved at the top of some trough cross-bedded sandstone, and is interpreted as macroforms (Eberth et al., 1990; Eberth, 2005). Paleocurrent data gathered from cross-beds indicates flow towards the east-southeast (Eberth et al., 1990; Gilbert et al., 2018).

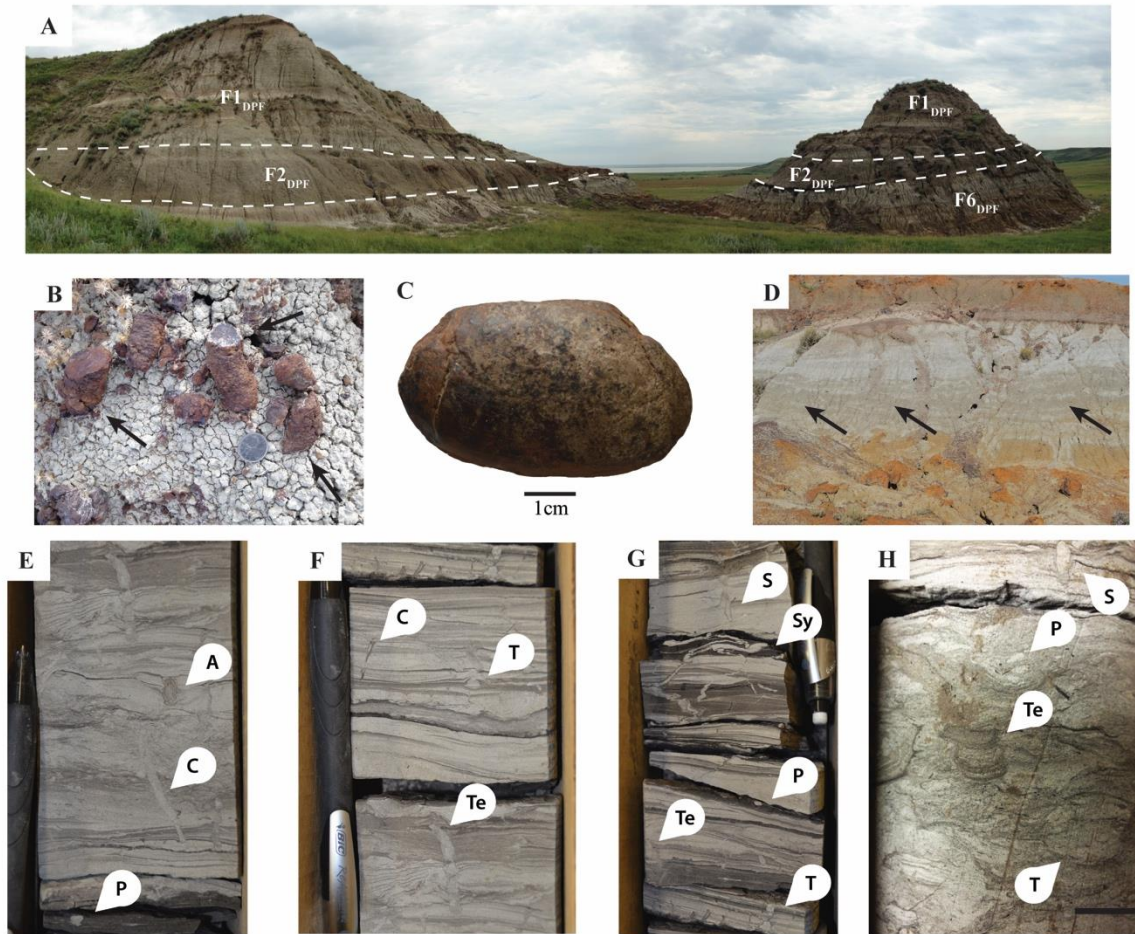


Figure 4.11: Selected photos from the Dinosaur Park Formation in both outcrop and core. **A.** Panoramic photograph of floodplain facies from the lowermost Dinosaur Park at Muddy Lake, Saskatchewan. Note the U-shaped geometry of F2_{DPF} truncating against inclined heterolithic stratification of F6_{DPF}. Deposits of F6_{DPF} in this photo are directly above the Oldman Formation contact. **B.** Nodular, siderite-encrusted root traces in F1_{DPF} at Muddy Lake, Saskatchewan indicate deposition took place in a waterlogged, anoxic environment. Canadian quarter for scale. **C.** Pelycopod (pisidiids) collected from U-shaped abandoned channel highlighted in A. **D.** Convolute bedding at the base of abandoned meander channels at Muddy Lake, Saskatchewan. **E.** Brackish-water trace fossils near the Dinosaur Park - Manâtakâw contact. Note the escape structures, indicating periods of heavy sedimentation. Carbonaceous laminae and double mud drapes are preserved at the base of the core (Core 07-02-004-27W3). **F.** Brackish-water trace fossils near the Dinosaur Park - Manâtakâw contact. Note the presence of both symmetrical and asymmetrical ripples, interpreted as wave and tide in origin, respectively (Core 07-02-004-27W3). **G.** Brackish-water trace fossils near the Dinosaur Park - Manâtakâw contact. Note the syneresis cracks near the lower contact of the Manâtakâw Member (Core 07-02-004-27W3). **H.** Brackish-water trace fossils from the upper Dinosaur Park Formation. All brackish-water forms were found in F6_{DPF} (Core 10-10-002-27W3). A - *Asterosoma* isp.; C - *Cylindrichnus* isp.; P - *Planolites* isp.; S - *Skolithos* isp.; Sy - syneresis cracks; T - *Thalassinoides* isp.; Te - *Teichichnus* isp. All scale bars = 1 cm. Pen for scale in photos E to G is xx cm long. See Table 4.4 for facies descriptions.

Overlying the basal sandstone, heterolithic deposits consisting of siltstones, mudstones, and shales alternate with thick- to thin-bedded, bright-banded to lignitic coal layers (Fig. 4.3). Pedogenesis is common throughout, and gleysol and siderite-cemented root development is present throughout several of the beds (Fig. 4.11B). Massive bedding, interbedded heterolithic sediments, horizontal lamination, and convolute bedding are pervasive (Fig. 4.11D). Trace fossils are rare, comprising simple, horizontal burrows and trails attributed mainly to *Planolites* isp., and *Mermia* isp. Local siderite-cemented *in situ* logs are present in fine-grained silty mudstones. Bivalves (pisidiids) and gastropods are common throughout this facies (Fig. 4.11C).

Up-section, organic-rich, upward-fining, inclined silty and muddy heterolithic sediments containing syneresis cracks, current-ripple lamination with mud drapes, and a diverse brackish-water trace-fossil assemblage (e.g., *Teichichnus* isp., *Cylindrichnus* isp., *Asterosoma* isp., *Planolites* isp.) mark the top of the DPF (Fig. 4.11F-H).

Sedimentary environments

The Dinosaur Park Formation was deposited in a low-lying coastal plain consisting of fluvio-estuarine channels, splays, and floodplains in a poorly drained lowland prone to marine incursion and tidal influence. Marine influence increases higher in the section, corresponding to transgression of the Western Interior Seaway (Fig. 4.12). Basal fluvial sandstone displays lateral accretion and inclined, mud-draped, unbioturbated heterolithic sandstone and mudstone, indicative of tidally influenced meandering channels. Overlying sandstone at the base of the formation, floodplain deposits contain fine- and very fine-grained sandstone laminae, siltstone and sandstone stringers, and convolute bedding, indicating periodic sediment influx resulting from crevasse-splay deposition (Elliot, 1986). Splay deposits are formed when levees are

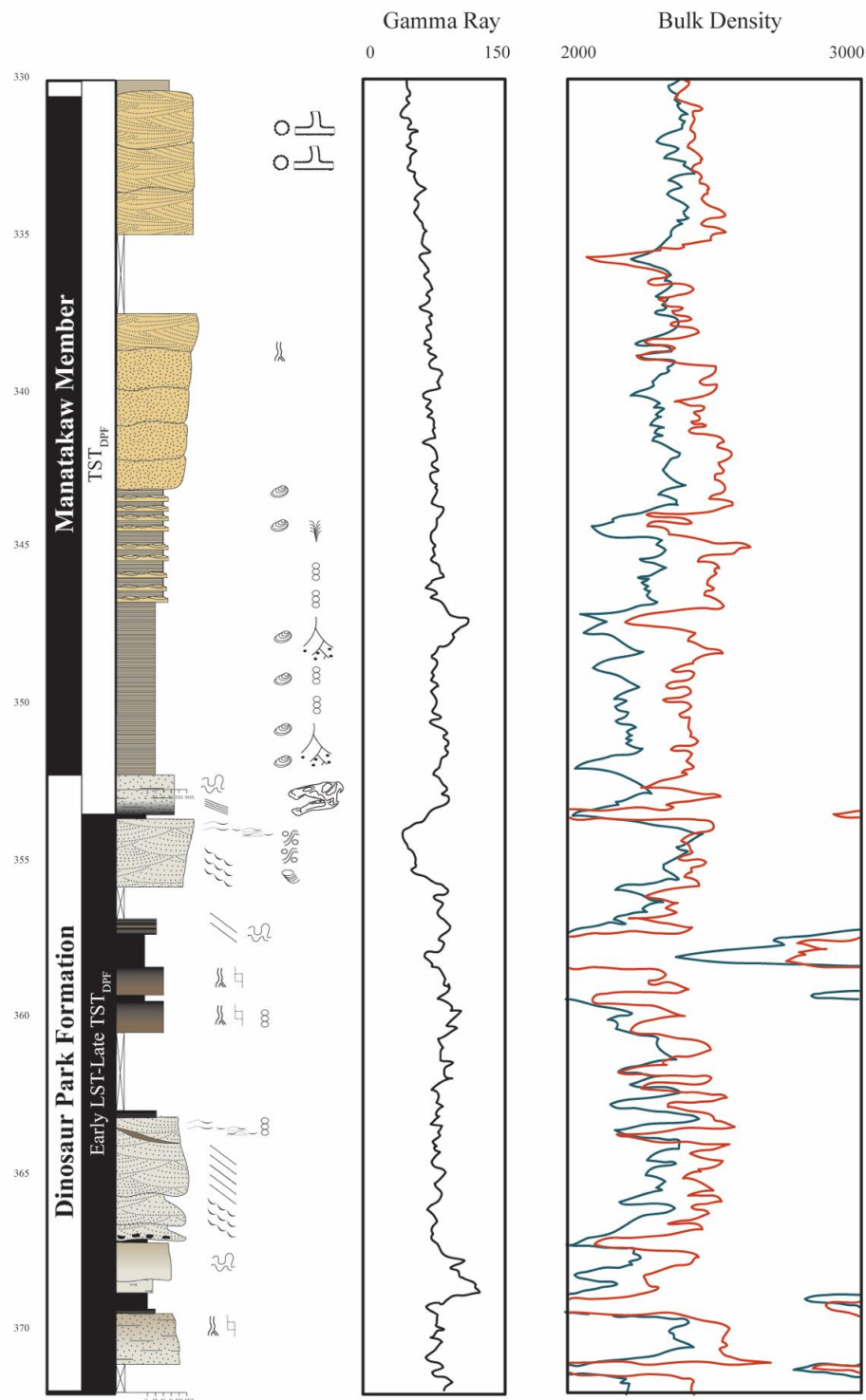


Figure 4.12: Representative lithostratigraphic log profiles of Canadian Landmaster Cypress Hills 06-31-06-25W3 and corresponding gamma (API) and bulk density log (K/M3). This core is proposed as the stratotype for the Manâtakâw Member in southwestern Saskatchewan. C - Coal; Sh - Shale/claystone; M - Mudstone; Si - Siltstone; FSS - Fine-grained sandstone; MSS - Medium-grained sandstone. See Figure 4.3 for symbol legend.

breached during flooding, and are common components of meandering stream environments, which frequently occur in areas with low gradients (Slingerland & Smith, 2004; Miall, 2010, 2013). Amalgamated fluvial channels overlain by heterolithic floodplain deposits indicate increasing accommodation throughout the Saskatchewan extent of the DPF.

The prevalence of mud, silt, and organic detritus in the DPF indicates deposition in a low-energy environment with considerable surrounding plant growth. Significant amounts of sediments were periodically deposited in overbank flooding events (Miall, 2013). Large peatmires, bogs, marshes and swamps developed into coal layers ranging in thickness from 0.1 to 3.3 m, which extend throughout the Cypress Hills region into Alberta and Montana (Frank, 2006). The extent of the coal beds indicates deposition in a low-lying, low-gradient environment. Siderite layers and nodules are a common feature in waterlogged soils (Retallack, 2008). The vegetation responsible for the coal beds most likely developed during periods of aggradation during 4th or 5th order sea-level rise. Subaerial exposure long enough to permit soil development is indicated by gleying, root traces, slickensides, and mottling. At Muddy Lake, siderite-encrusted root traces and siderite logs are found *in situ* in floodplain facies (Fig. 4.11B). Siderite-encrusted root traces have been linked to water-saturated environments with anoxic pore-water (Bojanowski et al., 2016).

Marginal-marine deposits at the top of the DPF are characterized by fining-upward successions of structureless, current-rippled, and/or cross-bedded sandstone, followed by inclined silty and muddy heterolithic deposits (Fig. 4.11E). This is interpreted as reflecting deposition in laterally migrating estuarine and intertidal channels. Syneresis cracks, current-ripple cross-lamination with mudstone drapes, and a brackish-water trace-fossil assemblage

indicate admixing of fresh and saline waters. Bioturbation was intermittent and dominated by diminutive infaunal ichnotaxa.

Formation geometry

The Dinosaur Park Formation (excluding the Manâtakâw Member) is 20.1–72.4 m thick, thinning towards the eastern and western margins of the study area (Fig. 4.8D). The formation is thickest in a vaguely sinuous northeast-southwest trend in the center of the study area. This is interpreted as paleovalleys carved by erosional downcutting into the underlying OF during base level fall. Thinning of the DPF towards the west reflects decreased accommodation due to proximity of the Sweetgrass Arch in southern Alberta and northern Montana. In the east, thinning is attributed to the DPF terminating against marine strata of the Bearpaw Formation.

4.4.4 Dinosaur Park Formation: Manâtakâw Member

Core from borehole Canadian Landmaster Cypress Hills W141/06-31-06-25W3 (Fig. 4.12) is herein proposed as the stratotype for the new Manâtakâw Member of the Dinosaur Park Formation, named from the traditional Plains Cree word for the Cypress Hills. Formally naming this unit will assist in referencing the transition from coastal plain and marginal-marine facies of the Dinosaur Park Formation, to shallow-marine successions of the Bearpaw Formation. The member consists of two distinct facies, and can be traced from core and the gamma ray - resistivity - density suite of logs in the subsurface from ranges 21 to 28W3, and townships 1 to 8.

Boundaries

The base of the Manâtakâw Member is placed at the top of a consistent rightward gamma deflection that coincides with a density deflection to the left (Fig. 4.12). This marks the lower boundary of estuarine basin and lagoon mudstone and shale. The upper contact is placed at the

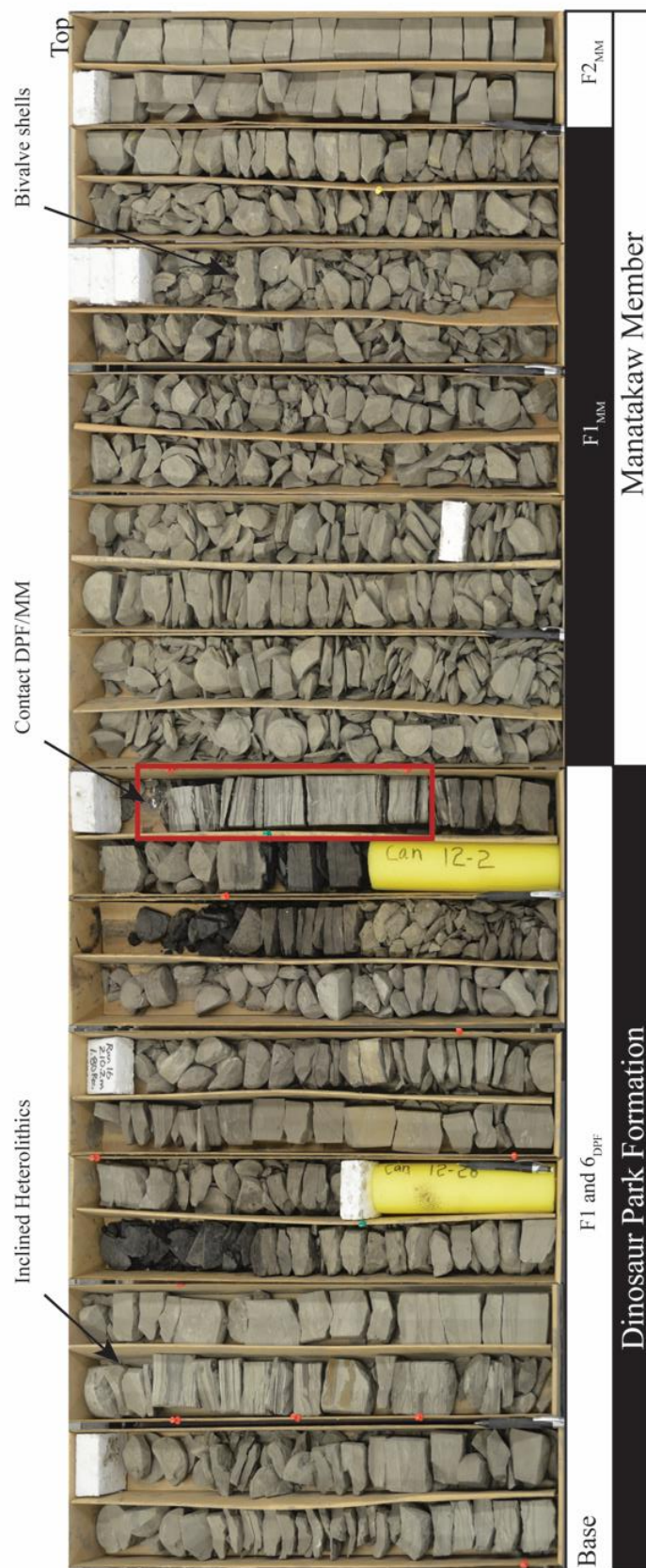


Figure 4.13: Representative core log from Nexen Battle Creek 07-02-004-27W/3. Core photos from Figure 11E-G were taken from this core in the uppermost DPF (red box). Note the Inclined heterolithic stratification of F6_{DPF} at the top of the Dinosaur Park Formation. These deposits are immediately overlain by F1-F2_{MM} of the Manatakaw Member. Note the presence of small bivalve shells in lagoon facies. See Tables 4.4 and 4.5 for descriptions of facies for DPF and MM.

top of barrier-island sandstone that corresponds to a sharp gamma-ray deflection to the left and a bulk density indication for sandstone. The top of the sandstone is locally capped by coal, as interpreted from bulk density logs. The upper boundary of the MM is indicated in gamma logs by a sharp shift to the right signaling transition to shallow-marine deposits of the Bearpaw Formation. The member thickens to the south and east and progressively thins to the west (Fig. 4.8E), terminating conformably against coastal plain and heterolithic deposits of the DPF east of the Alberta border.

Description

The Manâtakâw Member of the Dinosaur Park Formation consists of two facies and forms a coarsening-upward succession (Table 4.5). F1_{MM} consists of massive, medium to dark gray mudstone and shale with local siltstone and sandstone stringers and symmetrical ripples. Bioturbation is irregular, with *Planolites* isp. appearing throughout, and high occurrences (BI 4–5) of localized *Chondrites* isp. Small bivalves are preserved *in situ*, commonly occurring in distinct horizons.

F2_{MM} consists of fine- to medium-grained massive sandstone with localized trough- and planar cross-bedded sandstone with rare symmetrical ripples. Sporadic bioturbation, glauconite grains, carbonaceous laminae and coal clasts occur throughout F2_{MM}. Coal beds and coalified root trace fossils cap the top of the sandstone in places. The trace fossil *Macaronichnus* isp. appears in localized horizons within this facies (BI = 3).

Sedimentary environment

F1_{MM} to F2_{MM} overlie heterolithic tidally influenced sediments, and are attributed to estuarine and lagoonal basins and barrier island deposits, respectively. The presence of lagoons, barrier islands, and sand bars aligned parallel to the coast indicates that wave energy was the dominant

control on coastal morphology, with tides and fluvial processes contributing subordinately (Boyd et al., 1992; Dalrymple et al., 1992; Dalrymple, 2010). This member is interpreted as wave-dominated, tidally influenced estuary basins, lagoons and barrier island bars. *Macaronichnus* isp. is a trace fossil commonly associated with nearshore environments (Coates, 2002; Pemberton et al., 2001; Quiroz et al., 2010; Buatois & Mángano, 2011; Uchman et al., 2016). Coal and root traces at the top of these sands indicate subaerial exposure long enough to promote the growth of significant plants along the tops of the bars.

The appearance of localized *Chondrites* isp. suggests periods of lagoon anoxia and/or euxinia. This branching, dendritic trace fossil is found in poorly oxygenated environments and the trace maker(s) is believed to be able to live in anoxic sediments as a chemosymbiont (Seilacher, 1990; Bhattacharya & Banerjee, 2014). In modern lagoon environments, anoxia and euxinia are attributed to increased environmental temperatures, high organic content, and low water turbidity (Cioffi et al., 1995; Harzallah & Chapelle, 2002). Euxinia can develop when oxygen-depleted water is coupled with the presence of organic matter, sulfate ions, and sulfur-reducing bacteria. This commonly occurs in silled basins, such as barrier island and restricted saltwater bodies that have freshwater input from rivers and streams (Nägler et al., 2011). Due to the consistent distribution of this trace fossil, anoxia-euxinia in F1_{MM} is interpreted as linked to seasonal climate fluctuations. This interpretation is further supported by small *in situ* bivalves, with clustered occurrences representing death assemblages attributed to anoxic/euxinia pulses.

Formation geometry

Marginal-marine deposits of the Manâtakâw Member are 11.9–52.7 m thick and thicken towards the east. Facies of the MM terminate against DPF and BP sediments between ranges 27 and 28W3, but extend laterally to the north and south outside the study area (Fig. 4.8E). Termination

of lagoon and barrier island deposits reflects decreasing accommodation to the west against the paleotopographic “highlands” of the Sweetgrass Arch. The lack of the MM in the western portion of the study area, combined with the presence of conformable marine shales overlying heterolithic deposits of the DPF west of range 28W3, indicates the region underwent a rapid transgression at some point during the 2nd order Bearpaw Cycle.

4.4.5 Bearpaw Formation

The Bearpaw Formation is a southeastward-thickening fully marine deposit associated with the 2nd order transgressive-regressive Bearpaw Cycle of the Western Interior Seaway (Kauffman & Caldwell, 1993). The formation records wave-dominated, fluvial- and storm-influenced parasequences (Table 4.6) bound by marine flooding surfaces (Tsujita, 1995). The formation spans the late Campanian to early Maastrichtian (72–66 Ma), and records the final transgression of the Western Interior Seaway (Folinsbee et al., 1965; Caldwell, 1968). In Saskatchewan, the Bearpaw Formation is overlain by marginal-marine deposits of the Eastend Formation, and in central Alberta by the terrestrial Horseshoe Canyon Formation (Tsujita, 1995). In the study area, the Bearpaw Formation conformably overlies barrier island sandstone and marginal-marine heterolithics of the Dinosaur Park Formation. In outcrop, this is marked by an abrupt appearance of drab, greenish-gray, gray to dark gray shale, mudstone, and marine sandstone. In well logs, this is signaled by a gamma-ray shift to the right, which remains relatively consistent throughout much of the formation’s duration. A full treatment of the

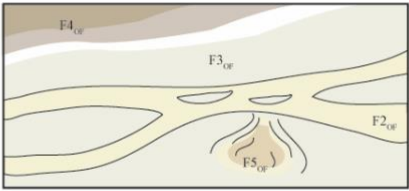

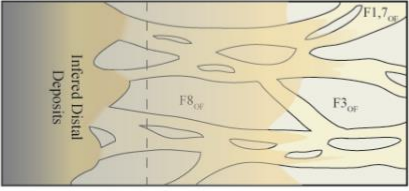
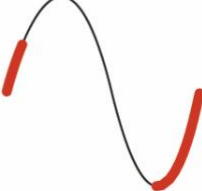
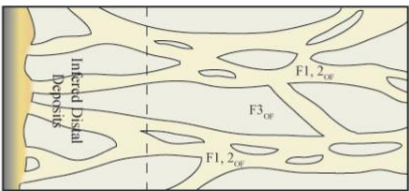
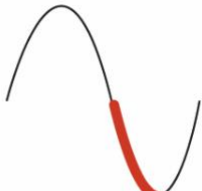

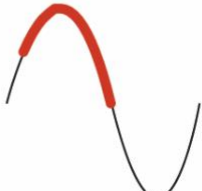

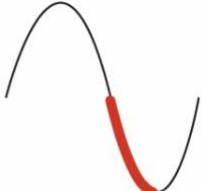


Systems Tract	Paleogeographic Setting	Lithostratigraphic Unit	Relative Sea-Level Curve
HST _{OF1}		Oldman Formation 'Lower Siltstone'	
TST _{OF1}		Oldman Formation	
LST _{OF1}		Oldman Formation 'Basal Sandstone'	
HST _{FF2}		Foremost Formation Upper Parasequences	
LST _{FF}		Foremost Formation Ribstone Creek Member	
HST _{FF1}		Foremost Formation Lower Parasequences	

Figure 4.14A: Diagram summarizing the sequence-stratigraphic evolution of the Belly River Group (lowermost units) and its associated formations and members in southwestern Saskatchewan, and the corresponding lithostratigraphic unit and paleoenvironmental settings that correspond to each systems tract.

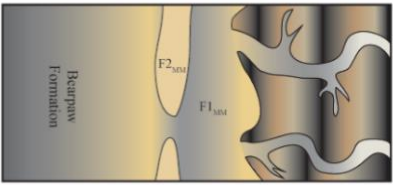



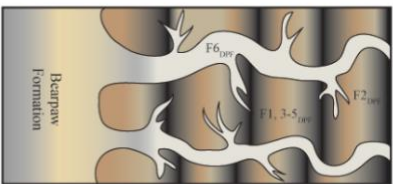

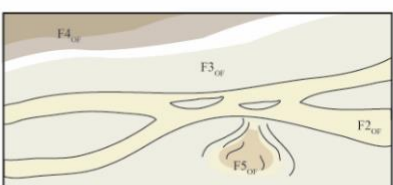

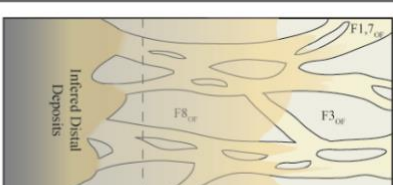

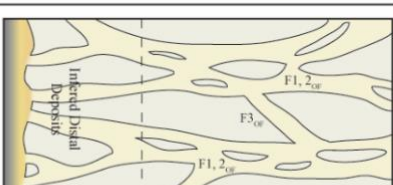
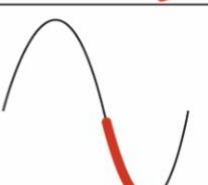
Systems Tract	Paleogeographic Setting	Lithostratigraphic Unit	Relative Sea-Level Curve
TST _{MM}		Manatakaw Member	
Late LST Early TST _{DPF}		Dinosaur Park Formation Coastal Plain	
LST _{DPF}		Dinosaur Park Formation Esuarine-Fluvio Channels	
HST _{OF2}		Oldman Formation 'Upper Siltstone'	
TST _{OF2}		Oldman Formation	
LST _{OF2}		Oldman Formation Comery Sandstone	

Figure 4.14B: Diagram summarizing the sequence-stratigraphic evolution of the Belly River Group (uppermost units) and its associated formations and members in southwestern Saskatchewan, and the corresponding lithostratigraphic unit and paleoenvironmental settings that correspond to each systems tract.

Bearpaw Formation in the southwestern plains is not within the scope of this study, but Tsujita (1995) provided a comprehensive overview of the formation.

4.5 Discussion

4.5.1 Sequence Stratigraphy

Variations in accommodation space, basin physiography, and sediment supply are the major controls on facies stacking patterns and their associated systems tracts (Catuneanu, 2006). The definition and mapability of systems tracts depends upon the depositional setting and the extent and types of data available to the study (Catuneanu et al., 2009). The depositional and sequence-stratigraphic model proposed herein is not placed within a high-frequency sequence-stratigraphic framework due to the poor lateral distribution and lack of reliable core and outcrop data available throughout the study area. The model proposed uses a simplified sea-level curve (Fig. 4.14A, B; Table 4.7) based on systems tracts outlined by Catuneanu et al. (2009): Falling Stage Systems Tract (FSST), Lowstand Systems Tract (LST), Transgressive Systems Tract (TST), and Highstand Systems Tract (HST).

The Belly River Group represents siliciclastic sedimentation in a foreland basin controlled by tectonic uplift, subsidence and climate. The Foremost and Oldman formations record a time of overall wedge progradation, with the Oldman representing the maximum regression of the Western Interior Seaway during the Campanian (Fig. 4.15). The Dinosaur Park Formation signals the onset of the last major transgression of the Western Interior Seaway across western Canada (Hamblin, 1997b; Eberth, 2005). Four transgressive-regressive 3rd order cycles are recognized in the Belly River Group in southwestern and west-central Saskatchewan. No FSST cycles were identified, likely due to sediment bypass, with FSST sedimentation occurring

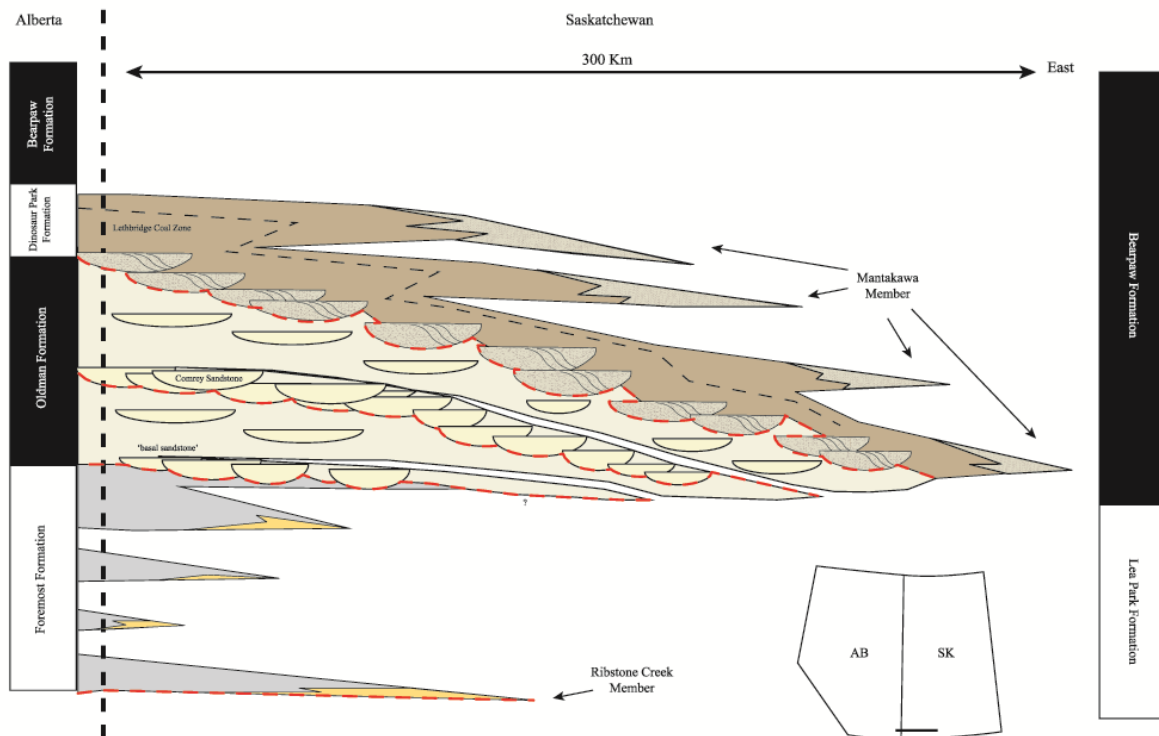


Figure 4.15: Regional schematic cross-section through the Belly River Group to demonstrate the contrasting geometries in southwestern Saskatchewan. This represents subsurface geometries from just west of the Alberta border, to Regina, Saskatchewan. The model has been highly vertically exaggerated to demonstrate formation relationships. Modified from Eberth (2005).

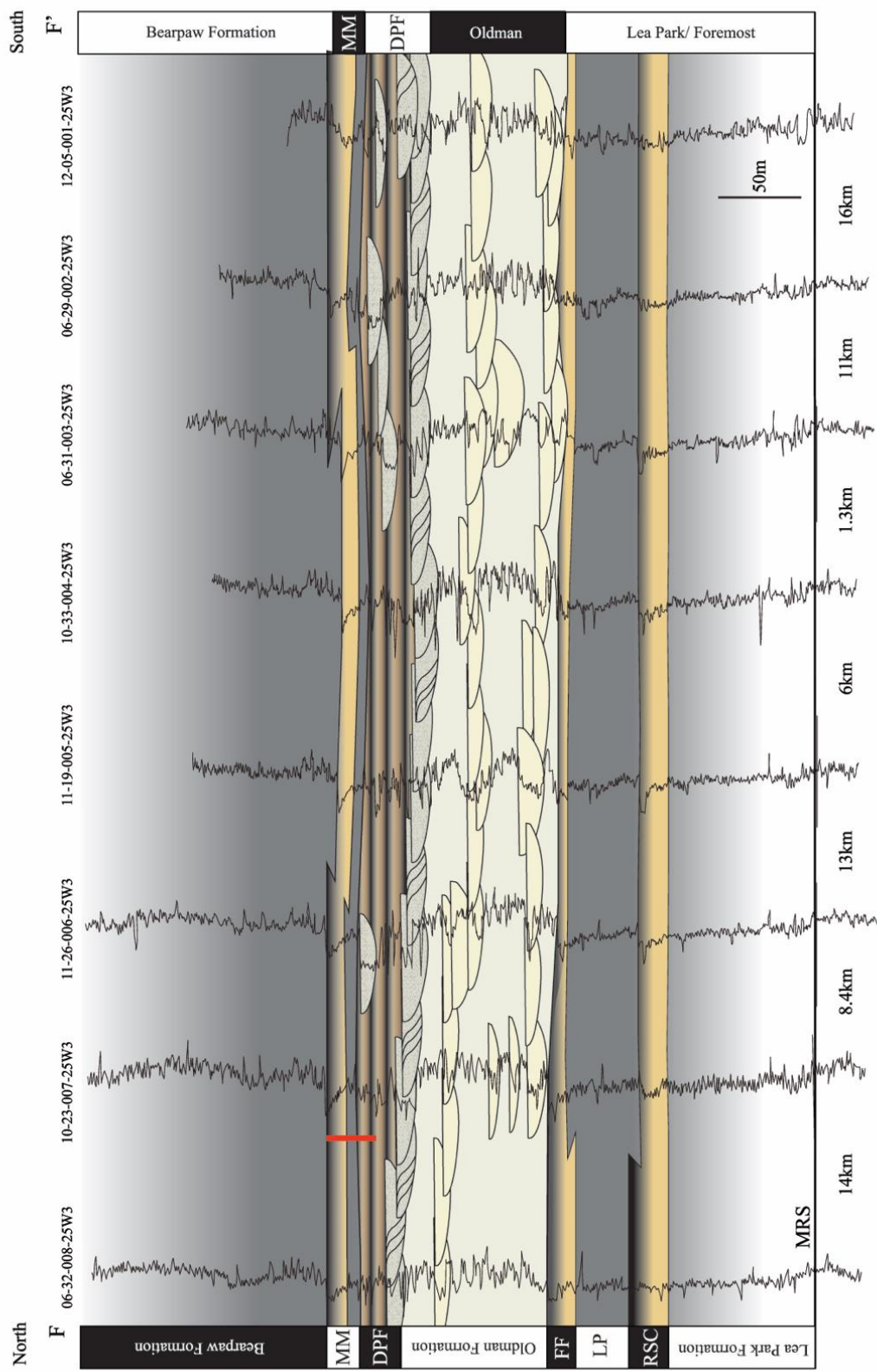


Figure 4.16: Cross-section F-F' (see Figure 2 for location) represents a strike-oriented (i.e., E-W) transect through range 25W3. DPF - Dinosaur Park Formation; FF - Foremost Formation; LP - Lea Park; MM - Manātākāw Member; MRS - Milk River Shoulder; RSC - Ribstone Creek Member.

farther basinward. Seven subsurface cross-sections were constructed to illustrate the subsurface parameters of each formation (Fig. 4.16, 4.17; Appendix D).

Foremost Formation

The Foremost Formation is composed of a series of coarsening-upwards parasequences bound by their associated flooding surfaces. These cycles consist of wave-dominated, shallow-marine successions and associated backshore shale and coal. Parasequences of the FF are progradational, conformably interfingering with fully marine shale of the Lea Park Formation, and represent highstand and lowstand systems tracts cycles (HST_{FF1} , LST/TST_{FF1} , HST_{FF2}). The lower FF is attributed to prograding HST_{FF1} shallow-marine, wave-dominated clastic wedges. The base of the Ribstone Creek Member (RSC) signals a major basinward shift of the FF. The lower contact of the RSC is treated as a sequence boundary and signals onset of a lowstand systems tract (LST/TST_{FF1}). The top of the carbonaceous shale and coal of the RSC indicates the start of transgression, with the transgressive surface placed at the top of these deposits. No outcrop or cored interval is known from the transgressive systems tract deposits in Saskatchewan, but estuarine facies are well documented in the FF in the Manyberries, Alberta region, near the Saskatchewan–Alberta border (Gordon, 2000; Cullen et al., 2016). Therefore, the lowstand and transgressive systems tracts are described together (LST/TST_{FF1}), with transgressive deposits defined as marine shale immediately overlying the RSC member. The maximum flooding surface (MFS) is arbitrarily placed between the top of the RSC and the next coarsening-upwards parasequence within shale of the overlying Lea Park Formation. The remaining FF consists of prograding HST_{FF2} parasequences, signaling a return of high accommodation conditions in the Western Canada Sedimentary Basin.

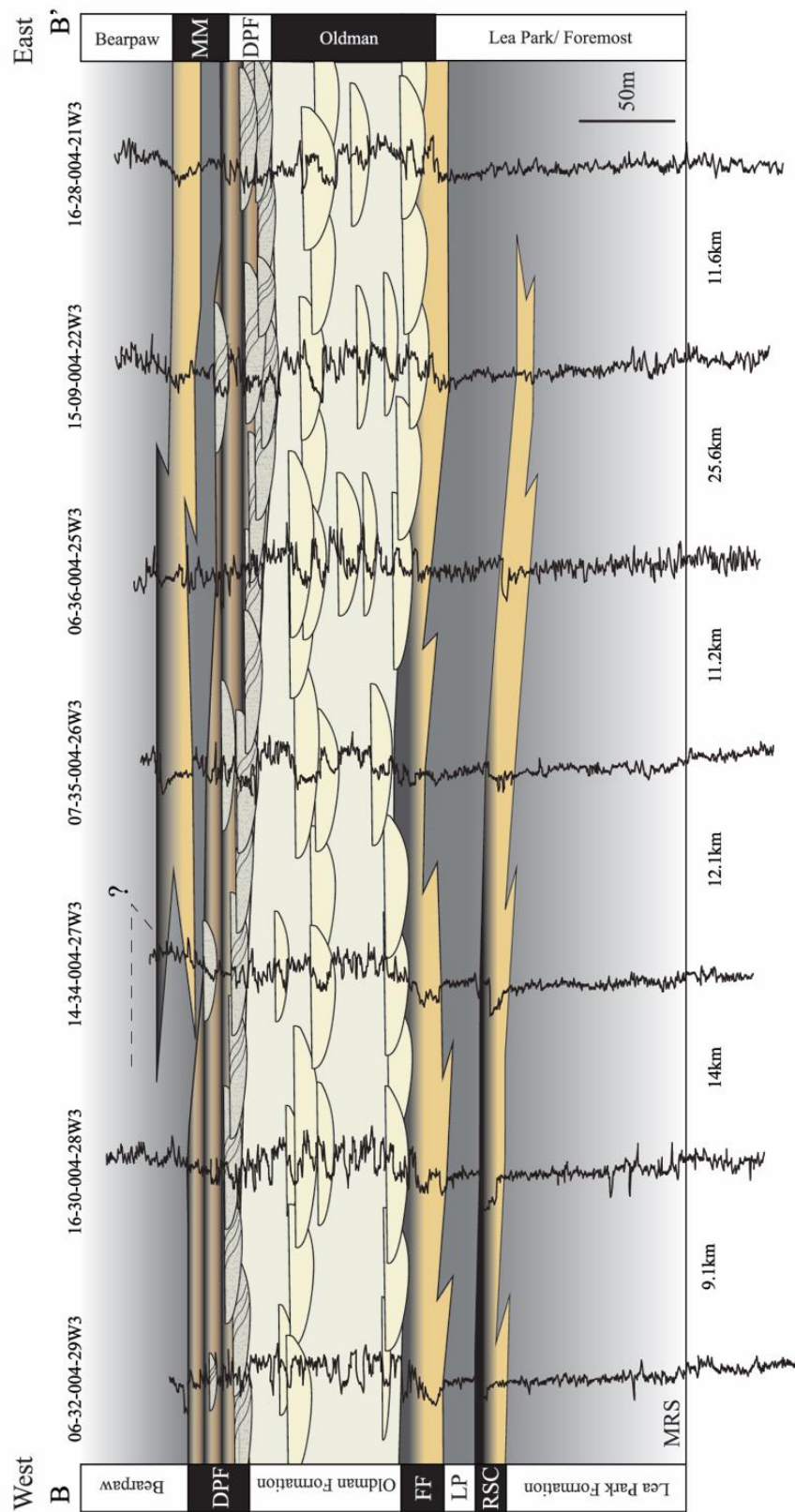


Figure 4.17: Cross-section B-B' (see Figure 2 for location) represents a dip-oriented transect (i.e., N-S) through township 4. Note the disappearance of the Manâtakâw Member west of range 28W3. DPF - Dinosaur Park Formation; FF - Foremost Formation; LP - Lea Park; MM - Manâtakâw Member; MRS - Milk River Shoulder; RSC - Ribstone Creek Member.

Oldman Formation

Facies of the Oldman Formation represent two full transgressive-regressive cycles (LST_{OF1} , TST_{OF1} , HST_{OF1} , LST_{OF2} , TST_{OF2} , HST_{OF2}). In Saskatchewan, the base of the Oldman Formation is marked by amalgamated paleochannels of the ‘basal sandstone’, which forms an erosional contact with the underlying Lea Park and Foremost formations. This represents a 3rd order sequence boundary, resulting from a relative drop in base level. Deposition of amalgamated fluvial channels have been attributed to low accommodation in regions undergoing regression (Catuneanu et al., 2009). The ‘basal sandstones’ and their associated siltstone-dominated floodplains are assigned to LST_{OF1} . A transgressive surface is placed at the base of muddy sandstone and greenish-gray to dark gray mudstone overlying deposits of the ‘basal sandstone’. This shift in deposition signals increasing accommodation during a time of minor transgression that achieved limited westward advancement. TST deposition never reached the Alberta–Saskatchewan border, as no definitive evidence of marine to marginal-marine encroachment has been documented in southeastern Alberta. This transgression is denoted as TST_{OF1} , and is composed of mudstone and shale of $F8_{OF}$. TST_{OF1} mudstone and shale are overlain by buff- and pale yellow-colored mudstones, siltstones, silty sandstones, and isolated, lenticular sandstone attributed to fluvial channels and associated overbank facies. The first OF maximum flooding surface is placed at the contact between these buff-colored deposits and the underlying mudstone and shale. These siltstone-dominated deposits are interpreted as lithostratigraphic equivalents to the informal lower siltstone member of the Oldman Formation observed in southeastern Alberta (Eberth, 2005). This “member” was interpreted as a LST by Eberth (2005), but in Saskatchewan, this unit represents deposition resulting from increased accommodation space and sediment supply, and the deposits are designated as HST_{OF1} . Isolated channel fill and associated

floodplains dominate deposits inland of transgressive marginal-marine facies (Catuneanu et al., 2009). When transgression ended, these facies began to be deposited basinwards, resulting in progradational to aggradational stacking patterns characteristic of highstand conditions.

The second Oldman Formation transgressive-regressive cycle is marked at the base by deposits of the Comrey Sandstone. This is a ~5–15 m succession of amalgamated paleochannels located roughly midsection in the Oldman Formation and is present throughout Saskatchewan and Alberta (Eberth & Hamblin, 1993; Hamblin, 1997a). Previous studies have assigned the CS to late transgressive systems tract deposition, with the base considered a cryptic sequence boundary in Alberta (Eberth, 2005). Amalgamated paleochannels are attributed to times of low accommodation, either due to changes in base level or arid environmental conditions (Catuneanu et al., 2009). Therefore, the CS is interpreted as LST_{OF2}, deposited during a time of low accommodation seasonal aridity (Eberth & Hamblin, 1993; Troke, 1993; Hamblin, 1997a). Marine incursion in the upper CS of southeastern Alberta has been previously suggested, as double drapes described by Troke (1993) were proposed as potential tidal influence signatures during a small-scale transgression of the Western Interior Seaway. In Saskatchewan, a 1.5 m interval of shale and mudstone immediately overlies the CS in Woodpile Coulee. This is interpreted as representing marine incursion during TST_{OF2}, with the transgressive surface placed at the base of the mudstone and shale. The ‘Upper Siltstone Member’ informally recognized in Alberta is observed in Saskatchewan. This interval consists of isolated fluvial channels, and siltstone- and mudstone-dominated overbank facies in a high accommodation setting. This indicates a shift to basinward progradation during HST_{OF2}, with the marine flooding surface placed at the base of this unit.

Facies analysis and stacking patterns indicate that the Oldman Formation was deposited in a semi-arid alluvial to coastal plain environment that underwent seasonal climate-driven flash flooding (Eberth & Hamblin, 1993; Hamblin, 1997a). Despite two minor 3rd order transgressive episodes, the OF records the maximum regressive extension of the BRG (Hamblin, 1997a; Eberth, 2005). This shows that the OF was deposited during a time of high accommodation and sediment supply. Paleochannels in the OF are distinct from those in the DPF, and are interpreted as representing braided river systems that experienced seasonal ephemeral flows and periodic subaerial exposure in a low-gradient alluvial plain (Eberth & Hamblin, 1993; Noad, 1993). As suggested by Eberth and Hamblin (1993), evidence from Saskatchewan corroborates that the OF was deposited under semi-arid conditions. This suggests paleoclimate was a major control on accommodation and base level at the time of OF deposition.

Dinosaur Park - Bearpaw transition

The Dinosaur Park – Bearpaw transition has been studied in more detail by Gilbert et al. (2019). The transition marks the last major 2nd order Bearpaw Cycle transgressive-regressive phase of the Western Interior Seaway. This transgression was extensive at its peak, effectively flooding all of Saskatchewan and most of southern Alberta east of the Rocky Mountains (Kauffman & Caldwell, 1993; Tsujita, 1995). A regional fall in base level triggered fluvial incision in the basin, creating a sequence boundary between the Oldman and Dinosaur Park formations. These incised valleys are filled at the base by amalgamated, laterally accreting paleochannels during an early LST_{DPF}. Inclined heterolithic deposits, mudstones, and coals immediately overlie isolated, lenticular channel sands and associated overbank facies in a coastal floodplain during late LST_{DPF} and early TST_{DPF}. The transgressive surface is placed at the top of the amalgamated channel sands.

Estuary and lagoon basin shale and mudstone, and barrier island sandstone of the Manâtakâw Member overlie Dinosaur Park Formation coals, heterolithic floodplain and point bar deposits. Initial transgression of the WIS was gradual, as evidenced by thick, stratigraphically continuous accumulations of successions of the MM east of range 28W3. Significant shoreline migration west of range 28W3 into Alberta is suggested by the sudden disappearance of the MM, with coal and heterolithics of the DPF being immediately overlain with shale of the Bearpaw Formation. This suggests transgression of the Western Interior Seaway happened in pulses, with times of relative shoreline stability followed by rapid transgressive episodes inundating significant distances westward. The maximum flooding surface is found higher within shale of the Bearpaw Formation and was not mapped in this study.

Facies analysis and stacking patterns in the DPF are consistent with deposition in a low-accommodation coastal plain environment (Eberth & Hamblin, 1993; Hamblin, 1997b). The Dinosaur Park Formation records a time of overall transgression of the WIS, which is reflected in laterally migrating channels, heterolithics, and coal deposits in a low-gradient coastal plain. The appearance of thick barrier island sandstone in the east indicates episodes of slow, stable transgression across the paleocoastline, punctuated by rapid transgressive advancement. This suggests the WIS occasionally progressed significant distances in a short amount of time.

Significance of incised vs. unincised lowstand systems tracts

Changes in base level is a major controlling factor of sedimentation style and geometry, which is reflected in the depositional environments preserved in regions close to the paleocoastline.

Gradients between the alluvial plain and adjacent shelf is critical in determining whether a river will respond to sea-level fall by forming an incised valley across the shelf or simply flowing across underlying deposits with little erosion and downcutting (Posamentier, 2001). Sea-level

fall causes incision if the seaward gradient is significantly steeper than that of the alluvial plain (Posamentier et al., 1992; Leeder & Stewart, 1996; Posamentier & Allen, 1999; Posamentier, 2001). If the shoreline migrates across surfaces steeper than the alluvial profile, fluvial channels will downcut into underlying deposits, forming incised valleys. Downcutting begins at the river mouth, and migrates upstream in the form of knickpoint migration (Posamentier, 2001). The extent of this downcutting is primarily in response to the magnitude of sea-level fall. Conversely, if shorelines are to migrate across surfaces with the same or lower gradient as the alluvial plain, valley incision does not occur (Posamentier, 2001). In either case, a lowstand alluvial system forms, and sedimentation only occurs in channels, point bars, and floodplains.

Valley incision has been well documented in the literature, especially since the advent of sequence stratigraphy (e.g., Dalrymple et al., 1992; Zaitlin et al., 1994; Eberth, 1996). Lowstand unincised alluvial systems have not been well documented, with little consideration being given to systems where sea-level fall has not resulted in significant incision of the underlying deposits to form a paleovalley. When sea-level fall is sufficient to expose the sea floor, but does not extend to the shelf, unincised fluvial deposition occurs (Posamentier, 2001). Lowstand unincised systems cover large geographic areas forming thick braided fluvial successions, often across midshelf settings (Posamentier, 2001). This is in direct contrast with lowstand incised systems, which are isolated, of small areal extent, and extend significant distances inland (Zaitlin et al., 1994; Posamentier, 2001).

A steep gradient and full exposure of the shelf is required to form significant incised valley systems. In systems where prolonged highstand conditions persist, highstand sedimentation could fill significant amounts of the available accommodation of the shelf. If sea level were to fall, a diminished water depth would require less sea-level fall to expose the shelf,

creating a gradient sufficient for valley incision to occur (Posamentier, 2001). Both the Foremost and Oldman formations document thick successions of prolonged highstand deposits. Both the ‘basal sandstone’ and Comrey Sandstone extend over large paleogeographic distances immediately overtop considerable highstand deposits. Both LST_{OF1} and LST_{OF2} lack evidence of incision, display sheet-like geometry, are of extensive lateral continuity, and are of significant thicknesses. This fits the criterion for unincised lowstand deposits described by Posamentier (2001). LST_{OF1} and LST_{OF2} are therefore interpreted as unincised lowstand deposits that accumulated due to a combination of slow tectonic tilting and climate aridity during the time of OF deposition. Slow tilting and dry climatic conditions would create the appropriate paleogeographic and paleoenvironmental conditions to circumvent incision during a relative sea-level fall (Fig. 4.18A).

In contrast, the Dinosaur Park Formation shows clear evidence of fluvial incision in the Cypress Hills study area (Fig. 4.18B). Isopach maps, formation geometry, fluvial structures and stacking patterns support a northwest-southeast-trending, tidally influenced fluvial incision at the base of the Dinosaur Park Formation (Gilbert et al., 2019). DPF incision has been previously suggested from lithostratigraphically equivalent deposits from Dinosaur Provincial Park in south-central Alberta (Eberth, 1996). Due to proximity to the paleocoastline, it is expected that fluvial incision would be far more pronounced in Saskatchewan than in more inland Alberta.

In southwestern Saskatchewan, DPF deposits were controlled in part by proximity to the Sweetgrass Arch, a paleotopographic high at the time of deposition. Incision skirts basinwards of the Arch, with associated floodplain deposits truncating westward due to lack of accommodation (Fig. 4.8D). Base level fall of sufficient magnitude to produce a gradient steep enough to create

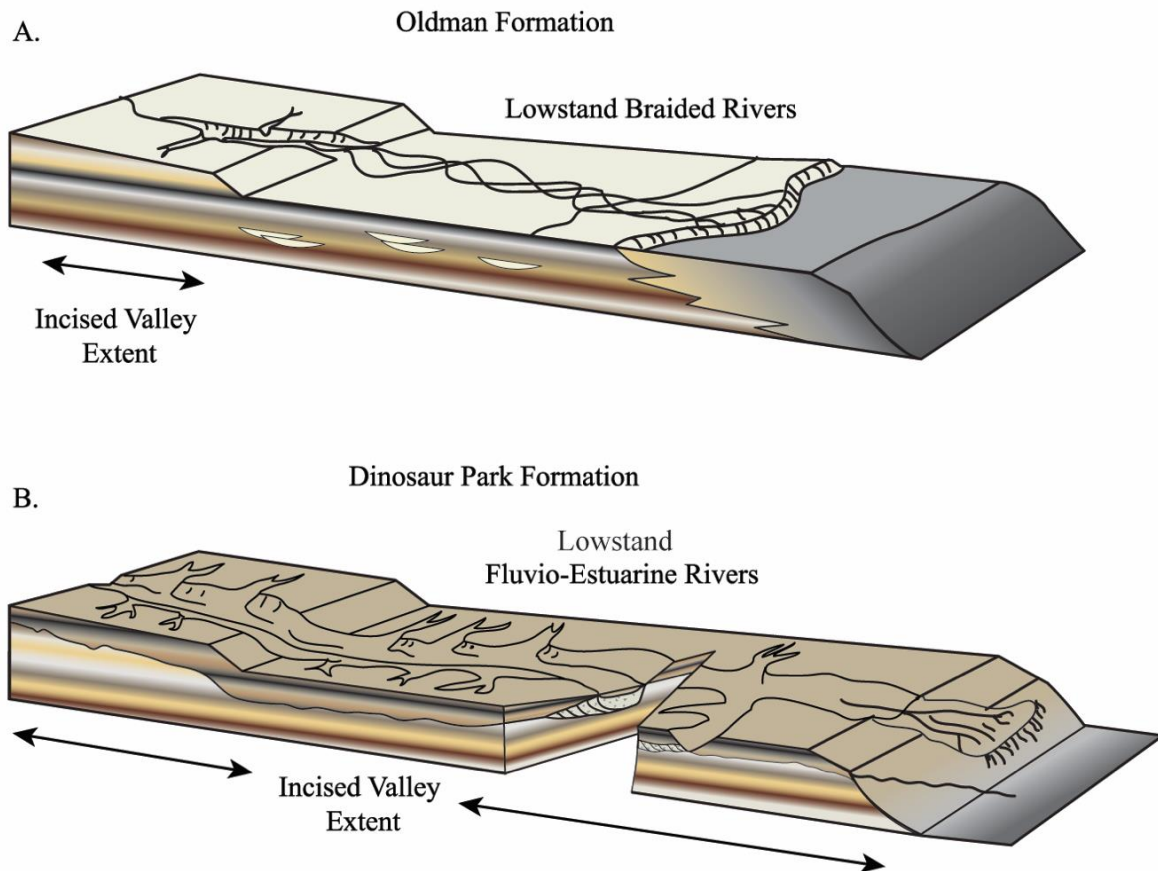


Figure 18: Schematic depiction of **A.** unincised lowstand deposition in the Oldman Formation and **B.** incised lowstand deposition in the Dinosaur Park Formation in southwestern Saskatchewan. According to this diagram, valley incision could occur farther upstream, depending on the steepness of the gradient created during base-level fall, but doesn't necessarily have to occur. Modified from Posamentier (2001).

fluvial incision is explained by regional tectonism. It is well established that paleochannel geometry, lithology, petrology, and flow direction change considerably across the Oldman–Dinosaur Park boundary (Eberth & Hamblin, 1993; Hamblin, 1997b; Eberth, 2005). Regional tectonic uplift is the most parsimonious answer for inducing slope gradient and sea-level change significant enough to prompt fluvial incision in a low-gradient coastal plain in a foreland basin.

Following lowstand fluvial deposition in the basal DPF, basin subsidence signals the onset of the 2nd order Bearpaw Cycle, and the last major transgression of the Western Interior Seaway across the western Canadian plains (Kauffman & Caldwell, 1993). Late LST_{DPF} and early TST_{DPF} deposits consisting of interbedded sandstone, siltstone, mudstone, shale, and coal replace fluvio-estuarine channels of the basal DPF. Increasing subsidence outstrips sediment supply, producing transgressive estuary basin, lagoon, and barrier island deposits of the Manâtakâw Member. Transgression occurred in a number of pulses, with stable shorelines persisting throughout the study area, only to be completely overtaken by a sudden pulse of sea-level rise that extended into Alberta. Complete disappearance of the MM west of range 28W3 indicates the paleoshoreline migrated considerable distances over a short period of geologic time. This is consistent with rapid basin subsidence induced by the Laramide Orogeny to the west. This interpretation is further supported by palynomorphs recovered from Woodpile Coulee. Species identified at the DPF-BP contact indicate an age of 75 Ma, which is more or less coincident with the contact in Dinosaur Provincial Park in central Alberta (Braman & Koppelhus, 2005).

The significance of recognizing incised vs. unincised terrain is critical to both paleoenvironmental reconstructions and the petroleum industry. Posamentier (2001) suggested that valley incision is relatively rare, characterizing only the lowest base-level falls. Given the

criteria required to produce incised valleys, unincised systems should be far more common in the sedimentologic record. In the Cretaceous of North America, unincised valleys should be relatively common, as the Western Canada Sedimentary Basin was deposited in a shallow foreland basin, where a high-gradient sea floor was likely absent. Slow basin tilting, combined with semi-arid climatic conditions would create enough slope to promote formation of a lowstand systems tract without requiring incision.

Valley incision generally requires a steep shelf slope, working to exaggerate the gradient required for incision. In the absence of a true shelf, such as in the WIS, regional tectonism could create a gradient significant enough to induce valley incision. Regional tectonism is undoubtedly responsible for incision observed in the DPF. Not only was this of large enough magnitude to promote valley incision, but it also reorganized drainage patterns in western Canada at the time of deposition. Re-evaluation of many incised valleys is strongly encouraged, as many are likely to have been misidentified. Though both serve as mechanisms for sediment bypass during lowstand conditions, incised and unincised systems have markedly different reservoir architecture (Posamentier, 2001). Recognizing these systems has significant implications for both paleoenvironmental reconstructions and petroleum exploration and development across the globe.

4.6. Summary and Conclusions

1) Previous nomenclature defining the terrestrial clastic sediments between the Lea Park and Bearpaw formations in Saskatchewan has been re-evaluated. The name Judith River Formation is dropped and is instead elevated to Group status. The name Belly River Group is adapted to conform with the nomenclature used in southern Alberta (Hamblin, 1997a, 1997b; Eberth, 2005). In southwestern Saskatchewan, the Belly River Group is composed of three formations: the

lowermost Foremost Formation (and the associated Ribstone Creek Member), Oldman Formation, and Dinosaur Park Formation (and the associated Manâtakâw Member). All three formations are separated by sequence boundaries, and represent varying stages of regression and subsequent transgression of the Western Interior Seaway.

2) A new stratigraphic unit, the Manâtakâw Member, has been proposed to subdivide the uppermost Dinosaur Park Formation. Formally naming this unit will assist in referencing the transition from coastal plain and marginal-marine facies of the Dinosaur Park Formation, to shallow-marine successions of the Bearpaw Formation. The member consists of two distinct facies and can be traced from core and the gamma ray - resistivity - bulk density suite of logs in the subsurface from ranges 21 to 28W3, and townships 1 to 8.

3) A wide range of clastic depositional environments and sub-environments are recorded throughout the Belly River Group. The lower Foremost Formation records shallow wave-dominated sedimentation during a highstand. The Ribstone Creek Member has been interpreted as LST_{FF1} , with overlying progradational shallow-marine successions interpreted as a return to highstand deposition. The transgressive systems tract is absent from this part of the basin.

4) The Oldman Formation erosionally overlies interfingering deposits of the Lea Park and Foremost formations and forms a sequence boundary. Braided fluvial channels denoted as the 'basal sandstones' represent unincised LST_{OF1} deposition. Unincised fluvial deposits indicate that drop in base level was not significant enough to produce widespread erosion across the exposed offshore and shelf. This suggests that this lowstand was induced by gradual basin tilt and semi-arid environmental conditions that persisted throughout the OF depositional history. Deposits of the LST_{OF1} are overlain by mudstones and shales of the TST_{OF1} , a minor marine

transgression that reached limited landward extent. Deposits of the TST_{OF1} are overlain by HST_{OF1} and indicate a return to high-accommodation depositional conditions.

5) A second transgressive-regressive cycle within the OF is recognized by amalgamated paleochannels of the Comrey Sandstone. These deposits are attributed to a second unincised LST_{OF2} event likely resulting from a second episode of basin tilting. At Woodpile Coulee in southwestern Saskatchewan, the Comrey is immediately overlain by mudstones and shales attributed to inundation by marine floodwaters during TST_{OF2} . Evidence suggests that flooding across the paleocoast was more extensive in this second episode, as tidal signatures have been recorded at the top of the Comrey Sandstone in southeastern Alberta (Troke, 1993). Once again, highstand (HST_{OF2}) conditions return, and siltstone- and sandstone-dominated isolated channel fill and associated floodplain deposits dominate the upper OF.

6) The Dinosaur Park Formation records a dramatic shift in basin evolution, with paleodrainage changing significantly between the Oldman and Dinosaur Park formations. Isopach maps indicate paleovalley incision took place at the Oldman-Dinosaur Park formation contact. This required a significant fall in base level and was initiated by tectonism. Stacked meandering paleochannels attributed to LST_{DPF} dominate the base of the formation. With the onset of late LST_{DPF} - early TST_{DPF} , channel deposits are replaced by coals and floodplain heterolithic sediments. As transgression continued, estuaries, lagoons, and barrier islands of the newly erected Manâtakâw Member backstepped across coastal plain deposits of the DPF. An abrupt rise in sea level drowns the coast, resulting in marine shales of the Bearpaw Formation immediately overlying coastal plain deposits of the DPF west of range 28W3. This indicates that the WIS underwent sudden, dramatic transgressive shifts that flooded substantial portions of the paleocoastline.

7) Recognizing unincised vs. incised lowstand systems is vital to understanding basin evolution in any depositional sequence. Unincised systems are under-represented in the literature, despite being more common in modern environments compared to their incised counterparts. The Belly River Group records both incised and unincised lowstand fluvial systems, and offers a contrasting example of the two systems in a single basin in a relatively short amount of geologic time. More care should be taken in the future in distinguishing between these systems, and a re-evaluation of depositional models characterized as incisive could reveal a confirmation bias in our geologic understanding of fluvial systems.

Acknowledgements

This research was funded by the University of Saskatchewan. MMG wishes to thank Zoë Vestrum who assisted with constructing the isopach maps. MMG also thanks Dennis Braman for palynology data provided in this study, and Tim Prokopiuk who assisted in the field at Sandy Point, Alberta. Special thanks to the Saskatchewan Geological Survey and Richard Wood at the Subsurface Geological Laboratory in Regina, Saskatchewan for providing research space and access to core tables.

Well Name	Location	Depths Cored
Nexen Battle Creek	W 111/07-02-04-27W3	185 – 243 m
Renaissance Senate	W 101/10-10-02-27W3	219 – 235 and 241 – 248 m
Nexen Vidora	W 111/06-04-05-25W3	225 – 280 m
Canadian Landmaster Cypress Hills	W 141/06-31-06-25W3	330 – 372 m
Renaissance Vidora	W 111/02-15-04-26W3	237 – 246 m
Canadian Landmaster Belanger	W141/10-23-07-25W3	385 – 415 m

Table 4.1: Summary of core logged for the purpose of this study.

Lithofacies Association	Lithofacies	Lithology, Sedimentary Structures and Body Fossil Content	Trace fossils	BI	Sedimentary Processes and Depositional Conditions	Sedimentary Environment
Foremost Formation FA 1 _{FF} : Wave-dominated shallow marine	F1 _{FF} Carbonaceous Shale and Coal	Dark grey to black fissile carbonaceous shale with sandy and silty stringers. Coalified wood, root traces, and abundant plant debris is preserved throughout. Contacts with over and underlying facies are sharp. F1 _{FF} overlies F4 _{FF} and underlies fully marine sands and shales. This facies ranges in thickness of 0.5-2m.	N/A	0	Backshore	Backshore and Coastal Plain
	F2 _{FF} Medium Grained Sandstone	Light grey to buff medium grained sandstone with low angled bedding. Parting lineation's observed at the top of the beds in outcrop. This facies overlies F3 _{FF} and underlies continental deposits of F1 _{FF} . Beds range in thickness from 0.4- 1m in thickness.	N/A	0	Shallow marine, near the top of fair weather wave base	Foreshore
	F3 _{FF} Medium grained sandstone with rare bioturbation	Light grey to buff, medium to fine grained trough cross-bedded sandstone. Rare carbonaceous debris locally present in troughs. F3 _{FF} displays gradational contacts, and commonly overlies F4 _{FF} and underlies F2 _{FF} . Ranges in thickness from 0.5-1.5m in thickness.	<i>Macaronichnus</i> isp.	0-3	Shallow marine shoreline with periodic storm activity. High energy, with predominant longshore currents producing 2D and 3D dunes in longshore bar deposits.	Upper Shoreface
	F4 _{FF} Amalgamated fine grained hummocky bedded sandstone	Amalgamated, light grey, fine to medium grained sandstone with localized siderite cementation. Commonly displays as massive, with rare low angled cross lamination, hummocky cross-stratification and symmetrical wave ripples. Carbonaceous debris and bivalve shells occur throughout the facies. Commonly gradationally overlies F5 _{FF} and underlies F5 _{FF} . Beds range in thickness from 0.3-0.8m in thickness.	<i>Ophiomorpha</i> isp., <i>Skolithos</i> isp.	0-1	Shallow marine wave dominated shoreline with periodic storm waves. High energy oscillatory flows. Storm surges result in unidirectional flow producing migrating 3D dunes	Lower Shoreface

	F5 _{FF} Hummocky bedded sandstone with shale interbeds	Light grey, fine to very-fine grained, sharp based, hummocky bedded sandstone with shale interbeds. Rare carbonaceous laminae are locally present. Sandstone is present in a 4:1 ratio compared to mudstone. Shale is thoroughly bioturbated. This facies overlies F? and underlies F4 _{FF} . Beds range in thickness from 0.5-1m thick.	<i>Planolites</i> isp., <i>Thalassinoides</i> isp.,	4-5	Shallow marine, wave dominated environment periodically affected by storms. Erosive sands are interpreted as tempestities, with siltstone deposited under fair-weather conditions.	Offshore Transition
	F6 _{FF} Interbedded sandstone and shale	Light grey fine to very-fine grained micro-hummocky and symmetrical rippled sandstone with interbedded shale and mudstone. Sand to mud typically occur in 1:1 or 1:2 ratios. Sandstone beds are erosive based and occur as discrete beds 0.2-0.4m thick, with shales and mudstones displaying similar thicknesses. This facies gradationally underlies F5 _{FF} . Shale and mudstone generally appears massive, but when visible, is entirely bioturbated.	<i>Chondrites</i> isp., <i>Planolites</i> isp.	2-6	Low energy suspension fallout punctuated by storms right above storm wave base.	Upper Offshore
	F7 _{FF} Shell Hash	Bioclastic, poorly consolidated marine bivalve and gastropod shells in a matrix of fissile mudstone and fine grained sandstone. Lower contact is always sharp and overlying F1 _{FF} , with the upper contact grading into F6 _{FF} where observed in core and outcrop. This facies is 0.2-0.3m in thickness.	<i>Thalassinoides</i> isp.	0-1	Reworked biogenic and clastic material during marine transgression.	Transgressive Lag

Table 4.2: Summary of facies, facies associations, and inferred depositional environments of the Foremost Formation. BI - Bioturbation index.

Lithofacies Association	Lithofacies	Lithology, Sedimentary Structures and Body Fossil Content	Trace fossils	BI	Sedimentary Processes and Depositional Conditions	Sedimentary Environment
Oldman Formation FA2 _{OF} : Alluvial Braided Channels	FI _{OF} Large- to medium-scale trough cross-bedded and current rippled amalgamated sandstone	<p>Very fine to fine grained light yellow, grey, and yellow-orange erosive based trough cross-bedded sandstone. Ironstone and mudstone clasts are occasionally observed at the base of channels and within individual troughs. Organic-rich claystone and carbonaceous laminae are preserved locally. Beds generally fine upwards, but occasionally display a coarsening upward trend. Beds are sheet and lenticular in shape, and display as both isolated and amalgamated and laterally extensive channel-fill. Siderite staining is common, sometimes leaving entire beds yellow-orange in appearance. Bedsets range in thickness of 0.5-1.3m thick and 2-6.5m in width. Paleocurrent analysis indicates flow from the south - southwest.</p>	N/A	0	<p>Migration of 3D-dunes in high energy, low sinuosity fluvial channels with unidirectional flow. The presence of organic detritus indicates a terrestrial setting.</p>	Lower braided fluvial channels
FA 3 _{OF} : Alluvial Coastal Plain	F2 _{OF} Cross-bedded and current rippled sandstone	<p>Fine-grained, light grey to light yellow lenticular to multi-storied cross-bedded, current rippled, and low angle parallel laminated sandstone. Basal contacts are both sharp and erosive. Siltstone, organic-rich claystone, and carbonaceous laminae are preserved throughout. Erosive surfaces are identified by mudstone pebbles and occasional ironstone clasts. Climbing ripples are noted, but rare. Unionid bivalves are preserved within some units. Beds fine upwards, are display as sheet shaped and more commonly lenticular. Beds range in thickness from 0.2-1.8m in thickness. Paleocurrent analysis indicates flow from the south - southwest.</p>	<i>Camborygma</i> isp., <i>Skolithos</i> isp., root traces	0-1	<p>Deposition resulting from quasi-steady, unidirectional flow in lower flow regime conditions. Rare climbing ripples indicate periods of increased sedimentation. Trace assemblage suggests alternating subaerial and subaqueous exposure.</p>	Lower to middle portions of channel-bars and fluvial channels

	F3 _{OF} Massive claystone and siltstone	<p>Massive light grey to buff mudstone and siltstone displaying both sharp and gradational bases.</p> <p>Carbonaceous detritus, coalified plant material, in situ coal laminae, and root traces are present locally.</p> <p>This unit is generally massive, but rarely exhibits planar bedding. This facies ranges in thickness of 0.3-2.6m thick.</p>	<i>Planolites</i> isp., <i>Skolithos</i> isp., <i>Taenidium</i> isp., root traces	0-1	Low energy, quite water environment with frequent subaerial exposure to allow pedogenenic development. The light color of this facies potentially indicates higher sedimentation rates, lower organic content, or organic oxidization.	Floodplain
	F4 _{OF} Siliceous muddy siltstone and sandstone	<p>Massive buff to whitish grey muddy siltstone/sandstone to sandy mudstone, This facies displays as massive, mottled, or planar laminated. Clay lined and siderite encrusted root traces with a tap-root appearance are common. Siderite staining is common throughout, and is often associated with the mottled appearance observed in this facies. This unit contains caliche, and high quartz grain and quartz cement content. This facies ranges in thickness from 0.8-1.5m.</p>	Root traces	0-1	Interfluvial floodplain paleosols, semialbic soil horizon with clear evidence of prolonged pedogenic development. Deep, clay lined root traces suggest a low water table.	Paleosol
	F5 _{OF} Horizontally stratified siltstone and Sandstone	<p>Fine grained buff to light yellow tabular, horizontally stratified siltstone and sandstone. Individual beds are generally massive, but do exhibit current ripples, planar lamination, and occasional clayey siltstone layers. This facies fine upwards and has gradational or sharp based contacts. Fragmented unionids and mudstone rip-up clasts are occasionally preserved within some packages. Vertebrate microfossils are common in this facies. Beds range in thickness from 0.3-3 meters, and are restricted to the upper OF.</p>	<i>Skolithos</i> isp., Root traces	0-1	Alternating periods of suspension fallout, clay flocculation, and subaerial exposure. Rip-up clasts and fragmented unionid shells indicate high energy flows that decrease over time, as indicated by clayey siltstone and planar lamination. Rare root traces indicate occasional pedogenesis.	Levee and crevasse splay deposits
	F6 _{OF} Coal	<p>Lignitic, friable coal. Rooting and clastic detritus is locally present in some</p>	Root traces	0-2		Swamps and floodplains

		seams. Seams range in thickness from 0.2-0.8m.				
	F7 _{OF} Inclined Heterolithic Stratification	Alternating fine-grained sandstone and mudstone with trough, parallel, and current ripple stratification. Millimeter to centimeter scale carbonaceous material comprised of comminuted plant fragments are locally abundant. This facies is 0.4-3.1m in thickness.	N/A	0	Point bar migration in seasonally flooded channels	Seasonally flooded meandering channels and streams
FA4 _{OF} : Marginal Marine	F8 _{OF} Massive Mudstone and Shale	Dark grey to greenish grey shale and mudstone. Beds are massive, and occasionally form fining upwards packages. Individual beds ranging in thickness from 0.5-1m in thickness and sets of 0.9-1.5m in thickness.	N/A	0	Quite waters in an inundated, low lying coastal to alluvial plain near sea level.	Marine encroachment on a low lying alluvial plain

Table 4.3: Summary of facies, facies associations, and inferred depositional environments of the Oldman Formation. BI - Bioturbation index.

Lithofacies Association	Lithofacies	Lithology, Sedimentary Structures and Body Fossil Content	Trace fossils	BI	Sedimentary Processes and Depositional Conditions	Sedimentary Environment
Dinosaur Park Formation FA5 _{DPF} : Wave-dominated tide influenced marginal marine fluvial affected	F3 _{DPF} Sparsely bioturbated heterolithic deposits	Medium to light grey, thinly laminated, tabular to lenticular, fine- to very fine-grained sandstone interbedded with light grey to grey-brown mudstone, silty mudstone, and silt. Cross-lamination and current ripples (locally wave reworked), syneresis cracks, slickensides and convolute bedding occur throughout. Coal clasts, carbonaceous laminae and plant debris occur throughout. Bed thickness ranges from 0.7-3.4 m.	<i>Asterosoma</i> isp., <i>Cylindrichnus concentricus</i> , <i>Palaeophycus</i> isp., <i>Planolites</i> isp., <i>Protovirgularia</i> isp., <i>Teichichnus rectus</i> , <i>Thalassinoides</i> isp., <i>Skolithos</i> isp.	0-3	Current ripples and low angle bedding indicate dominant unidirectional flow. Mud deposition during intermittent, slack water conditions between ebb and flow Low salinity brackish conditions.	Upper and middle estuarine channels, intertidal channels
	F4 _{DPF} Wave, current, and cross-stratified bioturbated sandstone	Medium to light grey, current, wave rippled, and cross stratified medium to fine-grained sandstone. Beds are erosionally based and reactivation surfaces are locally present. Mud drapes and horizontal mud laminae are present. Vertebrate microfossil assemblages are associated with this facies. When present, is always overlain by F7.	<i>Macaronichnus</i> isp., <i>Skolithos</i> isp	0-1	Migration of subaqueous, unidirectional flow dunes punctuated by slack-water conditions and occasional wind-driven oscillatory flows.	Bayhead delta
FA6 _{DPF} : Coastal Plain	F5 _{DPF} Rooted massive and thinly laminated carbonaceous mudstone and muddy siltstone	Medium to light grey and grey-brown massive mudstone and siltstone with abundant plant debris, coal clasts, slickensides, and soft sediment deformation. Lamination is thin alternating mud, silt, and carbonaceous debris and is unbioturbated. Commonly bounded by coal and containing coalified haloed root traces in places. Bed thickness ranges from 0.2-2.5 m.	Root traces, <i>Cochlichnus</i> isp., <i>Mermia</i> isp., <i>Planolites</i> isp.,	0-1	Suspension fallout of mud, silt and sand in a low energy environment. Gleysols indicate waterlogged conditions and a high water-table.	Floodplain

	F6 _{DPF} Current rippled and convolute bedded fine-grained sandstone	Light grey current ripple and trough cross bedded fine-grained sandstone and silty sandstone. Beds display both gradational and erosive bases with abundant carbonaceous debris, coal fragments, mudstone rip-up clasts, and convolute bedding. Rare Unionid bivalves and <i>Viviparus</i> sp., <i>Goniobasis</i> sp. and <i>Hydrobia</i> sp. gastropods are locally preserved both as isolated shells, and as coquina beds. Vertebrate microfossil assemblages are associated with this facies. Bed thickness ranges from 0.62-1.7 m.	Root traces, <i>Mermia</i> isp.	0-1	Episodic deposits due to levee failure along a fluvial channel resulting in sheetflooding onto the floodplain.	Lower fluvial and distributary channels and crevasse splays
	F7 _{DPF} Trough and current rippled sandstone	Light grey fine grained current rippled, trough cross bedded, and structureless sandstone. Carbonaceous detritus, mud rip-up clasts, and coal fragments are locally present. Vertebrate microfossil assemblages are associated with this facies. Erosive-based packages range in thickness from 0.45- 3.7 m.	Root traces, <i>Skolithos</i> isp.,	0-1	Lowermost portion of a meandering stream in a low gradient coastal plain environment. Rare evidence of intermittent tidal influence in channels.	Freshwater channels
	F8 _{DPF} Carbonaceous shale, silt, and coal	Highly variable, intercalated coal seams and coaly laminae. Coal ranges from shaly to bright-banded. Planar laminae, current ripples, slickensides, siderite, and convolute bedding. Thickness ranges from 0.38-3 m.	Root traces, <i>Cochlichnus</i> isp., <i>Mermia</i> isp., <i>Teredolites</i> isp.	0-1	High accumulation of plant debris in a coastal plain environment.	Floodplain, peat forming mires, swamps, and marshes.
	F9 _{DPF} Bentonitic mudstone	Seams of green-grey to light grey bentonite rich mudstone. Fissile to massive, with phenocrysts of biotite, quartz, and feldspar. Thickness ranges from 0.08-0.4 m.	N/A	0	Air fallout of ash from volcanic activity.	Sheltered, poorly drained swamps and marshes.

Table 4.4: Summary of facies, facies associations, and inferred depositional environments of the Dinosaur Park Formation. BI - Bioturbation index.

Lithofacies Association	Lithofacies	Lithology, Sedimentary Structures and Body Fossil Content	Trace fossils	BI	Sedimentary Processes and Depositional Conditions	Sedimentary Environment
Manâtakâw Member FA7 _{MM} : Wave-dominated, tide influenced marginal marine	F1 _{MM} Massive shale and mudstone and laminated silt	Massive medium to dark grey dominantly structureless shale with localized silt and sand stringers with rare oscillatory ripples 3-5mm in thickness. Small in situ bivalves are present throughout. Small Lucinidae and Ostreidae bivalves are preserved throughout. This facies is 0.5-5.2m thick.	<i>Chondrites</i> isp. <i>Planolites</i> isp.	0-1	Quite waters in a central basin catchment restricted from storms and tidal influence.	Restricted central estuary basin and coastal lagoons
	F2 _{MM} Fine to Medium grained bioturbated sandstone	Medium grey to greenish-grey, fine to medium grained sandstone. Low angle and cross bedding, and occasional glauconitic grains. Wave ripples, locally coal clasts, carbonaceous laminae, and occasional plant debris. Root traces at top of some beds. Bed thickness ranges from 1.4-6.3m.	<i>Macaronic hnus</i> isp., root traces	0-3	High-energy environment with unidirectional and oscillatory wave action produced by migration of dunes and ripples.	Outer estuarine mouth bar complex and barrier island bars

Table 4.5: Summary of facies, facies associations, and inferred depositional environments of the Manatakaw Member. BI - Bioturbation index.

Lithofacies Association	Lithofacies	Lithology, Sedimentary Structures and Body Fossil Content	Trace fossils	BI	Sedimentary Processes and Depositional Conditions	Sedimentary Environment
Bearpaw Formation FA8BP: Wave-dominated shallow marine	F1BP Shale	Fissile, thinly parallel-laminated, brown to grey shale. Sandy and/or silty stringers, and in situ marine bivalves. Thickness ranges from <1m to 5.2m.	<i>Chondrites</i> isp. <i>Phycosiphon incertum</i> , <i>Planolites</i> isp., <i>Zoophycos</i> isp.	4-6	Low energy suspension fallout below storm wave base.	Shelf
	F2BP Mudstone and interbedded siltstone	Brown to dark grey shale and mudstone with interbedded siltstone and rare very fine-grained sandstone laminae. Symmetrical ripples, carbonaceous laminae, shell debris and in situ bivalves are preserved throughout. Siltstone and sandstone laminae are 0.5 to 5.2 cm thick. This facies ranges in thickness from <2 to 4.5 m thick.	<i>Asterosoma</i> isp., <i>Chondrites</i> isp., <i>Nereites missouriensis</i> , <i>Planolites</i> isp., <i>Rhizocorallium</i> isp., <i>Zoophycos</i> isp.	2-5	Low energy suspension fallout punctuated by storms right above storm wave base.	Lower Offshore
	F3BP Bioturbated muddy and sandy siltstone	Fine-grained, light grey, alternating muddy and sandy siltstone. Rare micro-hummocky and symmetrical ripples, interstitial mudstone layers (>1-2.8 cm) and carbonaceous drapes. Bed thickness ranges from <1m to 2.5m.	<i>Asterosoma</i> isp., <i>Chondrites</i> isp., <i>Diplocraterion</i> isp., <i>Nereites missouriensis</i> , <i>Planolites</i> isp., <i>Rhizocorallium</i> isp., <i>Rosselia</i> isp.	3-5	Shallow marine, wave dominated environment between fair weather and storm weather wave base.	Upper Offshore
	F4BP Fine-grained sandstone and siltstone	Very fine- to fine-grained light grey sandstone and siltstone. When discernible, beds are erosive based, and preserve low angle lamination and wave ripples ranging in thickness from 0.5- 8 cm. Commonly, beds are heavily bioturbated at the top, with sedimentary structures discernible at the base of beds. Rare marine bivalve debris throughout. Mudstones ranging in thickness from 1.1-3.6cm and occur as discrete layers and drapes, but are rare. This facies ranges in thickness from 0.4-0.8m in thickness.	<i>Asterosoma</i> isp., <i>Chondrites</i> isp., <i>Diplocraterion</i> isp., <i>Planolites</i> isp., <i>Rhizocorallium</i> isp., <i>Skolithos</i> isp., <i>Thalassinoides</i> isp.	2-6	Shallow marine, wave dominated environment periodically affected by storms. Erosive sands are interpreted as tempestities, with siltstone deposited under fair-weather conditions.	Offshore Transition

	F5 _{BP} Amalgamated hummocky cross-stratified sandstone	Light grey to greenish-grey, fine-grained, hummocky cross-stratified sandstone. Rare trace fossils. Erosive bases and scours. Forms packages upwards of 6.8 m thick.	<i>Arenicolites</i> isp., <i>Ophiomorpha</i> isp., <i>Skolithos</i> isp.	0-1	Shallow marine wave dominated shoreline with periodic storm waves. High energy oscillatory flows. Storm surges result in unidirectional flow producing migrating 3D dunes	Lower Shoreface
	F6 _{BP} Amalgamated trough cross-stratified sandstone	Light grey to greenish-grey, tabular, cross-bedded and trough cross-bedded fine-grained sandstone beds 0.7-4.2m thick.. Both beds and bedsets coarsen upwards. Bed contacts are erosive based or gradational. Beds are amalgamated into packages 0.5-1m thick	<i>Macaronichnus</i> isp.	0-1	Shallow marine shoreline with periodic storm activity. High energy, with predominant longshore currents producing 2D and 3D dunes in longshore bar deposits.	Upper Shoreface

Table 4.6: Summary of facies, facies associations, and inferred depositional environments of the Bearpaw Formation. BI - Bioturbation index.

Belly River Group	Stratigraphic Unit	Facies Association	Facies	Environmental Interpretation	Systems Tract
	Bearpaw Formation	FA8 _{BP}	F1-6 _{BP}	Wave Dominated Shallow Marine	TST/HST
	DPF: Manâtakâw Member	FA7 _{MM}	F1-2 _{MM}	Estuary Bain, Lagoon, Barrier Islands	TST
	Dinosaur Park Formation	FA5/6 _{DPF}	F1-F6 _{DPF}	Coastal Plain Fluvial Channels and Associated Floodplain	LST/Early TST
	Oldman Formation	FA3 _{OF}	F2 _{OF} -7 _{OF}	Isolated Fluvial Channels and Associated Floodplain	HST
		FA4 _{OF}	F8 _{OF}	Marginal Marine Floodplain	TST
		FA2 _{OF}	F1 _{OF}	Braided Fluvial Channels	LST
		FA3 _{OF}	F2 _{OF} -7 _{OF}	Isolated Fluvial Channels and Associated Floodplain	HST
		FA4 _{OF}	F8 _{OF}	Marginal Marine Floodplain	TST
		FA2 _{OF}	F1 _{OF}	Braided Fluvial Channels	LST
	Foremost Formation	FA1 _{FF}	F1 _{FF} - F7 _{FF}	Wave Dominated Shallow marine	HST
	FF: Ribstone Creek Member		F1 _{FF} - F7 _{FF}		LST

Table 4.7: Summary of the sequence stratigraphic model applied to the Belly River Group of southwestern Saskatchewan.

References

- Bhattacharya, B., & Banerjee, S. (2014). *Chondrites* isp. indicating late Paleozoic atmospheric anoxia in eastern peninsular India. *The Scientific World Journal*, 2014, Article ID 434672, 9 p. <http://dx.doi.org/10.1155/2014/434672>
- Bojanowski, M. J., Jaroszewicz, E., Kořir, A., Łoziński, M., Marynowski, L., Wysocka, A., & Derkowski, A. (2016). Root-related rhodochrosite and concretionary siderite formation in oxygen-deficient conditions induced by a ground-water table rise. *Sedimentology*, 63(3), 523-551.
- Bowen, C. F. (1915). The stratigraphy of the Montana group, with special reference to the position and age of the Judith River Formation in north-central Montana. In *Shorter contributions to general geology, 1914* (pp. 95-153). U. S. Geological Survey, Professional Paper, 90-1.
- Boyd, R., Dalrymple, R., & Zaitlin, B. A. (1992). Classification of clastic coastal depositional environments. *Sedimentary Geology*, 80(3-4), 139-150.
- Braman, D. R., & Koppelhus, E. B. (2005). Campanian palynomorphs. In P. J. Currie & E. B. Koppelhus (Eds.), *Dinosaur Provincial Park: A spectacular ancient ecosystem revealed* (pp. 101-130). Bloomington & Indianapolis, IN: Indiana University Press.
- Buatois, L. A., & Mángano, M. G. (2011). *Ichnology: Organism-substrate interactions in space and time*. Cambridge, UK: Cambridge University Press.
- Caldwell, W. G. E. (1968). *The Late Cretaceous Bearpaw Formation in the South Saskatchewan River valley*. Saskatchewan Research Council, Geology Division, Report No. 8, 86 p.
- Cant, D. J., & Stockmal, G. S. (1989). The Alberta foreland basin: Relationship between stratigraphy and Cordilleran terrane-accretion events. *Canadian Journal of Earth Sciences*, 26(10), 1964-1975.
- Catuneanu, O. (2006). *Principles of sequence stratigraphy* (1st ed.). Amsterdam ; Boston: Elsevier.
- Catuneanu, O., Abreu, V., Bhattacharya, J. P., Blum, M. D., Dalrymple, R. W., Eriksson, P. G., . . . Winker, C. (2009). Towards the standardization of sequence stratigraphy. *Earth Science Reviews*, 92(1-2), 1-33.
- Catuneanu, O., Sweet, A. R., & Miall, A. D. (1997). Reciprocal architecture of Bearpaw TR sequences, uppermost Cretaceous, Western Canada Sedimentary Basin. *Bulletin of Canadian Petroleum Geology*, 45(1), 75-94.
- Catuneanu, O., Sweet, A. R., & Miall, A. D. (2000). Reciprocal stratigraphy of the Campanian–Paleocene western interior of North America. *Sedimentary Geology*, 134(3-4), 235-255.

- Cioffi, D., Di Eugenio, A., & Gallerano, F. (1995). A new representation of anoxic crises in hypertrophic lagoons. *Applied Mathematical Modelling*, 19(11), 685-695.
- Coates, L. (2002). *The ichnological-sedimentological signature of wave- and river-dominated deltas: Dunvegan and Basal Belly River formations, west-central Alberta* (Unpublished master's thesis). Simon Fraser University, Vancouver, Canada.
- Cobban, W. A., Walaszczyk, I., Obradovich, J. D., & McKinney, K. C. (2006). *A USGS zonal table for the Upper Cretaceous Middle Cenomanian–Maastrichtian of the western interior of the United States based on ammonites, inoceramids, and radiometric ages*. U.S. Geological Survey, Open-File Report 2006-1250.
- Cullen, T., Fanti, F., Capobianco, C., Ryan, M., & Evans, D. (2016). A vertebrate microsite from a marine-terrestrial transition in the Foremost Formation (Campanian) of Alberta, Canada, and the use of faunal assemblage data as a paleoenvironmental indicator. *Palaeogeography, Palaeoclimatology, Palaeoecology*, 444, 101-114.
- Dalrymple, R. W. (2010). Tidal depositional systems. In N. P. James & R. W. Dalrymple (Eds.), *Facies models* (4th ed., pp. 201-231). St. John's, Newfoundland: Geological Association of Canada.
- Dalrymple, R. W., Zaitlin, B. A., & Boyd, R. (1992). Estuarine facies models: Conceptual basis and stratigraphic implications. *Journal of Sedimentary Petrology*, 62(6), 1130-1146.
- Dawson, G. M. (1883). Glacial deposits of the Bow and Belly river country. *Science*, 1(17), 477-479.
- Dawson, F. M., Evans, C. G., Marsh, R., & Richardson, R. (1994). Uppermost Cretaceous and Tertiary strata of the Western Canada Sedimentary Basin. In G. D. Mossop & I. Shetsen (Comps.), *Geological atlas of the Western Canada Sedimentary Basin* (pp. 387-406). Calgary, Alberta: Canadian Society of Petroleum Geologists and Alberta Research Council.
- Dowling, D. B. (1917). *The southern plains of Alberta*. Geological Survey of Canada, Memoir 93. Ottawa, Ontario: Government Printing Bureau.
- Eberth, D. A. (1996). Origin and significance of mud-filled incised valleys (Upper Cretaceous) in southern Alberta, Canada. *Sedimentology*, 43(3), 459-477.
- Eberth, 2002 (section 4.5.1, Oldman Formation)
- Eberth, D. A. (2005). The geology. In P. J. Currie & E. B. Koppelhus (Eds.), *Dinosaur Provincial Park: A spectacular ancient ecosystem revealed* (pp. 54-82). Bloomington & Indianapolis, IN: Indiana University Press.

- Eberth, D. A., Braman, D. R., & Tokaryk, T. T. (1990). Stratigraphy, sedimentology and vertebrate paleontology of the Judith River Formation (Campanian) near Muddy Lake, west-central Saskatchewan. *Bulletin of Canadian Petroleum Geology*, 38(4), 387-406.
- Eberth, D. A., & Hamblin, A. P. (1993). Tectonic, stratigraphic, and sedimentologic significance of a regional discontinuity in the upper Judith River Group (Belly River wedge) of southern Alberta, Saskatchewan, and northern Montana. *Canadian Journal of Earth Sciences*, 30(1), 174-200.
- Elliot, T. (1986). Deltas. In H. G. Reading (Ed.), *Sedimentary environments and facies* (2nd ed., pp. 113-154). Oxford, UK: Blackwell Scientific Publications.
- Embry, A. (1990). A tectonic origin for third order depositional sequences in extensional basins - Implications for basin modeling. In *Quantitative dynamic stratigraphy* (pp. 491-501). New Jersey, NJ: Prentice Hall.
- Folinsbee, R. E., Baadsgaard, H., Cumming, G. L., Nascimbene, J., & Shafiqullah, M. (1965). Late Cretaceous radiometric dates from the Cypress Hills of Western Canada. In *Guidebook for the Alberta Society of Petroleum Geologists' 15th annual field conference, Part 1, Cypress Hills Plateau* (pp. 162-174).
- Frank, M. C. (2006). *Coal distribution in the Upper Cretaceous (Campanian) Belly River Group of southwest Saskatchewan*. Saskatchewan Industry and Resources, Open File Report 2005-33, CD-ROM.
- Frey, R. W., Curran, H. A., & Pemberton, S. G. (1984). Tracemaking activities of crabs and their environmental significance: The ichnogenus *Psilonichnus*. *Journal of Paleontology*, 58(2), 333-350.
- Frey, R. W., & Pemberton, S. G. (1987). The *Psilonichnus* ichnocoenose, and its relationship to adjacent marine and nonmarine ichnocoenoses along the Georgia coast. *Bulletin of Canadian Petroleum Geology*, 35(3), 333-357.
- geoLOGIC Systems Ltd. (2018) (section 4.2)
- Gilbert, M. M., Bamforth, E. L., Buatois, L. A., & Renault, R. W. (2018). Paleoeology and sedimentology of a vertebrate microfossil assemblage from the easternmost Dinosaur Park Formation (Late Cretaceous, Upper Campanian,) Saskatchewan, Canada: Reconstructing diversity in a coastal ecosystem. *Palaeogeography, Palaeoclimatology, Palaeoecology*, 495, 227-244.
- Gilbert, M. M., Buatois, L. A., & Renault, R. W. (2019). Ichnology and depositional environments of the Upper Cretaceous Dinosaur Park – Bearpaw Formation transition in the Cypress Hills region of Southwestern Saskatchewan, Canada. *Cretaceous Research*. Published online at doi: 10.1016/j.cretres.2018.12.017

- Gordon, J. (2000). *Stratigraphy and sedimentology of the Foremost Formation in southeastern Alberta and southwestern Saskatchewan* (Unpublished master's thesis). University of Regina, Canada.
- Gradstein, F. M., Ogg, J. G., Schmitz, M. D., & Ogg, G. M. (2012). *The geologic time scale 2012* (Vol. 1-2). Elsevier B.V.
- Hamblin, A. P. (1997a). Stratigraphic architecture of the Oldman Formation, Belly River Group, surface and subsurface of southern Alberta. *Bulletin of Canadian Petroleum Geology*, 45(2), 155-177.
- Hamblin, A. P. (1997b). Regional distribution and dispersal of the Dinosaur Park Formation, Belly River Group, surface and subsurface of southern Alberta. *Bulletin of Canadian Petroleum Geology*, 45(3), 377-399.
- Hamblin, A. P., & Abrahamson, B. (1996). Stratigraphic architecture of "Basal Belly River" cycles, Foremost Formation, Belly River Group, subsurface of southern Alberta and southwestern Saskatchewan. *Bulletin of Canadian Petroleum Geology*, 44(4), 654-673.
- Harzallah, A., & Chapelle, A. (2002). Contribution of climate variability to occurrences of anoxic crises 'malaïgues' in the Thau lagoon (southern France). *Oceanologica Acta*, 25(2), 79-86.
- Hayden, F. (1856). On the geology of the Missouri Valley. *Proceedings of the American Philosophical Society*, 292-296.
- Jerzykiewicz, T., & Norris, D. K. (1994). Stratigraphy, structure and syntectonic sedimentation of the Campanian 'Belly River' clastic wedge in the southern Canadian Cordillera. *Cretaceous Research*, 15(4), 367-399.
- Kauffman, E., & Caldwell, W. (1993). The Western Interior Basin in space and time. In W. G. E. Caldwell & E. G. Kauffman (Eds.), *Evolution of the Western Interior Basin* (pp. 1-30). Geological Association of Canada, Special Paper #39.
- Lambe, L. M. (1907). On a new crocodilian genus and species from the Judith River Formation of Alberta. *Proceedings and Transactions of the Royal Society of Canada, Third Series, Vol. 1*, 219-244.
- Leckie, D. A., & Smith, D. G. (1992). Regional setting, evolution, and depositional cycles of the Western Canada Foreland Basin. In R. W. Macqueen & D. A. Leckie (Eds.), *Foreland basins and fold belts* (pp. 9-46). American Association of Petroleum Geologists, AAPG Memoir 55.
- Leeder, M. R., & Stewart, M. D. (1996). Fluvial incision and sequence stratigraphy: Alluvial responses to relative sea-level fall and their detection in the geological record. In S. P. Hesselbro & D. N. Parkinson (Eds.), *Sequence stratigraphy in British geology* (pp. 25-39). Geological Society, London, Special Publications, 103.

- Lerbekmo, J. F., & Braman, D. R. (2002). Magnetostratigraphic and biostratigraphic correlation of late Campanian and Maastrichtian marine and continental strata from the Red Deer Valley to the Cypress Hills, Alberta, Canada. *Canadian Journal of Earth Sciences*, 39(4), 539-557.
- MathWorks (2018). (section 4.2)
- McLean, J. R. (1971). *Stratigraphy of the Upper Cretaceous Judith River Formation in the Canadian Great Plains*. Saskatchewan Research Council, Geology Division, Report No. 11.
- Meek, F. B., & Hayden, F. V. (1856). Descriptions of new species of Acephala and Gastropoda from the Tertiary formations of Nebraska Terr., with some general remarks on the geology of the country about the sources of the Missouri River. *Academy of Natural Sciences of Philadelphia, Proceedings*, 8, 111-126.
- Miall, A. D. (2010) Alluvial models. In N. P. James & R. W. Dalrymple (Eds.), *Facies models* (4th ed., pp. 201-231). St. John's, Newfoundland: Geological Association of Canada.
- Miall, A. D. (2013). *The geology of fluvial deposits: Sedimentary facies, basin analysis, and petroleum geology*. Springer.
- Nägler, T. F., Neubert, N., Böttcher, M. E., Dellwig, O., & Schnetger, B. (2011). Molybdenum isotope fractionation in pelagic euxinia: Evidence from the modern Black and Baltic seas. *Chemical Geology*, 289(1-2), 1-11.
- Noad, J. J. (1993). *An analysis of changes in fluvial architecture through the upper Oldman Member, Judith River Formation of the Upper Cretaceous, southern Alberta, Canada* (Unpublished master's thesis). Birkbeck College, University of London, UK.
- Peale, A. C. (1912). On the stratigraphic position and age of the Judith River Formation. *Journal of Geology*, 20(6), 530-549.
- Pemberton, S. G., Spila, M., Pulham, A. J., Saunders, T., MacEachern, J. A., Robbins, D., & Sinclair, I. K. (2001). *Ichnology & sedimentology of shallow to marginal marine systems. Ben Nevis and Avalon reservoirs, Jeanne d'Arc Basin*. Geological Association of Canada, Short Course Notes, 15. St. John's, Newfoundland: Geological Association of Canada.
- Posamentier, H. (2001). Lowstand alluvial bypass systems: Incised vs. unincised. *AAPG Bulletin*, 85(10), 1771-1793.
- Posamentier, H. W., & Allen, G. P. (1999). *Siliciclastic sequence stratigraphy: Concepts and applications*. SEPM Concepts in Sedimentology and Paleontology # 7. Tulsa, OK: Society for Sedimentary Geology.

- Posamentier, H. W., Allen, G. P., James, D. P., & Tesson, M. (1992). Forced regressions in a sequence stratigraphic framework: Concepts, examples, and exploration significance. *AAPG Bulletin*, 76(11), 1687-1709.
- Power, B. A., & Walker, R. G. (1996). Allostratigraphy of the Upper Cretaceous Lea Park-Belly River transition in central Alberta, Canada. *Bulletin of Canadian Petroleum Geology*, 44(1), 14-38.
- Price, R. A. (1994). Cordilleran tectonics and the evolution of the Western Canada Sedimentary Basin. In G. D. Mossop & I. Shetson (Comps.), *Geological atlas of the Western Canada Sedimentary Basin* (pp. 13-24). Calgary, Alberta: Canadian Society of Petroleum Geologists and Alberta Research Council.
- Quiroz, L. I., Buatois, L. A., Mángano, M. G., Jaramillo, C. A., & Santiago, N. (2010). Is the trace fossil *Macaronichnus* an indicator of temperate to cold waters? Exploring the paradox of its occurrence in tropical coasts. *Geology*, 38(7), 651-654.
- Retallack, G. J. (2008). *Soils of the past: An introduction to paleopedology*. John Wiley & Sons.
- Rogers, R. R. (1995). *Sequence stratigraphy and vertebrate taphonomy of the Upper Cretaceous Two Medicine and Judith River formations, Montana* (Unpublished doctoral dissertation). University of Chicago, U.S.A.
- Rogers, R. R., Kidwell, S. M., Deino, A. L., Mitchell, J. P., Nelson, K., & Thole, J. T. (2016). Age, correlation, and lithostratigraphic revision of the Upper Cretaceous (Campanian) Judith River Formation in its type area (north-central Montana), with a comparison of low- and high-accommodation alluvial records. *The Journal of Geology*, 124(1), 99-135.
- Russell, L. S., & Landes, R. W. (1940). *Geology of the southern Alberta plains*. Geological Survey of Canada, Memoir 221.
- Seilacher, A. (1990). Aberrations in bivalve evolution related to photo- and chemosymbiosis. *Historical Biology*, 4, 289-311.
- Slingerland, R., & Smith, N. D. (2004). River avulsions and their deposits. *Annual Review of Earth and Planetary Science*, 32, 257-285.
- Slipper, S. E., & Hunter, H. M. (1931). Stratigraphy of Foremost, Pakowki, and Milk River formations of southern plains of Alberta. *AAPG Bulletin*, 15(10), 1181-1196.
- Stanton, T., & Hatcher, J. (1905). Geology and paleontology of the Judith River beds. In T. Stanton, J. Hatcher & F. H. Knowlton, *Geology and paleontology of the Judith River beds, with a chapter on the fossil plants* (pp. 7-119). U. S. Geological Survey, Bulletin 257. Washington: Government Printing Office.

- Troke, C. (1993). *Sedimentology, stratigraphy and calcretes of the Comrey Member, Oldman Formation (Campanian), Milk River Canyon, southeastern Alberta* (Unpublished master's thesis). University of Calgary, Canada.
- Tsujita, J. C. (1995). *Stratigraphy, taphonomy and paleoecology of the Upper Cretaceous Bearpaw Formation in southern Alberta* (Unpublished doctoral dissertation). McMaster University, Hamilton, Canada.
- Uchman, A., Johnson, M. E., Rebelo, A. C., Melo, C., Cordeiro, R., Ramalho, R. S., & Ávila, S. P. (2016). Vertically-oriented trace fossil *Macaronichnus segregatis* from Neogene of Santa Maria Island (Azores; NE Atlantic) records vertical fluctuations of the coastal groundwater mixing zone on a small oceanic island. *Geobios*, 49(3), 229-241.
- Zaitlin, B., Dalrymple, R., & Boyd, R. (1994). The stratigraphic organization of incised-valley systems associated with relative sea-level change. In R. W. Dalrymple, R. Boyd & B. A. Zaitlin (Eds.), *Incised-valley systems: Origin and sedimentary sequences* (pp. 45-60). Society for Sedimentary Geology, SEPM Special Publication No. 51.

Transition

Chapter 5 presents a regional case study of the sedimentology, sedimentary environments, biostratigraphy, and vertebrate paleontology of the Lake Diefenbaker site in Saskatchewan Landing Provincial Park in southwestern Saskatchewan. This site inspired the author's initial investigation of the Belly River Group in Saskatchewan, with the vertebrate material being the focus of the author's undergraduate thesis. The sequence-stratigraphic and depositional environment overview presented in Chapters 3 and 4 provide the necessary framework from which to elucidate complex paleoecologic significance from the vertebrate remains recovered from the Lake Diefenbaker paleontologic assemblage. Not only does the site represent the easternmost surface expression of the Dinosaur Park Formation in Canada, but it is the first comprehensive within-site diversity study concerning Campanian vertebrate microfossil assemblages in Saskatchewan. M. Gilbert carried out the fieldwork, wrote the manuscript, and prepared all the figures and tables presented in the chapter. E. Bamforth contributed by assisting in specimen identification and alpha diversity analysis.

Paleoecology and Sedimentology of a Vertebrate Microfossil Assemblage from the Easternmost Dinosaur Park Formation (Late Cretaceous, Upper Campanian) Saskatchewan, Canada: Reconstructing Diversity in a Coastal Ecosystem

Abstract

A ~42 meter section of Late Cretaceous Upper Campanian sediments exposed along the northern shore of Lake Diefenbaker in Saskatchewan Landing Provincial Park, southwestern Saskatchewan, Canada, represents the easternmost outcrop of the Dinosaur Park Formation in the Western Canada Sedimentary Basin. Herein we document a new microvertebrate locality from the upper part of this formation that shows high diversity in a mixed coastal and marine assemblage. Palynology, ichnology, sedimentology, and vertebrate paleontology are integrated to determine paleoenvironmental and paleoecological conditions in the region. The site is interpreted as having been deposited under marginal-marine conditions near a shoreline undergoing transgression by the encroaching Bearpaw Sea. Though well-studied and -sampled in Alberta, the Dinosaur Park Formation is poorly exposed with little known associated vertebrate assemblages in Saskatchewan. These discoveries from the new microvertebrate site offer new insights into Late Cretaceous ecosystems near paleocoastlines, allowing for future studies of spatial diversity patterns relative to Albertan faunas. Herein is presented the first published occurrences of several Late Campanian vertebrate taxa in Saskatchewan.

5.1 Introduction

Changes in faunal composition and depositional environments in the alluvial and coastal plains flanking the Western Interior Seaway of North America have been widely documented in Late Cretaceous Campanian (76.9–75.8 Ma) deposits from southern Alberta (Dodson, 1971; Wood et al., 1988; Brinkman, 1990; Eberth, 1990; Brinkman et al., 1998, 2004, 2005a or 2005b?; Brown et al., 2013). Fossil-bearing Campanian deposits are present in Saskatchewan and hold a similar potential for the study of paleoecosystems at the time. These deposits have been under-studied compared to equivalent strata in Alberta, and it is not known if and how the paleofaunas of the two provinces vary. It is reasonable to suggest that faunal variations would occur between the two provinces. The ecosystems in Saskatchewan were closer to the paleoshoreline of the Western Interior Sea, and would have experienced marine influence for a greater period of time. Herein, we describe a fossil locality from Saskatchewan, presenting one of the first descriptions of the Campanian-aged terrestrial paleobiodiversity from the province.

Vertebrate microfossils (‘microvertebrates’) have played an important role in understanding paleoecology and community succession through the stratigraphic record (Shotwell, 1955; Estes & Berberian, 1970; Dodson, 1973; Sankey, 2008). Vertebrate microfossil assemblages (referred to here as ‘microsites’) are concentrations of fossilized vertebrate remains, including small bones, scales and teeth of multiple taxa, of which more than 75% are 5 cm in size or smaller (Rogers & Kidwell, 2007). These accumulations may be considered both thanatocoenoses (accumulations of *in situ* fossils in a single locality) and biocoenoses (biological communities at a single locality), providing a ‘snapshot’ of biodiversity over the period that the microsite was formed. These fossil deposits afford higher-resolution information about

paleocommunity structure than is available from any other geological or macro-paleontological source.

Campanian-aged (83.6–72.1 Ma) deposits of the Belly River Group (BRG) in southern and central Alberta include (from oldest to youngest), the Foremost, Oldman, and Dinosaur Park formations. In Montana, the BRG is equivalent to the Judith River Formation and upper portion of the Two Medicine Formation (Rogers, 1998). All group-equivalents yield rich microsite assemblages (Rogers & Brady, 2010; Eberth, 2015). Whereas the BRG in Alberta is well-exposed and -represented in core, BRG outcrops and associated microsites in Saskatchewan are generally sparse and poorly known. This lack of knowledge is problematic because Saskatchewan contains the eastern- and northeasternmost occurrences of this group in Canada (Eberth et al., 1990).

During the Campanian, Saskatchewan was situated at a slightly higher latitude than today, near the paleocoastline of the Western Interior Seaway. Based on climate-leaf analysis, the paleoclimate is suggested to have been warm temperate to subtropical, with a mean annual temperature of around 12.0°C ($\pm 2.1^\circ$) and a growing season precipitation of 1586 mm (± 280 mm) (Golovneva, 2000). In modern environments, salinity has been shown to be a primary factor in controlling the distribution and abundance of organisms (Remane & Schlieper, 1972; Basan et al., 1977; Dunson & Mazzotti, 1989; Dunson & Travis, 1991; MacEachern & Gingras, 2007; Buatois & Mángano, 2011; Torres-Dowdall et al., 2013), therefore, the easternmost deposits in Saskatchewan offer an opportunity to increase understanding of faunal turnover across the coastal and alluvial plains in response to marine transgression. Because they were nearer paleocoastline, paleocommunities in Saskatchewan should have been more influenced by

temporal fluctuations in sea level than those in more inland locations in southern Alberta (Eberth et al., 1990).

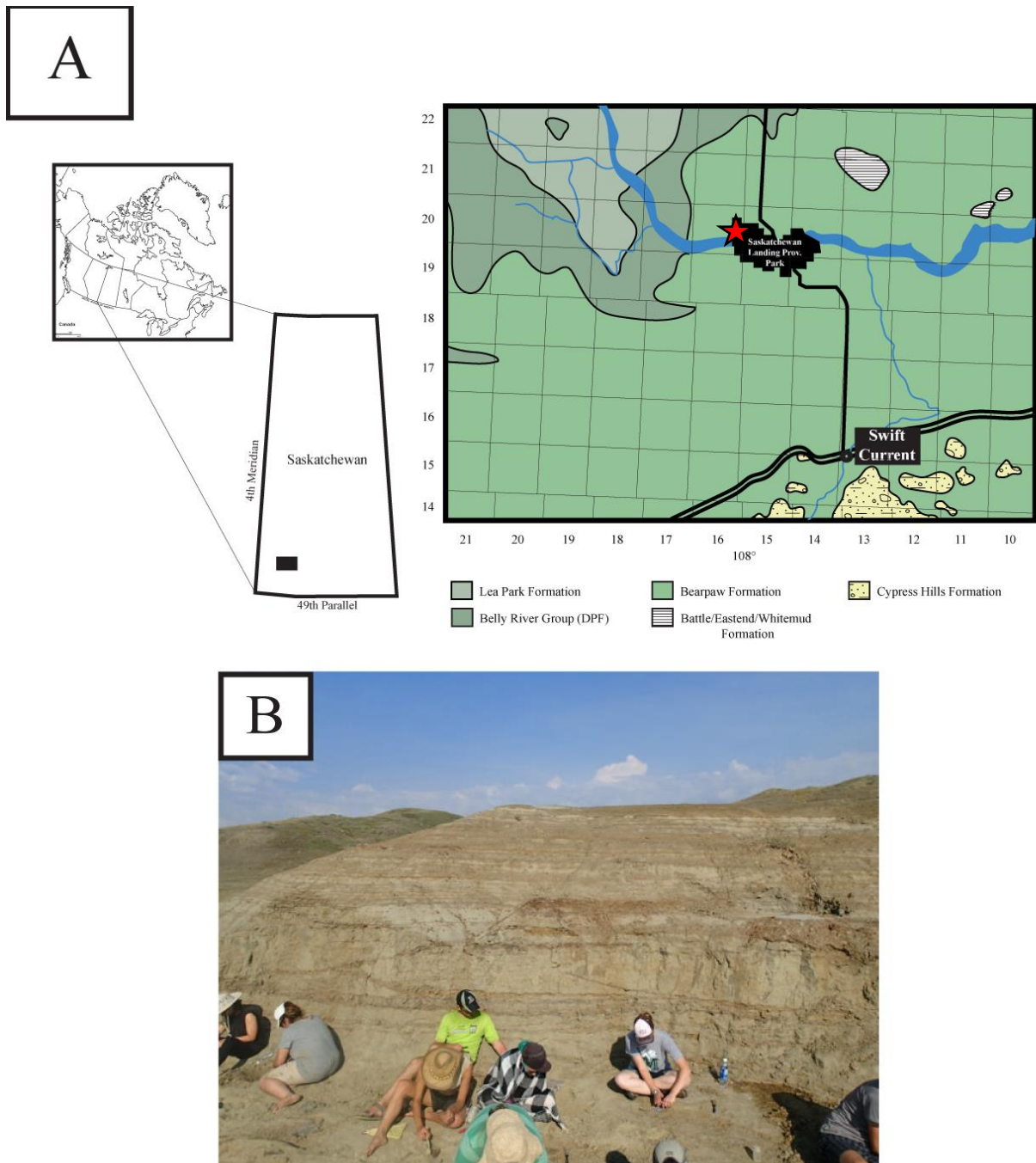


Figure 5.1: Location of the Lake Diefenbaker microsite (LD, red star) in Saskatchewan Landing Provincial Park, southwest Saskatchewan. **A.** Geographic location of Saskatchewan in context to regional landmarks. **B.** Photograph of outcrop where the majority of microsite material was collected. Note trough cross-bedding followed by beds containing flaser and wavy bedding.

In this paper, we describe the sediments and vertebrate paleontology of a fossil-rich locality at Saskatchewan Landing Provincial Park in southwestern Saskatchewan, Canada (Fig. 5.1), and interpret the depositional environment and associated microvertebrate assemblage. Interpretation of the depositional environments has been aided by ichnological analysis. The fossil taxa in this site constitute the easternmost occurrence of a Late Campanian terrestrial microvertebrate locality in the Western Interior Seaway. The fossil locality on Lake Diefenbaker ('Lake Diefenbaker site': LD) provides a rare opportunity to study the fauna in an ancient marginal-marine environment that responded to a sea-level rise.

5.2 Materials and Methods

5.2.1 Geological Setting

Deposition of Cretaceous and Paleogene sediments in the Western Canada Sedimentary Basin (Fig. 5.2) occurred in two depocenters separated by the Bow Island Arch: the Williston Basin to the east, and the Foreland Basin to the west (Dawson et al., 1994). During the Laramide Orogeny (~ 70–80 Ma), collisional accretion of microcontinents onto the west coast of North America caused thrust-sheet loading, resulting in formation of an orogenic belt (Price, 1994). This flexed the craton to produce a deeply subsiding asymmetric foredeep fed by sediments from the tectonically induced slope (Catuneanu et al., 2000). In west-central North America, this resulted in deposition of large amounts of marine and nonmarine clastic sediments in transgressive-regressive, tectonically controlled wedge-cycles (Leckie & Smith, 1992). The Belly River Group is the fourth of five recognized cycles of foreland basin deposition (Embry, 1990; Miall, 1991; Leckie & Smith, 1992).

Deposition of the Campanian Belly River Group resulted from large sediment supply to

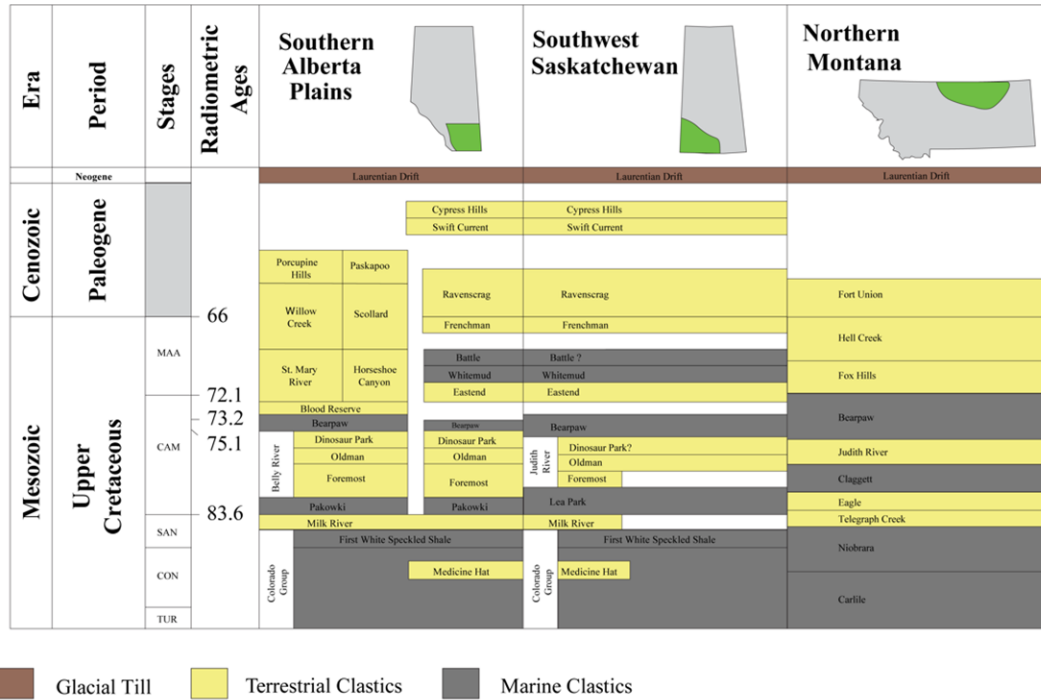


Figure 5.2: Stratigraphic nomenclature utilized in southeastern Alberta and southwestern Saskatchewan through the Upper Cretaceous Series in the Western Canada Sedimentary Basin. Radiometric and biostratigraphic dates: 66: K-T boundary (Gradstein et al., 2012); 72.1: Campanian – Maastrichtian boundary (Gradstein et al., 2012); 73.2 ± 0.4: Dorothy Bentonite (Lerbekmo & Braman, 2002); 75.1: *Exileloceras jenneyi* (Cobban et al., 2006); 83.6: Campanian – Santonian boundary (Gradstein et al., 2012). Modified from Braman and Sweet (2012). TUR - Turonian; CON - Coniacian; SAN - Santonian; CAM - Campanian; MAA - Maastrichtian.

the basin, producing an eastward-thinning paralic (interfingering marine and coastal) to nonmarine clastic succession (Cant & Stockmal, 1989). Three formations from this period are recognized formally in the western Canadian plains. In ascending order, these are the Foremost, Oldman and Dinosaur Park formations (Eberth & Hamblin, 1993). Each formation is bound by a disconformity, and has distinctive sedimentological and petrographic signatures that reflect tectonic controls of sediment supply (Fig. 5.3) (Eberth, 2005).

The Foremost Formation interfingers with the underlying marine Lea Park Formation, which is equivalent to the marine Pakowki and Claggett formations of Alberta and Montana, respectively, and records a period of regression. Maximum retreat of the Western Interior Seaway across Saskatchewan and Alberta is represented by the Oldman Formation. The transgressive sediments of the overlying Dinosaur Park Formation interfinger with sediments of the overlying, marine Bearpaw Formation (Eberth & Hamblin, 1993). Upper Belly River and Bearpaw exposures crop out along the South Saskatchewan River Valley in Alberta and Saskatchewan, with Dinosaur Park and Bearpaw formations exposed along the western bank of Lake Diefenbaker in Saskatchewan Landing Provincial Park. In earlier interpretations, McLean (1971) assigned the lowest terrestrial beds to the Judith River Formation, and Caldwell (1968) assigned the overlying marine sediments to the Bearpaw Formation.

Cretaceous deposits in the South Saskatchewan River Valley lie at the center of the Moose Jaw syncline (MJS), whose axis generally coincides with the Missouri Coteau, a narrow band of prairie uplands that runs through southern Saskatchewan to South Dakota (Caldwell, 1968). The MJS is a northwest-trending extension of the Williston Basin of northeastern Montana and North Dakota that flanks the Bowdoin Dome to the east (McCrossan & Glaister, 1964). The MJS is believed to have been caused by dissolution of Middle Devonian Prairie

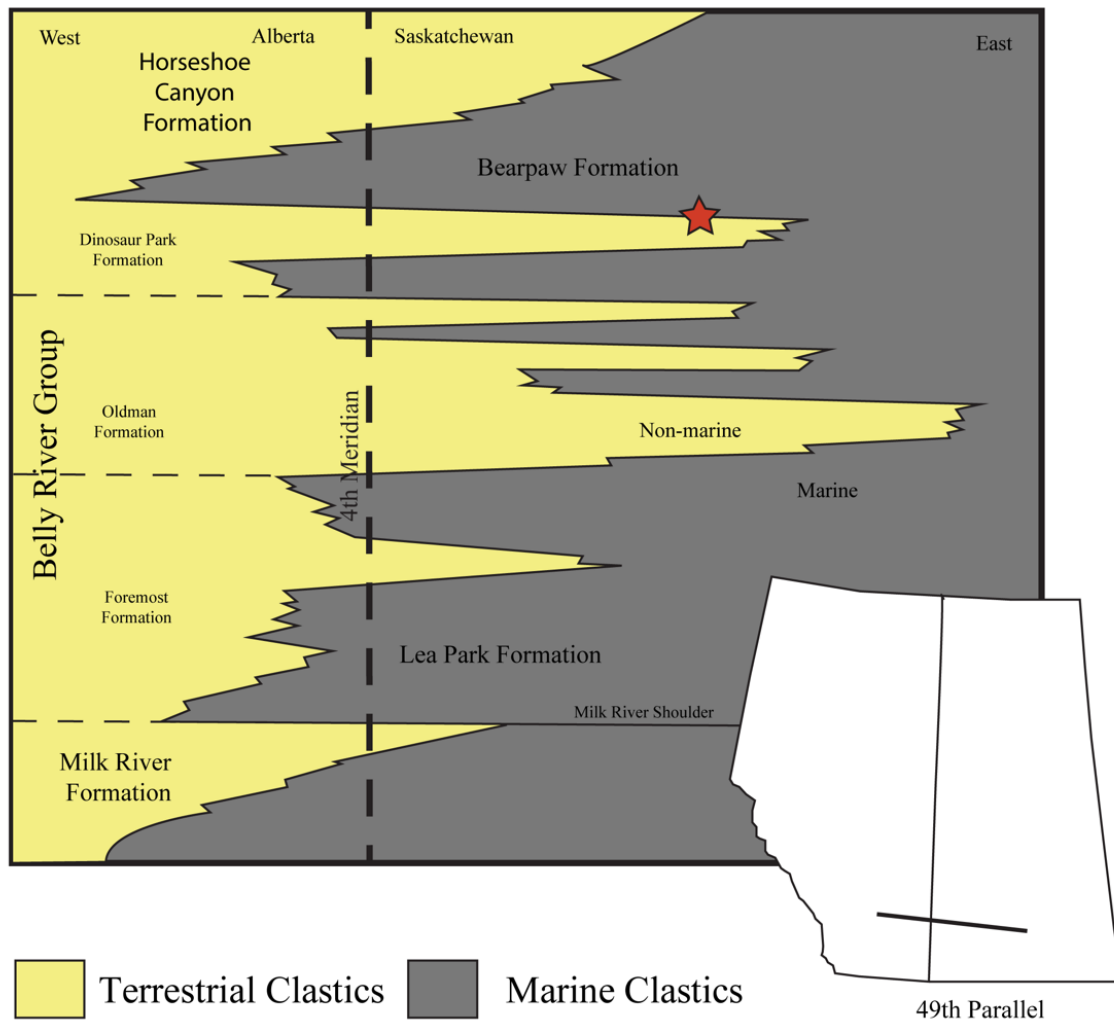


Figure 5.3: Simplified schematic cross-section of the Upper Cretaceous Series through southern Alberta and southern Saskatchewan. Modified from McLean (1971), and represents approximate location of site according to the schematic. The Saskatchewan–Alberta border runs concurrent with the 4th meridian (110°W longitude) along its entirety. Star represents approximate location of the Saskatchewan Landing Site in relation to relative transgressive-regressive cycles of the Dinosaur Park Formation.

Evaporite salts, which resulted in collapse of overlying strata (McLean, 1971). Slumping and rotational slump faulting has further complicated stratigraphy in the valley (McConnell, 1885; Caldwell, 1968). At the Lake Diefenbaker site (LD), all Cretaceous strata are laterally discontinuous making stratigraphic mapping difficult. Furthermore, construction of the Gardner Dam in 1971 led to flooding of most BRG exposures along the South Saskatchewan River valley.

BRG strata at the LD crops out on the north side of the river in Saskatchewan Landing Provincial Park. The Cretaceous strata dip gently at 8° to the north-northeast and strike west. Deformation of the bedrock at the site is attributed to salt-induced collapse (causing the MJS) during the Late Cretaceous to Holocene, and rotational slump faulting due to migration of the South Saskatchewan River.

5.2.2 History of Fossil Collection

Fossil material was originally surface-collected from the Lake Diefenbaker site in 1975 by N. Yurchyshyn. The material, which included champsosaurs, dinosaurs, turtles, crocodiles, fish, chondrichthyans, and a rare fossil of the toothed bird *Baptoris*, was assigned to the Royal Saskatchewan Museum (RSM) collection under catalogue number RSM P2306. The site was not revisited until 1990, when T. Tokaryk (RSM), D. Taylor and N. Yurchyshyn returned. Their surface-picked collection (catalogued under RSM P2199) included taxa similar to those collected in 1975, but added plesiosaur material. In 1992, the collection T. Tokaryk, J. Storer (RSM) and G. Schutte undertook (catalogued under RSM P2471), added shark and salamander taxa and elasmosaurs to the collections. Another surface collection (catalogued under RSM P2945) by W. Long (RSM) and M. Caldwell (University of Alberta) took place in 2002.

In 2012, H. Larsson (McGill University-Redpath Museum) and students visited the site.

They, with two of the authors (MG, EB), excavated the microsite between 2012 and 2015. That collection (P3217 at RSM) added new taxa. One thousand, one hundred and eighty-five vertebrate fossils have been collected from the LD, and the collection is still ongoing.

5.2.3 Data Collection and Specimen Identification

Detailed sedimentologic and stratigraphic information was recorded during summers of 2012 and 2013 after outcrop surfaces were cleaned. Sediment logs included Brunton© compass and Jacob's Staff measurements. Standard sedimentological information (grain size, clast shape, sedimentary structures, paleocurrent indicators, bed geometry, bed contacts, body fossils, trace fossils) was recorded. Sediment color was assigned using the Munsell color chart (Munsell, 2000).

Palynology samples were collected when stratigraphic measurements were made. Three sub-samples from each stratigraphic horizon were collected for palynological analysis and sent to Global Geolabs Ltd. (<http://www.globalgeolab.com>) in Medicine Hat, Alberta, for processing. The resulting slides were analysed and the palynomorphs identified by Dennis Braman of the Royal Tyrrell Museum in Drumheller, Alberta. The palynological samples are currently catalogued and stored at that location.

Microvertebrate fossil material was both picked at the surface and shovelled out in a mass, a strategy known as bulk collecting. Bulk material was screen-washed with a #18 U.S. standard size sieve with 1 mm openings, and picked under a dissection microscope. Fossil material was identified and catalogued at the RSM by Tim Tokaryk, John Storer, Meagan Gilbert and Emily Bamforth (authors), and at McGill University by Sarah Popov and Hans Larsson. All material was identified to the lowest possible taxonomic level and the abundance of each type of faunal element was determined. In total, 1185 elements were identified and included in this

study. The collections are housed at the Royal Saskatchewan Museum T. rex Discovery Centre in Eastend, Saskatchewan.

5.2.4 Diversity Analysis

In this study, alpha ('within site') diversity measurements were calculated using non-parametric species estimators. Non-parametric species estimators extrapolate the number of species that would be present in a sample, if that sample were 'complete' (Colwell & Coddington, 1994). The fossil record is by its nature incomplete, and rare taxa will inevitably be missing from any sample. This introduces inaccuracies when trying to establish species diversity in the fossil record. Species estimators aim to mitigate complications that arise from sample incompleteness by estimating how many taxa may be missing, and then adding that number to the observed diversity (Colwell & Coddington, 1994).

These estimators use the number of 'rare' taxa, represented by singletons or doubletons, in a sample to estimate how many species are theoretically missing (Vavrek, 2011). These estimators are often used in neo-ecological studies, but have recently been applied to the study of paleoecology (Hammer & Harper, 2006). These estimators have an advantage over the more common rarefaction method as they are not as prone to underestimating diversity in communities with low species evenness, and are generally not sensitive to the underlying pattern of species abundances (Gotelli & Colwell, 2001). Previous reviews of the performance of non-parametric species estimators (i.e., Colwell & Coddington, 1994; Hortal et al., 2006) suggest that the Chao-1 (Chao, 1984), Abundance-based Coverage Estimator (ACE) (Chao & Lee, 1992; Chao et al., 1993; Lee & Chao, 1994), and second-order jackknife estimator (Smith & van Belle, 1984) perform best for abundance-based paleontological databases. Equations for these species estimators (see Chapter 2), as well as future discussion of their application, can be found in the

references provided here.

Non-parametric species estimators were calculated using the ‘vegan’ package (Oksanen, 2010) and the ‘fossil’ package (Vavrek, 2011) in R Statistical Software (R Core Team, 2013), version 2.13.2.

5.3 Results

5.3.1 Facies Descriptions and Interpretations

Sedimentary deposits at the LD (Fig. 5.4) can be classed into seven lithofacies. A description and depositional interpretation for each lithofacies follows.

Facies 1: Silty and sandy inclined heterolithic stratification

Description

Facies 1 consists of inclined centimeter- to millimeter-scale, tabular to lenticular, parallel-laminated and current-ripple cross-laminated, light gray to buff, very fine-grained sandstone. This alternates with light brown to brownish-gray mudstone and claystone locally with carbonaceous laminae (Fig. 5.5B, C). This is consistent with the definition of inclined heterolithic stratification (Thomas, 1987). This facies is laterally extensive, is 0.3–4.7 m thick, and extends to both the east and west before dipping below the surface or being concealed by vegetation. Evidence of bidirectionality of paleocurrents is present locally, with ripple crests trending northwest and southeast. A fining-upward trend is apparent, with bedding changing gradationally up-section from flaser to wavy, to lenticular. Ironstone and claystone nodules are present in the sandstones. Trace fossils are found throughout the unit and include the ichnogenera *Planolites*,

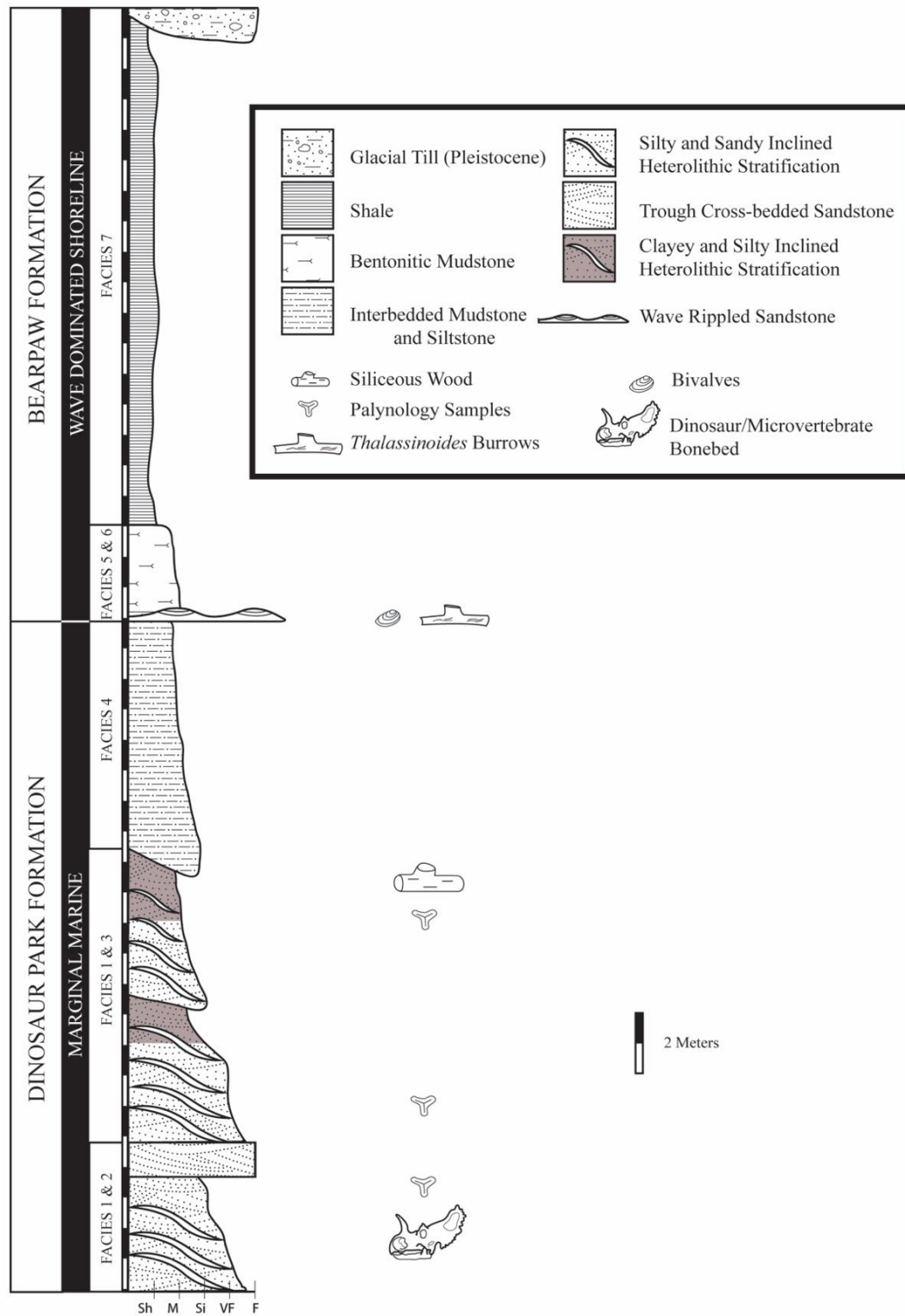


Figure 5.4: Measured section of the Dinosaur Park – Bearpaw Formation exposure at the Saskatchewan Landing Provincial Park, Lake Diefenbaker site. Sh - Shale; M - Mudstone; Si - Siltstone; VF - Very fine-grained sandstone; F - Fine-grained sandstone.

Palaeophychus, and *Teichichnus*. Most vertebrate fossils discussed here are present in this facies.

Interpretation

Inclined, parallel-laminated and ripple cross-laminated sandstone and mudstone, forming fining-upward intervals with erosive bases in this section are characteristic of tidally influenced point bar deposits. Bidirectional ripples with mudstone and carbonaceous drapes indicate changes in flow regime, and are commonly associated with a variety of tide-influenced settings, such as tidal flats and tidal sandbars (Wood, 1989; Eberth et al. 1990; Lettley & Pemberton, 2004; Dalrymple & Choi, 2007; Davis et al., 2011; Daidu et al., 2013). Inclined heterolithics with flaser, wavy, and lenticular bedding is typical of tidally influenced coastal plain channels (James & Dalrymple, 2010). This facies is interpreted as migrating tidally influenced point bars.

Facies 2: Trough cross-bedded sandstone

Description

Facies 2 comprises trough cross-bedded, light gray to buff, fine- to very fine-grained sandstone units with erosive bases, invariably overlying Facies 1. *In situ* detrital claystone and siderite intraclasts, 1.2–5 cm long, are preserved in individual troughs (Fig. 5.5C, D). Clay drapes and carbonaceous laminae are locally present between cross beds. Paleocurrent measurements indicate flow directions towards the east-southeast.

Interpretation

Trough cross-bedding commonly implies subaqueous migration of 3D dunes. Fine- to very fine-grained sandstone with clay and carbonaceous drapes suggests intervening periods of slack water and (or) variation in flow regime (James & Dalrymple, 2010). This sandstone facies is interpreted as intertidal channel fill. Sharp contacts with over- and underlying heterolithic beds

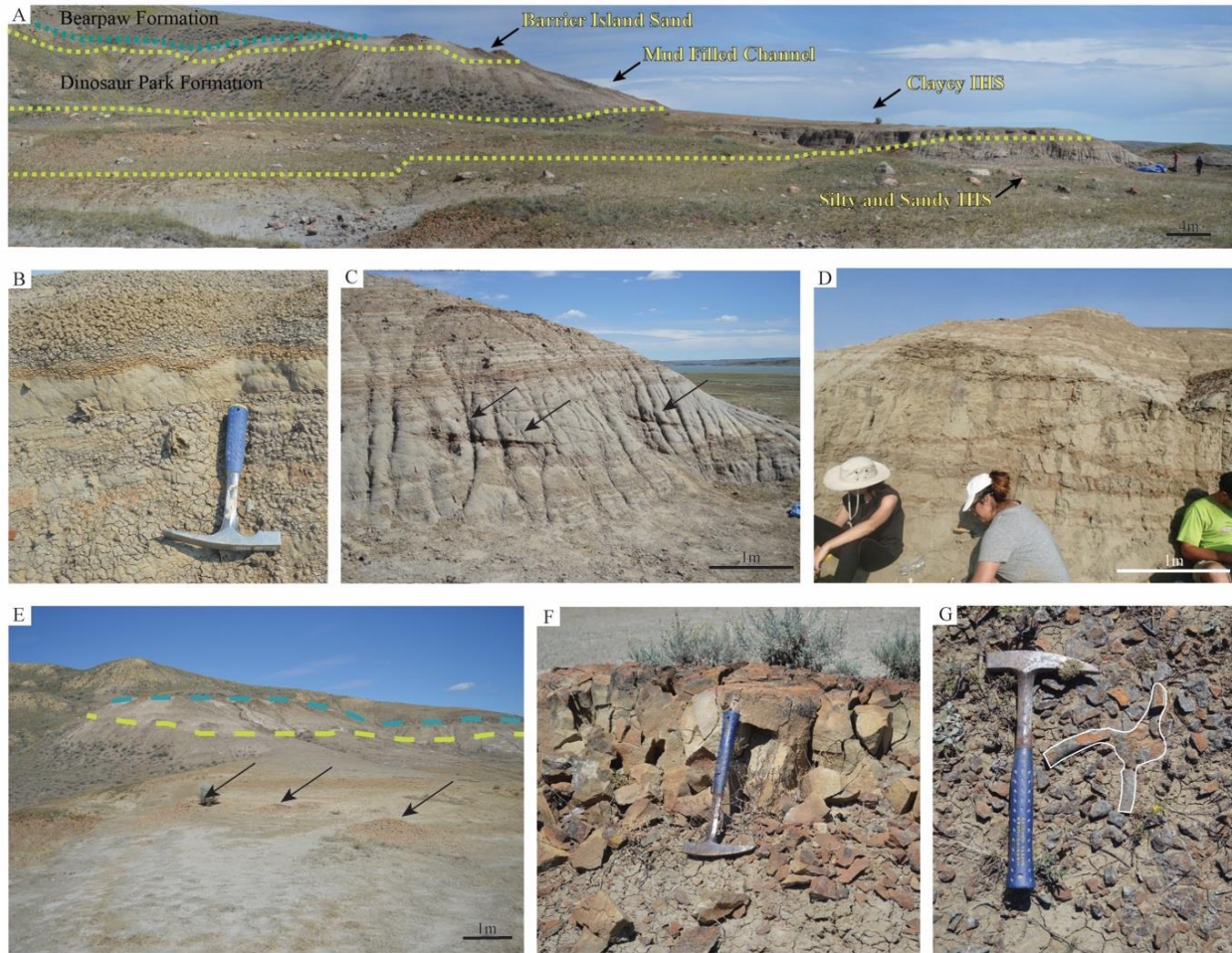


Figure 5.5: **A.** Panoramic photograph of the Saskatchewan Landing site. The yellow dashed lines indicate boundaries between IHS (inclined heterolithic stratification), mud-filled channel, and barrier island sand. The blue dashed line indicates the contact between the Dinosaur Park Formation and the Bearpaw Formation. **B.** Rippled sands and mudstone interbedding in Facies 1. **C.** IHS and trough cross-bedded sandstones of Facies 1 and 2. The arrows indicate carbonaceous laminae between troughs of Facies 2. **D.** Erosive-based trough cross-bedding of Facies 2 with ironstone clasts at the base (arrows). **E.** Mudstones with siliceous tree trunks (arrows) of Facies 3. Base of the U-shaped channel body of Facies 4 is outlined with yellow dashed line. Formation contact between the Dinosaur Park and the Bearpaw formations is shown with a dashed blue line. **F.** Iron-cemented, very fine-grained sandstone of Facies 5 separating terrestrial Dinosaur Park Formation deposits from overlying marine shales of the Bearpaw Formation. **G.** *Thalassinoides* isp. burrows with very fine-grained sandy infill directly underlying deposits of Facies 5. Trace fossil is outlined in white. Estwing chisel edge rock pick length – 28 cm (B); Estwing rock pick length – 33 cm (F, G).

of Facies 1 support this interpretation (Wood, 1985, 1989; Eberth, 1993, 2005).

Facies 3: Silty and clayey inclined heterolithic stratification

Description

This facies consists of massive green-gray mudstone with minor carbonaceous shale. Contacts between the shale and the underlying facies vary from gradual to abrupt. This facies is 2–6 m thick, with *in situ* fossilized wood and wood fragments common throughout (Fig. 5E). A monospecific trace-fossil assemblage consisting of sparse *Planolites* is present. Dinoflagellates were recovered in one of the sampled intervals.

Interpretation

Massive mudstone facies with *in situ* fossil logs and dinoflagellates imply deposition in a coastal region occasionally inundated with low-salinity waters (Boyd et al., 1992; Dalrymple et al., 1992; James & Dalrymple, 2010; Davis et al., 2011). *Planolites* is a facies-crossing ichnotaxon present in both continental and marine environments (Buatois & Mángano, 2007). However, in this context *Planolites* most likely represents the activity of a brackish-water infauna. In modern transgressive coastal systems, inclined, laminated mud deposits with abundant plant material exist in the upper reaches of tidally influenced estuaries and along intertidal channel margins in meandering channels (Buatois & Mángano, 2007; Daidu et al., 2013). This facies is interpreted as estuary channel fill located more seaward of Facies 1.

Facies 4: Lenticular interbedded mudstone and siltstone

Description

This facies is represented by a laterally extensive, broad U-shaped body of mudstone, with intercalated siltstone lenses near the top of the section. Muds are dark gray and mottled with

orange and rust-colored (Munsell 5R 4/6), laterally discontinuous centimeter-scale silts. This body is 0.5–6 m thick, and can be traced to its termination along the valley wall in an east-west orientation (Fig. 5E). Contact with the underlying Facies 3 is abrupt and erosional.

Interpretation

This lithofacies represents an estuary valley fill. The U-shaped geometry and fine sediments indicate a channel infilled due to transgression (mud-filled channel). Infill would have occurred during fallout of suspended sediment in a low-energy environment when the rising Bearpaw Sea drowned the coastline. Estuarine channel fills are commonly associated with heterolithics, which underlies this facies (James & Dalrymple, 2010).

Facies 5: Siderite-cemented sandstone

Description

Laterally continuous (54 m), very fine- to fine-grained sandstone with symmetrical ripple lamination with local siderite cementation (Fig. 5F). Cementation is discontinuous, but pervasive throughout the facies. The ichnogenus *Thalassinoides* with sandy infill is present both within the beds and in the mudstone directly underlying this facies (Fig. 5G). *In situ* marine bivalves were identified, further indicating transition to a fully marine environment.

Interpretation

Facies 5 is interpreted as a combination barrier island – wave ravinement surface. Barrier islands are typically found at the mouth of estuaries, acting as a buffer from open-marine processes.

Unlined *Thalassinoides* with infills similar to the overlying strata is diagnostic of the *Glossifungites* Ichnofacies (MacEachern & Pemberton, 1992). This would have effectively created the conditions necessary for low-energy suspension fallout in the central estuarine basin

(Boyd et al., 2006).

Facies 6: Bentonitic mudstone

Description

A laterally extensive, 2–3.6 m thick seam of gray-green bentonitic mudstone occurs below the contact between the Dinosaur Park and Bearpaw formations. This unit lies directly above Facies 5 throughout the modern river valley where these contacts can be traced. No bioturbation is apparent in this facies.

Interpretation

The bentonite in this unit originated from the early diagenetic alteration of volcanic ash (Lerbekmo, 2002). The absence of bioturbation indicates that this facies was deposited rapidly.

Facies 7: Shale

Description

This facies consists of black to dark grey, thinly parallel-laminated shale, in units 5–8 m thick. The shale is laterally extensive, and is disconformably overlain by Quaternary glacial till deposits. Marine ammonites were recovered from this facies (Caldwell, 1975).

Interpretation

Facies 7 records low-energy suspension fallout of sediment below storm wave-base (Davis & Hayes, 1984; Roy et al., 1994; Nichols, 2009; James & Dalrymple, 2010). This facies represents sedimentation in a siliciclastic shelf environment.

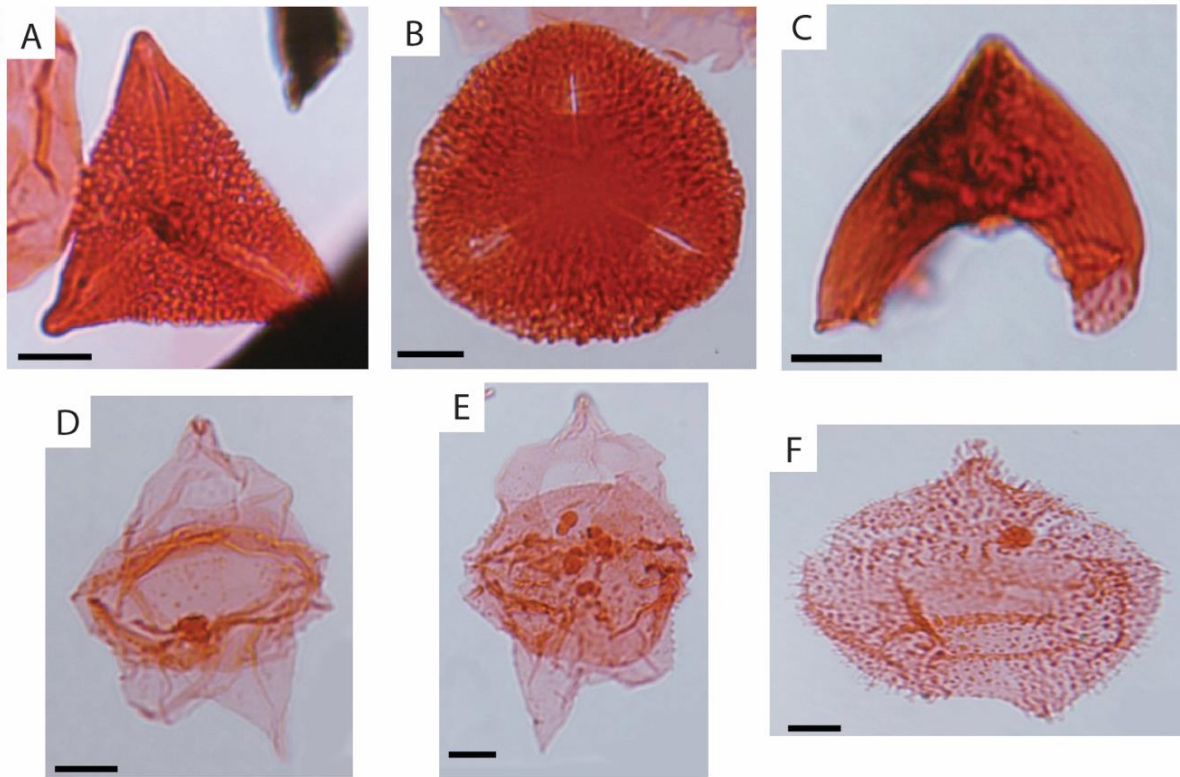


Figure 5.6: Biostratigraphically significant palynomorphs identified from the Saskatchewan Landing Lake Diefenbaker site. **A.** *Accuratipollis macrosolenoides*. **B.** *Expressipollis* sp. 1. **C.** *Mancicorpus tripodiformis*. **D.** *Chatangiella* sp. 1. **E.** *Chatangiella* sp. 2. **F.** *Chlamydophorella* sp. 1. All illustrated specimens are stored in the collections of the Royal Tyrrell Museum of Palaeontology, Drumheller, Alberta. All scale bars are 1 μm .

5.3.2 Palynology and Biostratigraphy

Palynomorphs recovered from the Lake Diefenbaker site are presented in Table 5.1, with biostratigraphically significant taxa illustrated in Figure 6. *Mancicorpus tripodiformis*, *Accuratipollis macrosolenoides*, and *Expressipollis* sp. 1 imply correlation with the middle to upper (but not uppermost) part of the Dinosaur Park Formation, relative to the type section in the Red Deer River Valley, Alberta (Braman & Sweet, 2012). The stratigraphic placement of this outcrop as not uppermost Dinosaur Park Formation is due to the absence of palynomorph species that characterize that portion of the formation in the type section. These palynomorphs are missing from nearby outcrops of Dinosaur Park Formation along the South Saskatchewan River to the west of the Lake Diefenbaker locality. All South Saskatchewan River sites are consistent with one another in both the presence and absence of palynomorph species, and provide a consistent picture across this area (D. Braman, personal communication, 2012). Dinoflagellates in sediment samples from the LD (Fig. 5.6) suggests marine seawater influence at the site. Integrating sedimentology and palynology indicates the Dinosaur Park – Bearpaw Formation contact occurs close to the top of the stratigraphic intervals sampled at the LD. The boundary is placed at the base of the iron-cemented sandstone facies. Relative to the type section of the Dinosaur Park Formation in Alberta this contact is geologically older in Saskatchewan (D. Braman, personal communication, 2012). This further corroborates the hypothesis that contact between the two formations is diachronous, with transgression of the Bearpaw Sea overtaking terrestrial regions in Saskatchewan before those in Alberta (Eberth, 2005).

The micropaleontological assemblage at the LD, consisting in part of spores from mosses, ferns, lycopods, tree ferns, and pollen from flowering plants and conifers, is similar to samples reported at Muddy Lake in west-central Saskatchewan (Eberth et al., 1990), and with

assemblages from Dinosaur Provincial Park (Braman & Sweet, 2012). Pollen identified for this study is included in Appendix E.

5.3.3 Vertebrate Paleontology

In total, 1185 identifiable elements were recovered from the Lake Diefenbaker site, representing 42 paleospecies. In terms of abundance, Reptilia comprise the largest group of animals 36% (n = 433). Champsosaurs make up 30% of the overall taxa recovered, and represent 83% of the reptilian component at LD. Chondrichthyans are the second most abundant group, making up 31% (n = 365) of the assemblage. Osteichthyans (Actinopterygii) are the most diverse group present, represented by at least 13 paleospecies. The remaining taxa consist of turtles, crocodiles, birds, mammals, salamanders, lizards, marine reptiles, theropod and ornithiscian dinosaurs (Table 5.2). Similar marginal-marine assemblages have been collected from Dinosaur Provincial Park in the Lethbridge Coal Zone (Brinkman et al., 2005a). The microvertebrate fossils at the Lake Diefenbaker locality represent the easternmost vertebrate assemblage known from the Belly River Group. Select taxa are represented in Figures 5.7 and 5.8, and descriptions are included in Appendix F.

5.4 Discussion

5.4.1 Paleoecology

Chondrichthyans

A highly diverse assemblage of cartilaginous fish was recovered from the microsite (Table 5.2). *Carcharias steineri* (Fig. 5.7D) is the most abundant (n = 87), followed by *Archaeolamna kopingensis* (n = 33) and *Meristodonoides montanensis* (n = 10) (Fig. 5.7A). *Meristodonoides montanensis* is the only shark in the assemblage not part of an extant lineage, and is commonly recovered from fluvial and marginal-marine beds in Dinosaur Provincial Park (Brinkman et al.,

2005a). *Carcharias*, *Archaeolamna*, and *Squalicorax* are all lamniforms, with modern representatives being sand tiger and mackerel sharks. These are large bodied, fast swimming sharks inhabiting nearshore environments (Compagno, 2001). *Cretorectolobus olsoni* (Fig. 5.7C), *Eucrossorhinus microcuspidatus* (Fig. 5.7B), and *Squalicorax* sp. (Fig. 5.7E) are represented by few or single specimens. *Cretorectolobus olsoni* and *E. microcuspidatus* are related to modern carpet and nurse sharks, which typically live in shallow- to moderate-depth ocean waters (Brinkman et al., 2005a). The paucity of deep-water taxa, coupled with higher numbers of species known from coastal or marginal-marine settings, implies a transitional depositional environment highly influenced by the coastal processes.

Myledaphus bipartitus (i.e., Fig. 5.7F) teeth are the most abundant element recovered from the site (n = 261). *Myledaphus* is a freshwater ray related to the modern guitar fish, and is commonly associated with nonmarine deposits in the Western Canada Sedimentary Basin (Beavan & Russell, 1999; Brinkman, 1990; Brinkman et al., 2005a; Neuman & Brinkman, 2005).

The Chondrichthyan component of the assemblage implies significant marine influence. *Archaeolamna*, *Carcharias*, *Eucrossorhinus*, and *Cretorectolobus* have been recovered from the Lethbridge Coal Zone in Alberta, a stratigraphic unit that is associated with marine transgression of the Bearpaw Sea (Eberth, 2005). The presence of numerous lamniforms further suggests a strong marine signature at the time of deposition because these sharks are associated with fully marine, open waters in the Late Cretaceous (Case, 1978).

Osteichthyans

A diverse assemblage of bony fishes, including Amiids (i.e., Fig. 5.7G), Acipenseriformes, Holostei, and teleosts, were collected from the site. The only extant amiid, *Amia calva*, is

restricted to completely freshwater environments, where it prefers quiet waters with low dissolved oxygen and significant vegetative overgrowth (Wheeler, 1985; Grande & Bemis, 1998). Modern sturgeon (Acipenseriformes) live in both freshwater and marine environments, with some marine species known to migrate upstream to spawn in freshwater (Wheeler, 1985). *Belonostomus* (i.e., Fig. 5.7H) is associated with both freshwater and marginal-marine deposits throughout the Upper Cretaceous of western Canada, and has been recovered from a range of depositional environments in Alberta (Brinkman, 1990; Neuman & Brinkman, 2005; Larson et al., 2010). *Enchodus* (i.e. Fig. 5.7I) is the only osteichthyan recovered from this assemblage that is found exclusively in marine to marginal-marine environments (Brinkman et al., 2005a; Cumbaa et al., 2006). The garfish, *Lepisosteus*, is unexpectedly absent from the assemblage. The enamel-covered ganoid scales of *Lepisosteus*, often called ‘garscales’, are ubiquitous in Late Cretaceous vertebrate microfossil sites (Brinkman et al., 2004, 2005a; Moran, 2011), and are often recovered in high abundances. The unexpected absence of *Lepisosteus* at the LD could have significant ecological implications, and warrants further study.

Teleost remains are an important, yet poorly understood component of Late Cretaceous terrestrial paleoecology in the Western Interior Basin (Neuman & Brinkman, 2005). Teleost remains at the LD comprise mainly isolated centra and fin spines. *Coriops* is thought to be an osteoglossomorph (Neuman & Brinkman, 2005), with modern representatives restricted to freshwater environments. *Paralbula* and related osteichthyans such as *Ostariostoma* are assigned to the Albulidae (bonefish), a type of elopomorph (Neuman & Brinkman, 2005; Brinkman et al., 2017). Esocoids (Salmoniformes), clupeomorphs such as *Horseshoeichthys*, and Ellimmichthyids such as *Diplomystus*, are also recovered from fluvial beds (Newbrey et al., 2010; Divay & Murray, 2016) and are considered part of a freshwater fluvial assemblage.

Amphibians

Somewhat counterintuitively for a site with strong marine influence, a robust assemblage of lissamphibians, including *Albanerpeton* (Fig. 5.7M), *Scapherpeton* (Fig. 5.7K), *Opisthotriton* (Fig. 5.7L) and *Lisserpeton*, were recovered from the Lake Diefenbaker site. Salamanders decrease in diversity and abundance up-section in Dinosaur Provincial Park, an observation thought to reflect encroachment of the transgressing Western Interior Seaway (Brinkman, 1990).

Lissamphibians, mainly salamanders, are the fifth most abundant taxonomic group recovered from LD. One anuran partial humerus (Fig. 5.7J) has been identified. Amphibians are considered to have a low tolerance of high salinity, restricting them to freshwater environments. Caudata are generally more restricted than Anura, with modern salamanders typically confined to aqueous freshwater environments (Hopkins & Brodie Jr., 2015). However, a few salamander species tolerate brackish water (Hopkins & Brodie Jr., 2015). Fossil salamanders are not only taxonomically diverse, but are abundant at the study site. Given the high abundance of salamander material, the high species diversity, and the nature of the sediments, transport from upstream environments is the simplest explanation. If that is the case, the possibility that taxa with freshwater affinity at the LD were also transported from upstream must be taken into account when considering the overall diversity.

Turtles

Of the four turtle families identified from this site, trionychids are dominant. Trionychids are soft-shelled, freshwater, carnivorous turtles that are still found worldwide today (Ernst et al., 1998). Their presence at the Lake Diefenbaker site is consistent with research conducted at microsites in Dinosaur Provincial Park, where the trionychid *Aspideretoides* (i.e., Fig. 5.8A, B) is found in former coastal deposits. Baenids (i.e., Fig. 5.7O) are an extinct group of paracryptodiran



Figure 5.7: Representative microvertebrates from the Saskatchewan Landing site. **A.** RSM P2199.107 *Meristodonoides montanensis* tooth. **B.** RSM P2945.119 *Eucrossorhinus microcuspidatus* tooth. **C.** RSM P2945.120 *Cretorectolobus olsoni* tooth. **D.** RSM P2945.122 *Carcharias steineri* tooth. **E.** RSM P2471.87 *Squalicorax* sp. tooth. **F.** RSM P2945.59 *Myledaphus biparticus* tooth. **G.** RSM P2199.42 Amiidae vertebrae. **H.** RSM P2945.21 *Belonostomus longirostris* partial dentary. **I.** RSM P2945.18 *Enchodus* sp. tooth. **J.** RSM P2945.262 *Anura* sp. distal humerus. **K.** RSM P2945.1 *Scapherpeton tectum* vertebrae. **L.** RSM P2471.75 *Opisthotriton kayi* vertebrae. **M.** RSM 2945.85 *Albanerpeton* sp. vertebrae. **N.** RSM P2945.169 Adocidea carapace fragment. **O.** RSM P2199.48 Baenidae carapace fragment. All scale bars are 2 mm.

turtle known only from North America (Lyson & Joyce, 2010), representing a clade of cryptodire. In the Hell Creek Formation, baenids are commonly found in large channel deposits, and are interpreted to have been carnivorous or durophagous riverine, bottom dwellers (Brinkman, 2005). Modern snapping turtles (Chelydridae) favor heavily vegetated freshwater channels and tolerate brackish water (Ernst et al., 1998). Brinkman (2005) suggested that chelydrids might have preferred coastal communities, based on evidence from Late Cretaceous deposits in Alberta. *Adocus* (i.e., Fig. 5.7N), the only genus represented from the Family Adocidea, is thought to have been mostly aquatic because its carapace implies a turtle adapted to an aquatic lifestyle (Hutchison & Archibald 1986; Brinkman, 2005).

Turtles from the studied assemblage are all aquatic or semi-aquatic, with the best-represented group being known to have tolerated brackish-water conditions. The genus *Basilemys*, which is the only fully terrestrial turtle confirmed from the Late Cretaceous (Holroyd & Hutchison, 2002), is absent from this assemblage, despite being relatively common in the Dinosaur Park Formation in Alberta (see Brinkman et al., 2004, 2005a, 2005b). Brinkman (1990) suggested that *Basilemys* might have occupied more inland habitats, supporting the interpretation of the LD as being an increasingly marginal-marine meandering-river system.

Marine reptiles

Plesiosauran remains are known from marine-influenced deposits (e.g., Lethbridge Coal Zone) as well as nonmarine deposits in Alberta (Sato et al., 2005). Most material is recovered from nonmarine fluvial beds in the Dinosaur Park Formation, while material found in the Lethbridge Coal Zone is primarily isolated elements (Sato et al., 2005). Articulated skeletons of numerous marine reptiles have been collected from the Bearpaw Formation in southwestern Saskatchewan (Sato, 2005). Isolated teeth and a single centrum collected from the Lake Diefenbaker locality were identified as belonging to a polycotyloid ('short-necked plesiosaur'). The vertebra has unfused epiphyses, implying that the animal was a juvenile when it died. A tooth from an elasmosaur ('long-necked plesiosaur'), also known from the marine Bearpaw Formation of Saskatchewan (i.e., Sato, 2003), was also recovered from the site. Polycotyloids and elasmosaurs are associated with marine deposits, so their presence in the LD implies brackish-water and marine influences.

Choristodera

Champsosaurus (i.e., Fig. 5.8C) make up 30% of material recovered from the site, and are the second best represented group. Champsosaurs are gavial-like piscivores with long, slender elongated skulls and needle-like teeth (Gao & Brinkman, 2005). They are recovered from many depositional environments in North America, ranging from freshwater to coastal marine (Brinkman, 1990; Eberth & Brinkman, 1997; Cullen et al., 2016). Champsosaurs, being almost fully aquatic, are thought to have favored open-water habitats such as ponds and lagoons (Brinkman, 1990; Currie & Koppelhus, 2005; Gao & Brinkman, 2005). Conversely, crocodiles might have preferred shoreline habitats during the Late Cretaceous (Brinkman, 1990). Their presence is compatible with the present environmental interpretation because champsosaurs are presumed to have inhabited channels and ponds, with crocodiles occupying niches nearer the

shoreline (Brinkman et al., 2005a or 2005b?).

Crocodylia

Crocodile material (i.e., Fig. 5.8D, E) is well represented at the Lake Diefenbaker site, primarily in the form of dermal scutes, though several well-preserved, isolated cranial elements have also been recovered. The crocodile genus is most like *Leidyosuchus* sp., the most common genus of crocodile in this size range from the Dinosaur Park Formation of Alberta (Wu, 2005).

Dinosaurs

Dinosaurs are represented in the microvertebrate assemblage by disarticulated bones, bone fragments, and shed or lost teeth. At least seven dinosaur species are present at the Lake Diefenbaker site (excluding birds), including three types of theropod. Brinkman et al. (1998) postulated that ceratopsians preferred coastal lowland habitats. Abundant ceratopsian material, represented mostly by teeth (i.e., Fig. 5.8H), supports this hypothesis. Hadrosaur fossils (i.e., Fig. 5.8I) are much less abundant at the study site. This fits with an interpretation of the LD being a coastal habitat because hadrosaurs are believed to have preferred inland environments more than coastal settings (Brinkman, 1990). The presence of at least one hypsilophodont (Fig. 5.8F) and ankylosaurid species, though only represented by a small number of elements, increases the known geographical range of these dinosaurs in the Campanian of North America. The ankylosaur material identified from the LD – a tooth and dermal scutes (Fig. 5.8F, G) – is the first recovered from Campanian rocks in Saskatchewan.

While only three small theropod teeth were recovered, the LD contained 28 complete and partial shed tyrannosaur teeth (i.e., Fig 5.8K). Although it is not possible to determine species from

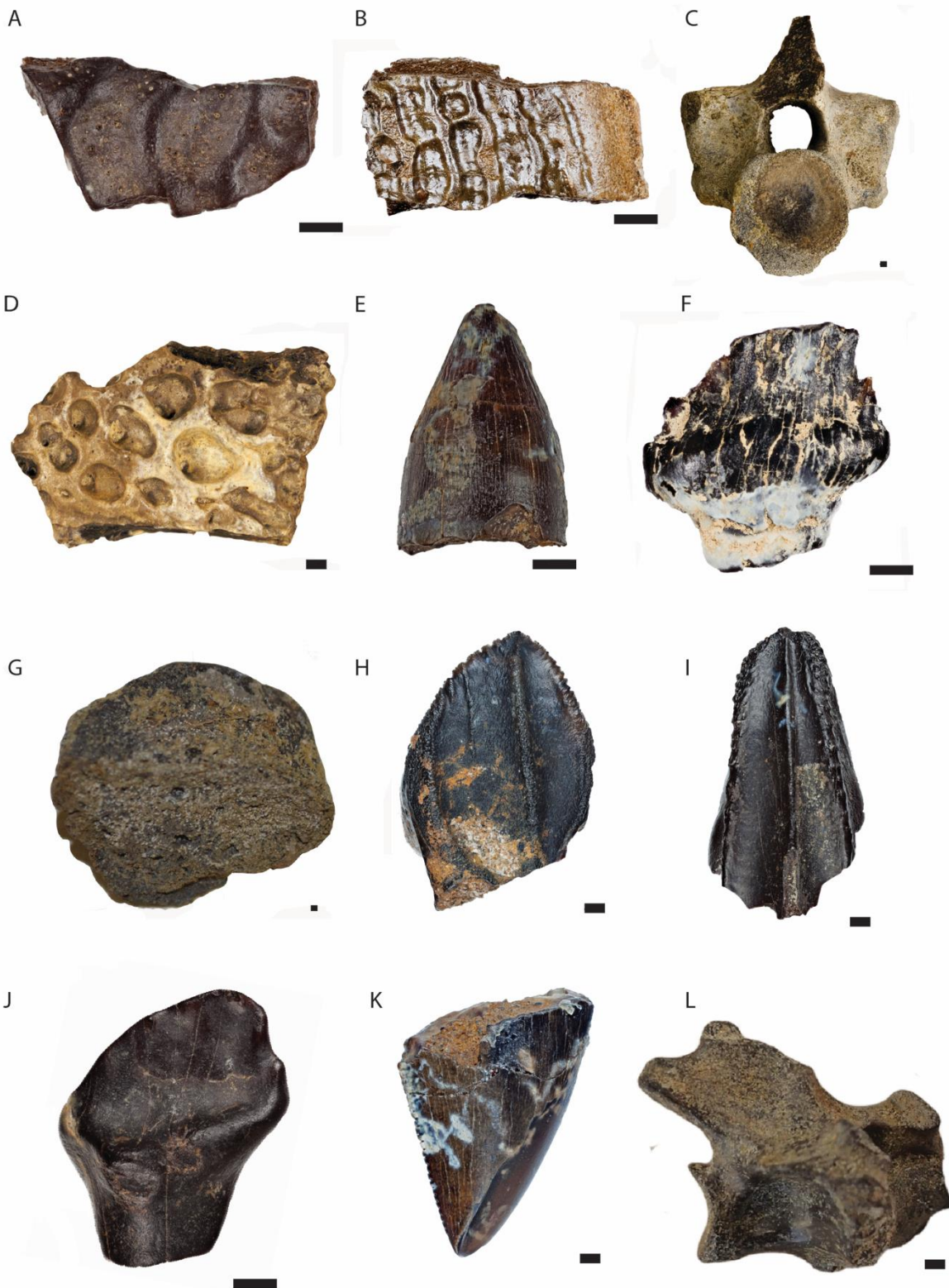


Figure 5.8: Representative microvertebrates from the Saskatchewan Landing site. **A.** RSM P2945.167 Trionychidae carapace fragment. **B.** RSM P2471.65 *Aspideretoides* sp. carapace fragment. **C.** RSM P2502.16 *Champsosaurus* sp. vertebrae. **D.** RSM P3222.4 *Leidyosuchus* sp. scute. **E.** RSM P2199.45 *Leidyosuchus* sp. tooth. **F.** RSM P2945.20 Ankylosauridae tooth. **G.** RSM P3222.1 Ankylosauridae scute. **H.** RSM P2471.32 Ceratopsidae tooth. **I.** RSM P2199.51 Hadrosauridae tooth. **J.** RSM P2945.535 Hypsilophodont tooth. **K.** RSM P2945.248 Tyrannosauridae tooth. **L.** RSM P3202.2 *Baptornis* sp. vertebrae. All scale bars 2 mm.

those teeth, they are probably from one of the two most common large theropods of the Late Campanian, *Daspletosaurus* sp. or *Gorgosaurus libratus* (Currie, 2003). While this may represent a preservation bias, it is possible that the LD represented an area where large theropods preferentially hunted and/or scavenged. In the Dinosaur Park Formation of Alberta, tyrannosaur teeth are among the most common theropod tooth type in microvertebrate sites (i.e., in Currie et al. 2008), ostensibly as a result of these animals scavenging. Two of the larger ornithischian bones at the LD suggest evidence of scavenging, displaying tooth marks and spiral fractures. More evidence is required to verify the nature and extent of the scavenging.

Small theopods are rare in the assemblage, and are represented by isolated teeth of *Dromaeosaurus* sp. and a troodontid (likely *Troodon*). The presence of a troodontid in the absence of *Saurornitholestes* is interesting, as the later genus is common in Dinosaur Provincial Park in Alberta, while the former is rare. Despite the small sample size of this collection, this may have implications for the paleoecology that warrants future investigation. The LD contains the first reported evidence of these small theropods in late Campanian deposits in Saskatchewan.

Birds

A fourth dorsal vertebra from *Baptornis* sp. (Fig. 5.8L) was recovered from the Lake Diefenbaker site in 1975 (Tokaryk & Harington, 1992). Three more *Baptornis* vertebrae were collected later. *Baptornis*, a toothed diving bird most commonly associated with the Niobrara

Chalk Formation in Kansas, is considered a marine diving bird. An isolated limb element from another different type of hesperornithoform was also recovered. The presence of these toothed birds in the Lake Diefenbaker assemblage not only extends the stratigraphic range of *Baptornis* (Tokaryk & Harington, 1992), but supports a marginal-marine interpretation for the preferred habitat of these birds.

5.4.2 *Estimated Species Diversity*

A summary of the diversity statistics is provided in Table 5.3. In general, the non-parametric species estimators suggested that there were between 6 and 17 species missing from the sample. The ACE returned the most conservative estimate, while the second-order jackknife provided the least conservative estimates. Although the second-order jackknife has been suggested to perform best for paleontological collections with low sample sizes, the ACE also performs very well when sample sizes are larger if rare taxa are not all represented by singletons (Hortal et al., 2006), as is the case here.

While beta diversity between this locality and coeval localities in Alberta is the subject of another ongoing study, it is worth briefly noting that the observed number of paleotaxa at the Lake Diefenbaker site is generally higher than at other microvertebrate sites of comparable age in Alberta, despite the fact that the dinosaur diversity is markedly depauperate (Brinkman et al., 2004). This increased diversity may have resulted from the Lake Diefenbaker microsite containing a higher diversity of more fully marine taxa, relative to assemblages found in Alberta's Dinosaur Park Formation. This may, in part, be because these animals lived in an environment nearer, and more heavily influenced by, the Western Interior Sea. The presence of a diverse salamander assemblage also suggests that the Lake Diefenbaker microsite contains both taxa that were deposited *in situ*, and taxa that were transported from farther inland. This

combination of inland and coastal taxa might also account for the higher than expected species diversity at the site. Further research is required to explore these results.

5.4.3 *Depositional Evolution*

During the Late Campanian, the Western Interior Seaway stretched from the Gulf of Mexico to the Canadian Arctic, bisecting North America into two distinct regions (Caldwell, 1975). Encroachment of this seaway played a major role in controlling both paleogeography and paleoenvironmental conditions, especially along regions directly under threat of frequent inundation by seawater. The climate was mild, with oxygen isotope values from molluscs indicating water paleotemperatures between 15° and 27° Celsius (Forester et al., 1977). Evidence from plant macrofossils of this age in Alberta indicates that the overall annual temperatures would have been between 5.0°C ($\pm 3.3^\circ$) in the cold season and 19.0°C ($\pm 3.1^\circ$) in the warm season (Golovneva, 2000). Although there are several similar locations in the world with comparable climates and similar flora types (i.e., the Florida Everglades), there is no direct modern analogue to this Late Cretaceous subtropical environment at high latitude. The seasonal photo period at the time would have been more comparable to that of Saskatchewan today, with long hours of darkness in the winter months and long hours of daylight in the summer months. When drawing conclusions about this paleoecosystem, these anomalies are important to bear in mind.

Integration of the many lines of evidence presented here implies that the site represents a coastal setting undergoing marine transgression. Biostratigraphically significant palynomorphs, such as *Mancicorpus tripodiformis*, *Accuratipollis macrosolenoides* and *Expressipollis* sp. 1, show that the site probably belongs to the upper Dinosaur Park Formation, which in Alberta records a phase of transgression (Eberth, 2005). The paleocoastline would have encroached on

Saskatchewan seaward of the more upland, western regions in Alberta. Palynomorphs substantiate this interpretation, as they date the site as slightly older than the type-section in the Red Deer River Valley in Alberta.

The Lake Diefenbaker site becomes increasingly marine influenced stratigraphically upward, with organic-rich mudstones and shales overlying coarser-grained heterolithic beds. As transgression continued, formerly freshwater meander-belts were submerged by seawater, creating brackish-water systems. An estuary is a transgressive coastal environment at the mouth of a river (Dalrymple et al., 1992; Davis et al., 2011). This environment receives sediment from both fluvial and marine sources, and is influenced by both fluvial and marine processes. An estuary is considered to extend from the landward limit of tidal facies at its head to the seaward limit of coastal facies at its mouth (Dalrymple, 2006). Estuaries are restricted to transgressive depositional settings and form during a relative rise in sea level. Although the Dinosaur Park Formation is poorly exposed along Lake Diefenbaker and faulting limits stratigraphic correlation, it is reasonable to conclude that low-lying, meandering fluvial channels and associated overbank areas would have been overtaken and drowned, leading to mud-filled brackish-water channels along a tide-dominated shoreline. This is reflected in the geometry of the upper mudstone lenticular bed. The final transgression of the Bearpaw Sea is interpreted as having occurred rapidly at the LD because a transgressive lag and a firmground delineated by the *Glossifungites* Ichnofacies mark the contact between the Dinosaur Park and Bearpaw formations. Interfingering of the nonmarine upper Belly River deposits with the Bearpaw Formation is well known in Saskatchewan (Caldwell, 1968), recording subtle changes in sea level that are not seen in Alberta. This interfingering complicates the stratigraphy and makes interpretation difficult. Faulting and rotational slump faulting throughout Saskatchewan further confuses stratigraphic

correlation. Ongoing studies will further refine the stratigraphy in this region.

A brackish-water faunal assemblage is expected in a marginal-marine environment. Many of the taxa recovered from the Lake Diefenbaker microsite, in terms of both diversity and numbers, are brackish to fully marine. The presence of amiids, amphibians, and other, more inland, taxa known for salinity intolerance imply that the environment was initially freshwater and became progressively more saline, or that these fossil remains were physically transported seawards from a more inland source.

5.5 Conclusions

The vertebrate fauna at the Lake Diefenbaker site represents the easternmost vertebrate microfossil assemblage from the Late Cretaceous Dinosaur Park Formation. This fauna provides the first glimpse of a marginal-marine, coastal fauna living during a time of transgression of the Bearpaw Sea in Saskatchewan. Diverse assemblages of terrestrial and marine taxa have been recovered from the locality, many of which are reported for the first time in the Campanian in the province. In total, 42 vertebrate taxa were identified, with non-parametric species estimators suggesting that there may have been 48 to 59 species present. Champsosaurs and cartilaginous fishes are the most abundant and diverse group recovered from the site, reinforcing a transgressive marginal-marine interpretation for the paleoenvironment. It is likely that there was some reworking of the shoreline, with coastal tidal channels reworking some of the sediments as transgression occurred.

Based on the integration of sedimentological and paleontological datasets, the depositional environment at this locality is interpreted as being a marginal-marine coastline undergoing transgression. The lowermost heterolithic sediments are considered to represent tidally influenced point bars and intertidal creeks dissecting the landscape. Up-section, muddy

point bars and mudflat deposits are replaced by estuarine channel fills. Final transgression of the Bearpaw Sea is signalled by a transgressive deposit associated with the *Glossifungites* Ichnofacies. The fauna corroborate this hypothesis, as aquatic taxa are freshwater, brackish water, and fully marine. A fining-upwards trend, marine trace fossils, and the presence of dinoflagellates indicate increased marine influence in the region, culminating in transgression of the Bearpaw Sea.

This work constitutes one of the first paleobiodiversity studies undertaken in the Campanian of Saskatchewan. When compared with the well-known Dinosaur Park Formation faunas of Alberta, this study and subsequent research will help to elucidate how environmental factors, such as the proximity to the paleocoastline, influenced paleobiodiversity patterns on broad spatial scales.

Acknowledgements

Thank you to Hans Larsson and the McGill field school crews (2013–2015), especially to Sarah Popov, for collecting and processing much of the microsite material that was used in this study. Wes Long and John Storer for collecting, processing and assigning initial identifications to parts of the collection. To Dennis Braman for providing analysis of the pollen samples. A very special thank you to Tim Tokaryk, without whom none of this would have been possible. Lastly, thanks to Mignon le Roux (University of Saskatchewan), who dedicated many hours in both the field and lab. Support for this project was provided by the University of Saskatchewan.

Class, Subclass, Clade or Division	Superorder and/or Order	Family	Genus	Species
Green and Blue Algae				
Chlorophyta	Zygnematales	Zygnemataceae	<i>Ovoidites</i>	<i>O. ligneolus</i>
			<i>Schizosporis</i>	<i>S. parvus</i>
		Unknown	<i>Sigmopollis</i>	<i>S. carbonis</i>
Dinoflagellates				
Pyrrhophyta	Dinophyceae	Uncertain	<i>Chlamydothorea</i>	C. sp.
		Uncertain	<i>Chatangiella</i>	C. sp. 1, 2
Mosses, Liverworts, and Hornworts				
Bryophyta	Anthocerotales	Anthocerotaceae	<i>Foraminisporis</i>	<i>F. asymmetricus</i>
Hepaticae	Sphaerocarpaceae	Sphaerocarpaceae	<i>Triporeletes</i>	<i>T. stellatus</i>
			<i>Zlivisporis</i>	<i>Z. cenomanianus</i> , <i>reticulatus</i> , <i>sinifer</i> , sp.
Musci	Sphagnales	Sphagnaceae	<i>Stereigranisporis</i>	<i>S. regius</i> , <i>antiquasporites</i>
			<i>Stereisporites</i>	<i>S. rodaensis</i>
Lycopodiophyta	Lycopodiales	Lycopodiaceae	<i>Camarozonosporites</i>	<i>C. ambiguus</i>
			<i>Cibitiidites</i>	<i>C. bettarius</i>
			<i>Retitriteles</i>	R. sp.
Isoetopsida	Selaginellales	Selaginellaceae	<i>Echinatisporis</i>	<i>E. sp 1, 2</i>
			<i>Heliosporites</i>	<i>H. kemensis</i>

			<i>Liburnisporis</i>	<i>L. adnacus</i>
			<i>Lusatisporis</i>	<i>L. dettmannae</i>
Ferns				
Polypodiophyta	Polypodiales	Osmundaceae	<i>Baculatisporites</i>	<i>B. comaumensis</i>
			<i>Osmundacidites</i>	<i>O. wellmanii</i>
			<i>Reticulosporis</i>	<i>R. foveolatus</i>
		Dicksoniaceae	<i>Laevigatosporites</i>	<i>L. haardti</i>
			<i>Leptolepidites</i>	<i>L. sp.</i>
			<i>Umbosporites</i>	<i>U. callosus</i>
		Salviniaceae	<i>Azolla</i>	<i>A. sp.</i>
Unclassified Trilete Spores				
			<i>Interulobites</i>	<i>I. sp.</i>
			<i>Polycingulatisporites</i>	<i>P. reduncus</i>
			<i>Varirugosisporites</i>	<i>V. tolmanensis</i>
			<i>Verrucosisporites</i>	<i>V. sp.</i>
Gymnosperms				
Pinophyta	Cycadales	Cycadaceae	<i>Cycadopites</i>	<i>C. fragilis</i>
			<i>Monosulcites</i>	<i>M. sp.</i>
	Pteridospermales	Caytoniaceae	<i>Vitreisporites</i>	<i>V. pallidus</i>
	Pinales	Pinaceae	<i>Alisporites</i>	<i>A. Bilateralis, grandis</i>
			<i>Pityosporites</i>	<i>P. constrictus, elongatus</i>
		Cupressaceae	<i>Sequoiapollenites</i>	<i>S. paleocenicus</i>
			<i>Taxodiaceapollenites</i>	<i>T. hiatus, vacuipites</i>

		Podocarpaceae	<i>Podocarpidites</i>	<i>P. sp.</i>
			<i>Pristinupollenites</i>	<i>P. microsaccus</i>
		Cheirolepidiaceae	<i>Circulina</i>	<i>C. parva</i>
Gneticae	Gnetopsida	Ephedraceae	<i>Equisetosporites</i>	<i>E. menakaе,</i> <i>multicostatus</i>
Angiosperms				
Magnoliophyta	Euphorbiales	Buxaceae	<i>Erdtmanipollis</i>	<i>E.</i> <i>procumbertiformis</i>
	Haloragales	Gunneraceae	<i>Tricolpites</i>	<i>T. reticulatis</i> , sp.
	Santalaceae	Olacaceae	<i>Pulcheripollenites</i>	<i>P. krempii</i>
		Loranthaceous	<i>Expressipollis</i>	<i>E. sp. 1</i>
	Proteales	Proteaceae	<i>Siberiapollis</i>	<i>S. montanensis</i> , sp.
Caryophyllidae	Caryophyllales	Chenopodiaceae	<i>Polyporina</i>	<i>P. cribraria</i>
Lilopsida	Liliales	Liliaceae	<i>Liliacidites</i>	<i>L. sp. 1, 2, 3</i>
	Cyperales	Cyperaceae	<i>Pentetrapites</i>	<i>P. inconspicuus</i>
Angiosperms: Parent Plant Uncertain				
			<i>Aquilapollenites</i>	<i>A. aptus</i> , <i>attenuatus</i> , <i>funkhouserii</i> , cf. <i>quadrilobus</i> , sp. 1, 2, 3, <i>trialatus</i> , <i>turbidus</i>
			<i>Integricorpus</i>	<i>I. clarireticulatus</i>

			<i>Manicorpus</i>	<i>M. anchoriforme, tripodiformis</i>
			<i>Translucentipollis</i>	<i>T. plicatilis</i>
Possible Triprojectate Affinities				
			<i>Accuratipollis</i>	<i>A. macrosolenoides</i>
			<i>Cranwellia</i>	<i>C. rumsevensis</i>
Oculates				
			<i>Azonia</i>	<i>A. pulchella</i>
Others				
			<i>Grewipollenites</i>	<i>G. canadensis</i>
			<i>Gunnaripollis</i>	<i>G. superbus</i>
			<i>Inaperturotetradites</i>	<i>I. scabratus</i>
			<i>Pleurospermaepollenites</i>	<i>P. sp.</i>
			<i>Subtriporopollenites</i>	<i>S. alpinus</i>
			<i>Tricolpopollenites</i>	<i>P. sp.</i>
			<i>Tricolporites</i>	<i>T. sp. 1, 2</i>
			<i>Virgo</i>	<i>V. amiantopollis</i>
Unknown				
			<i>Circumflexipollis</i>	<i>C. tilioides</i>
			<i>Dyadonapites</i>	<i>D. reticularis</i>

Table 5.1: Palynomorph taxa identified from samples recovered at the LD site.

Class; Subclass, Clade or Division	Superorder and/or Order	Family	Genus and species	Elements	Numb er of Elemen ts	Percenta ge (%) of Assembl age
Chondrichthyes						
Chondrichthyes Huxley, 1880; Elasmobranchii Bonaparte, 1838	Euselachii Hay, 1902	Hybodontidae Owen, 1837	<i>Meristodonoides montanensis</i> Underwood and Cumbaa, 2010	Teeth	10	0.85
	Orectolobiformes Applegate, 1972	Orectolobidae Jordan and Fowler, 1972	<i>Cretorectolobus olsoni</i> Case, 1978	Teeth	1	0.08
			<i>Eucrossorhinus microcuspidatus</i> Case, 1978	Teeth	1	0.08
	Lamniformes Berg, 1958	Odontaspidae Müller and Henle, 1839	<i>Carcharias steineri</i> Case, 1987	Teeth	87	7.33
		Cretoxyrinidae Glückman, 1958	<i>Archaeolamna kopingensis</i> Silverson, 1992	Teeth	33	2.78
		Anacoracidae Casier, 1947	<i>Squalicorax</i> <i>sp.</i> Whitley, 1939	Teeth	1	0.08

	Rajiformes Cappetta, 1992	Rhinobatidae Muller and Henle, 1837	<i>Myledaphus bipartitus</i> Cope, 1876	Teeth, Tooth plates	261	21.99
Osteichthyes						
Osteichthyes Huxley, 1880	Acipenseriformes Berg, 1940	Acipenseridae Bonaparte, 1831	<i>Acipenser sp.</i> Linnaeus, 1758	Cranial material, Vertebrae	17	1.43
	Amiiformes Hay, 1929	Amiidae Bonaparte, 1837	Indet.	Cranial material, Vertebra	30	2.53
	Aspidorhynchiformes Bleeker, 1859	Aspidorrhynchidae Nicholson and Lydekker, 1889	<i>Belonostomus longirostris</i> Lamb, 1902	Dentary fragment, Cranial material	2	0.17
Osteichthyes Indet.	Indet.	Indet.	Indet.	Bone, cranial fragments	105	8.85
Osteichthyes; Teleostei (Arratia, 1997)						
	Elopiformes Sauvage, 1875	Elopidae Romer, 1966	cf <i>Paratarpon</i> <i>sp.</i> Bardack, 1970	Centra	3	0.25
		Phyllodontidae Sauvage, 1875	cf <i>Paralbula</i> <i>sp.</i> Blake, 1940	Centra	2	0.17
		Ostariostomidae Schaeffer, 1949	cf <i>Ostariostoma</i>	Centra	3	0.25

			<i>sp.</i> Schaeffer, 1949			
	Aulopiformes Rosen, 1973	Enchodontidae Woodward, 1901	<i>Enchodus sp.</i> Agassiz, 1835	Tooth	1	0.08
	Salmoniformes Bleeker, 1859	Esocoidea Bleeker, 1859	cf <i>Escoid sp.</i> indet.	Centra	1	0.08
	Clupeomorpha; Ellimmichthyiformes Grande, 1985	Sorbinichthyidae Alvarado-Ortega et al., 2008	<i>Horseshoeichthys sp.</i> Newbery et al., 2010	Centra	3	0.25
		Ellimmichthyidae Grande 1982	<i>Diplomystus sp.</i> Cope, 1877	Centra	3	0.25
	Osteoglossomorpha Greenwood, Rosen, Weitzman, and Myers, 1966; Osteoglossiformes Berg 1940	Osteoglossidae Bonaparte 1832	cf <i>Cretophareodus sp.</i> Li 1996	Centra	3	0.25
		Hiodontidae Bleeker, 1859	Indet.	Centra	4	0.34
Teleost Indet.	Indet.	Indet.	Indet.	Centra	11	0.93
Amphibia						
Amphibia Linnaeus, 1758;	Anura Duméril, 1806	In det.	In det.	Humerus	1	0.08
	Caudata Scopoli, 1777	Scapherpetonidae Auffenberg and Goin, 1959	<i>Scapherpeton tectum</i> Cope, 1876	Cranial material, Vertebrae	34	2.86

			<i>Lisserpeton bairdi</i> Estes, 1965	Vertebra	4	0.34
		Batrachosauroidae Auffenberg, 1958	<i>Opisthotriton kayi</i> Auffenberg, 1961	Vertebra	17	1.43
	Allocaudata Fox and Naylor, 1982	Albanerpetontidae Fox and Naylor, 1982	<i>Albanerpeton sp.</i> Estes and Hoffstetter, 1976	Vertebra	6	0.51
Reptilia						
Reptilia Laurenti, 1768; Anapsida Williston, 1917	Testudines Batsch, 1788; Cryptodira Cope, 1868	Adocidae Cope, 1870	Indet.	Carapace fragment	1	0.08
		Baenidae Cope, 1882	Indet.	Carapace fragment	2	0.17
		Chelydridae Swainson, 1839	Indet.	Carapace fragment	2	0.17
		Trionychidae Gray, 1870	cf <i>Aspideretoides sp.</i> Leidy, 1856	Carapace fragment s	10	0.84
	Chelonia Indet.	Indet.	Indet.	Carapace / bone fragment s	21	1.77
Reptilia;						

Diapsida Osborn, 1903						
	Squamata Oppel, 1811	Varanidae Gray, 1827	<i>Palaeosaniwa</i> <i>sp.</i> Gilmore, 1928	Partial jaw, Vertebrae	2	0.17
	Choristodera Cope, 1876	Champsosaurida e Cope, 1884	<i>Champsosaur</i> <i>us sp.</i> Cope, 1876	Teeth, cranial fragment s, post- cranial elements, dentary	358	30.16
	Plesiosauria Blainville, 1835	Polycotylidae Wiliston, 1925	Indet.	Teeth and vertebrae	5	0.42
		Elasmosauridae Cope 1869	Indet.	Tooth	1	0.08
Reptilia; Archosauria Cope, 1870						
	Crocodylia Gmelin, 1788	Crocodylidae Cuvier, 1808	<i>Leidyosuchus</i> <i>sp.</i> Lambe, 1907	Osteoder ms, teeth, cranial material, vertebra	32	2.70
Reptilia; Archosauria ; Dinosauria Owen, 1842						
	Ornithischia Seeley, 1888;	Ankylosauridae Brown, 1908	Indet.	Osteoder ms (scutes)	2	0.17

	Ankylosauria Osborn, 1923					
	Ornithischia; Ceratopsia Marsh, 1890	Ceratopsidae Marsh, 1888	Indet.	Teeth, post- cranial elements	41	3.45
	Ornithischia; Ornithopoda Marsh, 1881	Hadrosauridae Cope, 1869	Indet.	Teeth, post- cranial elements	15	1.26
		Hypsolophodontidae Dollo 1882	Indet.	Tooth	1	0.08
	Ornithischia Indet.	Indet.	Indet.	Bone fragment s	13	0.10
	Saurischia Seeley, 1888; Theropoda Marsh 1881	Dromaeosaurida e Matthew and Brown, 1922	<i>Dromaeosaur us albertensis</i> Matthew and Brown, 1922	Teeth	2	0.17
		Tyrannosauridae Osborn, 1905	cf <i>Gorgosaurus sp.</i>	Teeth	28	2.36
		Troodontidae Gilmore, 1924	Indet.	Tooth	1	0.08
Aves						
Aves Linnaeus, 1758	Hesperornithifor mes Fürbringer 1888	Hesperornithidae Marsh 1880	<i>Baptornis sp.</i> Marsh, 1877	Vertebra, Post- cranial elements	4	0.34
	Hesperornithifor mes Indet.	Indet.	Indet.	Post- cranial element	1	0.08
Mammalia						

Mammalia	Multituberculata Cope, 1884	Cimolomyidae Marsh, 1889	<i>Meniscoessus</i> <i>sp.</i> Fox, 1980	Teeth	2	0.17
----------	--------------------------------	-----------------------------	--------------------------------------------------------------	-------	---	------

Table 5.2: Microvertebrate specimens (n = 1185) from the Saskatchewan Landing site, Dinosaur Park Formation. Bold text in each line of the table represents the lowest taxonomic designation for the group in the assemblage.

Number of Species Observed	Non-parametric Species Estimator	Number of Estimated Species
42.0		
	Choa-1	52.6
	Second-Order Jackknife	59.0
	Abundance-based Coverage Estimator (A	48.5

Table 5.3: Estimated alpha (within-site) species diversity at the LD site based on the microvertebrate collection. The estimated number of total species was calculated using three different non-parametric species estimators: Choa-1 (Choa, 1984), Jackknife-2 (Smith and van Belle, 1984), and Abundance-based Coverage Estimator (Choa and Lee, 1992). Methodologies and equations are provided in section 2.3.

References

- Auffenberg, W. (1961). A new genus of fossil salamander from North America. *American Midland Naturalist*, 66(2), 456-465.
- Auffenberg, W., Goin, C. J., & Cope, E. D. (1959). The status of the salamander genera *Scapherpeton* and *Hemitrypus* of Cope. *American Museum Novitates*, 1979.
- Basan, P., Frey, R., Crimes, T. P., & Harper, J. C. (1977). Actual-palaeontology and neoichnology of salt marshes near Sapelo Island, Georgia. *Geological Journal*, Special Issue, (9), 41-70.
- Baszio, S. (1997). Palaeoecology of dinosaur assemblages throughout the Late Cretaceous of south Alberta, Canada. *CFS Courier Forschungsinstitut Senckenberg*, 196, 1-31.
- Beavan, N. R., & Russell, A. P. (1999). An elasmobranch assemblage from the terrestrial-marine transitional Lethbridge Coal Zone (Dinosaur Park Formation: Upper Cambrian), Alberta, Canada. *Journal of Paleontology*, 73(3), 494-503.
- Boyd, R., Dalrymple, R., & Zaitlin, B. A. (1992). Classification of clastic coastal depositional environments. *Sedimentary Geology*, 80(3-4), 139-150.
- Boyd, R., Dalrymple, R., Zaitlin, B., Posamentier, H. W., & Walker, R. A. (2006). Estuarine and incised-valley facies models. In H. W. Posamentier & R. G. Walker (Eds.), *Facies models revisited* (pp. 171-235). Society for Sedimentary Geology, SEPM Special Publication No. 84.
- Braman, D., & Sweet, A. (2012). Biostratigraphically useful Late Cretaceous–Paleocene terrestrial palynomorphs from the Canadian Western Interior Sedimentary Basin. *Palynology*, 36(1), 8-35.
- Brinkman, D. B. (1990). Paleoecology of the Judith River Formation (Campanian) of Dinosaur Provincial Park, Alberta, Canada: Evidence from vertebrate microfossil localities. *Palaeogeography, Palaeoclimatology, Palaeoecology*, 78(1), 37-54.
- Brinkman, D. B. (2005). Turtles: Diversity, paleoecology, and distribution. In P. J. Currie & E. B. Koppelhus (Eds.), *Dinosaur Provincial Park: A spectacular ancient ecosystem revealed* (pp. 202-220). Bloomington & Indianapolis, IN: Indiana University Press.
- Brinkman, D. B., Braman, D. R., Neuman, A. G., Ralrick, P. E., & Sato, T. (2005a). A vertebrate assemblage from the marine shales of the Lethbridge Coal Zone. In P. J. Currie & E. B. Koppelhus (Eds.), *Dinosaur Provincial Park: A spectacular ancient ecosystem revealed* (pp. 486-500). Bloomington & Indianapolis, IN: Indiana University Press.
- Brinkman, D., & Neuman, A. (2002). Teleost centra from Uppermost Judith River Group (Dinosaur Park Formation, Campanian) of Alberta, Canada. *Journal of Paleontology*, 76(1), 138-155.

- Brinkman, D. B., Neuman, A. G., & Divay, J. D. (2017). Non-marine fish of the late Santonian Milk River Formation of Alberta, Canada – evidence from vertebrate microfossil localities. *Vertebrate Anatomy Morphology Palaeontology*, 3, 7-46.
- 5Brinkman, D. B., Russell, A., Eberth, D. A., & Peng, J.-H. (2004). Vertebrate palaeocommunities of the lower Judith River Group (Campanian) of southeastern Alberta, Canada, as interpreted from vertebrate microfossil assemblages. *Palaeogeography, Palaeoclimatology, Palaeoecology*, 213(3), 295-313.
- Brinkman, D. B., Russell, A. P., & Peng, J.-H. (2005b). Vertebrate microfossil sites and their contribution to studies of paleoecology. In P. J. Currie & E. B. Koppelhus (Eds.), *Dinosaur Provincial Park: A spectacular ancient ecosystem revealed* (pp. 88-98). Bloomington & Indianapolis, IN: Indiana University Press.
- Brinkman, D. B., Ryan, M. J., & Eberth, D. A. (1998). The paleogeographic and stratigraphic distribution of ceratopsids (Ornithischia) in the upper Judith River Group of western Canada. *Palaios*, 13(2), 160-169.
- Brown, C. M., Evans, D. C., Campione, N. E., O'Brien, L. J., & Eberth, D. A. (2013). Evidence for taphonomic size bias in the Dinosaur Park Formation (Campanian, Alberta), a model Mesozoic terrestrial alluvial-paralic system. *Palaeogeography, Palaeoclimatology, Palaeoecology*, 372, 108-122.
- Buatois, L. A., & Mángano, M. G. (2007). Invertebrate ichnology of continental freshwater environments. In *Trace Fossils* (pp. 285-323). Elsevier.
- Buatois, L. A., & Mángano, M. G. (2011). *Ichnology: Organism-substrate interactions in space and time*. Cambridge, UK: Cambridge University Press.
- Caldwell, M. W. (2005). The Squamates: Origins, phylogeny, and paleoecology. In P. J. Currie & E. B. Koppelhus (Eds.), *Dinosaur Provincial Park: A spectacular ancient ecosystem revealed* (pp. 235-248). Bloomington & Indianapolis, IN: Indiana University Press.
- Caldwell, W. G. E. (1968). *The Late Cretaceous Bearpaw Formation in the South Saskatchewan River valley*. Saskatchewan Research Council, Geology Division, Report No. 8, 86 p.
- Caldwell, W. G. E. (Ed.) (1975). *The Cretaceous system in the western interior of North America: The proceedings of an international symposium organized by the Geological Association of Canada and held at the University of Saskatchewan in Saskatoon, May 23-26, 1973*. Geological Association of Canada, Special Paper No. 13.
- Cant, D. J., & Stockmal, G. S. (1989). The Alberta foreland basin: Relationship between stratigraphy and Cordilleran terrane-accretion events. *Canadian Journal of Earth Sciences*, 26(10), 1964-1975.

- Cappetta, H. (1987). *Chondrichthyes II: Mesozoic and Cenozoic Elasmobranchii. Handbook of paleoichthyology* (v. 3B). Stuttgart ; New York: G. Fischer Verlag.
- Case, G. R. (1978). A new selachian fauna from the Judith River Formation (Campanian) of Montana. *Palaeontographica. Abteilung A: Palaeozoologie-Stratigraphie*, 160(1), 176-205.
- Catuneanu, O., Sweet, A. R., & Miall, A. D. (2000). Reciprocal stratigraphy of the Campanian–Paleocene western interior of North America. *Sedimentary Geology*, 134(3-4), 235-255.
- Chao, A. (1984). Non-parametric estimation of the number of classes in a population. *Scandinavian Journal of Statistics*, 11(4), 265-270.
- Chao, A., & Lee, S. M. (1992). Estimating the number of classes via sample coverage. *Journal of the American Statistical Association*, 87(417), 210-217.
- Chao, A., Ma, M. C., & Yang, M. C. K. (1993). Stopping rules and estimation for recapture debugging with unequal failure rates. *Biometrika*, 80(1), 193-201.
- Cobban, W. A., Walaszczyk, I., Obradovich, J. D., & McKinney, K. C. (2006). *A USGS zonal table for the Upper Cretaceous Middle Cenomanian–Maastrichtian of the western interior of the United States based on ammonites, inoceramids, and radiometric ages*. U.S. Geological Survey, Open-File Report 2006-1250.
- Colwell, R. K., & Coddington, J. A. (1994). Estimating terrestrial biodiversity through extrapolation. *Philosophical Transactions of The Royal Society of London, Series B-Biological Sciences*, 345(1311), 101-118.
- Compagno, L. J. V. (2001). *Sharks of the world. An annotated and illustrated catalogue of shark species known to date. Volume 2. Bullhead, mackerel and carpet sharks (Heterodontiformes, Lamniformes and Orectolobiformes)*. FAO Species Catalogue for Fisheries Purposes, No. 1, Vol. 2. Rome: Food and Agriculture Organization for the United Nations.
- Coombs Jr., W. (1988). The status of the dinosaurian genus *Diclonius* and the taxonomic utility of hadrosaurian teeth. *Journal of Paleontology*, 62(5), 812-817.
- Cope, E. (1876). Descriptions of some vertebrate remains from the Fort Union Beds of Montana. *Proceedings of the Academy of Natural Sciences of Philadelphia*, 28, 248-261.
- Cullen, T., Fanti, F., Capobianco, C., Ryan, M., & Evans, D. (2016). A vertebrate microsite from a marine-terrestrial transition in the Foremost Formation (Campanian) of Alberta, Canada, and the use of faunal assemblage data as a paleoenvironmental indicator. *Palaeogeography, Palaeoclimatology, Palaeoecology*, 444, 101-114.

- Cumbaa, S. L., Schröder-Adams, C., Day, R. G., & Phillips, A. J. (2006). Cenomanian bonebed faunas from the northeastern margin, Western Interior Seaway, Canada. In S. G. Lucas & R. M. Sullivan (Eds.), *Late Cretaceous vertebrates from the Western Interior* (pp. 139-155). New Mexico Museum of Natural History and Science, Bulletin 35. Albuquerque, NM; New Mexico Museum of Natural History.
- Currie, P. (2003). Cranial anatomy of tyrannosaurid dinosaurs from the Late Cretaceous of Alberta, Canada. *Acta Palaeontologica Polonica*, 48(2), 191-226.
- Currie, P. J., & Koppelhus, E. B. (Eds.) (2005). *Dinosaur Provincial Park: A spectacular ancient ecosystem revealed*. Bloomington & Indianapolis, IN: Indiana University Press.
- Currie, P. J., Langston Jr., W., & Tanke, D. H. (2008). A new horned dinosaur from an Upper Cretaceous bone bed in Alberta. e-book #49729: NRC Research Press.
- Currie, P. J., Rigby, J. K., & Sloan, R. E. (1991). Theropod teeth from the Judith River Formation of southern Alberta, Canada. In K. Carpenter & P. J. Currie (Eds.), *Dinosaur Systematics: Approaches and perspectives* (pp. 107-125). Cambridge, UK: Cambridge University Press.
- Daidu, F., Yuan, W., & Min, L. (2013). Classifications, sedimentary features and facies associations of tidal flats. *Journal of Palaeogeography*, 2(1), 66-80.
- Dalrymple, R. W. (2006). Incised valleys in time and space: An introduction to the volume and an examination of the controls on valley formation and filling. In R. W. Dalrymple, D. A. Leckie & R. W. Tillman (Eds.), *Incised valleys in time and space* (pp. 5-12). Society for Sedimentary Geology, SEPM Special Publication No. 85.
- Dalrymple, R. W., & Choi, K. (2007). Morphologic and facies trends through the fluvial-marine transition in tide-dominated depositional systems: A schematic framework for environmental and sequence-stratigraphic interpretation. *Earth Science Reviews*, 81(3-4), 135-174.
- Dalrymple, R. W., Zaitlin, B. A., & Boyd, R. (1992). Estuarine facies models: Conceptual basis and stratigraphic implications. *Journal of Sedimentary Petrology*, 62(6), 1130-1146.
- Davis Jr., R. A., & Hayes, M. O. (1984). What is a wave-dominated coast? *Marine Geology*, 60(1-4), 313-329.
- Davis et al., 2011 (sections 5.3.1, F1 and 5.4.3; unless you meant Davis and Dalrymple 2012.)
- Dawson, F. M., Evans, C. G., Marsh, R., & Richardson, R. (1994). Uppermost Cretaceous and Tertiary strata of the Western Canada Sedimentary Basin. In G. D. Mossop & I. Shetsen (Comps.), *Geological atlas of the Western Canada Sedimentary Basin* (pp. 387-406). Calgary, Alberta: Canadian Society of Petroleum Geologists and Alberta Research Council.

- Divay, J. D., & Murray, A. M. (2016). An early Eocene fish fauna from the Bitter Creek area of the Wasatch Formation of southwestern Wyoming, U.S.A. *Journal of Vertebrate Paleontology*, 36(5). Published online at doi: 10.1080/02724634.2016.1196211
- Dodson, P. (1971). Sedimentology and taphonomy of the Oldman Formation (Campanian), Dinosaur Provincial Park, Alberta (Canada). *Palaeogeography, Palaeoclimatology, Palaeoecology*, 10(1), 21-74.
- Dodson, P. (1973). The significance of small bones in paleoecological interpretation. *Contributions to Geology*, 12(1), 15-19.
- Dunson, W. A., & Mazzotti, F. J. (1989). Salinity as a limiting factor in the distribution of reptiles in Florida Bay: A theory for the estuarine origin of marine snakes and turtles. *Bulletin of Marine Science*, 44(1), 229-244.
- Dunson, W. A., & Travis, J. (1991). The role of abiotic factors in community organization. *The American Naturalist*, 138(5), 1067-1091.
- Eberth, D. (1990). Stratigraphy and sedimentology of vertebrate microfossil sites in the uppermost Judith River Formation (Campanian), Dinosaur Provincial Park, Alberta, Canada. *Palaeogeography, Palaeoclimatology, Palaeoecology*, 78(1), 1-36.
- Eberth, D. A. (1993). Depositional environments and facies transitions of dinosaur-bearing Upper Cretaceous redbeds at Bayan Mandahu (Inner Mongolia, People's Republic of China). *Canadian Journal of Earth Sciences*, 30(10), 2196-2213.
- Eberth, D. A. (2005). The geology. In P. J. Currie & E. B. Koppelhus (Eds.), *Dinosaur Provincial Park: A spectacular ancient ecosystem revealed* (pp. 54-82). Bloomington & Indianapolis, IN: Indiana University Press.
- Eberth, D. (2015). Origins of dinosaur bonebeds in the Cretaceous of Alberta, Canada. *Canadian Journal of Earth Sciences*, 52(8), 655-681.
- Eberth, D. A., Braman, D. R., & Tokaryk, T. T. (1990). Stratigraphy, sedimentology and vertebrate paleontology of the Judith River Formation (Campanian) near Muddy Lake, west-central Saskatchewan. *Bulletin of Canadian Petroleum Geology*, 38(4), 387-406.
- Eberth, D. A., & Brinkman, D. B. (1997). Paleocology of an estuarine, incised-valley fill in the Dinosaur Park Formation (Judith River Group, Upper Cretaceous) of southern Alberta, Canada. *Palaios*, 12(1), 43-58.
- Eberth, D. A., & Hamblin, A. P. (1993). Tectonic, stratigraphic, and sedimentologic significance of a regional discontinuity in the upper Judith River Group (Belly River wedge) of southern Alberta, Saskatchewan, and northern Montana. *Canadian Journal of Earth Sciences*, 30(1), 174-200.

- Embry, A. (1990). A tectonic origin for third order depositional sequences in extensional basins - Implications for basin modeling. In *Quantitative dynamic stratigraphy* (pp. 491-501). New Jersey, NJ: Prentice Hall.
- Erickson, G., Krick, B., Hamilton, M., Bourne, G., Norell, M., Lilleodden, E., & Sawyer, W. (2012). Complex dental structure and wear biomechanics in hadrosaurid dinosaurs. *Science*, 338(6103), 98-101.
- Ernst, C. H., Altenburg, R. G. M., & Barbour, R. W. (1998). Turtles of the world [CD-ROM]. ETI (Electronics Today International).
- Estes, R. (1964). University of California Publications in Geological Sciences, 49, University of California Publications in Geological Sciences, 1964, Vol.49.
- Estes, R., and Berberian, P. (1970). *Paleoecology of a late Cretaceous vertebrate community from Montana*. Breviora 343. Cambridge, MA: Museum of Comparative Zoology, Harvard University.
- Fiorillo, A. (1989). The vertebrate fauna from the Judith River Formation (Late Cretaceous) of Wheatland and Golden Valley counties, Montana. *The Mosasaur*, 4, 127-142.
- Forester, R., Caldwell, W., & Oro, F. (1977). Oxygen and carbon isotopic study of ammonites from the Late Cretaceous Bearpaw Formation in southwestern Saskatchewan. *Canadian Journal of Earth Sciences*, 14(9), 2086-2100.
- Frampton, E. (2007). *Taphonomy and palaeoecology of mixed invertebrate-vertebrate fossil assemblage in the Foremost Formation (Cretaceous, Campanian), Milk River Valley, Alberta* (Unpublished master's thesis). University of Calgary, Canada.
- Gao, K., & Brinkman, D. B. (2005). Choristoderes from the park and its vicinity. In P. J. Currie & E. B. Koppelhus (Eds.), *Dinosaur Provincial Park: A spectacular ancient ecosystem revealed* (pp. 221-234). Bloomington & Indianapolis, IN: Indiana University Press.
- Gao, C. L., Lu, J. C., Liu, J. Y., & Ji, Q. (2005). New Choristodera from the Lower Cretaceous Jiufotang Formation in Chaoyang area, Liaoning China. *Geological Review*, 51, 694-697.
- Gardner, J. D. (2005). Lissamphibians. In P. J. Currie & E. B. Koppelhus (Eds.), *Dinosaur Provincial Park: A spectacular ancient ecosystem revealed* (pp. 186-201). Bloomington & Indianapolis, IN: Indiana University Press.
- Gardner, J., & Russell, A. (1994). Carapacial variation among soft-shelled turtles (Testudines; Trionychidae), and its relevance to taxonomic and systematic studies of fossil taxa. *Neues Jahrbuch Fuer Geologie Und Palaeontologie. Abhandlungen*, 193(2), 209-244.

- Gardner, J., Russell, A., & Brinkman, D. (1995). Systematics and taxonomy of soft-shelled turtles (Family Trionychidae) from the Judith River Group (mid-Campanian) of North America. *Canadian Journal of Earth Sciences*, 32(5), 631-643.
- Golovneva, L. B. (2000). The Maastrichtian (Late Cretaceous) climate in the northern hemisphere. In M. B. Hart (Ed.), *Climates: Past and present* (pp. 43-54). Geological Society of London, Special Publication No. 181.
- Gotelli, N. J., & Colwell, R. K. (2001). Quantifying biodiversity: Procedures and pitfalls in the measurement and comparison of species richness. *Ecology Letters*, 4(4), 379-391.
- Gradstein, F. M., Ogg, J. G., Schmitz, M. D., & Ogg, G. M. (2012). *The geologic time scale 2012* (Vol. 1-2). Elsevier B.V.
- Grande, L. E., & Bemis, W. (1998). A comprehensive phylogenetic study of Amiid fishes (Amiidae) based on comparative skeletal anatomy. An empirical search for interconnected patterns of natural history. *Journal of Vertebrate Paleontology*, 18, 1-696.
- Grande, L., & Hilton, E. J. (2009). A replacement name for *Psammorhynchus* Grande & Hilton, 2006 (Actinopterygii, Acipenseriformes, Acipenseridae). *Journal of Paleontology*, 83(2), 317-318.
- Hammer, Ø., & Harper, D. A. T. (2006). *Paleontological data analysis*. Oxford, UK: John Wiley & Sons Ltd.
- Hilton, E. J., & Grande, L. (2006). Review of the fossil record of sturgeons, family Acipenseridae (Actinopterygii: Acipenseriformes), from North America. *Journal of Paleontology*, 80(4), 672-683.
- Holroyd, P. A., & Hutchison, J. H. (2002). Patterns of geographic variation in latest Cretaceous vertebrates: Evidence from the turtle component. In J. H. Hartman, K. R. Johnson & D. J. Nichols (Eds.), *The Hell Creek Formation and the Cretaceous-Tertiary boundary in the northern Great Plains: An Integrated continental record of the end of the Cretaceous* (pp. 177-190). Geological Society of America, GSA Special Papers, 361.
- Hopkins, G. R., & Brodie Jr., E. D. (2015). Occurrence of amphibians in saline habitats: A review and evolutionary perspective. *Herpetological Monographs*, 29(1), 1-27.
- Horner, J. R., & Goodwin, M. B. (2006). Major cranial changes during Triceratops ontogeny. *Proceedings of the Royal Society of London, Series B: Biological Sciences*, 273(1602), 2757-2761.
- Horner, H. R., Weishampel, D. B., & Forster, C. A. (2004). Hadrosauridae. In *The dinosauria* (2nd ed., pp. 438-463). University of California Press.

- Hortal, J., Borges, P. A., & Gaspar, C. (2006). Evaluating the performance of species richness estimators: Sensitivity to sample grain size. *Journal of Animal Ecology*, 75(1), 274-287.
- Hutchison, J. H., & Archibald, J. D. (1986). Diversity of turtles across the Cretaceous/Tertiary boundary in northeastern Montana. *Palaeogeography, Palaeoclimatology, Palaeoecology*, 55(1), 1-22.
- James, N. P., & Dalrymple, R. (Eds.) (2010). *Facies models* (4th ed.). St. John's, Newfoundland: Geological Association of Canada.
- Larson, D. W., Brinkman, D. B., & Bell, P. R. (2010). Faunal assemblages from the upper Horseshoe Canyon Formation, an early Maastrichtian cool-climate assemblage from Alberta, with special reference to the *Albertosaurus sarcophagus* bonebed. *Canadian Journal of Earth Sciences*, 47(9), 1159-1181.
- LeBlanc, A. R., Reisz, R. R., Evans, D. C., & Bailleul, A. M. (2016). Ontogeny reveals function and evolution of the hadrosaurid dinosaur dental battery. *BMC Evolutionary Biology*, 16(1), 152. Published online at doi: 10.1186/s12862-016-0721-1
- Leckie, D. A., & Smith, D. G. (1992). Regional setting, evolution, and depositional cycles of the Western Canada Foreland Basin. In R. W. Macqueen & D. A. Leckie (Eds.), *Foreland basins and fold belts* (pp. 9-46). American Association of Petroleum Geologists, AAPG Memoir 55.
- Lee, S. M., & Chao, A. (1994). Estimating population size via sample coverage for closed capture-recapture models. *Biometrics*, 50(1), 88-97.
- Lerbekmo, J. F. (2002). The Dorothy bentonite: An extraordinary case of secondary thickening in a late Campanian volcanic ash fall in central Alberta. *Canadian Journal of Earth Sciences*, 39(12), 1745-1754.
- Lerbekmo, J. F., & Braman, D. R. (2002). Magnetostratigraphic and biostratigraphic correlation of late Campanian and Maastrichtian marine and continental strata from the Red Deer Valley to the Cypress Hills, Alberta, Canada. *Canadian Journal of Earth Sciences*, 39(4), 539-557.
- Lettley, C. D., & Pemberton, S. G. (2003). Speciation of McMurray Formation inclined heterolithic strata: Varying depositional character along a riverine estuary system. In *Canadian Society of Petroleum Geologists Annual Core Conference, Calgary, Alberta, Abstract* (pp. 6-10).
- Lettley, C. D. (2004). Speciation of McMurray Formation inclined heterolithic strata: Varying depositional character along a riverine estuary system. In *CSPG/ CSEG / CWLS Convention 2004, Innovation, Collaboration, Exploration: Building to the Future, May 31 - June 4*, Calgary, Alberta, Proceedings.
- Lull, R. S., & Wright, N. E. (1942). *Hadrosaurian dinosaurs of North America*. Geological Society of America, Special Paper 40.

- Lyson, T. R., & Joyce, W. G. (2010). A new baenid turtle from the Upper Cretaceous (Maastrichtian) Hell Creek Formation of North Dakota and a preliminary taxonomic review of Cretaceous Baenidae. *Journal of Vertebrate Paleontology*, 30(2), 394-402.
- MacEachern, J. A., & Gingras, M. K. (2007). Recognition of brackish-water trace fossil suites in the Cretaceous Western Interior Seaway of Alberta, Canada. In R. G. Bromley, L. A. Buatois, G. Mángano, J. F. Genise & R. N. Melchor (Eds.), *Sediment-organism interaction: A multifaceted ichnology* (pp. 149-193). Society for Sedimentary Geology, SEPM Special Publication No. 88.
- MacEachern, J. A., & Pemberton, S. G. (1992). Ichnological aspects of Cretaceous shoreface successions and shoreface variability in the Western Interior Seaway of North America. In S. G. Pemberton (Ed.), *Applications of ichnology to petroleum exploration: A core workshop* (pp. 57-84). Society for Sedimentary Geology, SEPM Core Workshop No. 17.
- McConnell, R. G. (1885). *Report on the Cypress Hills, Wood Mountain and adjacent country: Embracing that portion of the district of Assiniboia, lying between the international boundary and the 51st parallel and extending from long. 106° to long. 100° 50'*. Geological and Natural History Survey of Canada. Montreal, Quebec: Dawson Brothers.
- McCrossan, R., & Glaister, R. P. (1964). *Geological history of Western Canada* (2nd ed.). Calgary, Alberta: Alberta Society of Petroleum Geologists.
- McLean, J. R. (1971). *Stratigraphy of the Upper Cretaceous Judith River Formation in the Canadian Great Plains*. Saskatchewan Research Council, Geology Division, Report No. 11.
- Miall, A. D. (1991). Stratigraphic sequences and their chronostratigraphic correlation. *Journal of Sedimentary Research*, 61(4), 497-505.
- Moran, S. M. (2011). *The taphonomy, paleoecology, and depositional environment of vertebrate microfossil bonebeds from the Late Cretaceous Hell Creek Formation in Garfield County, Montana*. College of William and Mary. Undergraduate Honors Theses, Paper 419. <https://scholarworks.wm.edu/honorstheses/419>
- Munsell, A. H. (2000). Munsell soil color charts, Munsell Color. New Windsor, NY: Gretag Macbeth.
- Neuman, A., & Brinkman, D. (2005). Fishes of the fluvial beds. In P. J. Currie & E. B. Koppelhus (Eds.), *Dinosaur Provincial Park: A spectacular ancient ecosystem revealed* (pp. 167-185). Bloomington & Indianapolis, IN: Indiana University Press.
- Newbrey, M. G., Murray, A. M., Brinkman, D. B., Wilson, M. V., & Neuman, A. G. (2010). A new articulated freshwater fish (Clupeomorpha, Ellimmichthyiformes) from the Horseshoe Canyon Formation, Maastrichtian, of Alberta, Canada. *Canadian Journal of Earth Sciences*, 47(9), 1183-1196.

- Nicholls, E. (1972). *Fossil turtles from the Campanian Stage of western North America*. (Unpublished master's thesis). University of Calgary, Canada.
- Nichols, G. (2009). *Sedimentology and stratigraphy* (2nd ed.). Chichester, UK ; Hoboken, NJ: Wiley-Blackwell.
- Oksanen, J. (2010). *Cluster analysis: Tutorial with R*. University of Oulu, Oulu, Finland.
- Peng, J. (1998). Palaeoecology of vertebrate assemblages from the Upper Cretaceous Judith River Group (Campanian) of southeastern Alberta, Canada. *Science*.
- Price, R. A. (1994). Cordilleran tectonics and the evolution of the Western Canada Sedimentary Basin. In G. D. Mossop & I. Shetsen (Comps.), *Geological atlas of the Western Canada Sedimentary Basin* (pp. 13-24). Calgary, Alberta: Canadian Society of Petroleum Geologists and Alberta Research Council.
- R Core Team. (2013). R: A language and environment for statistical computing. R Foundation for Statistical Computing, Vienna, Austria. URL <http://www.R-project.org/>.
- Remane A., & Schlieper, C. (1972). Biology of brackish water. *The Quarterly Review of Biology*, 47(4), 467.
- Rogers, R. R. (1998). Sequence analysis of the Upper Cretaceous Two Medicine and Judith River formations, Montana; nonmarine response to the Claggett and Bearpaw marine cycles. *Journal of Sedimentary Research*, 68(4), 615-631.
- Rogers, R. R., & Brady, M. E. (2010). Origins of microfossil bonebeds: Insights from the Upper Cretaceous Judith River Formation of north-central Montana. *Paleobiology*, 36(1), 80-112.
- Rogers, R. R., & Kidwell, S. M. (2007). A conceptual framework for the genesis and analysis of vertebrate skeletal concentrations. In R. R. Rogers, D. A. Eberth & A. R. Fiorillo (Eds.), *Bonebeds: Genesis, analysis, and paleobiological significance* (pp. 1-63). Chicago ; London: University of Chicago Press.
- Roy, P. S., Cowell, P. J., Ferland, M. A., & Thom, B. G. (1994). Wave-dominated coasts. In R. W. G. Carter & C. D. Woodroffe (Eds.), *Coastal evolution: Late Quaternary shoreline morphodynamics* (pp. 121-186). Cambridge, UK: Cambridge University Press.
- Sahni, A. (1972). The vertebrate fauna of the Judith River Formation, Montana. *Bulletin of the American Museum of Natural History*, 147, article 6, 323-412.
- Sankey, J. T. (2008). Vertebrate paleoecology from microsites, Talley Mountain, Upper Aguja Formation, (Late Cretaceous), Big Bend National Park, Texas, USA. In J. T. Sankey & S. Baszio (Eds.), *Vertebrate microfossil assemblages: Their role in paleoecology and paleobiogeography* (pp. 61-77). Bloomington, IN: Indiana University Press.

- Sato, T. (2003). Description of Plesiosaurs (Reptilia: Sauropterygia) from the Bearpaw Formation (Campanian-Maastrichtian) and a phylogenetic analysis of the elasmosauridae (doctoral thesis). University of Calgary, Canada. ProQuest Dissertations and Theses.
- Sato, T. (2005). A new polycotylid plesiosaur (Reptilia: sauropterygia) from the Upper Cretaceous Bearpaw Formation in Saskatchewan, Canada. *Journal of Paleontology*, 79(5), 969-980.
- Sato, T., Eberth, D., Nicholls, E., & Manabe, M. (2005). Plesiosaurian remains from non-marine to paralic sediments. In P. J. Currie & E. B. Koppelhus (Eds.), *Dinosaur Provincial Park: A spectacular ancient ecosystem revealed* (pp. 249-276). Bloomington & Indianapolis, IN: Indiana University Press.
- Shotwell, J. A. (1955). An approach to the paleoecology of mammals. *Ecology*, 36(2), 327-337.
- Smith, E. P., & van Belle, G. (1984). Nonparametric estimation of species richness. *Biometrics*, 40(1), 119-129.
- Thomas, R. G., Smith, D. G., Wood, J. M., Visser, J., Calverley-Range, E. A., & Koster, E. H. (1987). Inclined heterolithic stratification—terminology, description, interpretation and significance. *Sedimentary Geology*, 53(1-2), 123-179.
- Tokaryk, T. T., & Harington, C. R. (1992). *Baptornis* sp. (Aves: Hesperornithiformes) from the Judith River Formation (Campanian) of Saskatchewan, Canada. *Journal of Paleontology*, 66(6), 1010-1012.
- Torres-Dowdall, J., Dargent, F., Handelsman, C. A., Ramnarine, I. W., & Ghalambor, C. K. (2013). Ecological correlates of the distribution limits of two poeciliid species along a salinity gradient. *Biological Journal of the Linnean Society*, 108(4), 790-805.
- Underwood, C. J., & Cumbaa, S. L. (2010). Chondrichthyans from a Cenomanian (Late Cretaceous) bonebed, Saskatchewan, Canada. *Palaeontology*, 53(4), 903-944.
- Vavrek, M. J. (2011). Fossil: Palaeoecological and palaeogeographical analysis tools. *Palaeontologia Electronica*, 14(1), 16.
- Welton, B., & Farish, R. F. (1993). *The collector's guide to fossil sharks and rays from the Cretaceous of Texas*. Dallas, TX: Horton Printing.
- Wheeler, A. (1985). *World encyclopedia of fishes*. London: Macdonald.
- Wood, J. M. (1985). *Sedimentology of the Late Cretaceous Judith River Formation, "Cathedral" area, Dinosaur Provincial Park, Alberta* (Unpublished master's thesis). University of Calgary, Canada.

- Wood, J. M. (1989). Alluvial architecture of the Upper Cretaceous Judith River Formation, Dinosaur Provincial Park, Alberta, Canada. *Bulletin of Canadian Petroleum Geology*, 37(2), 169-181.
- Wood, J. M., Thomas, R. G., & Visser, J. (1988). Fluvial processes and vertebrate taphonomy: The Upper Cretaceous Judith River Formation, south-central Dinosaur Provincial Park, Alberta, Canada. *Palaeogeography, Palaeoclimatology, Palaeoecology*, 66(1-2), 127-143.
- Wu, X.-C. (2005). Crocodylians. In P. J. Currie & E. B. Koppelhus (Eds.), *Dinosaur Provincial Park: A spectacular ancient ecosystem revealed* (pp. 277-291). Bloomington & Indianapolis, IN: Indiana University Press.

Transition

Chapter 5 presents a regional case study of the sedimentology, sedimentary environments, biostratigraphy, and vertebrate paleontology of the Lake Diefenbaker site in southwestern Saskatchewan. Chapter 6 discusses Woodpile Coulee, the most stratigraphically complete outcrop of the BRG in Saskatchewan, and possibly the entire Western Canada Sedimentary Basin. A summary of the sedimentology and palynology of Woodpile Coulee is provided, as well as a discussion of the biostratigraphic framework. Detailed description of the Dinosaur Park Formation transition from lowstand to transgressive system tracts is highlighted. Alpha diversity of a vertebrate microfossil locality discovered at this transition is described and compared to the dataset provided in Chapter 3, at Diefenbaker Lake.

A New Dinosaur Park Formation (Campanian, Late Cretaceous)
Microvertebrate Locality from the Cypress Hills region of Southwest
Saskatchewan: Implications for paleoenvironmental controls on species alpha
diversity

Abstract

The Upper Cretaceous Belly River Group (BRG) of southern Alberta and its relative equivalent in Montana, the Judith River Formation, are widely known for their exceptional exposure and superb fossil content. Outcrops of the Belly River Group are far less common in Saskatchewan than in Alberta and Montana, but do record a variety of fossil material within the uppermost beds. These deposits and their associated fossil material are significant, as they represent the easternmost expression of the BRG in Canada, and are a geographic link between Alberta and Montana. On the extreme southwestern flanks of the Cypress Hills, surface exposures of the Belly River Group are investigated in detail for the first time since the 1930s.

A complete sequence of Belly River Group clastics, spanning the Lea Park Formation at the base to the Bearpaw Formation at the top, is exposed in the study area. These deposits represent the most complete continuous exposure from the upper Lea Park to lower Bearpaw formations in the Western Interior Basin. Though these deposits are extensive, the stratigraphy is complicated by structural tilting, faulting, and native prairie grass cover. The exposures are located in a glacial drainage channel trending northwest-southeast known as Woodpile Coulee, named for Woodpile Creek which flows through it. These deposits have been studied in detail, and the sedimentology, stratigraphy, ichnology, and biostratigraphy is presented herein. The Dinosaur Park Formation is particularly well exposed, consisting of a lower fluvio-estuarine

dominated and an upper lignite and mudstone dominated facies associations. A detailed discussion of the Dinosaur Park Formation provides context for an associated microfossil assemblage and establishes a framework for future studies concerned with between-site diversity trends during the Campanian of North America.

The Woodpile Coulee microsite contains at least 36 different fossil species including several taxa that are rare or unknown elsewhere in the province. Among the dinosaurs present are nodosaurs, which are known from only one other site in Saskatchewan. Hadrosaur, ceratopsian, and pachycephalosaur remains have been recovered from the site, as well as the small hypsolophodont *Thescelosaurus* sp. Tyrannosaurids are present, in addition to several small theropods, including *Troodon* sp. and *Dromaeosaurus* sp. Crocodile, champsosaur, turtle, amphibian, and a broad diversity of bony and cartilaginous fish have been identified. Studying the fossil life recovered from the Dinosaur Park Formation has permitted analysis of spatial alpha and beta diversity trends, particularly in relation to proximity to the paleocoastline as a biodiversity driver. By establishing a rigid geologic framework for these deposits, subtle nuances among the interplay of paleoecology, paleoenvironment, and paleotopography can be applied to our understanding of the fossil record and add to our understanding of organism response to natural changes over time.

1. Introduction

The Belly River Group (in particular the Oldman and Dinosaur Park formations) and the Judith River Formation of Alberta and Montana respectively are penecontemporaneous units, deposited within the same large-scale depositional system controlled by tectonics in the west, resulting in similar paleoenvironmental conditions along the western edge of the Western Interior coastline. The deposits themselves, and the taxa recovered within, have been the focus of countless studies concerning stratigraphy, sedimentology, paleoecology, paleobiogeography, and evolution. Newly described Dinosaur Park Formation deposits in southwestern Saskatchewan have yielded several microvertebrate fossil assemblages that have considerable potential to provide important new information on Campanian coastal ecosystems.

Turnover in faunal composition has been linked to fluctuations in sea level caused by inundation and the subsequent exposure of coastline due to transgressive-regressive cycles of the Western Interior Seaway (WIS) of North America. These tectonically controlled cycles are known to have occurred since the Jurassic, but Upper Cretaceous (Campanian: 83.6–72.1 Ma) deposits from southern Alberta and northern Montana are well exposed, accessible, and highly fossiliferous, leading to many significant vertebrate paleoecology studies throughout the last century (Dodson, 1971; Wood et al., 1988; Eberth, 1990; Brinkman, 1990; Brinkman et al., 1998, 2004, 2005; Rogers and Kidwell, 2000; Brady et al., 2005; Brown et al., 2013; Cullen et al., 2016; Gilbert et al., 2018). This work has largely been possible by utilizing microvertebrate fossil assemblages (microsites), which are concentrations of fossilized vertebrate remains, including small bones, scales and teeth of multiple taxa, of which more than 75% are 5 cm in size or smaller (Rogers and Kidwell, 2007). Vertebrate microfossil assemblages can provide insights into biodiversity over the period when the site was formed and fossils were

accumulating. This is important for understanding paleoecology through deep time and provides more data than is otherwise available from smaller or isolated paleontological datasets (Shotwell, 1955; Estes and Berberian, 1969; Dodson, 1973; Sankey, 2008).

In this paper, the sedimentology, invertebrate paleontology, and palynology of the Belly River Group, and in particular the DPF, is described from a regional outcrop in extreme southwestern Saskatchewan (Fig. 6.1). This site will be referred to hereafter as ‘Woodpile Coulee’ (WPC), after the name given to the glacial meltwater channel it was discovered in (referred to locally as a coulee). Additionally, we 1) interpret the depositional environment and associated palynology and faunal assemblages; 2) interpret and describe material collected from a vertebrate microfossil assemblage within the DPF; 3) conduct an alpha (within-site) diversity analysis of the microvertebrate material and contrast this material with the Lake Diefenbaker microsite to elucidate spatial and temporal patterns across the DPF of Saskatchewan.

2. Geological Setting

Cretaceous and Paleogene sedimentation (Fig. 6.2) in the Western Interior Sedimentary Basin occurred in two depocenters, the Williston Basin and the Alberta Foreland Basin, which are separated by the Bow Island Arch (Dawson et al., 1994). During the Laramide orogeny (~ 70 to 80 Ma), collisional accretion of microcontinents onto the western coast of North America caused thrust loading, forming an orogenic belt (Price, 1994). This flexed the craton to produce a deeply subsiding asymmetric foredeep fed by sediments from tectonically controlled slopes in the west (Catuneanu et al., 2000). In west-central North America, this resulted in deposition of extensive marine and non-marine clastic sediments in transgressive-regressive, tectonically-controlled wedge-cycles (Leckie and Smith, 1992). The BRG is the fourth of five recognized cycles of foreland basin deposition; the transition between the DPF and the Bearpaw Formation

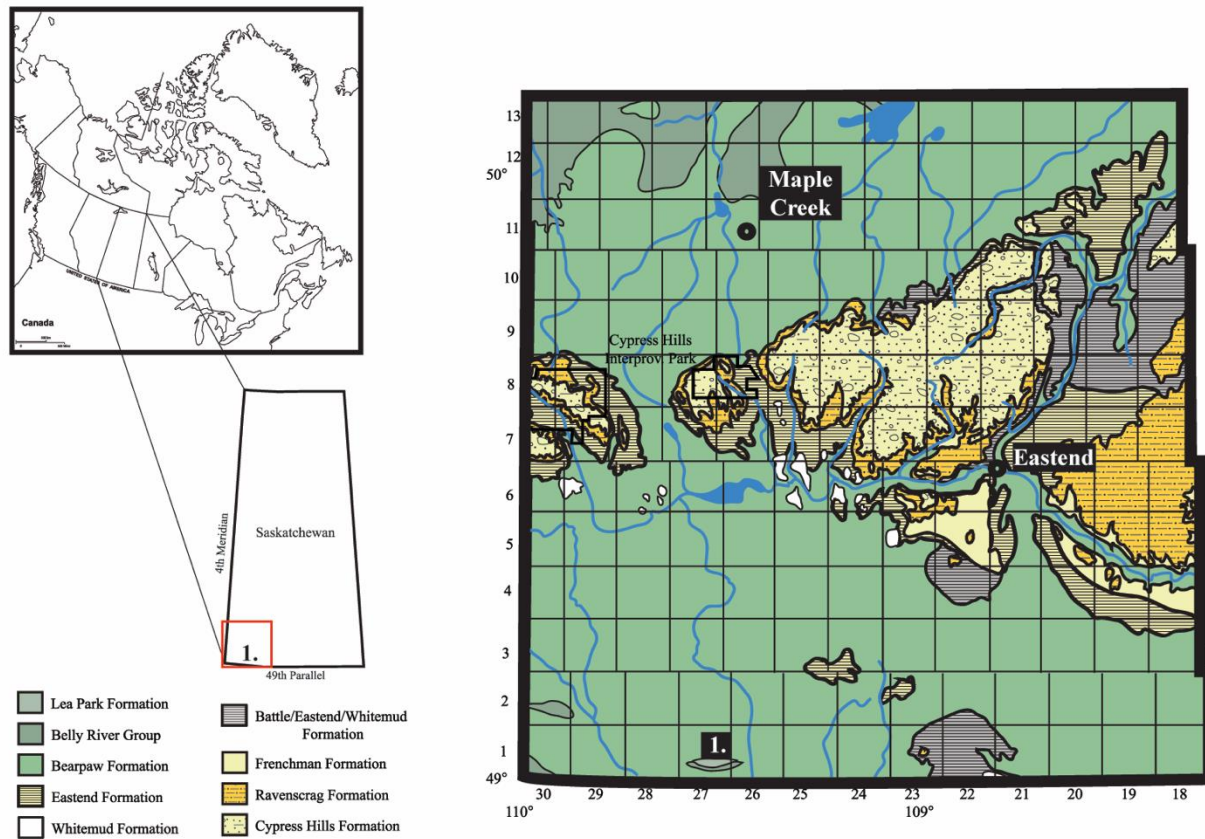


Figure 6.1: Left: Geographic location of Saskatchewan in context to regional landmarks and boundaries of the Cypress Hills region and location of exposed outcrop at 1. Woodpile Coulee. Right: Regional map of the Cypress Hills region in context to regional landmarks. Based on maps from the Saskatchewan Geological Survey.

(BP) marks the last major transgression of the Western Interior Seaway (Embry, 1990; Kauffman and Caldwell, 1993; Leckie and Smith, 1992).

The Belly River Group (BRG) in both Alberta and Saskatchewan is a terrestrial clastic wedge under and overlain by marine strata of the Lea Park (Clagette Formation of Alberta) and Bearpaw formations respectively (Eberth and Hamblin, 1993; McLean, 1971). In descending order, the BRG includes: the Foremost (FF) (and the associated Ribstone Creek Member), Oldman (OF), and Dinosaur Park (DPF) formations (Fig. 6.1) (Eberth and Hamblin, 1993). All formations are formally recognized in Saskatchewan (see Chapter 4), but show clear evidence of significant marine influence when compared to their Alberta equivalents, as most facies associations have a marginal marine component. In southwestern Saskatchewan, lagoon, estuary basin, and barrier-island deposits directly overlying coastal plain facies of the DPF have been designated the Manâtakâw Member, a unit included within the Dinosaur Park Formation (see Chapter 4).

In Montana, the BRG is equivalent to the Judith River Formation, which in ascending order is divided into the Parkman Sandstone, McClelland Ferry, Coal Ridge, and Woodhawk members (Rogers, 1998; Rogers et al., 2016). These members are very similar to the Foremost, Oldman, Dinosaur Park formations and Manâtakâw members respectively, and are considered by the author to be contemporary depositional systems deposited within similar environmental parameters and affected by the same tectonic controls. All group-equivalents yield rich vertebrate microsite assemblages (Eberth, 2015; Rogers and Brady, 2010).

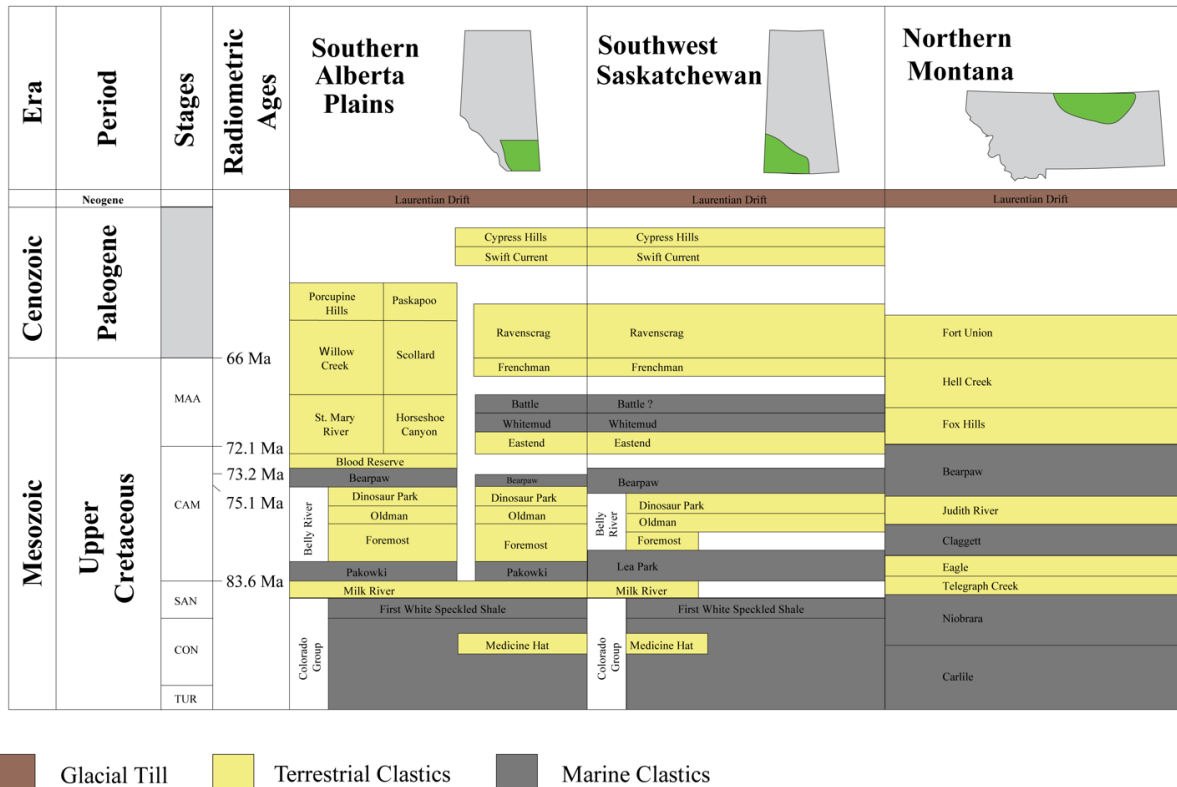


Figure 6.2: Stratigraphic nomenclature utilized in southeastern Alberta and southwestern Saskatchewan through the Upper Cretaceous Series in the Western Canada Interior Basin. Radiometric and biostratigraphic dates (Ma): 66: K-T Boundary (Gradstein et al., 2012); 72.1: Campanian Maastrichtian boundary (Gradstein et al., 2012); 73.2 ± 0.4: Dorothy Bentonite (Lerbekmo and Braman, 2002); 75.1: *Exileoceras jenneyi* (Cobban et al., 2006); 83.6: Campanian-Santonian boundary (Gradstein et al., 2012). After Gilbert et al. (2018). TUR - Turonian; CON - Coniacian; SAN - Santonian; CAM - Campanian; MAA - Maastrichtian.

3. Materials and Methods

3.1 Data Collection

Detailed sedimentologic and stratigraphic information was recorded during summers of 2014 and 2015. Outcrop was scraped to expose fresh surfaces, and sediment logs were recorded using a Brunton© compass and Jacob's Staff. Standard sedimentologic information (color, grain size, clast shape, sedimentary structures, paleocurrent indicators, bed geometry, bed contacts, invertebrate and vertebrate body fossils, and trace fossils) were recorded. Core logged from the Dinosaur Park Formation in the Cypress Hills was used as a proxy for Woodpile Coulee (Fig. 6.3). Due to the poor exposure and limited lateral extent of exposed facies, a composite section was constructed from multiple measured sections (Fig. 6.4).

Microvertebrate fossil material was surface-picked and bulk sampled in 1989 and 2018 by staff of the Royal Saskatchewan Museum, and in 2014 and 2015 by the senior author. Bulk material was screen-washed with a #18 U.S. standard size sieve with 1 mm mesh and picked under a dissection microscope. Fossil material was identified and catalogued at the RSM by Tim Tokaryk, Tara Lekach, Meagan Gilbert and Emily Bamforth. All material was identified to the lowest possible taxonomic level and the abundance of each type of faunal element was determined. In total, 327 elements were identified and included in this study. The collection is housed at the Royal Saskatchewan Museum T. rex Discovery Centre in Eastend, Saskatchewan, Canada. Diversity analysis was ran on the sample set, the results of which were compared to alpha diversity analysis conducted on another Saskatchewan microvertebrate site, Lake Diefenbaker (Chapter 5; Gilbert et al., 2018). The Lake Diefenbaker site was deposited at the contact between the DPF and the Bearpaw Formation.

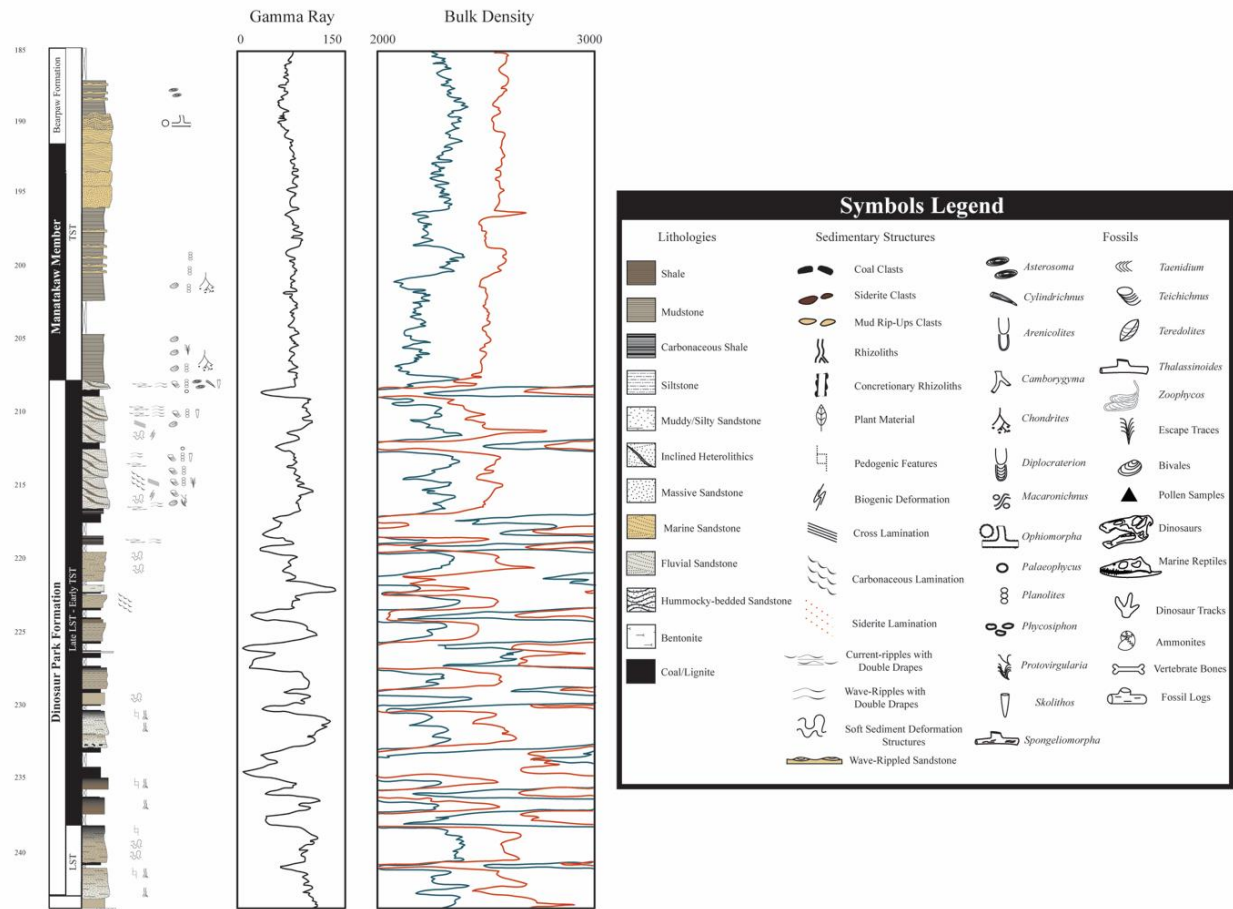


Figure 6.3: Representative lithostratigraphic log profiles of Nexen Battle Creek 07-02-004-27W3 and corresponding gamma (API) and bulk density log (K/M3) used to assist in identifying facies of the DPF at Woodpile Coulee. C - Coal; Sh - Shale/Claystone; M - Mudstone; Si - Siltstone; FSS - Fine-grained Sandstone; MSS - Medium-grained Sandstone. LST – Lowstand Systems Tract; TST – Transgressive Systems Tract.

Dennis Braman (Royal Tyrrell Museum of Paleontology; RTMP) collected 36 palynology samples from WPC in 1989. These samples were prepared using acid dissolution of mineral matter, oxidation, heavy-liquid separation, sieving, and dyeing of the residues, which were permanently mounted on glass slides. The studied preparations are stored in the permanent collection of the RTMP in Drumheller, Alberta, Canada.

3.2 Diversity Analysis

Alpha diversity is a local measurement referring to the average species diversity in a specific habitat or region (Whittaker, 1972). Alpha diversity measurements were calculated using non-parametric species estimators, which extrapolate the number of species that would be present in a sample, if that sample were complete (Colwell and Coddington, 1994). This approach is taken because rare taxa are often underrepresented or entirely absent from any given sample in the fossil record. Species estimators attempt to minimize these errors caused by incompleteness of the fossil record by statistically estimating how many taxa are missing (Colwell and Coddington, 1994; Vavrek, 2011). These estimators are more effective than rarefaction, as they are less likely to underestimate diversity in communities with low species evenness and are not as sensitive to the underlying pattern affecting species abundance (Gotelli and Colwell, 2001). Previous studies have indicated that Chao-1 (Chao, 1984), Abundance-based Coverage Estimator (ACE) (Chao and

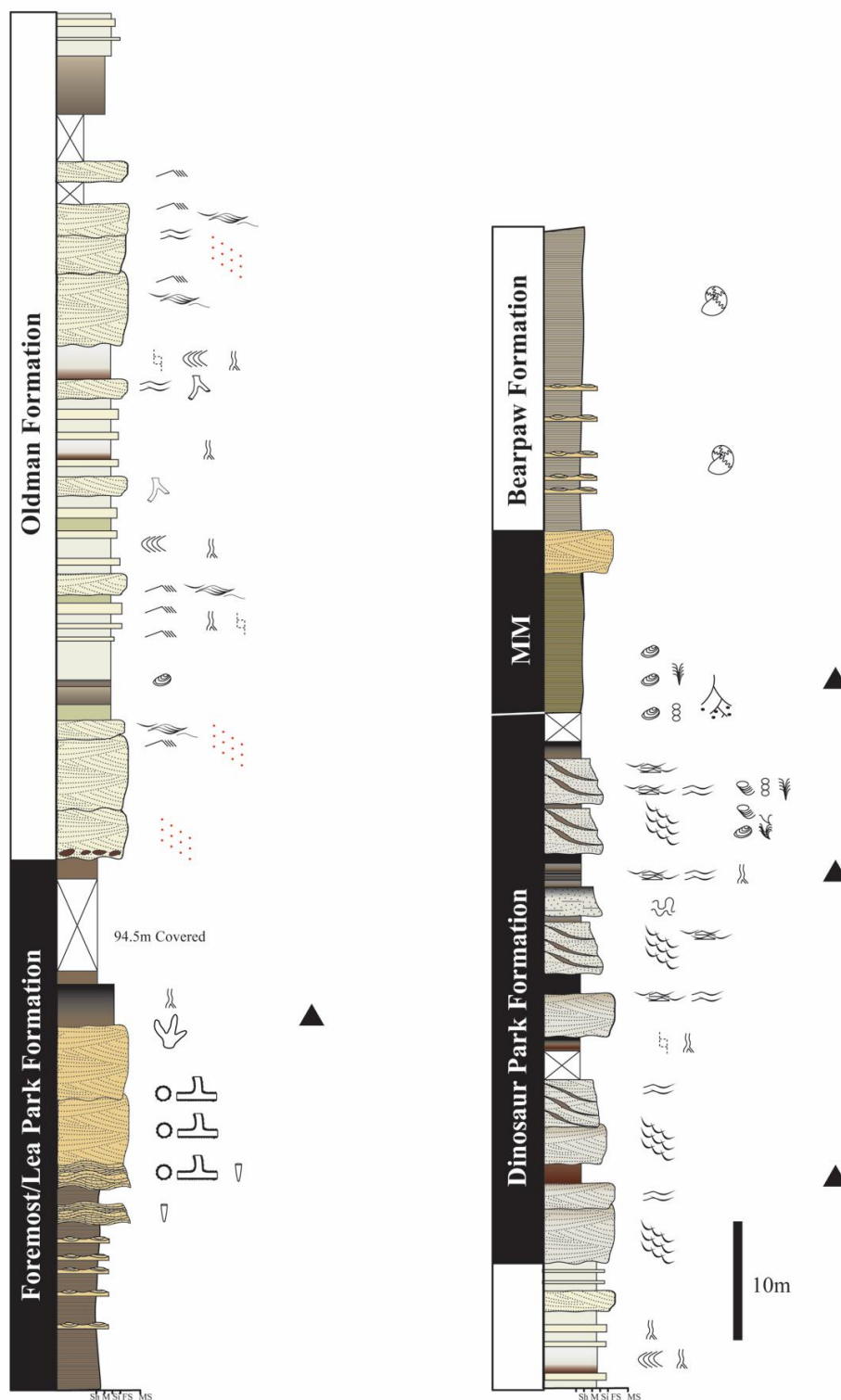


Figure 6.4: Representative composite lithostratigraphic log profile of exposed outcrop at Woodpile Coulee. C - Coal; Sh - Shale/Claystone; M - Mudstone; Si - Siltstone; FSS - Fine-grained Sandstone; MSS - Medium-grained Sandstone; MM - Manâtakâw Member.

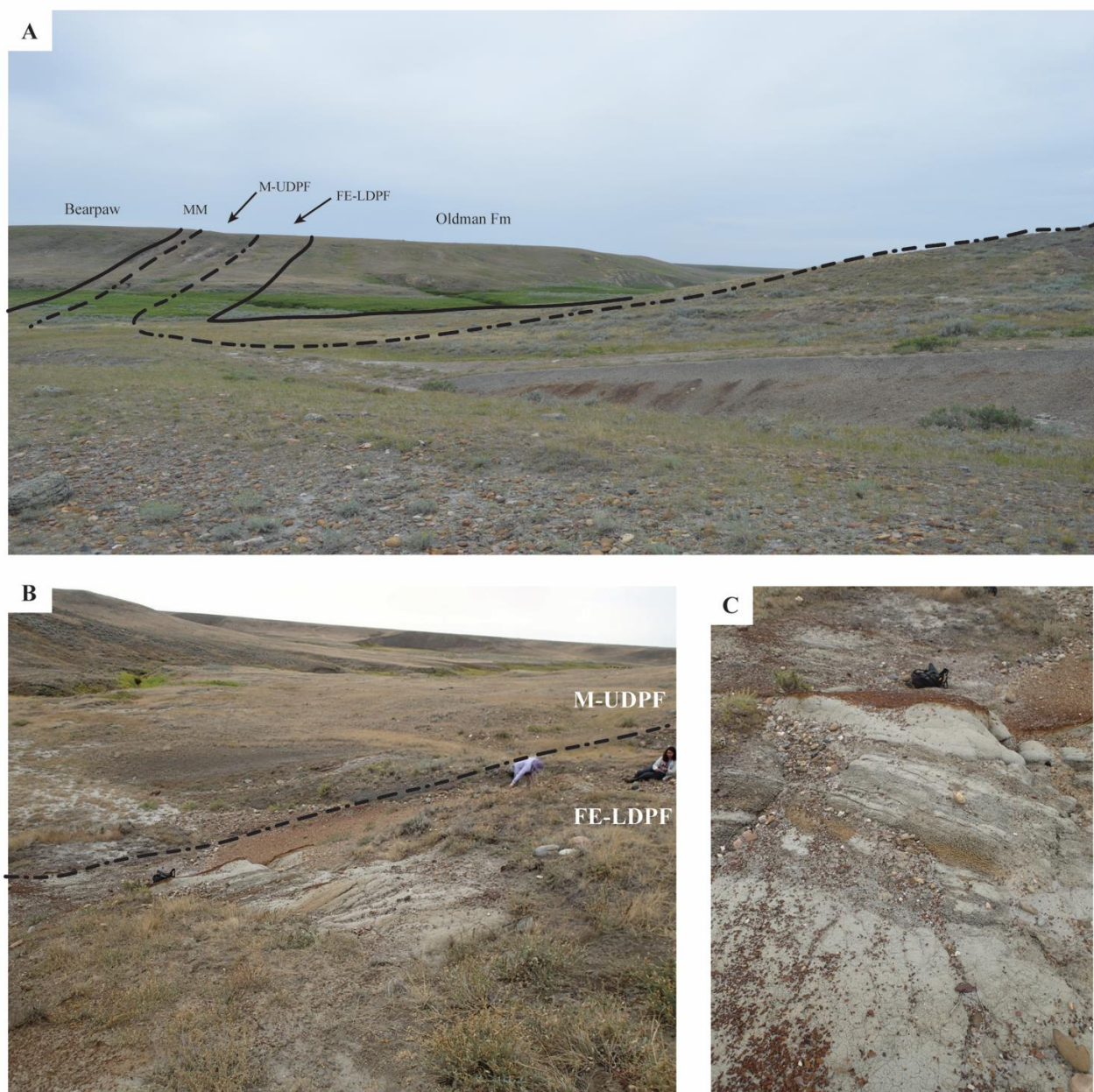


Figure 6.5: Selected photos of outcrop highlighting the Dinosaur Park Formation and the associated microvertebrate locality. A. Panoramic photograph (taken to the northwest) displaying the inclination of the beds. Formation contacts are denoted with a solid black line, and important stratigraphic surfaces within the Dinosaur Park Formation are denoted with dashed lines; B. Photograph taken from the microvertebrate site looking at the inclined contact between the lower sandstone dominated DPF and the upper mud dominated DPF; C. Photograph of the microvertebrate locality. FE-LDPF – Fluvio-estuarine lower Dinosaur Park Formation; M-UDPF – Muddy upper Dinosaur Park Formation; MM - Manâtakâw Member.

Lee, 1992; Chao and Yang, 1993; Lee and Chao, 1994), and second-order Jackknife (Smith and van Belle, 1984) perform best for abundance-based paleontologic datasets. Non-parametric species estimators were calculated using the vegan and fossil packages (Oksanen, 2010; Vavrek, 2011) in R Statistical Software (R Core Development Team, 2013), version 2.13.2.

4. Results

4.1 Site Description

Woodpile Coulee is located on the southernmost flanks of the Cypress Hills, a major topographic high in southeastern Alberta and southwestern Saskatchewan. With the onset of deglaciation, glacial meltwater channels drained to the south, carving a series of incised valleys into the surrounding landscape, exposing various Cenozoic and Cretaceous sediments throughout the region (McLean, 1971).

Strata of the BRG are exposed in their entirety at Woodpile Coulee and in patches along adjacent coulees to the east and west. The strata are tilted and faulted, dipping an average of 40° to the south and striking east (Fig. 6.5A). Resistant sandstones of the FF and OF can be traced laterally along the surface for hundreds of meters to both the east and west before terminating against their causative faults. The source of the faulting is not presently known, but two hypotheses have been proposed: 1) glacial thrust faulting during the last Pleistocene glaciation, and 2) displacement by intrusive volcanics related to uplift of the Bearpaw Mountains during the late Cenozoic (McLean, 1971). Outcrop exposure is generally poor due to the nearly vertical nature of the beds and extensive native prairie grass cover and soil creep.

The microsite is situated in a northeast-southwest trending tributary flank of Woodpile

Coulee (Fig. 6.5B). The fossil material is preserved within silty sandstone and mudstone near the top of sandstone-dominated deposits of the lower DPF (Fig. 6.5C). These deposits are overlain by lignites and mudstones of the upper DPF and are lithostratigraphically equivalent to the Lethbridge Coal Zone of Alberta (Eberth and Hamblin, 1993; Hamblin, 1997). Stratigraphically, the microsite is located in the mid- DPF at the transition from lowstand fluvio-estuarine channels of the lower DPF to lignites and heterolithic deposits of the transgressive upper DPF.

4.2 Sedimentology

4.2.1 Sedimentology of the Belly River Group at Woodpile Coulee

The BRG is fully exposed along WPC, including the Ribstone Creek Member, a terrestrial tongue of the Foremost Formation over- and underlain by marine shales of the Lea Park Formation (Gordon, 2000; Gilbert et al., in review). A representative geophysical well log was constructed to provide insights into depositional trends at Woodpile Coulee and southwestern Saskatchewan (Fig. 6.6) (see Chapter 4 for a regional treatment of the BRG in southwestern Saskatchewan).

The Foremost and upper Lea Park Formation is exposed in patches along WPC. The Ribstone Creek Member in particular is a prominent lithologic feature, reflecting the resistant nature of the sandstones (Fig. 6.7A-E). In the Cypress Hills, the FF interfingers with fully marine shales of the Lea Park, and is comprised of shallowing upwards successions of wave-dominated coastal deposits dominated by *Ophiomorpha* isp. and *Skolithos* isp (Fig. 6.7B), capped by backshore facies with dinosaur footprints (Fig. 6.7c and f). The uppermost FF is interpreted as

Canadian Landmaster Belanger
10-23-007-25W3

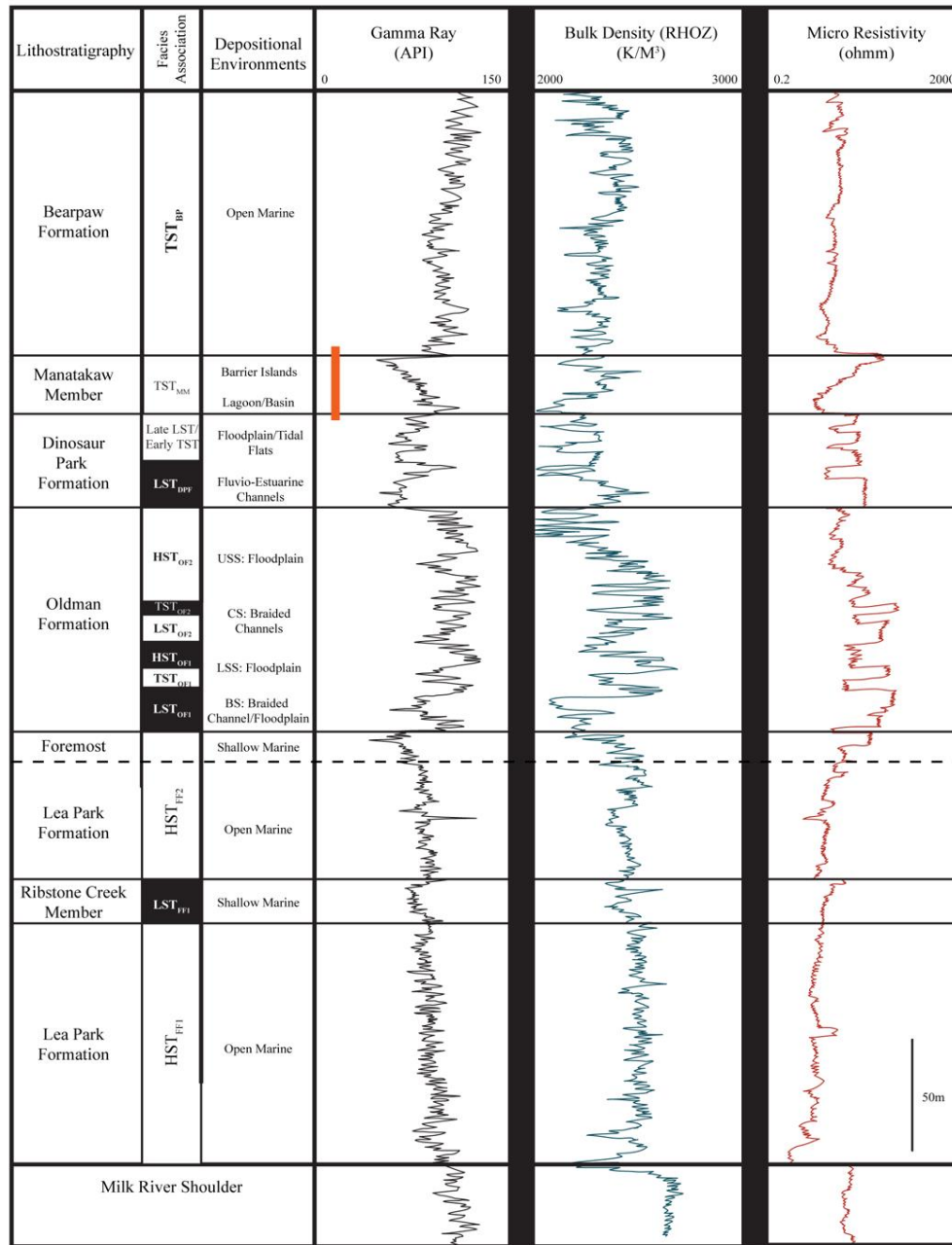


Figure 6.6: Representative well log highlighting stratigraphy, systems tracts, and depositional environments of the Belly River Group in the subsurface of southwestern Saskatchewan (Canadian Landmaster Belanger – 10-23-007-25W3). This well illustrates the typical gamma ray – bulk density – resistivity log signatures of the Belly River Group. Dashed line of the Foremost Formation indicates its sporadic occurrence throughout the study area. Red line indicates available core that was logged for this study. For systems tract information, see Chapter 4.

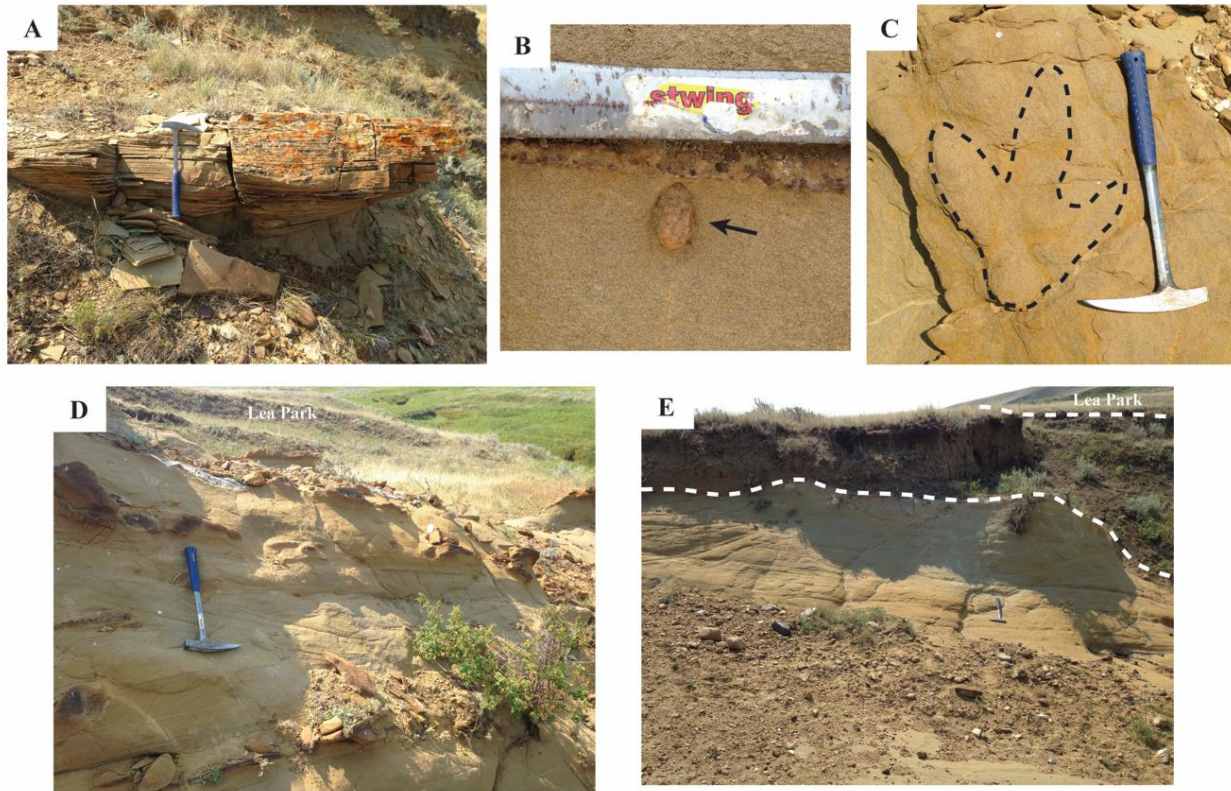


Figure 6.7: Selected photos of outcrop highlighting different facies and ichnofossils from the Foremost Formation (Ribstone Creek Member) in Woodpile Coulee, Saskatchewan. A. Hummocky cross-stratification from offshore transition deposits; B. *Ophiomopha* isp. burrows in lower shoreface sandstone; C. Dinosaur track preserved in foreshore facies; D. Foreshore, Upper shoreface, and lower shoreface deposits. Note the overlying Lea Park Formation in the background; E. Foreshore sandstones and backshore shales and coals of the Ribstone Creek Member immediately overlain by shales of the Lea Park Formation. Upper dashed line denotes a marine flooding surface.

reflecting highstand conditions at the end of the FF depositional cycle in the Cypress Hills.

The OF is the thickest and most well exposed formation at Woodpile Coulee. Deposits of the OF record two full T-R cycles, indicating a complex interplay between sediment supply and accommodation space at the time of deposition. The OF is characterized by buff and pale-yellow colored sandstone and siltstone. This formation records fluvial channels, levees, crevasse splays, floodplains, and paleosols, and is dominantly fully terrestrial, with only minor evidence of marine transgression 1) at the top of the ‘basal’ sandstones; 2) at the top of the Comrey Sandstone (Fig. 6.8a-b). Amalgamated sandstone of the ‘basal’ and Comrey Sandstones are attributed to lowstand conditions perpetuated by minimal slope and a lack of true deep marine (Gilbert et al submitted). Isolated lenticular channelized sandstone overlain by siltstone and mudstone are interpreted as fluvial channels and their associated floodplains deposited during a highstand. These deposits record bioturbation indicative of habitually dry conditions (e.g. *Taenidium*; Fig. 6.8c). Though the OF is relatively well exposed at WPC, detailed sedimentology is often obscured by soil development and grass cover.

The DPF and its associated Manâtakâw Member are the final terrestrial to marginal marine sediments of the BRG before inundation of the WIS. Terrestrial sediments of the BRG are subsequently replaced with shale and mudstone of the BF. Deposits of the DPF are discussed below.

4.2.2 Sedimentology of the Dinosaur Park Formation at Woodpile Coulee

Fluvial deposits at the base of the DPF at Woodpile Coulee represent meandering channel systems and associated heterolithic deposits in an incised fluvio-estuarine environment (Gilbert

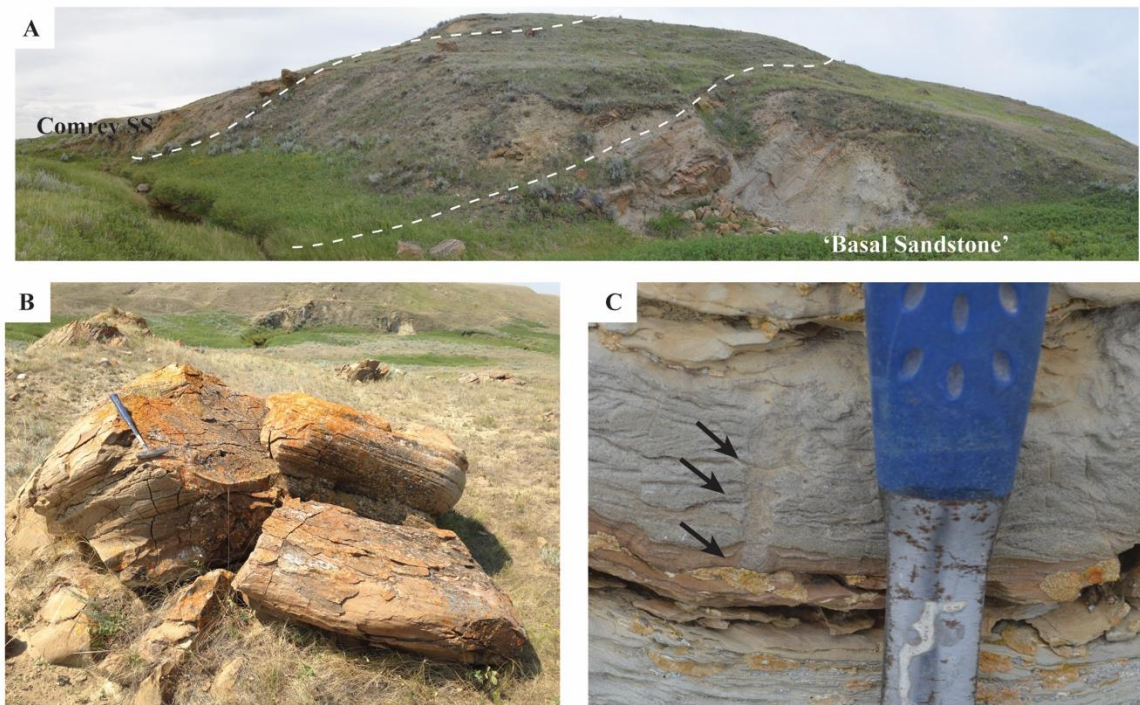


Figure 6.8: Selected panoramic outcrop photos of the Oldman Formations A. The lower ‘basal sandstone’ of southwestern Saskatchewan in Woodpile Coulee. This contact sits directly above shales of the Lea Park Formation. Note the basal contact of the Comrey Sandstone roughly 20m to the south. Both sandstones are resistant to weathering, and can be traced laterally for ~1km to the east and west before terminating against the faults edge. Formations are dipping at roughly 30°; B. Photograph taken facing west showing resistant braided fluvial sandstones assigned to the Comrey Sandstone known from southeastern and central Alberta. This sandstone unit has been identified as having been deposited in a unincised Lowstand Systems Tract; C. *Taenidium* isp. burrows crosscutting isolated braided sandstones in the upper Highstand Systems Tract at Woodpile Coulee. This trace was likely colonizing upper floodplain deposits, and downcutting into underlying fluvial deposits. These deposits directly underlie the Dinosaur Park Formation in the coulee.

et al., 2019). In the study area, the base of the DPF is composed of fine-grained siltstone and sandstone representing fluvial channel-fill deposited during a lowstand systems tract. Isopach maps constructed from subsurface well data indicate that the DPF underwent incision at its base, likely induced by tectonism in the Canadian Cordillera (Gilbert et al., 2019). These lower deposits show increasing tidal influence up-section before transitioning into mudstone- and lignite-dominated deposits of the upper DPF (Fig. 6.6). This transition signals increased accommodation and onset of the second-order Bearpaw Cycle in a transgressive systems tract. Facies analysis implies that the upper DPF accumulated in a swampy, low-energy setting dominated by organic-rich mudstone, heterolithic deposits, and coal seams.

The lower interval is characterized by 0.45–3.7 m thick fining-upward successions of trough cross-bedded and current rippled fine-grained sandstone. Paleocurrent indicators show a prevailing flow direction from the northeast. These deposits are overlain by beds with inclined heterolithic stratification (IHS) and are composed of interbedded successions of siltstone, mudstone and sandstone. Cross-lamination, current ripples, wave ripples and carbonaceous debris are common throughout these deposits.

In the upper DPF, brown and green mudstone and silty mudstone display localized siderite, root trace fossils, slickensides, ironstone lenses, and bentonitic layers (Fig. 6.9). These deposits represent abandoned meander channels and associated paleosols in a water-saturated environment. Parallel-laminated sandstone and siltstone layers are present throughout these deposits, and commonly show convolute bedding. These deposits indicate episodic deposition of coarser grained water-saturated sediments dominated by fine-grained sandstone. Bright banded coal and red lignite are abundant throughout the upper DPF.



Figure 6.9: Representative photographs of core from the Dinosaur Park Formation (Nexen Battle Creek Core 07-02-004-27W3; log shown in Figure 6.3). This log displays fluvio-estuarine sandstone and siltstone at the base, passing into upper mud and coal dominated deposits at the top, and finally into lagoon and barrier island deposits of the Manâtakâw Member at the top.

The transition between the upper and lower DPF is interpreted as a shift from low accommodation sedimentation during a lowstand systems tract, to high to moderate accommodation during a transgressive systems tract. The shift from sinuous meandering-channel fill to swampy, highly vegetated floodplain in the mid-DPF of Saskatchewan shows that transgression occurred earlier in Saskatchewan than in Alberta. This is expected because Saskatchewan was nearer the contemporary paleocoastline during the late Campanian (Caldwell, 1968; Eberth et al., 1990; Tsujita, 1995; Gilbert et al., 2018). The microfossil assemblage described here was recovered as a concentrated horizon at the base of an erosional contact between the upper and lower DPF in a crevasse-splay deposit. The rocks and fossils both imply a marginal marine influence during sedimentation.

4.3 Paleopedology

The upper DPF displays paleosols that give clues to paleoenvironmental conditions during sedimentation (Retallack, 1994, 2001; Retallack et al., 1987; Schaetzl and Anderson, 2005). Carbonaceous rooted mudstone, reddish-brown lignitic peat deposits, tabular bright-banded coal seams, ironstone layers, bentonitic mudstone, siderite, and slickensides (Fig. 6.9) can all help when interpreting ancient soils.

Up to 14 coal seams have been identified from the upper BRG in southwestern Saskatchewan, each from 0.1–3.3 m thick (Frank, 2006). Such coal seams have been attributed to 4th or 5th order transgressive events in a low-lying coastal plain environment prone to marine incursions (Gilbert et al., 2019). Three ~1 m thick reddish-brown lignitic peat accumulations are easily recognized in the DPF at Woodpile Coulee. Peat results from decomposition of significant accumulations of organic matter in low-energy environments under permanently water-saturated

settings (Retallack, 2001). Carbonaceous mudstone with abundant root trace fossils, slickensides, seeds, leaves, amber and coalified branches implies limited transport of organic material.

Siderite-cemented root traces and extensive ironstone cementation have been associated with anoxic soils in tropical to sub-tropical environments with high water-tables (e.g., Bojanowski et al., 2016).

4.4 Biostratigraphy

More than 200 species of terrestrial palynomorphs were identified from samples collected from Woodpile Coulee (Table 6.1; Appendix G). Much of the sampled section was covered by prairie grasses and unable to be sampled. Covered portions spanned intervals from the upper part of the LP and FF, much of the OF, and some of the DPF. Inferences developed here are in large part based on the biostratigraphic framework provided by Braman and Koppelhus (2005) for the Dinosaur Provincial Park area of Alberta, northwest of Woodpile Coulee, and personal communications between Dennis Braman and the senior author.

The range of *Aquilapollenites rigidus* Tschudy and Leopold 1971 is restricted to the basal part of the FF in the Onefour area of southeastern Alberta. The upper limit of the range is at the base of the Taber Coal zone, which is absent in Saskatchewan. *Fibulapollis scabratus* is restricted to the FF and LPF. The species *Mancicorpus tripodiformis*, *Cranwellia rumseyensis*, *Dyadonapites reticulatus*, and *Translucentipollis plicatilis* all first appear in the uppermost two meters of the OF in the Dinosaur Provincial Park area to the northwest. The species *Senipites drumhellerensis*, *Orbiculapollis globosus*, *Gleicheniidites* sp., *Expressipollis* sp., and *Aquilapollenites leucocephalus* first appear in the uppermost DPF or lowest BF in the Dinosaur Park area.

Eberth and Hamblin (1993) compared the stratigraphic section in the Dinosaur Provincial Park area to that exposed to the southeast along the Milk River. They showed that the DPF thinned in that direction while the OF thickened. The palynomorph biostratigraphic markers do not necessarily trace the lithostratigraphic boundaries but do define nearly synchronous events (Braman pers comm., 2018). Eberth and Hamblin (1993) and Eberth (2005) have provided radiometric dates through the section exposed at Dinosaur Provincial Park and the Onefour area. Based on their data, they placed the Dinosaur Park-Bearpaw formational contact at approximately 75 Ma. This coincides with the contact at Woodpile Coulee based on palynological correlation using the first appearances of *Senipites drumhellerensis*, *Orbiculapollis globosus*, *Gleicheniidites* sp., *Expressipollis* sp., and *Aquilapollenites leucocephalus*. The OF-DPF contact occurs at 76.4 Ma and *Mancicorpus tripodiformis*, *Cranwellia rumseyensis*, *Dyadonapites reticulatus*, and *Translucentipollis plicatilis* first appear just below this contact. In the measured section these species first appear near the 175 m level. Eberth (2005) provided a date of 79.1 Ma for a horizon near the base of the Foremost Formation and Eberth and Deino (1992) assigned a date of 78.3 Ma to the FF-OF contact. The last common occurrence of *Aquilapollenites rigidus* occurs near the base of the Taber coal zone, which lies in the upper part of the FF in Alberta. The last appearance of this species at Woodpile Coulee is at 43.5 m in the measured section, giving this level an age of approximately 78.5 Ma.

The lower 71.5 m of the measured section at Woodpile Coulee has marine indicators present in the form of dinoflagellates. This is also typical for the FF below the Taber coal zone in the Onefour area (Braman, unpublished data). Dinoflagellates are present in the samples taken in the BF.

Pollen samples were not taken from the vertebrate microsite itself, but lithostratigraphic

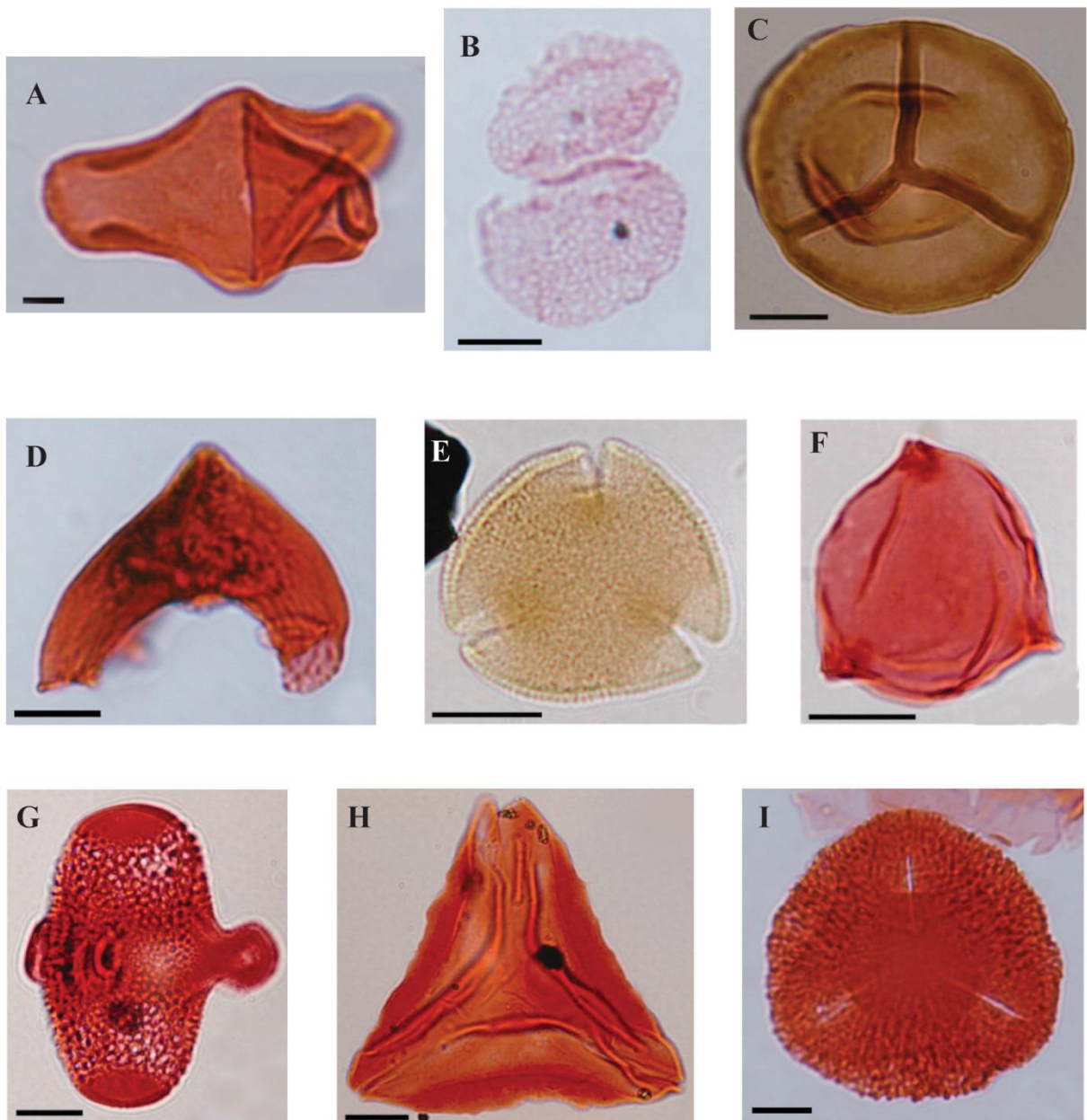


Figure 6.10: Biostratigraphically significant palynomorph species recovered from Woodpile coulee by Dennis Braman: A. *Translucentipollis plicatilis*; B. *Dyadonapites reticulatus*; C. *Cranwellia rumseyensis*; D. *Manicorpus tripodiformis*; E. *Senipites drumhellerensis*; F. *Orbiculapollis globosus*; G. *Aquilapollenites leucocephalus*; H. *Gleicheniidites* sp.; I. *Expressipollis* sp. Photographs by Dennis Braman.

correlation across the valley to the sample source was made. The samples contain biostratigraphically significant palynomorphs such as *Senipites drumhellerensis*, *Dyadonapites reticulatus*, and *Orbiculapollis globosus* (Fig. 6.9). They indicate an age of mid-DPF when compared with sampled intervals at Dinosaur Provincial Park in central Alberta (Braman and Koppelhus, 2005).

4.5 Paleontology

The Woodpile Coulee microsite preserves a small sample (n= 327) of diverse, broadly distributed taxa (Table 6.2). Reptiles (turtles, squamates, crocodiles, and Champsosaurs) account for the highest occurrences in the site, making up 26% of the total microvertebrate assemblage. They are followed by ray-finned fish (Actinopterygii: Osteichthyans), accounting for 22%. Amphibians, dinosaurs, chondrichthyes and mammals account for 17%, 16%, 14%, and 4% of the microvertebrate taxa at the site, respectively. An ammonite and fragments of dinosaur eggshell were also recovered.

Along with a diverse assemblage of microvertebrates, the site yielded many molluscs. Both bivalves and gastropods have been recovered from the microfossil layer and overlying beds. Molluscan faunas help when reconstructing paleoenvironments and identifying stratigraphic surfaces (Johnston and Hendry, 2005).

5. Discussion

5.1 Vertebrate paleontology

Cretorectolobus olsoni and the guitar fish *Myledaphus biparticus* were the only cartilaginous fish recovered from the Woodpile Coulee microsite. *Cretorectolobus olsoni* is characterized by its

small, piercing teeth, and is related to modern carpet- and nurse sharks that live in shallow to medium-depth tropical to temperate waters (Brinkman et al., 2005). *Myledaphus biparticus* is an extinct freshwater ray commonly associated with nonmarine deposits in the DPF (Beavan and Russell, 1999; Brinkman et al., 2005). Both species are common in the Lethbridge Coal Zone in Alberta (Brinkman et al., 2005).

A moderately diverse assemblage of bony fish, including *Lepisosteus* (garfish), amiids (bowfins), Acipenseriformes (sturgeons), Holostei, and teleosts were identified at the site (Table 6.2). All species are common throughout the DPF in Alberta, being recovered from both freshwater and marginal-marine environments. The garfish *Lepisosteus*, inexplicably absent at the Lake Diefenbaker microsite, was recovered in relatively high abundance from the WPC. The teleost *Paralbula*, commonly recovered from coastal settings in DPP (Brinkman et al., 2005) and the esocoid (Salmoniformes) *Diplomystus*, associated with freshwater fluvial assemblages, were both found at Woodpile Coulee.

A high abundance of lissamphibians is present at the Woodpile Coulee microsite, with frogs and several species of salamander identified, including *Scapherpeton*, *Opisthotriton*, and *Albanerpeton*. Lissamphibians decrease in abundance up-section at DPP, a trend that is believed to reflect an intolerance to increasing salinity induced by the encroaching Western Interior Seaway (Gardiner, 2005). The salamander *Opisthotriton kayi*, is the most abundant lissamphibian present at the site.

Four turtle families have been recovered from WPC, with the soft shelled trionychid turtles dominating. Trionychids are a freshwater carnivorous group that are still present today (Ernst et al., 1998). The trionychid *Aspideretoides splendidus* is a common component of coastal



Figure 6.11: Significant microvertebrate fossils recovered from the Woodpile Coulee site: A-D. *Nodosauridae* teeth; E. *Thescelosaurus* sp.; F. *Troodon* sp. Line = 5mm.

community assemblages collected from DPP. Chelydrids (snapping turtles) are widespread in the Cretaceous of western North America, and have been referenced as a common component of coastal assemblages in the Late Cretaceous (Brinkman, 2005). Baenids are an extinct group of primitive cryptodire found only in North America (Gaffney, 1972), and are commonly recovered from fluvial deposits in both the Hell Creek Formation of Montana and the Dinosaur Park Formation in Alberta (Hutchison, 1984; Brinkman, 2005). *Basilemys* is a large bodied turtle with robust limbs and short, stout digits, and has been suggested to be a tortoise-like terrestrial turtle (Brinkman, 2005).

Several semi-aquatic crocodile and crocodile-like taxa have been identified from the assemblage. Champsosaurs make up a small percentage of the material recovered from Woodpile Coulee. Champsosaurs are a common component of vertebrate microfossil assemblages in the DPF and have been recovered from both freshwater and coastal marine environments. These gavial-like piscivores are commonly associated with open-water depositional environments, such as freshwater channels and ponds. The alligatoroids *Leidyosuchus* and *Albertochampsia* account for a large percentage of non-dinosaurian archosaurs at WPC. In DPP, crocodiles occupy environments near coastlines (Brinkman et al., 2005).

Dinosaur taxa are represented by a number of groups, most of which are identified by teeth. At least nine dinosaur species are present at Woodpile Coulee. Of the ornithischians, nodosaurs are the most abundant, which is of particular interest (Fig. 6.11a-d). Nodosaurs are rare in the DPF and in Saskatchewan overall, but are commonly reported from nearshore terrestrial sediments throughout the Cretaceous (Arbour et al., 2016). Teeth attributed to pachycephalosaurids (Fig. 11e) and *Thescelosaurus* extend the paleogeographic range of both groups in the late Campanian of North America. According to samples collected from DPP,

pachycephalosaurids decrease in abundance up-section, and are interpreted as an inland taxa (Brinkman et al., 2005).

Three theropod taxa were identified on the basis of tooth morphology. Tyrannosauridae is the most abundant, which is consistent with patterns observed in microvertebrate sites in Alberta (Currie et al., 2008). Small theropods make up a smaller percentage of the assemblage, consisting of *Dromaeosaurus* and single example of *Troodon* (Fig. 6.11f).

Mammals are abundant, and are represented by multituberculates, marsupials, and possible placentals. The mammal family Didelphidae is present in the assemblage. These are speculated to be the ancestors of Cenozoic North American marsupials (Fox, 2005). The mammal distribution in DPP has been studied in detail by Sankey et al. (2005), who concluded that assemblages higher in sections tend to have higher abundance of marsupials and relatively fewer placental mammals).

5.2 Invertebrate paleontology

An extensive mollusk fauna is found in association with the vertebrate microfossil assemblage at WPC. The fauna is dominated by gastropods with subsidiary unionid bivalves. The gastropod assemblage is primarily made up of thousands of tiny ‘micromollusks’, only a few millimeters in length, which may be attributable to the hydrobiid and pluroceriid families. Fragmentary remains of a larger gastropod, approximately 60 mm in width were recovered from the site, but have yet to be identified. The mollusk genera identified from the microsite to date are known to occur in Dinosaur Provincial Park and are have been previously associated with crevasse splay deposits in the lower DPF (Johnston and Hendry, 2005). The genus *Anadara* was identified from the shell hash associated with the WPC microsite. This genus is a marine to marginal marine ark clam,

whose modern affiliates are known to frequent tidally influenced, brackish water environments (Broom, 1985). It implies a marine influence at the time of deposition, which is supported by the presence of marine sharks and ammonites within the assemblage.

Mudstone beds a few meters up section from the microvertebrate-bearing deposits contain the oyster *Crassostrea*. Specimens were found both disarticulated and articulated, suggesting little to no transport. Living *Crassostrea* species are restricted to coastal, marginal-marine environments with highly variable salinities and periodic subaerial exposure (Kirby, 2001). In Alberta, DPF assemblages containing brackish faunas are known to occur in the basal Lethbridge Coal Zone (Johnston and Hendry, 2005).

The presence of freshwater and marine to marginal-marine mollusks in the mid to upper DPF indicates an interplay between brackish-water and freshwater conditions within a short stratigraphic interval. The Woodpile Coulee microsite occurs near the transition from lower fluvio-estuarine influenced channels, to the upper mudstone and coal-dominated Saskatchewan expression of the Lethbridge Coal Zone. It is well established in both Alberta and Saskatchewan, that deposition of the Lethbridge Coal Zone was highly influenced by the effects of sea level rise. This indicates similarities in depositional environments in southwestern Saskatchewan and central Alberta, even though the sites are hundreds of kilometers apart, and the influence of sea level rise occurred earlier in Saskatchewan.

5.3 Palynological reconstruction

Cretaceous climates were considerably warmer than those in southwestern Saskatchewan today, being that of a temperate climate (Braman and Koppelhus, 2005). The landscape consisted of a low relief coastline cut by broad incised channels during the transition from the OF to the DPF,

with paleochannel flow towards the east and southeast (Eberth and Hamblin, 1993; Hamblin, 1997; Gilbert et al., 2019). Oxygen isotope analysis of fossil shells from the BF of Saskatchewan indicates that water temperatures were between 15° and 27° Celsius (Caldwell et al., 1983).

Palynomorphs show that gymnosperms were the dominant canopy-forming trees in the Woodpile Coulee region during deposition of the DPF (Table 6.1). The understory layer consisted of a wide variety of ferns and flowering shrubs, lichens, lycopods, and angiosperms. This is characteristic of the ‘*Aquilapollenites* Floral Province’, which is identified by the presence of angiosperm pollen of the Triprojectates, a taxonomic group of unknown modern affinity (Braman and Koppelus, 2005). Examples characteristic of this assemblage include *Aquilapollenites*, *Manicorpus*, and *Translucentipollis*, all of which are found at Woodpile Coulee. Other characteristic flora includes *Expressipollis*, an angiosperm whose modern relatives include parasitic trees such as mistletoe, and *Siberiapollis*, an angiosperm whose modern counterparts are commonly referred to as sugarbushes. Dinoflagellates have been recovered from the uppermost mudstone and lignite beds of the DPF in WPC, confirming the onset of marine incursion before total inundation of the WIS across Saskatchewan and Alberta.

5.4 Vertebrate Alpha Diversity of the Woodpile Coulee Microsite

A summary of statistics used to calculate species estimates for Woodpile Coulee and Lake Diefenbaker (see Chapter 5) is provided in Table 6.3. Species estimators predict that, given a complete sample of the Woodpile Coulee assemblage, between 4 and 15 more species would have been be present. The same estimators suggest that the Lake Diefenbaker microsite represents a more complete sample of the entire assemblage, suggesting that only 3 and 10 species could be recovered. In spite of estimators indicating that the WPC is less complete than

the Lake Diefenbaker site, it is representative of a higher diversity. In both samples, the aerial coverage estimator (ACE) returned the most conservative estimate, while the second-order Jackknife estimates (which are less biased by small sample sizes) were the most liberal. The species estimators suggest that the WPC assemblage is legitimately more diverse, despite the collection being a smaller, less complete sampling than the assemblage at Lake Diefenbaker. The second-order Jackknife has been suggested to perform best for paleontological collections with low sample sizes (Hortal et al., 2006).

While beta diversity between these localities and coeval sites in Alberta is the subject of another ongoing study, it is worth noting that the observed number of paleotaxa at both the Woodpile Coulee and Lake Diefenbaker sites is generally higher than at other microvertebrate sites of comparable age in Alberta reported by Brinkman et al. (2004). Increased biodiversity at Lake Diefenbaker can be attributed to the presence of several marine taxa, which are generally rare in terrestrial microsites recovered from the DPF in Alberta. The Lake Diefenbaker site was situated close to the paleocoastline of the WIS, at the DPF– BF transition, resulting in diversity being more heavily influenced by the presence of both terrestrial and marine taxa. A significant marine signature is not obviously present based on taxa present at Woodpile Coulee, suggesting that the high diversity at this site may be attributable to another factor.

5.5 Paleoecological Implications

During the Late Cretaceous, the WIS stretched from the Gulf of Mexico to the Arctic, effectively bisecting North America into distinct eastern and western regions (Caldwell, 1975). The transgressive and regressive cycles of this seaway were controlled by tectonics in the Canadian Cordillera, which played a fundamental role in shaping paleogeography, paleoenvironment, and paleoecology. Tectonics in the cordillera are believed to have tilted the basin between deposition

of the OF and overlying DPF. This tilting resulted in reorientation of paleochannel drainage and changes to climate patterns. A steeper paleoslope coupled with regression of the WIS resulted in the formation of incised valleys along the Saskatchewan extent of the paleocoastline (Gilbert et al., 2019). This signaled a shift in depositional environments across the OF-DPF contact, abruptly transitioning from braided alluvial channels and their associated floodplains in a semi-arid climate, to meandering channels and associated swamps and floodplains in an environment similar to the modern Florida Everglades.

Initial deposition of the DPF is represented by fluvial deposits within incised valleys cut and filled during a lowstand systems tract. The upper mudstone and coal dominated deposits of the DPF mark onset of the last major transgression of the WIS across the coastal and alluvial plains of western North America. The Woodpile Coulee site lies at the interchange between lowstand fluvial deposits of the lower DPF and transgressive mudstones and coals of the upper DPF. This interpretation is supported by palynomorphs recovered from the region, which would place the site stratigraphically in the mid-DPF.

The presence and abundance of nodosaurs recovered from the Woodpile Coulee microsite are of particular interest. Ankylosaurine dinosaurs are divided into two families, both of which were present in the Campanian of North America: Ankylosauridae and Nodosauridae. Nodosaurids are extremely rare in Saskatchewan, and yet they occur with high abundance at WPC, with members of the family Ankylosauridae entirely missing from the assemblage. Previous studies suggest that ankylosaurs had a preference for inland environments, with nodosaurs favoring marginal marine and fluvial settings (Brinkman et al., 1990; Butler and Barrett, 2008). Arbour et al. (2016) tested this hypothesis and found it to be statistically possible in North America, but not well supported based on the known occurrences of both groups. By subdividing transgressive-regressive cycles

into distinctive time bins, Arbour et al. (2016) found that this ‘positive’ association in North America was less certain when factoring in ankylosaurid extirpation. It is believed that North American ankylosaurids became extirpated during the Cenomanian, possibly due to loss of habitat at onset of a large transgression of the WIS. Following the Cenomanian extirpation, an Asian lineage of Ankylosauridae had immigrated into North America by the Campanian (Thompson et al., 2012; Arbour and Currie, 2016).

The presence and high abundance of nodosaurids at WPC is interpreted as reflecting true nodosaur affinity for coastal environments. The WPC microsite was deposited when the sequence stratigraphic cycle was switching from a lowstand to transgressive systems tract. Appearance of brackish and saltwater tolerant invertebrates, coupled with increased coal seam and mudstone deposits, provides evidence of this transition. This would have effectively transferred a relatively proximal coastal system to one more regularly affected by the incursion of the WIS.

Overall, the site contains an abundance of freshwater species and minor marine to marginal-marine taxa. The recovery of *Cretorectolobus olsoni*, a single ammonite, and *Anadara* bivalves, combined with tidal indicators in the sediments, is compelling evidence that the site was undergoing marine influence. It is possible that the onset of transgression, combined with seasonal storm events would drive marine taxa further upland into coastal plain fluvio-estuarine systems. The site is deposited at the shift from dominantly fluvial-estuarine channels, to marine influenced transgressive floodplains. It is reasonable to interpret this assemblage as a reflection of the shift in subsidence patterns at the time of deposition.

During the Campanian, Saskatchewan was situated at a slightly higher latitude than today (Caldwell, 1968), near the paleocoastline of the Western Interior Seaway. Oxygen isotope

analyses of fossil shells implies that water temperatures were between 15° and 27° C in the adjacent WIS (Caldwell et al., 1983). During the early stages of DPF deposition in southwestern Saskatchewan, basin tilting led to erosional downcutting, resulting in incised fluvio-estuarine valleys along a wave-dominated, tidally influenced, river-affected coastline (see Chapter 4). In modern environments, salinity, climate, and geographic barriers are primary controls of the distribution and abundance of organisms (Remane and Schlieper, 1972; Basan and Frey, 1977; Dunson and Mazzotti, 1989; Dunson and Travis, 1991; MacEachern and Gingras, 2007; Buatois and Mángano, 2011; Torres-Dowdall et al., 2013). Globally, temperature and precipitation have been considered secondary factors in controlling species distribution during the Cretaceous, because of low latitudinal climate gradients (Huber et al., 1995). Therefore, the easternmost DPF deposits of Saskatchewan provide an opportunity to examine hypotheses concerning terrestrial faunal turnover across a coastal and alluvial plain in a regional context, and the role that salinity, paleogeographic barriers, and potentially climate might have played in regional faunal diversity in the Campanian.

It has been suggested that uplift in the Cordillera rerouted fluvial drainage in the Western Interior Sedimentary Basin between deposition of the Oldman/McClelland and Dinosaur Park/Coal Ridge (Eberth and Hamblin, 1993; Gilbert et al., 2019). In southwestern Saskatchewan, the DPF experienced substantial tilting to the southeast, creating a fluvial drainage gradient sufficient to induce incision in southwestern Saskatchewan (see Chapter 4). It is reasonable to suggest that biological assemblages would vary across the alluvial and coastal plains in response to changing environmental gradients created by lowstand incision and subsequent transgressive infilling of fluvio-estuarine valleys. When compared with Alberta, ecosystems in Saskatchewan were nearer the eastern paleoshoreline of the WIS and experienced

greater marine influence for a longer time (e.g., Gilbert et al., 2018). Herein, we discuss the sedimentology and structural geology of the exposed section of the BRG, the biostratigraphically significant palynomorphs, the paleoenvironments of the DPF, and describe a new vertebrate microfossil locality from Woodpile Coulee in extreme southwestern Saskatchewan.

6. Conclusions

- 1) Sedimentology and biostratigraphy reveal that stratigraphic surfaces of the Belly River Group in Woodpile Coulee are diachronous, and generally younger than contemporaneous deposits in the Red Deer River Valley of Alberta.
- 2) Transition from lowstand fluvio-estuarine deposits of the lower Dinosaur Park Formation, to upper lignitic and mudstone deposits of the upper Dinosaur Park Formation are preserved at Woodpile Coulee. The increasing presence of Brackish and marine invertebrate and vertebrate fossils corroborate this interpretation.
- 3) Biostratigraphically significant palynomorphs are reported on for the entire section at Woodpile Coulee for the first time in the scientific literature, and place WPC within the *Aquilapollenites* Floral Province.
- 4) Alpha diversity analysis of the WPC vertebrate material implies the Woodpile Coulee microsite is less complete than the previously published Lake Diefenbaker site, but is more taxonomically diverse.
- 5) Nodosaurids recovered from the site are interpreted as reflecting a preference for fluvial and coastal plain environments.
- 6) Three field localities are now recognized as containing vertebrate microfossil assemblages in Saskatchewan, together representing the easternmost extension of the

BRG in Canada. Each of these three locations is found at a different stratigraphic horizon within the DPF: 1) Muddy Lake correlates to the lowermost DPF; 2) Lake Diefenbaker correlates to the upper to uppermost DPF; and 3) Woodpile Coulee correlates to the mid DPF. This provides possibility to study more complex biodiversity trends in the DPF of Saskatchewan.

Acknowledgements

The author wishes to thank Emily Bamforth significant collaboration on this project, including help with identification, sorting, and cataloguing many of the fossils recovered post 1989.

Special thanks to Terra Lekach for her assistance picking, sorting, and identifying much of the microvertebrate material collected from 2014-2015.

Palynomorphs recovered from Woodpile Coulee

Accuratipollis lactifluminis	Equisetosporites amabilis	Reticulosporis reticulatus
Accuratipollis macrosolenoides	Equisetosporites hughesii	Retitriteles austroclavatidites
Aequitriradites spinulosus	Equisetosporites mollis	Retitriteles mediocris
Alisporites bilateralis	Equisetosporites multicostatus	Retitriteles spp.
Alutisporites sp.	Equisetosporites multistriatus	Rogalskaisporites cicatricosus
Annulispora salsa	Equisetosporites spp.	Scabrastephanocolpites albertensis
Appendicisporites undosus	Erdtmanipollis procumbentiformis	Scabrastephanocolpites lepidus
Aquilapollenites amicus	Eucommiidites minor	Scabrastephanocolpites pentaaperturites
Aquilapollenites attenuatus	Eucommiidites troedssonii	Schizosporis parvus
Aquilapollenites augustus	Expressipollis sp.	Senipites drumhellerensis
Aquilapollenites bellus	Fibulapollis scabratus	Sequoiapollenites paleocenicus
Aquilapollenites clarireticulatus	Foraminisporis asymmetricus	Sequoiapollenites sp.
Aquilapollenites drumhellerensis	Foraminisporis undulatus	Sestrosporites pseudoalveolatus
Aquilapollenites funkhouseri	Foraminisporis sp.	Siberiapollis montanensis
Aquilapollenites leucocephalus	Foveosporites subtriangularis	Siberiapollis spp.
Aquilapollenites cf. leucocephalus	Foveosporites sp.	Sigmopollis carbonis
Aquilapollenites mtchedlishvili	Gabonisoris labyrinthus	Sigmopollis hispidus
Aquilapollenites notabile	Gleicheniidites delicatus	Stereigranisoris regius
Aquilapollenites quadrilobus	Gleicheniidites senonicus	Stereisporites ancoris
Aquilapollenites quadrilobus	Gleicheniidites stellatus	Stereisporites antiquasporites
Aquilapollenites rectus	Gleicheniidites sp.	Stereisporites antiquus
Aquilapollenites rigidus	Grewipollenites canadensis	Stereisporites cingulatus
Aquilapollenites senonicus	Grewipollenites radiatus	Stereisporites rodaensis
Aquilapollenites stelckii	Gunnaripollis suberbus	Stereisporites triangulopunctatus
Aquilapollenites trialatus	Hazaria sheoparii	Stoverisporites lunaris
Aquilapollenites turbidus	Heliosporites kemensis	Subtriporopollenites alpinus
Aquilapollenites spp.	Inaperturotetradites scabratus	Syncolpites sp.
Arecipites barakati	Interulobites sp.	Taxodiaceapollenites hiatus
Arecipites sp.	Klukisporites sp.	Taxodiaceapollenites vacuipites
Asterisporites chlonovae	Kurtzipites sp.	Tetranguladinium cruciformis
Azonia calvata	Kuylisporites scutatus	Tetranguladinium sp.
Azonia cribrata	Laevigatosporites haardtii	Tetraporina quadrata
Azonia jacutense	Laevigatosporites nitidulus	Tetraporina sp.
Azonia pulchella	Laevigatosporites nitidus	Todisporites minor
Azonia recta	Laevigatosporites undulatififormis	Translucentipollis plicatilis
Baculatisporites comaumensis	Liburnisporis adnacus	Tricolpites parvus
Baculatisporites papillosus	Liliacidites mirus	Tricolpites reticulatus
Baculatisporites spp.	Liliacidites variegatus	Tricolpites ringens
Biretisporites psilatus	Liliacidites spp.	Tricolpites spp.
Biretisporites sp.	Lusatisporis dettmannae	Tricolpopollenites elongatus
Camarozonosporites ambigens	Mancicorpus anchoriforme	Tricolpopollenites levitas
Camarozonosporites amplus	Mancicorpus glaber	Tricolpopollenites spp.
Camarozonosporites similis	Mancicorpus trapeziforme	Tricolporites spp.
Camarozonosporites spp.	Mancicorpus tripodiformis	Trifossapollenites ellipticus
Cibotiumspora clavatus	Mancicorpus sp.	Trilites bettianus
Cibotiumspora juncta	Marcellopites tolmanensis	Trilites sp.
Cicatricosisporites spp.	Mica hoodoensis	Trilobapollis laudabilis
Cingulatisporites dakotaensis	Monosulcites riparius	Triporoletes involucreatus
Circulina parva	Monosulcites sp.	Triporopollenites triplicatus
Circumflexipollis tilioides	Orbiculapollis globosus	Triporopollenites spp.
Cirratriradites luminosus	Ornamentifera baculata	Triquitrites absurdus
Classopollis classoides	Ovoidites ligneolus	Trochicola scollardiana

Conbaculatisporites sp.	Palaeoisoetes subengelmanni	Trudopollis meekeri
Concavisporites sp.	Pediastrum boryanum	Trudopollis sp.
Cranwellia rumseyensis	Penetetrapites inconspicuus	Tschudypollis retusus
cf. Cranwellia sp.	Pilosisorites sp.	Tschudypollis thalmanii
Crassipollis sp.	Pityosporites constrictus	Umbosporites callosus
Cyathidites australis rimalis	Pleurospermaepollenites sp.	Varirugosisporites tolmanensis
Cyathidites minor	Podocarpidites biformis	Verrucatotrilites sp.
Cycadopites fragilis	Podocarpidites spp.	Verrutricolpites sp.
Cycadopites spp.	Polycingulatisporites reduncus	Virgo amiantopollis
Deltoidospora diaphana	Polycingulatisporites sp.	Vitreisorites pallidus
Distaltriangulisorites costatus	Polyporina cribraria	Wulongospora sp.
Distaltriangulisorites mutabilis	Pristinupollenites microsaccus	Zlivisporis blanensis
Dyadonapites reticulatus	Pristinupollenites sp.	Zlivisporis cenomanianus
Echinatisporis solaris	Pulcheripollenites krempii	Zlivisporis novomexicanum
Echinatisporis spp.	Quadripollis krempii	Zlivisporis spp.
Enzonasporites bojatus	Reticuloidosporites pseudomurii	Dinoflagellates

Table 6.1: Comprehensive list of palynomorphs recovered from the Woodpile Coulee locality. For a complete list of stratigraphic intervals, see Appendix VII.

	Lake Diefenbaker	Woodpile Coulee
Taxa		
Chondrichthyes		
<i>Meristodonoides montanensis</i>	10	0
<i>Archaeolamna kopingensis</i>	33	0
<i>Carcharias steineri</i>	87	0
<i>Cretorectolobus olsoni</i>	1	10
<i>Eucrossorinus microcuspidatus</i>	1	0
<i>Squalicorax</i> sp.	1	0
<i>Myledaphus</i> sp.	262	28
Actinopterygii		
<i>Belonostomus longirostris</i>	2	0
<i>Acipenser</i> sp.	17	1
<i>Enchodus</i> sp.	1	0
<i>Amia</i> sp.	30	7
<i>Lepisosteus</i> sp.	0	27
Holostean A	0	14
Holostean B	0	4
cf. <i>Paratarpon</i> sp.	3	0
cf. <i>Paralbula</i> sp.	2	3
cf. <i>Ostariostoma</i> sp.	1	0
cf. Escoid sp. indet.	1	3
<i>Horseshoeichthys</i> sp.	3	0
<i>Diplomystus</i> sp.	3	2
cf. <i>Cretophareodus</i> sp.	3	0
Hiodontidae sp. indet.	4	0
Teleost centra various	11	26
Amphibia		
Caudata		
<i>Scapherpeton tectum</i>	34	13
<i>Opisthotriton kayi</i>	17	23
<i>Albanerpeton</i> sp.	6	1
<i>Lisserpeton bairdi</i>	4	0
Anura		
gen. sp. Indet.	1	7
Reptilia		
Testudines		
Adocidae	1	0

Basilemys	0	1
Trionychidae	10	8
Baenidae	2	2
Chelydridae	2	2
Chelonia sp. indet	21	4
Squamata		
<i>Palaeosaniwa</i> sp.	2	2
Crocodylidae		
<i>Leidyosuchus</i> sp.	32	38
<i>Brachychampsia</i> sp.	0	4
Choristodera		
Champsosaurus sp.	358	20
Sauropterygia		
Polycotylidae	5	0
Elasmosauridae	1	0
Archosauria		
Ankylosauridae	2	0
Nodosauridae	0	15
Ceratopsidae	41	5
Stegoceras	0	3
Hadrosauridae	15	16
Hypsolophodontidae	1	0
Thescelosauridae	0	1
Tyrannosauridae	28	9
Dromaeosauridae sp.	2	4
Troodon sp.	1	2
Ornithomimidae	0	0
Aves		
Baptornis sp.	4	0
Hesperornithoform sp. indet.	1	0
Mammalia		
Multituberculata	2	3
Marsupicarnivora	0	3
<i>Alphadon</i> sp.	0	2
Mammalia	0	2

Table 6.2: Microvertebrate taxa recovered from Lake Diefenbaker and Woodpile Coulee.

	Observed	Chao-1 Estimate	Jackknife-2 Estimate	ACE Estimate
Woodpile Coulee	46	54.0 ± 4.0	60.9 ± 5.7	50.2 ± 4.9
Saskatchewan Landing	37	42.3 ± 3.4	46.9 ± 4.3	39.5 ± 3.7

Errors are +/- 2 SD.

Table 6.3: Estimated Alpha diversity comparing Woodpile Coulee and Lake Diefenbaker based on microvertebrate taxa. The estimated number of total species was calculated using three different non-parametric species estimators: Chao-1, Jackknife-2, and Abundance-based Coverage Estimator.

References

- Arbour, V. M., & Currie, P. J. (2016). Systematics, phylogeny and palaeobiogeography of the ankylosaurid dinosaurs. *Journal of Systematic Palaeontology*, 14(5), 385-444.
- Arbour, V. M., Zanno, L. E., & Gates, T. (2016). Ankylosaurian dinosaur palaeoenvironmental associations were influenced by extirpation, sea-level fluctuation, and geodispersal. *Palaeogeography, Palaeoclimatology, Palaeoecology*, 449, 289-299.
- Basan, P., Frey, R., Crimes, T. P., & Harper, J. C. (1977). Actual-palaeontology and neoichnology of salt marshes near Sapelo Island, Georgia. *Geological Journal*, Special Issue, (9), 41-70.
- Bojanowski, M. J., Jaroszewicz, E., Košir, A., Łoziński, M., Marynowski, L., Wysocka, A., & Derkowski, A. (2016). Root-related rhodochrosite and concretionary siderite formation in oxygen-deficient conditions induced by a ground-water table rise. *Sedimentology*, 63(3), 523-551.
- Braman, D., & Koppelhus, E. B. (2005) Campanian Palynomorphs in *Dinosaur Provincial Park: A spectacular ancient ecosystem revealed*, Indiana University Press, Bloomington, Indiana, 54-82.
- Broom, M. J. (Ed.). (1985). *The biology and culture of marine bivalve molluscs of the genus Anadara* (Vol. 12). WorldFish.
- Buatois, L. A., & Mángano, M. G. (2011). *Ichnology: Organism-substrate interactions in space and time*. Cambridge University Press.
- Carpenter, K. (1982). Baby dinosaurs from the Late Cretaceous Lance and Hell Creek formations and a description of new species of theropod. *Contributions to geology*, 20(2), 123-134.
- Carpenter, K. (1999). *Eggs, nests, and baby dinosaurs: a look at dinosaur reproduction*. Indiana University Press.
- Cobban, W. A., Walaszczyk, I., Obradovich, J. D., & McKinney, K. C. (2006). A USGS Zonal Table for the Upper Cretaceous Middle Cenomanian--Maastrichtian of the Western Interior of the United States Based on Ammonites, Inoceramids, and Radiometric Ages. U.S. Geological Survey, Open-File Report 2006-1250, 46 p.
- Dodson, P. (1971). Sedimentology and taphonomy of the Oldman Formation (Campanian), Dinosaur Provincial Park, Alberta (Canada). *Palaeogeography, Palaeoclimatology, Palaeoecology*, 10(1), 21-74.
- Dodson, P. (1973). The significance of small bones in paleoecological interpretation. *Contributions to Geology*, 12(1), 15-19.

Beavan, Neil R., & Russell, Anthony P. (1999). An elasmobranch assemblage from the terrestrial-marine transitional lethbridge coal zone (Dinosaur Park Formation: Upper Cambrian), Alberta, Canada. *Journal of Paleontology*, 73(3), 494-503.

Brinkman, D. (1990). Paleooecology of the Judith River Formation (Campanian) of Dinosaur Provincial Park, Alberta, Canada: Evidence from vertebrate microfossil localities. *Palaeogeography, Palaeoclimatology, Palaeoecology*, 78(1), 37-54.

Brinkman, D. B. (2005). Turtles: Diversity, Paleoecology, and Distribution, in *Dinosaur Provincial Park: A spectacular ancient ecosystem revealed*, Indiana University Press, Bloomington, Indiana, 54-82.

Brinkman, D. B., Ryan, M. J., & Eberth, D. A. (1998). The paleogeographic and stratigraphic distribution of ceratopsids (Ornithischia) in the upper Judith River Group of western Canada. *Palaaios*, 13(2), 160-169.

Brinkman D. B., Russell A., Eberth, D. A. & Peng, J. H. (2004). Vertebrate palaeocommunities of the lower Judith River Group (Campanian) of southeastern Alberta, Canada, as interpreted from vertebrate microfossil assemblages. *Palaeogeography, Palaeoclimatology, Palaeoecology*, 213(3), 295-313.

Brinkman, D.B., Braman, D., Neuman, A., Ralrick, P., & Sato, T. (2005a) 5. A vertebrate assemblage from the marine shales of the Lethbridge Coal Zone, in *Dinosaur Provincial Park: A spectacular ancient ecosystem revealed*, Indiana University Press, Bloomington, Indiana, 88-98.

Brinkman, D. B., Russell, A. P., Peng, J. H., Currie, P. J., & Koppelhus, E. B. (2005b). 26. Vertebrate microfossil sites and their contribution to studies of paleoecology, in *Dinosaur Provincial Park: A spectacular ancient ecosystem revealed*, Indiana University Press, Bloomington, Indiana, 54-82.

Brinkman, Russell, Eberth, & Peng. (2004). Vertebrate palaeocommunities of the lower Judith River Group (Campanian) of southeastern Alberta, Canada, as interpreted from vertebrate microfossil assemblages. *Palaeogeography, Palaeoclimatology, Palaeoecology*, 213(3), 295-313.

Brown, C. M., Evans, D. C., Campione, N. E., O'Brien, L. J., & Eberth, D. A. (2013). Evidence for taphonomic size bias in the Dinosaur Park Formation (Campanian, Alberta), a model Mesozoic terrestrial alluvial-paralic system. *Palaeogeography, Palaeoclimatology, Palaeoecology*, 372, 108-122.

Butler, R. J., & Barrett, P. M. (2008). Palaeoenvironmental controls on the distribution of Cretaceous herbivorous dinosaurs. *Naturwissenschaften*, 95(11), 1027-1032.

- Caldwell, W. G. E. (1968). The late Cretaceous Bearpaw formation in the south Saskatchewan River valley Saskatchewan Research Council, Geology Division, 8, 86.
- Caldwell, W. G. (1975) *The Cretaceous system in the western interior of North America*, Waterloo, Ontario, Geological Association of Canada.
- Cant, D. J., & Stockmal, G. S. (1989). The Alberta foreland basin: relationship between stratigraphy and Cordilleran terrane-accretion events. *Canadian Journal of Earth Sciences*, 26(10), 1964-1975.
- Catuneanu, Sweet, & Miall. (2000). Reciprocal stratigraphy of the Campanian–Paleocene Western Interior of North America. *Sedimentary Geology*, 134(3), 235-255.
- Chao, A. (1984). Nonparametric Estimation of the Number of Classes in a Population. *Scandinavian Journal of Statistics*, 11(4), 265-270.
- Chao, A., & Lee, S. (1992). Estimating the Number of Classes via Sample Coverage. *Journal of the American Statistical Association*, 87(417), 210-217.
- Chao, A., & Yang, M. C. (1993). Stopping rules and estimation for recapture debugging with unequal failure rates. *Biometrika*, 80(1), 193-201.
- Colwell, R., & Coddington, J. (1994). Estimating terrestrial biodiversity through extrapolation *Philosophical Transactions of The Royal Society Of London Series B-Biologic*, 345(1311), 101-118.
- Cullen, T., Fanti, F., Capobianco, C., Ryan, M., & Evans, D. (2016). A vertebrate microsite from a marine-terrestrial transition in the Foremost Formation (Campanian) of Alberta, Canada, and the use of faunal assemblage data as a paleoenvironmental indicator. *Palaeogeography, Palaeoclimatology, Palaeoecology*, 444, 101-114.
- Dawson, F., Evans, C., Marsh, R., & Richardson, R. (1994). Uppermost Cretaceous and Tertiary strata of the Western Canada Sedimentary Basin, *Geological Atlas of the Western Canada Sedimentary Basin*, Alberta Research Council, Calgary, Alberta, 13-25.
- Dunson, W., Mazzotti, F., & Dunson, W.A. (1989). Salinity as a limiting factor in the distribution of reptiles in Florida Bay: A theory for the estuarine origin of marine snakes and turtles. *Bulletin of Marine Science*, 44(1), 229-244.
- Dunson, W., & Travis, J. (1991). The Role of Abiotic Factors in Community Organization. *The American Naturalist*, 138(5), 1067-1091.
- Eberth, D. A. (2005). The geology, in *Dinosaur Provincial Park: A spectacular ancient ecosystem revealed*, Indiana University Press, Bloomington, Indiana, 54-82.

- Eberth, D. (2015). Origins of dinosaur bonebeds in the Cretaceous of Alberta, Canada. *Canadian Journal of Earth Sciences*, 52(8), 655-681.
- Eberth, D. A., & Deino, A. L. (1992). A geochronology of the non-marine Judith River Formation of southern Alberta. In *SEPM Theme Meeting, Mesozoic of the Western Interior* (pp. 24-25).
- Eberth, D. A., & Hamblin, A. P. (1993). Tectonic, stratigraphic, and sedimentologic significance of a regional discontinuity in the upper Judith River Group (Belly River wedge) of southern Alberta, Saskatchewan, and northern Montana. *Canadian Journal of Earth Sciences*, 30(1), 174-200.
- Eberth, D. A., Braman, D. R., & Tokaryk, T. T. (1990). Stratigraphy, sedimentology and vertebrate paleontology of the Judith River Formation (Campanian) near Muddy Lake, west-central Saskatchewan. *Bulletin of Canadian Petroleum Geology*, 38(4), 387-406.
- Embry, A. (1990). *A tectonic origin for third order depositional sequences in extensional basins - Implications for basin modeling*. Quantitative dynamic stratigraphy: Prentice Hall, New Jersey, 491-501.
- Estes, R., and Berberian, P. (1970). Paleocology of a Late Cretaceous vertebrate community from Montana. Museum of Comparative Zoology, Breviora.
- Fox, R. C. (2005). Late Cretaceous Mammals, in *Dinosaur Provincial Park: A spectacular ancient ecosystem revealed*, Indiana University Press, Bloomington, Indiana, 54-82.
- Frank, M. (2006). Coal distribution in the upper cretaceous (Campanian) Belly River group of southwest Saskatchewan (*Open file report (Saskatchewan Geological Survey)*; 2005-33). Regina]: Saskatchewan Geological Survey.
- Gaffney, E. S., Parsons, T. S., & Williams, E. E. (1972). An illustrated glossary of turtle skull nomenclature. *American Museum novitates*; no. 2486.
- Gardner, J. D. (2005). Lissamphibians, in *Dinosaur Provincial Park: A spectacular ancient ecosystem revealed*, Indiana University Press, Bloomington, Indiana, 54-82.
- Gilbert, M. M., Bamforth, E. L., Buatois, L. A., & Renaut, R. W. (2018). Paleocology and sedimentology of a vertebrate microfossil assemblage from the easternmost Dinosaur Park Formation (Late Cretaceous, Upper Campanian,) Saskatchewan, Canada: Reconstructing diversity in a coastal ecosystem. *Palaeogeography, Palaeoclimatology, Palaeoecology*, 495, 227-244.
- Gilbert, M. M., Buatois, L. A., & Renaut, R. W. (2019). Ichnology and Depositional Environments of the Upper Cretaceous Dinosaur Park – Bearpaw Formation transition in the Cypress Hills region of Southwestern Saskatchewan, Canada. *Cretaceous Research* DOI 10.1016/j.cretres.2018.12.017

Gilbert, M. M., Buatois, L. A., & Renaut, R. W. (Submitted). Sequence Stratigraphy and Depositional Environments of the Belly River Group (Campanian) in southwestern Saskatchewan, Canada: Incised and Unincised Fluvial Systems along an Epicontinental Seaway. *Bulletin of Canadian Petroleum Geology*.

Gotelli, N. J., & Colwell, R. K. (2001). Quantifying biodiversity: procedures and pitfalls in the measurement and comparison of species richness. *Ecology letters*, 4(4), 379-391.

Hamblin, A. P. (1997). Regional distribution and dispersal of the Dinosaur Park Formation, Belly River Group, surface and subsurface of southern Alberta. *Bulletin of Canadian Petroleum Geology*, 45(3), 377-399.

Hortal, J., Borges, P. A., & Gaspar, C. (2006). Evaluating the performance of species richness estimators: sensitivity to sample grain size. *Journal of Animal Ecology*, 75(1), 274-287.

Huber, B. T., Hodell, D. A., & Hamilton, C. P. (1995). Middle–Late Cretaceous climate of the southern high latitudes: stable isotopic evidence for minimal equator-to-pole thermal gradients. *Geological Society of America Bulletin*, 107(10), 1164-1191.

Hutchison, J. H., & Archibald, J. D. (1986). Diversity of turtles across the Cretaceous/Tertiary boundary in northeastern Montana. *Palaeogeography, Palaeoclimatology, Palaeoecology*, 55(1), 1-22.

Johnston, P. A. & Hendry, A. J. W. (2005). Paleocology of Mollusks from the Belly River Group, in *Dinosaur Provincial Park: A spectacular ancient ecosystem revealed*, Indiana University Press, Bloomington, Indiana, 54-82.

Kauffman, E., & Caldwell, W. (1993). The Western Interior Basin in space and time. *Special Paper - Geological Association of Canada*, 39, 1-30.

Leckie, D. A., & Smith, D. G. (1992). Regional setting, evolution, and depositional cycles of the Western Canada Foreland Basin. *American Association of Petroleum Geologists*, 16(5), 9-46

Maceachern, J. A., & Gingras, M. K. (2007). Recognition of brackish-water trace-fossil suites in the cretaceous western interior Seaway of Alberta, Canada. *SEPM Special Publications*, 88, 149-19.

McLean, J. (1971). *Stratigraphy of the Upper Cretaceous Judith River Formation in the Canadian Great Plains*. Report/Saskatchewan Research Council, Geology Division, No. 11.

Oksanen, J. (2010). Cluster analysis: tutorial with R. *University of Oulu, Oulu*.

- Remane A. & Schlieper, C. (1972). Biology of Brackish Water. *Quarterly Review of Biology*, 47(4), 467.
- Retallack, G. J. (1988). Field recognition of paleosols. *Geological Society of America Special Paper*, 216, 1-20.
- Retallack, G. J. (2008). *Soils of the past: an introduction to paleopedology*. John Wiley & Sons.
- Rogers, R. R. (1998). Sequence analysis of the Upper Cretaceous Two Medicine and Judith River formations, Montana; nonmarine response to the Claggett and Bearpaw marine cycles. *Journal of Sedimentary Research*, 68(4), 615-631.
- Rogers, R. R., & Brady, M. E. (2010). Origins of microfossil bonebeds: insights from the Upper Cretaceous Judith River Formation of north-central Montana. *Paleobiology*, 36(1), 80-112.
- Rogers, R. R., & Kidwell, S. M. (2007). A conceptual framework for the genesis and analysis of vertebrate skeletal concentrations in *Bonebeds: genesis, analysis, and paleobiological significance*, 1-63.
- Rogers, R. R., Kidwell, S. M., Deino, A. L., Mitchell, J. P., Nelson, K., & Thole, J. T. (2016). Age, correlation, and lithostratigraphic revision of the Upper Cretaceous (Campanian) Judith River Formation in its type area (north-central Montana), with a comparison of low-and high-accommodation alluvial records. *The Journal of Geology*, 124(1), 99-135.
- Sankey, J. T., Brinkman, D. B., Guenther, M., & Currie, P. J. (2002). Small theropod and bird teeth from the late Cretaceous (late Campanian) Judith River Group, Alberta. *Journal of Paleontology*, 76(4), 751-763.
- Sankey, J. T., Brinkman, D. B., Fox, R. C., Eberth, D. A., Currie, P. J., & Koppelhus, E. (2005). Patterns of distribution of mammals in the Dinosaur Park Formation and their paleobiological significance, in *Dinosaur Provincial Park: A spectacular ancient ecosystem revealed*, Indiana University Press, Bloomington, Indiana, 436-449.
- Sankey, J. T. (2008). Vertebrate paleoecology from microsites, Talley Mountain, Upper Aguja Formation, (Late Cretaceous), Big Bend National Park, Texas, USA in *Vertebrate microfossil assemblages: their role in paleoecology and paleobiogeography*. Indiana University Press, 61-77.
- Schaetzl, R. (2005). *Soils: genesis and geomorphology*. Cambridge University Press.
- Shotwell, J. A. (1955). An approach to the paleoecology of mammals. *Ecology*, 36(2), 327-337.

Smith, E. P., & van Belle, G. (1984). Nonparametric estimation of species richness. *Biometrics*, 119-129.

Thompson, R. S., Parish, J. C., Maidment, S. C., & Barrett, P. M. (2012). Phylogeny of the ankylosaurian dinosaurs (Ornithischia: Thyreophora). *Journal of Systematic Palaeontology*, 10(2), 301-312.

Torres-Dowdall, J., Dargent, F., Handelsman, C. A., Ramnarine, I. W., & Ghalambor, C. K. (2013). Ecological correlates of the distribution limits of two poeciliid species along a salinity gradient. *Biological Journal of the Linnean Society*, 108(4), 790-805.

Tsujita, J. C. (1995). Stratigraphy, taphonomy and paleoecology of the Upper Cretaceous Bearpaw Formation in southern Alberta PhD. Dissertation, McMaster University, Hamilton.

Vavrek, M. J. (2011). Fossil: palaeoecological and palaeogeographical analysis tools: *Palaeontologia Electronica*, v. 14, no. 1, p. 16.

Wood, J. M., Thomas, R. G., & Visser, J. (1988). Fluvial processes and vertebrate taphonomy: the upper cretaceous Judith River formation, south-central dinosaur Provincial Park, Alberta, Canada. *Palaeogeography, Palaeoclimatology, Palaeoecology*, 66(1-2), 127-143.

Transition

This chapter reviews known hydrocarbon potential of the Belly River Group in southwestern Saskatchewan. This review of previously published data provides a comprehensive overview of known resources and future potential. This is significant, as the sand bodies in the Ribstone Creek Member, upper BRG, and lowermost Bearpaw Formation are known shallow gas pools believed to be derived from significant coal seams throughout the study area. The sequence stratigraphic component of this thesis has direct implications for prospective hydrocarbon development from BRG deposits in Saskatchewan.

Chapter 7

Review of Hydrocarbon Resources associated with the Belly River Group

The Belly River Group and Lower Bearpaw Formation is a known host for both shallow gas pools and extensive coal seams in southwestern Saskatchewan. Sandstones of the Belly River Group and lowermost Bearpaw Formation are the youngest deposits to host hydrocarbons in the province (Simpson, 1981). The Vidora Shallow Gas pool of the Whiteside field produces from the Ribstone Creek, Manâtakâw, Dinosaur Park, and Bearpaw Formations. Coal seams of varying qualities underlie approximately 13 800 km² in the Cypress Hills region, and has been speculated to be the source of the hydrocarbons within the Vidora pool (Figure 7.1; Frank, 2005).

Belly River oil and gas extraction and development is considerably more advanced in Alberta compared to Saskatchewan. Oil was discovered in the Belly River Group in the 1950s, with extensive development occurring in the 1970s and 1980s. Horizontal drilling triggered a second wave of production from the Group in Alberta starting in 2011 (Prairie Sky Royalty, 2017). In Alberta, the BRG produces coal, light oil, natural gas, and natural gas liquids. The Saskatchewan extension it is currently known to produce only shallow gas and coal. The Belly River Group in Saskatchewan is an active gas producer, and as of 2011 was the 10th most productive non-associated gas producing formation in Saskatchewan (Figure 7.2; Yang, 2011). In the 1920s and 1930s, coal was mined from the upper Dinosaur Park Formation at Woodpile Coulee. At present, no BRG coal is mined in Saskatchewan.

Frank (2005) mapped and quantified the coal content in the Cypress Hills region to determine volume estimates and net coal thickness. 150 townships were found to contain BRG coal seams in southwestern Saskatchewan, with an average thickness of 3.5 meters and a total

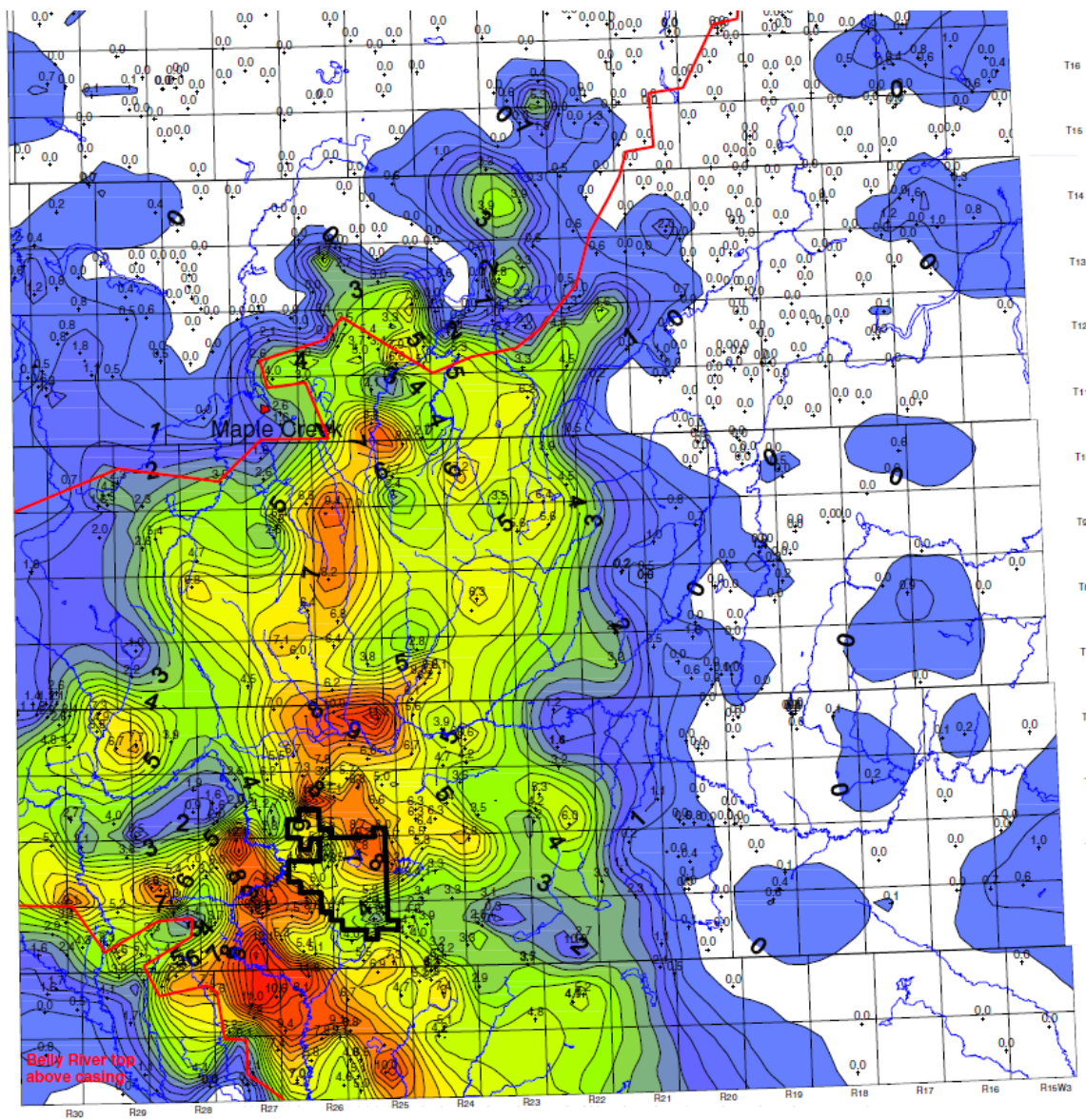


Figure 7.1: Total net coal isopach in meters, outline of the Vidora Gas Pool is outlined in black. Modified from Frank, 2005.

coal volume of $48 \times 10^9 \text{ m}^3$. The source of the gas pool in both the Ribstone Creek and the upper BRG – lowermost Bearpaw is likely sourced from coals within these units, and

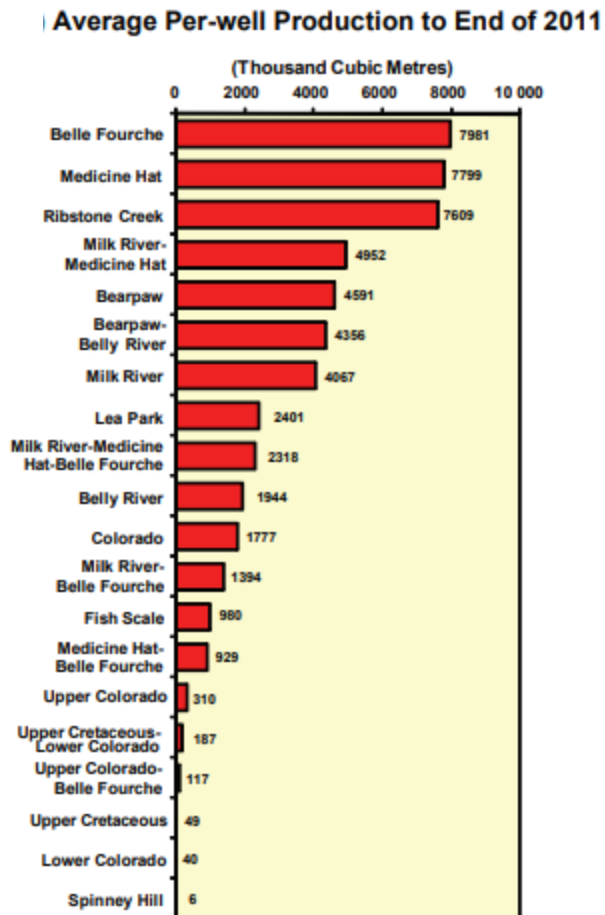


Figure 7.2: Top 20 Saskatchewan gas plays by average per-well gas production in the year 2011. From Yang, 2012.

organic accumulations within the Western Interior Seaway shale and mudstone deposits. In the Cypress Hills region, measured gas content from desorption studies of BRG coals have been done for both Nexen Battle Creek and Nexen Vidora wells, indicating 0.97 m^3 of gas present per cubic meter of coal. Overall, the Ribstone Creek Member is believed to host $1.3 \times 10^9 \text{ m}^3$, the Belly River Group $456.9 \times 10^6 \text{ m}^3$, the Belly River (Dinosaur Park) – Bearpaw transition $169.9 \times 10^6 \text{ m}^3$, and the Bearpaw $229.6 \times 10^6 \text{ m}^3$ (Table 7.1, 7.2; Yang, 2012) of gas. Capital investment has been stagnant in BRG shallow gas in recent years due to depressed natural gas prices, but the plays do hold significant potential if markets were to improve (Prairie Sky Royalty, 2017).

Future studies should focus on identifying specific petrographic properties of the coals from the Belly River Group. Upwards of 17 coal seams are known to occur in the Cypress Hills region of southwestern Saskatchewan (Frank, 2005), many of which will undoubtedly have different properties. Several bright banded coals were logged during the course of this study, and it would be of economic significance to quantify them. A hydrogeologic study of the Vidora Gas Pool would help elucidate flushing and trapping of hydrocarbons, and to firmly determine the source of the Vidora Gas Pool (microbial, coal, etc.).

Formation	Play Area	Gas Type	10 ⁹ m ³			Tcf		
			Low Case	Medium Case	High Case	Low Case	Medium Case	High Case
Belly River	1	NA	1.161	1.735	2.914	0.041	0.062	0.103

Table 7.1: Low, medium, and high case estimates for each play area. From National Energy Board, 2008.

Formation	Play Area	Gas Type	10 ⁹ m ³			Tcf		
			GIP	Producible	Marketable	GIP	Producible	Marketable
Belly River	1	NA	1.735	1.092	1.037	0.062	0.039	0.037

Table 7.2: Ultimate natural gas estimates by formation and play area – medium case. From National Energy Board, 2008.

References

- Frank, M. C. (2006). *Coal distribution in the Upper Cretaceous (Campanian) Belly River Group of southwest Saskatchewan*. Saskatchewan Industry and Resources, Open File Report 2005-33, CD-ROM.
- Prairie Sky Royalty Ltd. (2017). 2017 Royalty Playbook. Open File Report.
- Saskatchewan Ministry of Energy and Resources. (2008). *Saskatchewan's Ultimate Potential for Conventional Natural Gas*. Saskatchewan Ministry of Energy and Resources, Open File Report 2008-8.
- Simpson, F. (1979). Low-permeability gas reservoirs in marine, Cretaceous sandstones of Saskatchewan: 1. Project outline and rationale. Summary of Investigations, 79-10.
- Yang, C. (2012). Hydrocarbon play ranking and production trends in Saskatchewan to Year End 2011. *Summary of Investigations*, 1, 2012-4.

Conclusions

The purpose of this study was to investigate the sedimentology, sequence stratigraphy, ichnology, and paleontology of the Belly River Group in southwestern Saskatchewan. This was accomplished by integrating datasets from a number of different interdisciplinary sources, including well logs, subsurface core, available outcrop exposure, vertebrate and invertebrate body fossils, and trace fossils. A comprehensive investigation of the Belly River Group in Saskatchewan had not taken place since the 1970s (McLean, 1971). As such, this study sought to provide a comprehensive examination utilizing our modern understanding of sequence stratigraphic and paleoecologic concepts.

This work has re-examined and redefined many aspects of the Belly River Group in the province. The Belly River Group has now been placed into a modern nomenclature framework based on studies published in Montana and Alberta (e.g. Eberth and Hamblin, 1993; Rogers et al., 2016). This provides broader context to those wishing to study the Late Cretaceous in the Western Interior Sedimentary Basin and beyond. The Foremost, Oldman, and Dinosaur Park formations are now formally recognized in southern Saskatchewan. A new stratigraphic unit within the Dinosaur Park Formation, the Manâtakâw Member, has been created to facilitate understanding of the transition from terrestrial to marine deposition in the Late Campanian.

As a result of this study, several facies and facies associations have been recognized in the Saskatchewan expression of the Belly River Group (Chapter 3). Building from this, a sequence stratigraphic framework was erected to facilitate understanding of base level changes throughout deposition of the BRG clastic cycle. Due to Saskatchewan's proximity to the Western Interior Seaway paleocoastline, subtle changes in base level are more easily discernable in the Saskatchewan deposits. This has refined our understanding of facies changes in the BRG for not

only Saskatchewan, but equivalent deposits in Alberta and Montana. This study highlights how synthesis of multiple datasets that have historically been studied separately can elucidate complex depositional patterns in basin evolution.

Two microvertebrate sites from the Dinosaur Park Formation were studied and integrated with sedimentology, palynology, and invertebrate paleontology. This provided paleoenvironmental and paleoecologic context to the DPF in Saskatchewan. The DPF has been the subject of countless vertebrate paleontology studies in Alberta and Montana. The Saskatchewan extension of the DPF has provide valuable insight into paleoecologic variation and species response to sea level changes in lowland, coastal ecosystems.

Though this study presents an incredible amount of data covering many topics, several avenues remain to be explored. Such future directions include, but are not limited to:

- 1) An updated, detailed sedimentologic and sequence stratigraphic study of the Bearpaw Formation and associated overlying Cretaceous strata in Saskatchewan. This would constrain understanding of sea-level changes and the final retreat of the Western Interior Seaway from Saskatchewan. This should be expanded to tie in equivalent aged strata across North America.
- 2) Further Alpha diversity studies utilizing microsites (i.e. Muddy Lake, Saskatchewan) that were collected but never formally analyzed for this study.
- 3) Beta diversity analysis, or between site diversity analysis, based on the vertebrate microfossil data collected from the Dinosaur Park Formation of Saskatchewan.

Comparisons with other known late Campanian assemblages in North America and abroad would be of extreme value for understanding large-scale paleoecological trends.

- 4) Future studies focused on petrography and properties of the coals, and the nature of the hydrocarbon pools associated with the Belly River Group and Bearpaw Formation in not only the Cypress Hills, but across southern Saskatchewan.

Appendix A

Ichnology and Depositional Environments of the Upper Cretaceous Dinosaur Park – Bearpaw
Formation transition in the Cypress Hills region of Southwestern Saskatchewan, Canada

Dinosaur Park - Bearpaw Transition
Facies Picks

UWI	KB	Latitude	Longitude	DPF	OF	FA 2	FA 3/4	FA 3/4
141/06-27-001-23W3	987.4	49.06413N	109.00183W	309.70	402.8	309.70	349.5	402.8
131/11-33-001-24W3	957.7	49.08193N	109.15901W	252.40	342.2	252.40	294.9	342.2
101/12-32-001-24W3	927.9	49.08136N	109.18589W	215.70	294.6	215.70	261.4	294.6
141/06-15-001-25W3	909.7	49.03450N	109.26795W	188.80	271.2	188.80	212.8	271.2
111/01-18-001-25W3	889.4	49.03034N	109.32368W	159.30	216.4	159.30	175.4	216.4
141/12-05-001-25W3	878.5	49.01040N	109.31833W	131.6	187.9	131.6	158.2	187.9
141/12-19-001-25W3	908.7	49.05220N	109.33916W	193.50	238.5	193.50	205.4	238.5
121/07-12-001-26W3	889.2	49.01865N	109.35394W	155.40	217.5	155.40	182	217.5
101/10-24-001-26W3	903.4	49.05219N	109.35295W	180.40	236.4	180.40	196.9	236.4
141/10-34-001-26W3	884.6	49.08225N	109.39619W	157.50	198.9	157.50	171.1	198.9
101/11-15-001-27W3	892.5	49.03786N	109.53687W	112.8	182.5	112.8	154.7	182.5
101/10-25-001-27W3	921	49.06702N	109.48657W	157.90	221.9	157.90	182.5	221.9
141/14-36-001-28W3	924.9	49.08666N	109.62537W	166.4	207.5		166.4	207.5
101/05-20-002-21W3	906.2	49.13604N	108.78497W	314.40	360.1	314.40	335.9	360.1
111/04-12-002-21W3	916.7	49.10210N	108.69460W	309.40	371.6	309.40	334.9	371.6
131/09-25-002-21W3	905	49.15500N	108.67984W	293.00	380	293.00	345.7	380
121/07-35-002-21W3	906.6	49.16511N	108.70829W	300.50	380.5	300.50	336.6	380.5
131/07-16-002-22W3	952.7	49.12227N	108.88680W	328.60	376.8	328.60	352.7	376.8
111/03-22-002-22W3	930.3	49.13148N	108.86722W	307.20	363.2	307.20	333	363.2
131/13-01-002-23W3	965.1	49.10018N	108.96411W	342.00	390.2	342.00	358.5	390.2
131/15-35-002-23W3	958.8	49.17361N	108.97658W	316.50	368.6	316.50	344.4	368.6
101/08-04-002-24W3	963.7	49.09262N	109.14765W	308.00	350.7	308.00	330.3	350.7
141/08-05-002-24W3	937.1	49.09244N	109.16753W	275.50	317.9	275.50	297.1	317.9
101/11-11-002-24W3	962.6	49.11055N	109.11354W	282.30	357.3	282.30	325.4	357.3
131/10-13-002-24W3	973	49.12689N	109.08682W	285.80	363.4	285.80	322.1	363.4
141/15-14-002-24W3	974.7	49.13007N	109.10548W	285.60	366.6	285.60	326.1	366.6
141/10-30-002-24W3	980.5	49.15471N	109.19522W	274.80	346.6	274.80	304.9	346.6
141/06-32-002-24W3	1014.2	49.16600N	109.17909W	310.70	389.8	310.70	347.5	389.8
131/09-32-002-24W3	1009.6	49.17003N	109.17070W	304.70	379.6	304.70	342.2	379.6
111/05-15-002-25W3	933.6	49.12077N	109.27393W	224.30	310.8	224.30	252.2	310.8
141/10-25-002-25W3	986.2	49.15459N	109.21844W	281.90	354.8	281.90	310	354.8
141/06-28-002-25W3	950.9	49.15144N	109.29051W	222.10	297.1	222.10	246.3	297.1
141/06-29-002-25W3	941.4	49.15120N	109.31301W	193.90	285.3	193.90	215.5	285.3
101/09-33-002-25W3	988.2	49.16837N	109.28074W	273.40	339.5	273.40	303.9	339.5
101/06-06-002-26W3	905	49.09267N	109.47006W	155.90	219.5	155.90	178.8	219.5
101/12-13-002-26W3	920.7	49.12546N	109.36359W	143.10	230	143.10	173.6	230
131/11-14-002-26W3	917.6	49.12593N	109.38099W	135.20	212.7	135.20	156.2	212.7
121/11-33-002-26W3	919.4	49.16813N	109.42531W	195	239.8		195	239.8

121/10-15-002-26W3	895.4	49.12382N	109.39959W	131.00	199.5	131.00	152	199.5
101/09-20-002-26W3	900.6	49.13969N	109.43650W	157.50	225.4	157.50	183	225.4
121/06-22-002-26W3	905.8	49.13443N	109.40409W	170.20	232.4	170.20	195.6	232.4
131/06-05-002-27W3	923.3	49.09298N	109.58224W	143.20	208.8	143.20	167.4	208.8
141/06-05-002-27W3	924	49.09388N	109.57954W	142.70	213	142.70	170	213
101/11-15-001-27W3	892.5	49.03786N	109.53687W	112.8	182.5	112.8	154.7	182.5
141/14-03-002-28W3	909.5	49.10110N	109.66954W	115.10	182.7	115.10	137.4	182.7
101/11-24-002-28W3	910.1	49.13973N	109.62566W	125.00	190.6	125.00	154.2	190.6
101/10-32-002-28W3	927.2	49.16876N	109.70935W	110.80	170.2	110.80	136	170.2
131/07-12-003-21W3	908.7	49.19521N	108.70411W	260.80	320.5	260.80	296.5	320.5
101/14-34-003-21W3	925.1	49.26016N	108.75449W	262.30	325.8	262.30	302	325.8
101/02-26-003-22W3	920.8	49.23439N	108.86109W	240.30	312.7	240.30	286	312.7
101/05-11-003-22W3	905.3	49.19425N	108.87212W	272.80	329.2	272.80	296.1	329.2
121/13-07-003-23W3	991.4	49.20110N	109.09786W	288.80	375.2	288.80	326.5	375.2
101/11-20-003-23W3	948.9	49.22679N	109.06769W	252.70	335.2	252.70	288.4	335.2
101/13-20-003-23W3	953.5	49.23106N	109.07430W	255.90	338.8	255.90	290	338.8
111/11-28-003-23W3	937.4	49.24093N	109.04464W	242.80	325	242.80	275.8	325
131/13-02-003-24W3	997.1	49.18836N	109.14167W	287.30	370.1	287.30	327	370.1
101/06-03-003-24W3	998.6	49.17976N	109.15847W	296.30	374.7	296.30	332.7	374.7
131/10-18-003-24W3	1014.8	49.21337N	109.22078W	296.90	386.1	296.90	320.5	386.1
101/09-19-003-24W3	1008.3	49.22708N	109.21417W	305.60	372.4	305.60	334.8	372.4
131/12-19-003-24W3	1000.7	49.22748N	109.23100W	275.60	359.4	275.60	307.3	359.4
111/12-29-003-24W3	995.1	49.24084N	109.20717W	290.50	372.5	290.50	317.5	372.5
141/16-30-003-24W3	987.7	49.24579N	109.21375W	277.90	328.9	277.90	296.1	328.9
131/06-01-003-25W3	1066.6	49.18027N	109.24871W	365.9	417.6	365.9	387.7	417.6
101/06-31-003-25W3	991.8	49.25272N	109.35977W	233.20	303	233.20	268.1	303
141/03-35-003-25W3	990	49.25028N	109.26890W	254.60	315.5	254.60	271.1	315.5
111/11-35-003-25W3	971.9	49.25481N	109.26802W	233.90	311.4	233.90	254.2	311.4
121/06-11-003-26W3	930.8	49.19365N	109.40455W	183.90	256.2	183.90	206.7	256.2
101/14-25-003-26W3	1004.2	49.24526N	109.38198W	255.60	335.9	255.60	281.5	335.9
111/12-31-003-26W3	943	49.25551N	109.49880W	172.90	232.6	172.90	195.6	232.6
101/04-35-003-26W3	971.6	49.24874N	109.41064W	213.40	276.1	213.40	240	276.1
141/14-08-003-27W3	924.3	49.20277N	109.60370W	127.30	202.2	127.30	159	202.2
101/07-13-003-27W3	918.2	49.20890N	109.51150W	147.60	215.7	147.60	176.5	215.7
141/06-19-003-27W3	965.4	49.22482N	109.62656W	167.40	230.7	167.40	189.3	230.7
141/06-21-003-27W3	931.8	49.22445N	109.58278W	144.90	214.2	144.90	166.5	214.2
111/07-35-003-27W3	953.1	49.25185N	109.53256W	209	241.8		209	241.8
101/10-02-003-28W3	940.2	49.18349N	109.66801W	169.9	208.7		169.9	208.7
101/06-03-003-28W3	932	49.17982N	109.69601W	120.90	194.6	120.90	157.7	194.6

111/07-05-003-28W3	922.1	49.17918N	109.73434W	128.8	173.2		128.8	173.2
141/08-05-003-28W3	928.2	49.17971N	109.72758W	122.5	176		122.5	176
141/06-07-003-28W3	947.4	49.19575N	109.76129W	148.4	180.3		148.4	180.3
141/16-08-003-28W3	964	49.20277N	109.72758W	175.4	206.6		175.4	206.6
121/10-09-003-28W3	945	49.19652N	109.71356W	146.2	200.8		146.2	200.8
141/06-10-003-28W3	959.5	49.19515N	109.69473W	161.7	217.7		161.7	217.7
141/08-10-003-28W3	952.6	49.19574N	109.68284W	162.5	206.9		162.5	206.9
141/14-14-003-28W3	976	49.21693N	109.67259W	182.5	226.7		182.5	226.7
101/07-34-003-28W3	983.3	49.25255N	109.69047W	195.7	239.5		195.7	239.5
101/07-35-003-28W3	973.5	49.25258N	109.66813W	189	225.5		189	225.5
121/10-15-003-29W3	927	49.21134N	109.82734W	112	150		112	150
101/11-32-003-29W3	974.1	49.25617N	109.87536W	147.2	187.8		147.2	187.8
121/10-35-003-29W3	971.3	49.25482N	109.80474W	161.6	194.5		161.6	194.5
141/08-36-003-30W3	997.1	49.25313N	109.90860W	166.3	205.4		166.3	205.4
121/06-07-004-21W3	942.8	49.28156N	108.82280W	276.40	362.7	276.40	310.7	362.7
111/05-16-004-21W3	961.3	49.29529N	108.78112W	291.80	386.6	291.80	331.3	386.6
111/16-28-004-21W3	952.5	49.33269N	108.76496W	306.40	400.1	306.40	343.9	400.1
101/14-19-004-22W3	1034.5	49.31798N	108.95621W	333.40	410.8	333.40	376.6	410.8
101/15-09-004-22W3	987.2	49.28891N	108.90591W	306.9	398	306.9	348.8	398
101/16-33-004-22W3	1053.1	49.34713N	108.90037W	389.30	466.8	389.30	427.4	466.8
121/10-31-004-23W3	986.2	49.34190N	109.08800W	278.10	350.9	278.10	313.7	350.9
141/15-04-004-24W3	955.9	49.27571N	109.17364W	238.40	317.1	238.40	271.4	317.1
101/11-15-004-24W3	957.8	49.30010N	109.15856W	257.20	315.3	257.20	282.6	315.3
141/12-28-004-24W3	946	49.33076N	109.18472W	226.10	286.7	226.10	250.3	286.7
101/10-09-004-25W3	962.6	49.28525N	109.30938W	214.60	289.7	214.60	239.9	289.7
111/11-14-004-25W3	950.1	49.29857N	109.26793W	213.10	277.2	213.10	235.9	277.2
121/06-20-004-25W3	946.4	49.31073N	109.33857W	189.30	276.8	189.30	215	276.8
101/06-24-004-25W3	951.9	49.31054N	109.24733W	220.50	299	220.50	238.3	299
121/06-26-004-25W3	949.2	49.32467N	109.27117W	207.40	276.8	207.40	228	276.8
131/07-28-004-25W3	945.6	49.32674N	109.31133W	195.90	261.1	195.90	218	261.1
101/06-30-004-25W3	953	49.32544N	109.35975W	196.10	281.4	196.10	224.9	281.4
131/11-32-004-25W3	955.7	49.34404N	109.33801W	194.00	280.4	194.00	220	280.4
131/10-33-004-25W3	954.6	49.34426N	109.31168W	202.40	285.5	202.40	229.6	285.5
111/06-36-004-25W3	960.1	49.33987N	109.24591W	220.60	297.4	220.60	241.1	297.4
141/07-03-004-26W3	969.1	49.26892N	109.42037W	211.80	280.2	211.80	232	280.2
141/08-14-004-26W3	957.4	49.29692N	109.39149W	198.90	263.4	198.90	224	263.4
101/10-21-004-26W3	947	49.31437N	109.44379W	184.50	256.4	184.50	207.4	256.4
141/08-24-004-26W3	946.3	49.31081N	109.36899W	192.20	255.7	192.20	220.1	255.7
101/07-25-004-26W3	952.5	49.32539N	109.37664W	193.30	260.6	193.30	221.2	260.6

131/15-27-004-26W3	952	49.33312N	109.42158W	187.20	269.8	187.20	215	269.8
141/16-31-004-26W3	948.3	49.34752N	109.48217W	174.10	246.5	174.10	197	246.5
101/07-35-004-26W3	948.7	49.33987N	109.39911W	185.90	260.3	185.90	202.4	260.3
131/13-10-004-27W3	954.5	49.28998N	109.56898W	177.80	243.8	177.80	200.4	243.8
131/06-16-004-27W3	964.1	49.29720N	109.58398W	183.00	255.1	183.00	205.5	255.1
141/14-17-004-27W3	959.6	49.30454N	109.60436W	170.80	246.7	170.80	192	246.7
101/10-18-004-27W3	962.9	49.29993N	109.62318W	164.50	239.4	164.50	191.7	239.4
131/07-20-004-27W3	965.6	49.31114N	109.60168W	171.30	245	171.30	200.5	245
111/14-34-004-27W3	955.4	49.34659N	109.56048W	183.30	246.8	183.30	201	246.8
141/06-03-004-28W3	986.7	49.26780N	109.69497W	190.9	242.8		190.9	242.8
131/10-08-004-28W3	968.8	49.28603N	109.73593W	180	214.8		180	214.8
141/06-09-004-28W3	972.5	49.28307N	109.71628W	171.2	209		171.2	209
101/10-13-004-28W3	976.6	49.29981N	109.64585W	201	240.3		201	240.3
141/10-15-004-28W3	983	49.29999N	109.68946W	195.7	234.7		195.7	234.7
141/06-17-004-28W3	979.9	49.29767N	109.73876W	183	231.8		183	231.8
111/09-24-004-28W3	977.9	49.31331N	109.63843W	202.6	251.7		202.6	251.7
111/11-24-004-28W3	977.7	49.31377N	109.64939W	199.9	246		199.9	246
141/16-30-004-28W3	991.5	49.33402N	109.75008W	192.5	237.3		192.5	237.3
141/06-25-004-29W3	994.1	49.32681N	109.78356W	180	224.7		180	224.7
141/06-32-004-29W3	992.3	49.34116N	109.87513W	172.1	220.4		172.1	220.4
101/02-10-005-21W3	939.7	49.36505N	108.74905W	291.90	356.7	291.90	327.7	356.7
141/08-11-005-21W3	938	49.37012N	108.72011W	292.30	357	292.30	330.5	357
131/10-03-005-22W3	1061.1	49.35871N	108.88364W	406.30	481.2	406.30	441.9	481.2
141/14-06-005-22W3	1060.2	49.36279N	108.95620W	362.90	460.6	362.90	403.5	460.6
121/02-18-005-22W3	1044.5	49.37944N	108.95159W	354.70	449.9	354.70	399.8	449.9
141/08-19-005-22W3	1045.4	49.39862N	108.94386W	359.60	439.6	359.60	400.2	439.6
101/07-29-005-24W3	994.9	49.41233N	109.19740W	263.50	338.5	263.50	296.1	338.5
141/06-01-005-25W3	964.5	49.35588N	109.24556W	226.40	307.6	226.40	245.5	307.6
111/07-02-005-25W3	959.7	49.35365N	109.26328W	219.90	307.5	219.90	241.4	307.5
121/06-06-005-25W3	950.1	49.35404N	109.36046W	191.40	270.1	191.40	216	270.1
101/07-07-005-25W3	961	49.36904N	109.35423W	206.40	285.4	206.40	233.8	285.4
111/12-14-005-25W3	967.8	49.38586N	109.27552W	217.10	308.2	217.10	241.5	308.2
131/11-19-005-25W3	983.9	49.40249N	109.36079W	226.20	301.1	226.20	251.7	301.1
131/11-23-005-25W3	976.4	49.40190N	109.27124W	226.80	316.9	226.80	271.3	316.9
141/06-28-005-25W3	989.6	49.41431N	109.31352W	231.30	318.9	231.30	260.7	318.9
141/07-01-005-26W3	958.4	49.35609N	109.37654W	198.40	282.4	198.40	223.5	282.4
101/06-06-005-26W3	954	49.35453N	109.49355W	174.20	245.3	174.20	196.6	245.3
111/11-07-005-26W3	960.4	49.37169N	109.49371W	181.40	257.6	181.40	205.2	257.6
131/07-18-005-26W3	962.7	49.38457N	109.49018W	183.00	260.5	183.00	209.1	260.5

101/10-21-005-26W3	977.8	49.40182N	109.44401W	205.40	282.9	205.40	235.6	282.9
141/13-23-005-26W3	983.9	49.40652N	109.40751W	219.00	290.1	219.00	249.1	290.1
131/11-25-005-26W3	989.3	49.41714N	109.38316W	226.30	301.3	226.30	248.8	301.3
141/07-27-005-26W3	986.1	49.41404N	109.42038W	214.40	285.5	214.40	240	285.5
111/07-28-005-26W3	984	49.41211N	109.44384W	209.30	280.9	209.30	231	280.9
121/06-29-005-26W3	986	49.41238N	109.47263W	210.60	274.1	210.60	235	274.1
101/10-07-005-27W3	973.2	49.37264N	109.62317W	171.10	241	171.10	193.5	241
101/11-12-005-27W3	957.4	49.37257N	109.51667W	183.00	238.9	183.00	204.2	238.9
131/07-13-005-27W3	967.5	49.38451N	109.51252W	188.60	254	188.60	212	254
101/10-15-005-27W3	970.8	49.38699N	109.55640W	182.20	247	182.20	206.3	247
111/07-17-005-27W3	975	49.38308N	109.59976W	169.90	231.8	169.90	199.9	231.8
141/08-01-005-28W3	978.8	49.35496N	109.63799W	198.9	249.1		198.9	249.1
101/11-13-005-28W3	986.9	49.38729N	109.65123W	175.40	240.3	175.40	194.5	240.3
141/07-25-005-28W3	997	49.41424N	109.64556W	212	263		212	263
101/10-33-005-28W3	1030.2	49.43090N	109.71290W	234.10	275.2	234.10	252.3	275.2
141/14-07-005-29W3	1020.5	49.37681N	109.89676W	192	218.7		192	218.7
101/07-13-005-30W3	1030.2	49.38368N	109.91477W	200	229.3		200	229.3
101/07-21-006-21W3	944.3	49.48550N	108.77144W	288.10	350.1	288.10	330	350.1
101/14-08-006-21W3	968.3	49.46354N	108.79865W	302.50	366	302.50	343.1	366
101/16-14-006-21W3	907.1	49.47804N	108.72149W	246.00	308.2	246.00	286.6	308.2
101/03-11-006-22W3	1026.6	49.45270N	108.86645W	349.20	419.1	349.20	396.2	419.1
101/04-16-006-22W3	1072.3	49.46773N	108.91703W	385.20	458.9	385.20	425.8	458.9
101/08-03-006-22W3	1037.2	49.44198N	108.87787W	364.50	438.1	364.50	405.1	438.1
101/13-11-006-22W3	1028.7	49.46326N	108.87213W	348.70	418.5	348.70	390.6	418.5
101/16-12-006-22W3	983.9	49.46348N	108.83308W	307.50	368.5	307.50	348.2	368.5
141/16-05-006-22W3	1068.2	49.45044N	108.92067W	382.90	457.2	382.90	426.1	457.2
141/14-03-006-23W3	1060.1	49.45052N	109.02154W	369.80	443.4	369.80	406.6	443.4
141/14-12-006-23W3	1131.5	49.46484N	108.97702W	439.30	521.2	439.30	471.6	521.2
111/06-11-006-24W3	1029.5	49.45731N	109.13462W	304.40	387	304.40	350	387
121/04-11-006-24W3	1039.4	49.45297N	109.14302W	311.40	395.2	311.40	357.1	395.2
141/14-09-006-25W3	1064.4	49.46496N	109.31336W	321.50	407.8	321.50	346.9	407.8
141/16-22-006-25W3	1053.5	49.49341N	109.28032W	314.50	388.2	314.50	341.6	388.2
141/11-26-006-25W3	1052.5	49.50381N	109.26915W	319.20	384.5	319.20	344.7	384.5
141/06-31-006-25W3	1068.8	49.51467N	109.35772W	327.50	391.3	327.50	350.7	391.3
121/06-02-006-26W3	1017.9	49.44125N	109.40572W	249.90	323.9	249.90	276	323.9
101/03-03-006-26W3	1007.6	49.43862N	109.42764W	235.90	300.8	235.90	260.5	300.8
131/12-32-006-26W3	1097.3	49.51925N	109.47953W	334.00	414.6	334.00	357.7	414.6
101/10-10-006-27W3	1026.9	49.46007N	109.55585W	250.70	304.6	250.70	273.9	304.6
141/11-18-006-28W3	1089.1	49.47546N	109.76144W	284	337.9		284	337.9

101/07-19-006-28W3	1117.1	49.48563N	109.75803W	318.9	361		318.9	361
141/07-33-006-28W3	1140.6	49.51527N	109.71254W	346.9	393.3		346.9	393.3
101/07-12-006-29W3	1078.4	49.45621N	109.78073W	280.4	319.6		280.4	319.6
101/07-14-006-29W3	1089.8	49.47144N	109.80280W	277	328.2		277	328.2
101/11-18-006-29W3	1171.3	49.47469N	109.89870W	342.5	386.6		342.5	386.6
141/16-21-006-29W3	1113.6	49.49407N	109.84020W	306.2	378.6		306.2	378.6
131/11-27-006-29W3	1111	49.50424N	109.83191W	308.3	356.6		308.3	356.6
141/11-29-006-29W3	1137.5	49.50428N	109.87383W	316.8	362.4		316.8	362.4
121/06-32-006-29W3	1176.2	49.51391N	109.87792W	359	410		359	410
101/12-34-006-29W3	1121.3	49.51815N	109.83662W	322.5	359.1		322.5	359.1
121/10-14-006-30W3	1175	49.47287N	109.93941W	341	384.6		341	384.6
101/09-21-006-30W3	1172	49.48913N	109.97687W	339.7	382.2		339.7	382.2
141/11-25-006-30W3	1197.9	49.50405N	109.91857W	369	410.9		369	410.9
111/06-35-006-30W3	1230.3	49.51392N	109.94196W	412.5	449.5		412.5	449.5
141/11-36-006-30W3	1242.2	49.51882N	109.91808W	428	480.6		428	480.6
101/03-29-007-21W3	1111	49.58405N	108.81971W	437.80	509	437.80	472.1	509
101/05-33-007-21W3	1126.5	49.60191N	108.80180W	458.80	521.1	458.80	494.4	521.1
101/13-22-007-21W3	957.4	49.58000N	108.77938W	297.50	357.2	297.50	333	357.2
101/15-30-007-21W3	1142.7	49.59461N	108.83631W	463.40	535.8	463.40	501.5	535.8
121/04-22-007-21W3	941	49.56789N	108.78140W	276.80	346.7	276.80	319.2	346.7
131/03-34-007-21W3	1094.2	49.59891N	108.77480W	439.20	498.9	439.20	474.8	498.9
131/12-32-007-21W3	1139.1	49.60666N	108.82676W	469.60	535.6	469.60	501.4	535.6
131/13-34-007-21W3	1124	49.60987N	108.78121W	462.50	524.7	462.50	492.4	524.7
101/08-02-007-22W3	1050	49.52920N	108.87503W	370.90	445.8	370.90	405.4	445.8
101/02-28-007-23W3	1147	49.58381N	109.06147W	433.20	503.1	433.20	459.8	503.1
101/03-21-007-24W3	1084.5	49.56905N	109.20319W	358.60	412	358.60	391.6	412
121/06-15-007-24W3	1066.2	49.55750N	109.18326W	325.50	411.9	325.50	357.6	411.9
141/08-05-007-25W3	1078.1	49.52993N	109.34920W	337.20	402.3	337.20	361.6	402.3
101/05-32-007-25W3	1131.4	49.60195N	109.36711W	386.80	455	386.80	414.4	455
101/06-08-007-25W3	1101.7	49.54367N	109.36138W	359.50	433.3	359.50	384.7	433.3
141/10-23-007-25W3	1129.4	49.57647N	109.28703W	386.50	456.1	386.50	415.4	456.1
121/07-32-007-25W3	1176.2	49.60183N	109.35639W	427.90	489.9	427.90	449.6	489.9
101/06-26-007-26W3	1101.2	49.58798N	109.42911W	348.90	412	348.90	372.9	412
111/08-33-007-26W3	1196.1	49.60201N	109.46204W	437.20	496.3	437.20	462.7	496.3
121/16-12-007-27W3	1146.5	49.55100N	109.53179W	379.80	443.3	379.80	400.5	443.3
101/04-04-007-28W3	1161.3	49.52582N	109.75069W	374.3	424.4		374.3	424.4
101/07-10-007-28W3	1155.8	49.54398N	109.71762W	381.50	424.6	381.50	400.5	424.6
101/16-23-007-29W3	1269.5	49.58011N	109.82426W	461.4	509.7		461.4	509.7
121/10-06-007-29W3	1335.3	49.53225N	109.92160W	520.5	568.5		520.5	568.5

121/10-07-007-29W3	1383.4	49.54645N	109.92252W	562	608.9		562	608.9
101/02-23-007-30W3	1376.8	49.56909N	109.96517W	554.1	589.1		554.1	589.1
101/06-15-007-30W3	1388.4	49.55848N	109.99325W	556.7	592.1		556.7	592.1
101/10-01-007-30W3	1319.4	49.53255N	109.94339W	488.2	539.7		488.2	539.7
101/06-01-008-21W3	979.9	49.61655N	108.72812W	317.30	387.2	317.30	351.6	387.2
101/07-07-008-21W3	1136.3	49.63056N	108.83653W	451.20	523.5	451.20	488	523.5
101/11-04-008-21W3	1099.7	49.61988N	108.79643W	433.60	503.4	433.60	469.1	503.4
101/11-17-008-21W3	1128.4	49.64924N	108.81908W	453.70	526.1	453.70	491.8	526.1
141/16-07-008-21W3	1136.1	49.63954N	108.82870W	459.30	527.9	459.30	502.5	527.9
101/02-02-008-22W3	1145.4	49.61297N	108.88158W	458.20	531.9	458.20	487.4	531.9
101/03-23-008-22W3	1147.6	49.61297N	108.88158W	458.00	535.5	458.00	491	535.5
131/06-30-008-24W3	1218.3	49.67492N	109.24901W	479.30	540.6	479.30	502.1	540.6
101/01-23-008-25W3	1216.2	49.65630N	109.28255W	472.40	548.3	472.40	501.3	548.3
121/10-09-008-25W3	1136.6	49.63413N	109.33316W	388.00	448.2	388.00	415.2	448.2
131/06-32-008-25W3	1237.1	49.69072N	109.36198W	489.60	556.1	489.60	509.2	556.1
141/06-17-008-25W3	1163.3	49.64686W	109.36029W	416.40	472.3	416.40	439.3	472.3
101/06-18-008-26W3	1270.7	49.64584N	109.51935W	502.40	568.5	502.40	527.4	568.5
131/11-11-008-26W3	1152.8	49.63535N	109.43000W	397.10	454.2	397.10	419.9	454.2
141/16-01-008-26W3	1116.9	49.62530N	109.39340W	362.70	421.1	362.70	387	421.1
101/11-20-008-27W3	1134.2	49.66410N	109.63309W	344.80	398.3	344.80	364.5	398.3
121/10-10-008-27W3	1286.6	49.63451N	109.58253W	509.20	567.7	509.20	529.6	567.7
141/07-07-008-28W3	1238.7	49.63166N	109.78376W	439.8	471.7		439.8	471.7
101/10-34-008-29W3	1154.6	49.69288N	109.85234W	362	391.2		362	391.2
101/10-23-008-30W3	1286.6	49.66365N	109.96517W	482	513.7		482	513.7

Appendix B

Ichnology and Depositional Environments of the Upper Cretaceous Dinosaur Park – Bearpaw
Formation transition in the Cypress Hills region of Southwestern Saskatchewan, Canada

Supplementary Cross Sections

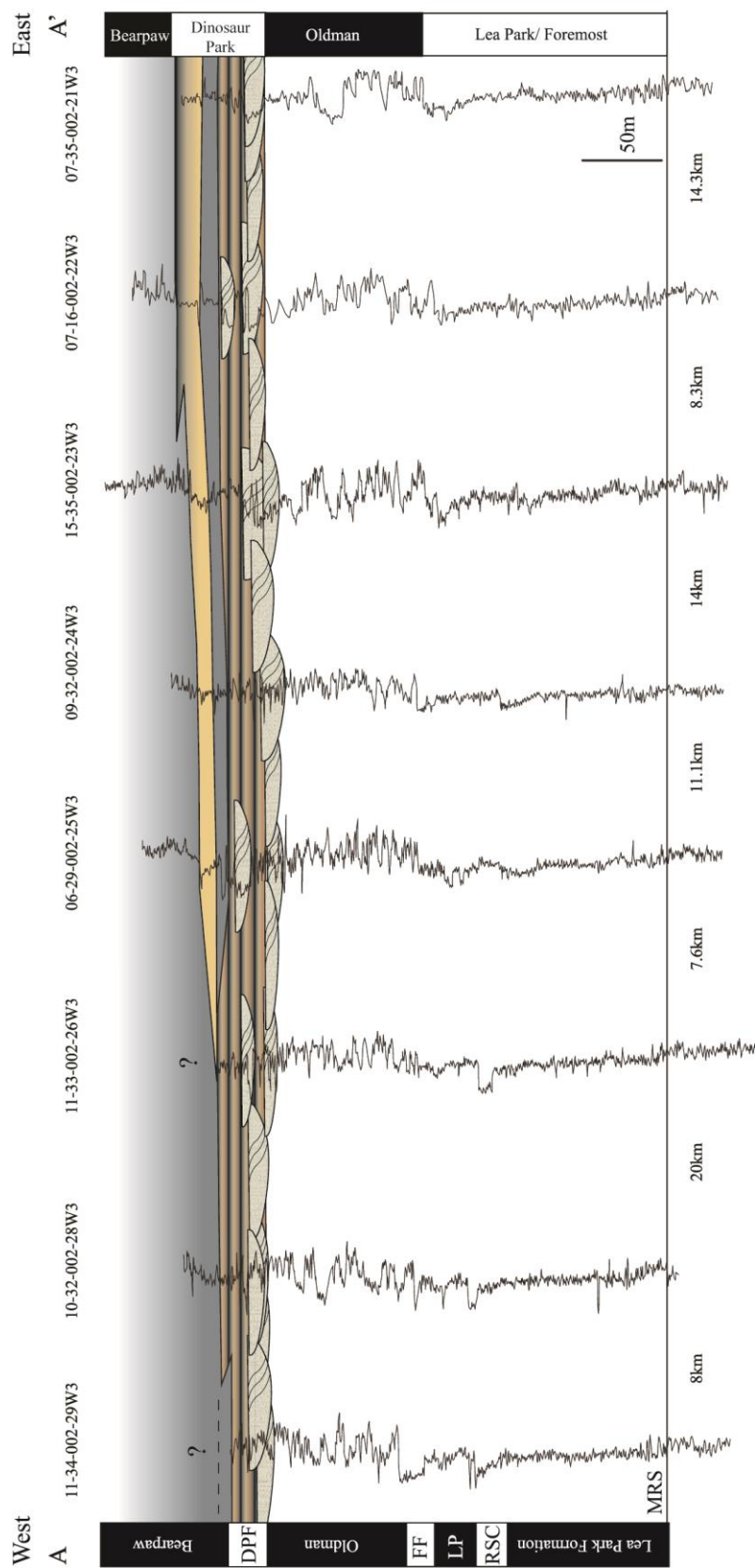


Figure B.1: Dip-oriented cross section through Township 2.

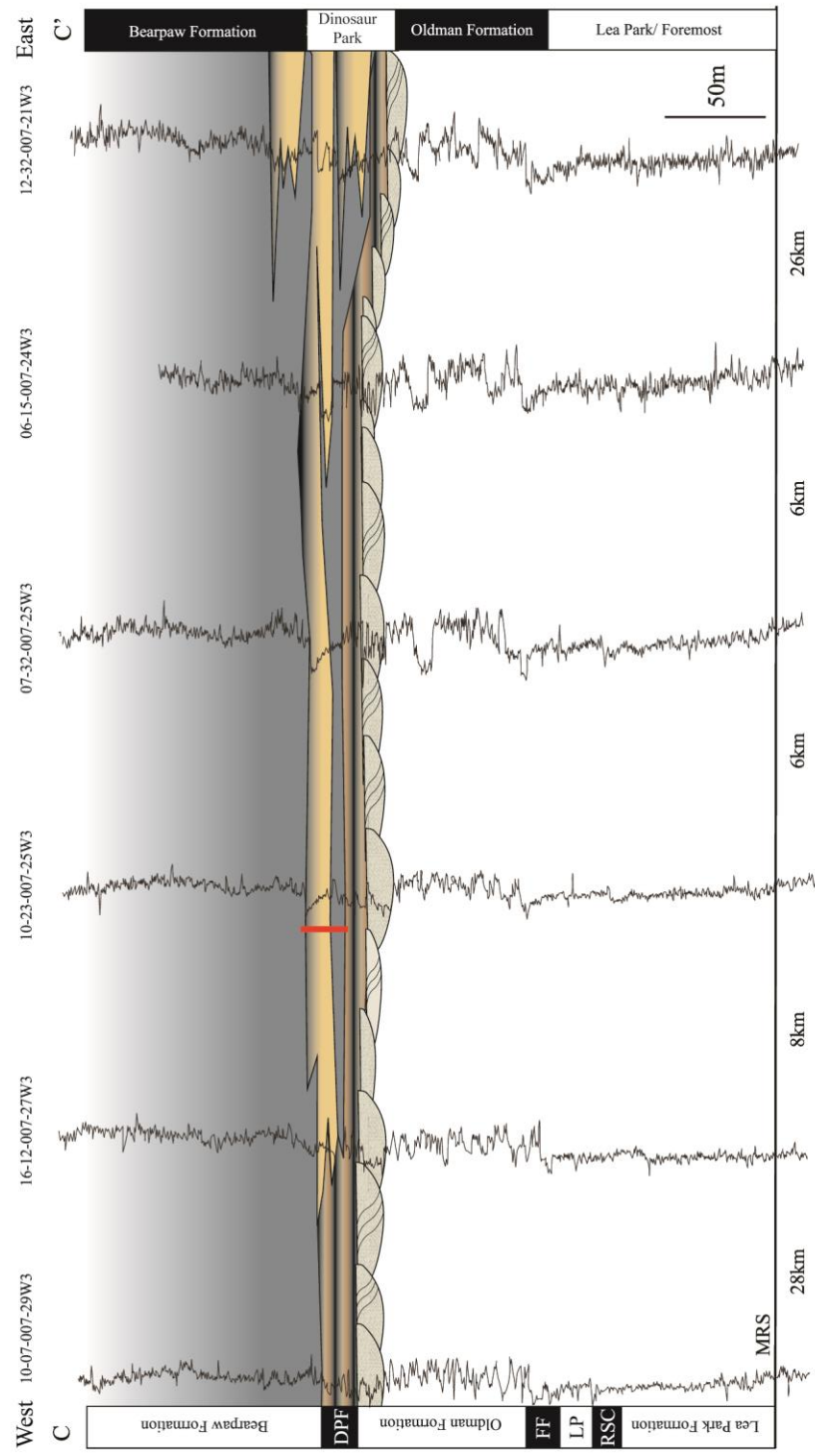


Figure B.2: Dip-oriented cross section through Township 7.

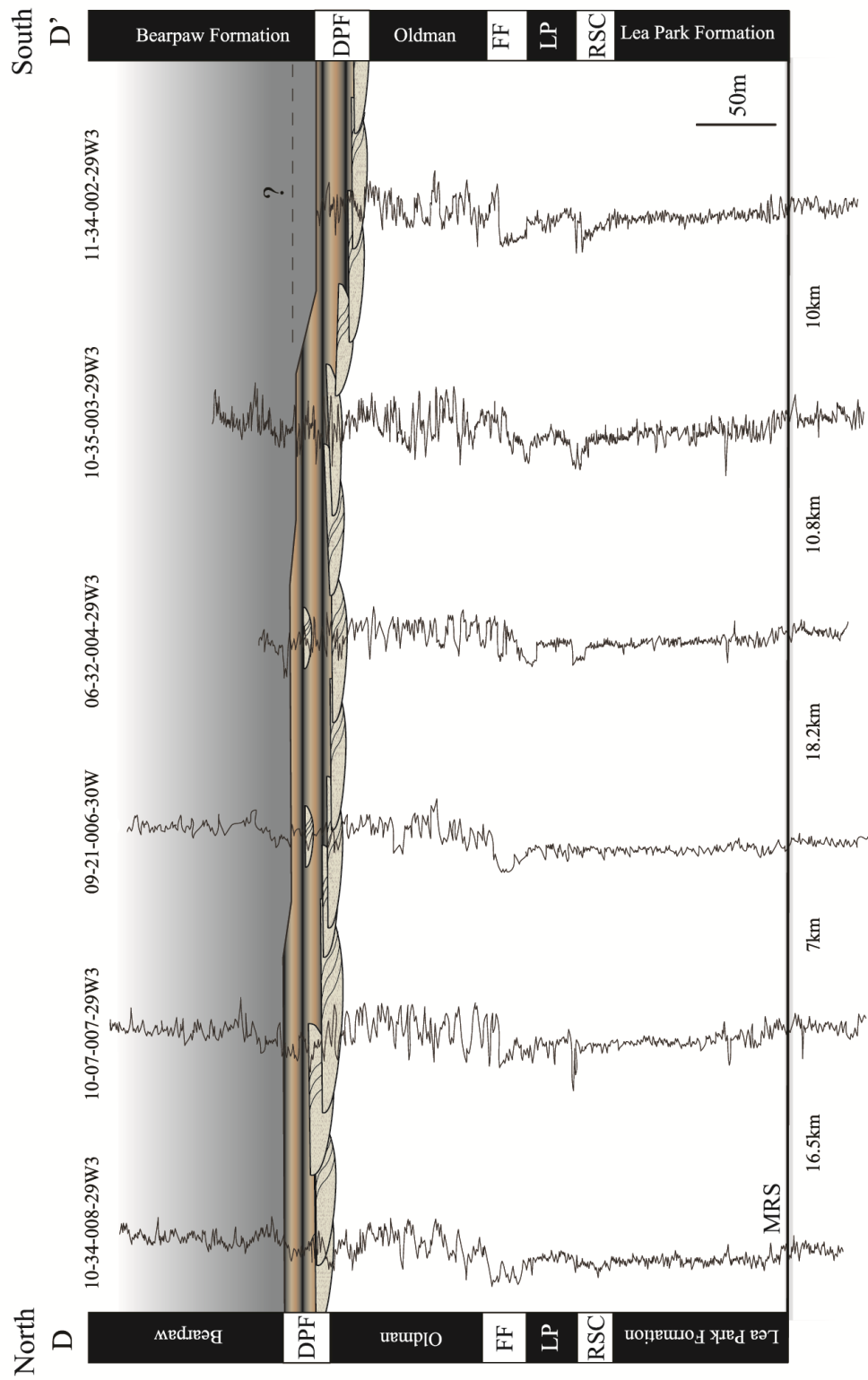


Figure B.3: Strike-oriented cross section through Range 29/30.

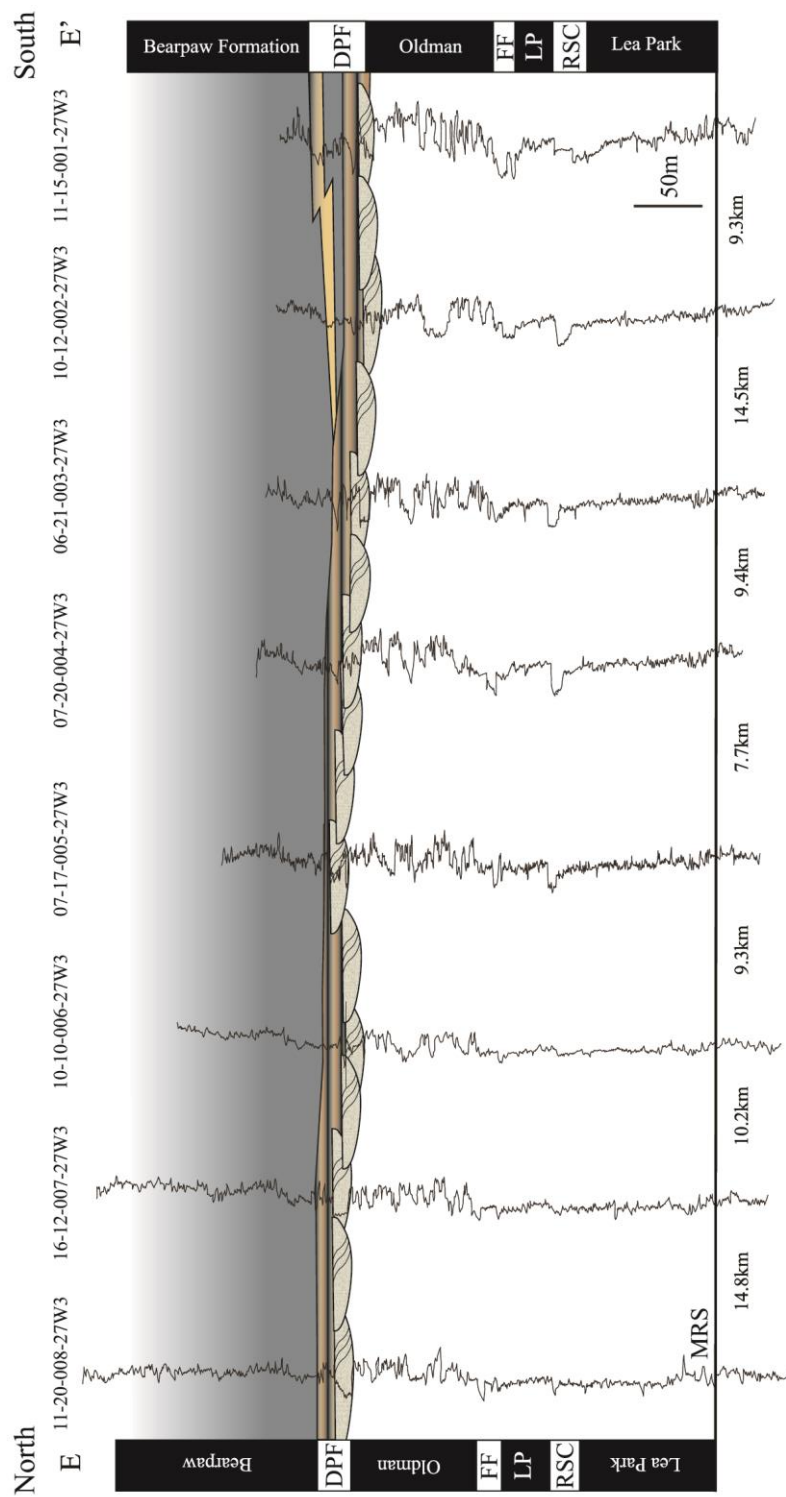


Figure B.4: Strike-oriented cross section through Range 27.

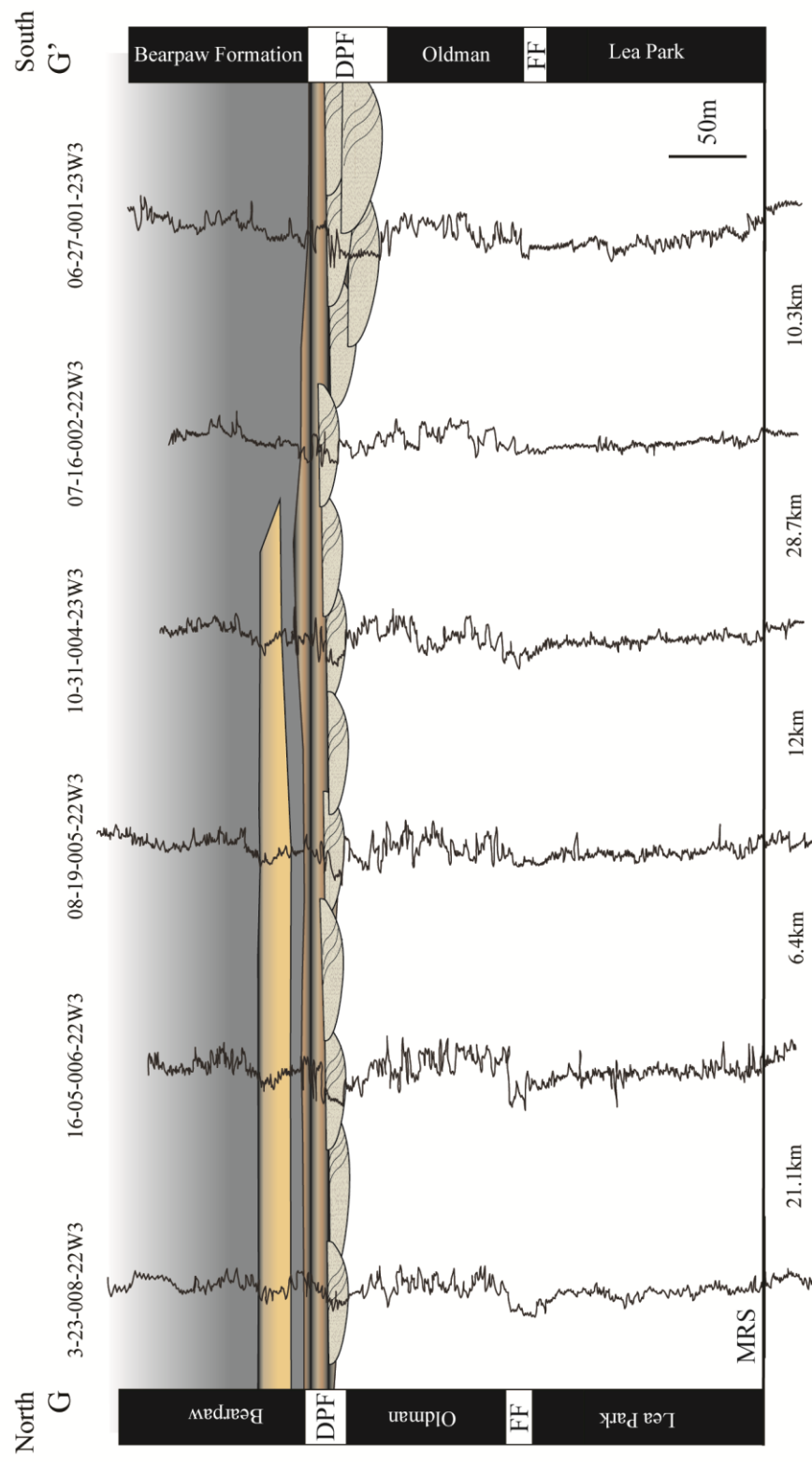


Figure B.5: Strike-oriented cross section through Range 22/23.

Appendix C

Sequence Stratigraphy and Depositional Environments of the Belly River Group (Campanian) in southwestern Saskatchewan, Canada: Incised and Unincised Fluvial Systems along an Epicontinental Seaway

Belly River Group Formation Picks

Well ID	Latitude	Longitude	MM	DPF	OF	FF	LP	RSC T	RSC B	MRS
141/06-27-001-23W3	49.06413N	109.00183W	309.70	349.5	402.8	501.3	514.5			694.3
131/11-33-001-24W3	49.08193N	109.15901W	252.40	294.9	342.2	433.9	449			638.2
101/12-32-001-24W3	49.08136N	109.18589W	215.70	261.4	294.6		413.6			602.4
141/06-15-001-25W3	49.03450N	109.26795W	188.80	212.8	271.2		389.2			577
111/01-18-001-25W3	49.03034N	109.32368W	159.30	175.4	216.4		347.2			519
141/12-05-001-25W3	49.01040N	109.31833W	131.6	158.2	187.9	321.8	332.5	395.5	415.5	519
141/12-19-001-25W3	49.05220N	109.33916W	193.50	205.4	238.5		350.6			553.7
121/07-12-001-26W3	49.01865N	109.35394W	155.40	182	217.5	323.6	343	361	369.9	538.3
101/10-24-001-26W3	49.05219N	109.35295W	180.40	196.9	236.4		324	356.2	366.4	546.5
141/10-34-001-26W3	49.08225N	109.39619W	157.50	171.1	198.9	308.8	319	363.1	371	519.3
101/11-15-001-27W3	49.03786N	109.53687W	112.8	154.7	182.5	293.8	313.8	351.1	368.7	508.4
101/10-25-001-27W3	49.06702N	109.48657W	157.90	182.5	221.9		324.7	384.5	401.7	545
141/14-36-001-28W3	49.08666N	109.62537W		166.4	207.5	319.6	338.9	366	382.1	525.9
101/05-20-002-21W3	49.13604N	108.78497W	314.40	335.9	360.1		462.2			623.6
111/04-12-002-21W3	49.10210N	108.69460W	309.40	334.9	371.6		477	536.7	553.5	632.6
131/09-25-002-21W3	49.15500N	108.67984W	293.00	345.7	380		453.7			620
121/07-35-002-21W3	49.16511N	108.70829W	300.50	336.6	380.5		463.6			621.7
131/07-16-002-22W3	49.12227N	108.88680W	328.60	352.7	376.8		482.3			664.5
111/03-22-002-22W3	49.13148N	108.86722W	307.20	333	363.2		466.4			643.5
131/13-01-002-23W3	49.10018N	108.96411W	342.00	358.5	390.2		500.6	560.4	574.4	677.9
131/15-35-002-23W3	49.17361N	108.97658W	316.50	344.4	368.6		480.4	542.6	555.3	657.5
101/08-04-002-24W3	49.09262N	109.14765W	308.00	330.3	350.7	452	465	509.3	529.7	644.6
141/08-05-002-24W3	49.09244N	109.16753W	275.50	297.1	317.9		417	481.3	501.6	614
101/11-11-002-24W3	49.11055N	109.11354W	282.30	325.4	357.3	463.1	473.4	531.2	550.2	655
131/10-13-002-24W3	49.12689N	109.08682W	285.80	322.1	363.4	471.3	481.8	539.8	553.8	662.4
141/15-14-002-24W3	49.13007N	109.10548W	285.60	326.1	366.6	473.5	481.3	539.2	552.3	663.4
141/10-30-002-24W3	49.15471N	109.19522W	274.80	304.9	346.6	442.4	453.9	523.7	540.2	653.9
141/06-32-002-24W3	49.16600N	109.17909W	310.70	347.5	389.8	471.4	487.2	557.1	574.9	686
131/09-32-002-24W3	49.17003N	109.17070W	304.70	342.2	379.6	486	496.7	548.6	568.9	680
111/05-15-002-25W3	49.12077N	109.27393W	224.30	252.2	310.8	418.8	423.2	463.1	479.6	594.5
141/10-25-002-25W3	49.15459N	109.21844W	281.90	310	354.8	450.8	460.9	520.1	543.5	654.6
141/06-28-002-25W3	49.15144N	109.29051W	222.10	246.3	297.1	395.7	406.3	471	490.1	602.5
141/06-29-002-25W3	49.15120N	109.31301W	193.90	215.5	285.3	377.5	389.5	444	474.6	589.5
101/09-33-002-25W3	49.16837N	109.28074W	273.40	303.9	339.5	419.8	432.2	496.1	519.8	636
101/06-06-002-26W3	49.09267N	109.47006W	155.90	178.8	219.5	316.6	332.5	378.8	397.2	535
101/12-13-002-26W3	49.12546N	109.36359W	143.10	173.6	230	336.7	357.5	401.2	431.4	560.3
131/11-14-002-26W3	49.12593N	109.38099W	135.20	156.2	212.7	305.2	319.9	374.3	389.2	532.1
121/11-33-002-26W3	49.16813N	109.42531W		195	239.8	338.7	352	397.5	430.4	549.5
121/10-15-002-26W3	49.12382N	109.39959W	131.00	152	199.5	304.4	314.7	364	374.9	519
101/09-20-002-26W3	49.13969N	109.43650W	157.50	183	225.4	335.6	353.8	388.5	398.8	540.4
121/06-22-002-26W3	49.13443N	109.40409W	170.20	195.6	232.4	337.2	346	377.3	389	548
131/06-05-002-27W3	49.09298N	109.58224W	143.20	167.4	208.8	326.9	340.5	379	390.9	532.5
141/06-05-002-27W3	49.09388N	109.57954W	142.70	170	213	323.9	348	380	389.1	532
101/11-15-001-27W3	49.03786N	109.53687W	112.8	154.7	182.5	293.8	313.8	351.1	368.7	508.4
141/14-03-002-28W3	49.10110N	109.66954W	115.10	137.4	182.7	295.1	308.5	340	350	498
101/11-24-002-28W3	49.13973N	109.62566W	125.00	154.2	190.6	304.9	317.9	353.6	370.1	513
101/10-32-002-28W3	49.16876N	109.70935W	110.80	136	170.2	277.4	298.4	338.6	357.2	507
131/07-12-003-21W3	49.19521N	108.70411W	260.80	296.5	320.5	447.4	463.2			622.1
101/14-34-003-21W3	49.26016N	108.75449W	262.30	302	325.8	447.5	463			626.2
101/02-26-003-22W3	49.23439N	108.86109W	240.30	286	312.7	439.7	454.5			624.5
101/05-11-003-22W3	49.19425N	108.87212W	272.80	296.1	329.2	434.5	447.8	507	513.3	610.8
121/13-07-003-23W3	49.20110N	109.09786W	288.80	326.5	375.2	479.8	492.3	549.2	564.4	673

101/11-20-003-23W3	49.22679N	109.06769W	252.70	288.4	335.2	444.5	459.5	515.6	525.7	635.6
101/13-20-003-23W3	49.23106N	109.07430W	255.90	290	338.8	442.3	455.3	518.8	531.5	640.1
111/11-28-003-23W3	49.24093N	109.04464W	242.80	275.8	325	435.8	445	508.3	517.1	627
131/13-02-003-24W3	49.18836N	109.14167W	287.30	327	370.1	485.8	490.2	544	555.3	671.5
101/06-03-003-24W3	49.17976N	109.15847W	296.30	332.7	374.7	480.5	488.6	542.1	559.2	671.6
131/10-18-003-24W3	49.21337N	109.22078W	296.90	320.5	386.1	484.5	492.6	547	561	678.5
101/09-19-003-24W3	49.22708N	109.21417W	305.60	334.8	372.4	478.7	487	541.6	554.6	673.3
131/12-19-003-24W3	49.22748N	109.23100W	275.60	307.3	359.4	461.2	468	526.2	542.3	658.5
111/12-29-003-24W3	49.24084N	109.20717W	290.50	317.5	372.5	462.3	473	530.5	544.9	659.8
141/16-30-003-24W3	49.24579N	109.21375W	277.90	296.1	328.9	457.8	465.3	520.9	532.2	649.8
131/06-01-003-25W3	49.18027N	109.24871W	365.9	387.7	417.6	518.9	531.4	586.4	606.1	722.3
101/06-31-003-25W3	49.25272N	109.35977W	233.20	268.1	303	418.7	424	476	500	622.5
141/03-35-003-25W3	49.25028N	109.26890W	254.60	271.1	315.5	432.4	444	503.8	520	636.2
111/11-35-003-25W3	49.25481N	109.26802W	233.90	254.2	311.4	413.1	424.9	483.8	501.9	616.8
121/06-11-003-26W3	49.19365N	109.40455W	183.90	206.7	256.2	355.2	366	413.8	425.2	566.8
101/14-25-003-26W3	49.24526N	109.38198W	255.60	281.5	335.9	432.5	442	486.6	508.4	636
111/12-31-003-26W3	49.25551N	109.49880W	172.90	195.6	232.6	337.2	359.5	395.2	420.5	545.6
101/04-35-003-26W3	49.24874N	109.41064W	213.40	240	276.1	392.2	401	448	472.5	596.3
141/14-08-003-27W3	49.20277N	109.60370W	127.30	159	202.2	314	323.9	364.1	386.4	516.6
101/07-13-003-27W3	49.20890N	109.51150W	147.60	176.5	215.7	330.4	350	385	407.9	533
141/06-19-003-27W3	49.22482N	109.62656W	167.40	189.3	230.7	334.8	356.7	391	418.8	549
141/06-21-003-27W3	49.22445N	109.58278W	144.90	166.5	214.2	319.3	334.5	373	396.3	526.5
111/07-35-003-27W3	49.25185N	109.53256W		209	241.8	362	370.5	409.6	434.4	559.5
101/10-02-003-28W3	49.18349N	109.66801W		169.9	208.7	311.2	323.5	362.2	373.8	516
101/06-03-003-28W3	49.17982N	109.69601W	120.90	157.7	194.6	291.1	304.8	346.1	366	503.8
111/07-05-003-28W3	49.17918N	109.73434W		128.8	173.2	280.5	293.9	325.4	344.7	485
141/08-05-003-28W3	49.17971N	109.72758W		122.5	176	269.7	285.3	329.7	342.5	489.1
141/06-07-003-28W3	49.19575N	109.76129W		148.4	180.3	272.3	294.2	344.2	359.5	499.9
141/16-08-003-28W3	49.20277N	109.72758W		175.4	206.6	287.9	313.3	367.6	383.1	526
121/10-09-003-28W3	49.19652N	109.71356W		146.2	200.8	310	332.8	353.3	374.7	510
141/06-10-003-28W3	49.19515N	109.69473W		161.7	217.7	337.5	355.3	371	394.7	527.4
141/08-10-003-28W3	49.19574N	109.68284W		162.5	206.9	324.6	344.5	369.4	380	525.5
141/14-14-003-28W3	49.21693N	109.67259W		182.5	226.7	329.9	351	389.3	404	541.8
101/07-34-003-28W3	49.25255N	109.69047W		195.7	239.5	346.2	367.9	395.2	403.5	548
101/07-35-003-28W3	49.25258N	109.66813W		189	225.5	335.4	353.6	391.5	414.4	547.1
121/10-15-003-29W3	49.21134N	109.82734W		112	150	272.3	277.8	313.4	327.2	469
101/11-32-003-29W3	49.25617N	109.87536W		147.2	187.8	308	327.7	353	369.5	513.6
121/10-35-003-29W3	49.25482N	109.80474W		161.6	194.5	317.6	337.2	360.9	383.7	522.8
141/08-36-003-30W3	49.25313N	109.90860W		166.3	205.4	332.6	355.5	363.1	387.3	531.4
121/06-07-004-21W3	49.28156N	108.82280W	276.40	310.7	362.7		451.7			641.5
111/05-16-004-21W3	49.29529N	108.78112W	291.80	331.3	386.6		489.4			656.9
111/16-28-004-21W3	49.33269N	108.76496W	306.40	343.9	400.1		495.1			669
101/14-19-004-22W3	49.31798N	108.95621W	333.40	376.6	410.8	526.4	543.2			732.9
101/15-09-004-22W3	49.28891N	108.90591W	306.9	348.8	398	509.7	512.7			687.3
101/16-33-004-22W3	49.34713N	108.90037W	389.30	427.4	466.8	586.2	601.7			760.8
121/10-31-004-23W3	49.34190N	109.08800W	278.10	313.7	350.9	463.4	474.6	534	543.5	657.2
141/15-04-004-24W3	49.27571N	109.17364W	238.40	271.4	317.1	418.7	433	491	502.5	620
101/11-15-004-24W3	49.30010N	109.15856W	257.20	282.6	315.3	430.9	436.3	494	502.3	622.3
141/12-28-004-24W3	49.33076N	109.18472W	226.10	250.3	286.7	403.9	415.5	468.7	482.7	597.6
101/10-09-004-25W3	49.28525N	109.30938W	214.60	239.9	289.7		398.9	462.1	481.3	602.6
111/11-14-004-25W3	49.29857N	109.26793W	213.10	235.9	277.2	377.5	405	460	481	594.7
121/06-20-004-25W3	49.31073N	109.33857W	189.30	215	276.8	374.3	383.5	439	452.2	576
101/06-24-004-25W3	49.31054N	109.24733W	220.50	238.3	299	396.4	407	464.8	479.6	597.1
121/06-26-004-25W3	49.32467N	109.27117W	207.40	228	276.8	389.8	406.8	453	470.3	589
131/07-28-004-25W3	49.32674N	109.31133W	195.90	218	261.1	373.1	389.4	435.5	459.3	578

101/06-30-004-25W3	49.32544N	109.35975W	196.10	224.9	281.4	372.6	389.1	442	456.4	579
131/11-32-004-25W3	49.34404N	109.33801W	194.00	220	280.4	377.6	383.5	443	460.7	582
131/10-33-004-25W3	49.34426N	109.31168W	202.40	229.6	285.5	376.1	387	443	460.2	584
111/06-36-004-25W3	49.33987N	109.24591W	220.60	241.1	297.4	398.4	415.6	470.9	484.8	603.5
141/07-03-004-26W3	49.26892N	109.42037W	211.80	232	280.2	395.6	402.5	443.7	455.5	592
141/08-14-004-26W3	49.29692N	109.39149W	198.90	224	263.4	357.4	373.9	439.9	460.3	587.9
101/10-21-004-26W3	49.31437N	109.44379W	184.50	207.4	256.4	354.7	362.3	413.8	433.5	561.1
141/08-24-004-26W3	49.31081N	109.36899W	192.20	220.1	255.7	368.4	376.1	434.7	448.7	573.8
101/07-25-004-26W3	49.32539N	109.37664W	193.30	221.2	260.6	373.4	379.5	436.2	453.6	574.9
131/15-27-004-26W3	49.33312N	109.42158W	187.20	215	269.8	373.9	388.5	434.3	447.6	567.6
141/16-31-004-26W3	49.34752N	109.48217W	174.10	197	246.5	351.9	367.2	403.5	425.6	554.5
101/07-35-004-26W3	49.33987N	109.39911W	185.90	202.4	260.3	361.3	372.5	428.5	444.9	567.5
131/13-10-004-27W3	49.28998N	109.56898W	177.80	200.4	243.8	349	358.2	396.5	416.5	546.7
131/06-16-004-27W3	49.29720N	109.58398W	183.00	205.5	255.1	354.8	368.7	402.3	421.8	554.5
141/14-17-004-27W3	49.30454N	109.60436W	170.80	192	246.7	331.7	348.9	392.8	411.7	545.7
101/10-18-004-27W3	49.29993N	109.62318W	164.50	191.7	239.4	333.4	352.5	391.7	412.1	547.4
131/07-20-004-27W3	49.31114N	109.60168W	171.30	200.5	245	344.9	359.4	405.9	427.8	550.4
111/14-34-004-27W3	49.34659N	109.56048W	183.30	201	246.8	348.2	363.4	402	419.5	556
141/06-03-004-28W3	49.26780N	109.69497W		190.9	242.8	346.9	359.6	399	420.6	552
131/10-08-004-28W3	49.28603N	109.73593W		180	214.8	334.8	357	383	401	535
141/06-09-004-28W3	49.28307N	109.71628W		171.2	209	327.2	342	383.9	400.8	534.8
101/10-13-004-28W3	49.29981N	109.64585W		201	240.3	342.1	362.4	402.7	421.9	555.9
141/10-15-004-28W3	49.29999N	109.68946W		195.7	234.7	343.5	362.5	403	421	555
141/06-17-004-28W3	49.29767N	109.73876W		183	231.8	341	350.9	389	403.2	541
111/09-24-004-28W3	49.31331N	109.63843W		202.6	251.7	343.2	359.9	399.1	420.6	555.9
111/11-24-004-28W3	49.31377N	109.64939W		199.9	246	347.2	364	402.8	422.6	554
141/16-30-004-28W3	49.33402N	109.75008W		192.5	237.3	347.6	370.5	397	411.4	553
141/06-25-004-29W3	49.32681N	109.78356W		180	224.7	332	351.5	392	408.2	548.5
141/06-32-004-29W3	49.34116N	109.87513W		172.1	220.4	330.9	347.6	373.7	389.3	532.2
101/02-10-005-21W3	49.36505N	108.74905W	291.90	327.7	356.7	467.1	486.2			653.2
141/08-11-005-21W3	49.37012N	108.72011W	292.30	330.5	357	473.9	495			657.4
131/10-03-005-22W3	49.35871N	108.88364W	406.30	441.9	481.2	596.2	618			772.7
141/14-06-005-22W3	49.36279N	108.95620W	362.90	403.5	460.6	562.3	575			752.2
121/02-18-005-22W3	49.37944N	108.95159W	354.70	399.8	449.9	554	556.9			740.1
141/08-19-005-22W3	49.39862N	108.94386W	359.60	400.2	439.6	541.2	565.3			745
101/07-29-005-24W3	49.41233N	109.19740W	263.50	296.1	338.5	434.7	446.5	508.6	527.7	640.1
141/06-01-005-25W3	49.35588N	109.24556W	226.40	245.5	307.6	409	419	474.8	489.3	608
111/07-02-005-25W3	49.35365N	109.26328W	219.90	241.4	307.5	397.7	409.9	466	484	601.5
121/06-06-005-25W3	49.35404N	109.36046W	191.40	216	270.1	359.9	377.5	435	444.4	573
101/07-07-005-25W3	49.36904N	109.35423W	206.40	233.8	285.4	373.5	389.2	449.9	464.2	588
111/12-14-005-25W3	49.38586N	109.27552W	217.10	241.5	308.2	391.6	408	463	481.2	602.5
131/11-19-005-25W3	49.40249N	109.36079W	226.20	251.7	301.1	393.5	405.9	463.1	477.7	601.5
131/11-23-005-25W3	49.40190N	109.27124W	226.80	271.3	316.9	408.3	421.5	478	493.5	611
141/06-28-005-25W3	49.41431N	109.31352W	231.30	260.7	318.9	405.5	419.5	478.9	495.4	618
141/07-01-005-26W3	49.35609N	109.37654W	198.40	223.5	282.4	376.7	387	441.5	457.4	580
101/06-06-005-26W3	49.35453N	109.49355W	174.20	196.6	245.3	354.6	369.8	407.8	425.7	558.4
111/11-07-005-26W3	49.37169N	109.49371W	181.40	205.2	257.6	373.1	387.1	416	434.1	563
131/07-18-005-26W3	49.38457N	109.49018W	183.00	209.1	260.5	374.8	386.2	418.8	438.3	567.2
101/10-21-005-26W3	49.40182N	109.44401W	205.40	235.6	282.9	377.9	387.1	446.7	460.7	588.3
141/13-23-005-26W3	49.40652N	109.40751W	219.00	249.1	290.1	377.6	394.2	459	469.2	593
131/11-25-005-26W3	49.41714N	109.38316W	226.30	248.8	301.3	388.9	405.7	470.6	482.8	605.4
141/07-27-005-26W3	49.41404N	109.42038W	214.40	240	285.5	380.8	395	458	470.9	593.5
111/07-28-005-26W3	49.41211N	109.44384W	209.30	231	280.9	379.9	392	456.5	469.7	593.5
121/06-29-005-26W3	49.41238N	109.47263W	210.60	235	274.1	381	396.1	449	464.4	591
101/10-07-005-27W3	49.37264N	109.62317W	171.10	193.5	241	349.6	365.8	397.5	415	555.3
101/11-12-005-27W3	49.37257N	109.51667W	183.00	204.2	238.9	346.5	356	409.7	430.7	559.6
131/07-13-005-27W3	49.38451N	109.51252W	188.60	212	254	352.4	369	417.5	435	569
101/10-15-005-27W3	49.38699N	109.55640W	182.20	206.3	247	344.5	360.9	415.1	434.9	565.1

111/07-17-005-27W3	49.38308N	109.59976W	169.90	199.9	231.8	339.8	359	405.2	424.9	557.6
141/08-01-005-28W3	49.35496N	109.63799W		198.9	249.1	342.2	362.1	403	419.3	559.6
101/11-13-005-28W3	49.38729N	109.65123W	175.40	194.5	240.3	346.3	359.7	410	428.1	567.2
141/07-25-005-28W3	49.41424N	109.64556W		212	263	355.5	370	422.1	442.2	580
101/10-33-005-28W3	49.43090N	109.71290W	234.10	252.3	275.2	392	405.4	446.5	463.2	603.5
141/14-07-005-29W3	49.37681N	109.89676W		192	218.7	347.5	367	397.5	416.4	556.7
101/07-13-005-30W3	49.38368N	109.91477W		200	229.3	351.2	370	397.8	418.5	563.9
101/07-21-006-21W3	49.48550N	108.77144W	288.10	330	350.1	476.1	500.8			650.7
101/14-08-006-21W3	49.46354N	108.79865W	302.50	343.1	366	486.6	498.7			672.7
101/16-14-006-21W3	49.47804N	108.72149W	246.00	286.6	308.2	432.7	459			620
101/03-11-006-22W3	49.45270N	108.86645W	349.20	396.2	419.1	537.2	557.2			724.5
101/04-16-006-22W3	49.46773N	108.91703W	385.20	425.8	458.9	578.2	594.4			768.1
101/08-03-006-22W3	49.44198N	108.87787W	364.50	405.1	438.1	548.6	566.4			738.5
101/13-11-006-22W3	49.46326N	108.87213W	348.70	390.6	418.5	548.1	556			730.3
101/16-12-006-22W3	49.46348N	108.83308W	307.50	348.2	368.5	495.5	511.5			682.8
141/16-05-006-22W3	49.45044N	108.92067W	382.90	426.1	457.2	577.9	590.3			767.1
141/14-03-006-23W3	49.45052N	109.02154W	369.80	406.6	443.4	560.3	567.6			747.6
141/14-12-006-23W3	49.46484N	108.97702W	439.30	471.6	521.2	638	654.5			822.8
111/06-11-006-24W3	49.45731N	109.13462W	304.40	350	387	493	501.6	539.4	554.6	688.6
121/04-11-006-24W3	49.45297N	109.14302W	311.40	357.1	395.2	494.3	513.4	551.5	566.7	695.6
141/14-09-006-25W3	49.46496N	109.31336W	321.50	346.9	407.8	492.7	504.3	561.2	576.7	699.3
141/16-22-006-25W3	49.49341N	109.28032W	314.50	341.6	388.2	477.1	497.8	553.3	573.6	691.1
141/11-26-006-25W3	49.50381N	109.26915W	319.20	344.7	384.5	495.7	518.6	559.6	578.3	694.5
141/06-31-006-25W3	49.51467N	109.35772W	327.50	350.7	391.3	491.6	504.9	554.5	575.4	698
121/06-02-006-26W3	49.44125N	109.40572W	249.90	276	323.9	409.9	425	488.5	500	622.6
101/03-03-006-26W3	49.43862N	109.42764W	235.90	260.5	300.8	400.8	408.9	472.6	482.7	605.3
131/12-32-006-26W3	49.51925N	109.47953W	334.00	357.7	414.6	502.9	515.6	568.2	585.5	701.7
101/10-10-006-27W3	49.46007N	109.55585W	250.70	273.9	304.6	433.9	442.3	485.2	504.7	627.3
141/11-18-006-28W3	49.47546N	109.76144W		284	337.9	433.7	450.6	491.2	504.1	649.5
101/07-19-006-28W3	49.48563N	109.75803W		318.9	361	463.9	480.1	521	540.1	677.9
141/07-33-006-28W3	49.51527N	109.71254W		346.9	393.3	496.6	517.6	557.5	577	705.9
101/07-12-006-29W3	49.45621N	109.78073W		280.4	319.6	420.6	441.4	483.1	508.1	639.5
101/07-14-006-29W3	49.47144N	109.80280W		277	328.2	413.4	435.3	491.8	507.2	647.5
101/11-18-006-29W3	49.47469N	109.89870W		342.5	386.6	495.2	519.1	547.8	568.2	706
141/16-21-006-29W3	49.49407N	109.84020W		306.2	378.6	453.2	475	503.2	521.1	664
131/11-27-006-29W3	49.50424N	109.83191W		308.3	356.6	445	469.2	512.7	532	666
141/11-29-006-29W3	49.50428N	109.87383W		316.8	362.4	465.1	487	531	551.5	684.2
121/06-32-006-29W3	49.51391N	109.87792W		359	410	518.1	528	566	587.5	725.3
101/12-34-006-29W3	49.51815N	109.83662W		322.5	359.1	464.5	483.6	523.2	545.8	679.8
121/10-14-006-30W3	49.47287N	109.93941W		341	384.6	477.6	507	542.5	564.9	707.8
101/09-21-006-30W3	49.48913N	109.97687W		339.7	382.2	482.7	503.5	526.2	549.1	698.3
141/11-25-006-30W3	49.50405N	109.91857W		369	410.9	525.2	553	579.8	593.8	737.9
111/06-35-006-30W3	49.51392N	109.94196W		412.5	449.5	557.3	578.8	606	620.8	766.2
141/11-36-006-30W3	49.51882N	109.91808W		428	480.6	582.6	603.5	630	650.8	783.5
101/03-29-007-21W3	49.58405N	108.81971W	437.80	472.1	509	627.1	645.6			814.4
101/05-33-007-21W3	49.60191N	108.80180W	458.80	494.4	521.1	643	664.6			830.3
101/13-22-007-21W3	49.58000N	108.77938W	297.50	333	357.2	477.8	491.8			671.5
101/15-30-007-21W3	49.59461N	108.83631W	463.40	501.5	535.8	657.8	674.3			840

121/04-22-007-21W3	49.56789N	108.78140W	276.80	319.2	346.7	462.2	483.9			652.1
131/03-34-007-21W3	49.59891N	108.77480W	439.20	474.8	498.9	620.9	641.3			803.1
131/12-32-007-21W3	49.60666N	108.82676W	469.60	501.4	535.6	655.5	675			836
131/13-34-007-21W3	49.60987N	108.78121W	462.50	492.4	524.7	655.9	673			828.9
101/08-02-007-22W3	49.52920N	108.87503W	370.90	405.4	445.8	556	571.5	633.8	655.4	744.9
101/02-28-007-23W3	49.58381N	109.06147W	433.20	459.8	503.1	599.3	609.6	683.4	697.4	804.7
101/03-21-007-24W3	49.56905N	109.20319W	358.60	391.6	412	533.9	547.8	597.4	611.3	721.2
121/06-15-007-24W3	49.55750N	109.18326W	325.50	357.6	411.9	511.3	519	579.5	594.7	708.4
141/08-05-007-25W3	49.52993N	109.34920W	337.20	361.6	402.3	509.6	516.9	568.3	584.8	711.2
101/05-32-007-25W3	49.60195N	109.36711W	386.80	414.4	455	550.3	560.4			745.2
101/06-08-007-25W3	49.54367N	109.36138W	359.50	384.7	433.3	538.9	547.7	591.9	608.4	732.2
141/10-23-007-25W3	49.57647N	109.28703W	386.50	415.4	456.1	564	571.6	625	647.8	757.7
121/07-32-007-25W3	49.60183N	109.35639W	427.90	449.6	489.9	599.4	612.1	656.5	674.3	791.8
101/06-26-007-26W3	49.58798N	109.42911W	348.90	372.9	412	513	527.9	573.7	588.9	714
111/08-33-007-26W3	49.60201N	109.46204W	437.20	462.7	496.3	591	602.4	658.3	672.2	798.6
121/16-12-007-27W3	49.55100N	109.53179W	379.80	400.5	443.3	540.2	547.6	608.4	622.4	750
101/04-04-007-28W3	49.52582N	109.75069W		374.3	424.4	526	534.9	565.1	578.1	727.3
101/07-10-007-28W3	49.54398N	109.71762W	381.50	400.5	424.6	516.1	533.9	574.5	588.5	728.8
101/16-23-007-29W3	49.58011N	109.82426W		461.4	509.7	627.8	630.3	671	688.8	820.2
121/10-06-007-29W3	49.53225N	109.92160W		520.5	568.5	678	695.5	727.9	741.2	881.5
121/10-07-007-29W3	49.54645N	109.92252W		562	608.9	715.8	732.3	767.7	784.2	922
101/02-23-007-30W3	49.56909N	109.96517W		554.1	589.1	708.5	726.6	753	772	918.7
101/06-15-007-30W3	49.55848N	109.99325W		556.7	592.1	712.7	729.1	757.7	776.2	922.9
101/10-01-007-30W3	49.53255N	109.94339W		488.2	539.7	647	663	695	713.7	854
101/06-01-008-21W3	49.61655N	108.72812W	317.30	351.6	387.2	519.3	530.4			688.8
101/07-07-008-21W3	49.63056N	108.83653W	451.20	488	523.5	655.3	664.5			823.9
101/11-04-008-21W3	49.61988N	108.79643W	433.60	469.1	503.4	630.4	645.3			802.5
101/11-17-008-21W3	49.64924N	108.81908W	453.70	491.8	526.1	648	659.9			823.9
141/16-07-008-21W3	49.63954N	108.82870W	459.30	502.5	527.9	651.4	667.1			827
101/02-02-008-22W3	49.61297N	108.88158W	458.20	487.4	531.9	647.5	659.6			829.7
101/03-23-008-22W3	49.61297N	108.88158W	458.00	491	535.5	647.2	664.5			833.3
131/06-30-008-24W3	49.67492N	109.24901W	479.30	502.1	540.6	657.4	664.5	711.7	726.9	840.6
101/01-23-008-25W3	49.65630N	109.28255W	472.40	501.3	548.3	641	654.1	699.5	717.2	830.9
121/10-09-008-25W3	49.63413N	109.33316W	388.00	415.2	448.2	554.9	563.9	615.8	633.8	749.8
131/06-32-008-25W3	49.69072N	109.36198W	489.60	509.2	556.1	653.9	662.1	711.1	728.9	843.8
141/06-17-008-25W3	49.64686W	109.36029W	416.40	439.3	472.3	572.5	583.2	642.5	657.7	773.9
101/06-18-008-26W3	49.64584N	109.51935W	502.40	527.4	568.5	672.6	684	723.4	745	865
131/11-11-008-26W3	49.63535N	109.43000W	397.10	419.9	454.2	546.9	557.1	611.7	630.7	757.1
141/16-01-008-26W3	49.62530N	109.39340W	362.70	387	421.1	524.6	546.9	586.2	598.9	725.3
101/11-20-008-27W3	49.66410N	109.63309W	344.80	364.5	398.3	510.7	531.6	567	586.1	709.9
121/10-10-008-27W3	49.63451N	109.58253W	509.20	529.6	567.7	674.3	692.8	732.8	751.8	876
141/07-07-008-28W3	49.63166N	109.78376W		439.8	471.7	583.4	601.1	641.3	659.6	794.9
101/10-34-008-29W3	49.69288N	109.85234W		362	391.2	500.5	523	558.9	570.2	713.2
101/10-23-008-30W3	49.66365N	109.96517W		482	513.7	633.1	647.7	680.1	699.1	838.2

Appendix D

Sequence Stratigraphy and Depositional Environments of the Belly River Group (Campanian) in southwestern Saskatchewan, Canada: Incised and Unincised Fluvial Systems along an Epicontinental Seaway

Supplementary Cross Sections

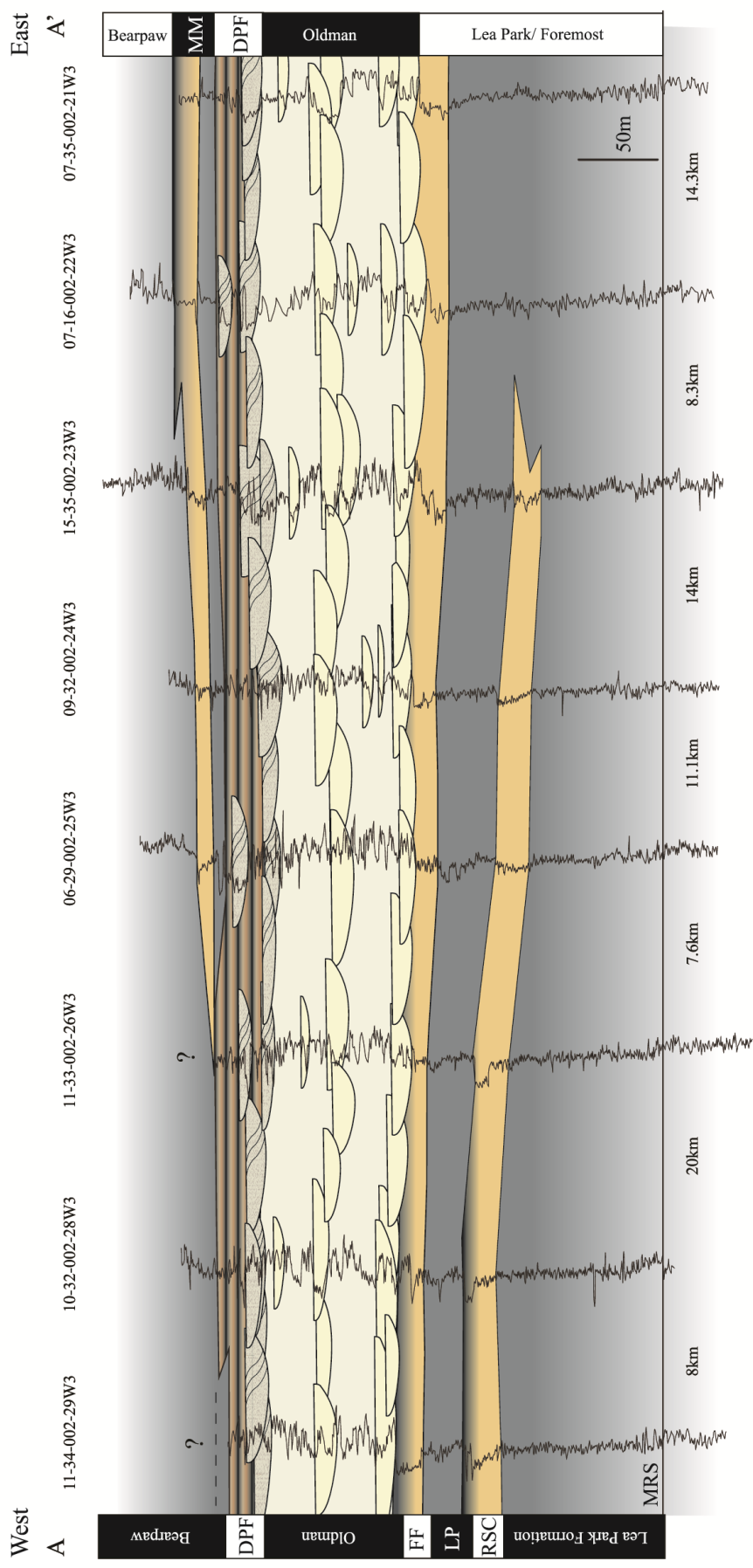


Figure D.1: Dip-oriented cross section through Township 2.

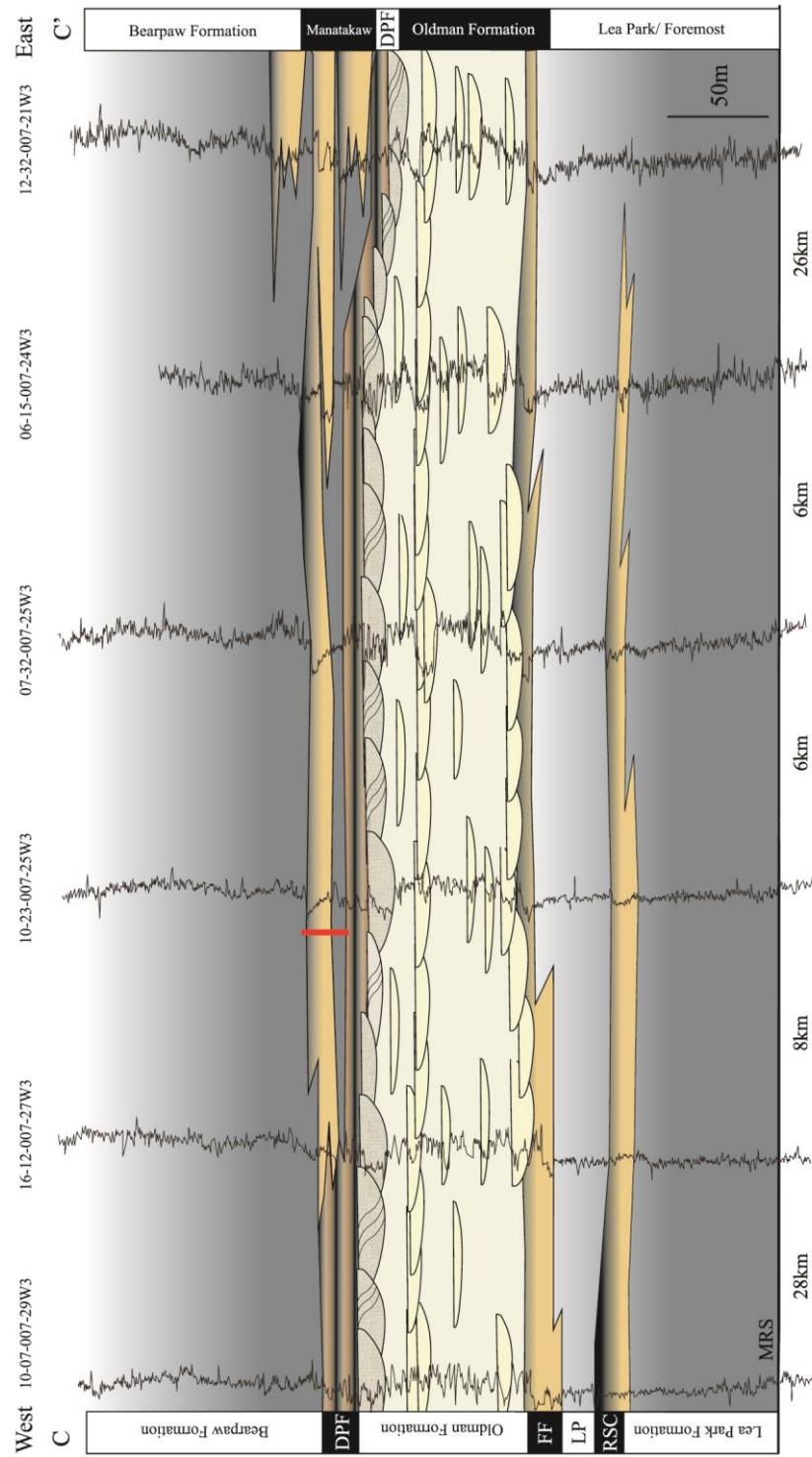


Figure D.2: Dip-oriented cross section through Township 7.

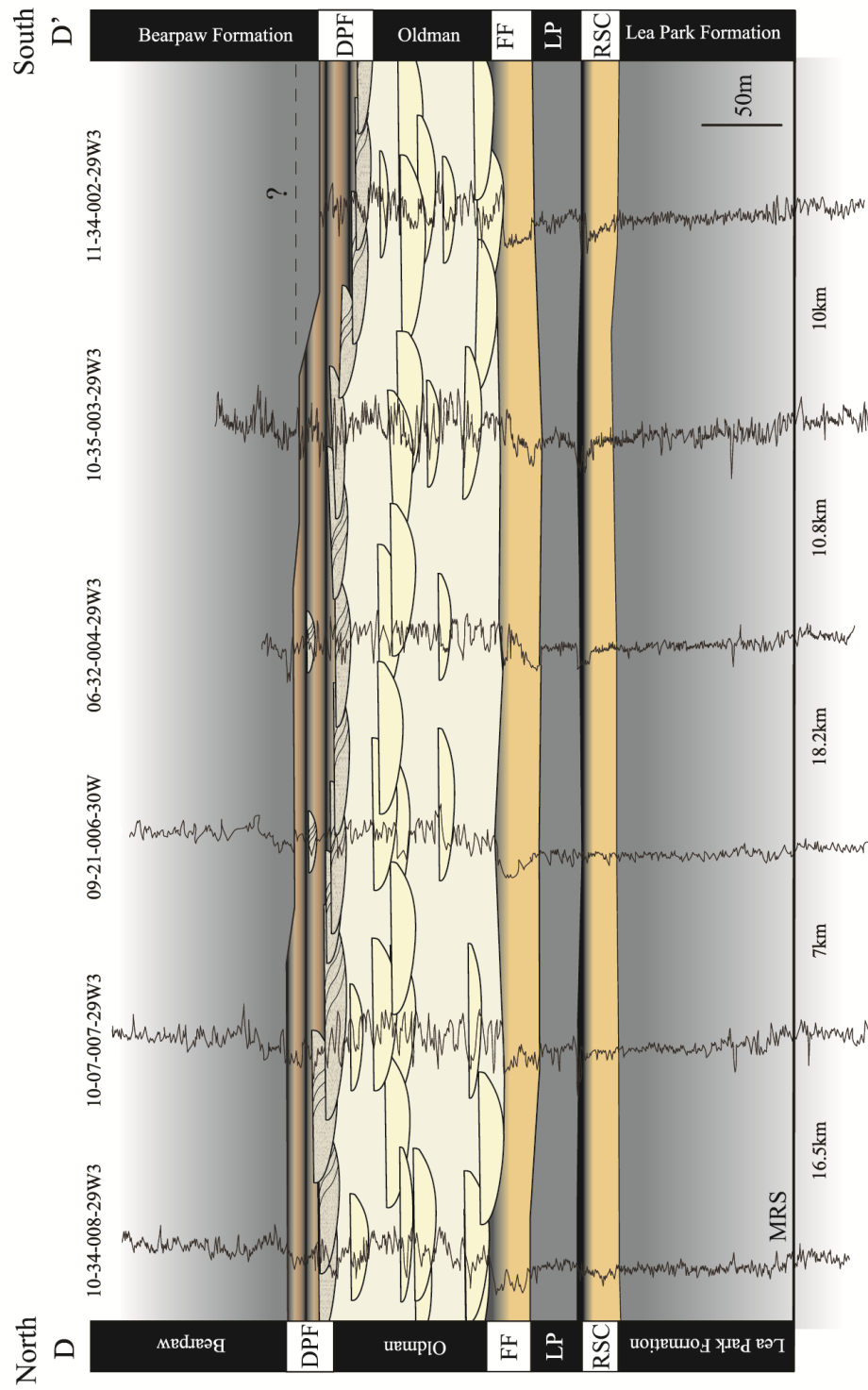


Figure D.3: Strike-oriented cross section through Range 29/30.

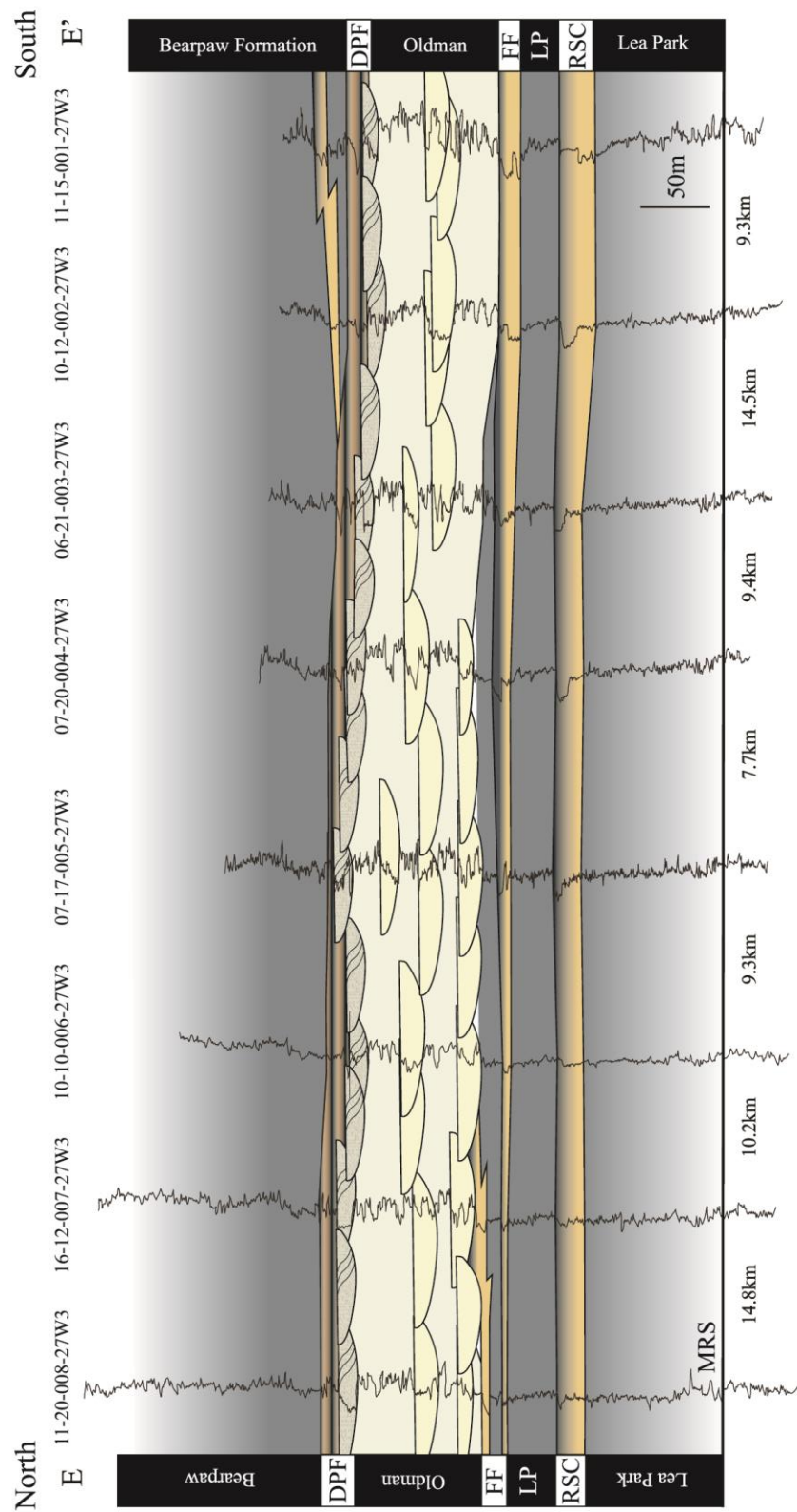


Figure D.4: Strike-oriented cross section through Range 27.

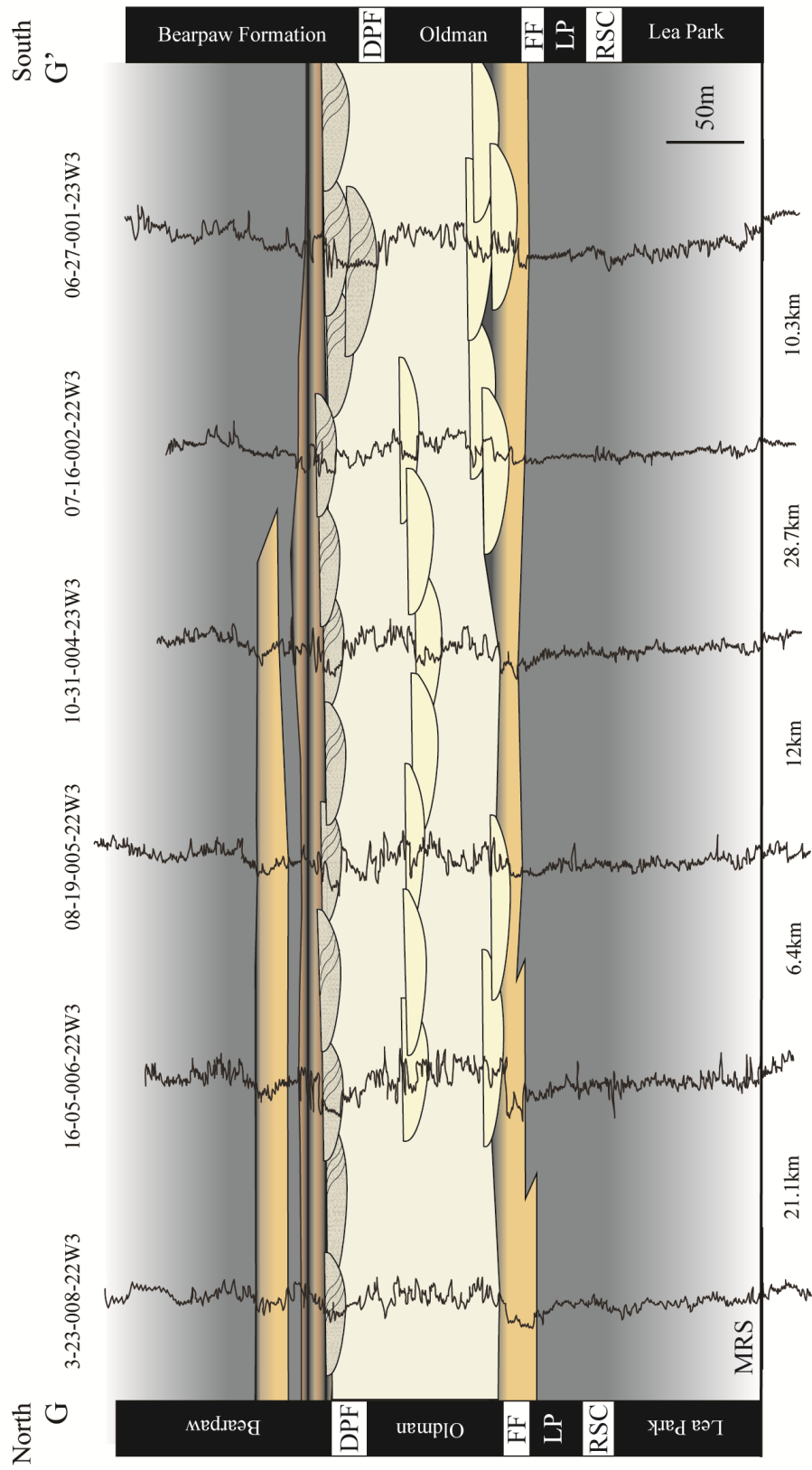


Figure D.5: Strike-oriented cross section through Range 22/23.

Appendix E

A New Dinosaur Park Formation (Campanian, Late Cretaceous) Microvertebrate Locality
from the Cypress Hills Region of Southwestern Saskatchewan: Implications for
paleoenvironmental controls on species alpha diversity

Supplementary Palynology Data

Samples	1	2	3	4	5	6	7	8	9	10
Meterage	0	3	7.5	10.5	13.5	18	24	36	43.5	52.5
<i>Accuratipollis lactifluminis</i>	x									
<i>Accuratipollis macrosolenoides</i>										
<i>Aequitriradites spinulosus</i>				x		x		x	x	
<i>Alisporites bilateralis</i>			x			x	x			
<i>Alutisporites</i> sp.	x									
<i>Annulispora salsa</i>										
<i>Appendicisporites undosus</i>									x	
<i>Aquilapollenites amicus</i>									x	
<i>Aquilapollenites attenuatus</i>	x		x	x	x			x		
<i>Aquilapollenites augustus</i>										
<i>Aquilapollenites bellus</i>										
<i>Aquilapollenites clarireticulatus</i>		x	x	x	x	x	x	x		
<i>Aquilapollenites drumhellerensis</i>										
<i>Aquilapollenites funkhouseri</i>		x			x					x
<i>Aquilapollenites leucocephalus</i>										
<i>Aquilapollenites</i> cf. <i>leucocephalus</i>										
<i>Aquilapollenites mtchedlishvili</i>			x	x						
<i>Aquilapollenites notabile</i>										
<i>Aquilapollenites quadrilobus</i>										
<i>Aquilapollenites quadrilobus</i>	x	x	x		x	x	x	x	x	x
<i>Aquilapollenites rectus</i>					x					
<i>Aquilapollenites rigidus</i>	x	x	x	x	x	x	x	x	x	
<i>Aquilapollenites senonicus</i>		x				x				
<i>Aquilapollenites stelckii</i>	x		x	x	x	x	x	x		x
<i>Aquilapollenites trialatus</i>	x	x	x	x	x	x	x	x	x	x
<i>Aquilapollenites turbidus</i>	x	x	x	x	x	x	x	x	x	x
<i>Aquilapollenites</i> spp.	x	x	x	x	x	x	x			x
<i>Arecipites barakati</i>										x
<i>Arecipites</i> sp.										
<i>Asterisporites chlonovae</i>	x									
<i>Azonia calvata</i>	x								x	
<i>Azonia cribrata</i>	x	x	x		x	x			x	
<i>Azonia jacutense</i>					x					
<i>Azonia pulchella</i>		x	x	x	x		x	x		
<i>Azonia recta</i>		x	x	x						
<i>Baculatisporites comaumensis</i>										
<i>Baculatisporites papillosus</i>						x		x	x	
<i>Baculatisporites</i> spp.		x		x						x
<i>Biretisporites psilatus</i>				x				x		
<i>Biretisporites</i> sp.										
<i>Camarozonosporites ambigens</i>		x	x	x	x	x		x		x

<i>Camarozonosporites amplus</i>						x				
<i>Camarozonosporites similis</i>					x					

<i>Camazonosporites</i> spp.			x							
<i>Cibotiumspora clavatus</i>			x							
<i>Cibotiumspora juncta</i>					x					
<i>Cicatricosisporites</i> spp.			x	x	x	x		x	x	
<i>Cingulatisporites dakotaensis</i>						x				
<i>Circulina parva</i>			x		x		x	x		
<i>Circumflexipollis tilioides</i>		x	x	x	x			x	x	x
<i>Cirratiradites luminosus</i>			x							x
<i>Classopollis classoides</i>			x					x		
<i>Conbaculatisporites</i> sp.									x	
<i>Concavisporites</i> sp.	x									
<i>Cranwellia rumseyensis</i>										
cf. <i>Cranwellia</i> sp.	x		x			x				
<i>Crassipollis</i> sp.							x			
<i>Cyathidites australis rimalis</i>		x		x	x	x			x	x
<i>Cyathidites minor</i>	x	x	x	x	x	x		x	x	x
<i>Cycadopites fragilis</i>	x	x	x	x	x			x		
<i>Cycadopites</i> spp.										
<i>Deltoidospora diaphana</i>				x						
<i>Distaltriangulisporites costatus</i>										
<i>Distaltriangulisporites mutabilis</i>			x							
<i>Dyadonapites reticulatus</i>										
<i>Echinatisporis solaris</i>					x	x		x	x	x
<i>Echinatisporis</i> spp.				x						
<i>Enzonalasporites bojatus</i>		x		x		x	x		x	x
<i>Equisetosporites amabilis</i>				x						x
<i>Equisetosporites hughesii</i>				x						
<i>Equisetosporites mollis</i>										
<i>Equisetosporites multicostatus</i>				x						
<i>Equisetosporites multistriatus</i>			x							
<i>Equisetosporites</i> spp.										
<i>Erdtmanipollis procumbentiformis</i>		x		x	x		x	x		
<i>Eucommiidites minor</i>						x		x	x	
<i>Eucommiidites troedssonii</i>				x						
<i>Expressipollis</i> sp.										
<i>Fibulapollis scabratus</i>	x	x	x	x	x	x	x	x	x	x
<i>Foraminisporis asymmetricus</i>						x		x	x	
<i>Foraminisporis undulatus</i>	x	x	x	x	x	x	x		x	x
<i>Foraminisporis</i> sp.										
<i>Foveosporites subtriangularis</i>				x	x	x				
<i>Foveosporites</i> sp.										
<i>Gabonisporis labyrinthus</i>		x	x	x						
<i>Gleichenioidites delicatus</i>			x	x						
<i>Gleichenioidites senonicus</i>		x	x	x	x	x	x	x		x
<i>Gleichenioidites stellatus</i>	x		x	x					x	
<i>Gleichenioidites</i> sp.										

<i>Grewipollenites canadensis</i>								X	X	
<i>Grewipollenites radiatus</i>	x		x	x	x			x		
<i>Gunnaripollis suberbus</i>										
<i>Hazaria sheopiarrii</i>										
<i>Heliosporites kemensis</i>		x	x	x	x	x			x	
<i>Inaperturotetradites scabratus</i>	x	x	x	x	x	x			x	
<i>Interulobites</i> sp.			x	x	x	x	x		x	x
<i>Klukisporites</i> sp.									x	
<i>Kurtzipites</i> sp.				x	x				x	
<i>Kuylisporites scutatus</i>			x							x
<i>Laevigatosporites haardti</i>	x	x	x	x	x		x	x	x	x
<i>Laevigatosporites nitidulus</i>						x				
<i>Laevigatosporites nitidus</i>										
<i>Laevigatosporites undulatiformis</i>										
<i>Liburnisporis adnacus</i>				x		x				
<i>Liliacidites mirus</i>										
<i>Liliacidites variegatus</i>		x			x					x
<i>Liliacidites</i> spp.	x		x	x		x				
<i>Lusatisporis dettmannae</i>			x							x
<i>Mancicorpus anchoriforme</i>					x		x		x	x
<i>Mancicorpus glaber</i>										
<i>Mancicorpus trapeziforme</i>	x									
<i>Mancicorpus tripodiformis</i>										
<i>Mancicorpus</i> sp.						x				
<i>Marcelloporites tolmanensis</i>										
<i>Mica hoodooensis</i>										
<i>Monosulcites riparius</i>	x		x							x
<i>Monosulcites</i> sp.				x		x				
<i>Orbiculapollis globosus</i>										
<i>Ornamentifera baculata</i>		x								
<i>Ovoidites ligneolus</i>										
<i>Palaeoisoetes subengelmanni</i>						x		x	x	
<i>Pediastrum boryanum</i>	x	x								
<i>Penetetrapites inconspicuus</i>			x	x	x	x		x	x	x
<i>Pilosporites</i> sp.										
<i>Pityosporites constrictus</i>		x		x	x				x	
<i>Pleurospermaepollenites</i> sp.	x			x	x	x	x	x	x	x
<i>Podocarpidites biformis</i>		x								
<i>Podocarpidites</i> spp.	x		x	x		x	x	x		x
<i>Polycingulatisporites reduncus</i>	x	x	x	x	x	x		x	x	x
<i>Polycingulatisporites</i> sp.	x									
<i>Polyporina cribraria</i>										
<i>Pristinupollenites microsaccus</i>	x	x	x	x	x	x		x		x
<i>Pristinupollenites</i> sp.		x								
<i>Pulcheripollenites krempii</i>	x	x	x	x		x			x	x
<i>Quadripollis krempii</i>						x				

<i>Reticuloidosporites pseudomurii</i>	x	x		x		x	x		x	
<i>Reticulospores reticulatus</i>								x		
<i>Retitriletes austroclavatidites</i>										
<i>Retitriletes mediocris</i>						x		x	x	
<i>Retitriletes spp.</i>		x	x	x	x	x		x		
<i>Rogalskaisporites cicatricosus</i>			x	x	x	x				x
<i>Scabrastephanocolpites albertensis</i>										
<i>Scabrastephanocolpites lepidus</i>										
<i>Scabrastephanocolpites pentaaperturites</i>										
<i>Schizosporites parvus</i>						x				
<i>Senipites drumhellerensis</i>										
<i>Sequoiapollenites paleocenicus</i>				x	x	x		x	x	
<i>Sequoiapollenites sp.</i>										x
<i>Sestrosporites pseudoalveolatus</i>					x					x
<i>Siberiapollis montanensis</i>										
<i>Siberiapollis spp.</i>		x	x	x	x					
<i>Sigmopollis carbonis</i>										
<i>Sigmopollis hispidus</i>							x			
<i>Stereigranisorites regius</i>						x				
<i>Stereisporites ancoris</i>										
<i>Stereisporites antiquasporites</i>	x	x	x	x	x	x		x	x	x
<i>Stereisporites antiquus</i>										
<i>Stereisporites cingulatus</i>		x	x	x	x	x		x	x	x
<i>Stereisporites rodaensis</i>			x							
<i>Stereisporites triangulopunctatus</i>										
<i>Stoverisporites lunaris</i>									x	
<i>Subtriporopollenites alpinus</i>										
<i>Syncolpites sp.</i>			x			x				
<i>Taxodiaceapollenites hiatus</i>	x	x	x	x	x	x	x	x	x	x
<i>Taxodiaceapollenites vacuipites</i>		x	x	x	x	x		x	x	x
<i>Tetranguladinium cruciformis</i>										
<i>Tetranguladinium sp.</i>										
<i>Tetraporina quadrata</i>	x									
<i>Tetraporina sp.</i>										
<i>Todisporites minor</i>										
<i>Translucentipollis plicatilis</i>										
<i>Tricolpites parvus</i>	x						x			
<i>Tricolpites reticulatus</i>	x									
<i>Tricolpites ringens</i>			x							
<i>Tricolpites spp.</i>	x	x	x	x	x	x				x
<i>Tricolpopollenites elongatus</i>					x					
<i>Tricolpopollenites levitas</i>										
<i>Tricolpopollenites spp.</i>										
<i>Tricolporites spp.</i>				x		x		x	x	x
<i>Trifossapollenites ellipticus</i>										
<i>Trilites bettianus</i>				x						

<i>Trilites</i> sp.	x							x		
<i>Trilobapollis laudabilis</i>										
<i>Triporoletes involucratus</i>	x	x	x	x	x	x		x	x	x
<i>Triporopollenites triplicatus</i>	x	x	x	x	x	x	x		x	x
<i>Triporopollenites</i> spp.		x	x		x		x	x	x	x
<i>Triquitrites absurdus</i>		x	x	x	x	x				
<i>Trochicola scollardiana</i>	x	x	x	x	x	x	x			
<i>Trudopollis meekeri</i>		x			x		x			x
<i>Trudopollis</i> sp.						x	x		x	x
<i>Tschudypollis retusus</i>								x		
<i>Tschudypollis thalmannii</i>	x	x	x		x	x				x
<i>Umbosporites callosus</i>	x	x	x	x	x	x	x	x	x	x
<i>Varugosporites tolmanensis</i>			x							
<i>Verrucatotrilites</i> sp.	x									
<i>Verrutricolpites</i> sp.								x		
<i>Virgo amiantopollis</i>										
<i>Vitreisporites pallidus</i>	x	x	x	x	x	x	x	x	x	x
<i>Wulongspora</i> sp.										
<i>Zlivisporis blanensis</i>				x						
<i>Zlivisporis cenomanianus</i>			x		x	x		x	x	x
<i>Zlivisporis novomexicanum</i>									x	
<i>Zlivisporis</i> spp.				x						x
Dinoflagellates	x	x	x	x	x	x	x	x	x	x

Samples	11	12	13	14	15	16	17	18	19	20
Meterage	66	67	71.5	136	174	178	188.5	217.5	229	233
<i>Accuratipollis lactifluminis</i>					x					
<i>Accuratipollis macrosolenoides</i>										
<i>Aequitriradites spinulosus</i>										
<i>Alisporites bilateralis</i>										
<i>Alutisporites</i> sp.										
<i>Annulispora salsa</i>						x				
<i>Appendicisporites undosus</i>										
<i>Aquilapollenites amicus</i>										
<i>Aquilapollenites attenuatus</i>								x	x	
<i>Aquilapollenites augustus</i>										
<i>Aquilapollenites bellus</i>						x				
<i>Aquilapollenites clarireticulatus</i>			x		x					
<i>Aquilapollenites drumhellerensis</i>						x				
<i>Aquilapollenites funkhouserii</i>										
<i>Aquilapollenites leucocephalus</i>										
<i>Aquilapollenites</i> cf. <i>leucocephalus</i>										
<i>Aquilapollenites mtchedlishvili</i>							x			
<i>Aquilapollenites notabile</i>										
<i>Aquilapollenites quadrilobus</i>								x		x
<i>Aquilapollenites quadrilobus</i>					x	x	x	x	x	
<i>Aquilapollenites rectus</i>										
<i>Aquilapollenites rigidus</i>										
<i>Aquilapollenites senonicus</i>										x
<i>Aquilapollenites stelckii</i>										
<i>Aquilapollenites trialatus</i>			x			x	x	x		
<i>Aquilapollenites turbidus</i>			x	x	x	x	x	x	x	
<i>Aquilapollenites</i> spp.			x		x		x	x		
<i>Arecipites barakati</i>										
<i>Arecipites</i> sp.										
<i>Asterisporites chlonovae</i>										
<i>Azonia calvata</i>										
<i>Azonia cribrata</i>			x							
<i>Azonia jacutense</i>										
<i>Azonia pulchella</i>										
<i>Azonia recta</i>										
<i>Baculatisporites comaumensis</i>										
<i>Baculatisporites papillosus</i>										
<i>Baculatisporites</i> spp.										
<i>Biretisporites psilatus</i>										
<i>Biretisporites</i> sp.							x			
<i>Camarozonosporites ambigens</i>			x						x	
<i>Camarozonosporites amplus</i>										
<i>Camarozonosporites similis</i>										

<i>Camarozonosporites</i> spp.							x			
<i>Cibotiumspora clavatus</i>										
<i>Cibotiumspora juncta</i>						x				
<i>Cicatricosporites</i> spp.										
<i>Cingulatisporites dakotaensis</i>										
<i>Circulina parva</i>	x		x			x				
<i>Circumflexipollis tilioides</i>					x					
<i>Cirratriradites luminosus</i>										
<i>Classopollis classoides</i>			x							
<i>Conbaculatisporites</i> sp.										
<i>Concavisporites</i> sp.										
<i>Cranwellia rumseyensis</i>					x		x	x	x	
cf. <i>Cranwellia</i> sp.					x			x		
<i>Crassipollis</i> sp.										
<i>Cyathidites australis rimalis</i>										
<i>Cyathidites minor</i>			x		x	x	x	x		
<i>Cycadopites fragilis</i>	x			x	x	x	x	x	x	
<i>Cycadopites</i> spp.								x	x	
<i>Deltoidospora diaphana</i>								x		
<i>Distaltriangulisporites costatus</i>										
<i>Distaltriangulisporites mutabilis</i>										
<i>Dyadonapites reticulatus</i>					x	x		x		
<i>Echinatisporis solaris</i>										
<i>Echinatisporis</i> spp.										
<i>Enzonalasporites bojatus</i>			x	x	x	x	x			
<i>Equisetosporites amabilis</i>										
<i>Equisetosporites hughesii</i>										
<i>Equisetosporites mollis</i>										
<i>Equisetosporites multicoatus</i>										
<i>Equisetosporites multistriatus</i>										
<i>Equisetosporites</i> spp.										
<i>Erdtmanipollis procumbentiformis</i>					x	x	x	x		
<i>Eucommiidites minor</i>										
<i>Eucommiidites troedssonii</i>										
<i>Expressipollis</i> sp.										
<i>Fibulapollis scabratus</i>			x							
<i>Foraminisporis asymmetricus</i>										
<i>Foraminisporis undulatus</i>			x		x	x	x	x		
<i>Foraminisporis</i> sp.						x				
<i>Foveosporites subtriangularis</i>										
<i>Foveosporites</i> sp.										
<i>Gabonispors labyrinthus</i>			x			x				
<i>Gleicheniidites delicatus</i>			x							
<i>Gleicheniidites senonicus</i>	x		x		x	x	x	x		
<i>Gleicheniidites stellatus</i>										
<i>Gleicheniidites</i> sp.										

<i>Grewipollenites canadensis</i>										
<i>Grewipollenites radiatus</i>										
<i>Gunnaripollis suberbus</i>				x						
<i>Hazaria sheopiarrii</i>			x				x			
<i>Heliosporites kemensis</i>					x	x				
<i>Inaperturotetradites scabratus</i>					x	x				
<i>Interulobites</i> sp.		x					x			
<i>Klukisporites</i> sp.										
<i>Kurtzipites</i> sp.										
<i>Kuylisporites scutatus</i>										
<i>Laevigatosporites haardti</i>			x	x	x	x	x		x	
<i>Laevigatosporites nitidulus</i>										
<i>Laevigatosporites nitidus</i>										
<i>Laevigatosporites undulatifomis</i>										
<i>Liburnisporis adnacus</i>										
<i>Liliacidites mirus</i>								x		
<i>Liliacidites variegatus</i>								x		
<i>Liliacidites</i> spp.	x			x			x	x	x	x
<i>Lusatisporis dettmannae</i>						x	x	x	x	
<i>Mancicorpus anchoriforme</i>			x	x	x	x	x	x	x	x
<i>Mancicorpus glaber</i>										
<i>Mancicorpus trapeziforme</i>										
<i>Mancicorpus tripodiformis</i>					x					
<i>Mancicorpus</i> sp.			x							
<i>Marcellopites tolmanensis</i>										
<i>Mica hoodoensis</i>		x								
<i>Monosulcites riparius</i>				x		x		x		
<i>Monosulcites</i> sp.		x								
<i>Orbiculapollis globosus</i>										
<i>Ornamentifera baculata</i>			x							
<i>Ovoidites ligneolus</i>	x									
<i>Palaeoisoetes subengelmanni</i>										
<i>Pediastrum boryanum</i>	x	x								
<i>Penetetrapites inconspicuus</i>						x				
<i>Pilosisorites</i> sp.										
<i>Pityosporites constrictus</i>			x			x	x	x	x	
<i>Pleurospermaepollenites</i> sp.			x							
<i>Podocarpidites biformis</i>										
<i>Podocarpidites</i> spp.										
<i>Polycingulatisporites reduncus</i>			x		x		x	x		
<i>Polycingulatisporites</i> sp.										
<i>Polyporina cribraria</i>	x	x		x	x	x	x	x	x	x
<i>Pristinupollenites microsaccus</i>				x		x				
<i>Pristinupollenites</i> sp.										
<i>Pulcheripollenites krempii</i>						x	x	x	x	
<i>Quadripollis krempii</i>										

<i>Reticuloidosporites pseudomurii</i>			x		x					
<i>Reticulosporites reticulatus</i>										
<i>Retitriteles austroclavatidites</i>										
<i>Retitriteles mediocris</i>										
<i>Retitriteles spp.</i>			x							
<i>Rogalskaiisporites cicatricosus</i>										
<i>Scabrastephanocolpites albertensis</i>										
<i>Scabrastephanocolpites lepidus</i>					x					
<i>Scabrastephanocolpites pentaaperturites</i>										
<i>Schizosporites parvus</i>						x		x		x
<i>Senipites drumhellerensis</i>										
<i>Sequoiapollenites paleocenicus</i>			x		x					
<i>Sequoiapollenites sp.</i>										
<i>Sestrosporites pseudoalveolatus</i>			x							
<i>Siberiapollis montanensis</i>						x				
<i>Siberiapollis spp.</i>										
<i>Sigmopollis carbonis</i>	x		x		x	x		x	x	x
<i>Sigmopollis hispidus</i>	x	x	x						x	
<i>Stereigranisorites regius</i>										
<i>Stereisporites ancoris</i>										
<i>Stereisporites antiquasporites</i>	x		x		x	x	x			
<i>Stereisporites antiquus</i>										
<i>Stereisporites cingulatus</i>										
<i>Stereisporites rodaensis</i>										
<i>Stereisporites triangulopunctatus</i>										
<i>Stoverisporites lunaris</i>										
<i>Subtriporopollenites alpinus</i>	x		x	x		x	x	x	x	x
<i>Syncolpites sp.</i>										
<i>Taxodiaceapollenites hiatus</i>	x	x	x	x	x	x	x	x	x	x
<i>Taxodiaceapollenites vacuipites</i>					x	x				
<i>Tetranguladinium cruciformis</i>	x									
<i>Tetranguladinium sp.</i>	x									
<i>Tetraporina quadrata</i>	x	x						x	x	x
<i>Tetraporina sp.</i>										x
<i>Todisporites minor</i>						x				
<i>Translucentipollis plicatilis</i>						x	x			
<i>Tricolpites parvus</i>										
<i>Tricolpites reticulatus</i>				x		x		x	x	x
<i>Tricolpites ringens</i>										
<i>Tricolpites spp.</i>	x				x	x	x	x	x	x
<i>Tricolpopollenites elongatus</i>										
<i>Tricolpopollenites levitas</i>								x	x	x
<i>Tricolpopollenites spp.</i>							x	x	x	x
<i>Tricolporites spp.</i>			x			x	x	x	x	
<i>Trifossapollenites ellipticus</i>					x	x	x			
<i>Trilites bettianus</i>							x			

<i>Trilites</i> sp.										
<i>Trilobapollis laudabilis</i>										
<i>Triporoletes involucratus</i>										
<i>Triporopollenites triplicatus</i>					x	x				
<i>Triporopollenites</i> spp.				x	x	x	x	x	x	x
<i>Triquitrites absurdus</i>			x							
<i>Trochicola scollardiana</i>				x	x	x	x			
<i>Trudopollis meekeri</i>										
<i>Trudopollis</i> sp.			x							
<i>Tschudypollis retusus</i>										
<i>Tschudypollis thalmannii</i>			x	x	x	x	x	x		
<i>Umbosporites callosus</i>						x				
<i>Varugosporites tolmanensis</i>										
<i>Verrucatotriletes</i> sp.										
<i>Verrutricolpites</i> sp.						x	x	x	x	
<i>Virgo amiantopollis</i>				x	x	x				
<i>Vitreisporites pallidus</i>					x	x				
<i>Wulongspora</i> sp.						x				
<i>Zlivisporis blanensis</i>										
<i>Zlivisporis cenomanianus</i>						x				
<i>Zlivisporis novomexicanum</i>										
<i>Zlivisporis</i> spp.						x				
Dinoflagellates		x	x							

Samples	21	22	23	24	25	26	27	28	29	30
Meterage	234.5	239	243	244.5	250	251	251.5	254.5	261	264.5
<i>Accuratipollis lactifluminis</i>										
<i>Accuratipollis macrosolenoides</i>				x						
<i>Aequitriradites spinulosus</i>										
<i>Alisporites bilateralis</i>										
<i>Alutisporites</i> sp.										
<i>Annulispora salsa</i>										
<i>Appendicisporites undosus</i>										
<i>Aquilapollenites amicus</i>										
<i>Aquilapollenites attenuatus</i>				x	x	x	x	x		
<i>Aquilapollenites augustus</i>								x	x	
<i>Aquilapollenites bellus</i>										
<i>Aquilapollenites clarireticulatus</i>									x	x
<i>Aquilapollenites drumhellerensis</i>										
<i>Aquilapollenites funkhouseri</i>						x	x			x
<i>Aquilapollenites leucocephalus</i>										
<i>Aquilapollenites</i> cf. <i>leucocephalus</i>										
<i>Aquilapollenites mtchedlishvili</i>						x				
<i>Aquilapollenites notabile</i>								x		
<i>Aquilapollenites quadrilobus</i>	x	x	x		x	x	x	x	x	x
<i>Aquilapollenites quadrilobus</i>				x						
<i>Aquilapollenites rectus</i>						x				
<i>Aquilapollenites rigidus</i>										
<i>Aquilapollenites senonicus</i>	x		x	x	x		x			
<i>Aquilapollenites stelckii</i>										
<i>Aquilapollenites trialatus</i>										
<i>Aquilapollenites turbidus</i>			x	x		x	x	x		x
<i>Aquilapollenites</i> spp.			x	x	x	x	x	x		x
<i>Arecipites barakati</i>										
<i>Arecipites</i> sp.										
<i>Asterisporites chlonovae</i>										
<i>Azonia calvata</i>										
<i>Azonia cribrata</i>										
<i>Azonia jacutense</i>										
<i>Azonia pulchella</i>										
<i>Azonia recta</i>										
<i>Baculatisporites comaumensis</i>								x		
<i>Baculatisporites papillosus</i>										
<i>Baculatisporites</i> spp.										
<i>Biretisporites psilatus</i>						x				
<i>Biretisporites</i> sp.										
<i>Camarozonosporites ambigens</i>			x	x		x	x	x		
<i>Camarozonosporites amplus</i>										
<i>Camarozonosporites similis</i>										

<i>Camazonosporites</i> spp.										
<i>Cibotiumspora clavatus</i>										
<i>Cibotiumspora juncta</i>										
<i>Cicatricosisporites</i> spp.							x			
<i>Cingulatisporites dakotaensis</i>										
<i>Circulina parva</i>						x				x
<i>Circumflexipollis tilioides</i>	x									
<i>Cirratriadites luminosus</i>										
<i>Classopollis classoides</i>						x				
<i>Conbaculatisporites</i> sp.										
<i>Concavisporites</i> sp.										
<i>Cranwellia rumseyensis</i>		x	x	x	x	x	x	x		x
cf. <i>Cranwellia</i> sp.										
<i>Crassipollis</i> sp.										
<i>Cyathidites australis rimalis</i>										
<i>Cyathidites minor</i>						x	x	x		x
<i>Cycadopites fragilis</i>	x			x	x	x	x	x	x	x
<i>Cycadopites</i> spp.										
<i>Deltoidospora diaphana</i>					x				x	
<i>Distaltriangulisporites costatus</i>										
<i>Distaltriangulisporites mutabilis</i>										
<i>Dyadonapites reticulatus</i>	x	x	x	x	x	x	x	x	x	x
<i>Echinatisporis solaris</i>										
<i>Echinatisporis</i> spp.										
<i>Enzonalasporites bojatus</i>				x			x	x		
<i>Equisetosporites amabilis</i>		x								
<i>Equisetosporites hughesii</i>										
<i>Equisetosporites mollis</i>						x				
<i>Equisetosporites multicostatus</i>										
<i>Equisetosporites multistriatus</i>										
<i>Equisetosporites</i> spp.						x	x			
<i>Erdtmanipollis procumbentiformis</i>						x		x		x
<i>Eucommiidites minor</i>		x								
<i>Eucommiidites troedssonii</i>										
<i>Expressipollis</i> sp.										
<i>Fibulapollis scabratus</i>										
<i>Foraminisporis asymmetricus</i>										
<i>Foraminisporis undulatus</i>						x	x	x		
<i>Foraminisporis</i> sp.				x						
<i>Foveosporites subtriangularis</i>										
<i>Foveosporites</i> sp.			x							x
<i>Gabonisoris labyrinthus</i>							x			
<i>Gleichenioidites delicatus</i>						x	x	x		x
<i>Gleichenioidites senonicus</i>	x		x	x		x	x	x		
<i>Gleichenioidites stellatus</i>										x
<i>Gleichenioidites</i> sp.										x

<i>Grewipollenites canadensis</i>										
<i>Grewipollenites radiatus</i>										
<i>Gunnaripollis suberbus</i>										
<i>Hazaria sheopiarrii</i>				x			x	x		
<i>Heliosporites kemensis</i>										x
<i>Inaperturotetradites scabratus</i>							x	x		
<i>Interulobites</i> sp.					x		x			
<i>Klukisporites</i> sp.										
<i>Kurtzipites</i> sp.										
<i>Kuylisporites scutatus</i>								x		
<i>Laevigatosporites haardtii</i>			x	x		x	x	x		x
<i>Laevigatosporites nitidulus</i>					x					
<i>Laevigatosporites nitidus</i>										
<i>Laevigatosporites undulatiformis</i>										
<i>Liburnisporis adnacus</i>										
<i>Liliacidites mirus</i>			x	x	x		x			
<i>Liliacidites variegatus</i>							x			
<i>Liliacidites</i> spp.	x		x	x	x		x	x	x	x
<i>Lusatisporis dettmannae</i>		x							x	x
<i>Mancicorpus anchoriforme</i>	x	x	x	x	x	x	x	x	x	x
<i>Mancicorpus glaber</i>										
<i>Mancicorpus trapeziforme</i>										
<i>Mancicorpus tripodiformis</i>								x		x
<i>Mancicorpus</i> sp.										
<i>Marcelloporites tolmanensis</i>								x		
<i>Mica hoodoensis</i>	x				x					
<i>Monosulcites riparius</i>										
<i>Monosulcites</i> sp.	x				x		x	x		x
<i>Orbiculapollis globosus</i>						x				x
<i>Ornamentifera baculata</i>										
<i>Ovoidites ligneolus</i>		x								
<i>Palaeoisoetes subengelmanni</i>							x			
<i>Pediastrum boryanum</i>										
<i>Penetetrapites inconspicuus</i>										
<i>Pilosporites</i> sp.										
<i>Pityosporites constrictus</i>		x				x				
<i>Pleurospermaepollenites</i> sp.			x			x	x		x	
<i>Podocarpidites biformis</i>										
<i>Podocarpidites</i> spp.										
<i>Polycingulatisporites reduncus</i>							x			x
<i>Polycingulatisporites</i> sp.										
<i>Polyporina cribraria</i>		x				x	x		x	x
<i>Pristinupollenites microsaccus</i>							x			
<i>Pristinupollenites</i> sp.										
<i>Pulcheripollenites krempii</i>		x						x		x
<i>Quadripollis krempii</i>										

<i>Reticuloidosporites pseudomurii</i>			x			x	x	x		x
<i>Reticulospores reticulatus</i>										
<i>Retitriteles austroclavatidites</i>										
<i>Retitriteles mediocris</i>										
<i>Retitriteles spp.</i>						x	x	x		
<i>Rogalskaiasporites cicatricosus</i>							x			
<i>Scabrastephanocolpites albertensis</i>									x	x
<i>Scabrastephanocolpites lepidus</i>							x			x
<i>Scabrastephanocolpites pentaaperturites</i>							x		x	
<i>Schizosporites parvus</i>		x		x						
<i>Senipites drumhellerensis</i>			x	x		x		x		
<i>Sequoiapollenites paleocenicus</i>			x	x			x	x		
<i>Sequoiapollenites sp.</i>										
<i>Sestrosporites speudoalveolatus</i>										
<i>Siberiapollis montanensis</i>										
<i>Siberiapollis spp.</i>						x	x			
<i>Sigmopollis carbonis</i>	x	x			x		x	x	x	
<i>Sigmopollis hispidus</i>								x		
<i>Stereigranisorites regius</i>							x			
<i>Stereisporites ancoris</i>							x	x		
<i>Stereisporites antiquasporites</i>				x		x	x	x		
<i>Stereisporites antiquus</i>										
<i>Stereisporites cingulatus</i>								x		
<i>Stereisporites rodaensis</i>										
<i>Stereisporites triangulopunctatus</i>										
<i>Stoverisporites lunaris</i>										
<i>Subtriporopollenites alpinus</i>	x	x	x	x		x	x			x
<i>Syncolpites sp.</i>				x				x		
<i>Taxodiaceapollenites hiatus</i>			x	x	x	x	x	x	x	x
<i>Taxodiaceapollenites vacuipites</i>			x	x	x	x	x	x		x
<i>Tetranguladinium cruciformis</i>										
<i>Tetranguladinium sp.</i>										
<i>Tetraporina quadrata</i>		x		x	x			x	x	
<i>Tetraporina sp.</i>	x									
<i>Todisporites minor</i>						x		x		
<i>Translucentipollis plicatilis</i>										
<i>Tricolpites parvus</i>										
<i>Tricolpites reticulatus</i>		x		x		x	x	x		x
<i>Tricolpites ringens</i>									x	x
<i>Tricolpites spp.</i>	x	x	x	x	x		x	x	x	x
<i>Tricolpopollenites elongatus</i>										
<i>Tricolpopollenites levitas</i>	x	x	x	x	x	x	x	x	x	x
<i>Tricolpopollenites spp.</i>	x	x			x	x	x	x		x
<i>Tricolporites spp.</i>		x		x	x	x	x	x	x	x
<i>Trifossapollenites ellipticus</i>				x		x				x
<i>Trilites bettianus</i>										

<i>Trilites</i> sp.										
<i>Trilobapollis laudabilis</i>										x
<i>Triporoletes involucratus</i>										
<i>Triporopollenites triplicatus</i>						x				
<i>Triporopollenites</i> spp.		x	x	x	x	x	x	x	x	x
<i>Triquitrites absurdus</i>										
<i>Trochicola scollardiana</i>						x				x
<i>Trudopollis meekeri</i>										x
<i>Trudopollis</i> sp.								x		x
<i>Tschudypollis retusus</i>										
<i>Tschudypollis thalmannii</i>			x			x	x	x		x
<i>Umbosporites callosus</i>	x		x	x	x		x	x	x	x
<i>Varirugosporites tolmanensis</i>										
<i>Verrucatotrilites</i> sp.										
<i>Verrutricolpites</i> sp.		x	x			x	x			
<i>Virgo amiantopollis</i>							x			x
<i>Vitreisporites pallidus</i>						x	x			
<i>Wulongspora</i> sp.										
<i>Zlivisporis blanensis</i>	x									
<i>Zlivisporis cenomanianus</i>						x	x			
<i>Zlivisporis novomexicanum</i>										
<i>Zlivisporis</i> spp.										
Dinoflagellates										x

Samples	31	32	33	34	35	36
Meterage	269	273.5	278	284	290	297.5
<i>Accuratipollis lactifluminis</i>						
<i>Accuratipollis macrosolenoides</i>						
<i>Aequitriradites spinulosus</i>						
<i>Alisporites bilateralis</i>						
<i>Alutisporites</i> sp.						
<i>Annulispora salsa</i>						
<i>Appendicisporites undosus</i>						
<i>Aquilapollenites amicus</i>						
<i>Aquilapollenites attenuatus</i>	x		x	x		
<i>Aquilapollenites augustus</i>						
<i>Aquilapollenites bellus</i>						
<i>Aquilapollenites clarireticulatus</i>		x		x	x	x
<i>Aquilapollenites drumhellerensis</i>						
<i>Aquilapollenites funkhouserii</i>		x			x	
<i>Aquilapollenites leucocephalus</i>				x		
<i>Aquilapollenites</i> cf. <i>leucocephalus</i>			x			
<i>Aquilapollenites mtchedlishvili</i>						
<i>Aquilapollenites notabile</i>						
<i>Aquilapollenites quadrilobus</i>	x	x		x	x	x
<i>Aquilapollenites quadrilobus</i>				x	x	
<i>Aquilapollenites rectus</i>				x		
<i>Aquilapollenites rigidus</i>						
<i>Aquilapollenites senonicus</i>						
<i>Aquilapollenites stelckii</i>			x			
<i>Aquilapollenites trialatus</i>		x		x	x	
<i>Aquilapollenites turbidus</i>		x		x	x	x
<i>Aquilapollenites</i> spp.	x	x		x		
<i>Arecipites barakati</i>						
<i>Arecipites</i> sp.					x	
<i>Asterisporites chlonovae</i>						
<i>Azonia calvata</i>						
<i>Azonia cribrata</i>						
<i>Azonia jacutense</i>						
<i>Azonia pulchella</i>						
<i>Azonia recta</i>						
<i>Baculatisporites comaumensis</i>				x		
<i>Baculatisporites papillosus</i>		x				
<i>Baculatisporites</i> spp.		x	x			
<i>Biretisporites psilatus</i>			x			
<i>Biretisporites</i> sp.						
<i>Camarozonosporites ambigens</i>		x	x	x	x	x
<i>Camarozonosporites amplus</i>						
<i>Camarozonosporites similis</i>						

<i>Camarozonosporites</i> spp.						
<i>Cibotiumspora clavatus</i>						
<i>Cibotiumspora juncta</i>					x	
<i>Cicatricosporites</i> spp.		x	x	x	x	
<i>Cingulatisporites dakotaensis</i>					x	
<i>Circulina parva</i>						
<i>Circumflexipollis tilioides</i>						
<i>Cirratriradites luminosus</i>			x	x	x	
<i>Classopollis classoides</i>					x	x
<i>Conbaculatisporites</i> sp.						
<i>Concavisporites</i> sp.						
<i>Cranwellia rumseyensis</i>	x	x	x	x	x	x
cf. <i>Cranwellia</i> sp.						
<i>Crassipollis</i> sp.						
<i>Cyathidites australis rimalis</i>						
<i>Cyathidites minor</i>	x	x	x			x
<i>Cycadopites fragilis</i>						
<i>Cycadopites</i> spp.	x				x	
<i>Deltoidospora diaphana</i>						
<i>Distaltriangulisporites costatus</i>				x	x	
<i>Distaltriangulisporites mutabilis</i>						
<i>Dyadonapites reticulatus</i>					x	
<i>Echinatisporis solaris</i>				x		
<i>Echinatisporis</i> spp.						
<i>Enzonalasporites bojatus</i>	x					
<i>Equisetosporites amabilis</i>	x					
<i>Equisetosporites hughesii</i>						
<i>Equisetosporites mollis</i>						
<i>Equisetosporites multicostatus</i>						
<i>Equisetosporites multistriatus</i>						
<i>Equisetosporites</i> spp.		x			x	
<i>Erdtmanipollis procumbentiformis</i>		x	x			x
<i>Eucommiidites minor</i>						
<i>Eucommiidites troedssonii</i>						
<i>Expressipollis</i> sp.		x	x	x	x	x
<i>Fibulapollis scabratus</i>						
<i>Foraminisporis asymmetricus</i>						
<i>Foraminisporis undulatus</i>				x	x	x
<i>Foraminisporis</i> sp.						
<i>Foveosporites subtriangularis</i>						
<i>Foveosporites</i> sp.						
<i>Gabonispors labyrinthus</i>						
<i>Gleicheniidites delicatus</i>	x				x	x
<i>Gleicheniidites senonicus</i>	x	x	x		x	x
<i>Gleicheniidites stellatus</i>	x		x		x	x
<i>Gleicheniidites</i> sp.	x	x	x	x	x	

<i>Grewipollenites canadensis</i>						
<i>Grewipollenites radiatus</i>						
<i>Gunnaripollis suberbus</i>						
<i>Hazaria sheopiarui</i>						
<i>Heliosporites kemensis</i>		x			x	
<i>Inaperturotetradites scabratus</i>						
<i>Interulobites</i> sp.					x	
<i>Klukisporites</i> sp.						
<i>Kurtzipites</i> sp.						
<i>Kuylisporites scutatus</i>		x		x	x	
<i>Laevigatosporites haardtii</i>	x			x		
<i>Laevigatosporites nitidulus</i>						
<i>Laevigatosporites nitidus</i>		x	x			
<i>Laevigatosporites undulatiformis</i>						x
<i>Liburnisporis adnacus</i>				x	x	
<i>Liliacidites mirus</i>	x					
<i>Liliacidites variegatus</i>						
<i>Liliacidites</i> spp.	x					
<i>Lusatisporis dettmannae</i>			x		x	x
<i>Mancicorpus anchoriforme</i>	x	x	x	x	x	x
<i>Mancicorpus glaber</i>			x	x		
<i>Mancicorpus trapeziforme</i>						
<i>Mancicorpus tripodiformis</i>	x	x	x	x	x	x
<i>Mancicorpus</i> sp.						
<i>Marcellopites tolmanensis</i>						
<i>Mica hoodoensis</i>						
<i>Monosulcites riparius</i>						
<i>Monosulcites</i> sp.	x			x		x
<i>Orbiculapollis globosus</i>					x	x
<i>Ornamentifera baculata</i>		x				
<i>Ovoidites ligneolus</i>						
<i>Palaeoisoetes subengelmanni</i>						
<i>Pediastrum boryanum</i>						
<i>Penetetrapites inconspicuus</i>						
<i>Pilosisorites</i> sp.			x	x	x	
<i>Pityosporites constrictus</i>						x
<i>Pleurospermaepollenites</i> sp.						
<i>Podocarpidites biformis</i>						
<i>Podocarpidites</i> spp.				x		
<i>Polycingulatisporites reduncus</i>	x	x			x	
<i>Polycingulatisporites</i> sp.						
<i>Polyporina cribraria</i>	x	x	x		x	x
<i>Pristinupollenites microsaccus</i>	x		x		x	x
<i>Pristinupollenites</i> sp.						
<i>Pulcheripollenites krempii</i>	x			x	x	x
<i>Quadripollis krempii</i>				x		

<i>Reticuloidosporites pseudomurii</i>	x	x	x		x	x
<i>Reticulosporis reticulatus</i>						
<i>Retitriletes austroclavatidites</i>		x				
<i>Retitriletes mediocris</i>						
<i>Retitriletes spp.</i>			x		x	
<i>Rogalskaisporites cicatricosus</i>					x	
<i>Scabrastephanocolpites albertensis</i>						
<i>Scabrastephanocolpites lepidus</i>						
<i>Scabrastephanocolpites pentaaperturites</i>	x			x		x
<i>Schizosporis parvus</i>						
<i>Senipites drumhellerensis</i>			x			
<i>Sequoipollenites paleocenicus</i>		x				
<i>Sequoipollenites sp.</i>						
<i>Sestrosporites pseudoalveolatus</i>					x	
<i>Siberiapollis montanensis</i>				x		
<i>Siberiapollis spp.</i>						
<i>Sigmopollis carbonis</i>	x	x	x			
<i>Sigmopollis hispidus</i>						
<i>Stereigranisporis regius</i>				x		
<i>Stereisporites ancoris</i>			x	x	x	
<i>Stereisporites antiquasporites</i>		x	x	x	x	x
<i>Stereisporites antiquus</i>				x	x	
<i>Stereisporites cingulatus</i>		x	x	x	x	
<i>Stereisporites rodaensis</i>						
<i>Stereisporites triangulopunctatus</i>					x	
<i>Stoverisporites lunaris</i>						
<i>Subtriporopollenites alpinus</i>	x					
<i>Syncolpites sp.</i>						
<i>Taxodiaceapollenites hiatus</i>		x	x	x	x	x
<i>Taxodiaceapollenites vacuipites</i>		x	x	x		
<i>Tetranguladinium cruciformis</i>						
<i>Tetranguladinium sp.</i>						
<i>Tetraporina quadrata</i>	x					
<i>Tetraporina sp.</i>	x					
<i>Todisporites minor</i>						
<i>Translucentipollis plicatilis</i>			x	x	x	x
<i>Tricolpites parvus</i>						
<i>Tricolpites reticulatus</i>			x		x	x
<i>Tricolpites ringens</i>						
<i>Tricolpites spp.</i>	x	x	x	x	x	x
<i>Tricolpopollenites elongatus</i>						
<i>Tricolpopollenites levitas</i>						
<i>Tricolpopollenites spp.</i>					x	x
<i>Tricolporites spp.</i>	x		x			
<i>Trifossapollenites ellipticus</i>						x
<i>Trilites bettianus</i>						

<i>Trilites</i> sp.						
<i>Trilobapollis laudabilis</i>						
<i>Triporeletes involucratus</i>					x	
<i>Triporopollenites triplicatus</i>						
<i>Triporopollenites</i> spp.	x	x	x	x	x	x
<i>Triquitrites absurdus</i>						
<i>Trochicola scollardiana</i>					x	
<i>Trudopollis meekeri</i>			x		x	x
<i>Trudopollis</i> sp.	x			x	x	
<i>Tschudypollis retusus</i>						
<i>Tschudypollis thalmannii</i>	x	x	x	x	x	x
<i>Umbosporites callosus</i>	x			x		
<i>Varirugosporites tolmanensis</i>	x					
<i>Verrucatotriletes</i> sp.						
<i>Verrutricolpites</i> sp.			x			x
<i>Virgo amiantopollis</i>	x	x				
<i>Vitreisporites pallidus</i>				x	x	x
<i>Wulongspora</i> sp.						
<i>Zlivisporis blanensis</i>						
<i>Zlivisporis cenomanianus</i>						
<i>Zlivisporis novomexicanum</i>						
<i>Zlivisporis</i> spp.						
Dinoflagellates	x	x	x	x	x	x

Appendix F

Paleoecology and sedimentology of a vertebrate microfossil assemblage from the easternmost
Dinosaur Park Formation (Late Cretaceous, Upper Campanian) Saskatchewan, Canada:
Reconstructing diversity in a coastal ecosystem

Systematic Paleontology of the Lake
Diefenbaker Microsite

Class Chondrichthyes Huxley, 1880

Subclass Elasmobranchii Bonaparte, 1838

Order Euselachii Hay, 1902

Family Hybodontidae Owen, 1837

Genus *Meristodonoides* Underwood & Cumbaa, 2010

Meristodonoides (Hybodus) montanensis Agassiz, 1837

Description and discussion. Fig. 7a. Tooth is identified by a mesio-distally expanded crown, and a straight, high, principal cusp rounded in cross section. Lateral cusplets may or may not be present. Roots are straight and flat exhibiting multiple foramina, and are not bilobed.

Meristodonoides montanensis in Dinosaur Provincial Park is found in association with marine sharks, indicating that it may have been a brackish water species (Brinkman et al., 2005a; Neuman and Brinkman, 2005).

Order Orectolobiformes Applegate, 1972

Family Orectolobidae Jordan and Fowler, 1972

Genus *Cretorectolobus* Case, 1978

Cretorectolobus olsoni Case, 1978

Description and discussion. Fig. 7c. Tooth is wider than it is high, with a slender central cusp tapering to cusplless shoulders. Both lingual and labial crown faces are smooth, with a well-developed labial flange and lingual protuberance. Roots are short, with a basal attachment that is triangular in shape and slightly concave. This is the first documented occurrence of this genus in

Saskatchewan. This species has commonly been found associated with estuarine deposits in Alberta (Beavan and Russell, 1999; Peng et al, 2001).

Genus *Eucrossorhinus* Regan, 1908

Eucrossorhinus microcuspidatus Case, 1978

Description and discussion. Fig. 7b. Tooth is slightly higher than it is wide, with a sigmoidal aspect to the lingual part of the crown. A labial flange extends basally, beyond the foot of the crown. Shoulders exhibit lateral cusplets. The roots are short, with the basal surface slightly concave and triangular (Beavan and Russell, 1999). A nutrient foramen is present on the labial protuberance. This is the first occurrence of this genus in Saskatchewan.

Order Lamniformes Berg, 1958

Family Odontaspidae Müller and Henle, 1839

Genus *Carcharias* Rafinesque, 1810

Carcharias steineri Case, 1987

Description and discussion. Fig. 7d. Tooth displays tall, slender, sigmoid-shaped central cusp flanked on each side by a single lateral cusp (Frampton, 2006). The edges of the central cusp are well defined with thin enamel. The lingual face of the tooth is smooth, with a pronounced nutrient groove on the lingual protuberance. The roots are strongly bilobed, creating a concave appearance at the base of the tooth. *Carcharias steineri* is separated from the similar *Odontaspis* by the presence of multiple pairs of cusplets in the latter. It has been suggested that *Odontaspis* favored open waters, whereas the similar *Carcharias* lived in more coastal settings (Welton and Farish, 1993).

Family Cretoxyrhinidae Glückman, 1958

Genus *Archaeolamna* Siverson, 1992

Archaeolamna kopingensis Silverson, 1992

Description and discussion. Teeth are similar to that of *Synodontaspis*, but possess a broad-based, triangular, distally curved central cusp, which is strongly labio-lingually compressed. Each side bears a single lateral cusp varying in development (well to poor) that is slightly divergent from the main central cusp (Peng et al, 2001). A lingual protuberance is present, and bears several nutrient pits.

Family Anacoracidae Casier, 1947

Genus *Squalicorax* Whitley, 1939

Sp. indet.

Description and discussion. Fig. 7e. Single incomplete tooth is assigned to *Squalicorax* on the basis of a large, low, distally angled crown with the apex of the cusp being acutely angled (Cappetta, 1987). Serrations along the tooth margin are continuous. No nutrient groove or pit is present.

Order Rajiformes Cappetta, 1992

Family Rhinobatidae Muller and Henle, 1837

Genus *Myledaphus* Cope, 1876

Myledaphus bipartitus Cope, 1876

Description and discussion. Fig. 7f. Teeth are hexagonal with a bifid root smaller than the crown. A transverse ridge that is slightly arched labially divides the occlusal surface. That surface bears numerous folds running parallel and extend labio-lingually. The sides of the crown are marked with prominent vertical grooves, commonly continuous with the enameloid folds of the occlusal surface. *Myledaphus* teeth are among the most widespread elasmobranch fossils in the Upper Cretaceous of North America (Estes, 1964; Sahni, 1972; Peng et al, 2001; Neuman and Brinkman, 2005).

Class Osteichthyes Huxley, 1880

Subclass Actinopterygii Cope, 1887

Order Acipenseriformes Berg, 1940

Family Acipenseridae Bonaparte, 1831

Genus *Acipenser* Linnaeus, 1758

Sp. indet.

Description and discussion. Fin spines display longitudinal grooves along the spine, indicating fusion, at least in part, of the first several lepidotrichia to produce the pectoral spine (Grande and Hilton, 2009; Hilton and Grande, 2006).

Order Amiiformes Hay, 1929

Family Amiidae Bonaparte, 1837

Gen. et. sp. indet.

Description and discussion. Fig. 7g. Anteriorly-posteriorly shortened centra with the dorsal portion thicker than the ventral. Amphicoelous as in teleosts with oval ends and a small notochordal foramen on each centra (Grande and Bemis, 1998). Sparse material precludes identification at a lower taxonomic level.

Order Aspidorhynchiformes Bleeker, 1859

Family Aspidorrhynchidae Nicholson and Lydekker, 1889

Genus *Belonostomus* Agassiz, 1834

Belonostomus longirostris Lamb, 1902

Description and discussion. Fig. 7h. Jaw fragments are the most diagnostic, being long and narrow, laterally compressed and rounded ventrally. Teeth are conical, and widely spaced in a single row.

Division Teleostei (*sensu* Arratia, 1997)

Order Elopiformes Sauvage, 1875

Family Elopidae Romer, 1966

Genus *Paratarpon* Bardack, 1970

Morphoseries IA-1: *Paratarpon*

Description and discussion. Precaudal centra are antero-posteriorly shorter than high. Parapophyseal and neural arch pits are shallow with fine, evenly spaced bone fibers interlacing between articular ends of the centrum (feature absent in *Parabula*, below). This morphoseries

can be assigned to *Paratarpon* based on the narrow, plate-like portions of the centra and overall size (average size 6.0 mm).

Order Elopiformes Sauvage, 1875

Family Phyllodontidae Sauvage, 1875

Genus *Paralbula* Blake, 1940

Description and discussion. *Paralbula* represented by centra described as Morphotype 1A-2 by Brinkman and Neuman, 2010. Deep neural arch and parapophyseal pits, and lacking a second pit ventral to the parapophyseal pit. Fibers extend between the ends of the centra, and are grouped together into distinctive bundles. This series occurs in two localities within the Lethbridge Coal Zone of the Dinosaur Park Formation in Alberta, where *Paralbula* teeth are abundant. Therefore, 1A-2 has been assigned to *Paralbula* by association (Neuman and Brinkman, 2005). Teeth, also present in the assemblage, are small (average size 1 mm), ridged and dome-shaped to subspherical

Order Aulopiformes Rosen, 1973

Family Enchodontidae Woodward, 1901

Genus *Enchodus* Agassiz, 1835

Sp. indet.

Description and discussion. Fig. 7i. Tooth is broken off, lacking a root, but has diagnostically distinct distal and mesial cutting blades.

Order Salmoniformes Bleeker, 1859

Suborder Esocoidea Bleeker, 1859

Family Escoidae Cuvier, 1817

Morphospecies IB-2: ?escoid

Description and discussion. Represented by centra described as Morphospecies IB-2 in Brinkman and Neuman, 2000. Neuman and Brinkman (2005) assigned this series as potentially belonging to an escoid fish based upon abundance and size frequency data.

Order Ellimmichthyiformes Grande, 1985

Family Sorbinichthyidae Alvarado-Ortega et al., 2008

Order Clupiformes Bleeker 1859

Horseshoeichthys sp. Newbery et al., 2010

Description and discussion. Represented by centra described as Morphospecies IB-1 in Brinkman and Neuman, 2000. Simple spools with unfused transverse processes. Neural arch and parapophyseal pits are located close together. Referred to *Horseshoeichthyes* based on the redescription of this Morphospecies in Newbery et al., 2010.

Family Ellimmichthyidae Grande 1982

Genus *Diplomystus* Cope, 1877

Description and discussion. Represented by centra described by Brinkman and Neuman (2010) as Morphospecies IIA-1, redescribed by Divay and Murray (2016) as *Diplomystus*. Precaudal

centra with deep neural arch articular pits. Long, laterally directed transverse processes and mid-dorsal and midventral pits.

Superorder Osteoglossomorph Greenwood, Rosen, Weitzman, and Myers, 1966

Family Osteoglossidae Bonaparte 1832

Morphoseries IIA-2: ?*Cretophareodus*

Description and discussion. Morphoseries IIA-2 is similar to IIA-1, differing only in having a mid-dorsal bar that extends between the end of the centrum and the absence of a midventral pit. Neuman and Brinkman (2005) tentatively assigned this series to *Cretophareodus* based on the size of the centra. See Brinkman and Neuman (2002) for further discussion.

Family Hiodontidae

Morphoseries IIB-1: Hiodontidae

Description and discussion. Amphicoelous precaudal centra. Shallow pits for articulation of ribs on the body of the centrum are characteristic of this series.

Order Elopiformes Sauvage, 1875

Family Ostariostomidae Schaeffer, 1949

Genus Ostariostoma (?) Schaeffer, 1949

Description and discussion. Represented by centra described by Brinkman and Neuman (2010) as Morphospecies IIIA-1, redescribed by Brinkman et al (2017) as Ostariostoma. Small, elongated centra, oval in end view and wider than they are high. Separate parapophyses are present on the sides of the centra.

Class Amphibia Linnaeus, 1758

Order Anura Duméril, 1806

Family indet.

Gen. et. sp. indet.

Description and discussion. Fig. 7j. Distal humeri with large, ball-like articulating condyle.

Order Caudata Scopoli, 1777

Family Scapherpetonidae Auffenberg and Goin, 1959

Scapherpeton tectum Cope, 1876

Description and discussion. Fig. 7k. Amphicoelous trunk vertebrae with teardrop-shaped cotyles. Basapophyses are absent, but a well-developed subcentral keel is present on the ventral surface of the vertebrae. Atlantes have a characteristically large odontoid process and two lateral condyles for articulation with the skull.

Of the several species of *Scapherpeton* described by Cope (1876), only one, *S. tectum*, is considered valid (Auffenberg and Goin, 1959). Isolated remains have been found throughout Upper Cretaceous sediments of the Western Interior Basin (Cope, 1876; Estes, 1964; Fiorillo, 1989; Brinkman, 1990; Peng et al., 2001; Gardner, 2005). Some isolated atlantes described as

having a scooped shaped odontoid process with variably flattened, subcircular anterior cotyles have been referred to this taxon (Gardner, 2005). Dentaries assigned to this taxon are described as slender, elongated, and medially curved (Peng et al., 2001).

Family Scapherpetontidae Auffenberg and Goin, 1959

Lisserpeton bairdi Estes, 1965

Description and discussion. Arrow-shaped odontoid processes and compressed anterior cotyles

Family Batrachosauroididae Auffenberg, 1958

Opisthotriton kayi Auffenburg, 1961

Description and discussion. Fig. 7l. Opisthocoelous centra with a poorly developed pitted anterior condyle, and prominent posteroventral basapophyses and subcentral keel.

Opisthotriton was first described from isolated vertebrae recovered from the Lance Formation of Wyoming by Auffenburg (1961) and expanded upon by Estes (1964). Material assigned to this genus has been recovered throughout the Western Interior (Fiorillo, 1989; Brinkman, 1990; Peng et al., 2001; Gardner, 2005).

Order Allocaudata Fox and Naylor, 1982

Family Albanerpetontidae Fox and Naylor, 1982

Genus *Albanerpeton* Estes and Hoffstetter, 1976

sp. indet

Description and discussion. Fig. 7m. Trunk vertebrae are small and elongated. Both ends of the centra are rounded and deeply concave. Centra are ventrally smooth, lacking a subcentral keel typical of *Opisthotriton*. Neural spines are underdeveloped and neural arches are low.

Class Reptilia Laurenti, 1768

Order Testudines Batsch, 1788

Suborder Cryptodira Cope, 1868

Family Adocidae Cope, 1870

Gen. et. sp. indet.

Description and discussion. Fig. 7n. Shell fragment bearing fine ornamentation of many regularly-arranged shallow pits was recovered. This genus is distinguished from trionychids based on wavy undulations and less orderly arrangement of pits present in the latter (Peng et al., 2001).

Family Baenidae Cope, 1882

Gen. et. sp. indet.

Description and discussion. Fig. 7o. Carapace fragments have relatively smooth surfaces lacking ornamentation, and are heavily constructed, with small sulci (Peng et al, 2001). Three genera are recognized in the Dinosaur Park Formation of Alberta (*Plesiobaena*, *Boremys*, and *Neurankyles*) but material at the Diefenbaker site is too fragmentary to diagnose below family level.

Family Chelydridae Swainson, 1839

Gen. et. sp. indet.

Description and discussion. Carapace fragments are thin shelled with deep sulci, ridges, and a roughened, corrugated texture. Four shell fragments recovered from the site were consistent with this diagnosis.

Family Trionychidae Gray, 1870

Genus *Aspideretoides* (?) Leidy, 1856

sp. indet.

Description and discussion. Fig. 8a-b. Sculpture patterns consist of pitting, irregular, wavy ridges and grooves, which may vary throughout ontogeny (Gardner and Russell, 1994). Five trionychid species have been described from the Belly River Group, but are difficult to distinguish based on fragmentary remains (Gardner et al., 1995). Though ornamentation is distinctive of the trionychids to family, it is of less significance at taxonomic levels (Estes, 1964; Nicholls, 1972; Gardner and Russell, 1994; Peng et al., 2001).

Subclass Diapsida Osborn, 1903

Order Squamata Oppel, 1811

Family Varanidae Gray, 1827

Genus *Palaeosaniwa* Gilmore, 1928

sp. indet.

Description and discussion. Tooth bases with plicidentine morphology. Teeth are laterally compressed and sharply pointed with crenulated bases. Vertebrae assigned to this genus exhibit

large zygopophyses and a median depression on the ventral surface of the centrum.

Palaeosaniwa is known from the Dinosaur Park Formation in Alberta, where it is considered to be a terrestrial varanid favouring meandering river-floodplain environments (Caldwell, 2005).

Order Choristodera Cope, 1876

Family Champsosauridae Cope, 1884

Genus *Champsosaurus* Cope, 1876

sp. indet.

Description and discussion. Fig. 8c. Precaudal vertebra cylindrical and amphiplatyan, a feature characteristic of the genus. Where neural arch is preserved, it is square to rectangular in outline, high vaulted, and with a medial neural spine. Rib and limb material is also common and abundant. No pathologies are evident, though taphonomic processes might have obscured their identification.

Choristoderes are an extinct group of crocodilian-like diapsid reptiles known from the Late Triassic to the Oligocene (Gao et al., 2005). Two species of *Champsosaurus* are known from the Belly River Group of Alberta: *Champsosaurus natator* and *Champsosaurus lindoei*. *C. lindoei* is more gracile than *C. natator*, with the former exhibiting a more slender snout with an expanded anterior tip. Distinction between the two is reduced to cranial features because postcranial elements are non-diagnostic.

Suborder Plesiosauria Blainville, 1835

Family Polycotylidae Wiliston, 1925

Gen. et. sp. indet.

Description and discussion. Teeth are pointed and slender, with fine striations along the lingual surface of the crown and a smooth labial surface. A single fragmented centrum shows an amphicoelous condition with a slight notochord depression in the middle of the articular face.

Family Elasmosauridae Cope 1869

Gen et. sp. indet.

Description and discussion. Long, curved tooth with fine striations on the crown. Tooth differs from that of polycotylids in lacking striations and possessing a notched tooth base.

Superorder Archosauria Cope, 1870

Clade Eusuchia Huxley, 1875

Order Crocodylia Gmelin, 1788

Family Crocodylidae Cuvier, 1808

Genus *Leidyosuchus* Lambe, 1907

sp. indet.

Description and discussion. Fig. 8e. Teeth are cone-shaped with smooth, faint grooves running perpendicular along the crown. Such conical teeth indicate anterior positions, whereas posterior crushing teeth oval-shaped, flat, and low-crowned in this taxon.

Two types of osteoderms (scutes) present (Fig. 8d): The first type, likely dorsal scutes, large, thick and deeply ornamented with large pits. The second type, likely ventral scutes, smaller and thinner, with shallow pits along the surface. Scutes cannot be identified to genus, although likely

represent *Leidyosuchus*. Several pieces of *Leidyosuchus* cranial material, including squamosal, frontal and jugal fragments, were recovered . These pieces display characters consistent with those described for *Leidyosuchus* from Dinosaur Provincial Park (Wu, 2005)

Clade Dinosauria Owen, 1842

Order Ornithischia Seeley, 1888

Suborder Ankylosauria Osborn, 1923

Family Ankylosauridae Brown, 1908

Gen. et sp. indet.

Description and discussion. Fig. 8f. Tooth with phylliform crown and a simple, peg- like root . Tooth has a low cingula on one side, with vertical grooves on one side of the tooth (the other being smooth sided). A single ankylosaur scute was also discovered at the site (Fig. 8g).

Suborder Ceratopsia Marsh, 1890

Family Ceratopsidae Marsh, 1888

Gen et. sp. indet.

Description and discussion. A laterally compressed nasal horncore with fusion of the midline suture Distinct partial basioccipitals with complete condyles. Teeth (Fig. 8h) with a dorso-ventral ridge located on the anterior half of the occlusal surface of the crown are indicative of family.

Conclusive genus identification of isolated ceratopsian remains is largely restricted to parietals and squamosals. Horner and Goodwin (2006) determined that species identification of ceratopsians by conical nasal horn cores is inconclusive, because vast ontogenetic changes occurred throughout life, and nasal horns are highly variable in size and profile in adult skulls. Abundant macrofossils have since been recovered from the site, and are being studied separately.

Suborder Ornithopoda Marsh, 1881

Family Hadrosauridae Cope, 1869

Gen et. sp. indet.

Description and discussion. Hadrosaur dentition of tooth batteries; close packing of small teeth, with three to five replacement teeth per tooth position. Teeth (Fig. 8l) are taller than they are wide and composed mainly of mantle dentine and orthodentine (Erickson et al. 2012, LeBlanc et al. 2016). The crown bears enamel only on one side (buccal for maxillary teeth, lingual for dentary teeth), and exhibits a strong median carina (Horner et al, 2004).

Hadrosaur teeth are not thought to be specific to genus, though this question has not been considered in any great detail (Lull and Wright, 1942; Coombs, 1988). However, it has been noted that crown morphologies of the two subfamilies, Hadrosaurinae and Lambeosaurinae, are not the same. In lambeosaurines, this carina is often sinuous and the crown-root angle is greater than 145°. This is in contrast to the hadrosaurine condition in which the median carina is straight or only slightly curved and the crown-root angle ranges from 120° to 140° (Horner et al., 2004).

All teeth recovered from the Diefenbaker site lack roots, making it impossible to distinguish between the two subfamilies, but they are diagnostic as Hadrosauridae gen. indet.

Family Hypsilophodontidae Dollo 1882.

Hypsilophodont, Gen. et. sp. indet.

Description and discussion. Fig. 8f. Referred to hypsilophodontidae based on descriptions in Brown et al. (2013). Tooth is small with a triangular crown that is labio-lingually compressed. A cingulum is well developed on the anterior and posterior aspect of the tooth. Tooth root is broken off, but what remains is peg-like.

Order Saurischia Seeley, 1888

Suborder Theropoda Marsh 1881

Family Dromaeosauridae Matthew and Brown, 1922

Dromaeosaurus albertensis Matthew and Brown, 1922

Description and discussion. Referral to *Dromaeosaurus* based on Currie et al. (1990). Teeth are large, recurved, laterally compressed, and sharply tapered. As in most other theropods, the carinae are serrated; however denticles on the distal carina are larger than those of the mesial carina. *D. albertensis* teeth can be recognized in microsites by an anterior serrated carina twisting towards the lingual surface, a feature unknown in other theropods. *Dromaeosaurus* is a relatively rare theropod throughout the BRG (Currie et al., 1990; Baszio, 1997; Peng et al., 1997).

Family Tyrannosauridae Osborn, 1905

cf Gorgosaurus libratus Lambe, 1914

Description and discussion. Fig. 8k. Large, thick teeth with elongated and recurved crowns and chisel-like denticles. Premaxillary teeth are characteristically D-shaped in cross section. Teeth

recovered exhibit fragmentary crowns, making lower taxonomic assignment difficult. Refereed tentatively to *Gorgosaurus libratus* based on the similarity of the teeth with this taxon, and because *Gorgosaurus* was the only tyrannosaurid known in this stratigraphic level of the Dinosaur Park Formation (Hans Larsson, pers comm..)

Family Troodontidae Gilmore, 1924

Gen and sp. Indet.

Single tooth tentatively referred to Troodontidae based on one recurved tooth with distinctive striations and wide, flared denticles on the posterior edge only.

Class Aves

Order Hesperornithiformes Fürbringer 1888

Family Hesperornithidae Marsh 1880

Genus *Baptornis* Marsh, 1877

Sp. indet.

Description and discussion. Fig. 81. See Tokaryk and Harington (1992) for full description.

Hesperornithiformes are regarded as open marine diving birds, so their presence in this assemblage is of paleoenvironmental significance.

Class Mammalia

Order Multituberculata

Family Cimolomyidae Marsh, 1889

Genus *Meniscoessus* Fox, 1980

Description and discussion. A Tooth is two rooted and longer than it is wide. The tooth has five cusps, three lingually and two labially. The sides of the cusps are ornamented with well-developed ridges.

Appendix G

Paleoecology and sedimentology of a vertebrate microfossil assemblage from the
easternmost Dinosaur Park Formation (Late Cretaceous, Upper Campanian)
Saskatchewan, Canada: Reconstructing diversity in a coastal ecosystem

Palynology Dataset

Genus and Species	1	2	3
<i>Accuratipollis lactifluminis</i> Braman 2002		X	
<i>Accuratipollis macrosolenoides</i> (Mtchedlishvili) Krutzsch 1970		X	X
<i>Aequitriradites baculatus</i> Doring 1964			
<i>Aequitriradites conulatus</i> Hunt 1985		X	
<i>Aequitriradites reticulatus</i> Kotova 1968			
<i>Aequitriradites spinulosus</i> (Cookson & Dettmann) Cookson & Dettmann 1961			
<i>Aequitriradites verrucosus</i> (Cookson & Dettmann) Cookson & Dettmann 1961			
<i>Aequitriradites</i> sp. 3			
<i>Alisporites bilateralis</i> Rouse 1959		X	
<i>Alisporites grandis</i> (Cookson) Dettmann 1963	X		X
<i>Alnipollenites quadernaria</i> (Stanley) Oltz 1969			
<i>Alnipollenites verus</i> (Potonié) Potonié 1934		X	
<i>Anacolosidites grandis</i> Bondarenko 1966		X	
<i>Annulisporea salsa</i> Braman 2002			
<i>Aquilapollenites aptus</i> Srivastava 1969			
<i>Aquilapollenites kentii</i> Braman 2013	X		X
<i>Aquilapollenites manifestus</i> (Takahashi & Shimono) Braman 2013			
<i>Aquilapollenites quadrilobus</i> Rouse 1957	X	X	X
<i>Aquilapollenites triangulus</i> (Yu, Guo & Mao) Braman 2013			
<i>Aquilapollenites</i> sp. 8			
<i>Arecipites</i> sp. 1			
<i>Arecipites</i> sp. 2			
<i>Asterisporites chlonovae</i> (Doring) Venkatachala & Rawat 1971		X	
<i>Asterisporites montanensis</i> (Tschudy) Li 2001			
<i>Asterisporites</i> sp. 3	X		
<i>Atospora</i> sp. 1			
<i>Azonia calvata</i> (Samoilovitch) Wiggins 1976			
<i>Azonia cribrata</i> Wiggins 1976			
<i>Azonia fabacea</i> Samoilovitch 1961			
<i>Azonia pulchella</i> Felix & Burbridge 1973			
<i>Azonia recta</i> (Bolkhovitina) Samoilovitch 1961			
<i>Azonia</i> sp. 2			
<i>Baculatisporites comaumensis</i> (Cookson) Potonié 1956		X	
<i>Baculatisporites papillosus</i> Takahashi 1964			
<i>Baculatisporites</i> sp. 4			
<i>Baculatisporites</i> sp. 6			
<i>Baculatisporites</i> sp. 13			
<i>Betulaceipollenites infrequens</i> (Stanley) Oltz 1969		X	

<i>Biretisporites deltoideus</i> (Rouse) Dettmann 1963			
<i>Biretisporites psilatus</i> (Groot & Penny) Dettmann 1963			
<i>Biretisporites</i> sp. 1			
<i>Biretisporites</i> sp. 2			
<i>Biretisporites</i> sp. 6			
<i>Botryococcus</i> sp. 1		X	
<i>Calamospora mesozoica</i> Couper 1958			
<i>Camarozonosporites ambigens</i> (Fradkina) Playford 1971	X	X	
<i>Camarozonosporites amplus</i> (Stanley) Dettmann & Playford 1968	X	X	
<i>Camarozonosporites</i> sp. 1			
<i>Cibotioidites bettianus</i> (Srivastava) Srivastava 1975	X	X	X
<i>Cibotioidites</i> sp. 2			
<i>Cibotiumspora clavata</i> Lei 1978		X	
<i>Cibotiumspora dicksoniaeformis</i> (Kara-Murza) Zhang 1984			
<i>Cibotiumspora juncta</i> (Kara-Murza) Singh 1983			
<i>Cicatricosisporites baconicus</i> Deak 1963			
<i>Cicatricosisporites coconinoensis</i> Agasie 1969			
<i>Cicatricosisporites mohrioides</i> Delcourt & Sprumont 1955			
<i>Cicatricosisporites myrtellii</i> Burger 1966			
<i>Cicatricosisporites ornatus</i> Srivastava 1972			
<i>Cicatricosisporites potomacensis</i> Brenner 1963			
<i>Cicatricosisporites radiatus</i> Krutzsch 1959	X	X	
<i>Cicatricosisporites spiralis</i> Singh 1971			
<i>Cicatricosisporites stoveri</i> Pocock 1964			
<i>Cicatricosisporites</i> sp. 9			
<i>Cicatricosisporites</i> sp. 17			
<i>Cicatricosisporites</i> sp. 24	X		
<i>Cicatricosporites norrisii</i> Srivastava 1971			
<i>Cingulatisporites dakotaensis</i> Stanley 1965			
<i>Circulina parva</i> Brenner 1963			
<i>Circumflexipollis tilioides</i> Chlonova 1961			
<i>Cirratiradites luminosus</i> Chlonova 1961			
<i>Cirratiradites</i> sp. 1			
<i>Clavatitricolpites</i> sp. 1			
<i>Clavatitricolpites</i> sp. 2			
<i>Concavissimisporites</i> sp. 1			
<i>Costatoperforosporites tuberculicostalis</i> (Stelmak) Davies 1985			
<i>Cranwellia rumseyensis</i> Srivastava 1966	X	X	X
<i>cf. Cranwellia</i> sp. 1			
<i>Cupanieidites terrestris</i> Braman 2002			X
<i>Cyathidites australis</i> Couper 1953			
<i>Cyathidites australis</i> var. <i>rimalis</i> Balme 1957			

<i>Cyathidites minor</i> Couper 1953	X	X	X
<i>Cyathidites rarus</i> (Bolkhovitina) Deak 1964			
<i>Cyathidites</i> sp. 1			
<i>Cyathidites</i> sp. 2			
<i>Cycadopites follicularis</i> Wilson & Webster 1946			
<i>Cycadopites fragilis</i> Singh 1964		X	
<i>Cycadopites scabratus</i> Stanley 1965	X		
<i>Cycadopites</i> sp. 5			
<i>Deltoidospora diaphana</i> Wilson & Webster 1946	X		
<i>Deltoidospora</i> sp. 2			
<i>Deltoidospora</i> sp. 3			
<i>Distaltrianglisporites perplexus</i> (Singh) Singh 1971			
<i>Droseridites</i> sp. 1			
<i>Dyadonapites reticulatus</i> Tschudy 1973	X	X	X
<i>Echimonocolpites</i> sp. 2			
<i>Echinatisporis caudatis</i> (Krasnova) Braman 2002			
<i>Echinatisporis solaris</i> Braman 2002			
<i>Echinatisporis Varispinosus</i> (Pocock) Srivastava 1975			
<i>Echinatisporis</i> sp. 1			
<i>Echinatisporis</i> sp. 4			
<i>Echinatisporis</i> sp. 6			
<i>Echinatisporis</i> sp. 12			
<i>Echinatisporis</i> sp. 19			
<i>Echinatisporis</i> sp. 20			
<i>Echinatisporis</i> sp. 22			
<i>Echinatisporis</i> sp. 25			
<i>Echitricolpites</i> sp. 1			
<i>Echitricolpites</i> sp. 2			
<i>Enzonalasporites bojatus</i> Braman 2002	X	X	
<i>Enzonalasporites</i> sp. 2			
<i>Ephedripites mediolobatus</i> Bolkhovitina 1953			
<i>Ephedripites notensis</i> (Cookson) Krutzsch 1961			
<i>Equisetosporites amabilis</i> Srivastava 1965			
<i>Equisetosporites hughesii</i> Pocock 1964			
<i>Equisetosporites menakae</i> Srivastava 1968			
<i>Equisetosporites mollis</i> Srivastava 1968			
<i>Equisetosporites multicostatus</i> (Brenner) Norris 1967			
<i>Equisetosporites</i> sp. 2	X	X	
<i>Equisetosporites</i> sp. 5			
<i>Erdtmanipollis procumbentiformis</i> (Samoilovitch) Krutzsch 1966	X	X	X
<i>Expressipollis</i> sp. 1	X	X	X
<i>Farabeipollis extendus</i> Braman 2013			

<i>Fibulapollis scabratus</i> Tschudy 1969			
<i>Foraminisporis asymmetricus</i> (Cookson & Dettmann) Dettmann 1963			
<i>Foraminisporis simiscalaris</i> (Paden-Phillips & Felix) Braman 2002	X		
<i>Foraminisporis undulatus</i> Leffingwell 1971	X	X	X
<i>Foraminisporis</i> sp. 4			
<i>Foveotricolpites</i> sp. 1			
<i>Foveotriteles subtriangularis</i> Brenner 1963			
<i>Gabonisporis labyrinthus</i> Srivastava 1972		X	
<i>Glaberprojectus celetus</i> Braman 2013			
<i>Glaberiprojectus</i> sp. 1			
<i>Gleicheniidites delicatus</i> (Bolkhovitina) Krutzsch 1959			X
<i>Gleicheniidites senonicus</i> Ross 1949	X	X	X
<i>Gleicheniidites stellatus</i> (Bolkhovitina) Krutzsch 1959			
<i>Gleicheniidites</i> sp. 1		X	X
<i>Gnetaceaepollenites oreadis</i> Srivastava 1968			
<i>Graminidites ulkapites</i> Srivastava 2011			
<i>Graminidites</i> sp. 1			
<i>Grewipollenites canadensis</i> Srivastava 1969			
<i>Grewipollenites radiatus</i> Tschudy 1973			
<i>Gunnaripollis superbus</i> Srivastava 1969		X	
<i>Hamulatisporis</i> sp. 1			
<i>Hannisporis scollardensis</i> Srivastava 1972			
<i>Hazaria sheopiarai</i> Srivastava 1971			X
<i>Heliosporites breviculus</i> (Balme) Wingate 1980	X	X	
<i>Hymenoreticulisporites</i> sp. 1			
<i>Hymenoreticulisporites</i> sp. 3			
<i>Inaperturotetradites scabratus</i> Tschudy 1973	X	X	X
<i>Integricorpus bellus</i> Mtchedlishvili 1961			
<i>Integricorpus clarireticulatus</i> Samoilovitch 1964	X	X	
<i>Interulobites</i> sp. 1	X		X
<i>Jarzenipollenites</i> sp. 1			
<i>Klukisporites</i> sp. 1			
<i>Kuprianipollis</i> sp. 1			
<i>Kurtzipites primitivus</i> Braman 2013			
<i>Laevigatosporites haardtii</i> (Potonié & Venitz) Thomson & Pflug 1953	X	X	X
<i>Laevigatosporites nitidus</i> Mamczar 1960			
<i>Laevigatosporites undulatiformis</i> Beilstein 1994		X	
<i>Leptolepidites tenuis</i> Stanley 1965			X
<i>Leptolepidites</i> sp. 7			
<i>Leptolepidites</i> sp. 10			
<i>Liburnisporis adnacus</i> Srivastava 1972			
<i>Liliacidites complexus</i> (Stanley) Leffingwell 1971			

<i>Liliacidites creticus</i> Mtchedlishvili 1961			
<i>Liliacidites intermedius</i> Couper 1953			
<i>Liliacidites morrinensis</i> Srivastava 1969			
<i>Liliacidites pollucibilis</i> Chmura 1973		X	
<i>Liliacidites variegatus</i> Couper 1958			
<i>Liliacidites</i> sp. 1			
<i>Liliacidites</i> sp. 2			
<i>Liliacidites</i> sp. 3	X		
<i>Liliacidites</i> sp. 5			
<i>Liliacidites</i> sp. 8	X		
<i>Liliacidites</i> sp. 12			
<i>Liliacidites</i> sp. 18			
<i>Lusatisporis dettmannae</i> (Drugg) Srivastava 1972		X	
<i>Lycopodiacidites</i> sp. 1			
<i>Maculatisporites</i> sp. 3			
<i>Maculatisporites</i> sp. 4			
<i>Mancicorpus anchoriforme</i> Mtchedlishvili 1961	X	X	X
<i>Mancicorpus tripodiformis</i> (Tschudy & Leopold) Tschudy 1973	X	X	X
<i>Mancicorpus</i> sp. 10			
<i>Marcelloporites tolmanensis</i> Srivastava 1969			
<i>Marcelloporites</i> sp. 2			
<i>Mica hoodooensis</i> Braman 2002			
<i>Monosulcites riparius</i> Braman 2002		X	
<i>Monosulcites</i> sp. 1	X		X
<i>Monosulcites</i> sp. 2			
<i>Multinodisporites</i> sp. 1			
<i>Orbiculapollis globosus</i> (Chlonova) Chlonova 1961		X	
<i>Osmundacidites wellmanii</i> Couper 1953		X	
<i>Osmundacidites</i> sp. 1			
<i>Ovoidites ligneolus</i> (Potonié) Thompson & Pflug 1953			
<i>Ovoidites</i> sp. 3			
<i>Pandaniidites typicus</i> (Norton) Sweet 1986	X		
<i>Parviprojectus amicus</i> (Srivastava) Braman 2013			
<i>Parviprojectus amygdaloides</i> (Srivastava) Braman 2013			
<i>Parviprojectus dolium</i> Samoilovitch 1964	X		
<i>Parviprojectus fasciatus</i> Braman 2013			
<i>Parviprojectus formosus</i> (Srivastava & Rouse) Braman 2013			X
<i>Parviprojectus funkhouseri</i> (Srivastava) Braman 2013	X	X	X
<i>Parviprojectus marionii</i> Braman 2013			
<i>Parviprojectus oblatum</i> (Srivastava) Braman 2013			
<i>Parviprojectus reticulatus</i> Mtchedlishvili 1961			
<i>Parviprojectus saginatus</i> (Felix & Burbridge) Braman 2013			

<i>Parviprojectus stelckii</i> (Srivastava) Braman 2013			X
<i>Parviprojectus trialatus</i> (Rouse) Braman 2013	X	X	X
<i>Parviprojectus validus</i> (Srivastava) Braman 2013			
<i>Parviprojectus</i> sp. 11			
<i>Pediastrum</i> sp. 1	X	X	X
<i>Penetetrapites inconspicuus</i> Sweet 1986	X		
<i>Pilosisorites</i> sp. 1		X	
<i>Pilosisorites</i> sp. 2			
<i>Pityosporites alipollenites</i> (Rouse) Krutzsch 1971			X
<i>Pityosporites constrictus</i> (Pierce) Krutzsch 1971	X	X	X
<i>Pityosporites</i> sp. 2			
<i>Pleurospermaepollenites</i> sp. 1		X	X
<i>Plicapollis</i> sp. 1			
<i>Podocarpidites cretaceus</i> Kara-Murza 1954			
<i>Podocarpidites crispus</i> (Chlonova) Krutzsch 1971			
<i>Podocarpidites kainarensis</i> (Bolkhovitina) Krutzsch 1971		X	
<i>Podocarpidites maximus</i> (Stanley) Norton 1969	X		X
<i>Podocarpidites minisculus</i> Singh 1964		X	
<i>Podocarpidites multesimus</i> (Bolkhovitina) Pocock 1962			
<i>Podocarpidites</i> sp. 1			
<i>Podocarpidites</i> sp. 2			
<i>Podocarpidites</i> sp. 3			
<i>Polycingulatisporites reduncus</i> (Bolkhovitina) Playford & Dettmann 1965	X	X	X
<i>Polycingulatisporites</i> sp. 5			
<i>Polypodiisporites amplus</i> Srivastava 1971	X		
<i>Polypodites</i> sp. 3			
<i>Polyporina cribraria</i> Srivastava 1969		X	
<i>Polyporina</i> sp. 1			
<i>Polyporina</i> sp. 3			
<i>Pristinupollenites microsaccus</i> (Couper) Tschudy 1973	X	X	X
<i>Pristinupollenites</i> sp. 3			
<i>Pristinupollenites</i> sp. 4			
<i>Proteacidites bellus</i> Samoilovitch 1961			
<i>Pseudoaquilapollenites parallelus</i> (Tschudy) Braman 2013			X
<i>Pulcheripollenites krempii</i> Srivastava 1969	X		X
<i>Quadripollis krempii</i> Drugg 1967			
<i>Quadripolls</i> sp. 2			
<i>Retibrevitricolporites beccus</i> Sweet 1986			
<i>Reticorpus senonicus</i> (Mtchedlishvili) Braman 2013	X	X	X
<i>Reticorpus superus</i> Braman 2013			
<i>Reticorpus trapeziforme</i> (Mtchedlishvili) Braman 2013			

<i>Reticuloidosporites pseudomurii</i> Elsik 1968	X	X	
<i>Reticulosporis foveolatus</i> (Pierce) Skarby 1978	X		
<i>Reticulosporis reticulatus</i> (Cookson) Jameossaniae 1987			
<i>Retitriletes austroclavatidites</i> (Cookson) Krutzsch 1963			
<i>Retitriletes globosus</i> Pierce 1961			
<i>Retitriletes mediocris</i> (Bolkhovitina) Krutzsch 1963		X	
<i>Retitriletes</i> sp. 1	X	X	
<i>Retitriletes</i> sp. 2	X		
<i>Retitriletes</i> sp. 6			
<i>Retitriletes</i> sp. 13			X
<i>Rogalskaisporites cicatricosus</i> (Rogalska) Danzé-Corsin & Laveine 1963			
<i>Rosannia manika</i> Srivastava emend. Srivastava & Braman 2010	X		
<i>Rousea</i> sp. 6			
<i>Rousea</i> sp. 11			
<i>Rugubivesiculites</i> sp. 1			
<i>Satishia</i> sp. 1			
<i>Scabrastephanocolpites lepidus</i> Srivastava 1968			
<i>Scabrastephanocolpites pentaaperturites</i> Venkatachala & Sharma 1974		X	X
<i>Schizocystia laevigata</i> Cookson & Eisenack 1962			
<i>Schizophacus parvus</i> (Cookson & Dettmann) Pierce 1976	X	X	X
<i>Schizophacus spriggii</i> (Cookson & Dettmann) Pierce 1976			X
<i>Schizophacus</i> sp. 1			X
<i>Senipites drumhellerensis</i> Srivastava 1969		X	
<i>Sequoipollenites paleocenicus</i> Stanley 1965			
<i>Siberiapollis montanensis</i> Tschudy 1971			
<i>Siberiapollis</i> sp. 8			
<i>Siberiapollis</i> sp. 13			
<i>Siberiapollis</i> sp. 14			
<i>Siberiapollis</i> sp. 20			
<i>Siberiapollis</i> sp. 21	X		
<i>Siberiapollis</i> sp. 24			
<i>Siberiapollis</i> sp. 27			
<i>Siberiapollis</i> sp. 28			
<i>Siberiapollis</i> sp. 34			
<i>Siberiapollis</i> sp. 36			
<i>Siberiapollis</i> sp. 39			
<i>Siberiapollis</i> sp. 45			
<i>Siberiapollis</i> sp. 52			
<i>Sigmopollis carbonis</i> (Newman) Srivastava 1984			X
<i>Sigmopollis hispidus</i> Hedlund 1968	X	X	

<i>Sparganium</i> sp. 1			
<i>Stereigranisoris regius</i> (Drozastichich) Ravn & Witzke 1995		X	
<i>Stereisporites ancoris</i> Krutzsch 1963	X		
<i>Stereisporites antiquasporites</i> (Wilson & Webster) Dettmann 1963		X	
<i>Stereisporites antiquus</i> Krutzsch 1966	X	X	
<i>Stereisporites cingulatus</i> Krutzsch 1963		X	
<i>Stereisporites rodaensis</i> Krutzsch 1966			
<i>Stereisporites triangulopunctus</i> Krutzsch 1966			
<i>Striatopollis trochuensis</i> (Srivastava) Farabee & Canright, 1986			
<i>Striatopollis</i> sp. 2			
<i>Striatopollis</i> sp. 5			
<i>Striatopollis</i> sp. 10			
<i>Striatopollis</i> sp. 12			
<i>Striatopollis</i> sp. 13			
<i>Subtriporopollenites alpinus</i> (Wolf) Tschudy 1973	X	X	X
<i>Taxodiaceapollenites hiatus</i> (Potonié) Kremp 1949	X	X	X
<i>Taxodiaceapollenites vacuipites</i> (Wodehouse) Wingate 1980	X	X	X
<i>Tetracolpites pulcher</i> Srivastava 1969			
<i>Tetracolpites reticulatus</i> Srivastava 1966			
<i>Tetranguladinium cruciformis</i> Yu, Guo & Mao 1983			
<i>Tetraporina quadrata</i> Bolkhovitina 1953	X		X
<i>Todisporites minor</i> Couper 1958			
<i>Todisporites</i> sp. 3			
<i>Translucentipollis plicatilis</i> Chlonova 1961			
<i>Tricolpites confossipollis</i> Srivastava 1975			
<i>Tricolpites crassireticulatus</i> Dutta & Sah 1970			
<i>Tricolpites explanatus</i> (Anderson) Drugg 1967			
<i>Tricolpites favosus</i> Ward 1986			
<i>Tricolpites foveolatus</i> Norton 1969			
<i>Tricolpites hokkaidoanus</i> Takahashi 1991			
<i>Tricolpites matauraensis</i> Couper 1953			
<i>Tricolpites occidentalis</i> Srivastava 1969			
<i>Tricolpites parvus</i> Stanley 1965			
<i>Tricolpites platyreticulatus</i> Groot, Penny & Groot 1961	X		
<i>Tricolpites reticulatus</i> Cookson 1947	X	X	X
<i>Tricolpites sphaeroides</i> Takahashi & Sugiyama 1990			
<i>Tricolpites</i> sp. 1	X	X	X
<i>Tricolpites</i> sp. 2			
<i>Tricolpites</i> sp. 5			
<i>Tricolpites</i> sp. 7			
<i>Tricolpites</i> sp. 12			
<i>Tricolpites</i> sp. 13			

<i>Tricolpites</i> sp. 14	X		
<i>Tricolpites</i> sp. 16			
<i>Tricolpites</i> sp. 17			
<i>Tricolpites</i> sp. 18			
<i>Tricolpites</i> sp. 21			
<i>Tricolpites</i> sp. 22			
<i>Tricolpites</i> sp. 23			
<i>Tricolpites</i> sp. 25	X		
<i>Tricolpites</i> sp. 29			
<i>Tricolpites</i> sp. 32	X		
<i>Tricolpites</i> sp. 38			
<i>Tricolpites</i> sp. 47			
<i>Tricolpites</i> sp. 48			
<i>Tricolpites</i> sp. 52			
<i>Tricolpites</i> sp. 54			
<i>Tricolpites</i> sp. 55			
<i>Tricolpites</i> sp. 65			
<i>Tricolpites</i> sp. 76			
<i>Tricolpopollenites levitas</i> Tschudy 1973	X	X	
<i>Tricolpopollenites parvulus</i> Groot & Penny 1960			
<i>Tricolpopollenites tenuiformis</i> Groot, Penny & Groot 1961			
<i>Tricolpopollenites</i> sp. 1			
<i>Tricolpopollenites</i> sp. 4			
<i>Tricolpopollenites</i> sp. 8			
<i>Tricolpopollenites</i> sp. 9			
<i>Tricolpopollenites</i> sp. 10			
<i>Tricolpopollenites</i> sp. 12			
<i>Tricolpopollenites</i> sp. 16			
<i>Tricolpopollenites</i> sp. 17	X		
<i>Tricolporites</i> sp. 1			
<i>Tricolporites</i> sp. 2			
<i>Tricolporites</i> sp. 4			
<i>Tricolporites</i> sp. 6			
<i>Tricolporites</i> sp. 7			
<i>Tricolporites</i> sp. 10			
<i>Tricolporites</i> sp. 20			
<i>Tricolporites</i> sp. 31	X	X	
<i>Tricolporites</i> sp. 35			
<i>Tricolporites</i> sp. 37			
<i>Tricolporites</i> sp. 49			
<i>Tricolporites</i> sp. 51			
<i>Tricolporites</i> sp. 73			

<i>Trifossapollenites ellipticus</i> Rouse 1957			
<i>Trilobapollis laudabilis</i> Braman 2002			
<i>Triporoletes involucratus</i> (Chlonova) Playford 1971	X	X	
<i>Triporoletes stellatus</i> Srivastava 1972	X	X	
<i>Triporopollenites rugatus</i> Newman 1965	X		
<i>Triporopollenites triplicatus</i> (Anderson) Nichols 2002			
<i>Triporopollenites</i> sp. 1			
<i>Triporopollenites</i> sp. 2			
<i>Triporopollenites</i> sp. 4			
<i>Triporopollenites</i> sp. 6			X
<i>Triporopollenites</i> sp. 13			X
<i>Triporopollenites</i> sp. 30			
<i>Triporopollenites</i> sp. 34			
<i>Triporopollenites</i> sp. 36			
<i>Triporopollenites</i> sp. 40			
<i>Triporopollenites</i> sp. 43			
<i>Triporopollenites</i> sp. 44			
<i>Triprojectus attenuatus</i> (Funkhouser) Braman 2013	X	X	X
<i>Triprojectus augustus</i> (Srivastava) Braman 2013			
<i>Triprojectus drumhellerensis</i> (Srivastava) Braman 2013			X
<i>Triprojectus geminatus</i> Braman 2013			
<i>Triprojectus pugnaefluminis</i> Braman 2013			
<i>Triprojectus rectus</i> (Tschudy) Braman 2013			
<i>Triprojectus turbidus</i> (Tschudy & Leopold) Braman 2013	X	X	X
<i>Triquitrites absurdus</i> Braman 2002	X		
<i>Trisectoris</i> sp. 1			
<i>Trochicola scollardiana</i> Srivastava 1972	X	X	
<i>Trudopollis meekeri</i> Newman 1965	X	X	X
<i>Tschudypollis thalmannii</i> (Anderson) Nichols 2002			
<i>Umbosporites callosus</i> Newman 1965		X	
<i>Undulatisporites</i> sp. 2			
<i>Varirugosporites tolmanensis</i> Srivastava 1972		X	
<i>Verrucosisporites</i> sp. 1		X	
<i>Verrucosisporites</i> sp. 2			
<i>Verrucosisporites</i> sp. 6	X		
<i>Verrucosisporites</i> sp. 7			
<i>Verrucosisporites</i> sp. 12			
<i>Verrucosisporites</i> sp. 14			
<i>Verrucosisporites</i> sp. 21			
<i>Verrutricolpites</i> sp. 2			
<i>Verrutricolpites</i> sp. 6			
<i>Verrutricolpites</i> sp. 13		X	

<i>Virgo amiantopollis</i> (Srivastava) Ward 1986	X	X	
<i>Vitreisporites pallidus</i> (Reissinger) Nilsson 1958	X	X	
<i>Zlivisporis blanensis</i> Pacltova 1959			
<i>Zlivisporis cenomanicus</i> (Agasie) Braman 2002	X	X	
<i>Zlivisporis novomexicanum</i> (Anderson) Leffingwell 1971			
<i>Zlivisporis reticulatus</i> (Pocock) Pacltova & Simoncsics 1970			
<i>Zlivisporis signifer</i> (Chlonova) Pacltova & Simoncsics 1970			
<i>Zlivisporis</i> sp. 5			
<i>Zlivisporis</i> sp. 6			
<i>Zlivisporis</i> sp. 8			
Unknown 31			
Unknown 62			
Dinoflagellates	X		X

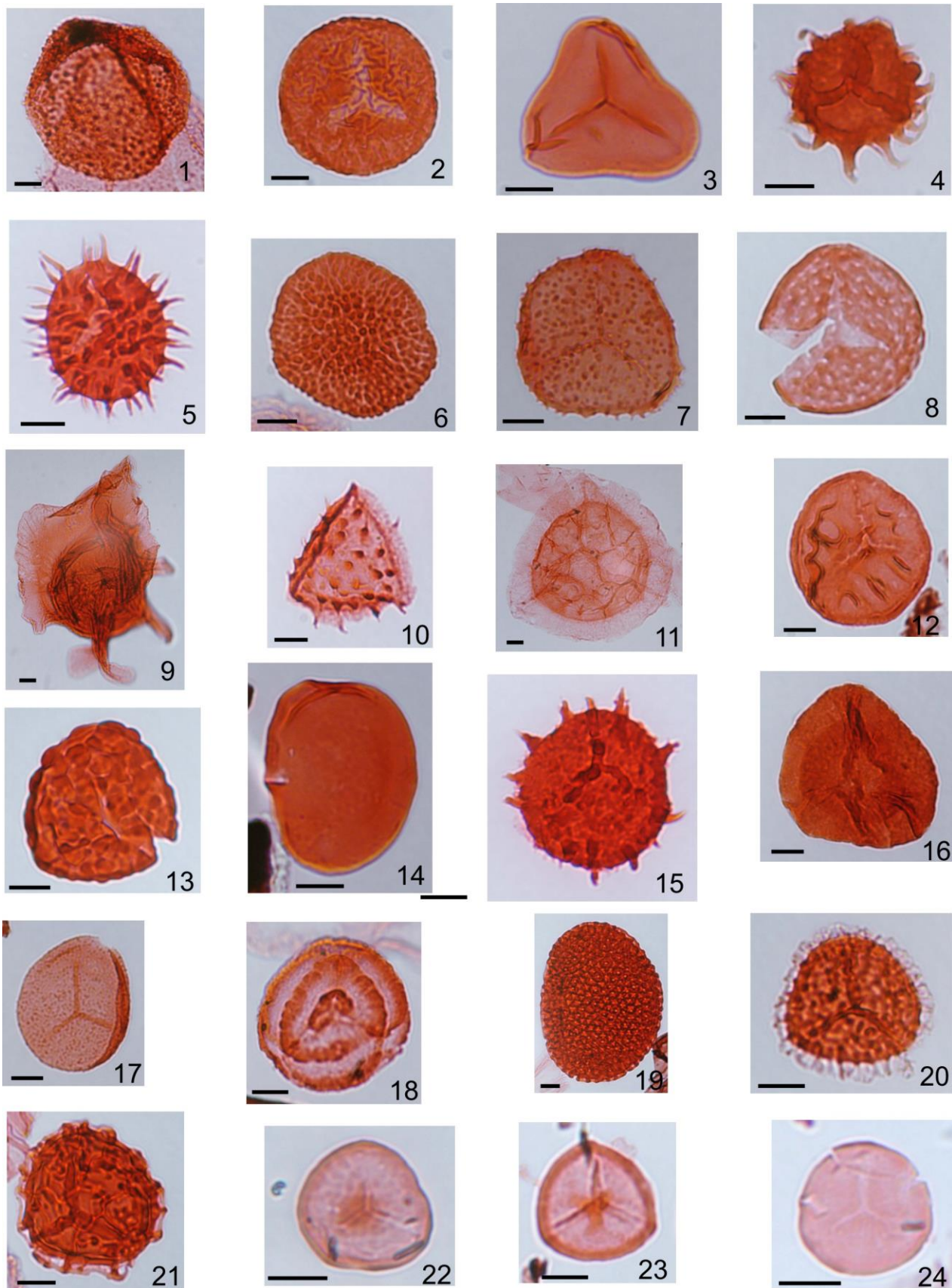


PLATE G.1

- Figure 1: *Baculatisporites comaumensis* (Cookson) Potonié 1956
- Figure 2: *Camarozonosporites ambigens* (Fradkina) Playford 1971
- Figure 3: *Cyathidites minor* Couper 1953
- Figure 4: *Echinatisporis* sp. 1
- Figure 5: *Echinatisporis* sp. 2
- Figure 6: *Foraminisporis asymmetricus* (Cookson & Dettmann) Dettmann 1963
- Figure 7: *Foraminisporis undulatus* Leffingwell 1971
- Figure 8: *Foveasporis triangulus* Stanley 1965
- Figure 9: *Ghoshispora* sp.
- Figure 10: *Heliosporites kemensis* (Chlonova) Srivastava 1972
- Figure 11: *Hymenoreticulisporites* sp.
- Figure 12: *Interulobites* sp.
- Figure 13: *Leptolepidites tenuis* Stanley 1965
- Figure 14: *Laevigatosporites haardti* (Potonié & Venitz) Thomson & Pflug 1953
- Figure 15: *Liburnisporis adnacus* Srivastava 1972
- Figure 16: *Lusatisporis dettmannae* (Drugg) Srivastava 1972
- Figure 17: *Osmundacidites wellmanii* Couper 1953
- Figure 18: *Polycingulatisporites reduncus* (Bolkhovitina) Playford & Dettmann 1965
- Figure 19: *Reticulosporis foveolatus* (Pierce), Skarby 1978
- Figure 20: *Retitriletes mediocris* (Bolkhovitina) Krutzsch 1963
- Figure 21: *Retitriletes* sp.
- Figure 22: *Stereigranisporis regius* (Drozhashtichich) Ravn & Witzke 1995
- Figure 23: *Stereisporites ancoris*
- Figure 24: *Stereisporites antiquasporites* (Wilson & Webster) Dettmann 1963

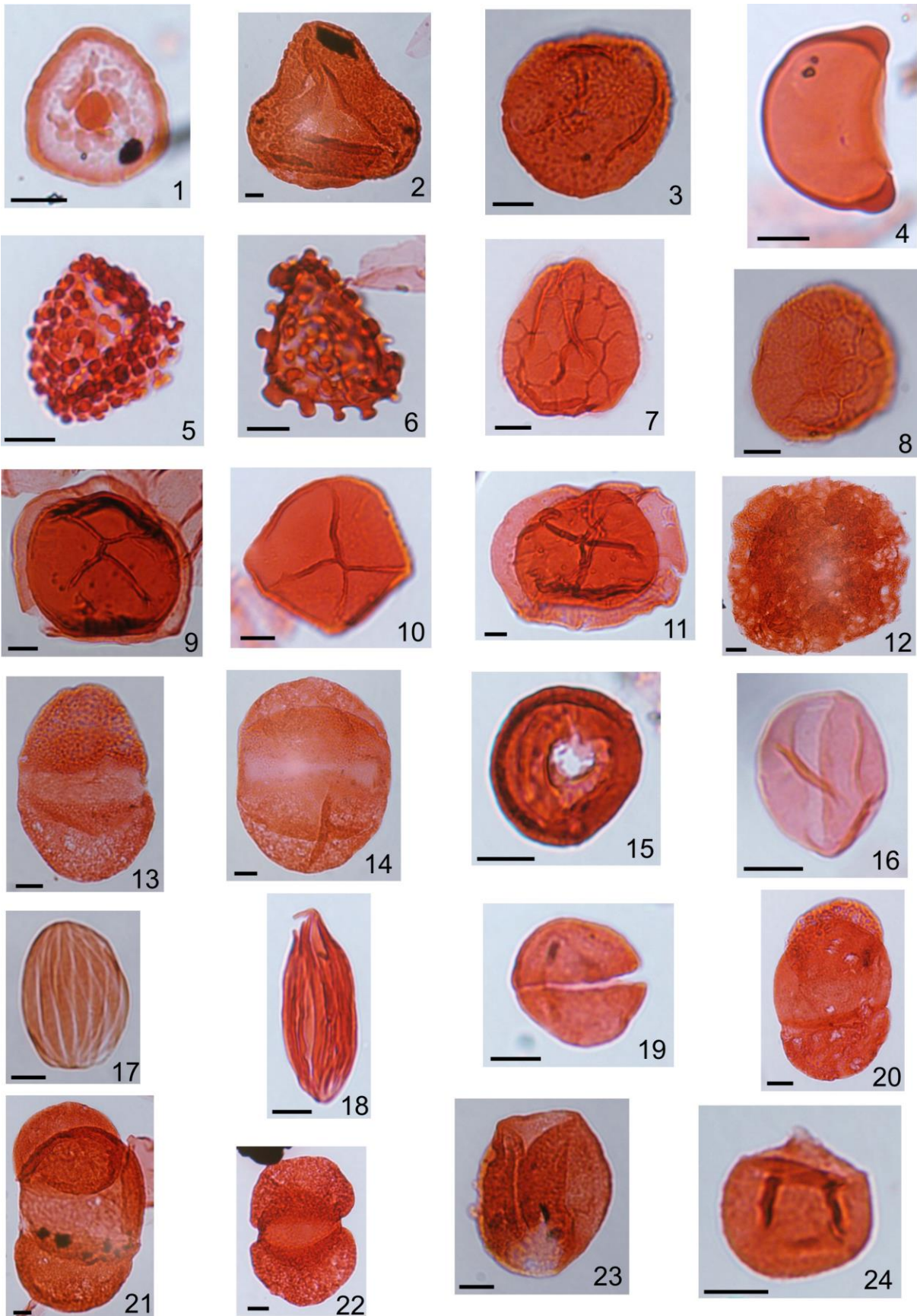


PLATE G.2

Figure 1: *Stereisporites rodaensis* Krutzsch in Doring, Krutzsch, Schulz & Timmermann 1966

Figure 2: *Cibotioidites bettianus* (Srivastava) Srivastava 1975

Figure 3: *Trisolissporites* sp.

Figure 4: *Umbosporites callosus* Newman 1965

Figure 5: *Varirugosisporites tolmanensis* Srivastava 1972

Figure 6: *Verrucosisporites* sp.

Figure 7: *Zlivisporis cenomanianus* (Agasie) Braman 2002

Figure 8: *Zlivisporis reticulatus* (Pocock) Pacltova & Simoncsics 1970

Figure 9: *Zlivisporis signifer* (Chlonova) Pacltova & Simoncsics 1970

Figure 10: *Zlivisporis* sp.

Figure 11: *Triporoletes stellatus* Srivastava 1972

Figure 12: *Azolla* sp.

Figure 13: *Alisporites bilateralis* Rouse 1959

Figure 14: *Alisporites grandis* (Cookson) Dettmann 1963

Figure 15: *Circulina parva* Brenner 1963

Figure 16: *Cycadopites fragilis* Singh 1964

Figure 17: *Equisetosporites menakae* Srivastava 1968

Figure 18: *Equisetosporites multicostatus* (Brenner) Norris 1967

Figure 19: *Monosulcites* sp.

Figure 20: *Pityosporites constrictus* (Pierce) Krutzsch 1971

Figure 21: *Pityosporites elongatus* var. *grandis* Tschudy 1973

Figure 22: *Podocarpidites* sp.

Figure 23: *Pristinupollenites microsaccus* (Couper) Tschudy 1973

Figure 24: *Sequoiapollenites paleocenicus* Stanley 1965

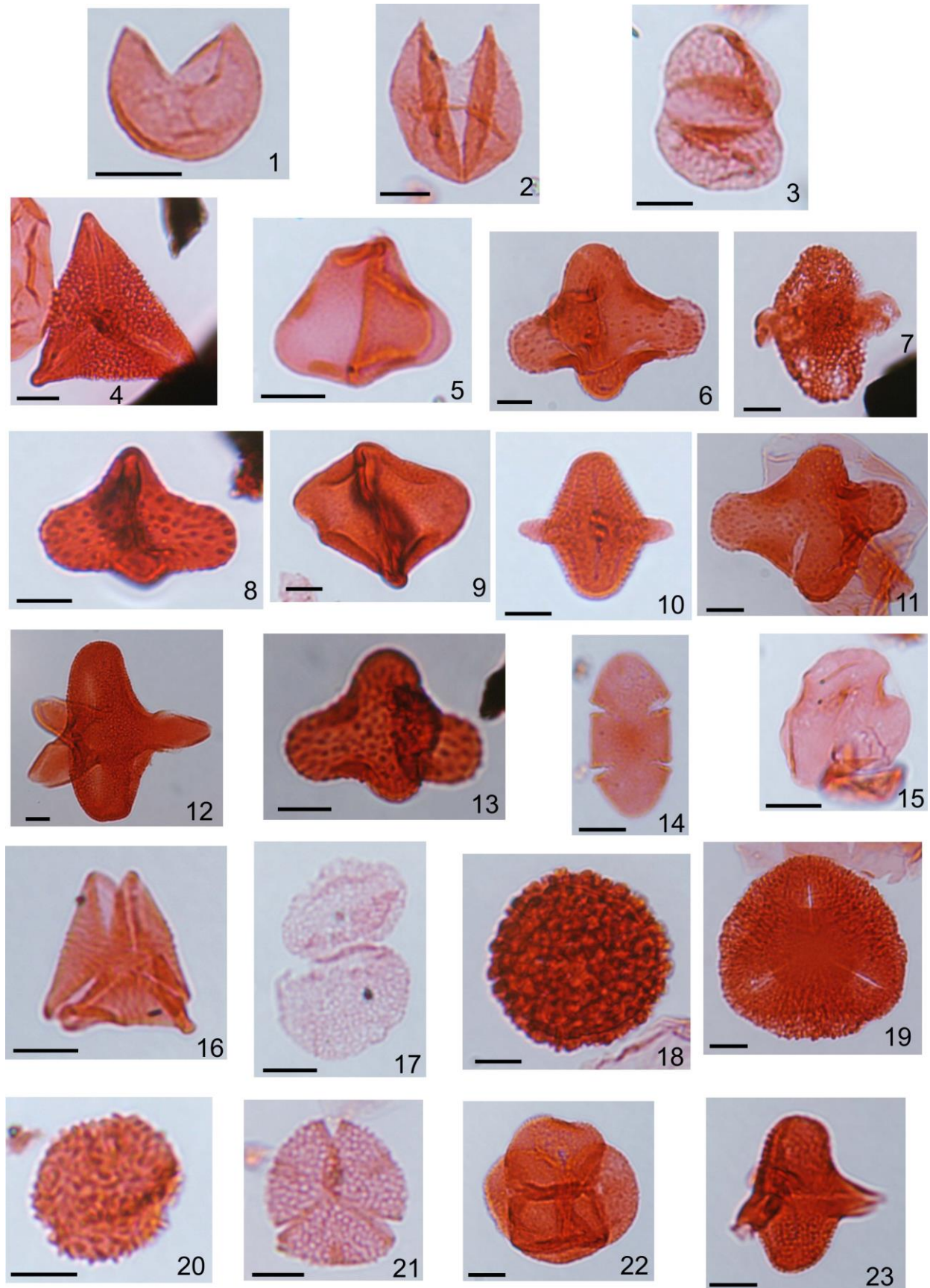


PLATE G.3

- Figure 1: *Taxodiaceapollenites hiatus* (Potonié) Kremp 1949
- Figure 2: *Taxodiaceapollenites vacuipites* (Wodehouse) Wingate 1980
- Figure 3: *Vitreisporites pallidus* (Reissinger) Nilsson 1958
- Figure 4: *Accuratipollis macrosolenoides* (Mtchedlishvili) Krutzsch 1970
- Figure 5: *Aquilapollenites aptus* Srivastava 1969
- Figure 6: *Aquilapollenites attenuatus* Funkhouser 1961
- Figure 7: *Aquilapollenites funkhouseri* Srivastava 1966
- Figure 8: *Aquilapollenites cf. quadrilobus* Rouse 1957
- Figure 9: *Aquilapollenites* sp. 1
- Figure 10: *Aquilapollenites* sp. 2
- Figure 11: *Aquilapollenites* sp. 3
- Figure 12: *Aquilapollenites trialatus* Rouse 1957
- Figure 13: *Aquilapollenites turbidus* Tschudy & Leopold 1971
- Figure 14: *Azonia pulchella* Felix & Burbridge 1973
- Figure 15: *Circumflexipollis tilioides* Chlonova 1961
- Figure 16: *Cranwellia rumseyensis* Srivastava 1966
- Figure 17: *Dyadonapites reticulatus* Tschudy 1973
- Figure 18: *Erdtmanipollis procumbentiformis* (Samoilovitch) Krutzsch 1966
- Figure 19: *Expressipollis* sp. 1
- Figure 20: *Grewipollenites canadensis* Srivastava 1969
- Figure 21: *Gunnaripollis superbus* Srivastava 1969
- Figure 22: *Inaperturotetradites scabratus* Tschudy 1973
- Figure 23: *Integricorpus clarireticulatus* Samoilovitch 1965

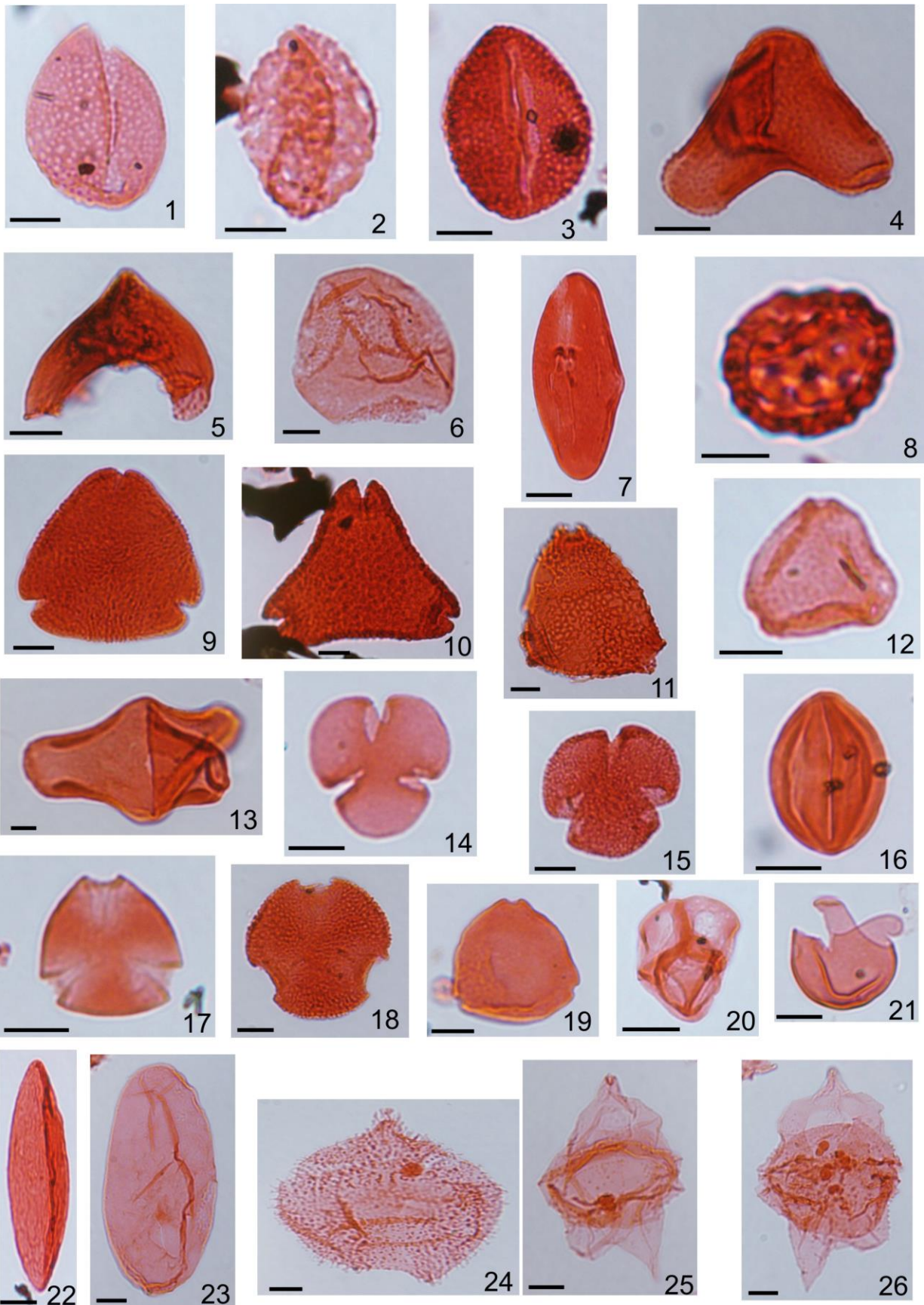


PLATE G.4

Figure 1: *Liliacidites* sp. 1

Figure 2: *Liliacidites* sp. 2

Figure 3: *Liliacidites* sp. 3

Figure 4: *Mancicorpus anchoriforme* Mtchedlishvili in Samoilovitch & Mtchedlishvili
1961

Figure 5: *Mancicorpus tripodiformis* (Tschudy & Leopold) Tschudy 1973

Figure 6: *Penetetrapites inconspicuus* Sweet 1986

Figure 7: *Pleurospermaepollenites* sp.

Figure 8: *Polyporina cribraria* Srivastava 1969

Figure 9: *Pulcheripollenites krempii* Srivastava 1969

Figure 10: *Siberiapollis montanensis* Tschudy 1971

Figure 11: *Siberiapollis* sp.

Figure 12: *Subtriporopollenites alpinus* (Wolf) Tschudy 1973

Figure 13: *Translucentipollis plicatilis* Chlonova 1961

Figure 14: *Tricolpites reticulatus* Cookson ex Couper 1953

Figure 15: *Tricolpites* sp.

Figure 16: *Tricolpopollenites* sp.

Figure 17: *Tricolporites* sp. 1

Figure 18: *Tricolporites* sp. 2

Figure 19: *Triporites* sp.

Figure 20: *Virgo amiantopollis* (Srivastava) Ward, p. 65, pl. 19, figs. 10-14.

Figure 21: *Sigmopollis carbonis* (Newman) Srivastava 1984

Figure 22: *Ovoidites ligneolus* (Potonié) Thomson & Pflug 1953

Figure 23: *Schizosporis parvus* Cookson & Dettmann 1959

Figure 24: *Chlamydophorella* sp.

Figure 25: *Chatangiella* sp. 1

Figure 26: *Chatangiella* sp. 2